

TIGHT BINDING BOOK

UNIVERSAL
LIBRARY

OU_158465

UNIVERSAL
LIBRARY

OUP—2273—19-11-79—10,000 Copies.

OSMANIA UNIVERSITY LIBRARY

Call No. 535.84

Accession No. 29946

Author J63I

Johnson, Raynor. C.

Title Introduction to molecular spectra.

This book should be returned on or before the date last marked below.

An Introduction to MOLECULAR SPECTRA

by

RAYNOR C. JOHNSON

M.A. (OXON), D.SC. (LOND.)

Master of Queen's College, University of Melbourne.
Sometime Lecturer in Physics in Queen's University, Belfast,
and the University of London, King's College

With 8 plates
and 151 text diagrams



METHUEN & CO. LTD., LONDON
36 Essex Street, Strand, W.C.2

First published in 1949

CATALOGUE NO. 3461/U

PRINTED IN GREAT ~~BRITAIN~~ ^{BRITAIN}

TO
MY FATHER AND MOTHER

PREFACE

THE student of atomic spectra has many books at his disposal; the student of molecular spectra has but few at present. This is to be expected in view of the greater complexity of the latter, and that its theoretical development came later. I have attempted to provide a text-book for the student who has graduated in Physics or Chemistry—or who is approaching graduation—and desires an understanding of the subject within the limits of ordinary mathematical equipment at that stage. Thus, at one or two points I have introduced the results of wave-mechanics, but I have not assumed familiarity in the use of this method. Again, in dealing with the electronic structures of polyatomic molecules, I have considered it outside the scope of the present book to introduce matters involving a knowledge of Group Theory.

In preparing a book of this kind the author is indebted for diagrams and illustrative material to the original papers of many workers who have contributed to the advancement of the subject. Wherever possible permission has been obtained from either author or publisher, and acknowledgement of the source is made in the text.

No writer on molecular spectra can fail to record his indebtedness to Prof. R. S. Mulliken's outstanding contributions to the subject. In addition to this I particularly desire to thank Dr. W. Jevons, whose *Report on Band Spectra of Diatomic Molecules*, published by the Physical Society in 1932, has proved of the utmost help. I am grateful also to Dr. F. A. Jenkins for the use of several of his fine grating spectra, and to Miss I. Arnott for her secretarial assistance.

R. C. JOHNSON

December, 1945

CONTENTS

	PAGE
I. INTRODUCTION	1
(a) The energy of atoms and molecules.	
(b) The general structure of band systems.	
(c) The fine structure of bands.	
(d) Infra-red band spectra.	
II. THE GROSS STRUCTURE OF BAND SYSTEMS	15
(a) Representation of bands.	
(b) The interval between band head and origin.	
(c) The assignment of vibrational quantum numbers.	
(d) The origin of multiplicity in band heads.	
(e) Formation of ' tails ' in band sequences.	
III. THE DISTRIBUTION OF INTENSITY IN A SYSTEM	31
✓(a) The Franck-Condon theory.	
(b) Some typical intensity distributions.	
(c) Intersection of $U(r)$ curves : Pre-dissociation.	
(d) Variability in intensity distributions.	
(e) Considerations based on wave-mechanics.	
(f) Continuous spectra.	
IV. THE INTER-NUCLEAR LAW OF FORCE	50
(a) The $U(r)$ function of Kratzer.	
(b) The $U(r)$ function of Morse.	
(c) The $U(r)$ function of Rydberg.	
(d) Some empirical relations between molecular constants.	
(e) The vibrational-rotational interaction.	
V. THE DISSOCIATION OF MOLECULES	59
(a) General principles.	
(b) The ionic type of binding.	
(c) The atomic type of binding (' homopolar ').	
(d) The Van der Waals type of binding.	
(e) The $G(v) : \omega_v$ relation : Birge's second method.	
(f) Dissociation through rotation.	

VI. THE ELECTRONIC STATES OF MOLECULES

- (a) The correlation of band systems of a molecule.
- (b) Description of the electronic states of atoms.
- (c) Description of the electronic states of molecules : selection rules.
- (d) Detailed electronic configurations.
- (e) Heitler and London's method.
- (f) The method of Hund, Herzberg, and Mulliken.
- (g) Valency.

VII. ROTATIONAL TERMS AND VECTOR COUPLINGS 95

- (a) Hund's Case (a).
- (b) Hund's Case (b).
- (c) Hund's Case (b').
- (d) Stages intermediate between (a) and (b).
- (e) Hund's Case (c).
- (f) Hund's Case (d).
- (g) Λ -type doubling.

VIII. FINE STRUCTURE: GENERAL CONSIDERATIONS 105

- (a) Types of branches.
- (b) Positive and negative rotational levels.
- (c) The combination principle.

IX. THE FINE STRUCTURE OF TYPICAL BANDS 110

- | | |
|-----------------------------------------------|---------------------------------------------------|
| (a) $^1\Sigma \rightarrow ^1\Sigma$ bands | (h) $^2\Delta \rightarrow ^2\Pi$ bands |
| (b) $^1\Pi \rightleftharpoons ^1\Sigma$ bands | (i) $^3\Sigma \rightarrow ^3\Sigma$ bands |
| (c) $^1\Pi \rightarrow ^1\Pi$ bands | (j) $^3\Pi \rightleftharpoons ^3\Sigma$ bands |
| (d) $^1\Pi \rightleftharpoons ^1\Delta$ bands | (k) $^3\Pi \rightarrow ^3\Pi$ bands |
| (e) $^2\Sigma \rightarrow ^2\Sigma$ bands | (l) Mixed Transition $^3\Pi \rightarrow ^1\Sigma$ |
| (f) $^2\Pi \rightleftharpoons ^2\Sigma$ bands | (m) Perturbations |
| (g) $^2\Pi \rightarrow ^2\Pi$ bands | |

X. INTENSITY DISTRIBUTION WITHIN BANDS 147

- (a) General considerations.
- (b) Intensity factors (i).
- (c) Temperature determinations from band data.
- (d) Factors on which 'effective' temperature depends.
- (e) Abnormal molecular rotation (OH and HgH).
- (f) Alternating intensities of band lines.

XI. THE EFFECT OF ISOTOPY ON MOLECULAR SPECTRA	169
(a) The vibrational effect.	
(b) The rotational effect.	
(c) The electronic effect.	
(d) Deuteride spectra.	
XII. EFFECTS OF APPLIED MAGNETIC FIELDS	184
(a) Weak fields : the Zeeman effect.	
(b) Strong fields : the Paschen-Back effect.	
(c) Zeeman effect in the Ångström CO bands ($^1\Sigma \rightarrow ^1\Pi$)	
(d) Perturbed terms in the Ångström CO bands.	
(e) Zeeman effect in doublet bands ($^2\Pi \rightleftharpoons ^2\Sigma$).	
(f) Spin doubling and Λ -type doubling.	
XIII. THE SPECTRA OF POLYATOMIC MOLECULES	201
(a) Introduction.	
(b) the vibrations of molecules.	
(c) The rotation of molecules.	
(d) Envelopes of infrared absorption bands.	
(e) Isotopic effects.	
(f) Electronic bands of triatomic molecules.	
(g) Electronic structures of molecules.	
XIV. THE RAMAN EFFECT	254
(a) Nature of the effect.	
(b) The structure of Raman bands.	
(c) Raman spectra of CO_2 , OCS , NH_3 , H_2O , &c.	
(d) Raman spectra of some acids.	
(e) Some organic compounds.	
XV. VARIOUS APPLICATIONS OF MOLECULAR SPECTROSCOPY	272
(a) Astrophysics.	
(1) The night sky and aurorae.	
(2) Cometary spectra.	
(3) Planetary spectra.	
(4) Stellar spectra.	
(b) Chemistry.	
(c) Biochemistry.	
(1) Proteins.	
(2) Hormones.	
(3) Enzymes.	
(4) Vitamins.	

PLATES AT END

- I. Gross structure of 'Swan bands' of C_2 molecule
- II. Ångström band (0,3) at λ 5610, showing fine structure analysis
- III. Fortrat diagram for the (13,13) band at λ 3991.11 of the CN band system $^2\Sigma \longrightarrow ^2\Sigma$
- IV. (1) High-pressure C_2 bands, being a $^3\Pi \longrightarrow ^3\Pi$ system
 (2) Comet-tail bands, being a $^2\Pi \longrightarrow ^2\Sigma$ system of CO^+
 (3) The Ångström system of CO, $^1\Sigma \longrightarrow ^1\Pi$
 (4) The 'Triplet' system of CO $^3\Pi \longrightarrow ^3\Pi$
- V. Ultra-violet system of O_2^+ ($^2\Pi \longrightarrow ^2\Pi$)
- VI. Band systems in emission and absorption of BaF (first order of 21-ft. concave grating)
- VII. CN 'Tail' bands in the second order of a 21-ft. concave grating
- VIII. Two bands of the red CN system ($^2\Pi \longrightarrow ^2\Sigma$)

INTRODUCTION

(a) THE ENERGY OF ATOMS AND MOLECULES

AN understanding of molecular structure must necessarily be built upon a reasonable knowledge of that simpler unit—the atom. An understanding of molecular spectra is also much more easily achieved from a prior knowledge of the principles of atomic spectra. The student is therefore advised before proceeding farther to refresh his memory at this point.*

Anyone who has examined with a direct-vision spectroscope the light from a bunsen flame into which certain salts have been introduced, or the light from the common neon discharge tube, will be familiar with the characteristic appearance of an atomic spectrum, viz. sharp bright lines on a dark background. Each of these radiated frequencies (ν) is the result of a particular electronic transition in a particular element, and is accounted for by the well-known Bohr equation $E' - E'' = h\nu$. Here E' and E'' are the total energies of the electron which makes the transition, when it is in the higher and the lower states respectively. Atomic spectroscopy has been concerned for many years (and in broad outline has completed its task) to take each of the chemical elements and record accurately the possible frequencies which can be emitted by electronic excitation. These data have then been sifted and expressed in mathematical formulae, and from these formulae can be inferred the so-called energy levels E' , E'' , &c., which the outermost electron in the atom is capable of occupying when displaced. The same can be done for singly ionized atoms, for doubly ionized atoms, &c., and from all these data has been constructed a picture of the architecture of each of the ninety-two chemical elements.

If with a direct-vision spectroscope the blue cone of a bunsen flame is examined, or the light from the incandescent vapour between the poles of a carbon arc burning in air, a different type of spectrum will be seen. The former is commonly called the 'Swan' spectrum, and it arises from a C_2 molecule. The latter is from a CN molecule, and causes the well-known violet colour of the vapour between the poles of an arc. Plate I of the Swan system should be carefully examined. It will be observed that instead of a number of sharp lines we have a pattern of bands or flutings. Such is characteristic of a molecular spectrum. Each of the bands in Plate I will be observed to be sharp on the red (or less refrangible) side and shade off towards the violet (or more refrangible) end of the spectrum. Briefly, we say this spectrum is degraded towards the violet. Other molecular spectra may degrade the opposite way. Sometimes, for reasons which will be understood later, no sharp band heads are formed, and the direction of degradation is not apparent. Another feature of Plate I which is

* A small monograph by the present author, *Atomic Spectra* (Methuen and Co., 1946), provides all that is essential for this purpose.

immediately evident is that the bands fall into natural groups: there are clearly regularities and relationships here such as one can seldom discern in the line spectra of atoms. It is true that sometimes this regular grouping of bands is not obvious (see Plates IV and V) and can be determined only after mathematical work has been done on the band-head frequencies.

How is the marked difference in appearance between atomic and molecular spectra accounted for? A diatomic molecule has, like an atom, an electron-cloud, and displacement of the most loosely bound electron from one possible orbit to another will correspond in both cases to emission or absorption of radiation. The molecule has, however, two kinds of energy which are not appropriate to the atom: energy of vibration and of rotation. The quantum theory must be applied to each of these. As regards vibrational energy, a change of this may take place concurrently with the electronic transition in a molecule. If the vibrational energy possessed by the molecule diminishes, this will correspond to an emission of energy; if it increases, this corresponds to an absorption of energy. Again, all molecules are rotating, and there is a distribution of angular velocities among the molecules of a gas, just as there is a distribution of linear velocities—both being affected by temperature. The rotational energy is quantized, so that concurrently with an electronic plus a vibrational transition, the rotational quantum number may also change. If the rotational quantum number diminishes, this means an emission of energy, and if it increases, an absorption of energy.

For a molecule we may therefore write its total quantizable energy at any instant as

$$E = E_e + E_v + E_K \quad . \quad . \quad . \quad (1)$$

If E' and E'' are the energies of a higher and lower state of excitation between which a transition takes place, we know $E' - E'' = h\nu$, &c., so that we may write

$$E' - E'' = (E_e' - E_e'') + (E_v' - E_v'') + (E_K' - E_K''),$$

and therefore

$$\nu = \nu_e + \nu_v + \nu_K \quad . \quad . \quad . \quad (2)$$

The order of magnitude of these terms is $\nu_e > \nu_v > \nu_K$. Indeed, if a rotational change took place on its own, ν_K , being only quite a small frequency, would correspond to a wave-length in the far infra-red (in the region of 100 μ). If vibrational and rotational changes occurred together this would raise the frequency into the near infra-red region. If, however, simultaneously with these an electronic transition occurs, the magnitude of this (ν_e) raises the frequency of the emitted radiation into the visible or ultra-violet region as a general rule.

Let us now apply these general principles to obtain an understanding of the typical band spectrum of Plate I. It is a spectrum in which electronic, vibrational, and rotational changes have all taken place. The frequency ν_e is known as the 'origin' of the band system. Although we shall see later that it does not exactly coincide with any particular band 'line' or band 'origin', it is approximately coincident with the strong band near the middle ($v' = 0$ to $v'' = 0$).

We have constructed below the spectrum two groups of vibrational energy levels. The upper group is associated with the state of higher *electronic* excitation, and the lower group with that of lower *electronic* excitation. The individual levels of each group correspond to different amounts of vibrational energy possessed by the molecule, the actual numbers of vibrational quanta being given by v' and v'' for the upper and lower electronic states. If a particular vibrational energy level of the upper state corresponds to greater vibrational energy of the molecule than a level of the lower group, and a transition takes place between them, then clearly ν_i of equation (2) is positive and the corresponding radiation $\nu = \nu_e + \nu_i$ will be on the high-frequency side of the system origin at ν_e . If, however, the vibrational energy is less in the upper than in the lower electronic state, then ν_i will be negative, and the corresponding radiation $\nu_e + \nu_i$ will be on the low-frequency side of ν_e . The whole array of bands which is found in the spectrum is thus accounted for by a single electronic transition, which, however, may be associated in different molecules with any one of the many possible vibrational changes. The various band 'origins', as they are called, are given by the various values of $\nu = \nu_e + \nu_i$ arising from the possible values of ν_i . Each band is thus defined by two vibrational quantum numbers, v' of the upper electronic state and v'' of the lower electronic state, and is usually described as the ($v' \rightarrow v''$) or simply the (v', v'') band. This assemblage of bands on both sides of the system origin is collectively called the gross structure of the system.

Each band, if this were all, might be expected to consist of a single line. Careful examination of any individual band shows that it is a complex cluster of fine lines. These arise from rotational changes in the molecule, and are called the fine structure of the band system. These fine lines are grouped round each band 'origin' on both the high- and low-frequency sides. They cannot be studied satisfactorily on such a photograph as Plate I, for the dispersion and resolving power of the spectrograph used was not great enough. Plates II and III show, however, the detailed fine structure of a single band: these were both obtained by Dr. F. A. Jenkins with the help of a powerful concave-grating spectrograph. Viewed under this high power we can see that the reason why bands under low power appear as flutings, sharp on one side and shading off on the other, is due to the peculiar distribution of the fine lines. We can, in fact, imagine that built above each of the vibrational energy levels on Plate I is a pile of rotational energy levels, each of which is associated with a rotational quantum number K . The electronic and vibrational change which defines a particular band will in general be associated also with a change in the rotational energy. If the rotational energy diminishes in the transition, the corresponding fine line will be on the high-frequency side of the band origin; if the rotational energy increases, on the low-frequency side. This is clear from equation (2). Fortunately, the rotational quantum number is not free to change except by one unit, i.e. ± 1 . Hence the fine structure of a band such as that of Plate III consists of two series of lines, known as branches. The fine structure of the band of Plate II has a third branch corresponding to no change in the rotational quantum number. (Although

there is no change in the quantum number there is change in the rotational energy arising from a change of molecular size. Otherwise the Q branch would be a single strong line.)

The complete band system, such as Plate I depicts, thus arises from a single electronic transition associated with all the possible vibrational and rotational changes which can arise. Billions of atoms are participating in any light emission, and every possible combination of transitions will receive support according to certain statistical laws. The counterpart of such a band system in an atom is a single frequency arising from the electron transition only.

The units commonly used to express energy changes in atoms and molecules are either wave-numbers or volts. The wave-number ($1/\lambda$), for which the symbol ν will in future be used, is the number of waves per cm. Frequencies $c\nu$ are much larger and in practice unwieldy. If wave-numbers are used, the energy is understood to be that of the corresponding quantum of radiation :

$$E_{\text{ergs}} = hc\nu_{\text{cm.}^{-1}},$$

from which we have

$$1 \text{ wave-number unit (cm.}^{-1}\text{)} = 1.9627 \times 10^{-16} \text{ erg.}$$

If volts are used, the energy of an electron which has been accelerated through this voltage is intended. The relation between ν (cm.^{-1}) and V (volts) is found from $h\nu = eV \times 10^8/c$ (1 volt = 8106 wave-number units).

(b) THE GENERAL STRUCTURE OF BAND SYSTEMS

It will form a useful introduction to the study of gross structure of band systems if we consider the Swan system of Plate I in some detail. The photograph shown is an enlargement of the spectrum obtained by using a medium-size dense flint-glass prism instrument. This well-known spectrum is radiated by a C_2 molecule: it can be observed in the light of a candle flame, in the blue cone of a bunsen burner, in the carbon arc burning in an atmosphere of hydrogen, when discharges are passed through hydrocarbons, and with great brilliance in a discharge tube having carbon electrodes and containing 20–30 mm. of argon, to which from time to time small quantities of hydrogen are admitted. The two thick energy levels on Plate I represent two electronic energy levels of the vibrationless C_2 molecule (or, strictly, they include the residual $\frac{1}{2}$ -quantum of vibrational energy). The lower one, $\nu'' = 0$, is associated with the ground state of the electron in the molecule; the upper one, $\nu' = 0$, represents the molecule with its outer electron in an excited state. We have already explained that each electronic state may be associated with various quanta of vibrational energy, and these levels are depicted in Plate I.

Since each band of a system has two vibrational quantum numbers and corresponds to a transition $\nu' \rightarrow \nu''$ from one level to another, the wave-numbers of the band origins, once determined, can be placed in a table such as that given on p. 5.

WAVE-NUMBERS OF ORIGINS OF SWAN BANDS
(Below) Estimated relative intensities on a scale (1-10)

$v' \backslash v''$	0 (1618.21)	1 (1594.87)	2 (1571.53)	3 (1548.19)	4 (1524.85)	5 (1501.51)	6
0 (1754.07)	19373.9 (10)	17755.7 (7)	16160.8 (3)	14589.3			
1 (1715.37)	21127.9 (9)	19509.7 (6)	17914.0 (6)	16343.3 (4)	14795.1		
2 (1676.67)	22843.3 (2)	21225.1 (8)	19630.2 (1)	18058.7 (5)	16510.5 (3)	14985.7 (1)	
3 (1637.97)		22901.8 (4)	21306.9 (7)	19735.4	18187.2 (4)	16662.2 (3)	15160.8 (1)
4			22944.9 (5)	21373.3 (4)	19825.1 (2)	18300.3 (2)	16798.8 (2)

If molecules were simple harmonic vibrators, theory predicts that the only changes of vibrational quantum number which would take place would be ± 1 or 0. Since no molecule fulfils this condition in practice, we find that many values of $v' \sim v''$ occur. In the table given, the wave-number differences between adjacent rows necessarily correspond to the intervals between the adjacent v' levels on Plate I, and the wave-number differences between the columns correspond to the intervals between adjacent v'' levels on Plate I.

Once the band wave-numbers have been assigned satisfactorily in a table as shown, an expression can be found to represent the whole array. In the above case the formula following is a good representation :

$$\nu = 19373.9 + (1773.42 v' - 19.35 v'^2) - (1629.88 v'' - 11.67 v''^2).$$

The quadratic term, as we have mentioned, arises from the anharmonic character of the molecular vibration. If the C_2 molecule had been a true simple harmonic oscillator there would have been only three sequences of bands corresponding to $v' - v'' = \pm 1, 0$, and they would have been expressed by $\nu = 19373.9 + 1773.42 v' - 1629.88 v''$.

In Plate I we observe that bands corresponding to a particular change in v (i.e. a particular value of $v' - v''$) appear to form natural groups. These are technically called 'sequences'. Bands which arise from the same initial level are said to form a v'' -progression. Those which go to the same final level are said to form a v' -progression. Thus the bands marked * on Plate I are a v'' -progression from $v' = 0$. Progressions are rows and columns of the above table; sequences are diagonals. Passing outwards from the band-system origin along a row, we observe that the wave-numbers diminish; in passing down a column they increase. This is, of course, expressed by the above formula for the Swan system. In general a formula of this type,

$$\nu_{v'v''} = \nu_{00} + (\omega'v' - \omega'x'v'^2) - (\omega''v'' - \omega''x''v''^2) . . . (3)$$

expresses with reasonable accuracy the bands of most systems. Here ω' and x' are constants for the upper electronic state and ω'' and x'' are constants for the final electronic state.

It will also be noticed that as we pass outwards from the origin of the band system there is a general tendency for the intensities to fall off. Although this is not invariably the case, it is often a helpful characteristic in trying to assign vibrational quantum numbers to a new band system.

A band system such as that shown in Plate I is very simple to analyse (i.e. to assign to a (v', v'') table as on p. 5). This is by no means always easy to do. Sometimes different sequences, instead of standing out separately, overlap a good deal. A little reflexion will show from equation (3) that the sequences will stand out fairly clear of each other if $\omega' \sim \omega''$ is small compared to ω' or ω'' . In the Swan system of C_2 shown above, $1773.4 - 1629.9 = 143.5$ is a reasonably small quantity compared with either of them.

Comparing atomic and molecular radiation with each other, we observe that each line of an atomic spectrum is the counterpart of an elaborate band system in a molecule. When we recall the many hundreds of lines arising from various electron transitions in a typical atom, the question arises whether the spectrum of a typical molecule will not be an unmanageably complex affair of hundreds of complex band systems. Fortunately, in practice we find only a few electronic transitions taking place in molecules. In the helium molecule, which along with that of hydrogen is the most prolific in this respect, not more than a score or two of band systems have been found. Three or four known band systems is much more typical of the average molecule. This is because, as we shall see later in the book (Chapter III (a)), electronic transitions often result in the generation of substantial vibrational energy, and this may cause dissociation of the molecule, flinging the component atoms apart.

(c) THE FINE STRUCTURE OF BANDS

Even in Plate I, at some distance from the band heads, traces of the fine structure may be seen. In general, however, a powerful grating type of spectrograph is essential for the study of fine structure, and Plates II and III may be taken as examples of such photographs of two very simple bands. The band whose fine structure is shown in Plate II occurs also in Plate IV, which was taken by using a glass prism spectrograph, and the student will appreciate the marked contrast in resolving power of the two instruments.

We are now concerned to understand in general terms how fine structure arises. Chapters VIII and IX will deal in considerable detail with the many types which are found: here we consider only the basic principles. The vibrational levels of Plate I may be regarded as due to non-rotating molecules, and in reality a pile of rotational levels might be imagined associated with each of those levels. To make clear, however, the relative magnitudes of the different kinds of energy—electronic, vibrational, and rotational—we have constructed in Fig. 1 a scale diagram for a particular band system.

The state of a molecule taking into account its whole energy would

therefore be represented by one of these 'fine' rotational levels, and the fine structure of a band (v' , v''), is accounted for by transitions from the rotational levels of the upper v' state to the rotational levels of the lower v'' state. Each rotational level is distinguished by a rotational quantum number K which measures the number of units of angular momentum ($\hbar/2\pi$) the molecule possesses. Fortunately, theoretical considerations show that for rotational changes the quantum number

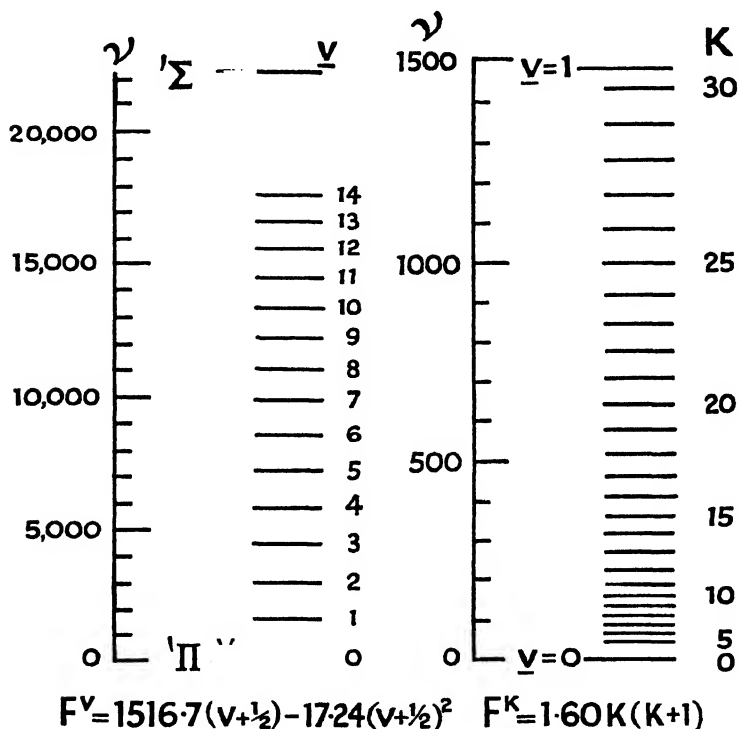


Fig. 1. Scale diagram of energy levels for the Ångström system of CO, illustrating the relative magnitude of v , v' , and v'' in a typical case.

K can only change by ± 1 or 0. (We shall find later that 'selection principles' of this kind govern many of the quantum numbers with which we are concerned in molecules.) As a result, a simple band may have three sets of lines. These are the so-called 'branches', and are named as follows:

$$\left. \begin{aligned}
 K + 1 &\rightarrow K && R \text{ branch (or Positive branch),} \\
 K &\rightarrow K && Q \text{ branch (or Zero branch),} \\
 K - 1 &\rightarrow K && P \text{ branch (or Negative branch).}
 \end{aligned} \right\} \quad (4)$$

Fig. 2 illustrates the transitions giving rise to these branches. One of the striking features of Plates II and III is the character of these

branches. The lines in any one branch are distributed in such a way that if the wave-number of each line is plotted against its rotational quantum number, they lie on a parabola. The *P* and *R* branches appear indeed to form parts of one and the same parabola. To account for this theoretically we may consider an idealized case—a rigid

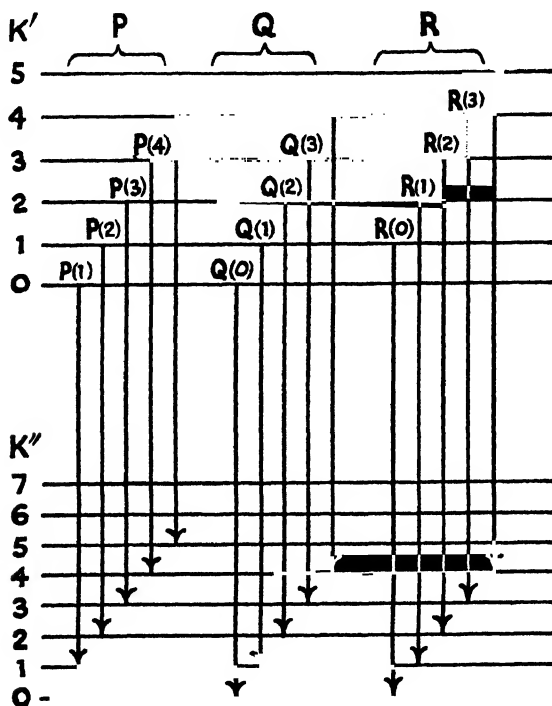


Fig. 2. Rotational transitions which will give rise to *P*, *Q*, and *R* branches in a simple band.

diatomic molecule rotating about a line perpendicular to the inter-nuclear axis and through the centre of gravity.

If *I* is the moment of inertia, and Ω the angular velocity

$$I\Omega = K \frac{h}{2\pi} \quad \dots \quad (5)$$

The rotational energy of the molecule is

$$E_K = \frac{1}{2}I\Omega^2 = K^2 \frac{h^2}{8\pi^2 I} \quad \dots \quad (6)$$

When an electronic transition takes place in a molecule, the molecular 'constants', such as the moment of inertia, frequency of nuclear vibration, &c., all change their values. This would be anticipated, in general, since the inter-nuclear distance represents an equilibrium between electrostatic repulsive forces of the nuclei and the binding

action of the negative electron-cloud. If an electron undergoes a transition from one orbit to another, its contribution to the binding forces of the molecule will change, and a new equilibrium must be established. If I' and I'' are the values of the moment of inertia in the initial and final states of the molecule, and if $h\nu_0$ represents the energy output from electronic and vibrational change (the values of ν_0 being given by equation (3)), then the wave-numbers due to rotational transitions $K' \rightarrow K''$ will be given by

$$\nu = \nu_0 + \frac{h}{8\pi^2 I' c} K'^2 - \frac{h}{8\pi^2 I'' c} K''^2 \quad . \quad . \quad . \quad (7)$$

If we substitute the permitted changes in K of (4) we have :

$$\left. \begin{aligned} \nu &= \nu_0 + B' + 2B'K + CK^2 & . \quad . \quad . & \quad R \text{ branch,} \\ \nu &= \nu_0 + CK^2 & . \quad . \quad . & \quad Q \text{ branch,} \\ \nu &= \nu_0 + B' - 2B'K + CK^2 & . \quad . \quad . & \quad P \text{ branch,} \end{aligned} \right\} \quad . \quad (8)$$

where the following abbreviations are used :

$$B' = \frac{h}{8\pi^2 I' c}, \quad B'' = \frac{h}{8\pi^2 I'' c}, \quad C = B' - B'' \quad . \quad (9)$$

The formulae (8) can best be understood with an actual case before us. In Plate II is a photograph of the (0,3) band of the Ångström system of CO. The three branches have been picked out, and the diagram above the spectrogram is a graph of wave-number (ν) against rotational quantum number (K). It portrays in a clear manner the significance of the three branches, which, as we see from (8), correspond to a parabolic distribution of lines. (This is usually called a Fortrat diagram.)

We observe that the band of Plate II degrades to the high-frequency side. The condition that it should do so is that the coefficient C of (9) should be positive, for the term CK^2 is the dominating one for the large values of K . If C were negative, then the band would degrade to the low-frequency side. If C is positive, then it is the P branch which forms the head; if C is negative, it is the R branch (see equation (8)). On Plate III we have the spectrogram of the (13,13) band of the CN molecule—a very simple type of band which has no Q branch, and which is degraded to the less refrangible or low-frequency side. It may be of interest to note that for the Ångström CO bands of Plate II, $B_0' = 1.942$ and $B_3'' = 1.538$ (i.e. $B' > B''$) and for the CN band of Plate III, $B_{13}' = 1.596$ and $B_{13}'' = 1.659$, i.e. $B' < B''$. We may summarize our remarks thus :

Direction of degradation to	Branch forming head	Changes in molecular constants		Inter-nuclear distance
		B	I	
High-frequency side .	P	$B_0' > B_0''$	$I_0' < I_0''$	Increases
Low-frequency side .	R	$B_0' < B_0''$	$I_0' > I_0''$	Decreases

We observe further from equation (8), as well as from Plates II and III, that, as regards the *P* and *R* branches, one branch is the continuation of the other branch for negative values of *K*.

The *P* and *R* branches intersect on the ν -axis at the point $\nu_0 + B'$ for $K = 0$. The *Q* branch head, it will be noticed, is at ν_0 , a wave-number close to, but not identical with, the above. The 'origin' of a band is defined by ν_0 , the wave-number of the radiation arising from electronic and vibrational change only. The *Q* head, if present, marks this point. The point of intersection of the *P* and *R* branches at $\nu_0 + B'$ is often called the null line of the band, for the reason that it is absent from the band structure. We see therefore that a band's origin will always lie within the band structure at some distance from the band head. On low-dispersion spectrograms (Plate I) only the position of the head is measurable: the origin can as a rule be located only if highly resolved bands are available.

Strictly, it is only band *origins* that are expressible by equation (3); but if these data are not available the band *heads* can usually be fitted to such a formula with fair accuracy. (Further detail is given in Chapter II, Sections (a) and (b).)

By fitting the fine-structure lines to equations (8), the moments of inertia of the emitting molecule are calculable for both the initial and final electronic states. The moment of inertia of a rotating diatomic molecule consisting of two masses m_1 and m_2 distant r apart is

$$I = \frac{m_1 m_2}{m_1 + m_2} r^2 = \frac{M_1 M_2}{M_1 + M_2} m_1 r^2 \quad . \quad . \quad (10)$$

where M_1 and M_2 are nuclear masses (whole numbers) and m_1 is the mass of an atom of unit atomic weight, viz.

$$m_1 = \frac{\text{mass of H atom}}{\text{atomic weight of H}} = \frac{1.662 \times 10^{-24}}{1.0077} = 1.649 \times 10^{-24} \text{ gm.}$$

Thus if the chemical nature of the emitter is known, the internuclear distance can be calculated (often to an accuracy of 0.001 A.U.) from

$$r = \frac{16.774}{B} \left(\frac{M_1 + M_2}{M_1 M_2} \right),$$

where r is measured in A.U. and B is measured in cm.^{-1} . In practice, however, the evaluation of the molecular constants B' , B'' , &c., is not done by fitting the fine-structure lines to the branch formulae (8), but by using certain mathematical relations between corresponding lines of different branches. These methods are collectively called the combination principle (see Chapter VIII, Section (c)).

(d) INFRA-RED BAND SPECTRA

We have seen in the preceding section what the structure of a simple type of 'electronic' band may be expected to be. The association of an electronic jump with vibrational and rotational changes has two major consequences: (1) because of the magnitude of ν_e it usually causes bands to be in the visible or ultra-violet region, and (2) because of the change of size of the molecule it creates bands with the para-

bolic type of branch. If no electronic transition takes place ($v_e = 0$), vibration-rotation bands may nevertheless occur. These are usually in the near infra-red region. This region can be investigated photographically up to about 12,000 A.U. ($= 1.2 \mu$), and beyond this the thermopile and galvanometer may be used. If prism spectrographs are employed the optical system has to be changed to deal effectively with different regions of the infra-red, such as quartz (1μ - 3.5μ), fluorite (1μ - 7μ), rocksalt (7μ - 15μ) or potassium bromide (12μ - 22μ).

In Fig. 3 we have represented the group of vibrational levels which is associated with the ground state of the C_2 molecule on Plate I.

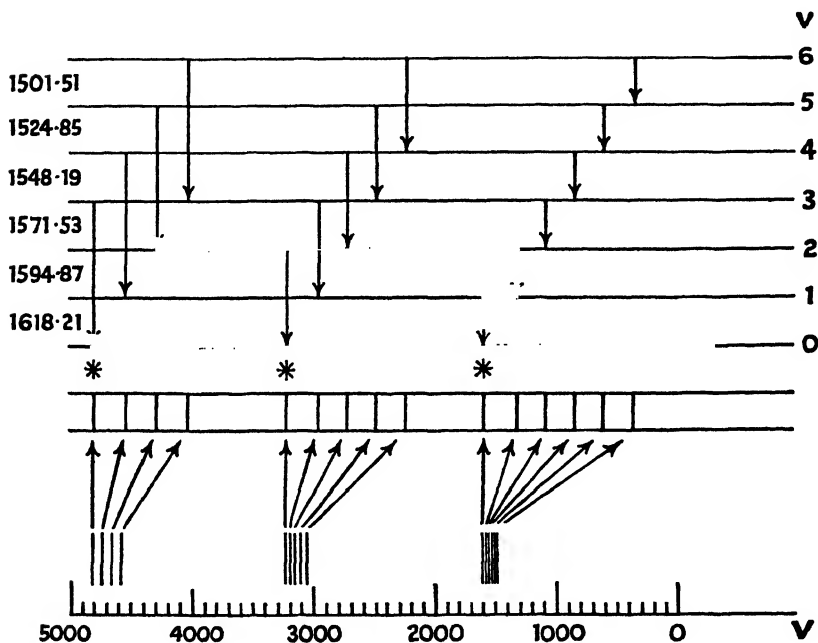


Fig. 3. Typical vibration-rotation band spectrum in emission.

Transitions between these would be expected to give rise to vibration-rotation bands, and all these bands should be expressible by the formula $\nu = 1629.88 (v' - v'') - 11.67 (v'^2 - v''^2)$. There are special reasons (see Chapter X) why molecules of the type X_2 , such as C_2 , N_2 , O_2 , Cl_2 , which have no electric moment, cannot give rise to vibration-rotation bands, but for purposes of illustrating the general features of such spectra we disregard the fact that the levels depicted in Fig. 3 are for a C_2 molecule. We have already remarked that the anharmonic vibrator can permit any change in v , so that arrows may be placed as shown to illustrate possible emission bands. The absorption spectrum of the cold gas or vapour would inevitably be simpler. The only bands to be expected are marked by *, and would correspond to absorption of energy from the ground level $v'' = 0$ to various

higher levels. The absorption band ($1 \leftarrow 0$) is usually called the 'fundamental', while ($2 \leftarrow 0$), ($3 \leftarrow 0$), &c., may be called 'overtones', and are approximately multiples of the fundamental wave-number (in the above case 1618.21 cm.^{-1}).

Infra-red bands commonly differ in appearance from electronic bands in not showing fine structure converging to the formation of a band head. The mean size of a molecule, and therefore the moment of inertia, is going to vary only slightly with vibrational amplitude, so that infra-red bands will almost invariably be headless. If $B' = B''$ in equation (8), the coefficient $C = B' - B''$ will vanish, and the

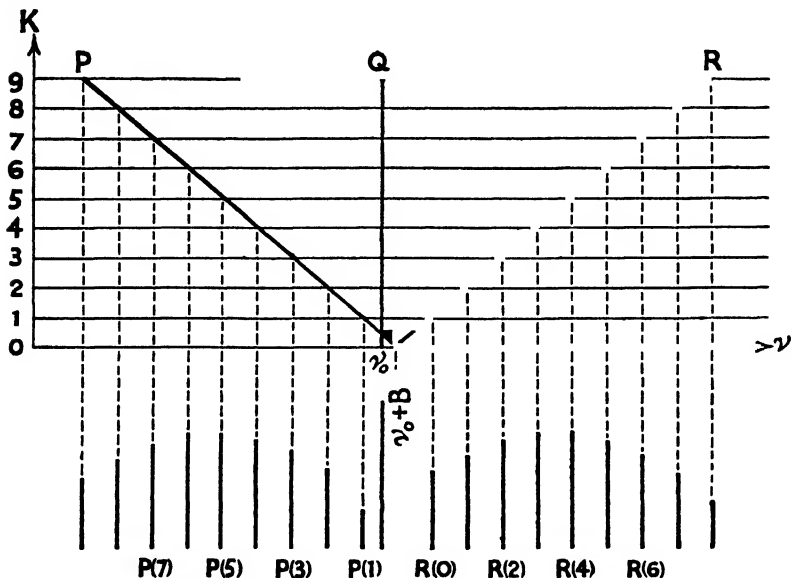


Fig. 4. Fortrat diagram for a simple vibration-rotation band where $C = 0$.

result will be a linear distribution of fine structure on both sides of the band origin. Examination of Plate VII, which is an *electronic* band system, will disclose a certain number of headless bands due to the fact that B' and B'' have become almost equal for these particular bands. This rather exceptional state of affairs for electronic bands is the rule for vibration-rotation bands. The formulae of equation (8) would degenerate in the special case $B' = B''$ to :

$$\left. \begin{aligned} \nu &= \nu_0 + B' + 2B'K & \dots & R \text{ branch,} \\ \nu &= \nu_0 & \dots & Q \text{ branch,} \\ \nu &= \nu_0 + B' - 2B'K & \dots & P \text{ branch.} \end{aligned} \right\} \dots (11)$$

This corresponds to degeneration of the parabolae into straight lines as in Fig. 4.

The Q branch, if present, becomes a single strong line at the band origin.

The moment of inertia of a molecule, as we have remarked above, will be expected to vary only slightly with vibrational amplitude, compared with the magnitude of the change which commonly occurs because of electronic displacement. The effect of vibration will be to increase slightly the mean square of the inter-nuclear distance, and thus to increase the moment of inertia. The constant B of (11) thus very slowly diminishes as v increases, and to a close approximation the relationship is linear :

$$B_i = B_0 - \alpha v \quad . \quad . \quad . \quad . \quad . \quad (12)$$

The constant α is comparatively small: for the upper and lower electronic states of the C_2 molecule these values have been found to be $\alpha' = 0.03$ and $\alpha'' = 0.025$. Because the constant $C = B_v - B_{v'}$, which is $\alpha(v'' - v')$ for vibration-rotation bands, is so small, these

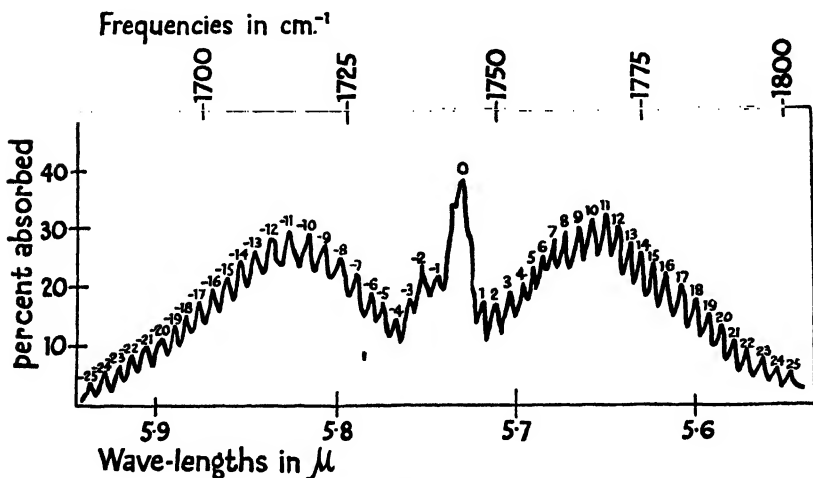


Fig. 5

bands will seldom if ever have a head. Because this has a negative value, however, the *tendency* to head formation will necessarily be in the R branch (see equation (8)).

Fig. 5 shows a recording of a typical vibration-rotation band made by the use of a slit-thermopile and galvanometer.

We now come to the matter of pure-rotation bands. For most molecules in an ordinary state, v_r and v_e of equation (2) are both zero. If sufficiently stimulated by electrons or radiation or by thermal agitation at high temperatures, then electronic and vibrational energy may be imparted. The common absence of vibrational energy in ordinary molecules is supported by the evidence of specific heats which at ordinary temperatures are adequately accounted for by the translational and rotational energy of most molecules. Both these types of energy are governed by the temperature which gives to the molecules an appropriate (probability) distribution of linear velocities and angular velocities. If a gas is unexcited (i.e. in temperature

equilibrium with its surroundings), then there will be a constant interchange of energies between individual molecules, some going up and some going down the energy scale, but the net result so far as radiation of the gas to its surroundings is concerned will be zero. If, however, the gas is above the temperature of its surroundings, thermal radiation will be emitted. A continuous spectrum will presumably be radiated as the kinetic energy of translation falls, but discrete band lines will arise from the quantized rotational energy. The equation (7) becomes :

$$\begin{aligned} \nu &= \frac{h}{8\pi^2 I c} [(K+1)^2 - K^2] \\ &= B(2K+1) \quad . \quad . \quad . \quad . \quad (13) \end{aligned}$$

This radiation is, of course, in the far infra-red region, and is difficult to analyse spectroscopically. Such a pure-rotation band, we observe, consists of one branch only of equidistant lines separated by the interval $h/4\pi^2 I c$ (see Fig. 6). In a few favourable cases (HCl and HBr) some of these lines have been observed experimentally.

THE GROSS STRUCTURE OF BAND SYSTEMS

(a) REPRESENTATION OF BANDS

WE now amplify the matter introduced briefly in Chapter I (b). Using the Swan system of C_2 as an example, we saw that the gross-structure of a typical band system could be represented by equation (3). The typical vibrational term was taken to be the function

$$G(v) = \omega_e v - \omega_e x_e v^2 + \omega_e y_e v^3 \dots \quad (14)$$

where as a rule no term higher than v^2 is necessary. The vibrational energy of the molecule is expressed by the values of $hcG(v)$. The 'origin' of the band system was defined as the wave-number ν_e . This is almost identical with the 'origin' of the (0,0) band but we shall see shortly that it is not quite the same.

According to the New Quantum Theory the typical vibrational term is

$$G(v) = \omega_e(v + \frac{1}{2}) - \omega_e x_e(v + \frac{1}{2})^2 + \omega_e y_e(v + \frac{1}{2})^3 \dots \quad (15) *$$

where v takes values 0, 1, 2, 3, &c. It is sometimes said that the New Quantum Theory introduces half-integral quantum numbers, but this is not so. The quantum numbers remain integral: it is the expression for the vibrational energy of an oscillation which is modified. As a result of this, the vibrational energy never vanishes but has a minimum value $hcG(0)$, where $G(0) = \frac{1}{2}\omega_e - \frac{1}{4}\omega_e x_e + \frac{1}{8}\omega_e y_e$. This vibrational energy is residual, and cannot be removed from the molecule. It follows therefore that the (0,0) band of a system has its origin at

$$\begin{aligned} \nu^{0r} &= \nu_e + G'(0) - G''(0) \\ &= \nu_e + (\frac{1}{2}\omega_e' - \frac{1}{4}\omega_e' x_e') - (\frac{1}{2}\omega_e'' - \frac{1}{2}\omega_e'' x_e'') \quad (16) \end{aligned}$$

which is not coincident with the system origin ν_e .

The nuclear vibration frequency is easily derived from the expression for the vibrational energy. Thus in cm^{-1}

$$\omega_e = \frac{1}{hc} \frac{\partial E}{\partial v} = \frac{\partial G}{\partial v} \quad (17) \dagger$$

According to the Old Quantum Theory we should therefore have

$$\omega_v = \omega_0 - 2\omega_0 x v + \dots \quad (18)$$

According to the New Quantum Theory we should have from (15) and (17)

$$\omega_v = \omega_e - 2x_e \omega_e(v + \frac{1}{2}) + 3y_e \omega_e(v + \frac{1}{2})^2 \dots \quad (19)$$

* The subscript e of ω_e is used to remind us that ω_e is the frequency of infinitesimal vibrations about the equilibrium position—a theoretical quantity, of course.

† A rigorous proof is rather too long to present. A simple proof follows from regarding v as continuously variable, when we should have for the energy of an oscillator of frequency ω_v , $E = hc f \omega_v dv$.

So that we have for the vibration frequency (ω_0) in the lowest state, where $v = 0$,

$$\omega_0 = \omega_e - x_e \omega_e + \frac{1}{2} y_e \omega_e (20)$$

The theoretical frequency ω_e about the equilibrium position does not actually exist for the molecule: it is deduced from (19) by extrapolation of ω_v to $v = -\frac{1}{2}$.

We postpone to Section (c) the criteria by which a correct assignment of vibrational quantum numbers to bands can be made, but, assuming this has been done, we may consider how a satisfactory formula such as (3) is obtained to express the system. We take as an example the band-head data of BeO, a spectrum lying in the visible region and easily obtained by burning an arc in air between beryllium poles. In the two accompanying tables are shown, first, the experimental data to which quantum numbers (v' , v'') have been assigned, and secondly, the first differences between the wave-numbers of the band heads. Examining this table of first differences we note that $\Delta G''$ is not quite constant down a particular column, but is a function of v' , and similarly $\Delta G'$ along a particular row is a function of v'' . This lack of constancy arises through the use of data on band *heads* as distinct from band *origins*. A small term $k(v' + \frac{1}{2})(v'' + \frac{1}{2})$ is usually adequate to meet this difficulty, and the bands can be fitted to a formula:

$$\nu^H = \nu_e + [\omega_e'(v' + \frac{1}{2}) - \omega_e'x'(v' + \frac{1}{2})^2] - [\omega_e''(v'' + \frac{1}{2}) - \omega_e''x''(v'' + \frac{1}{2})^2] - k(v' + \frac{1}{2})(v'' + \frac{1}{2}) . . (21)$$

For the sake of brevity we shall write $\Delta G(v + \frac{1}{2})$ for $G(v + 1) - G(v)$. From equation (21) we then derive

$$\left. \begin{aligned} \Delta G'(v + \frac{1}{2}) &= \omega_e' - 2\omega_e'x'(v' + 1) - k(v'' + \frac{1}{2}), \\ \Delta G''(v + \frac{1}{2}) &= \omega_e'' - 2\omega_e''x''(v'' + 1) + k(v' + \frac{1}{2}). \end{aligned} \right\} . . (22)$$

By taking the intervals between successive members in the same row or column in the second table we can find the best value of k . It is in this case 5.4. The third table is then prepared, giving the values of $\Delta G'(v' + \frac{1}{2}) + 5.4(v'' + \frac{1}{2})$ and $\Delta G''(v'' + \frac{1}{2}) - 5.4(v' + \frac{1}{2})$, in which table we now see that within the limits of experimental error there is constancy in particular rows or columns. Had this not been so, it would have indicated the necessity for terms in $y_e' \omega_e'(v' + \frac{1}{2})^3$ or $y_e'' \omega_e''(v'' + \frac{1}{2})^3$. The mean values of the corrected differences are indicated at the top and side of the third table. They are expressed by the formulae:

$$\begin{aligned} \Delta G'(v' + \frac{1}{2}) + 5.4(v'' + \frac{1}{2}) &= 1352.6 - 11.77 v', \\ \Delta G''(v'' + \frac{1}{2}) - 5.4(v' + \frac{1}{2}) &= 1448.0 - 30.0 v''. \end{aligned}$$

Comparing these with (22), we see at once that

$$\begin{aligned} \omega_e' &= 1364.4, & \omega_e'x' &= 5.88, \\ \omega_e'' &= 1478.0, & \omega_e''x'' &= 15.0. \end{aligned}$$

To find ν_e we have from (21), putting $v' = 0$, $v'' = 0$,

$$\nu^H = \nu_e + \frac{1}{2}(\omega_e' - \omega_e'') - \frac{1}{4}(\omega_e'x' - \omega_e''x'') - \frac{1}{4}k,$$

We proceed to consider upon what factors this variable interval depends.

(b) THE INTERVAL BETWEEN BAND HEAD AND ORIGIN

We should expect a variable interval of this kind to occur from the variation of moment of inertia with vibrational quantum number, expressed empirically by such formulae as (11). Let us consider this in detail.

Regarding a molecule as 'rigid' so far as the centrifugal effects of rotation are concerned (see Chapter IV (d) for a refinement), we have the fine structure of an electronic band given, according to the New Quantum Theory, by

$$\nu = \nu_0 + \frac{h}{8\pi^2 I' c} K'(K' + 1) - \frac{h}{8\pi^2 I'' c} K''(K'' + 1) \quad (23)$$

This may be compared with (7) on the Old Quantum Theory. The corresponding branches are :

$$\left. \begin{aligned} \nu &= \nu_0 + (B' + B'')(K + 1) + C(K + 1)^2 & (K + 1 \rightarrow K), \\ \nu &= \nu_0 - \frac{C}{4} + C(K + \frac{1}{2})^2 & (K \rightarrow K), \\ \nu &= \nu_0 - (B' + B'')K + CK^2 & (K - 1 \rightarrow K). \end{aligned} \right\} \quad (24)$$

Here $C = B' - B''$

The R and P branches clearly form part of the same function, the sequence of lines in the neighbourhood of the origin ν_0 being labelled $R(2), R(1), R(0)$, null line, $P(1), P(2)$, &c. The value of K corresponding to the head of the P branch is given by $\frac{\partial \nu}{\partial K} = 0$

$$K_{II} = \frac{B' + B''}{2(B' - B'')} \quad \dots \dots \dots (25)$$

Upon substitution in the P branch formula we have for the interval between head and origin

$$\nu^{Or} - \nu^{II} = \frac{(B' + B'')^2}{4(B' - B'')} \quad \dots \dots \dots (26)$$

Now, as we have already seen, B' and B'' are functions respectively of v' and v'' . In place of (11), we should now write

$$B_i = B_e - \alpha(v + \frac{1}{2}) \quad \dots \dots \dots (27)$$

so that $B_e = B_0 + \alpha/2$ of the old expression.

Substituting expressions for B_e' and B_e'' in (26), we have, using as abbreviations $C = B_e' - B_e''$ and $\theta = \frac{B_e' + B_e''}{2C}$, and bearing in mind in the expansion that $\alpha'(v' + \frac{1}{2}) - \alpha''(v'' + \frac{1}{2})$ is small compared with C ,

$$\begin{aligned} \nu^{Or} - \nu^{II} &= C\theta^2 + \alpha'\theta(\theta - 1)(v' + \frac{1}{2}) - \alpha''\theta(\theta - 1)(v'' + \frac{1}{2}) \\ &+ \frac{\alpha'^2}{C}(\frac{1}{4} - 0 + 0^2)(v' + \frac{1}{2})^2 + \frac{\alpha''^2}{C}(\frac{1}{4} + 0 + 0^2)(v'' + \frac{1}{2})^2 \\ &- \frac{2\alpha'\alpha''}{C}(\theta^2 - \frac{1}{4})(v' + \frac{1}{2})(v'' + \frac{1}{2}) \quad \dots \dots \dots (28) \end{aligned}$$

FIRST DIFFERENCES (CORRECTED) $\left\{ \begin{array}{l} \Delta G''(v'' + \frac{1}{2}) - 5.4(v'' + \frac{1}{2}) \\ \Delta G'(v' + \frac{1}{2}) + 5.4(v' + \frac{1}{2}) \end{array} \right\}$
 $\Delta G''(\frac{1}{2}) - 5.4(v' + \frac{1}{2})$ $\Delta G''(1\frac{1}{2}) - 5.4(v' + \frac{1}{2})$ $\Delta G''(2\frac{1}{2}) - 5.4(v' + \frac{1}{2})$ $\Delta G''(3\frac{1}{2}) - 5.4(v' + \frac{1}{2})$ $\Delta G''(4\frac{1}{2}) - 5.4(v' + \frac{1}{2})$ $\Delta G''(5\frac{1}{2}) - 5.4(v' + \frac{1}{2})$ $\Delta G''(6\frac{1}{2}) - 5.4(v' + \frac{1}{2})$

$v'' \backslash v'$	0	1	2	3	4	5	6	7
	(1448.0)	(1418.1)	(1388.7)	(1359.3)	(1325.7)	(1295.5)	(1267.8)	
0	1448.4	1420.4						
$\Delta G'(\frac{1}{2}) + 5.4(v'' + \frac{1}{2})$	(1362.6)	1351.8	1354.3					
1	1448.6	1417.7	1389.1					
$\Delta G'(1\frac{1}{2}) + 5.4(v'' + \frac{1}{2})$	(1340.8)	1339.1	1340.8	1342.4	1341.0			
2	1447.0	1416.1	1390.5	1356.4				
$\Delta G'(2\frac{1}{2}) + 5.4(v'' + \frac{1}{2})$	(1329.3)	1330.5	1328.2	1330.8	1327.7			
3		1418.4	1388.3	1359.5	1321.4			
$\Delta G'(3\frac{1}{2}) + 5.4(v'' + \frac{1}{2})$	(1315.6)		1316.5	1318.3	1316.0	1311.7		
4			1387.0	1360.9	1325.7			
$\Delta G'(4\frac{1}{2}) + 5.4(v'' + \frac{1}{2})$	(1305.4)			1306.7	1307.0	1302.6		
5				1360.6	1330.1	1293.6		
$\Delta G'(5\frac{1}{2}) + 5.4(v'' + \frac{1}{2})$	(1298.8)					1300.7	1296.8	
6						1297.5	1267.8	

We observe that if $B_c' + B_c'' > 2(B_c' - B_c'')$ (i.e. if $3B_c'' > B_c'$ which will always be the case), $\theta > 1$. Moreover, θ is + or - according as C is + or -. We may therefore summarize signs of the various coefficients in (28) as follows :

	Constant	$v' + \frac{1}{2}$	$v'' + \frac{1}{2}$	$(v' + \frac{1}{2})^2$	$(v'' + \frac{1}{2})^2$	$(v' + \frac{1}{2})(v'' + \frac{1}{2})$
Degraded to ultra-violet	+	+	-	+	+	-
Degraded to infra-red.	-	+	-	-	-	+

The expression for $\nu^{\text{Or}} - \nu^{\text{H}}$ of the BeO bands (which are degraded towards the red) accords with these predictions as to signs. In Fig. 6 is shown diagrammatically how the interval $\nu^{\text{Or}} - \nu^{\text{H}}$ will vary

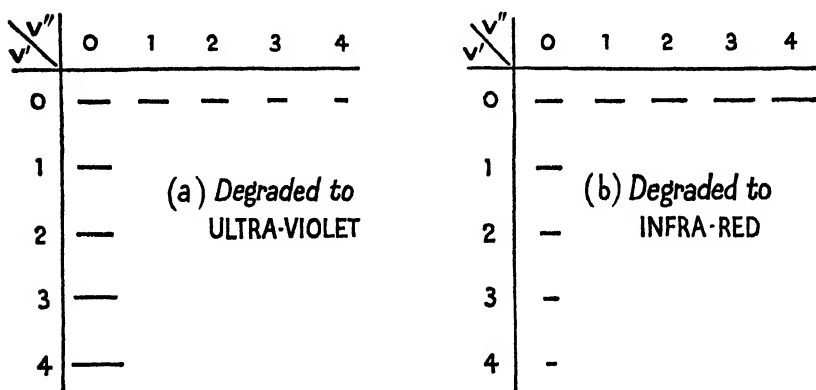


Fig. 6. Variation of the interval $\nu^{\text{Or}} - \nu^{\text{H}}$ in band systems.

throughout typical band systems degraded (a) to the ultra-violet, and (b) to the infra-red.

Sometimes the nature of bands is such that even on low-dispersion plates the interval between band origin and band head is measurable. In such a case there is no reason why these data for four bands should not be substituted in (28) and the four equations solved to give C , θ , α' , and α'' . Thus B_c'' and B_c' could be approximately determined (without a fine-structure analysis). If a Q branch is present, the head of which (see (24)) is at the band origin, the interval $\nu^{\text{Or}} - \nu^{\text{H}}$ should not be difficult to determine experimentally.

We note from (28) that the condition that the coefficient of $(v' + \frac{1}{2})(v'' + \frac{1}{2})$ shall be large is that C is small. Such arises if I' and I'' are nearly equal. In the spectra of CaF , SrF , BaF , &c., where this is the case (see Plate VI), and where two or perhaps three long sequences constitute the system, it is for this reason very difficult to express them by an accurate vibrational function.

(c) THE ASSIGNMENT OF VIBRATIONAL QUANTUM NUMBERS

When a new band system has been found, the wave-lengths of the heads (or origins) measured, and corresponding wave-numbers *in vacuo* obtained from tables, the problem arises of assigning (v' , v'') values to the bands. In a case such as the Swan system of C_2 (see Plate I and the corresponding table), or in the case of BeO, this is quickly done, and there are many other band systems of this type. The (0,0) sequence can sometimes be picked out by the sharp intensity fall in this sequence. In many band systems the intensity distribution is not of this type (see Plates IV and V) and inspection of spectrograms is of little help. Sometimes the data are incomplete by reason of the spectrum lying partly in the infra-red or the far ultra-violet. In other cases (see BaF bands of Plate VI), the interpretation of the various heads may complicate the process. In this section are enumerated features that are a guide in assigning vibrational quantum numbers. Reference may be made by way of illustration to the two tables of the C_2 and BeO systems.

(1) As v' increases v increases; as v'' increases v diminishes.

(2) The first differences between adjacent rows or adjacent columns should be approximately constant. If $\Delta G'(v)$ is a function of v'' , or $\Delta G''(v)$ of v' , this indicates an appreciable value of k (see (21) and (22)).

(3) The second differences should be approximately constant, viz. $\Delta^2 G(v'') = 2\omega_e''x''$ and $\Delta^2 G(v') = 2\omega_e'x'$. If there is an appreciable drift, the third difference (see (15)) should be $6y_e\omega_e$.

(4) Where Q branches are present, the direction of variation of the $v' - v''$ interval as in Fig. 6 provides a check on the arrangement of the bands.

(5) In many systems the (v' , v'') array has strong boundary progressions $v' = 0$ and $v'' = 0$. In contrast with this, observe the ultra-violet band system of the O_2^+ molecule shown on Plate V. The progression $v' = 0$ is well marked and the v' -numbering is therefore reliable, but the $v'' = 0$ progression is faint, being far in the ultra-violet. The most that can here be done is to take prolonged photographic exposures with suitably sensitive plates to see if there is any evidence of a progression still farther in the ultra-violet than the last observed. If we were not dealing with an ionised molecule (but a neutral one), and if the lower electronic state of the band system was the normal state of the molecule, then the absorption spectrum of the cold gas would consist of such bands as (0,0), (1,0), (2,0), (3,0), &c., and this would fix unequivocally the correct assignment of v'' .

The correctness of the assignment of initial quantum numbers can sometimes be conveniently determined by irradiation of the gas or vapour with a convenient monochromatic wave-length, and photography of the fluorescent spectrum. For example, if O_2 were irradiated with the strong Hg line λ 2536 ($= 39412 \text{ cm}^{-1}$), this would permit the band ($0 \rightarrow 0$) at 38620 cm^{-1} , but not the (1,0) band at 39491 cm^{-1} to be emitted in fluorescence.

(6) Another criterion is available if an isotope effect is present. If one of the atoms in the molecule has two isotopes, a duplication

of the gross structure of the band system results. The separation of corresponding bands of the two isotopes varies almost linearly with the wave-number separation of the band from the common system origin. (This is not quite identical with the origin of the (0,0) band : see (16).) The isotope effect is dealt with later in Chapter XI.

(7) When several band systems of the same molecule are known they are almost certain to share some of the electronic levels (and therefore the associated vibrational levels) in common. The correct assignment of v' or v'' values to a system is therefore assisted by the knowledge of other band systems that may be better developed or in a more convenient part of the spectrum. For example, the so-called Second Positive N_2 system has its heads expressed by

$$\begin{aligned} \nu^{\text{II}} = & 29653 + [2044.7(v' + \tfrac{1}{2}) - 26.047(v' + \tfrac{1}{2})^2] \\ & - [1732.84(v'' + \tfrac{1}{2}) - 14.437(v'' + \tfrac{1}{2})^2]. \end{aligned}$$

There is no doubt about the correctness of the assignment of (v' , v'') values here. The so-called First Positive N_2 system lies, however, to a substantial extent in the near infra-red, and some uncertainty as to the (v' , v'') assignment arises. Since some of the $\Delta G(v')$ intervals of this system are clearly identical with $\Delta G(v'')$ intervals of the Second Positive system, the (v' , v'') values can be assigned confidently. Thus the First Positive system is then expressed by :

$$\begin{aligned} \nu^{\text{I}} = & 9519 + [1732.84(v' + \tfrac{1}{2}) - 14.437(v' + \tfrac{1}{2})^2] \\ & - [1460.39(v'' + \tfrac{1}{2}) - 13.93(v'' + \tfrac{1}{2})^2]. \end{aligned}$$

As another example take the 'High-Pressure Carbon' system of Plate IV. The assignment of vibrational quantum numbers, and the nature of the emitting molecule, were determined by observing that some of the band intervals were identical with those of $\Delta G(v'')$ of the Swan C_2 system. These two systems have in fact a common final electronic state, the normal state of this molecule.

(d) THE ORIGIN OF MULTIPLICITY IN BAND HEADS

Examination of the Plates IV-VI shows many examples of multiplicity in the gross band structure. The chief causes of this will be summarized here. They are : multiplicity of the electronic levels (i.e. ν_e), Q branches, Λ -type doubling, and isotopy.

Multiplicity of ν_e

Multiplicity in ν_e does not mean, however, a duplication or triplication of the gross structure, displaced by some *constant* interval. Electronic and vibrational motions interact, and the $\Delta \nu_e$ doublet interval which is obvious in the Comet-Tail (CO^+) system (${}^2\Pi \rightarrow {}^2\Sigma$) of Plate IV, or the ultra-violet O_2^+ bands (${}^2\Pi \rightarrow {}^2\Pi$) of Plate V, shows a small but definite change in value through the system. Again, the electronic and rotational motions are in some molecules strongly linked together, and large doublet or triplet intervals at the band origins may diminish rapidly with increase of rotational quantum number. An example of this is seen in Fig. 7. When this variation

takes place very rapidly, the gross structure (low-dispersion plates) usually shows no multiplicity of the heads (see Plate I). Where, as

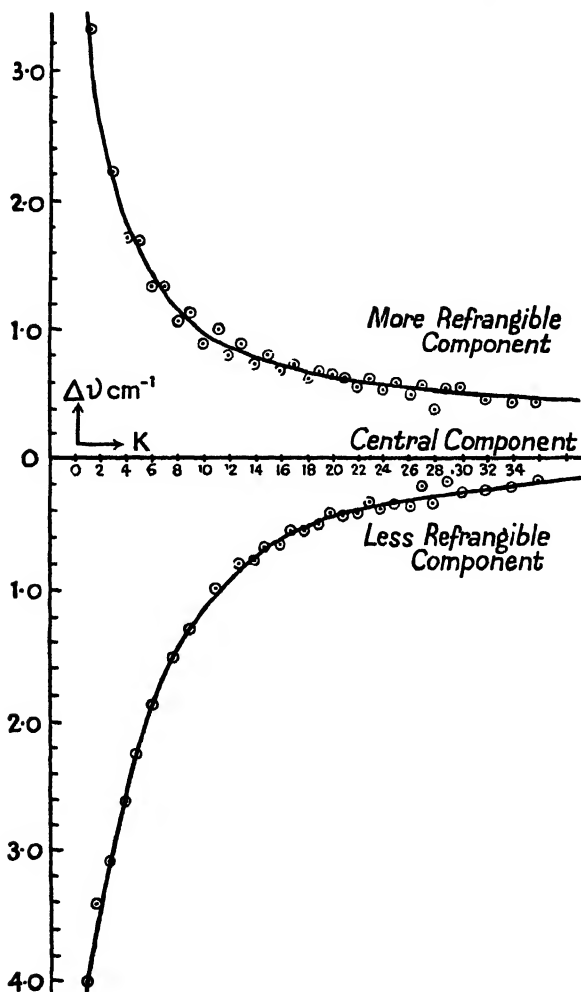


Fig. 7. Variation of the triplets of the R branch of $(0,0)$ band of the Swan C_2 ($^3\Pi \rightarrow ^3\Pi$) system.

in the 'Triplet' System of CO (Plate IV), the variation is less rapid, the heads may be visible.

Q branches

Doubling arising from the presence of Q branches is usually easily distinguishable. As a typical case we observe the *minor* doublet interval in the Comet-Tail (CO^+) bands of Plate IV. The faint outer

head is an *R* head, the stronger inner one a *Q* head. Much, however, depends on the intensity distribution in the fine structure of the branches. Thus (in Plate II) the Angström CO bands have *Q* branches, but they are not apparent under the low dispersion on Plate IV. When the inter-nuclear distance remains practically the same in the initial and final states, it is clear from (26) that a *Q* branch, if present, may be widely separated from the corresponding *P* or *R* head. Plate VI of BaF shows this effect. In the green (0,0) band (Spectrum II) the interval of about three bands of the sequence separates *R* and *Q* heads.

It is instructive to observe the type of error which may easily arise in interpreting the nature of band heads (Fig. 8). In some of the earliest plates taken of the BeF band system, triple band heads only were visible. Being an odd-electron molecule like BO, CN, CO⁺, and N₂⁺, an even multiplicity was expected, and analogy with the spectra of these other molecules indicated as the electron transition ${}^2\Pi \rightarrow {}^2\Sigma$ which should have *Q* branches. (This will be clear in later sections.) That the second interpretation in Fig. 8 is correct is shown by the following evidence: (a) the interval between the first and third heads varies through the

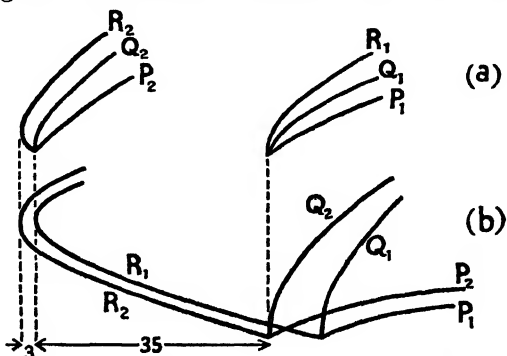


Fig. 8. (a) Incorrect, (b) correct, interpretation of heads of BeF system (${}^2\Pi \rightarrow {}^2\Sigma$).

system, as would be anticipated from Fig. 6 (for a system degraded to the red); (b) the interval between the first and second heads does not vary in this manner, and (c) while the expression of first and second heads by a formula requires a big coefficient of $(v' + \frac{1}{2})(v'' + \frac{1}{2})$, the third head requires no such term.

Λ -type doubling

A brief note as to Λ -type doubling will here suffice, since its nature will be fully appreciated only when fine structure is studied in detail in Chapters VII, VIII, and IX. A good example is seen in Spectrum III of Plate VI, which is the (1,0) sequence of the extreme red ${}^2\Sigma \rightarrow {}^2\Sigma$ system of BaF. It is characterized by a splitting of the rotational levels into two components, of which the separation *increases* with rotational quantum number. The effect of this will be seen from Fig. 9. Assuming only low-dispersion plates available, Λ -type doubling might possibly be confused with two *R* heads of an electronic doublet, as in Fig. 8 (b), especially if the *Q* branches are too faint to see. The differential diagnosis can, however, be made by examining heads known to be formed at lower *K*-values. Thus the (1,0) band must have its head formed at a lower *K*-value than the (0,0) band, for a system degraded to the red. For, since $B_1' = B_0' - \alpha'$,

we have $B_0'' - B_1' > B_0'' - B_0'$, and by (25) this result follows. At the lower K -value the separation of two heads arising from Λ -type doubling will be less. On the other hand, the separation of the two R heads would be greater (see Fig. 7) at the lower K -value. In a similar manner for a system degraded to the violet, for the (0,1) band $B_0' - B_1'' > B_0' - B_0''$ so that by (25) the head is formed at a smaller value of K than in the (0,0) band. Thus for the (0,1) band the Λ -type doubling would be smaller, but the separation of two P heads would be greater.

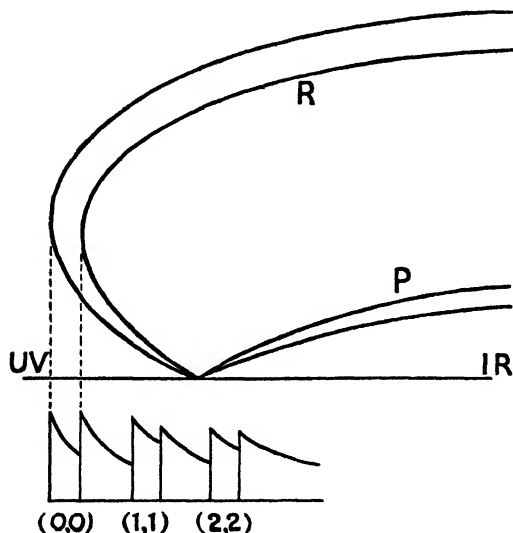


Fig. 9. Λ -type doubling in the $2\Sigma \rightarrow 2\Sigma$ system of BaF.

There is another differential diagnosis to be made—between Λ -type doubling and an ordinary Q - R (or P - Q) branch doublet. Upon reference to Fig. 6 it will be seen that this interval varies in just the same way as does the Λ -type doubling. The following criteria must therefore be used:

- (a) Express each of the heads in a vibrational formula such as (21). If both behave in a similar way and require a substantial coefficient k it is probably Λ -type doubling. On the other hand, if one of them is a Q head it should require no k to express it.
- (b) The type of intensity distribution is some guide to the magnitude of the Q - R or P - Q interval to be expected. A dominant and very prolonged (0,0) sequence indicates $\omega_e' \doteq \omega_e''$ and $B' \doteq B''$, and therefore by (26) the Q - R or P - Q interval should be large.
- (c) If an odd-electron atom is involved, Λ -type doubling in a $2\Sigma \rightarrow 2\Sigma$ system is an almost certain diagnosis.

Isotopic Multiplicity

The subject of isotopy is dealt with in Chapter XI. No confusion should arise from this cause, since the multiplicity vanishes at the system origin and the pattern intervals vary almost linearly with wave-number separation from the origin. If the nature of the molecular emitter is known, the factor governing the isotopic separation can be calculated. Finally, the relative abundance of isotopes (if known) is a guide to the relative intensities of corresponding band heads. The existence of all three isotopes of silicon (28, 29, and 30) is shown in the SiN band systems. Similarly CuCl bands show

evidence of quadruple systems corresponding to the four possible molecules from Cu (63 and 65) and Cl (35 and 37).

(e) FORMATION OF 'TAILS' IN BAND SEQUENCES

In most band systems of which we may take Plate I as a type, the convergence of successive bands in a sequence is not very marked, and the intensity decrement down any sequence is such as to cause it to fade out after the first few members. Occasionally (as may be observed in Plate VII) the intensity appears to revive in higher members of a sequence which has converged, and, so to speak, doubled back on itself. These higher members of the sequence, moreover, may degrade in the opposite sense to the early members. This phenomenon we must now endeavour to understand.

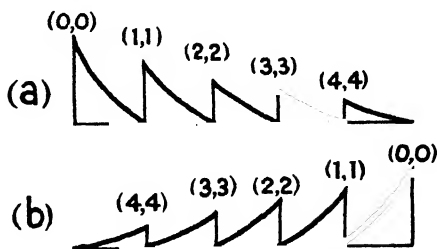


Fig. 10. Sequences (a) degraded to red, (b) degraded to violet.

Turning to (21), which expresses the band heads of a system, let us write $v'' - v' = C$ and substitute for v' say. We obtain

$$v^H = \text{Const} + (v'' + \frac{1}{2})[\omega_c' - \omega_c'' + C(2\omega_c'x_c' + k)] - (v'' + \frac{1}{2})^2[\omega_c'x_c' - \omega_c''x_c'' + k] \quad (29)$$

This is a quadratic in $(v'' + \frac{1}{2})$ in which for most band systems the coefficient of $(v'' + \frac{1}{2})$ is substantially greater than that of $(v'' + \frac{1}{2})^2$. Several observations may be made from (29):

(1) If $\omega_c' > \omega_c''$ successive members of a sequence are on the high-frequency side. If $\omega_c' < \omega_c''$ successive members are on the low-frequency side. Since $I\omega$ is approximately constant (see Chapter IV (e)), it follows that if $\omega' > \omega''$, then $I' < I''$, and $B' > B''$, so that the bands will degrade to the violet, and vice versa. In other words, as Fig. 10 indicates, the early members of a sequence will always lie on that side of the leading head towards which the bands are degraded.

(2) We observe that it is the magnitude of $\omega_c' \sim \omega_c''$ which principally controls the separation of successive members of a sequence. Where, as in the BaF $(^2\Pi \rightarrow ^2\Sigma)$ system of Plate VI ($\omega_c' = 456.0$, $\omega_c'' = 468.9$), the vibrational change is small, the succeeding heads in each sequence are close together. The same approximation of ω_c' and ω_c'' leads consequentially to that of I' and I'' , and therefore (see (26)) to a separation of the Q and R heads. Another associated feature (Chapter III (b)) is the concentration of energy largely in the (0,0) sequence.

(3) Since the coefficients of $(v'' + \frac{1}{2})$ and $(v'' + \frac{1}{2})^2$ have opposite signs, higher members of a sequence will theoretically converge to a limit, and still higher members will subsequently return upon themselves. We say 'theoretically' because the intensity fall down the sequence may cause the bands to fade out before this point is reached.

If the intensity is sustained, however, we have what is commonly called a 'tail' formation. The critical value of v'' corresponding to this is given by $\frac{\partial v}{\partial v''} = 0$ from (29), viz.

$$(v'' + \frac{1}{2})_{\text{crit}} = \frac{\omega_e' - \omega_e'' + C(2\omega_e'x' + k)}{2(\omega_e'x_e' - \omega_e''x_e'' + k)} \quad . \quad . \quad (30)$$

For tails to be possible v'' must be a positive integer. We can formulate

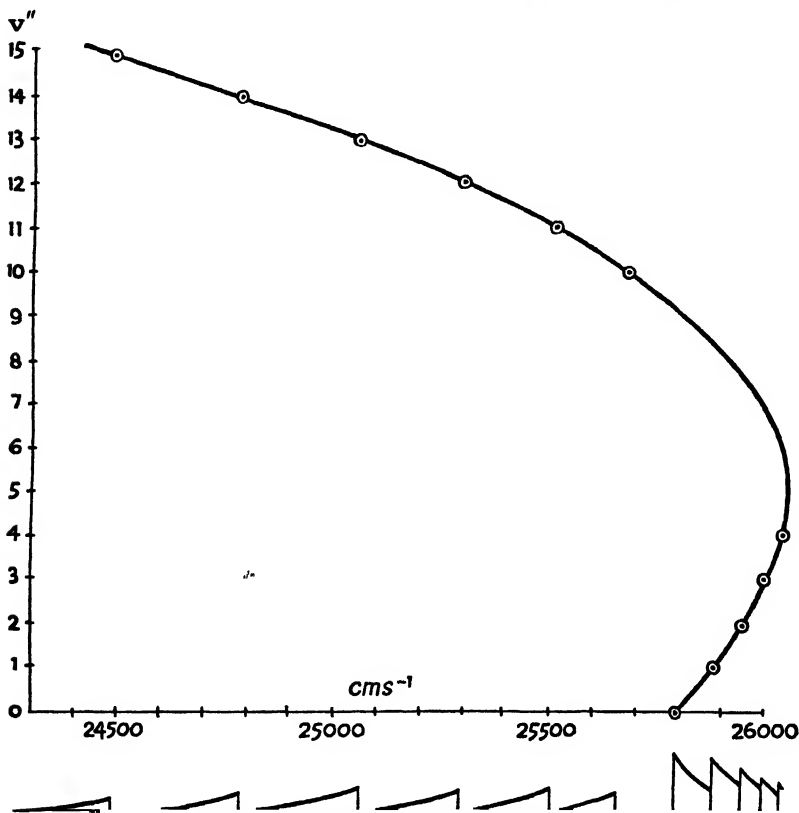


Fig. 11. Graph of $v : v''$ for the origins of the (0,0) sequence of CN bands.

a simple rule that covers the large majority of cases. Tails are possible when $(\omega_e'x_e' + k) - \omega_e''x_e''$ has the same sign as $(\omega_e' - \omega_e'')$.

By reason of the intensity fall down a sequence, a tail is more likely to be formed in practice if the above critical value of v'' is not too large. Thus we can say that favourable conditions are found if ω_e' and ω_e'' are not widely different while $\omega_e'x_e'$ and $\omega_e''x_e''$ differ considerably. Also we note from (30) that when $C (= v'' - v')$ is negative, conditions will be more favourable than for C positive.

We shall take as an example of 'tail' formation the violet CN

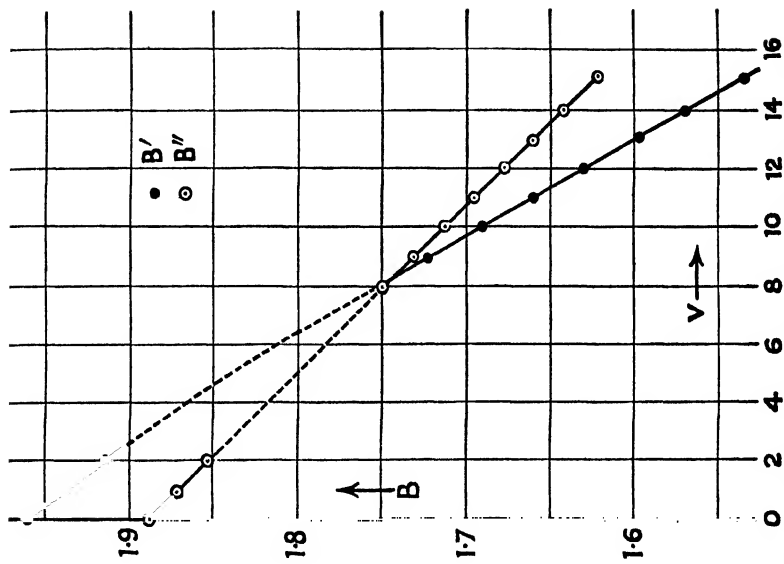
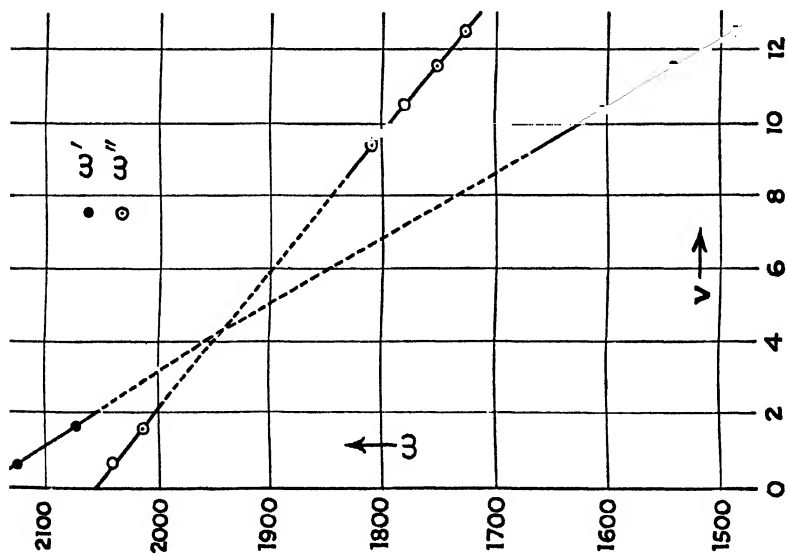


Fig. 12. ω , and B , for both initial and final electronic states as a function of ν (from Jenkins' paper, p. 551).

($^2\Sigma \rightarrow ^2\Sigma$) system which was studied in detail by F. A. Jenkins.* Photographs taken by him in the second order of a 20-ft. grating are shown in Plate VII. The main system degrades to *short* wavelengths: spectrum (C) shows the (0,1) sequence at λ 4216, spectrum (B) shows at the left, part of the (0,0) sequence at λ 3883, and spectrum (A) shows the (1,0) sequence at λ 3585. On the long-wave side of the (1,0) sequence are a number of headless bands, which are now known to be higher members of this sequence which has doubled back on itself. Similarly, spectrum (B) shows on the long-wave side of the (0,0) sequence, a number of bands degraded to the *long* wavelength side which are now known to be higher members of this sequence which has doubled back (and changed its direction of degradation). In Fig. 11 the band origins of the (0,0) sequence have been plotted against v'' . It is in fact a parabola such as would be expected by graphing equation (29). Intermediate members of the sequence are of course obscured by the strong early members.

By making a fine-structure analysis of the 'tail' bands, Jenkins was able to show that the final vibrational function $\omega_r'' : v''$ was virtually a linear extrapolation of that previously derived from analysis of the violet system. The function $\omega_r' : v'$ is not, however, linear (see Fig. 12). In a similar way it is seen that the rotational constants B_r'' of the final electronic state are very closely expressed by a linear formula $B_r'' = 1.8944 - 0.0181 v''$, but to express B_r' would require a cubic in v' .

The intersection of these two rotational term functions in Fig. 12 shows why the early members of the violet bands are degraded to the short-wave side (for $B_r' > B_r''$) while the so-called 'tail' bands are degraded to the long-wave side (for $B_r' < B_r''$). Bands in the neighbourhood of the intersection ($B_r' = B_r''$) will be headless. Such bands as (9,8) at λ 3616, and (10,9) at λ 3638 are clearly seen on Plate VII A.

It is not, of course, inevitable that tail bands should degrade in the opposite direction to that of low- v members of the system. In the event of the B_v' and B_v'' functions intersecting at a larger value of v than the observed tail bands, they would all have degraded in the same direction.

Numerous other examples of tail formations have been investigated, e.g. in N_2^+ bands by Herzberg,† and in the CaF and SrF bands by Johnson and Harvey.‡

* *Phys. Rev.*, vol. 31, p. 539 (1928).

† *Ann. d. Phys.*, vol. 86, p. 189 (1928).

‡ *Proc. Roy. Soc.*, vol. 122, p. 161 (1929), and vol. 133, p. 336 (1931).

CHAPTER III

THE DISTRIBUTION OF INTENSITY IN A SYSTEM

(a) THE FRANCK-CONDON THEORY

THE nuclei of a particular diatomic molecule have, as we know, a characteristic inter-nuclear distance r_e corresponding to stable equilibrium, and anharmonic oscillations are possible about this position. The equilibrium position must obviously correspond to that of minimum potential energy of the nuclei, and the restoring force when they are replaced from this position must arise as the resultant of (1) a force of mutual repulsion of the two nuclei, and (2) a binding force arising from the electron-cloud.

There is no difficulty in appreciating that the potential energy function $U(r)$ plotted as a function of r has a certain general form which is shown in Fig. 13. We have here constructed hypothetical $U(r)$ curves for two electronic states of a molecule. The general form of the curve follows from the following considerations: (1) there must be a minimum at r_e , the equilibrium inter-nuclear distance; (2) as r increases considerably, $U(r)$ must rise asymptotically to a value equal to the energy of dissociation (D) of the molecule; (3) as r diminishes considerably, $U(r)$ must rise rapidly corresponding to the strong inter-nuclear repulsion. A few typical vibrational energy levels associated with the lower electronic state are shown. Consider a typical vibrational level ab . As r oscillates from the value at a to that at b , it is clear that the kinetic energy of the nuclei is measured at any point k en route by the distance kc of the curve below k . Since the total energy of this particular vibration is constant in the absence of a quantum jump, clearly a fall kc of the nuclear potential energy involves a gain of this amount of kinetic energy.

Franck's original ideas* were directed to explaining the mechanism of photochemical dissociation (i.e. how a molecule could dissociate by absorption of a photon of suitable energy), but his conceptions apply equally to the reverse process of chemical association accompanied by light emission, to the problem of intensity distributions in both absorption and emission spectra, and to an understanding of continuous spectra. Condon† later developed Frank's ideas quantitatively, in the first instance from the old quantum standpoint, and later using wave-mechanics.

Consider a typical level ab of the lower electronic state. At some point of its oscillation in this energy level suppose a photon is absorbed and the molecule is transferred to the upper electronic state. Owing to the rapidity of this electronic change compared with the period of vibration of the nuclei, the nuclei possess the same distance and kinetic energy immediately after the transition as they had before. The net effect is the instantaneous substitution of one law of force

* *Trans. Faraday Soc.*, vol. 21, p. 536 (1925).

† Condon, *Phys. Rev.*, vol. 28, p. 1182 (1926); vol. 32, p. 858 (1928).

ing appreciably from the 'allowed' values of the old theory (see Fig. 24). For practical purposes we may reasonably suppose the transition is to the *nearest* quantized energy level.

Since the vibrating nuclei spend a considerable part of their time at the turning points a and b (i.e. adjacent to r_{\max} and r_{\min}) it is more probable that the electronic transition will take place from these positions than intermediately (from such a point as k). We see, then, that for any chosen value of v'' there will be two favoured v' values in the v' -progression which arises from it in absorption. In other words, there will be two maxima of intensity in the progression. The same conclusion holds, of course, in the emission process. In

$v' \backslash v''$	0	1	2	3	4	5	6	7
0	100	29.4	20.4					
1	31.3	31.0	17.2	13.6				
2	1.9	20.7	3.0	10.4	6.0			
3		3.4	18.5	0.6	8.0	7.7		
4			4.0	11.9		2.4	4.8	
5					6.5		1.5	2.7
6						2.5		0.6

Fig. 14. Measured intensities of Swan (C_2) bands occurring in the blue cone of a Bunsen flame.

this case, by dropping vertical lines from the ends (g, h) of a typical initial vibrational state v' , two favoured values of v'' are obtained.

In Fig. 14 the occurrence of such a two-branched curve—a parabola of maximum probability of transition—is apparent in a typical case (the system of Plate I). As another example, take the single v'' -progression ($v' = 0$) constituting the high pressure C_2 bands (see Plate IV). Rough estimates of the intensities of bands of the progression ranging from (0,0) to (0,11) are

1, 1, 1, 2, 7, 15, 1, 5, 10, 8, 6, 4.

Should a maximum occur in the gdj locus (considering the case of absorption) it is possible that a secondary maximum may occur in a few of the v' -progressions near the value of v' to which the point d corresponds in Fig. 13. This is because absorption transitions from

quite a substantial part of the initial range of amplitude ab will, where d is a maximum, all contribute to the same value of v' .

In emission the problem is similar. From the ends of a particular initial vibrational level, lines may be dropped to the lower $U''(r)$ curve, and a locus constructed for transitions from intermediate parts of the initial range. If this locus has a maximum, then a subsidiary maximum of intensity may be observed in some of the v'' -progressions. In the table below are intensities, estimated roughly by eye, on a scale 0 to 10, of the so-called β -system of NO (${}^2\Pi \rightarrow {}^2\Pi$), which illustrates this feature. More complicated intensity fluctuations are found in some cases, and the explanation of these in terms of wave-mechanics is given in Chapter III (d).

NO β -SYSTEM ${}^2\Pi \rightarrow {}^2\Pi$ INTENSITIES

$v'' \backslash v'$	0	1	2	3	4	5	6	7	8	9	10	11	12	13	14	15	16	17
0				0	6	9	10	10	10	10	10	6	3					
1				0	5	7	4	3	0	—	2	4	5	4	2			
2			0	1	7	6	1	—	1	3	3	—	—	2	4	3	1	
3			1	3	7	—	—	3	4	0	—	1	—	—	0	3	5	2
4			0	0							2	0						

From Fig. 13 we can see what conditions will give rise to the dissociation of a molecule following upon absorption of light. If r_e'' is considerably less than r_e' , then absorption of light from the r_{min} side of various v'' levels will result in dissociation. In Fig. 13 all v' -progressions arising from $v'' = 5$ and higher values of v'' will thus have a continuous spectrum which begins at the convergence point of the v' -progression. The presence of a continuous absorption spectrum for molecules is evidence of dissociation. The excess of energy over the dissociation value endows the resulting atoms with kinetic energy. The $U(r)$ curves for the halogens show this feature. Each v' -progression in the absorption spectrum of Cl_2 has a continuum on the short wave-length side of its convergence limit.

(b) SOME TYPICAL INTENSITY DISTRIBUTIONS

We now consider some typical intensity distributions in band spectra as interpreted through the $U(r):r$ curves of the electronic states

involved. For purposes of clarity the spacing of vibrational levels (which measures ω) in the potential basins of Fig. 15, &c., has been exaggerated.

Type I. In Fig. 15 is the case where $r_e' \doteq r_e''$ (and $\omega_e' \doteq \omega_e''$).

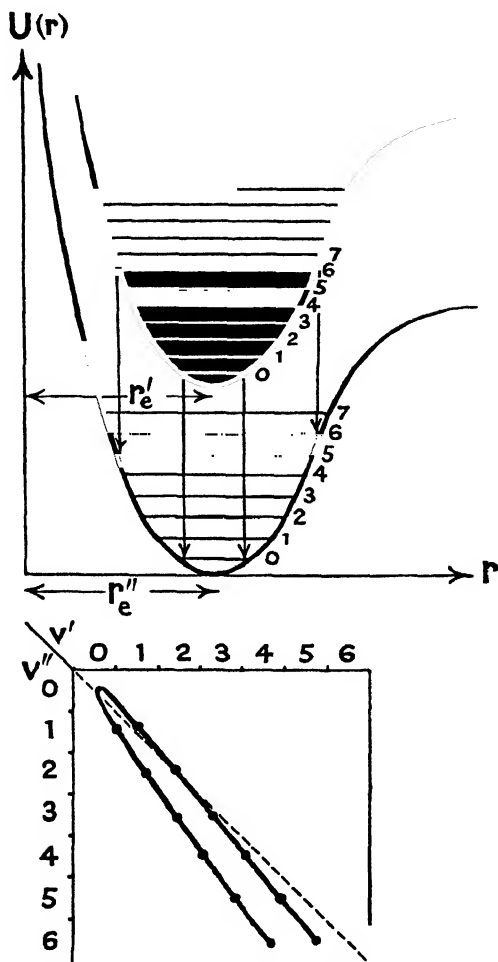


Fig. 15. $U(r) : r$ curves, Type I ($r_e' \doteq r_e''$).

By projecting downwards from the ends of the different initial vibrational levels we discover the most favoured values of v'' . It is clear that in this case the most probable transitions are where $v' = v''$. The (0,0) sequence will be dominant with perhaps the (1,0) and (0,1) sequences weakly developed. The Franck-Condon parabola of most-favoured transitions consists therefore of two almost coincident branches along the diagonal of the (v', v'') diagram. A good example of this is

in the ${}^2\Pi \rightarrow {}^2\Sigma$ green system of BaF on Plate VI. The inter-nuclear distances are not known for these two states, but we know $\omega_e' = 456.0$, $\omega_e'' = 468.9$.

Type II. In Fig. 16 we have the case of $r_e' < r_e''$ (and $\omega_e' > \omega_e''$)

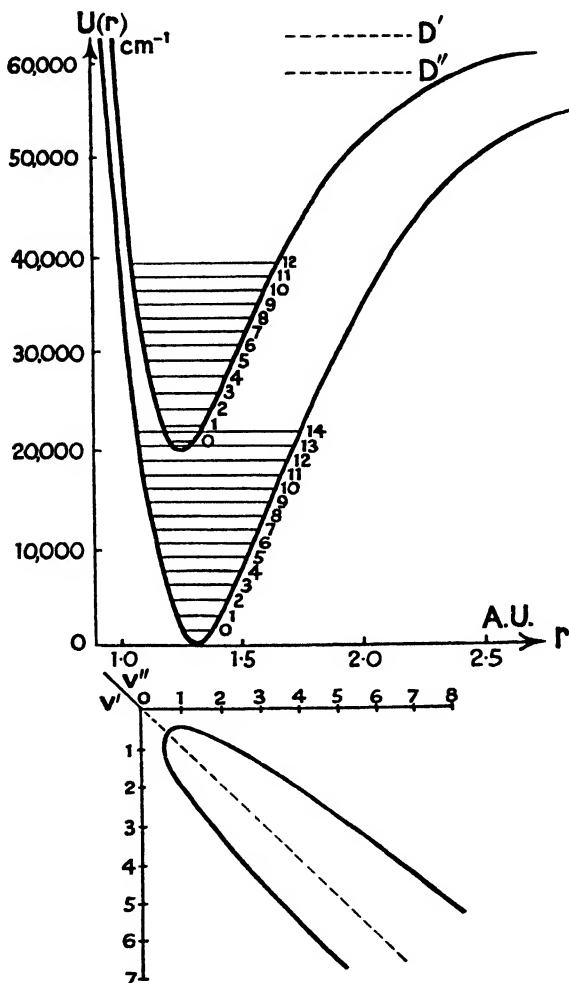


Fig. 16. $U(r) : r$ curves, Type II ($r_e' < r_e''$). The Swan (C_2) system shown in Plate I provides this illustration.

corresponding to a system degraded to the violet. The difference in r_e is not too large, however, so that we have a Franck-Condon parabola with moderately separated branches. Fig. 16 shows (to scale) the $U(r)$ curves characteristic of the two ${}^3\Pi$ states of the Swan band system, for which $r_e' = 1.261$ A.U. and $r_e'' = 1.308$ A.U.

A similar type of intensity distribution would arise for $r_e' > r_e''$ and $\omega_e' < \omega_e''$ provided the differences were not too great, but such a system would degrade to the red side.

Type III. Here r_e' is substantially less than r_e'' , and ω_e' substantially greater than ω_e'' . As Fig. 17 shows, a (0,0) band is impossible, and in the neighbourhood of the system origin there will be several weak bands. The 'parabola' of most-favoured transitions has widened out so that its two branches almost tend to follow the low v' - and v'' -progressions. In Fig. 17 it will be noted that a transition from $v' = 8$ (or more) is capable of producing molecular dissociation. All v'' -progressions arising from $v' \geq 8$ will therefore have a continuum associated with them on the *less refrangible* (i.e. long wave-length) side of the convergence limit (see Fig. 18). If we consider a transition from a point X to Y this energy transition will contribute to a continuous spectrum beyond the convergence limit of the $v' = 10$ progression. The excess of energy YZ over and above that required to effect dissociation of the molecule will be used up as kinetic energy of the separate atoms.

Fig. 18 exhibits the v'' -progression and continuum associated with $v' = 10$. If we had taken $v' = 18$, the maximum intensity of the continuum would have been at the convergence limit in our particular case. A rapid displacement of the continuous maximum towards the infra-red with increasing v' results, if numerically $\frac{dU''}{dr} > \frac{dU'}{dr}$. It will be observed that this process of photochemical dissociation with light *emission* depends on a considerably smaller inter-nuclear distance in the excited state than in the ground state. By reversing the direction of the arrow on YX we see that a converse process is possible under these conditions, viz. the formation of an excited molecule from two atoms, accompanied by a light absorption. H_2 presents a continuous ultra-violet spectrum of this type, of which considerable practical use is made. It arises through transitions down to a $1^3\Sigma$ state, which by the Pauli principle is unstable. Interpreted in terms

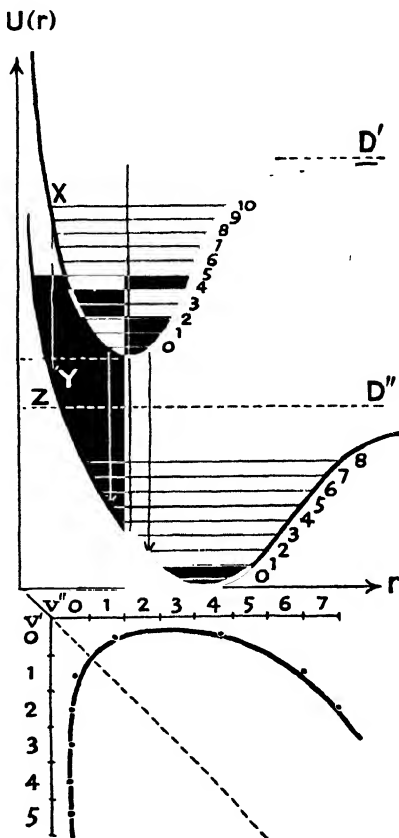


Fig. 17. $U(r) : r$ curves, Type III
($r_e' \ll r_e''$).

of the $U(r)$ curve, we may say that such is a permanently repulsive energy state of the atoms, so that its $U(r)$ curve is characterized by a vanishingly small D'' , or even by the absence of a minimum altogether. We may summarize the principal features of a Type III molecular spectrum thus :

(1) The intensity tends to follow the progressions rather than the sequences, corresponding to a Franck-Condon parabola with very wide branches.

(2) Bands in the neighbourhood of the origin *may* be impossible, and are generally weak.

Type IV. This is represented in Fig. 19, and differs from Type III in that $r_e' > r_e''$ and $\omega_e' < \omega_e''$. Like Type III, it represents an extreme case, in which there is a very considerable change in both r_e and ω_e . An intensity distribution similar to that of Type III is found. The table of intensities of the NO β system on p. 34 is an

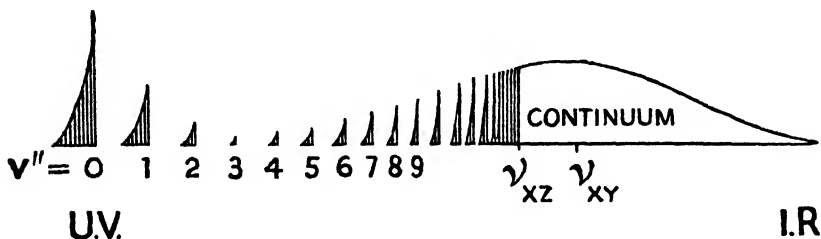


Fig. 18. Diagram of transitions from $v' = 10$, constructed from Fig. 17 data.

example of this. The symmetrical character of the Franck-Condon curve about the diagonal has also largely disappeared.

Type IV represents the case where molecular dissociation results from *absorption* of light of suitable frequency. Considering absorption (i.e. transitions from the ground state to the upper one in Fig. 19), we observe that all v' -progressions (i.e. from whatever v'' -level they derive) will have a continuum associated with them. If we consider a typical transition such as XYZ in absorption, this corresponds to a frequency in the continuous spectrum which lies on the *high-frequency side* of the convergence point of the v' -progression. This will be understood by considering Figs. 19 and 20 in conjunction. Of the energy $h\nu_{xz}$ which is absorbed by the molecule, the part $h\nu_{xy}$ is used up in exciting and dissociating the molecule, and the residuum $h\nu_{yz}$ becomes kinetic energy of the resulting atoms. Absorption spectra of this type are well known for the halogens Cl_2 , Br_2 , I_2 , ICl , IBr , &c., and the characteristic uncertainty involved in making a correct assignment of v' -values is clear from Fig. 20. Types both less and more extreme than that of Fig. 19 actually occur in practice. If either r' is still greater than r'' , or D' very much less than D'' , or both, then it is clear that *only* continuous spectra will be observed. Such is the case for the ultra-violet absorption spectra of HCl , HBr , &c., and the alkali halides NaCl , KBr , &c.

The converse aspect, viz. the emission spectrum, is also clear from Fig. 19. It is possible for two atoms with varying kinetic energies to associate to form a stable molecule with the emission of a con-

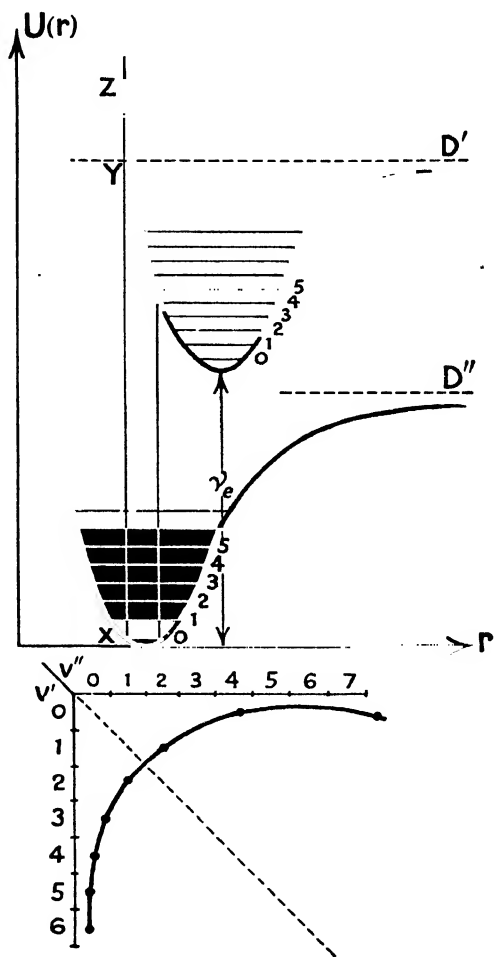


Fig. 19. $U(r) : r$ curve, Type IV ($r_e' \gg r_e''$).

tinuous spectrum. Such 'recombination' spectra are well known for the halogens, CH_3Cl , &c.

There is one general feature of intensity distributions which can be mentioned here. Typical $U(r)$ curves are approximately symmetrical about r_e for *small* oscillations of r . With increasing r (i.e. increasing v) the asymmetry becomes marked, however: especially will this be the case if D (the energy of dissociation) is small and r_e rather small. It follows that the nuclei will spend a greater time in the extended

phase $r > r_e$ than in the contracted phase ($r < r_e$), so that by the general principles of the Franck-Condon theory transitions will be more probable from (or to) the one side than the other. A study of typical cases, Figs. 15-19, shows that for a system degraded to the

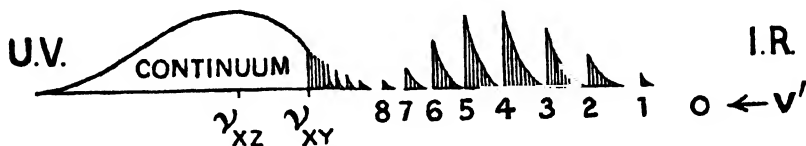


Fig. 20. Diagram of absorption transitions from $v'' = 0$ of Fig. 19.

violet ($r' < r''$) the left branch of the Condon parabola will be the stronger. For systems degraded to the red ($r' > r''$) the right branch will be stronger. This effect may, of course, be obscured in absorption systems by the rapid falling off in population of the initial vibrational states with increasing v'' .

(c) INTERSECTION OF $U(r)$ CURVES: PRE-DISSOCIATION

In Fig. 21 are shown a number of intersecting $U(r)$ functions. Of these 21 (d) includes a common but unstable type which we have

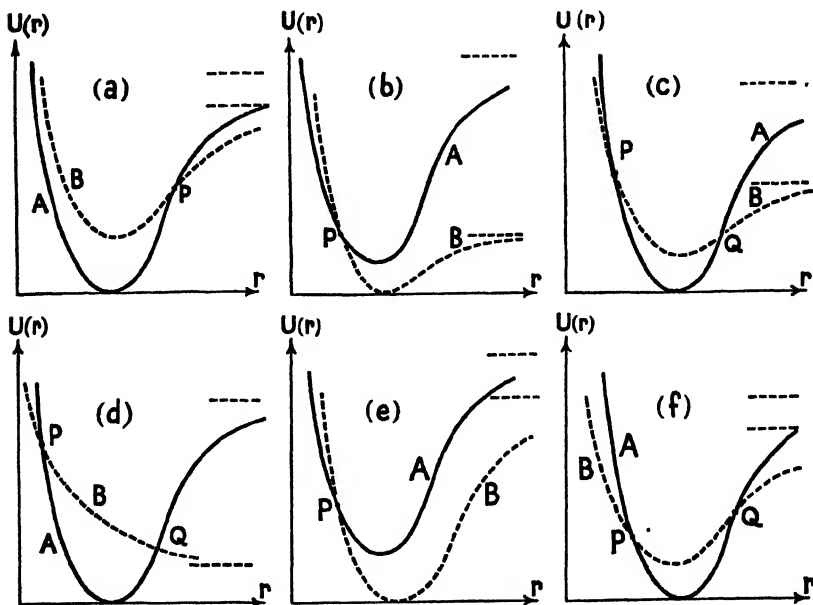


Fig. 21. Intersection of $U(r)$ curves of a molecule.

not hitherto encountered. Such states were first recognized theoretically by Heitler and London. The wave-equation for a system of two atoms has two solutions, one of which (E negative and quantized)

corresponds to a stable molecule with a $U(r)$ function having a minimum, the other (E positive and unquantized) indicates repulsion of the atoms at all distances. Such pairs of solutions are shown in Fig. 22 for two nitrogen atoms. These repulsive states reveal themselves experimentally in several ways, discussed later in this chapter. They are undoubtedly responsible for most continuous spectra. They would constitute the lower state for a continuous emission spectrum or the upper state for a continuous absorption spectrum. Kaplan made some early and informative studies of such states.*

The intersection of $U(r)$ curves of states between which selection principles would allow transitions to occur (see Chapter VI (b)) makes possible a radiationless transition of the molecule from one state to the other. Thus in Fig. 21 transfer from state A to state B will be possible when the vibrational energy in state A rises above the level of the point of intersection of the $U(r)$ curves. A draining of molecules away from state A to B will thus take place when $v \geq q$, the critical quantum number of the intersections. In Fig. 21 (e) and (f) dissociation will not arise, but in the other cases (a) to (d) the molecules 'drained away' will suffer dissociation.

Consider first the case where state A is the *initial* state of a band system. In both emission and absorption this means that at $v' = q$, and for a little above it, there will be a definite weakening and/or perturbation of the bands. Examples of this are found in the First Positive system of N_2 (see Fig. 22) at $v' = 3$, at $v' = 13, 14, 15, 16$, and at $v' = 19, 20$, and 21. In other more severe cases a system may be completely terminated at the progression $v' = q$. Thus the Second Positive N_2 system sharply terminates with the progression $v' = 4$ (due to the ${}^2D + {}^2D$ repulsive level). The Fourth Positive N_2 system consists of only one progression from $v' = 0$ (due to the ${}^2D + {}^2P$ repulsive level). The 2D and 2P nitrogen atoms have energies of 2.37 volts and 3.56 volts, respectively. Numerous other examples can be found: it is quite a common phenomenon. It will be noticed that four pairs of $U(r)$ curves (one stable and the other unstable) are shown in Fig. 22. These are the pairs of solutions of the wave-equation of two atoms already referred to.

Consider now the case where state A of Fig. 21 (a) to (d) is the *final* state of an emission band system. We have the phenomenon known as 'pre-dissociation'. This term was first used by Henri in 1924 to describe a phenomenon observed in the *absorption* band system of sulphur (S_2). In passing along a v' -progression in the direction of increasing v' , Henri found that the fine structure became suddenly diffuse, and the diffuseness persisted for greater values of v' than this critical one to a diminishing extent. In some systems two regions of pre-dissociation were observed, corresponding to two points such as P and Q of Fig. 21 (c) and (d). We may say, then, that for values of v' (in absorption) equal to (and greater than) a critical value, quantization of the rotational energy ceases or becomes very imperfect. In an emission spectrum the intersecting levels must be the lower ones, and pre-dissociation will be observed at a critical value of v'' (extending to higher values). The effect of the intersecting curve B is to reduce considerably the life period of the molecule in state A (if it

* *Phys. Rev.*, vol. 37, p. 1406 (1931); vol. 38, p. 1079 (1931).

has vibrational energy at or a little above the intersection point). The life period is presumably reduced to the same order of time as the rotation period of the molecule, so that rotational quantization begins to lose its significance. The vibration frequency, since it is

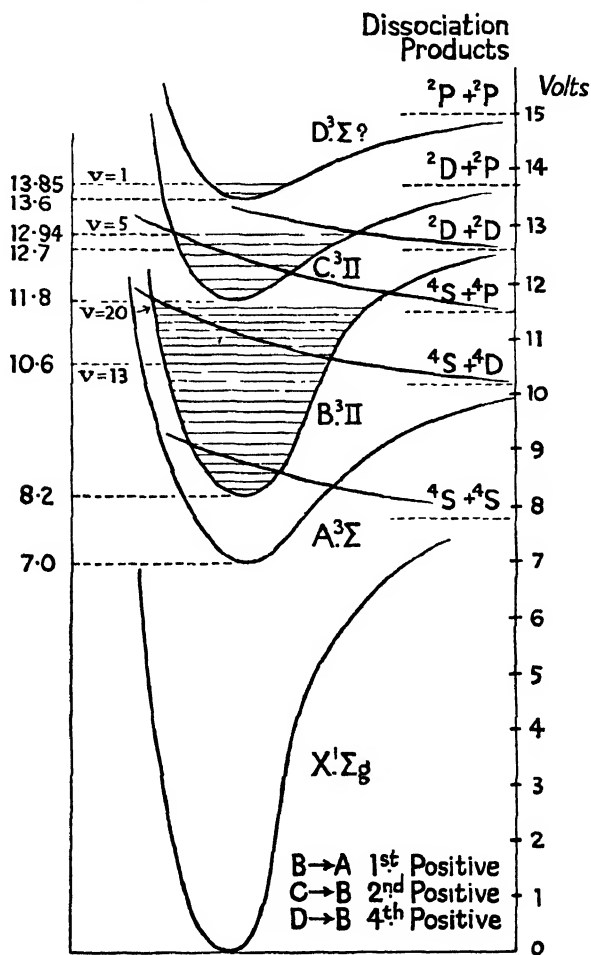


Fig. 22. $U(r)$ curves for some states of the N_2 molecule together with Heitler-London curves inferred from observations on pre-dissociation. The curves are not accurately drawn, and are intended only to show the correlation of dissociation energies and products.

much higher, remains unaffected by the shortened life period. (For the excited state of the S_2 molecule the rotational period is 0.52×10^{-10} sec. while the vibrational period is about 0.78×10^{-13} sec.—about 700 times smaller.)

There is, from the standpoint of the New Quantum Theory, not a precise point, but a region of finite probability of transfer surrounding

P and Q . For this reason the acuteness of the angle at which the $U(r)$ curves intersect at P as compared with Q in 21 (c) and (d) will lead to more pronounced pre-dissociation in the region of the former than of the latter.

As examples of pre-dissociation reference may be made to Herzberg * on P_2 , Martin † on SO, Brown and Gibson ‡ on ICl, Henri and Harris § on NO_2 , and Herzberg || on H·CHO.

There appears to be a displacement of pre-dissociation towards long wave-lengths with rise of temperature. It is also subject sometimes to modification in the presence of inert gases.

(d) VARIABILITY IN INTENSITY DISTRIBUTIONS

Differences in the intensity distributions within certain limits occur in most band systems, as the experimental conditions are varied. By way of illustrating this we shall briefly consider the First Positive band system of the nitrogen molecule ($B^3\Pi \rightarrow A^3\Sigma$ of Fig. 22). Most of it lies in the near infra-red region, but three sequences, the leading members of which are (3,0), (4,0), and (5,0), lie in the visible region, and eye-estimates of their intensities are recorded in Fig. 23. The explanation of all the variations represented would involve prolonged discussion: we shall here only indicate briefly the probable causation.

We observe that all sequences terminate sharply at $v' = 12$. This is presumably due to the intersecting ($^1S + ^2D$) repulsive level shown in Fig. 22. Apart from this the intensity distribution of Fig. 23 (a) is a part of the normal Condon parabolic type.

Fig. 23 (d) of the nitrogen afterglow spectrum is very striking. Briefly the experimental facts are, that if a condensed discharge is passed through pure N_2 a yellow glow persists for several seconds after the discharge is cut off. If nitrogen is streamed through a discharge tube the glowing nitrogen is carried away with the stream. It is called 'active' nitrogen because of its ability to excite the spectra of other substances. Thus when traces of $SiCl_4$ vapour are introduced into the stream, SiN band systems are produced. Similarly, passed over sulphur, iodine, or copper iodide, band systems of these molecules are excited. If N_2 of 100% purity is used, the spectrum of the nitrogen afterglow is solely that of Fig. 23 (d). If <1% oxygen is present the brilliancy of this spectrum is enhanced, but in addition the β -bands of $NO(^2\Pi \rightarrow ^2\Pi)$ (see p. 34) and the γ -bands ($^2\Sigma \rightarrow ^2\Pi$) of NO are also present in the ultra-violet. If the amount of admixed oxygen is increased, the First Positive bands of N_2 are reduced in intensity and finally disappear, but the spectra of NO persist in the now invisible afterglow, and chemical activity also persists. By introduction of BCl_3 vapour into a stream of this active 'nitrogen', band systems of BO are then developed strongly.

The nature of active nitrogen has been the subject of much

* *Nature*, Aug. 16 (1930); *Ann. d. Phys.*, vol. 15, p. 677 (1932).

† *Phys. Rev.*, vol. 41, p. 167 (1932).

‡ *Phys. Rev.*, vol. 40, p. 530 (1932).

§ Debye, *The Structure of Molecules* (Blackie, 1932).

|| *Trans. Faraday Soc.*, vol. 27, p. 378 (1931).

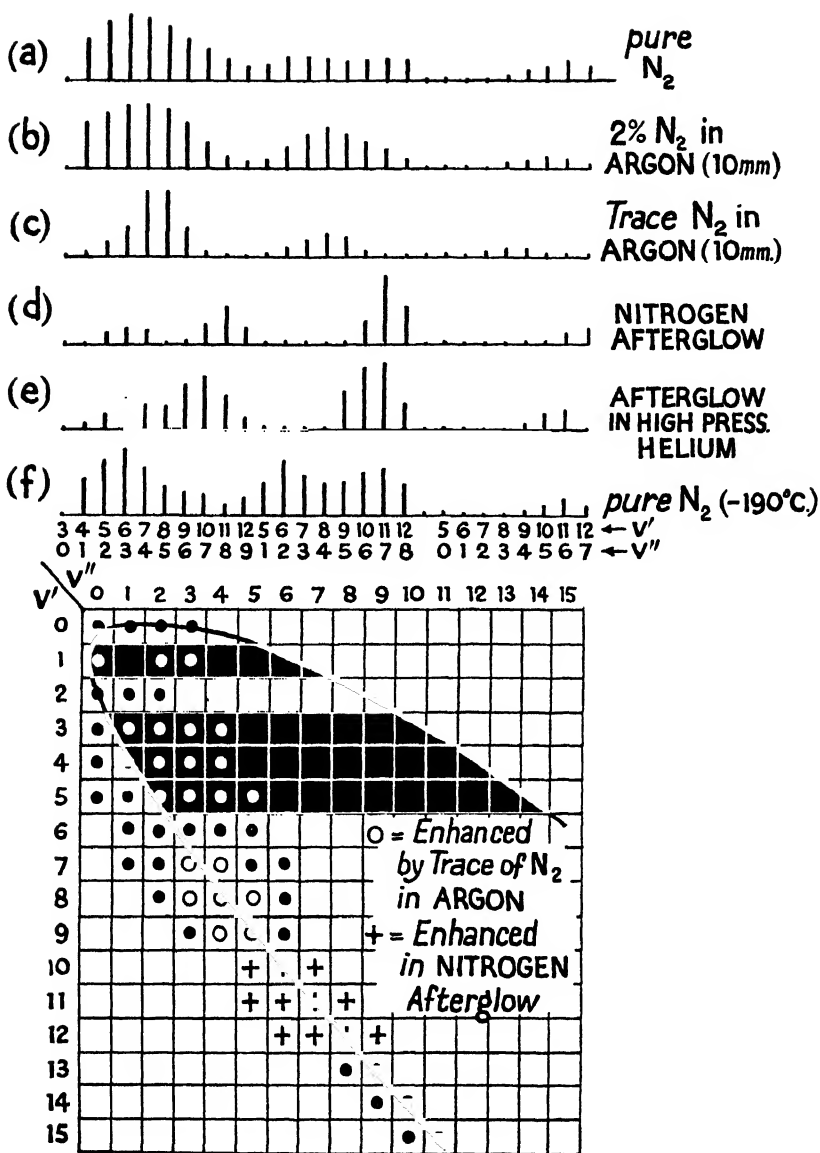


Fig. 23. Intensity variations in the First Positive band system of N_2 . The observed bands of this system are marked by dots in (v', v'') diagram. Enhanced bands are marked by suitable symbols. The parabola of maximum probability of transition has been constructed to scale from the data of Fig. 26.

controversy.* It probably consists of a mixture of metastable \dagger N_2 molecules (in the electronic state $A^2\Sigma$ of Fig. 22) and metastable N atoms in states 2D (2.37 volts) and 2P (3.56 volts). Fig. 23 (d) indicates that substantially only the levels $v' = 10, 11$, and 12 are populated. The band (6,3) indicates a smaller but appreciable population of $v' = 6$. The evidence of electronic-impact experiments suggests an energy of about 7.0 volts for metastable N_2 molecules in the state $A^3\Sigma$. If metastable 2D or 2P atoms collide with these molecules and give up their energy the resulting energies of about 9.4 or 10.6 volts correspond approximately to the regions $v' = 6$ and $v' = 11$ of the $B^3\Pi$ state. The Franck-Condon principle (see Fig. 26) indicates that the final states of $v'' = 7$ or 8 in $A^3\Sigma$ are to be expected from the above initial states.

Fig. 23 (f) is a record of the ordinary discharge in N_2 at low temperatures. At low-current densities, but over a substantial range of pressure, Okubo and Hamada record a selective enhancement of $v' = 6$ and 11 of the $B^3\Pi$ state. These are the same vibrational levels as are enhanced in the afterglow, but, as Fig. 23 suggests, the effects are markedly different. It has been suggested that if electronic excitation of the nitrogen molecule from the ground state ($v = 0$, $X^1\Sigma$ of Fig. 26) follows the same principle as light absorption, then a transition to $v = 7$ or 8 $A^3\Sigma$ is likely. This, being metastable, might be further raised by electronic impact to $v = 11$, $B^3\Pi$. This, however, leaves the more prominent enhancement of $v = 6$, $B^3\Pi$ unaccounted for.

Fig. 23 (e) shows the afterglow spectrum developed by a discharge through a N_2 -He mixture. There is a definite displacement of energy to the smaller quantum numbers, and this increases as the proportion of inert gas increases. The effects are specific, and different if neon or argon replace helium. Presumably the vibrational energy of metastable molecules in the state $v = 7$, $A^3\Sigma$ is allowed to 'leak away' to rare-gas atoms upon collision with them; but clearly the detail is obscure.

Modifications arising from various nitrogen-argon mixtures have been studied quantitatively. \ddagger It is tempting to suppose that the effect in Fig. 23 (c) might be due to collisions between excited argon atoms (loaded with the resonance potential energy $\begin{Bmatrix} 11.8 \\ 11.6 \end{Bmatrix}$ volts) and unexcited N_2 molecules. If this mechanism was responsible for lifting the N_2 molecule to state $v = 7$ or 8 of $B^3\Pi$ (see Fig. 22), then unfortunately the level $v = 0$, $A^3\Sigma$ would have to be at about 9.0 volts instead of 7.0 volts.

It is clear that we are far from a complete understanding of intensity variations. Papers by Duffendack § and others discuss these problems in detail and will repay study.

* Cf. Kaplan, *Phys. Rev.*, vol. 42, p. 97 (1932); Okubo and Hamada, *ibid.*, p. 795 (1932).

\dagger A metastable atom or molecule is one in an energy level above the normal, yet unable to return to the normal by the emission of radiation since a selection principle forbids it. They have a life period therefore of perhaps 10^3 or 10^4 times the normal until by collision with another body (or photon) they acquire energy to raise them to a level from which return to the normal is possible.

\ddagger Johnson, *Phil. Mag.*, vol. 48, p. 1069 (1924).

§ *Phys. Rev.*, vol. 34, p. 68 (1929); vol. 45, 807 (1934).

(e) CONSIDERATIONS BASED ON WAVE-MECHANICS

The solution of the wave-equation for a simple oscillator is well known.* It can also be shown that the probability of a transition from one state to another depends on the integral of the product of the ψ -functions for the two states. Thus the

$$\text{Probability of transition } v' \rightarrow v'' \text{ is } \int \psi'(r)\psi''(r)dr. \quad (31)$$

where $\psi(r)$ represents the radial (i.e. the nuclear-vibrational) part of the ψ -function.

In Fig. 24 we show typical wave-functions for a few vibrational

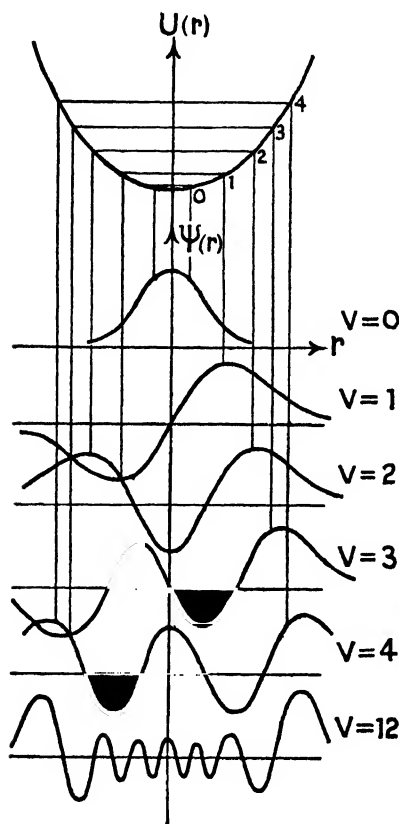


Fig. 24. Wave-functions of simple harmonic oscillator for various vibrational states.

states of a simple harmonic oscillator. The square of the displacement is a measure of the nuclei being found at any particular point of the range. It will be observed that outside the classical range the displacement falls rapidly to zero. Within the classical range the function is oscillatory in character. The normal state $v = 0$ corresponds to a Gaussian error function, representing therefore maximum probability in the middle of the range. All the functions for values of $v > 0$ are characterized by two broad peaks which coincide with the extremes of the classical range. In between these there are v nodes and $(v - 1)$ subsidiary peaks (i.e. maxima of probability). These subsidiary maxima diminish in amplitude and crowd together towards the centre of the range. The broad maxima of probability coincident with the two ends of the classical range correspond to the considerable time spent near the turning points, and which was recognized as an essential feature of the Franck-Condon theory of intensities. The subsidiary maxima within the range were unsuspected on the Old Quantum Theory or from a classical standpoint. The crowding together of the subsidiary maxima towards the centre

of the range accords with the fact that the nuclei have now acquired considerable momentum. If we try to think in the pictorial fashion of de Broglie, the oscillatory motions of Fig. 24 are a picture of the

* E.g., Ruark and Urey, *Atoms, Molecules, and Quanta*, p. 531 (McGraw Hill Book Co., 1930).

phase waves of the moving nuclei. Alternate nodes approximately give the wave-length λ , where $\lambda = h/p$, so that as the momentum p increases we should expect λ to diminish and the nodes to close together.

As we have already mentioned, the $|\psi|^2$ function is non-oscillatory outside the classical range and falls off fairly rapidly to zero. This accounts for the bands which occur *outside* the Condon parabola (see Figs. 14, 20, 23, &c.). The Old Quantum Theory had no explanation to offer of the existence of bands outside this parabola of maximum probability of transition.

Consider now the probability of a vibrational transition $v' \rightarrow v''$ from one electronic state to another. We may imagine two $U(r)$ curves such as are given in Fig. 24. Imagine transitions from $v' = 0$ to a final state of which the inter-nuclear distance is approximately the same. The $0 \rightarrow 0$ transition will be very probable, for since the two Gaussian error curves are located symmetrically round their respective equilibrium positions, there is a big r -range of overlapping, and the product under the integral in equation (31) will be large. On the other hand, we can see that a transition from $0 \rightarrow v''$ (where v'' is large) would be negligible, for the function $\psi''(r)$ is rapidly oscillatory in the range of r where it overlaps $\psi'(r)_{r=0}$, so that the integral of the product would be very small. If we take as a further example transitions from the state $v = 0$ to a final state with quite a different inter-nuclear distance, then the most-favoured transition will be to that v'' -level which has a wave-function whose maximum overlaps the Gaussian error curve of $v' = 0$. The wave-functions of smaller values of v'' will overlap only to a very slight extent, corresponding to a part of it lying outside the classical range. The wave-functions of large values of v'' , where they overlap the function $\psi(r)_{r=0}$, will be oscillating rapidly, and hence the value of (31) is small.

We see, then, that it is possible through the New Quantum Theory to make quantitative predictions of the transition probabilities of a band system. It is clear also that the Franck-Condon curve of maximum probability is adequately explained by this method. In addition, however, it provides a straightforward explanation of the subsidiary maxima which are a notable feature of the β NO bands (Chapter III (a)) and some other systems. Such maxima are the natural result of 'beats' between the oscillatory functions of the initial and final states. That is, if there is a coincidence in the r -range of a loop of the initial function with a loop of the final one—even though not of very large area—the integral of the product (equation 31) may be appreciable. Unfortunately the characteristic functions in practical cases of anharmonic-rotating molecules are usually not known to an accuracy which allows quantitative prediction of the phenomenon.

(f) CONTINUOUS SPECTRA

We have already indicated how continuous spectra arise, in terms of the $U(r)$ curves of the two electronic states involved. Figs. 18 and 20 illustrate typical continuous spectra in emission and absorption located beyond the convergence limit of a v' - and v'' -progression

respectively. We may confine ourselves for purposes of discussion to Figs. 17 and 18, which deal with continuous *emission* spectra. In Fig. 17 the v'' -progressions from $v' \geq 7$ possess continua. If D'' had been considerably smaller or r_e' still smaller relative to r_e'' , it is clear that every v'' -progression might have a continuum associated with it beyond its convergence limit and extending towards the infra-red. Of course if the final electronic state is an unstable repulsive one, only a continuous spectrum would be possible for this electronic transition. In Fig. 25 consider the continuum produced by transitions from $v' = 0$. The dotted curve represents the Gaussian error curve, which is the ψ -function corresponding to $v' = 0$. Suppose this

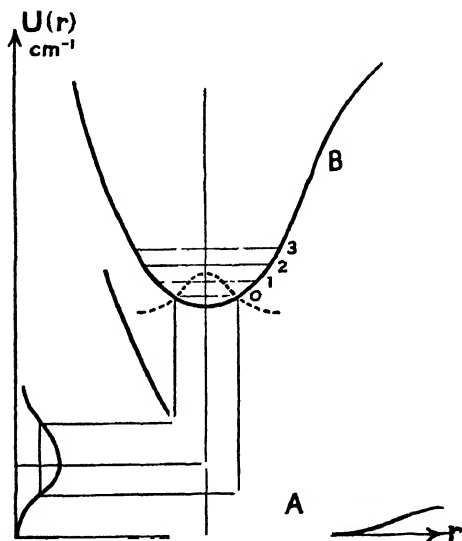


Fig. 25. Probability of transitions for the emission continuum from $v' = 0$.

has been accurately drawn, and also $U'(r)$ and $U''(r)$, then the intensity distribution in the continuum can be predicted. The expression (31) is still applicable to the determination of transition probabilities. We can infer from the ψ -functions of Fig. 24 that in the case of large values of v'' the final ψ -function only has appreciable amplitude in the immediate region of the $U''(r)$ curve. The only appreciable values of the integral are obtained in the region found by projecting downwards from the Gaussian curve $\psi_{v'}(r)$ on to $U''(r)$. As shown in Fig. 25, the transition probabilities for the continuum are thus obtained by 'reflecting' $\psi_{v'}(r)$ in $U''(r)$ on to the wave-

number axis. (The intensity distribution is derived from the probability distribution by multiplying its ordinates by factors v^4 .)*

It will be recognized that in a practical case the observed continuous *emission* spectrum of a gas will result from the superposition of continua derived from the various initial vibrational levels by the method outlined. The continuous *absorption* spectrum of a cold gas or vapour where the molecules are all likely to be in the state $v' = 0$ should, however, have the simple structure indicated. If curve A

* For proof of this, reference may be made to Ruark and Urey, *Atoms, Molecules, and Quanta*, Chapter XX (McGraw Hill Book Co.). We may remind ourselves, however, of the classical radiation from an accelerated charge e , the acceleration of which is \ddot{x} . Its rate of radiation of energy is easily shown to be $\frac{2e^2}{3c^3} \ddot{x}^2$ (see Ruark and Urey, Appendix VIII). For an oscillator of frequency ν the equation of which is $x = A \cos 2\pi\nu t$ the rate of energy radiation becomes $\frac{(2\pi\nu)^2 e^2 A^2}{3c^3} \cos^2 2\pi\nu t$ the time-average value of $\frac{1}{2}$.

be considered approximately linear in the region overlapped by the projectors from $B(v = 0)$, the transition-probability distribution in the continuum should be approximately a Gaussian one. Where curve A is a repulsive Heitler-London type, or, as in Fig. 25, is an approximation thereto, accurate quantitative determinations of the intensity distribution in the continuum are the only means available of determining the $U(r)$ function by which it is represented. If the curve happens to intersect another $U(r)$ function, as do those in Fig. 21, then one or possibly two points on its curve can be located, independently of the intensity-determination method. Very little quantitative research has so far been done on continuous spectra, or the intensity distribution within them.

Condon * has pointed out that in certain circumstances the New Quantum Theory predicts periodic intensity variations within a continuous spectrum, but we refer readers to the original paper

* *Phys. Rev.*, vol. 32, p. 866 (1928).

THE INTER-NUCLEAR LAW OF FORCE

IN Chapter II (a) we have seen that the gross structure of band systems can be represented by formulae. The experimentally determined constants ω_e , $\omega_e x_e$, $\omega_e y_e$ must be related to the law of force under which the nuclei vibrate. What is usually done is to make some reasonable assumption as to the mathematical form of the law of force (or, more usually, of $U(r)$), and then to calculate from it an expression for the vibrational energy of such a molecule. Comparison with the empirical data of (15) then gives the constants of the functions $U'(r)$ and $U''(r)$ for the two electronic states involved.

In Chapter III (a) we have observed that $U(r)$ must satisfy certain essential conditions. As $r \rightarrow \infty$, $U(r)$ must approach a finite value, the energy of dissociation (D). Also as $r \rightarrow 0$, $U(r) \rightarrow \infty$. In addition, for some intermediate value $r = r_e$, $U(r)$ must have a minimum. In this section we consider briefly some of the forms proposed for $U(r)$.

(a) THE $U(r)$ FUNCTION OF KRATZER

In 1920 Kratzer did pioneer work in this field. He suggested a power series

$$U(r) = -D + (2\pi\omega_0)^2 \mu r_0^2 \left[\frac{x^2}{2r^2} + \frac{c_3}{r_0^3} x^3 + \frac{c_4}{r_0^4} x^4 + \dots \right] \quad (32)$$

Here $x = r - r_0$, where r_0 was defined by $\frac{dU}{dr} = 0$. (We should call it r_e .) The minimum value $U(r_0) = -D$. Also $U(0) = \infty$. $U(\infty)$, however, is not a finite constant, so that Kratzer's function can be applicable only to small oscillations such as normally occur in the emission of band systems. For such oscillations of small amplitude, (32) represents a simple harmonic motion of frequency ω_0 . The final expression obtained* for the energy of the vibrating-rotating molecule is (neglecting an additive constant)

$$E = h(\omega_0 v - \omega_0 x v^2) + \frac{h}{8\pi^2 I_0} K^2 (1 - u^2 K^2) - h\alpha K^2 v \quad (33)$$

where

$$u = \frac{h}{4\pi^2 I_0 \omega_0}, \quad \alpha = \frac{3\omega_0 u^3}{2} (1 + 2c_3 \dots),$$

$$x = u \left(\frac{3}{2} + \frac{15}{2} c_3 + \frac{3}{2} c_4 + \frac{15}{4} c_3^2 \right).$$

The first two terms of (33) are the familiar expression for an anharmonic vibrator. The third term is the rotational energy of a rigid molecule. The fourth term takes account of the non-rigid character

* See Ruark and Urey, *Atoms, Molecules, and Quanta*, pp. 129 and 741.

of the molecule which distends under the action of centrifugal force. The fifth term takes account of the interaction of vibration and rotation and may be grouped with the third term, which might be written $\hbar B_r K^2$, where $B_r = B_0 - \alpha v$ (see equation (11)).

A number of inter-relationships of the constants of (33) are easily derived. Thus

$$u = \frac{2B_0}{\omega_0}, \quad \alpha = \frac{6B_0^2}{\omega_0} (1 + 2c_3 \dots) \quad (34)$$

If we write the rotational energy $\hbar(B_0 K^2 - D_0 K^4 \dots)$ we have a simple relation between these constants, viz.

$$\omega_0^2 = +4B_0^3/D_0. \quad (35)$$

Thus from the constants B_0 and D_0 , which are obtained from purely rotational data (i.e. analysis of fine structure), the nuclear vibration frequency can be calculated. The examples in the following table illustrate this.

	B_0 cm. ⁻¹	D_0 cm. ⁻¹	ω_0 (calc.)	ω_0 (obs.)
CuH $A \ ^1\Sigma$. .	6.7445	4.55×10^{-4}	1642	1655
$X \ ^1\Sigma$. .	7.8105	5.08×10^{-4}	1936	1903
BeF $^2\Pi$. .	1.4106	8.301×10^{-6}	1163	1164
$^2\Sigma$. .	1.4793	8.209×10^{-6}	1256	1256
AlO $B \ ^2\Sigma$. .	0.6019	1.163×10^{-6}	866	864
$X \ ^2\Sigma$. .	0.6386	1.109×10^{-6}	969	970

(b) THE $U(r)$ FUNCTION OF MORSE

Morse * has suggested a function involving only three constants which appears to give satisfactory agreement with experimental data over a wide range. Apart from an additive constant it is :

$$U(r) = De^{-2a(r-r_e)} - 2De^{-a(r-r_e)} \quad (36)$$

The first of these terms represents a repulsive force and the second an attractive force. This gives $U(\infty) = 0$, $U(r_e) = -D$, and although for $r = 0$, $U(r)$ is not infinite, it is nevertheless a satisfactorily large quantity. The constant D is clearly the energy of dissociation of the molecule.

Now $F_{r+\Delta r} = F_r + \left(\frac{\partial F}{\partial r}\right) \Delta r + \dots$, so that the restoring force for a small displacement Δr from the equilibrium position is $\left(\frac{\partial F}{\partial r}\right) \Delta r$ or $\left(\frac{\partial^2 U}{\partial r^2}\right) \Delta r$, where $r = r_e$. From (36) this is $2a^2 D \Delta r$. Hence the vibration frequency is

$$c\omega_e = \frac{a}{2\pi} \sqrt{\frac{2D}{\mu}} \quad (37)$$

* *Phys. Rev.*, vol. 34, p. 57 (1929).

The vibrational energy of a non-rotating diatomic molecule under this $U(r)$ function is evaluated by wave-mechanics to be

$$E = -D + \frac{ah}{2\pi} \sqrt{\frac{2D}{\mu}} (v + \frac{1}{2}) - \frac{a^2 h^2}{8\pi^2 \mu} (v + \frac{1}{2})^2,$$

or from (37).

$$E = -D + hc\omega_e(v + \frac{1}{2}) - \frac{c^2 h^2 \omega_e^2}{4D} (v + \frac{1}{2})^2 \quad . \quad . \quad (38)$$

The constants a and D of Morse's function are thus deducible from the data of vibrational analysis of a band system. From (37) and (38):

$$\left. \begin{aligned} a &= \sqrt{\frac{8\pi^2 c \mu \omega_e x}{h}} = 0.2454 \sqrt{\mu \omega_e x}, \\ D &= \omega_e^2 / 4\omega_e x. \end{aligned} \right\} \quad . \quad . \quad (39)$$

Here r and r_e are in Ångström units, ω_e , $\omega_e x$, D , and $U(r)$ are in cm^{-1} and $\mu = \frac{M_1 M_2}{M_1 + M_2} m_0$ is the reduced mass of the molecule (sec (10)). The value of r_e strictly requires fine-structure data for its evaluation, but an approximate value can be obtained through certain empirical relations discussed later in Chapter V (e).

(c) THE $U(r)$ -FUNCTION OF RYDBERG

Rydberg* has suggested the potential function:

$$U(r) = -D(1 + bx)e^{-bx} \quad . \quad . \quad . \quad (40)$$

where $x = r - r_e$. This satisfies the general requirements $U(\infty) = 0$, and $U(r_e) = -D$. As shown previously for the Morse function the vibration frequency for small oscillations about r_e can be easily obtained

$$c\omega_e = \frac{b}{2\pi} \sqrt{\frac{D}{\mu}} \quad . \quad . \quad . \quad (41)$$

The vibrational energy expression is similar to (38), so that D has the same value as given in (39), and for the constant b we have the formula

$$b = \sqrt{\frac{16\pi^2 c \mu \omega_e x}{h}} = 0.3468 \sqrt{\mu \omega_e x} \quad . \quad . \quad . \quad (42)$$

Intensity measurements do not furnish a direct test of the accuracy of any particular $U(r)$ function, although there is a strong presumption in favour of such a function if two constructed curves give an accurate prediction of the distribution of most-favoured transitions in the band system. In Fig. 26 have been constructed the $U(r)$ curves

* *Zeit. f. Phys.*, vol. 73, p. 376 (1931).

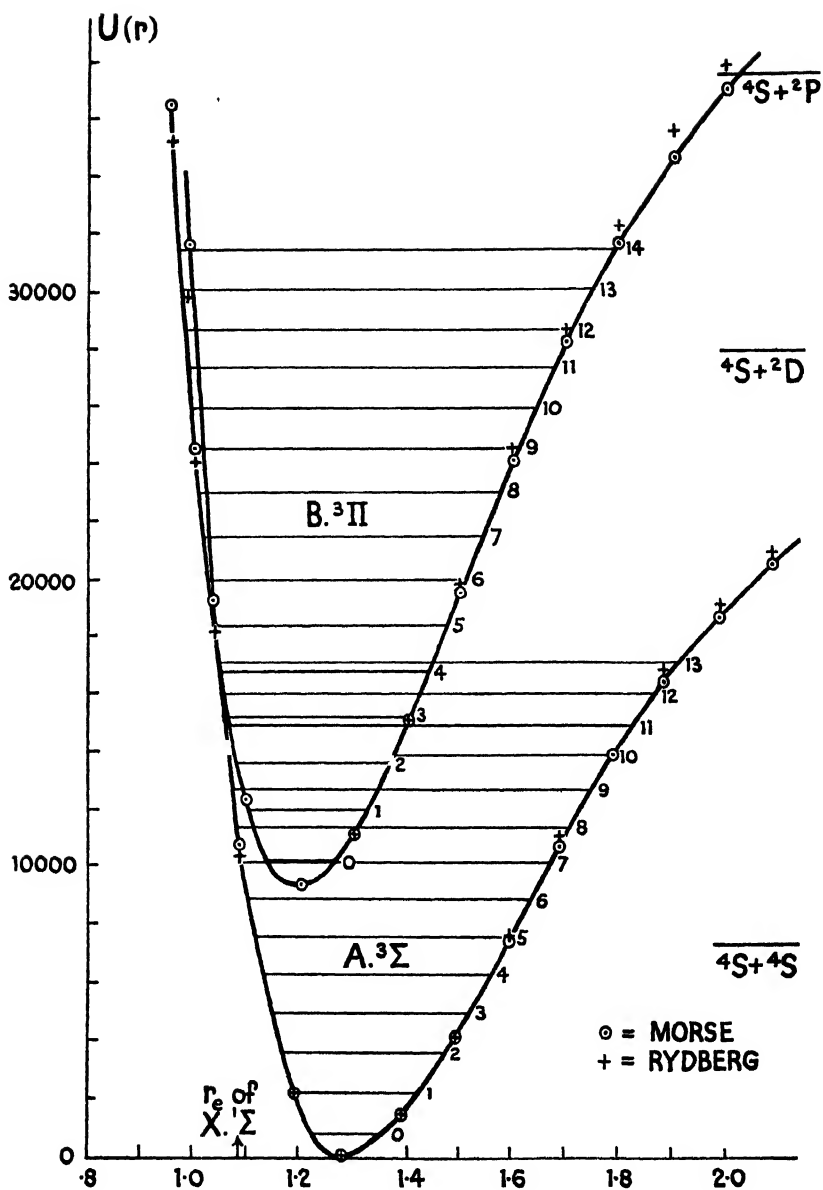


Fig. 26. Scale diagrams of the initial $B(^3\Pi)$ and final $A(^3\Sigma)$ states of nitrogen functions according to Rydberg and Morse. (r_e of ground level $X(^1\Sigma)$ is marked.)

for initial and final states of the First Positive bands of N_2 ($B^3\Pi \rightarrow A^3\Sigma$). The data used were

Rydberg :

$$U'(r) = 46995 - 37612(1 + 3.471x)e^{-3.471x}$$

Morse :

$$U'(r) = 9383 + 37612(1 - e^{-2.455x})^2$$

Rydberg :

$$U''(r) = 28128 - 28128(1 + 3.402x)e^{-3.402x}$$

Morse :

$$U''(r) = 28128(1 - e^{-2.411x})^2$$

$$\left. \begin{array}{l} \\ \\ \end{array} \right\} \begin{array}{l} x = (r' - 1.201) \text{ A.U.} \\ \\ x = (r'' - 1.291) \text{ A.U.} \end{array}$$

It is clear that the two functions are in very close agreement except in the region of large quantum numbers. From Fig. 26 a locus of most-favoured transitions can be constructed, and is plotted in Fig. 23, and it is consistent with that part of the band system in the visible region.

Oldenberg * has devised a graphical method by which an experimentally correct $U(r)$ curve may be constructed for high vibrational quantum numbers provided we can first construct one which is reliable up to say $v = 2$.

(d) SOME EMPIRICAL RELATIONS BETWEEN MOLECULAR CONSTANTS

Examination of the constants of the various electronic states of a molecule shows that increasing moment of inertia corresponds to decreasing vibration frequency. Many people have sought for empirical relationships between the molecular constants. Birge and Mecke have suggested the semi-quantitative relationship ω_e/B_e or $\omega_e I_e$ or $\omega_e r_e^2 = \text{constant}$. It is a useful relationship, but considerable deviations are found—not arising from any experimental inaccuracy. The value of ω_e/B_e is in the range 190–210 for hydrides of the first row of the periodic table, 230–320 for other hydrides, 1000–1600 for alkali metal molecules (X_2), and 800–1200 for the majority of lighter molecules with atoms of comparable mass.

Morse † has suggested the empirical relationship

$$r_0^3 \omega_0 = 3000 \text{ cm.}^{-1} \quad . \quad . \quad . \quad (43)$$

where the constant has a probable deviation of about ± 120 , corresponding to 1.3% in r_e . The constancy of this implies that $I^3 \omega_0^2$ and therefore B_0^3 / ω_0^2 is constant, which by (35) implies that D_0 is constant. The constancy of D is not well marked and would imply equal elastic distention of different molecules by rotation.

Clark ‡ has made a valuable modification of Morse's rule based upon a broad classification of molecules in two respects. Firstly, they are divided into 'periods' which are designated as KK , KL , KM , LL , LM , &c., according to the electronic shells which remain

* *Zeit. f. Phys.*, vol. 56, p. 563 (1929).

† *Phys. Rev.*, vol. 34, p. 61 (1929).

‡ *Phil. Mag.*, vol. 18, p. 459 (1934); vol. 19, p. 476 (1935).

attached to the component atoms (i.e. not shared by the molecule as a whole). Secondly, molecules are assigned a 'group number' n ranging from 0 to 14, according to the number of shared electrons. Thus CO is (KK , 10), O_2 is (KK , 11), AlO is (KL , 9), He_2 is (KK , 0). Clark's suggestion is

$$\omega_e r_e^3 \sqrt{n} = k - k' \quad . \quad . \quad . \quad (44)$$

where n is the group number, k a constant characteristic of the period, and k' is a correction for singly ionized molecules of that period (zero for neutral molecules). Clark gives as values of k

$$KK, 9,550; \quad KL, 12,850; \quad KM, 13,500.$$

The particular case of the hydride molecules involves k -values :

$$KH, 8,050; \quad LH, 15,250; \quad MH, 18,800.$$

In the LII period the formula does not present such good results as in other cases, probably because of uncertainty in the number of electrons really shared by the molecule. For this period Clark proposed to use an 'effective' group number (n') derived from n by the following empirical rule. For $n = 4$, $n' = n$. For $n < 4$ take as n' the next even number above n ; for $n > 4$ take as n' the next even number below n . (If molecular ions of this period are involved the word 'odd' is substituted for 'even' in this rule.) Thus

$$MgH, n = 3, n' = 4; \quad AlH, n = 4, n' = 4; \quad ClH, n = 8, n' = 6;$$

$$MgH', n = 2, n' = 3; \quad ClH', n = 7, n' = 5.$$

The degree of accuracy of the Morse and Clark formulae may be judged from the table on p. 56.

Allen and Longair* have pointed out that Clark's formula is not general enough to include isotopic molecules, which would be members of the same period and group number. Since for isotopes ω_e varies as μ^{-1} , where $\mu = \frac{M_1 M_2}{M_1 + M_2}$, they suggest instead of using a group number n the formula

$$\omega_e r_e^3 \sqrt{\mu} = \text{constant} \quad . \quad . \quad . \quad (45)$$

The values of the constant for different molecular periods are KK , 10,602; KL , 16,844; KM , 20,150; LL , 23,250; MM , 31,280; NN , 41,260. The formula is moderately successful, but gives errors somewhat greater than that of Clark. It has not been applied, however, to hydrides.

Another empirical rule due to Birge† is frequently of use for getting an approximate value of α when B and x are known :

$$\frac{2Bx}{\alpha} = 1.4 \pm 0.2 \quad . \quad . \quad . \quad (46)$$

From (33) and (34) we find that

$$\frac{2Bx}{\alpha} = \frac{1 + 5c_3 + c_4}{1 + 2c_3 + \dots} \doteq 1 + 3c_3 + \dots,$$

so that this approximate rule implies c_3 of Kratzer's formula is of the order 0.13 for most molecules.

* *Phil. Mag.*, vol. 19, p. 1032 (1935).

† *Phys. Rev.*, vol. 31, p. 919 (1927).

Mole- cule	Periodic group number	Elec- tronic state	ω_e cm. ⁻¹	r_e A.U. Expt.	r_e A.U.		% errors	
					Morse	Clark	Morse	Clark
KK period								
BeO	8	$C^1\Sigma^+$	1370.8	1.359	1.298	1.350	— 4.5	— 0.7
		$B^1\Pi$	1079	1.50	1.406	1.463	— 6.3	— 2.5
		$A^1\Sigma^+$	1487.5	1.328	1.266	1.316	— 4.7	— 0.9
BeF	9	$A^2\Pi$	1172.6	1.390	1.368	1.395	— 1.6	+ 0.4
		$X^2\Sigma^+$	1265.6	1.357	1.333	1.360	— 1.8	+ 0.2
CN	9	$B^2\Sigma^+$	2164.2	1.148	1.115	1.137	— 2.9	— 1.0
		$A^2\Pi_{inv}$	1788.7	1.236	1.188	1.212	— 3.9	— 1.9
		$X^2\Sigma^+$	2068.8	1.169	1.132	1.154	— 3.2	— 1.3
N ₂	10	$B^3\Pi$	1732.8	1.201	1.200	1.203	— 0.1	+ 0.2
		$A^3\Sigma$	1460.4	1.291	1.272	1.275	— 1.5	— 1.2
		$X^1\Sigma_g^+$	2359.6	1.094	1.083	1.086	— 1.0	— 0.7
NO	11	$B^3\Pi$	1037.6	1.413	1.424	1.406	+ 0.8	— 0.5
		$A^2\Sigma^+$	2375.3	1.060	1.081	1.066	+ 2.0	— 0.6
		$X^3\Pi$	1906.5	1.146	1.163	1.148	+ 1.5	— 0.2
O ₂	12	$B^4\Sigma_u^-$	710.1	1.599	1.616	1.571	+ 1.1	— 1.8
		$A^1\Pi_u$	1432.6	1.223	1.279	1.244	+ 4.6	+ 1.7
		$X^3\Sigma_g^-$	1584.9	1.204	1.237	1.202	+ 2.7	— 0.2
KL period								
AlO	9	$B^2\Sigma^+$	868.2	1.663	1.512	1.702	— 10.0	+ 2.3
		$X^2\Sigma^+$	977	1.614	1.453	1.637	— 10.0	+ 1.4
SiN	9	$B^2\Sigma^+$	1034.4	1.576	1.426	1.604	— 9.5	+ 1.1
		$X^2\Sigma^+$	1151.7	1.568	1.376	1.549	— 12.3	— 1.2
SO	12	$B^3\Sigma$	628.7	1.769	1.684	1.807	— 4.8	+ 2.1
		$X^3\Sigma$	1123.7	1.489	1.387	1.489	— 6.8	0.0
Hydrides (KH period)								
LiH	2	$1\Sigma^+$	1406.1	1.6	1.622	1.593	+ 1.3	— 0.4
BeH	3	2Π	2087.6	1.330	1.421	1.305	+ 6.8	— 1.9
		$2\Sigma^+$	2058.5	1.340	1.429	1.312	+ 6.6	— 2.1
BH	4	1Π	(2450)	1.213	1.348	1.180	+ 11.1	— 2.7
		$1\Sigma^+$	(2230)	1.226	1.391	1.217	+ 13.5	— 0.7
OH	7	$2\Sigma^+$	3182.5	1.009	1.235	0.986	+ 20.7	— 2.1
FH	8	1Σ	4037	0.864	1.141	0.890	+ 32.1	+ 3.0

Rydberg * has provided another empirical formula : if the squares of the first differences $\Delta G(v)$ (see equation (22)) are plotted against B^3_{v+1} , the relation is linear for all electronic states of the molecule :

$$\frac{[\Delta G(v)]^2}{B^3_{v+1}} = \text{constant} \quad . \quad . \quad . \quad . \quad . \quad (47)$$

* *Zeit. f. Phys.*, vol. 73, p. 376 (1931).

By substitution and approximation we find

$$\frac{[\Delta G(v)]^2}{B_{v+1}^3} = \frac{\omega_0^2}{B_0^3} \left[1 + \frac{3\alpha}{B_0} + v \left(\frac{3\alpha}{B_0} - 4x \right) \dots \right] \doteq -\frac{1}{4D_0} [1 + 4x]$$

(see (35)). We have, as a close approximation, put $\frac{2Bx}{\alpha} = 1.5$ (see (46)). The constancy for *different* molecules would be expected to be no greater than for that of Morse's rule (43).

Finally we may mention an empirical relation due to Badger* between the force-constant for unit displacement $k_i (= \frac{1}{2}(2\pi\omega_i)^2\mu)$ and the equilibrium inter-nuclear distance (r_i in A.U.)

$$k_i(r_i - d_i)^3 = 1.86 \times 10^5 \quad . \quad . \quad . \quad (48)$$

Here d_i is constant for a class of molecules obtained by taking one atom from the i th row and one from the j th row of the periodic table. A table of these constants may be found in the original papers.

(e) THE VIBRATIONAL-ROTATIONAL INTERACTION

As we indicated early in this chapter (see equations (11) and (27)), the moment of inertia will be expected to increase slowly with the vibrational amplitude. The constant α involved in the relation $B_v = B_e - \alpha(v + \frac{1}{2})$ was expressed in terms of the other constants of Kratzer's $U(r)$ function (see (34)). We did not similarly evaluate α using Morse's function (Section (b)), and we proceed to do so now by an approximate method.

Expanding $U(r) = -2De^{-\alpha\rho} + De^{-2\alpha\rho}$ in powers of $\rho = r - r_e$ we have

$$U(r) = -D(1 - \alpha^2\rho^2 + \alpha^3\rho^3 \dots).$$

The kinetic (rotational) energy may likewise be expanded in powers of ρ :

$$\begin{aligned} Er &= \frac{h^2}{8\pi^2\mu r^2} K(K+1) = \frac{h^2}{8\pi^2\mu r_e^2} K(K+1) \left(1 + \frac{\rho}{r_e}\right)^{-2} \\ &= F \left(1 - \frac{2\rho}{r_e} + \frac{3\rho^2}{r_e^2} \dots\right). \end{aligned}$$

The total energy, kinetic and potential, is thus

$$Er + U = -D + F - \frac{2F\rho}{r_e} + \rho^2 \left(\alpha^2 D + \frac{3F}{r_e^2} \right) \dots \quad (49)$$

Since Er is small compared to U , we may regard the effect of rotation as a perturbation of the potential function U . Let us suppose that the constants D and r_e of Morse's function are changed by small quantities γ and β .

$$\left. \begin{aligned} Er + U &= -2(D + \gamma)e^{-\alpha(\rho + \beta)} + (D + \gamma)e^{-2\alpha(\rho + \beta)} \\ \text{Expanding:} \\ &= -(D + \gamma)[1 - \alpha^2\beta^2 - (2\alpha^2\beta - 3\alpha^3\beta^2)\rho - (\alpha^2 - 3\alpha^3\beta)\rho^2] \end{aligned} \right\} \quad (50)$$

* *Jour. Chem. Phys.*, vol. 2, p. 138 (1924); *Phys. Rev.*, vol. 48, p. 284 (1935).

Comparing (49) and (50) we have :

$$\beta = -\frac{F}{a^2 r_c D}, \quad \gamma = -F + \frac{F^2}{a^2 r_c^2 D} \quad . \quad . \quad (51)$$

The value of r_c has therefore been increased by $F/a^2 r_c D$, and the value of D , the energy of dissociation, diminished by $(F - F^2/a^2 r_c^2 D)$. Both effects are in the direction we should anticipate as a result of rotation of the molecule.

Substituting this new value of $D + \gamma$ for D in (38) we have for the energy of the vibrating-rotating molecule

$$E = -D + F - \frac{F^2}{a^2 r_c^2 D} + \frac{ah}{\pi} \sqrt{\frac{2(D-F)}{\mu}} (v + \frac{1}{2}) - \frac{a^2 h^2}{8\pi^2 \mu} (v + \frac{1}{2})^2.$$

Expand the root, keeping first powers only of F/D , and we have finally

$$E = -D + hB_c K(K+1) - h \frac{4B_c^3}{\omega_c^2} K^2(K+1)^2 + h\omega_c (v + \frac{1}{2}) - \frac{h^2 \omega_c^2}{4D} (v + \frac{1}{2})^2 - \frac{h^2 \omega_c B_c}{2D} (v + \frac{1}{2}) K(K+1) \quad . \quad . \quad (52)$$

This is in agreement with Kratzer's formula (33), modified according to the New Quantum Theory. We observe that according to (52)

$\alpha = \frac{h\omega_c B_c}{2D}$ and $x_c = \frac{h\omega_c}{4D}$. Thus $\alpha = 2B_c x_c$. This is not consistent with experimental data (see (46)). The discrepancy arises from the method of approximation used. The direct solution of the wave-equation by Pekeris * gives for α

$$\alpha = 2x_c B_c \left(3 \sqrt{\frac{B_c}{x_c \omega_c}} - 3 \frac{B_c}{x_c \omega_c} \right) \quad . \quad . \quad . \quad (53)$$

and this formula yields good results.

* *Phys. Rev.*, vol. 45, p. 98 (1934).

THE DISSOCIATION OF MOLECULES

(a) GENERAL PRINCIPLES

BY the energy of dissociation of a diatomic molecule we mean the energy required to separate it into two unexcited atoms. Usually, though not necessarily, dissociation of a molecule from its ground (electronic) state yields two normal, i.e. unexcited, atoms, while often an excited molecule gives atoms of which one or both are excited. If there is evidence as to the amount of energy in the atomic products we can calculate the true energy of dissociation as defined above.

In Chapter III we have examined the mechanism by which a molecule may be dissociated. A brief summary is here appropriate :

(1) When $r' < r''$ to a sufficient extent, especially if D'' is small, dissociation may arise with emission of light for all values of v' above a critical one (see Fig. 17). An emission continuum would then accompany such v'' -progressions on the low-frequency side as is shown in Fig. 18. If a Heitler-London repulsive state is the lower one, only a continuum will occur.

(2) When $r' > r''$ to a sufficient extent, especially if D' is small, dissociation may arise likewise by absorption of light, for all values of v'' above a critical one (see Fig. 19). An absorption continuum will be associated with the various v' -progressions on the high-frequency side (see Fig. 20). If a Heitler-London state is the upper one, only an absorption continuum will occur.

(3) If by light absorption or emission an atom passes to a state A (see Fig. 21 ($a-c$)) above an intersection, such that the pre-dissociation phenomenon is found in band structure, molecular dissociation will begin. This is dealt with in more detail in Chapter V (g).

At first sight it may appear strange that the dissociation of a molecule necessarily takes place indirectly because of an electronic transition. As we have just seen, a favourable electronic transition may lead to the production of so much vibrational energy, according to the Franck-Condon principle, that dissociation results. Why cannot light-energy be absorbed as vibrational or rotational energy in sufficient quantity to do this? If a molecule has an electric moment* we can easily visualize the classical picture of a plane polarized light wave with its alternating electromagnetic field inducing increased vibration of the molecule, and of circularly or elliptically polarized inducing also rotation of the molecule. A molecule which has no electric moment would not be influenced in this way. But why does a molecule *with* electric moment not dissociate if placed in a strong

* Electric moment is analogous to magnetic moment and is measured in exactly the same way, viz. by the product of electric charge and distance between them. The condition that a molecule has electric moment is that the 'centre of gravity' of the negative (electronic) charge should not coincide with that of the positive (nuclear) charges.

enough beam of light of the appropriate (infra-red) frequency? With regard to the acquisition of rotational energy the selection principle for rotation quantum numbers limits changes to $\Delta K = \pm 1$ or 0, and the possibility of increasing K to the required point in steps of unity is theoretically possible but highly improbable. For an anharmonic oscillator the changes in v , the vibration quantum number, are not limited in this way, but jumps (Δv) of increasing magnitude diminish rapidly in probability.

It is appropriate to define at this point a number of terms applied to the classification of molecules. The terms polar and non-polar are used to denote molecules with and without electric moments respectively. The terms therefore refer to the charge distribution, the separation or otherwise of the positive and negative centres of charge. The great majority of molecules probably have an electric moment (i.e. are polar). On the other hand, most, if not all, 'elementary' molecules Cl_2 , I_2 , C_2 , N_2 , O_2 , &c., are non-polar. For the reasons which we have explained above (in a pseudo-classical manner), the non-polar class do not give rise to vibration-rotation bands or pure-rotation bands; they possess only electronic band spectra.

The term 'homopolar' was first used by the chemist Abegg, and has since been widely employed to denote molecules which may be regarded as synthesized from, or which will dissociate into, atoms. 'Heteropolar' is similarly used to denote molecules which can be regarded as built from ions: the precise criterion is given later. Franck has used the alternative terms 'atomic molecule' and 'ionic molecule' to make the distinction clear. The above two classifications, one based on electric charge distribution, and the other on dissociation products, are not mutually exclusive, e.g.:

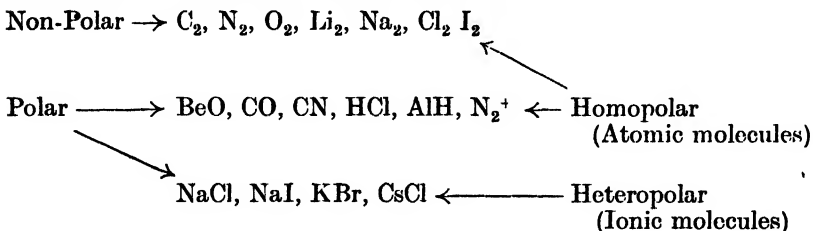


Fig. 27 has been constructed to make clear that there is a distinction between the energy of dissociation, D_0'' for the ground state, and D_0' for the upper state, and the more theoretical quantities D_c'' and D_c' . The energy of dissociation for a particular state whose potential function is $U(r)$ is

$$D_0 = U(r = \infty) - U(r = 0),$$

while clearly

$$D_c = U(r = \infty) - U(r = r_c)$$

so that

$$D_0 = D_c - G(0) \text{ in cm.}^{-1} \quad . \quad . \quad . \quad . \quad (54)$$

The quantity D of equations (36) and (40) is of course D_c and not D_0 , the true energy of dissociation. We have indicated at the right-hand side of Fig. 27 that from the ground state the molecule (AB) is supposed

to dissociate into two unexcited atoms A and B , while from the upper electronic state it dissociates into A' (an excited atom) and B . The quantity D_0'' is the energy of dissociation of the normal molecule as defined in the first sentence of this chapter. If the nature of the atomic products is known, then such values as D_0' derived for excited states

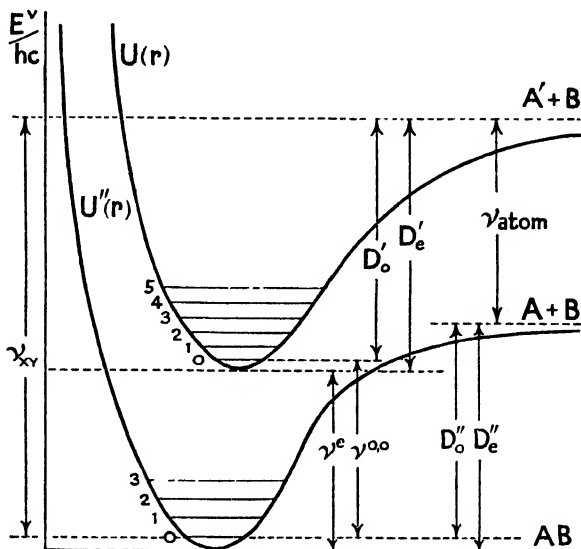


Fig. 27

of the molecule can be used as shown below to calculate D_0'' , the energy of dissociation of the normal molecule into two unexcited atoms.

It is useful to remember in working out problems of this type that

$$1 \text{ volt-electron} = 8106 \text{ cm}^{-1}$$

From Avogadro's number 6.064×10^{23} we derive also

$$8106 \text{ (cm}^{-1}\text{)} = 23,055 \text{ calories/gm. mol.} \quad . \quad . \quad (55)$$

Fig. 27 resembles Fig. 19 in that the various v' -progressions arising in absorption from the lower state to the higher will be associated with continua (as in Fig. 20). Where the intensity distribution is such that the convergence point (ν_{XY} of Figs. 20 and 27) can be traced experimentally, or where it can be located by a very short extrapolation of the progression, the conditions are as favourable as possible for an accurate determination of D_0' . From Fig. 27 it is clear that

$$D_0' = \nu_{XY} - \nu^{(0,0)},$$

where $\nu^{(0,0)}$ is the wave-number of the (0,0) band. More generally, if the convergence wave-number ν_{XY} is that of the v' -progression associated with an initial level v'' , then

$$D_0' = \nu_{XY} - \nu^{(0,v'')}.$$

If the electronic levels of the atom A are known from analysis of its line spectrum, then

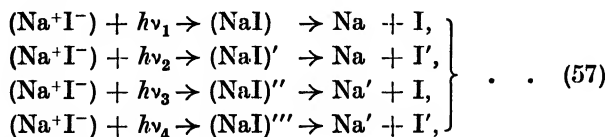
$$D_0'' = \nu_{XY} - \nu_{\text{atom}} + [G''(v'') - G''(0)] \quad . \quad . \quad (56)$$

Unfortunately, the possibility of determining the convergence wave-number of a progression by experiment or by a short extrapolation is far from being very common. We find that for the great majority of molecules the known band systems are covered by small values of v' and v'' , and that calculation of the point of convergence of the v' - or v'' -progressions from the observed data, which is represented by an equation such as (15), implies an extrapolation of very great extent. In spite of this the method is, however, of wide application, and is discussed in Section (e) of this chapter.

Where the 'cutting-off' phenomenon or pre-dissociation occurs, this obviously locates for us a point on the energy scale a little above a dissociation level (e.g. see Fig. 22). It provides a maximum limit for D and, if the intersecting Heitler-London curve is nearly horizontal at the point, gives an approximate value for D .

(b) THE IONIC TYPE OF BINDING

We may take the alkali metal halides as representative. The absorption spectrum is continuous only: there are no discrete progressions. Absorption of light effects dissociation of the molecules, not excitation to a stable state. As a consequence we find that no electronic emission band spectra are known. For this reason the Birge-Sponer extrapolation method, and evidence from the pre-dissociation phenomenon, are not available to help us in determining the energy of dissociation. We may make use, however, of observations of the wave-length at which fluorescence of the vapours of the alkali halides can be excited. As the exciting wave-length is gradually diminished, it is found that at certain critical values particular spectral lines of one of the radicles are excited. Knowing the energy required to do this, and the energy of the incident quantum, the dissociation energy of the molecule can at once be inferred as the difference. By definition, ionic molecules are regarded as separable into ions by increase of vibrational energy, but this process does not seem to be realized in practice. On the other hand, there is no theoretical reason why excitation of an electron in one of the shells should not take place and effect dissociation into one excited ion and one normal ion, just as a similar process of dissociation into a neutral atom and an excited atom is the general rule when light is absorbed by a suitable homopolar molecule. In practice the optical dissociation of ionic molecules certainly does occur, but the excited electron is transferred thereby from the acidic shell to the metallic shell, and two *neutral* atoms result. The atomic products may be unexcited, or one or both may be excited to different levels, depending on the frequency of the incident light. Thus:



symbolize typical observed processes.

How, then, in practice can one distinguish a molecule as of the true ionic type? The distinction is not easy. Such molecules as BeO ,

HCl, and other halogen acids, and polyatomic molecules such as H_2CO , &c., might from the numbers of electrons satisfying all the valency bonds be thought to be ionic. The evidence, however, classifies them as homopolar or atomic-type molecules. What is this evidence? In general, ionic molecules give ionic-type lattices in the crystalline state, and ionize strongly in solution and in the molten state. Spectroscopically, ionic molecules are always capable of dissociation by absorption of light into two *unexcited* atoms, as in the first example of (57). Some normal homopolar molecules also dissociate by light absorption into two unexcited atoms (see the next section), but the more usual

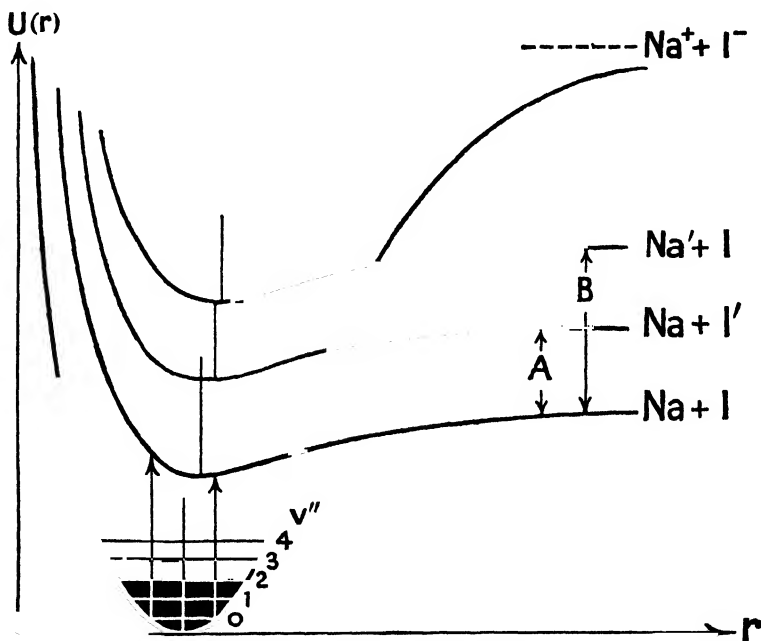


Fig. 28. $U(r)$ curves for NaI.

products include at least one *excited* atom. It is upon this spectroscopic evidence that the hydrogen halides are classed as homopolar, and differentiated from the alkali metal halides, which are heteropolar.

Before considering the alkali halides in detail, let us consider the general characteristics of their $U(r)$ curves. Firstly, the convergence of the vibration levels of the fundamental state should give dissociation into two ions. The stability of this class of molecule, and also the relatively large energy in the *ionized* atom as compared with the *excited* atom, show that the $U(r)$ curve of the fundamental state must intersect those of the higher electronic states. The $U(r)$ curves of these latter are such as account for absorption continua in transitions from the ground level. They are not Heitler-London curves of the repulsive type, but are each represented as having a slight minimum, to account for a phenomenon described below. Their trends on the

r_{\max} side are approximately parallel, for it is observed that the frequency intervals between the maxima of the two or three absorption continua usually observed correspond closely to the frequencies of the low-energy spectral lines of one (or both) of the products. It is, of course, upon the identification of these intervals (A and B in Figs. 28 and 29) with those of the atomic spectral lines that the nature of the dissociation products is in part based. The other part of the evidence is the particular fluorescence spectrum (a single line, of course) which is radiated when the excited atom (Na' or I' , for example) returns to the normal.

The phenomenon above referred to, upon which is based the form of the $U(r)$ curves of excited states in Fig. 28, was discovered by Sommermeyer.* It is illustrated diagrammatically in Fig. 29. Super-

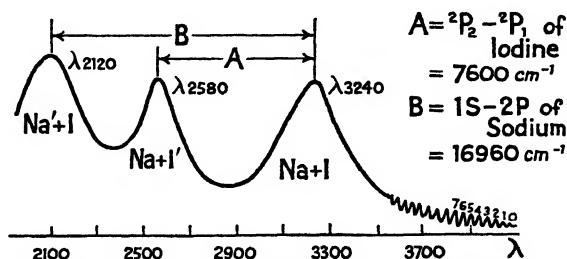


Fig. 29. Absorption spectrum of NaI vapour. (After Sommermeyer.)

posed on the less refrangible end of the first continuum were found intensity fluctuations resembling diffuse band heads. As indicated in Fig. 28, while absorption transitions from r''_{\min} and the immediate neighbourhood of r''_{\min} lead to absorption well in the continuum (about λ 3240, &c.), the shallow character of the minimum in the higher state means that transitions from the greater part of the r'' -range give almost the same absorbed frequency. For each vibrational state $v'' = 0, 1, 2, \dots$, there consequently results a peak of absorption, and it is these peaks which are shown on the right-hand side of Fig. 29. The non-appearance of similar peaks on the less refrangible side of the continua around λ 2580 and 2120 is probably due to the obscuring effect of the strong overlaid continuum, or may be improbable by reason of the r_c' for these excited states being too large relative to r_c'' (see Fig. 28). Sommermeyer measured the intervals between these peaks, and, in view of the interpretation given, these clearly provide data of $\Delta G''(v)$, and hence of the vibration frequency of the molecule. A list of such interval-data for NaI is appended. (Care must, however, be taken in deducing the vibration frequency from the observed intervals, and in particular in making any inference as to energy of dissociation from the convergence of these intervals. For it will be seen that if the curve $U'(r)$ is sufficiently displaced to the right in Fig. 28, then the peak intervals will at first converge much more rapidly and afterwards a little less rapidly than the true coefficient $2\omega_e x$ would indicate.)

* *Zeit. f. Phys.*, vol. 56, p. 548 (1929).

Quantum number v''	$\Delta G_v''$ interval	Quantum number v''	$\Delta G_v''$ interval
1	279	8	239
2	272	9	234
3	266	10	229
4	261	11	225
5	255	12	220
6	249	13	215
7	244	14	211

The main features of Fig. 29 are these :

(1) The absorption spectrum consists of three observed continua with maxima at λ 3240, 2580, and 2120 (overlapping), and others probably occur in the ultra-violet. The least refrangible of these corresponds to dissociation of the molecule into neutral unexcited atoms of sodium and iodine. The second continuum about λ 2580 gives an unexcited sodium atom and an excited atom of iodine raised from the normal $^2P_{3/2}$ state to a metastable $^2P_{1/2}$ state. The third continuum about λ 2120 corresponds to an unexcited iodine atom and an excited sodium atom.

(2) The evidence for the various dissociation products is found in that the frequency intervals A and B correspond to the frequency differences $^2P_{3/2} - ^2P_{1/2}$ of I and $1, \mu_s - 2, \mu_p$ of Na. Evidence is also available from fluorescence. Thus Terenin* and Kondratjew† have observed D -line emission when NaI vapour is illuminated by wave-lengths shorter than about λ 2450.

(3) The energy of dissociation is determinable from the low-frequency edge of the least refrangible absorption continuum (the peak marked o in Fig. 29), for this corresponds to the lowest frequency which will effect dissociation into normal atoms.

(4) The vibration frequencies of the alkali halides are determinable from the intervals of the absorption peaks superposed on the continuum on its less refrangible side.

When a salt molecule absorbs a quantum of higher frequency than the minimum required to effect the dissociation process, the energy excess appears as energy of translation of the atomic products. A considerable Döppler broadening of the yellow sodium lines emitted by a fluorescence of NaI vapour when illuminated by light of λ 2026 (much shorter than λ 2450) has been recorded by Franck and Hogness.‡

Terenin found that fluorescence experiments with triatomic salt molecules such as HgCl_2 , HgBr_2 , HgI_2 , TiCl_2 , &c., produced band systems characteristic of diatomic molecules together with a normal or excited halogen atom.

The case of thallium iodide (TII) may be presented as an example of a molecule with features of special interest. Terenin§ and others

* *Zeit. f. Phys.*, vol. 37, p. 98 (1926); vol. 44, p. 713 (1927).

† *Ibid.*, vol. 39, p. 191 (1926).

‡ *Ibid.*, vol. 44, p. 26 (1927).

§ *Phys. Zeit. der Sowjetunion*, vol. 2, pp. 299 ff., 377 ff. (1932).

have studied the absorption (and emission) spectra of this molecule in detail. A few of the $U(r)$ curves of TlI are pictured in Fig. 30. TlI has a normal band system observable in absorption and fluorescence in the region λ 3750–4200 (3.3–2.95 volts). There is a continuum associated with it in absorption. The bands and continuum arise from transitions from the normal state of the molecule to one above it with very loose binding. There are several other continua—as a type of which we may take that in the region λ 3200–2800

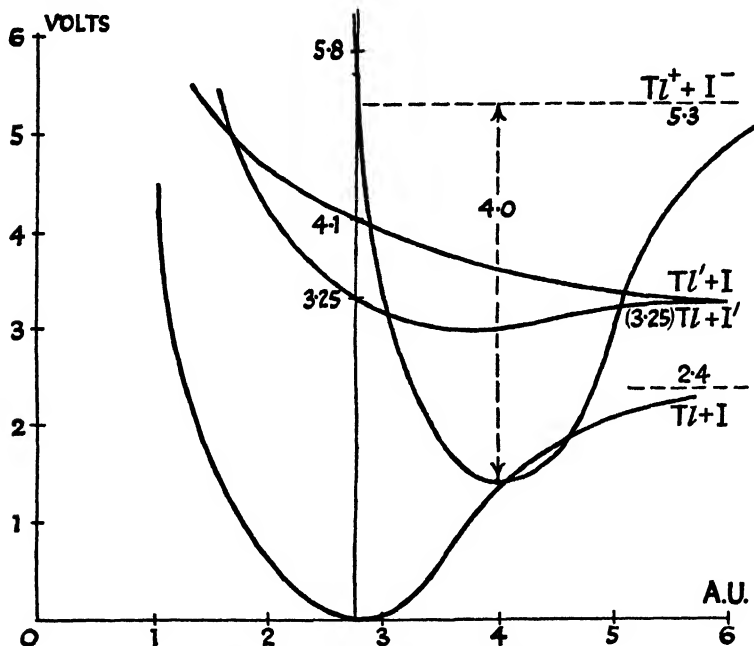


Fig. 30. Some $U(r)$ curves of TlI.

(3.9–4.4 volts) arising by transition from the normal to unstable (repulsive) states.

Upon illumination of the salt vapour with light in the region λ 2130 (5.8 volts) there is strong absorption corresponding to dissociation of the molecule into ions Tl^+ and I^- . This has been proved by magnetic mass analysis of the products by Terenin and Popov. Moreover, the photo-ionization current was shown to be proportional to the first power of the vapour pressure, so that the ionization was clearly a primary process in the molecule, and not due to collisions or other such secondary cause.

It appears that the thallium halide molecules are in their normal state homopolar or atomic-type molecules. By absorption of light of suitable wave-length we have seen that the molecule may be transferred to an ionic type of binding from which it is dissociated into ions. This is in notable contrast with the alkali metal halides (such as NaI), which are ionic-type molecules in the normal state but which

upon absorption of light are transferred to an atomic type of binding and dissociate into normal atoms (see Fig. 28). The behaviour of TII is explained by Fig. 30: it remains to present the data upon which the relative disposition of these $U(r)$ curves of TII are based.

If D_i is the energy required to dissociate the normal molecule into ions, D to dissociate it into atoms, I the ionization potential of TI, and E the electron affinity of the halogen atom:

$$D_i = D + I - E,$$

giving for TII the value $(2.4 + 6.1 - 3.2)$ volts, viz. 5.3 volts. The wave-length of maximum photo-ionization $\lambda 2130$, corresponding to 5.8 volts, indicates that the most-favoured ionization corresponds to about 0.5 volt kinetic energy in the ionic products. The value of r_0 for the normal state is 2.7 A.U. as derived from Morse's formula $r_0^3 \omega = 3000$, where $\omega = 150 \text{ cm.}^{-1}$. The value of r_0 for the ionic state may (less accurately) be deduced from the known ionic radii TI^+ (1.5 A.U.) and I^- (2.2 A.U.) in the crystalline state. Assume it to be 3.7 A.U. This value may be substituted in e^2/r to obtain an approximate value of the dissociation energy from the ionic-type binding. We thus obtain 4.0 volts. The relative disposition of the curves as in Fig. 30 is thus accounted for in a general way.

(c) THE ATOMIC TYPE OF BINDING ('HOMOPOLAR').

In this category fall the majority of diatomic molecules. For most of these dissociation in the ground state yields normal atoms, and in the first excited state of the molecule usually one excited and one normal atom. In contrast with this, the ionic molecule dissociates in its ground state into ions, and in its excited state into normal atoms. Occasionally both the ground state and first excited state of a homopolar molecule have $U(r)$ curves converging to the same dissociation level, and therefore both giving the same products. We cannot therefore class a molecule as homopolar or heteropolar on the basis of one kind of evidence (e.g. dissociation products) only.

One of the simplest methods of determining the energy of dissociation was suggested by Birge and Sponer.* From equations (17)–(19), we see that, if $G(v)$ is a quadratic within the limits of accuracy, ω_r is linear, thus

$$\omega_r = \omega_e - 2x_e \omega_e (v + \frac{1}{2}) \dots$$

Presumably dissociation corresponds to $\omega_r = 0$, which occurs when $v + \frac{1}{2} = \frac{\omega_e}{2x_e \omega_e}$. Substituting this particular value of v in the expression for the vibrational energy (15), we have

$$D_e = \frac{\omega_e^2}{4x_e \omega_e} \dots \dots \dots (57)$$

or by (54)

$$D_0 = \frac{\omega_e^2}{4x_e \omega_e} - \frac{\omega_e}{2} + \frac{\omega_e x_e}{4} \dots \dots \dots (58)$$

The value of this simple procedure depends entirely on the con-

* *Phys. Rev.*, vol. 28, p. 259 (1926).

fidence which can be placed in what is often a very long linear extrapolation. If ω_r is plotted against ν (as in Fig. 31), then, as equation (17) indicates, the energy of dissociation is the area $\int \omega_r d\nu$ under the line. For D_0 it is the area above the axis $\nu = 0$, for D_r the area above $\nu = -\frac{1}{2}$.

In Fig. 31 the curves of $\omega_r : \nu$ have been constructed for a few cases.* It is clear that the assumption of linearity may be only a rough approximation, and that a small curvature not apparent from low- ν data may lead to a large error in D . We conventionally describe curvature towards the axes as negative, and away from the axes as positive (based on the sign of the second derivative). A common type of $\omega_r : \nu$ curve has a small negative curvature for the greater

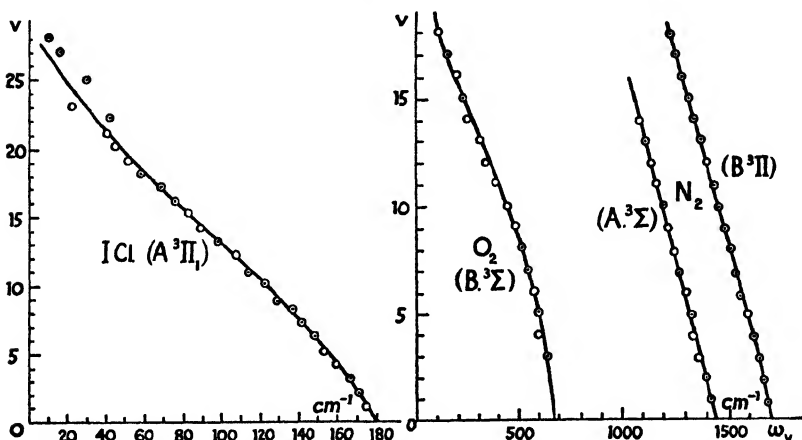


Fig. 31. $\omega_r : \nu$ graphs for ICl ($^3\Pi_1$), O_2 ($^3\Sigma$), N_2 ($^3\Pi$ and $^3\Sigma$).

part of the range, changing to a positive curvature in the later part. Some of the *ground* states of molecules, such as $X^2\Pi$ (β -system of NO), and $X^1\Sigma$ (Fourth Positive CO system), appear to have a strictly linear graph over the *observed* range.

From Fig. 27 we derive an important relationship between D' and D'' of two electronic states of a molecule.

$$D_0' + \nu^{(0,0)} = D_0'' + \nu_{\text{atom}} \quad . \quad . \quad . \quad (59)$$

If a knowledge of molecular structure makes known the probable nature of the atomic products ν_{atom} is known, and if either D' or D'' is reliably determined the other can be calculated.

Another useful relationship permits us to calculate D^+ the energy of dissociation of the ionized molecule if I_m , the ionization potential of the molecule, and I_a , that of the atom, are known.

$$D^+ + I_m = D + I_a \quad . \quad . \quad . \quad (60)$$

Energetically, it is clearly the same whether we first ionize a molecule

* Data on O_2 from Leifson (*Astrophys. Jour.*, vol. 63, p. 74 (1926)); data on ICl from Wilson (*Phys. Rev.*, vol. 32, p. 611 (1928)).

and then dissociate it, or first dissociate it and then ionize one of the atoms.

Among numerous possible examples we consider the oxygen molecule as a homopolar type. We shall limit ourselves to the best-known

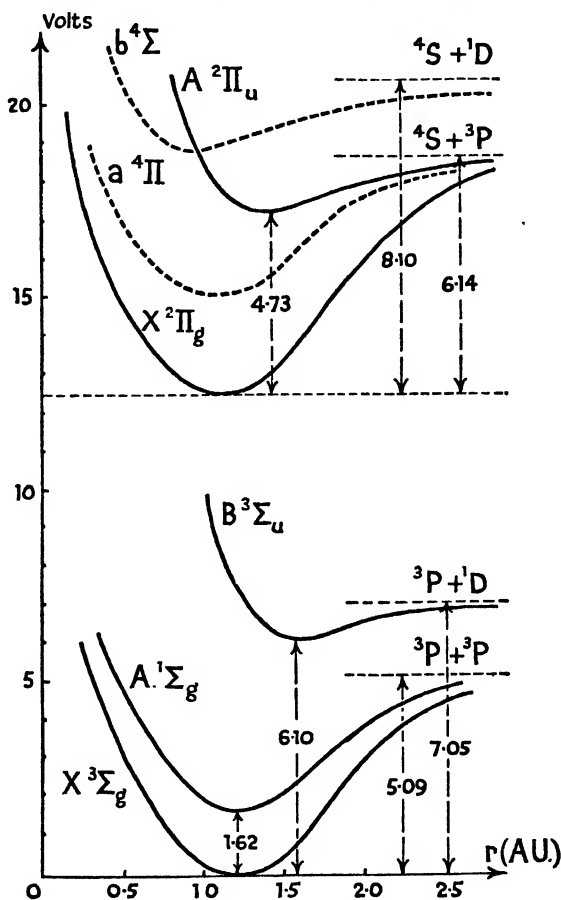


Fig. 32. $U(r)$ levels of O_2 and O_2^+ .

levels of oxygen. These are given in Fig. 32, and are principally familiar through the band systems

$A^1\Sigma \leftarrow X^3\Sigma$ Atmospheric absorption.

$B^3\Sigma \rightleftharpoons X^3\Sigma$ Schumann-Runge.

$A^2\Pi \rightarrow X^2\Pi$ Ultra-violet negative.

$b^4\Sigma \rightarrow a^4\Pi$ Visible negative.

The information about the visible negative bands of O_2^+ is more scanty than for the other systems, and these levels have therefore been indicated by broken lines. Fig. 32 is not intended to be quanti-

tatively accurate, but is merely a diagram with the important quantitative data marked in. The absorption data of the Schumann-Runge system are very extensive, and we have already seen (Fig. 31) that the v' -progressions of the $B^3\Sigma$ level have been followed almost up to the convergence point. (It is this absorption system which gives a continuum * below λ 1750, and which necessitates the use of *vacuum* spectrographs in all work in the Schumann region.) The value of D' for this level has thus been accurately determined as 0.95 volt. Using equation (59), it follows that

$$D'' = 0.95 + 6.10 - 1.96 = 5.09 \text{ volts.}$$

If we make use of the v'' -data provided by $G(v'')$ of the Schumann-Runge system, derived from the bands (0,11) to (0,17), we obtain by a long extrapolation about 6.0 volts. The discrepancy between this and the accepted value of 5.09 volts indicates the inaccuracy of such long extrapolations.

Applying (59), to find D' for the $A^1\Sigma$ level it is $5.09 - 1.62 = 3.47$ volts, since on theoretical grounds of molecular structure (see Chapter VI), there is no doubt the dissociation products in states X and A are the same. On the other hand, an evaluation of D' from (57), where $\omega_e = 1432.6$ and $\omega_e x_e = 13.925$, gives 4.46 volts, showing again the inaccuracy in relying on a long linear extrapolation.

Adopting $I_m = 12.5$ volts (from critical potential experiments) and $I_a = 13.55$ volts from the oxygen line spectrum, equation (60) gives $D' = 5.09 + 13.55 - 12.5 = 6.14$ volts. Calculating from (57), where $\omega_e = 1876.4$ and $\omega_e x_e = 16.53$, we have $D' = 6.45$ volts (of course a less reliable value).

Again applying (59) to find D' of the $A^2\Pi$ state of O_2^+ , we derive $6.14 - 4.37 = 1.41$ volts. Calculation from the vibrational data of this state gives the less reliable value 1.76 volts. It is interesting to note that the whole of the accepted values for the various electronic levels are based upon the reliable determination of D' ($= 0.95$ volt) for the upper electronic state of the Schumann-Runge system.

(d) THE VAN DER WAALS TYPE OF BINDING

The existence of a class of molecules of which the atoms are very loosely bound has been demonstrated by spectroscopic work. Of this type are the molecules Hg_2 , Cd_2 , Zn_2 , and mixed molecules which these elements are capable of forming with the alkali metals Na, K, Rb, and Cs, also with Tl and In. The existence of such molecules is supposed to be due to a shallow potential minimum formed by the balancing of Heitler-London repulsion and Van der Waals attracting forces (i.e. polarization forces), since the latter will sometimes fall off more slowly with increase of inter-nuclear distance than the former.† The result of atomic collisions is therefore expressed by a shallow potential curve such as those of Fig. 28. In contrast with Fig. 28, this forms the *normal* state of the molecule, and we shall see that there is evidence that the $U(r)$ curves of some of the *excited* states of these molecules are of the stable strongly bound type.

* See *Phys. Rev.*, vol. 40, p. 1018 (1932); vol. 42, p. 518 (1932).

† Proof due to Eisenschitz and London, *Zeit. f. Phys.*, vol. 60, p. 515 (1930).

We consider for purposes of illustration cadmium vapour. The curves of Fig. 33 are adapted from Mrozowski * and Fig. 34 from the paper of Winans,† whose interpretation we follow here.

First we describe the experimental facts. As is clear from Fig. 33,

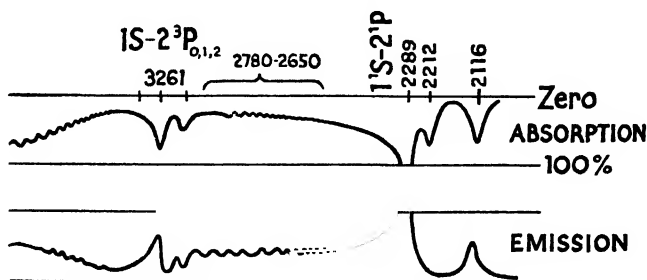


Fig. 33. Absorption and emission spectra of Cd_2 vapour. (After Mrozowski.)

there are two resonance lines $1^1S \rightarrow 2^3P$ (λ 3261), and $1^1S \rightarrow 2^1P$ (λ 2289). For purposes of illustration we shall confine ourselves to the latter. At low pressures of Cd vapour λ 2289 appears as a narrow line in absorption. With increasing pressure of vapour it at first broadens symmetrically, and two bands at λ 2212 and λ 2116 appear and broaden to a small extent. The band at λ 2212 broadens towards the long-wave side. The extensive broadening of the λ 2289 line with increasing pressure does not proceed beyond the band at λ 2212 on the short-wave side, but proceeds some 500 Å.U. towards the long-wave side. At vapour pressures over 130 mm. diffuse flutings make their appearance between about λ 2780 and 2650 converging towards the ultra-violet. In emission the band at λ 2212 does not appear at all.

The explanation of these facts is understood from Fig. 34 if we apply the principles of Franck and Condon. Absorption of the line λ 2289 is accounted for by Cd atoms ((a) in Fig. 34). The band at λ 2212 may be due to light absorption by the molecules from their lowest (non-vibrating) position (b). With increasing temperature there is increased

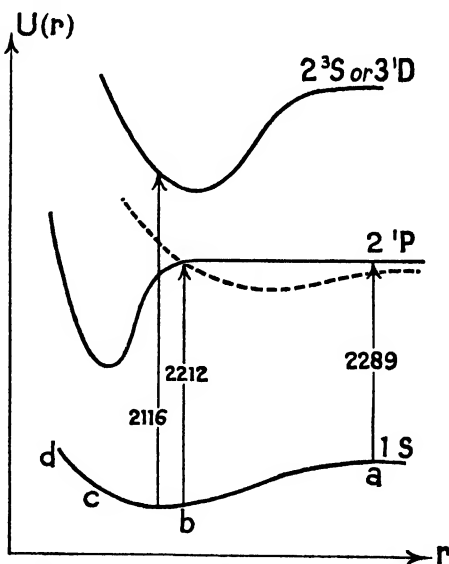


Fig. 34. $U(r)$ curves of the cadmium molecule (Cd_2). (After Winans.)

* *Zeit. f. Phys.*, vol. 62, p. 314 (1930).

† *Phil. Mag.*, vol. 7, p. 555 (1929).

vibrational amplitude in the ground electronic states, as well as an increasing number of Cd molecules present, so that clearly broadening to the low-frequency side is inevitable. Further, it is clear that absorption of λ 2212 corresponds to dissociation of the molecule in Fig. 34, so that this band would not occur in emission. There remains the broadening (with increasing pressure) of λ 2289 to explain. When two cadmium atoms collide, the curve of their mutual potential energy is the lowest curve 1^1S of Fig. 34. The colliding system of two atoms—a quasi-molecule—may at any point of the energy path absorb light of appropriate frequency and pass to the upper excited state. At first for low temperatures and low colliding velocities the most probable position of the system for absorption is near (*b*) of Fig. 34. The effect of increasing temperature is to make absorption develop appreciably from all points of the potential basin *abc*; also the effect of increased kinetic energy of the colliding components will result in a point such as (*d*) being attained by the system. As a result, appreciable absorption extends a considerable way on the low-frequency side of λ 2289, but not farther than λ 2212 on the high-frequency side.

The occurrence of the band λ 2116 in both emission and absorption is accounted for by a higher electronic state which must necessarily be approximately in the position and of the type shown.

If the curve of the 2^1P state were supposed to be as portrayed by the broken line in Fig. 34, instead of as we have hitherto assumed, then clearly a broadening of the band λ 2212 in absorption would occur symmetrically on both sides, and not as observed to the low-frequency side only.

The fluctuating intensities in the region λ 2780–2650 are explained along the same lines as the similar phenomenon in the alkali halides (Fig. 29). Their existence proves that the binding of the excited state is much stronger than the ground state—which latter must be a shallow basin for the phenomenon to arise at all. The direction of convergence of the diffuse bands should be towards the high-frequency side, as is found. Owing to the slope of the ground curve, the intervals between the diffuse bands will be greater than that of the spacing of vibrational levels of the upper state 2^1P . For this reason an extrapolation of the bands to the convergence limit to determine the energy of dissociation from the 2^1P state is liable to error. Mrozowski* by this method derived an energy of dissociation in the case of Hg_2 of 0.74 volt from the 2^1P state. Winans† deduced the energy of dissociation D'' from the ground state 1^1S of Hg_2 as 0.15 volt. For Cd_2 Winans gives 1600 cm^{-1} or 0.20 volt. Winans deduced these values for the normal state of these two molecules as the equivalent of the energy difference between points (*b*) and (*a*) in Fig. 34. Thus in Cd_2 it is the frequency difference of λ 2289 and 2212. For further detail a paper by S. W. Cram‡ on the molecular spectrum of cadmium may be consulted.

The existence of loosely bound molecules of the above type has now been established for a great many molecules of the alkali metals—pure molecules of the type X_2 , and mixed molecules of the type XY .

* *Zeit. f. Phys.*, vol. 55, p. 338 (1929); *Phys. Rev.*, vol. 36, p. 1168 (1930).

† *Phys. Rev.*, vol. 37, p. 897 (1931).

‡ *Ibid.*, vol. 48, p. 205 (1934).

The proof of their existence is found in the development of diffuse bands on the high-frequency side of the resonance lines of the metal in just the same way as λ 2212 appeared relative to the Cd resonance line λ 2289. Oldenberg* has discovered the possibility of Van der Waals molecules being formed by atoms uniting with atoms of the inert gases (such as HgA). The characteristics of these are similar to those molecules above described.

Glockler and Martin† have also described diffuse bands which appear on the long wave-length side of the Hg line λ 2536 (attributed to a methane-Hg molecule) when a mixture of methane and mercury vapour was illuminated by a mercury discharge tube.

(e) THE $G(v) : \omega$ RELATION: BIRGE'S SECOND METHOD.

In Section (c) it was stated that the common form of the $\omega_r : v$ curve was that of slight negative curvature (i.e. concave towards the axes) for low v -values and positive curvature in its latter part for the high v -range (cf. Fig. 31). This indicates, of course, that a quadratic expression for $G(v)$ which implies a linear expression for v (cf. equation (17)) is but a first approximation. Birge‡ has remarked that even a fourth degree polynomial in v fails to express ω_r satisfactorily over the whole range. Instead of plotting ω_r against v , Birge subsequently suggested plotting $\omega_r : G(v)$. ($G(v)$ is the vibrational term of (15)). Such a graph which was constructed by Birge for the $B^3\Sigma$ vibrational data of oxygen was apparently like a parabola, and on this assumption he could write

$$G = a + b\omega + c\omega^2 \quad . \quad . \quad . \quad (61)$$

If it is a true parabola its gradient should be linear for :

$$\Delta G = \frac{dG}{d\omega} = b + 2c\omega \quad . \quad . \quad . \quad (62) \S$$

Upon constructing experimentally the curve $\Delta G : \omega$ it was found not to be one straight line, but two quite distinct straight lines of different gradients. The apparent parabola obtained by plotting $G : \omega$ was in reality a synthesis of two parabolae—although to the eye this feature was not apparent. The point of inflexion of the former $\omega_r : v$ curve is really a junction of two curves and corresponds to this point of discontinuity where the two $G : \omega$ parabolae are contiguous. Fig. 35, which is adapted from Birge's paper, makes this clear. If we wish, we can obtain from equations (62) and (17) a true relation between ω and v . Equation (62) can be written $\frac{dG}{dv} \frac{dv}{d\omega} = b + 2c\omega$ or $\omega \frac{dv}{d\omega} = b + 2c\omega$. Multiply through by $\frac{d\omega}{\omega}$ and integrate. We have

$$v = b \log \omega + 2c\omega + d \quad . \quad . \quad . \quad (63)$$

This unfortunately cannot be solved except by approximate methods,

* *Zeit. f. Phys.*, vol. 55, p. 1 (1929).

† *Jour. Chem. Phys.*, vol. 2, p. 46 (1934).

‡ *Trans. Faraday Soc.*, vol. 25 p. 707 (1929).

§ ΔG means in words: the change in G due to unit change in ω .

otherwise we could obtain ω as a function of v and calculate the critical value of v corresponding to $\omega \rightarrow 0$. Although (63) has no practical value, we can deduce from it several points of interest.

(1) If the $\omega : v$ relation is strictly linear, then by equation (63) it follows that $b = 0$. Hence by equation (61) the $G : \omega$ parabola has its vertex at $\omega = 0$, and by equation (62) the $\Delta G : \omega$ graph must pass through the origin. This latter deduction is a sensitive practical criterion of the $\omega : v$ linearity.

(2) If the $\omega : v$ relation has negative curvature ($d^2v/d\omega^2$ is negative),

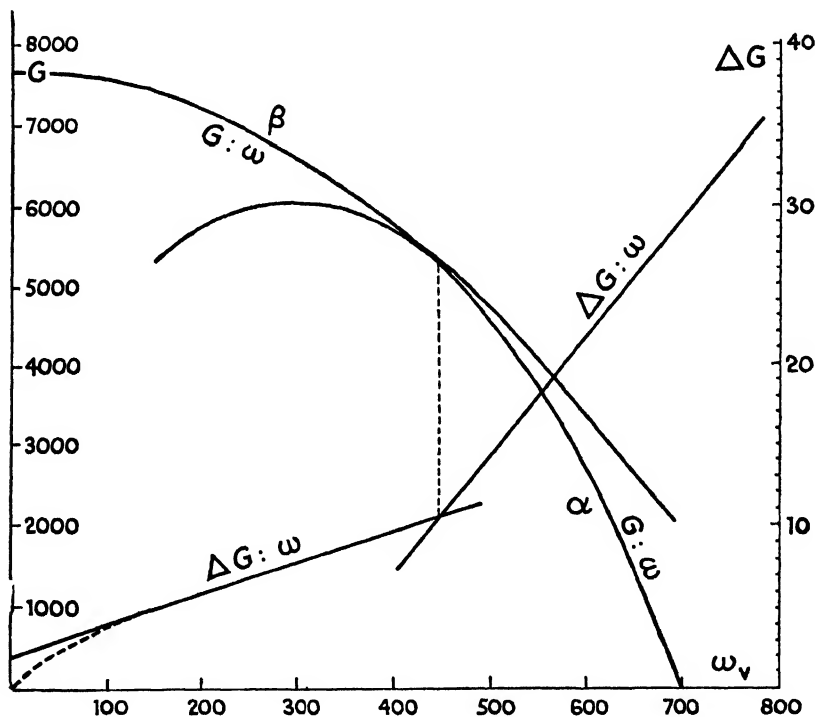


Fig. 35. $G : \omega$ and $\Delta G : \omega$ curves for the $B^2\Sigma$ state of O_2 . (After Birge.)

then from equation (63), b is positive, and by equation (61), which can be written $G = a - \frac{b^2}{4c} + c\left(\omega + \frac{b}{2c}\right)^2$, we see that the vertex occurs at a positive value of ω , viz. $\omega = -b/2c$. (This is a positive value of ω , since c is always negative, the $G : \omega$ parabola being inverted.) The parabola (α) of Fig. 35 corresponds to the negative curvature of the $\omega : v$ graph.

(3) If the graph $\omega : v$ has positive curvature (which is commonly found as we approach the dissociation point), then $d^2v/d\omega^2$ is positive, so that b is negative from equation (63). We see therefore that the vertex corresponds to a negative value of ω , viz. $-b/2c$, where now both b and c are negative. Parabola (β) of Fig. 35 is of this type.

(4) Consider the value of v given by equation (63) as $\omega \rightarrow 0$. As just considered, the curvature is generally positive in this region, so that b is negative. Let $b = -k$, where k is the numerical value of b . The term $b \log \omega$ can be written $\log (1/\omega^k)$, so that we see that $v \rightarrow \infty$ as $\omega \rightarrow 0$. This is the behaviour to be anticipated for ionic molecules, but not, according to Kratzer,* for the atomic type of binding. It is therefore considered probable that b actually becomes zero as ω approaches zero, so that v has a finite value. This corresponds in Fig. 35 to a slight departure from the parabolic form of $G : \omega$ close to the axis $\omega = 0$, so as to bring the vertex actually on this axis. It corresponds in the $\Delta G : \omega$ graph to a bending towards the origin, as indicated by the broken line there. This hypothesis is difficult either to confirm or disprove experimentally, since the vibrational levels close to the dissociation point are inevitably difficult to locate accurately.

The impossibility of $\omega : v$ having negative curvature as it approaches the dissociation point $\omega = 0$ follows from equation (63). For, with b positive, $\log (0)$ corresponds to $v = -\infty$, which is impossible. To be physically possible, the graph $\Delta G : \omega$ must intercept *above* the origin or, more probably, pass through it. Where its extrapolation to $\omega = 0$ would take it below the origin it is clear that it must be assumed to curve round so as to pass through it.

The energy of dissociation is the value of G corresponding to the intersection of the $G : \omega$ parabola with the $\omega = 0$ axis, or, alternatively, it is the area under the $\Delta G : \omega$ curve (see equations (61) and (62)).

For the $B^3\Sigma$ level of O_2 discussed in detail, the value of D' is 7700 cm^{-1} (0.95 volt). The discontinuity occurs at about 5400 cm^{-1} , which corresponds to about 68% of the dissociation energy of the molecule.

The phenomenon has been recorded for a number of other electronic levels of various molecules, as shown in the accompanying table. It

Molecule and level	Dissociation energy D (volts)	Energy level of discontinuity (volts)	% of D	Reference
O_2 ($B^3\Sigma$) . . .	0.95	0.67	68	<i>Trans. Faraday Soc.</i> , vol. 25, p. 707 (1929).
H_2 (Normal $^1\Sigma$) . .	4.465	4.06	91	<i>Trans. Faraday Soc.</i> , vol. 25, p. 707 (1929).
I_2 (Upper state) . .	0.85	0.57	68	<i>Trans. Faraday Soc.</i> , vol. 25, p. 707 (1929).
Br_2 (Upper state)	0.462	0.25	54	<i>Phys. Rev.</i> , vol. 38, p. 1187 (1931).
Cl_2 (Upper state)	0.39	0.23	59	<i>Proc. Roy. Soc.</i> , vol. 127, p. 638 (1930).
ICl	0.455	0.227	50	<i>Phys. Rev.</i> , vol. 40, p. 366 (1932).
		0.344	76	<i>Trans. Faraday Soc.</i> , vol. 27, p. 77 (1931).
IBr ($A^3\Pi_1$) . . .	0.167	0.114	68	<i>Phys. Rev.</i> , vol. 37, p. 1548 (1931).

* *Zeit. f. Phys.*, vol. 26, p. 40 (1925).

points to some change in the internal molecular structure (i.e. in the Law of Force), which takes place suddenly when the molecule is loaded to a certain critical point with vibrational energy.

We shall see when we consider (in Chapter VI (c)) the detailed electronic structure of molecules that, in the formation of a molecule from two atoms, some of the electrons must necessarily have their principal quantum numbers raised. This process, described as 'promotion of the electrons' by Mulliken, is required by the Pauli principle when it is applied to the molecular system. The converse process to this must take place in molecular dissociation, and the discontinuity in the $U(r)$ function may be an indication of the point

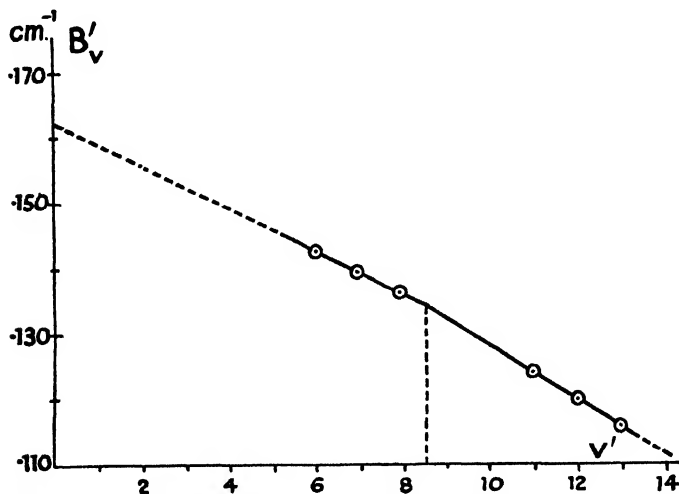


Fig. 36. $B_v : v$ graph for the upper state of the Cl absorption system. (After Elliott.)

beyond which true atomic conditions (as prescribed by the Pauli principle) are restored in the component atoms.

Since there is a sudden change in the Law of Force, we should expect to find, as a consequence, that the constant α of equation (27) in Chapter IV (e), $B_v = B_e - \alpha(v + \frac{1}{2})$ undergoes also a sudden change at the critical value of v . This expectation has been confirmed by Elliott * in the case of the Cl_2 absorption system ($\text{O}_u^+ \leftarrow {}^1\Sigma_g^+$). The case of ICl in the table is of special interest, in that two points of discontinuity have been recorded for the $A {}^3\Pi$ level. These occur at about $v' = 10$ and $v' = 17$ or 18 . Three parabolæ of the type (61) are thus required to cover the vibrational behaviour of the molecule.

(f) DISSOCIATION THROUGH ROTATION

In Chapter IV (e) we wrote for the total energy of the vibrating-rotating molecule

$$E = U(r) + \frac{h^2}{8\pi^2\mu r^2} K(K+1) \quad . \quad . \quad . \quad (64)$$

* *Proc. Roy. Soc.*, vol. 127, p. 638 (1930).

and showed that the effect of the rotational term was to cause an increase in r_e and a decrease in D (the energy of dissociation). In Fig. 37 we represent the energy curves $E : r$ for a series of values of K . For large values of r the function $U(r)$ approaches zero more rapidly than the rotational term in r^{-2} , hence maxima are produced above the dissociation level of the non-rotating molecule. As K increases and the potential basins get shallower, it is clear that the number of their contained vibrational levels will be fewer. In Fig. 37 we observe that no band can in fact exist for which $K \geq 30$: thus the molecule dissociates through its rotational instability.

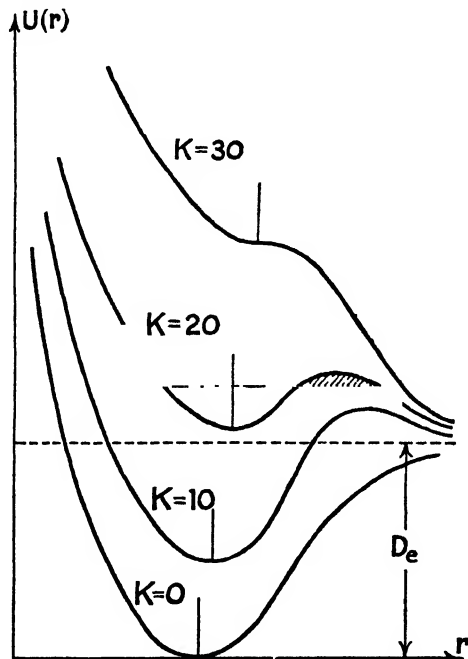


Fig. 37. $U(r)$ curves of a rotating-vibrating molecule.

Beginning at the top of Fig. 37 and travelling downwards, we pass through successive $U_K(r)$ curves which will contain at first only one vibrational level, $v = 0$, then through curves containing two vibrational levels, $v = 0, 1$, and so forth. It is clear that the total energy at the dissociation point, which corresponds to the summit of the potential barrier, will be greatest for $v = 0$, a little less for $v = 1$, still less for $v = 2$, &c., although all three are greater than D_e of the non-rotating molecule. These features are displayed in Fig. 38. The phenomenon of rotational instability has been noted for certain electronic states of many hydride molecules, HgH , AlH , CaH , &c. Once the minimum of the potential basin is above the dissociation level D_e (above $K = 18$ in Fig. 37), there is, according to wave-mechanics, a finite probability of rotational dissociation. Thus for any value of v there is a value of K at which the band structure

will suddenly terminate (Fig. 38). For a few K -values below these terminal values (and above AB) the finite probability of rotational dissociation shows itself as a diffuseness of the band lines (incidentally providing direct experimental evidence of the validity of wave-mechanics).

Mulliken* in 1925 first recorded a case of rotational instability in the CaH band at λ 3563. Photographs of the effect in AlH are given by Bengtsson and Rydberg,† and in SO by Martin.‡ Oldenberg§

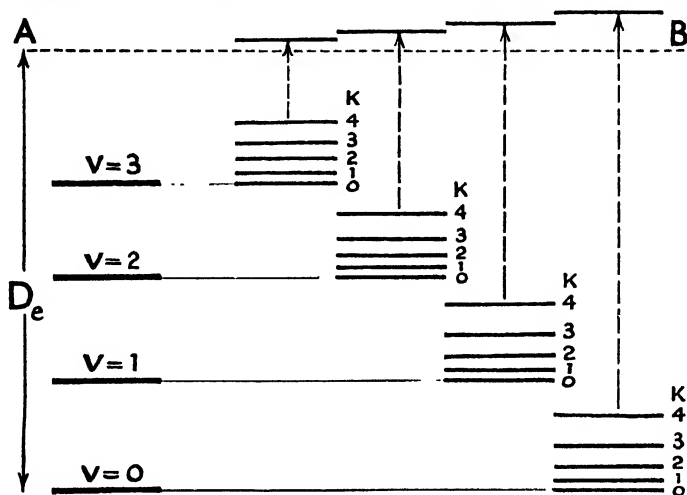


Fig. 38. Vibration-rotation levels from Fig. 37.

was the first to account in detail for the phenomenon. Others|| have subsequently applied wave-mechanics successfully.

The half-width of band lines has been shown by Kronig¶ to be

$$\Delta\nu = \frac{h\omega}{4\pi} \exp \left[-\frac{4\pi}{h} \int \sqrt{2\pi(E - U)} dr \right] \quad . \quad . \quad (65)$$

The integration is taken through the potential barrier at the appropriate vibration-rotation level: ω is the vibration frequency for this level. Thus in Fig. 37 for the particular vibration level shown, the integral $\int (E - U) dr$ would be the area shaded. It is apparent that for K -levels near the crest of the barrier the integral will be small in value and the half-width considerable. Rydberg has quantitatively verified this.** The problem of 'leakage' through the potential barrier is closely analogous in mechanism to that of the emission of α -particles from radioactive nuclei which Gamow has treated in his book.††

* *Phys. Rev.*, vol. 25, p. 509 (1925).

† *Zeit. f. Phys.*, vol. 59, p. 548 (1930).

‡ *Phys. Rev.*, vol. 41, p. 167 (1932).

§ *Zeit. f. Phys.*, vol. 56, p. 563 (1929).

|| *Phys. Rev.*, vol. 35, p. 1028 and p. 1538 (1930).

¶ *Zeit. f. Phys.*, vol. 62, p. 300 (1930).

** *Ibid.*, vol. 80, p. 514 (1932).

†† *Atomic Nuclei and Nuclear Transformations*. O.U.P. (1937).

THE ELECTRONIC STATES OF MOLECULES

(a) THE CORRELATION OF BAND SYSTEMS OF A MOLECULE

WE have seen that the bands of a system can be represented by a formula such as (3) or (21): $\nu = \nu_e + G'(v') - G''(v'')$. If different band systems of the same molecule have $G'(v')$ or $G''(v'')$ in common, this information makes possible the construction of a scheme of electronic energy levels for the molecule. Thus there are three known band systems of CO^+ represented by formulae

$$\begin{aligned}\nu &= 44782.7 + 1722.1(v' + \tfrac{1}{2}) - 24.33(v' + \tfrac{1}{2})^2 \\ &\quad - 2212(v'' + \tfrac{1}{2}) + 15.17(v'' + \tfrac{1}{2})^2, \\ \nu &= 19_{667.4}^{602.9} + 1564.5(v' + \tfrac{1}{2}) - 14.07(v' + \tfrac{1}{2})^2 \\ &\quad - 2212(v'' + \tfrac{1}{2}) + 15.17(v'' + \tfrac{1}{2})^2, \\ \nu &= 25_{089.8}^{215.3} + 1722.1(v' + \tfrac{1}{2}) - 24.33(v' + \tfrac{1}{2})^2 \\ &\quad - 1564.5(v'' + \tfrac{1}{2}) + 14.07(v'' + \tfrac{1}{2})^2,\end{aligned}$$

and this clearly corresponds to the scheme of electronic levels represented in Fig. 39. The significance of the description of these levels by $^2\Sigma$ and $^2\Pi$ is discussed later. The CO^+ molecule has thirteen electrons, and would be expected closely to resemble the molecules CN , N_2^+ , BO , and BeF , which all have this number of electrons. We might perhaps visualize these molecules as follows: each nucleus retains its own K -shell of two electrons ($n = 1$), the molecule as a whole has an L -shell of eight electrons ($n = 2$), while a valence electron ($n = 3$) moves in an outer orbit. In external electronic structure all these molecules would thus resemble the Na atom. With one or two exceptions the systems of Fig. 39 have been found in all the above-mentioned molecules, and the external resemblance to the Na atom led originally to the suggestion that the three levels were precisely analogous to the three lowest electronic states ($3s$ 2S , ($3p$ 2P , and ($4s$ 2S of the Na atom. Similarly the 21-electron molecules SiN , AlO , and MgF all have analogous systems and their external structure resembles the 19-electron potassium atom. Likewise CO and N_2 , with two valence electrons, have Mg as 'corresponding' atom; NO and O_2^+ , with three valence electrons, would have Al as 'corre-

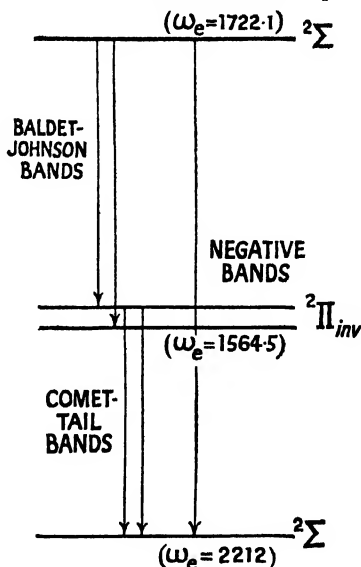


Fig. 39. Electronic levels of the CO^+ molecule (not drawn to scale).

sponding' atom. Closer examination shows, however, that there is no precise correspondence between the electronic levels of these atoms and molecules. It is found that there are in general many electronic levels in molecules which have no counterpart in the 'corresponding atom'. Moreover, transitions such as ${}^2S \rightarrow {}^2S$ are certainly disallowed by the selection principle ($\Delta L = \pm 1$) in atoms. The key to a correct description and understanding of the electronic states of molecules is found in the Stark effect on atoms.

(b) DESCRIPTION OF THE ELECTRONIC STATES OF ATOMS

It is obvious that an understanding of the electronic states of molecules must be built upon a prior knowledge of the electronic states of atoms. The student who has a clear understanding of the latter should be able to appreciate the significance of the molecular quantum numbers now to be introduced. It has been found necessary to make reference in subsequent sections to *Atomic Spectra* (Methuen's 'Monographs on Physical Subjects') by the present writer, and some time spent on this monograph at the present stage will greatly facilitate a further study of molecules. The present section is not intended as more than a summary of the quantum numbers occurring in atoms.

Every electron in an atom is defined precisely by four quantum numbers n, l, j, m , or five quantum numbers, if the spin $s = \frac{1}{2}$ is counted. The principal quantum number n determines in which shell the electron is found: $n = 1$ (K); $n = 2$ (L); $n = 3$ (M); $n = 4$ (N), &c. This quantum number primarily controls the energy and the major axis of the orbit, and by excitation it may take a series of values from a certain minimum up to infinity.

The subsidiary quantum number l is associated with the orbital angular momentum of the electron $\sqrt{l(l+1)} \frac{h}{2\pi}$. It divides up the electrons in the K, L, M shells into sub-groups, each of which has a characteristic value of l . The possible values of l range from 0 to $n - 1$. Thus in the M -shell ($n = 3$) there are three sub-groups having $l = 0, 1$, and 2 respectively. Electrons having $l = 0$ are labelled 'sharp', $l = 1$ are labelled 'principal', $l = 2$ are labelled 'diffuse', $l = 3$ are labelled 'fundamental'. Orbits having the same n but different values of l have different energy values. The s -electrons ($l = 0$) are most tightly bound, corresponding to the greatest degree of orbital eccentricity, and therefore greatest penetration of the atom core. This diminishes as l increases. The maximum number of electrons in these sub-groups is s (2), p (6), d (10), f (14), &c.

Each electron has a spin quantum number $s = \frac{1}{2}$ corresponding to spin momentum $\sqrt{s(s+1)} \frac{h}{2\pi}$, and this combines vectorially with $\sqrt{l(l+1)} \frac{h}{2\pi}$ to give $\sqrt{j(j+1)} \frac{h}{2\pi}$, the total* electronic angular momentum, i.e. the resultant momentum arising from orbital revolution and axial spin. For every complete shell or sub-group $\Sigma j = 0$. In the absence of a magnetic field, each of the electronic

* j is sometimes called the 'inner' quantum number.

states characterized by (n, l, j) is to be ascribed a statistical weight $2j + 1$, because in the presence of a field this number of specific orientations of the j -vector relative to the field arises. We therefore introduce m , a magnetic quantum number, so that the vector $m \frac{h}{2\pi}$ represents the projection of the j -vector momentum on the field, m taking the $2j + 1$ values between $+j$ and $-j$. All this refers to the quantum numbers of a single electron.

When we consider atoms with several electrons outside a complete shell, we have a resultant spin S' arising from the coupling of the individual electronic spins.* We have also a resultant orbital quantum number L from the individual l 's and a resultant total quantum number J which takes integral or half-integral values according as $L \pm S'$ is integral or half integral. J has $2S' + 1$ values lying between $L + S'$ and $L - S'$. The electron configuration of the atom thus gives rise to a resultant state or 'term' which is described as S ($L = 0$), P ($L = 1$), D ($L = 2$), &c. The multiplicity $2S' + 1$ is written as a prefix, thus 2P , 3S , &c. The value of S' would be either $\frac{1}{2} + \frac{1}{2}$ or $\frac{1}{2} - \frac{1}{2}$ for an atom with two electrons outside a closed shell. S' would be either $\frac{1}{2} + \frac{1}{2} + \frac{1}{2}$ or $\frac{1}{2} + \frac{1}{2} - \frac{1}{2}$ for three electrons. S' would be $\frac{1}{2} + \frac{1}{2} + \frac{1}{2} + \frac{1}{2}$ or $\frac{1}{2} + \frac{1}{2} + \frac{1}{2} - \frac{1}{2}$ or $\frac{1}{2} + \frac{1}{2} - \frac{1}{2} - \frac{1}{2}$ for four electrons, &c. The value of J is indicated as a suffix, thus, e.g. ${}^2P_{1\frac{1}{2}}$ implies $S' = \frac{1}{2}$, $L = 1$, $J = 1\frac{1}{2}$.

Individual spectral lines of an atom thus arise by the transition of an electron (sometimes of two electrons concurrently), and the lines are expressed in terms of the initial and final states, e.g. ${}^2P_{1\frac{1}{2}} \rightarrow {}^2S_1$. Only certain types of transition can take place, and (these for a one-electron transition) may be expressed by the following selection rules:

$$\Delta L = \pm 1,$$

$$\Delta J = \pm 1, \text{ or } 0 \text{ (excluding } 0 \rightarrow 0),$$

$$\Delta S' = \pm 1, \text{ or } 0.$$

The first of these means that such transitions as $S \rightleftharpoons P$, and $P \rightleftharpoons D$ are possible, but not $S \rightarrow S$, $P \rightarrow P$, or $S \rightleftharpoons D$. The second means that ${}^2P_{1\frac{1}{2}} \rightarrow {}^2S_1$ and ${}^2P_{\frac{1}{2}} \rightarrow {}^2S_1$ are possible, but not ${}^3P_2 \rightarrow {}^3S_0$ or ${}^3P_0 \rightarrow {}^3S_0$. The third of these indicates that inter-combination lines (${}^3P \rightarrow {}^1S$) corresponding to $\Delta S' = 1$ are possible. Some of these are found in spectra of the heavier elements. Transitions $\Delta S' = 0$ between spectral 'terms' of the same multiplicity are, however, the general rule.

(c) DESCRIPTION OF THE ELECTRONIC STATES OF MOLECULES: SELECTION RULES

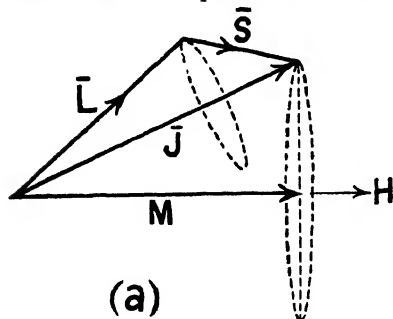
A molecule can be regarded as produced by two opposite processes: either by the bringing together of two separate atoms, or by the fictitious process of splitting the nucleus of a 'united atom' into two parts (and separating them). Thus, for example, the silicon atom of mass 28 might be regarded as split to give the CO molecule (C, 12 and O, 16). From whatever aspect we regard molecule formation it is clear that the system of two nuclei, with an electron-cloud penetrating

* In this brief summary other types of coupling are not mentioned.

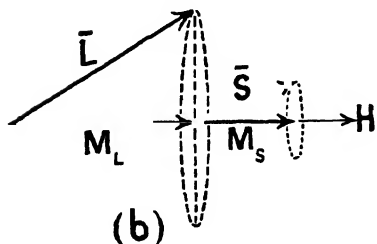
between them, implies the existence of a strong axial electric field. The appropriate rotation for *molecular* electronic states can therefore be most simply derived by examining the effect on the electronic states of an *atom* of a strong superposed electric field. In *Atomic Spectra*, Fig. 28 and the appropriate Section 6 (e) should be studied closely at this stage. The effect of a 'weak' electric field is to induce precession of \bar{J} ($\bar{J} \frac{h}{2\pi}$ is written briefly for $\sqrt{J(J+1)} \frac{h}{2\pi}$, the total electronic angular momentum) round the field axis. It can only orientate itself at certain angles to the field (F) given by

$$\bar{J} \cos(\bar{J}F) = M,$$

where M is a quantum number which takes those values* lying



(a)



(b)

Fig. 40. Precession of atomic vectors in a field: (a) weak, (b) strong.

$$\bar{L} = \sqrt{L(L+1)},$$

$$\bar{S} = \sqrt{S(S+1)},$$

$$\bar{J} = \sqrt{J(J+1)}.$$

relation to molecular electronic states as L and S do for atomic states.

Just as S, P, D, F states of atoms correspond to $L = 0, 1, 2, 3$, so $\Sigma, \Pi, \Delta, \Phi$ states of molecules correspond to $\Lambda = 0, 1, 2, 3$. The

* M is integral or half-integral according as J is integral or half-integral.

† A Σ -state ($\Lambda = 0$), the molecular equivalent of a sharp term in atomic spectra, will not in practice be confused with Σ , the quantum number which is the projection of S on the axis of the molecule.

between $+J$ and $-J$. Where a magnetic field is applied to an atom these $2J+1$ positions all have different energy values, but in an electric field those with opposite sign have the same energy, so that there are only $J+1$ different component levels (or $J+\frac{1}{2}$ levels if J is half-integral) in a weak field. Instead of M the Greek Ω is used for this quantum number in molecular notation. In Fig. 41 these levels have been plotted by using a formula due to Pauli $F(\Omega) = b_J[3\Omega^2 - J(J+1)]$, which has, however, no strict quantitative significance.

In a strong electric field the coupling of L and S to give J is broken down, so that \bar{L} and \bar{S} precess independently round the field axis. Two quantum numbers M_L and M_S now arise, bearing a similar relation to L and S as M did to J . These are called Λ and Σ in the molecular notation. Strong-field conditions are found in the majority of molecules, and these two quantum numbers Λ and Σ play the same part in

value of Λ ranges between $+L$ and $-L$, but there are only $L + 1$ energy levels, since those corresponding to $+\Lambda$ and $-\Lambda$ are energetically equivalent. The quantum number Σ , however, has $2S + 1$ values, ranging between $+S$ and $-S$.

Summing up (see Fig. 41), each atomic multiplet, characterized by an L -value, gives rise in a molecule to $L + 1$ multiplets, each characterized by a value of Λ ranging from 0 to L . These have the same

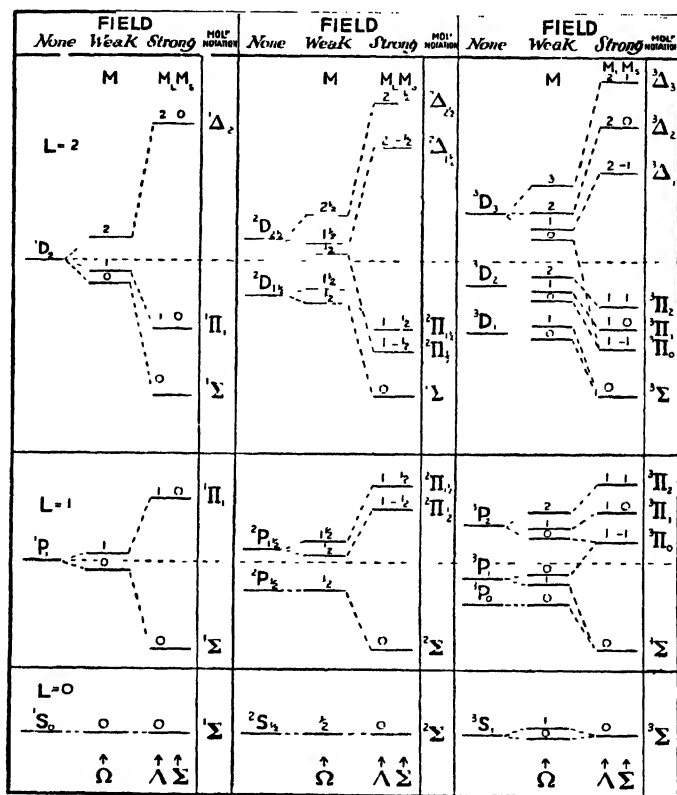


Fig. 41. Effect of (a) weak, (b) strong, electric fields on typical electronic states of an atom. (After Jevons.)

multiplicity $2S + 1$, i.e. the same number of component levels as in the atomic case. Each component is distinguished by a value of Ω ranging from $\Lambda - \Sigma$ to $\Lambda + \Sigma$. For example, the atomic state 3D_1 corresponds to $S = 1$, $L = 2$, $J = 1$; the molecular state $^3\Delta_1$ corresponds to $S = 1$, $\Lambda = 2$, $\Omega = 1$.

In Fig. 41 the strong-field levels have been plotted from $F(\Lambda) + A\Lambda\Sigma$, where the semi-quantitative expression $F(\Lambda) = a[3\Lambda^2 - L(L + 1)]$ has been adopted. It will be observed from the figure that the ratios of the intervals between the component levels of an

atomic multiplet follow the Landé interval rule. (Referring to *Atomic Spectra*, Chapter IV (g), it will be seen that the interval between the two levels characterized by J and $J - 1$ is proportional to J . Thus the three intervals between the four levels of 4D characterized by $J = 3\frac{1}{2}, 2\frac{1}{2}, 1\frac{1}{2}, \frac{1}{2}$ are in the ratio $7:5:3$.) But it will be observed from $\bar{F}(\Lambda) + A\Delta\Sigma$ that the corresponding intervals within a *molecular* multiplet are constant and equal to $A\Lambda$. The selection rules for molecular electronic transitions are as follows. They are identical with those for S , M_L , and M_S , for an atom in a strong electric field.

$$\left. \begin{array}{l} \Delta S = 0 \text{ (commonly), } \Delta S = 1 \text{ (occasionally), } \\ \Delta \Lambda = \pm 1 \text{ or } 0 \\ \Delta \Sigma = 0 \end{array} \right\} \Delta \Omega = \Delta \Lambda \quad . \quad . \quad (66)$$

Since change of Σ is not allowable, it follows that since Ω ranges from $\Lambda + \Sigma$ to $\Lambda - \Sigma$, the change in Ω must be identical with that in Λ .

As an example of $\Delta\Lambda = 0$, $\Delta S = 0$ we have $^2\Pi_1 \rightarrow ^2\Pi_1$, $^3\Delta_1 \rightarrow ^3\Delta_1$, &c. As an example of $\Delta\Lambda = 1$, $\Delta S = 0$ we have $^2\Pi_1 \rightarrow ^2\Sigma$, $^3\Delta_1 \rightarrow ^3\Pi_0$, &c. As an example of $\Delta S = 1$ we have $^3\Sigma \rightarrow ^1\Sigma$ of O_2 and $^3\Pi \rightarrow ^1\Sigma$ of CO , &c. Thus a $^3\Pi \rightarrow ^3\Pi$ transition is threefold with components $^3\Pi_3 \rightarrow ^3\Pi_3$, $^3\Pi_2 \rightarrow ^3\Pi_2$, and $^3\Pi_1 \rightarrow ^3\Pi_1$. Again, $^2\Delta \rightarrow ^2\Pi$ is twofold with components $^2\Delta_{3/2} \rightarrow ^2\Pi_{1/2}$ and $^2\Delta_{5/2} \rightarrow ^2\Pi_{3/2}$. In the case of Σ states no subscript is used, for since $\Lambda = 0$ there is no magnetic field along the inter-nuclear axis to orientate the spin, and hence no quantum number M_S or Σ exists. (The electronic spin vector \bar{S} is orientated, not by the axial field, but by the magnetic field created by \bar{L} which measures the orbital electronic momentum. Since \bar{L} precesses round the electric field along the molecular axis, this is the mean direction of the resulting magnetic field which controls the spin vector.) All Σ states $^1\Sigma$, $^2\Sigma$, or $^3\Sigma$ are single in fact.

We are now in a position to return to our two processes of molecule formation. Consider two atoms associated with the quantum numbers (L_1, S_1) , (L_2, S_2) , both subjected to an electric field and brought together. Each of them has a group of Λ -values

$$\Lambda_1 = 0, 1, 2, 3, \dots, L_1,$$

$$\Lambda_2 = 0, 1, 2, 3, \dots, L_2,$$

and the possible pairs of values combine together to give atomic multiplets whose values of Λ range from $L_1 - L_2$ to $L_1 + L_2$. Likewise each of these multiplets has a range of multiplicities derived from $S_1 - S_2 \dots$ to $S_1 + S_2$. For example, if a carbon atom in its ground state $(1s)^2(2s)^2(2p)^2 : ^3P$ combines with a nitrogen atom in its ground state $(1s)^2(2s)^2(2p)^3 : ^4S$, the possible values of Λ are 1 and 0, and of S are $\frac{1}{2}, \frac{3}{2}, \frac{5}{2}$, giving as possible molecular states $^2\Pi$, $^2\Sigma$, $^4\Pi$, $^4\Sigma$, $^6\Pi$, $^6\Sigma$. Usually only a few of these theoretically possible states are found in practice: in CN only $^2\Sigma$ and $^2\Pi$.

The alternative method of molecule formation is to consider the 'united atom' consisting of the fused atomic nuclei, which are subsequently separated. The values of Λ and Σ derived from L and S of the united atom when it is subject to an axial field are easily stated:

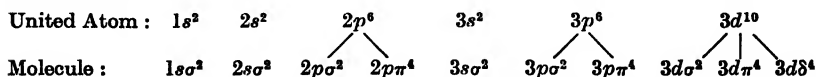
$\Lambda = 0, 1, 2, \dots, L$; Σ takes $2S + 1$ values from $+S$ to $-S$, the multiplicity remaining the same as in the united atom (see Fig. 41). Thus the 'united atom' Al with thirteen electrons $(1s)^2(2s)^2(2p)^6(3s)^2(2p): {}^2P$ gives, when subject to a field, the two molecular states ${}^2\Pi$ and ${}^2\Sigma$. Again, a 4P atomic state would give ${}^4\Pi$ and ${}^4\Sigma$ molecular states, the former of which has four components ${}^4\Pi_{3/2}$, ${}^4\Pi_{1/2}$, ${}^4\Pi_{-1/2}$, and ${}^4\Pi_{-3/2}$ obtained from $\Lambda = 1$ and $\Sigma = 1\frac{1}{2}, \frac{1}{2}, -\frac{1}{2}, -1\frac{1}{2}$.

(d) DETAILED ELECTRONIC CONFIGURATIONS

In order to understand more precisely the grouping and disposition of electrons in molecules we must ascribe quantum numbers to the individual electrons as we did in the atomic case (see Chapter VII (a) of *Atomic Spectra*). Let us imagine the case of a *very* strong field along the inter-nuclear axis so that even \bar{L} breaks down, and the \bar{l} of each electron precesses round the axis independently. The projection of \bar{l} on the axis will give to each individual electron a new quantum number λ . For $\lambda = 0, 1, 2, \dots$, we shall speak of $\sigma, \pi, \delta, \dots$, electrons. The resulting spin S is found to maintain its identity, however strong the axial field, while Λ is the sum of the individual values of λ . In addition to the quantum number λ , each electron has associated with it values of n and l which it strictly assumes only in the limiting case of the united atom. We can thus describe an electron in a molecule as $1s\sigma, 2s\sigma, 2p\pi, \dots$, &c. As an alternative we could associate with λ the values of n and l which the electron will assume in the other limiting case, of dissociation into atoms. These are not, in general, the same as the previous (n, l) values (see Section (f) later, on the 'promotion' of electrons). In this latter case we indicate an electron as $\sigma 1s, \sigma 2s, \pi 2p, \dots$, &c. Since in a molecule we are between the two limiting cases above mentioned, the assignment of precise values of n and l is not regarded as realistic by some writers who prefer to be non-committal and write $w\sigma, u\pi, x\sigma, \dots$, &c. As long as it is realized, however, that at a certain value of the inter-nuclear distance there must be a change from molecular to atomic conditions (see Chapter V (e)), we may conventionally use either of the above more precise notations.

It is important to know how many electrons are assignable to a particular state according to the Pauli principle. For a σ -state for which $\lambda = 0$ the maximum is two, corresponding to the two orientations of the spin. For a π -state the maximum is four, corresponding to each orientation of spin combined with $\lambda = \pm 1$. Similarly it is four for δ -electrons ($\lambda = \pm 2$), and for all other types. The 'closed' λ -group in molecules thus has four electrons (except for $\lambda = 0$, which has two electrons), and for such closed λ -groups $\Lambda = 0$ and $S = 0$; just as in the closed *atomic* group $L = 0, S = 0$.

The electrons of the 'united atom' are thus re-allocated in molecules as follows:



The molecular state resulting from closed λ -groups will be, of

atomic multiplet follow the Landé interval rule. (Referring to *Atomic Spectra*, Chapter IV (g), it will be seen that the interval between the two levels characterized by J and $J - 1$ is proportional to J . Thus the three intervals between the four levels of 4D characterized by $J = 3\frac{1}{2}, 2\frac{1}{2}, 1\frac{1}{2}, \frac{1}{2}$ are in the ratio 7:5:3.) But it will be observed from $\bar{F}(\Lambda) + A\Lambda\Sigma$ that the corresponding intervals within a molecular multiplet are constant and equal to $A\Lambda$. The selection rules for molecular electronic transitions are as follows. They are identical with those for S , M_L , and M_S , for an atom in a strong electric field.

$$\left. \begin{aligned} \Delta S &= 0 \text{ (commonly), } \Delta S = 1 \text{ (occasionally),} \\ \Delta \Lambda &= \pm 1 \text{ or } 0 \\ \Delta \Sigma &= 0 \end{aligned} \right\} \Delta \Omega = \Delta \Lambda \quad . \quad . \quad (66)$$

Since change of Σ is not allowable, it follows that since Ω ranges from $\Lambda + \Sigma$ to $\Lambda - \Sigma$, the change in Ω must be identical with that in Λ .

As an example of $\Delta\Lambda = 0$, $\Delta S = 0$ we have $^2\Pi_1 \rightarrow ^2\Pi_1$, $^3\Delta_1 \rightarrow ^3\Delta_1$, &c. As an example of $\Delta\Lambda = 1$, $\Delta S = 0$ we have $^2\Pi_1 \rightarrow ^2\Sigma$, $^3\Delta_1 \rightarrow ^3\Pi_0$, &c. As an example of $\Delta S = 1$ we have $^3\Sigma \rightarrow ^1\Sigma$ of O_2 and $^3\Pi \rightarrow ^1\Sigma$ of CO, &c. Thus a $^3\Pi \rightarrow ^3\Pi$ transition is threefold with components $^3\Pi_3 \rightarrow ^3\Pi_3$, $^3\Pi_2 \rightarrow ^3\Pi_2$, and $^3\Pi_1 \rightarrow ^3\Pi_1$. Again, $^2\Delta \rightarrow ^2\Pi$ is twofold with components $^2\Delta_{3/2} \rightarrow ^2\Pi_{3/2}$ and $^2\Delta_{5/2} \rightarrow ^2\Pi_{5/2}$. In the case of Σ states no subscript is used, for since $\Lambda = 0$ there is no magnetic field along the inter-nuclear axis to orientate the spin, and hence no quantum number M_S or Σ exists. (The electronic spin vector \bar{S} is orientated, not by the axial field, but by the magnetic field created by \bar{L} which measures the orbital electronic momentum. Since \bar{L} precesses round the electric field along the molecular axis, this is the mean direction of the resulting magnetic field which controls the spin vector.) All Σ states $^1\Sigma$, $^2\Sigma$, or $^3\Sigma$ are single in fact.

We are now in a position to return to our two processes of molecule formation. Consider two atoms associated with the quantum numbers (L_1, S_1) , (L_2, S_2) , both subjected to an electric field and brought together. Each of them has a group of Λ -values

$$\Lambda_1 = 0, 1, 2, 3, \dots, L_1,$$

$$\Lambda_2 = 0, 1, 2, 3, \dots, L_2,$$

and the possible pairs of values combine together to give atomic multiplets whose values of Λ range from $L_1 - L_2$ to $L_1 + L_2$. Likewise each of these multiplets has a range of multiplicities derived from $S_1 - S_2$. . . to . . . $S_1 + S_2$. For example, if a carbon atom in its ground state $(1s)^2(2s)^2(2p)^2 : ^3P$ combines with a nitrogen atom in its ground state $(1s)^2(2s)^2(2p)^3 : ^4S$, the possible values of Λ are 1 and 0, and of S are $\frac{1}{2}, \frac{3}{2}, \frac{5}{2}$, giving as possible molecular states $^2\Pi$, $^2\Sigma$, $^4\Pi$, $^4\Sigma$, $^6\Pi$, $^6\Sigma$. Usually only a few of these theoretically possible states are found in practice: in CN only $^2\Sigma$ and $^2\Pi$.

The alternative method of molecule formation is to consider the 'united atom' consisting of the fused atomic nuclei, which are subsequently separated. The values of Λ and Σ derived from L and S of the united atom when it is subject to an axial field are easily stated:

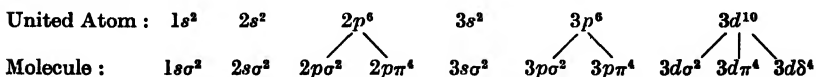
$\Lambda = 0, 1, 2, \dots, L$; Σ takes $2S + 1$ values from $+S$ to $-S$, the multiplicity remaining the same as in the united atom (see Fig. 41). Thus the 'united atom' Al with thirteen electrons $(1s)^2(2s)^2(2p)^6(3s)^2(2p):^2P$ gives, when subject to a field, the two molecular states $^2\Pi$ and $^2\Sigma$. Again, a 4P atomic state would give $^4\Pi$ and $^4\Sigma$ molecular states, the former of which has four components $^4\Pi_{3/2}$, $^4\Pi_{1/2}$, $^4\Pi_{-1/2}$, and $^4\Pi_{-3/2}$ obtained from $\Lambda = 1$ and $\Sigma = 1\frac{1}{2}, \frac{1}{2}, -\frac{1}{2}, -1\frac{1}{2}$.

(d) DETAILED ELECTRONIC CONFIGURATIONS

In order to understand more precisely the grouping and disposition of electrons in molecules we must ascribe quantum numbers to the individual electrons as we did in the atomic case (see Chapter VII (a) of *Atomic Spectra*). Let us imagine the case of a *very* strong field along the inter-nuclear axis so that even \bar{L} breaks down, and the \bar{l} of each electron precesses round the axis independently. The projection of \bar{l} on the axis will give to each individual electron a new quantum number λ . For $\lambda = 0, 1, 2, \dots$, we shall speak of $\sigma, \pi, \delta, \dots$, electrons. The resulting spin S is found to maintain its identity, however strong the axial field, while Λ is the sum of the individual values of λ . In addition to the quantum number λ , each electron has associated with it values of n and l which it strictly assumes only in the limiting case of the united atom. We can thus describe an electron in a molecule as $1s\sigma, 2s\sigma, 2p\pi, \dots$, &c. As an alternative we could associate with λ the values of n and l which the electron will assume in the other limiting case, of dissociation into atoms. These are not, in general, the same as the previous (n, l) values (see Section (f) later, on the 'promotion' of electrons). In this latter case we indicate an electron as $\sigma 1s, \sigma 2s, \pi 2p, \dots$, &c. Since in a molecule we are between the two limiting cases above mentioned, the assignment of precise values of n and l is not regarded as realistic by some writers who prefer to be non-committal and write $w\sigma, u\pi, x\sigma, \dots$, &c. As long as it is realized, however, that at a certain value of the inter-nuclear distance there must be a change from molecular to atomic conditions (see Chapter V (e)), we may conventionally use either of the above more precise notations.

It is important to know how many electrons are assignable to a particular state according to the Pauli principle. For a σ -state for which $\lambda = 0$ the maximum is two, corresponding to the two orientations of the spin. For a π -state the maximum is four, corresponding to each orientation of spin combined with $\lambda = \pm 1$. Similarly it is four for δ -electrons ($\lambda = \pm 2$), and for all other types. The 'closed' λ -group in molecules thus has four electrons (except for $\lambda = 0$, which has two electrons), and for such closed λ -groups $\Lambda = 0$ and $S = 0$; just as in the closed *atomic* group $L = 0, S = 0$.

The electrons of the 'united atom' are thus re-allocated in molecules as follows:



The molecular state resulting from closed λ -groups will be, of

or — state is whether $L + \Sigma l$ (or $L_1 + \Sigma l_1 + L_2 + \Sigma l_2$) is even or odd. (Here Σl is summed over the electrons, and the above alternatives are according as we derive the molecule from the united atom or the component atoms.) Examples of this are found in (69).

There is, moreover, a selection rule which limits electron transitions in Σ states to others of the same sign :

$$\Sigma^+ \rightarrow \Sigma^+ \text{ and } \Sigma^- \rightarrow \Sigma^- \quad . \quad . \quad . \quad . \quad . \quad (67)$$

In the process of molecule building (Section (f)), Σ^+ states of the component atoms must be conserved as Σ^+ states in the united atom : the same applies to Σ^- states. In non-radiating transitions (such as may arise through intersection of the $U(r)$ curves of Fig. 21) this same conservation must be maintained : + states remain + and — states remain —.

The recognition of + and — states hence determines which $\Sigma \rightarrow \Sigma$ band systems are possible according to (67).

In states other than of the Σ type ($\Lambda = 0$) we have seen in Section (c) that $F(\Lambda) = F(-\Lambda)$ so that all these coincident levels have a double statistical weight. We then assumed we were dealing with a 'frozen' molecule (non-vibrating and non-rotating). The interaction of vibration and rotation with electronic motion removes this coincidence, however, and a separation may result, giving a pair of sub-levels, one of which is + and the other —. These features will be discussed later (see Chapter VII (g) and Fig. 50), and the phenomenon is called Λ -type doubling.

In addition to the distinction between positive and negative states and levels, there is a further distinction to be made in the special case of *elementary* molecules (of the type X_2). Here it is clearly possible for the first atom to be in state A and the second atom in state B , or for the first atom to be in state B and the second in state A , and these states will be indistinguishable one from the other. There will thus arise twice as many states as in the ordinary molecule of type XY . Each energy level occurs twice : once as an 'even' and once as an 'odd' state. In wave-mechanics parlance even states permit reflexion of the wave-function at the centre-point of the inter-nuclear axis unchanged : odd states give rise to change of sign of the wave-function if this is done. In practice the criterion used is that even states of a molecule are those for which Σl of the component electrons is even ; odd states those for which Σl is odd. Even states are distinguished by the subscript g (German 'gerade') ; odd states by the subscript u ('ungerade'). An additional selection rule for *elementary molecules* then arises :

$$u \text{ (odd)} \nrightarrow g \text{ (even)} \quad . \quad . \quad . \quad . \quad . \quad (68)$$

It is the same selection rule as we found for atoms (see equation (28)).

As an example of these rules we may take the three known electronic states of the CO^+ molecule (Fig. 67). The probable structures of the molecule expressed as a derivation of the thirteen-electron united atom are :

$$\left. \begin{aligned} (B) : 1s\sigma^2 \cdot 2p\sigma^2 \cdot 2s\sigma^2 \cdot 3p\sigma \cdot 2p\pi^4 \cdot 3d\sigma^2 : {}^2\Sigma_u^+ & \quad (\Sigma l = 11), \\ (A) : 1s\sigma^2 \cdot 2p\sigma^2 \cdot 2s\sigma^2 \cdot 3p\sigma^2 \cdot 2p\pi^3 \cdot 3d\sigma^2 : {}^2\Pi_u & \quad (\Sigma l = 11), \\ (X) : 1s\sigma^2 \cdot 2p\sigma^2 \cdot 2s\sigma^2 \cdot 3p\sigma^2 \cdot 2p\pi^4 \cdot 3d\sigma : {}^2\Sigma_g^+ & \quad (\Sigma l = 10). \end{aligned} \right\} \quad (69)$$

The evidence on which such structure is based will be given in Section (e). The description as g or u follows from the summation Σl as even or odd. The fact that both Σ states are labelled + is based on a knowledge of the atomic dissociation products of the above states. They are:

(B) : $(1s)^2(2s)^2(2p)^2 : ^3P$ of C and $(1s)^2(2s)^2(2p)^3 : ^2D$ of O^+ ,

(A) and (X) : $(1s)^2(2s)^2(2p)^2 : ^3P$ of C and $(1s)^2(2s)^2(2p)^3 : ^4S$ of O^+ .

Thus for (B) $L_1 + \Sigma l_1 + L_2 + \Sigma l_2 = 1 + 2 + 2 + 3 = 8$, while for (A) and (X) $L_1 + \Sigma l_1 + L_2 + \Sigma l_2 = 1 + 2 + 0 + 3 = 6$.

Alternatively from the united atom Al :

$(1s)^2(2s)^2(2p)^6(3s)^2(3p) : ^2P$ [$L + \Sigma l = 8$] gives rise to states (A) and (X) ;
 $(1s)^2(2s)^2(2p)^6(3s)(3p)^2 : ^2S$ [$L + \Sigma l = 8$] gives rise to state (B).

Both methods indicate that the two Σ states are + in character so that by (67) a transition between them is permitted. Most Σ states are found in practice to be Σ^+ .

It may be remarked that while the three possible band systems $B \rightarrow X$, $A \rightarrow X$, $B \rightarrow A$ all occur in CO^+ (see Fig. 39), only the first two are known for the molecule N_2^+ . This we should anticipate from the restriction (68).

(e) HEITLER AND LONDON'S METHOD

It has been already mentioned that the nature of the electronic states arising in a molecule with a given number of electrons can be predicted (either from the 'united atom' or the component atoms), but that we lack a criterion for the stability of these states. Heitler and London * have developed a mathematical method by which the energy of a system of two atoms separated by a large distance can be expressed. They found it possible to infer the nature of the variation of $U(r)$ as the atoms approached making r smaller, and so to determine whether a state will be repulsive, or stable (with a minimum). Thus they determined that while the $^3\Sigma$ state was unstable, the $^1\Sigma$ state was stable for H_2 , Li_2 , Na_2 , LiH , &c. On the other hand, they found that no stable molecules Hc_2 , Bc_2 , HeH , &c., would be formed from their unexcited component atoms. This conforms with experimental evidence.

The general conclusions to which these investigators came was, that for two atoms whose resultant spins S_1 and S_2 differed from zero, molecule formation was always possible, and the lowest electronic state corresponded to a maximum of spin compensation (i.e. $S_1 \sim S_2$) in the molecule. Where either S_1 or S_2 was zero (or if both were zero), no molecule would be formed. Valency bonds were interpreted as uncompensated spins. Thus the valency of the above atoms would be $2S_1$ and $2S_2$ and the number of free valency bonds in the molecule formed would be $2(S_1 \sim S_2)$. This conception of valency is, however, clearly not adequate, nor is it always true that 1S atoms cannot take part in molecule formation. Thus BeH , ZnH , CdH , and HgH molecules are known, but all the atoms from which they are derived have

* *Zeit. f. Phys.*, vol. 44, p. 455 (1927).

1S states as the normal ones. It is, however, true that these metals all have 3S states very near to the normal, and these may account for the molecular formation. The examples given below show that when one or both atoms are in S states ($L = 0$), Heitler and London's conditions for molecule formation are generally satisfied. When neither molecule is in an S state there are many exceptions to their rule.

	Li (2S)	Be (1S)	B (2P)	C (3P)	N (4S)	O (3P)	F (2P)
H (2S) O (3P)	LiH ($^1\Sigma$) None	-BeH ($^2\Sigma$) BeO ($^1\Sigma$)	BH ($^1\Sigma$) -BO ($^2\Sigma$)	-CH ($^2\Pi$) CO ($^1\Sigma$)	=NH ($^3\Sigma$) -NO ($^2\Pi$)	-OH ($^2\Pi$) O $_2$ ($^3\Sigma$)	HF ($^1\Sigma$) None

(f) THE METHOD OF HUND, HERZBERG, AND MULLIKEN

One of our primary needs is a knowledge not only of the stability of the various molecular electronic states which may arise from a molecule with a known number of electrons, but also some idea of how their energy value depends on Λ and S . As is the case for atomic terms (*Atomic Spectra*, Chapter IV (c)), and for the same reasons, where terms of differing multiplicity derive from the same configuration and Λ -value, those with the larger multiplicity are the deeper. Thus, for example, $\sigma\pi : ^3\Pi$ is below $\sigma\pi : ^1\Pi$. Of terms with the same multiplicity and differing Λ we see from the energy expression $F(\Lambda) + \Lambda\Lambda\Sigma$ of Section (c) and Fig. 41 that those with the smaller values of Λ are deeper.

Apart from this, however, we need the more detailed information of the order of the strength of binding of individual electron orbits. In the process of *atom-building*, in which we visualize electrons being added one by one to a nucleus, we know that the order of binding is: $1s, 2s, 2p, 3s, 3p, 4s, 3d, 4p, 5s, 4d, 5p$, &c. We need some similar guide in molecule building. The problem is in several ways much more complex in the case of molecules. There is the greater variety of orbit-type (i.e. the λ -subdivision), and moreover the order of binding of these electron types differs with the atomic numbers of the atoms and the degree of disparity between them. We can, however, classify molecules, in a variety of ways, such that within each group there is a definite and characteristic order of binding. The hydrides form one such natural group. Again, the molecules $BO, CO^+, CO, N_2, N_2^+, NO, O_2, O_2^+, BeO, BeF$, &c., having twelve to sixteen electrons, and nuclei not very unequal, may all be expected to show a similar order of electronic binding.

The work which Hund, Herzberg, Mulliken,* and others have done in this field is an attempt to correlate electron orbits in the separate atoms with those in the actual molecules and also with those which occur in the limiting case of the united atom. In other words, it is an attempt to trace the type of energy change in different orbits as the inter-nuclear distance varies from ∞ to zero. The nature of this method can best be understood by illustration.

* The work most easily available to English readers is Mulliken's summary: *Reviews of Modern Physics*, vol. 2, pp. 60-115; vol. 3, pp. 90-155; vol. 4, pp. 1-86.

correlated with stable molecular configurations—and must necessarily be repulsive unstable states. In Fig. 42 are constructed $U(r)$ curves of the NH molecule. Those with the full line are derived from observed data; those with broken lines are placed in arbitrary positions, not having been observed as yet. On the left of the diagram are indicated the states of the united atom oxygen to which the $U(r)$ curves would link for $r = 0$. On the right are given the states of the nitrogen atom into which the $U(r)$ curves would dissociate as $r \rightarrow \infty$.

The method illustrated above for hydrides is possible only because of the close similarity expected to exist between orbits of such molecules and the 'united atom in a field'. In molecules which have comparable nuclei, then in the change from separate atoms to molecular conditions it is obvious that approximately half the electrons must be 'promoted', i.e. have their (n, l) values raised, in order to satisfy the Pauli principle which requires each electron to have a unique set of quantum numbers. On the right-hand side of Fig. 43 are given the various kinds of electron-orbit found in two widely separated atoms (in the presence of a superposed electric field). On the left-hand side are the types which would occur in the other limiting conditions ($r = 0$), of the united atom. Now, while in actual practice molecular conditions will be intermediate between these limiting cases, it is possible by examining experimental data to see how these extremes may be correlated. In constructing Fig. 43 it is firstly assumed that λ is conserved, i.e. σ electrons remain σ , π remain π , &c. Secondly, travelling from right to left ($r = \infty$ to $r = 0$), a step down means a lower energy and tighter binding, while a step up means higher energy and looser binding. These are described respectively as bonding electrons and anti-bonding electrons. The precise correlations of Fig. 43 are based upon this type of argument:

UNITED ATOM ($r \rightarrow 0$)		SEPARATE ATOMS ($r \rightarrow \infty$) 1 & 2	Nº OF ELECTRONS IN EACH ATOM	MOLECULAR NOTATION
4p σ		$\sigma_2 3p$	2	o σ
4s σ		$\pi_1 3p$	4	q π
3d δ		$\sigma_1 3s$	2	r σ
3d π		$\sigma_2 3s$	2	t σ
3d σ		$\sigma_1 2p$	2	u σ
3p π		$\pi_2 2p$	4	v π
3p σ		$\sigma_2 2p$	2	x σ
3s σ		$\pi_1 2p$	4	w π
2p π		$\sigma_1 2s$	2	y σ
2p σ		$\sigma_2 2s$	2	z σ
2s σ		$\sigma_1 1s$	2	K
1s σ		$\sigma_2 1s$	2	K

Fig. 43. The correlation of atomic electrons with those of the united atom (two comparable nuclei).

First four electrons : Excitation is necessary to produce the molecule which is unstable compared with its atomic products.

Fifth and sixth electrons : The Li_2 molecule is stable, hence $\sigma_2 2s$ is bonding.

Seventh and eighth electrons : Be_2 is unstable—no spectrum known, hence $\sigma_1 2s$ is anti-bonding.

Ninth to twelfth electrons : $(\pi_1 2p)^4$ must be bonding, for BeO is stable with a known band system.

Thirteenth and fourteenth electrons : BeO ($\omega_e = 1487$), BO ($\omega_e = 1885$), CO ($\omega_e = 2167$) show that $(\sigma_2 2p)^2$ are bonding electrons. The tightly bound fourteen-electron CO molecule has such great stability because its electrons fill up all the lowest states.

Fifteenth and sixteenth electrons : NO ($\omega_e = 1906$), O_2 ($\omega_e = 1556$) compared with CO show the $\pi_2 2p$ electrons are anti-bonding.

Nineteenth and twentieth electrons : There are no neon compounds, hence $(\sigma_1 2p)^2$ are anti-bonding. And so we might continue. The electrons which we have distinguished by the subscripts 1 and 2 should in the case of elementary molecules (type X_2) be properly labelled u and g (odd and even). Thus labels u and g distinguish the electrons of the two similar atoms. Travelling from the right side to the left side of Fig. 43 we note that the g -electrons of the atoms are linked with s or d electrons of the united atom (for which l is even), while u electrons are linked with p electrons (l odd).

In addition to the selection rules (66), (67), and (68), already given, we must add for the individual transition electron :

$$\Delta\lambda = \pm 1 \text{ or } 0 \quad . \quad . \quad . \quad . \quad . \quad (70)$$

To illustrate this section we conclude with a table of the probable structures of the N_2 molecule in its chief states, and a brief account of how we arrive at them. Reference back to Fig. 22 shows some of the $U(r)$ curves for N_2 .

Molecular state	Configurations of N_2 molecule	ω_e	Atomic products
$D \ ^3\Sigma_u^-$	$KK (z\sigma)^2(y\sigma)(w\pi)^4(x\sigma)(v\pi)^2$?	$^2P + ^2P$
$C \ ^3\Pi_u$	$KK (z\sigma)^2(y\sigma)(w\pi)^4(x\sigma)^2(v\pi)$	2045	$^2D + ^2P$
$B \ ^3\Pi_g$	$KK (z\sigma)^2(y\sigma)^2(w\pi)^4(x\sigma)(v\pi)$	1733	$^2D + ^2D$
$a \ ^1\Sigma_u^+$	$KK (z\sigma)^2(y\sigma)^2(w\pi)^2(x\sigma)^2(v\pi)$	1692	} $^4S + ^2D$
$A \ ^3\Sigma_u^+$	$KK (z\sigma)^2(y\sigma)^2(w\pi)^2(x\sigma)^2(v\pi)$	1460	
$X \ ^1\Sigma_g^+$	$KK (z\sigma)^2(y\sigma)^2(w\pi)^4(x\sigma)^2$	2360	

In explanation of the configurations given, numerous facts have to be weighed. The ground state is generally known to be $^1\Sigma$, and the very stable closed-shell configuration is the only reasonable one. Being closed, it is both g and $+$.

Next, we know from analysis that the First Positive system, $B \rightarrow A$, is $^3\Pi \rightarrow ^3\Sigma$, either $^3\Pi_u \rightarrow ^3\Sigma_u^+$ or $^3\Pi_u \rightarrow ^3\Sigma_g^-$ are possible. Now, $^3\Sigma$ is almost certainly $(w\pi)^3(x\sigma)^2(v\pi)$ which from Fig. 43 ($3\pi_u + \pi_g$) is odd. It is $+$, since $l_1 + l_2 + L_1 + L_2 = 3 + 1 + 0 + 2$. Hence state B is $^3\Pi_g$, which is consistent with $(w\pi)^4(x\sigma)(v\pi)$. The state labelled a , which is the initial state of the Lyman system $a \rightarrow X$, has

sometimes been described as ${}^1\Pi$, but if so it must be ${}^1\Pi_u$ to permit transition to $X\ {}^1\Sigma_g$. If so, it cannot derive from $(w\pi)^4(x\sigma)(v\pi)$, which would necessarily give ${}^1\Pi_g$ (see Fig. 43). It is therefore interpreted as ${}^1\Sigma_u^+$ with the configuration shown. The upper state $C\ {}^3\Pi$ must be labelled u , since $C\ {}^3\Pi \rightarrow B\ {}^3\Pi$ is the Second Positive system of nitrogen. The configuration given accounts for this. $D \rightarrow B$ is the Fourth Positive system, and a state ${}^3\Sigma_u$ is accounted for as shown. All the best-known band systems are thus accounted for by the movement of a single electron.

The student may verify (1) that the configurations of the above table give the molecular states of column 1 (see p. 92); (2) that the chief systems satisfy the selection rules given; (3) that the electronic displacements are of bonding or anti-bonding electrons (as ω_e shows, Fig 43 records); and (4) that from the atomic products given in the last column can be synthesized, as in Section (c), groups of molecular states, among which those of the first column are found.

(g) VALENCY

In Fig. 43 we described molecular electrons as bonding, anti-bonding, or non-bonding. Herzberg has suggested that the number of valence bonds in a molecule is equal to the difference between the number of pairs of bonding electrons and the number of pairs of anti-bonding electrons. (This excludes from consideration ionic molecules in which the valency is polar in character.) This rule gives a remarkable measure of agreement with chemical evidence as to the number of valence bonds in molecules, although in the case of odd-electron molecules it gives a half-integral number of bonds. Mulliken has drawn attention to the fact that the energies of molecular dissociation D (from the ground state) are for the most part proportional to the number of valence bonds (N), derived from Herzberg's definition. In the table of data (prepared by Mulliken) the values of D are so uncertain in many cases as to make more than

VALUES OF D AND N

Mol.	D (volts)	N	D/N	Mol.	D (volts)	N	D/N
H_2^+	2.64	$\frac{1}{2}$	5.28	CO^+	7.1	$2\frac{1}{2}$	2.8
H_2	4.44	1	4.44	CO	10.0	3	3.3
He_2^+	2.6	$\frac{1}{2}$	5.2	N_2	9.1	3	3.0
Li_2	1.14	1	1.14	NO^+	10.3	3	3.4
C_2	5.5	2	2.7	NO	6.1	$2\frac{1}{2}$	2.5
BO	6.6	$2\frac{1}{2}$	2.6	O_2^+	6.2	$2\frac{1}{2}$	2.5
CN	7.1	$2\frac{3}{2}$	2.8	O_2	5.09	2	2.54
N_2^+	6.8	$2\frac{1}{2}$	2.7	F_2	2.9	1	2.9

approximate agreement unexpected. The student may verify from Fig. 43 that the numbers of valence bonds ascribed to various molecules are as given in the table. In determining N (the number of bonds linking the atoms) the two pairs of K -electrons are regarded as non-bonding (except in the case of H_2^+ , H_2 , He_2^+ , and He_2 , where $\sigma_g 1s$ is bonding and $\sigma_u 1s$ is anti-bonding). The subject of valency is

an extensive study, being fundamental to the whole of chemistry. It may profitably be studied in such a monograph as *The Quantum Theory of Valency* by W. G. Penney (Methuen), or in Chapter XXV of *Organic Chemistry* edited by Gilman (John Wiley and Sons), or in *The Nature of the Chemical Bond* by Pauling (Cornell Univ. Press).

ROTATIONAL TERMS AND VECTOR COUPLINGS

IN equation (1) of this book the total molecular energy was to a first approximation regarded as made up of three independent parts $E = E_e + E_v + E_K$. In reality electronic, vibrational, and rotational motions are coupled together, and smaller terms such as E_{ev} , E_{eK} , and E_{vK} might properly have been included. The last of these was investigated in Chapter IV (e). The first can be neglected, since the general form of E , (see equation (15)) is independent of the electronic state. E_{eK} represents the interaction of electronic motion and rotation and is the most complex of these effects. The electronic orbital and spin angular momenta may in some cases be so strongly linked with the nuclear angular momentum that such electronic quantum numbers as Λ and Σ lose their validity. We are concerned here with the various types and strengths of coupling of these vectors and with the forms which the typical rotational term will take under these conditions. The simple form $BK(K+1)$ holds strictly only for $^1\Sigma$ states, and the refinements introduced in (52), as we have mentioned, are those arising from vibration-rotation coupling.

Hund has distinguished four cases commonly described by the letters (a), (b), (c), and (d). The first two of these cases are commonly found, the last two are much less usual. We now consider them in detail.

(a) HUND'S CASE (a)

It should be stated first, that all these cases are extreme or limiting cases and that in practice many intermediate stages are found. In Case (a) Λ is associated with a sufficiently strong magnetic field to 'couple' S (the spin vector) strongly with it. S then precesses round the inter-nuclear axis at certain angles θ such that

$$\Sigma = \sqrt{S(S+1)} \cos \theta,$$

where Σ is a quantum number which has $2S+1$ values ranging from $-S$ to $+S$. The total electronic angular momentum along the nuclear axis is given by the quantum number Ω , which is the algebraic sum $\Lambda + \Sigma$, and which therefore has a series of $2S+1$ values ranging from $\Lambda + S$ to $\Lambda - S$. The vector angular momentum $\Omega \frac{h}{2\pi}$ which

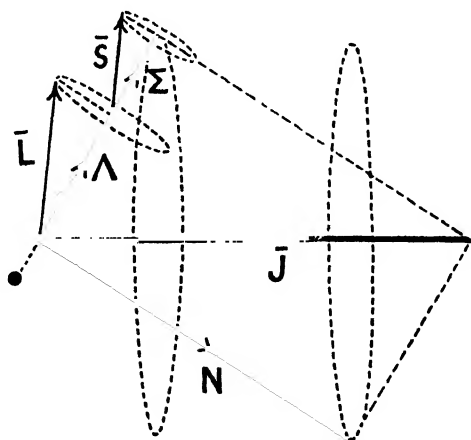


Fig. 44. Hund's Case (a).

is electronic in origin unites with the nuclear angular momentum $N \frac{h}{2\pi}$ to give a resultant $\bar{J} \frac{h}{2\pi}$ ($\bar{J} = \sqrt{J(J+1)}$). J is a quantum number which takes a series of values $\Omega, \Omega + 1, \Omega + 2, \dots$, with increasing rotational speed. N is not a quantum number, but is related to J and Ω , which are quantum numbers by

$$N = \sqrt{J(J+1) - \Omega^2} \quad (71)$$

Both N and Ω will, as expected, precess round their resultant \bar{J} . We note that J will be integral or half-integral, according as S is integral or half-integral.

As an example take $\Lambda = 1, S = 1$. We have three sub-states ${}^3\Pi_0, {}^3\Pi_1$, and ${}^3\Pi_2$ distinguished by $\Omega = 0, 1$, and 2 . Associated with each of these electronic sub-states is a pile of rotational levels, each of which has a characteristic J -value. Since the minimum value of J is Ω , there will appear to be one missing rotational level $J = 0$ in the pile associated with ${}^3\Pi_1$ and two missing levels $J = 0$ and 1 in the pile associated with ${}^3\Pi_2$.

In Case (a) precession of $\bar{L} (= \sqrt{L(L+1)})$ and $\bar{S} (= \sqrt{S(S+1)})$ takes place symmetrically round the inter-nuclear axis as in Fig. 44. It is not, however, uncommon in practice for the axis of precession to be somewhat displaced from the latter axis. If this is the case we may have an appreciable component L_{perp} , where $L_{\text{perp}}^2 = \bar{L}^2 - \Lambda^2$ perpendicular to the inter-nuclear axis. (We shall see later that in the limiting Case (d) the vector \bar{L} is completely uncoupled from the inter-nuclear axis and coupled with the axis of rotation.) Where L_{perp} exists it will combine vectorially with N to give a resultant $N \pm L_{\text{perp}}$, and it will then be $(N \pm L_{\text{perp}})^2$ which equals $J(J+1) - \Omega^2$ (see (71)). Hence

$$N^2 = J(J+1) - \Omega^2 - L_{\text{perp}}^2 \mp 2NL_{\text{perp}}.$$

The last term normally represents a small quantity but grows in importance as the uncoupling of the precession to the nuclear axis proceeds. If we write it for simplicity $\phi(J)/B_i$, then a typical rotational term would be

$$F = B_i N^2 = B_i [J(J+1) - \Omega^2 - L_{\text{perp}}^2] + \phi_i(J) \quad (72)$$

Of course for any one sub-state the term $-B_i(\Omega^2 + L_{\text{perp}}^2)$ is merely an additive constant. The term $\phi(J)$ has the form $\delta(J+1)J$ if the uncoupling is small: its effect therefore is a small correction to B_i , which becomes $B_i + \delta$. If the uncoupling is large $\phi(J)$ takes the form $\zeta + \epsilon J + \delta J(J+1)$, so that its effect on the rotational term may be written $\zeta + B_i^*[J^*(J^*+1)]$, where B_i^* differs slightly from B_i and J^* differs slightly from an integer.

We shall see in Section (g) that due to so-called Λ -type doubling where $\Lambda > 0$, $\phi(J)$ is double valued.

In the same way as we have considered \bar{L} uncoupling from the inter-nuclear axis, we may consider \bar{S} doing so. (We shall see later that in the limit this gives Case (b) of Hund.) In equation (72) we

should then have S_{perp} in place of L_{perp} , where $S^2_{\text{perp}} = S(S+1) - \Sigma^2$. The part $-B_v[S(S+1) + \Omega^2 - \Sigma^2]$ in equation (72) is again, of course, an additive constant for a particular sub-state. It varies from one sub-state to another, and since B_v is a function of v (see equation 27), it varies with the vibrational quantum number also.

(b) HUND'S CASE (b)

Here the magnetic field associated with Λ is so weak that the spin vector S is no longer coupled to it. The rotating nuclei create a magnetic field of their own, and the resultant of these two magnetic fields is along the line of $\bar{K} (= \sqrt{K(K+1)})$ which is the resultant of Λ and N . K is a quantum number which takes the values $\Lambda, \Lambda+1,$

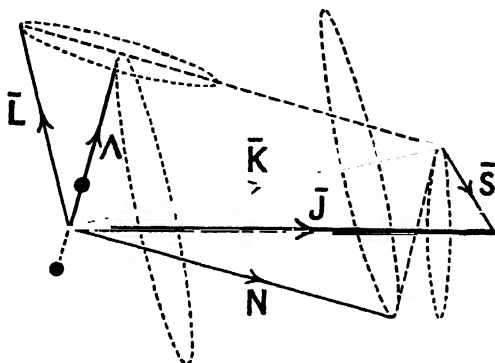


Fig. 45. Hund's Case (b).

$\Lambda+2, \dots$, so that it has a minimum value 0 for Σ states, 1 for Π states, 2 for Δ states, &c. Λ and N will precess round \bar{K} , as we should anticipate. N , which is not a quantum number, will be given by $\sqrt{K(K+1)} - \Lambda^2$. The spin vector \bar{S} will precess at various inclinations round \bar{K} which is the direction of the resultant magnetic field. \bar{S} and \bar{K} will combine vectorially to form a total angular momentum \bar{J} , so that effectively \bar{K} and \bar{S} precess round \bar{J} . The total (rotational) quantum number J will take $2S+1$ values * ranging between $K+S$ and $K-S$. The degree of multiplicity thus arising is of course the same as in Case (a), but it is sometimes described specifically as Case (b) spin multiplicity. In double states $J = K + \frac{1}{2}$ and $K - \frac{1}{2}$ (these are labelled by Mulliken F_1 and F_2 sub-states). In triplet states $J = K+1, K$, and $K-1$ (Mulliken labels these arbitrarily F_1, F_2 , and F_3 sub-states). Again it is clear that certain low rotational levels will be 'missing'. Thus in $^3\Pi$ states since $\Lambda=1, K_{\min}=1$ and the values of J_{\min} are $F_1(2), F_2(1)$, and $F_3(0)$.

The rotational energy term, which if there were no spin vector would have a form similar to (72), viz.

$$F = B_v N^2 = B_v [K(K+1) - \Lambda^2 - L^2_{\text{perp}}] + \phi(K) \quad (73)$$

has further energy terms due to the spin vector \bar{S} .

* Unless $K < S$ when there may be only $2K+1$.

(1) There is energy due to the linkage of \bar{S} with the magnetic field of \bar{L} (due to orbital motion).

(2) There is energy due to linkage of \bar{S} with the magnetic field along \bar{K} . This arises from the molecular rotation of the whole electron system and nuclei round \bar{K} .

(3) If there is more than one electron outside a closed shell there is the energy of interaction of these individual spins with each other. These three terms are given by Mulliken* as:

$$f(K, S) = \frac{1}{2} \{ A \Lambda^2 / K(K+1) \} + \gamma [J(J+1) - K(K+1) - S(S+1)] + w(K, S) \quad (74)$$

Note the first term vanishes if $\Lambda = 0$ —that is, for Σ states of any multiplicity. Note also that the third term $w(K, S)$ vanishes if there are no electrons, or only one electron outside a closed group—that is, for singlet and doublet states. We thus have in special cases:

Singlet States: $S = 0, J = K$, hence $f(K, S) = 0$.

Doublet States: ${}^2\Sigma, \Lambda = 0, S = \frac{1}{2}, J = K + \frac{1}{2}$, and $K - \frac{1}{2}$. The interval between the doublet components is therefore $\gamma(K + \frac{1}{2})$.

${}^2\Pi, \Lambda = 1$ and the separation of the components would be

$$\left[\frac{A}{K(K+1)} + \gamma \right] (K + \frac{1}{2}).$$

Triplet States: The third term $w(K, S)$ is now appreciable. Kramers† gives for it: $w_1(K, +1) = -\epsilon \left[1 - \frac{3}{2K+3} \right]; w_2(K, 0) = +2\epsilon; w_3(K, -1) = -\epsilon \left[1 + \frac{3}{2K-1} \right]$. For ${}^3\Sigma$ states we have $S = 1, \Lambda = 0, J = K + 1, K$, and $K - 1$. Upon substitution in (74) we find $f(K, S)$ for the three components has values

$$F_1(K+1) = K \left(\gamma - \frac{2\epsilon}{2K+3} \right), \quad F_2(K) = -\gamma + 2\epsilon, \\ F_3(K-1) = -(K+1) \left(\gamma + \frac{2\epsilon}{2K-1} \right).$$

These are triplet levels of increasing separation as K increases: the overall width for large values of K is $(2K+1)\gamma$ while the mid-point of the two outer components is approximately at a constant distance of $2\epsilon - \frac{\gamma}{2}$ from the middle component.

Hund's Case (b) must clearly obtain in all Σ states ($\Lambda = 0$), for these have no axial magnetic field to control \bar{S} . It may obtain for states where $\Lambda = 1, 2, 3$, etc., if the axial magnetic field is weak.

(c) HUND'S CASE (b')

This is the special case of all singlet states (for which $S = 0$). When $S = 0$ Cases (a) and (b) of Hund both degenerate to this one, which is represented in Fig. 46. Here $J = K, \Omega = \Lambda$, and

$$N = \sqrt{J(J+1) - \Lambda^2}.$$

* *Rev. Mod. Phys.*, vol. 2, p. 107 (1930).

† *Zeit. f. Phys.*, vol. 53, p. 422 (1929).

In the special case of $^1\Sigma$ states $N = \sqrt{J(J+1)}$ which was the simple assumption made in the early sections of this chapter (e.g.

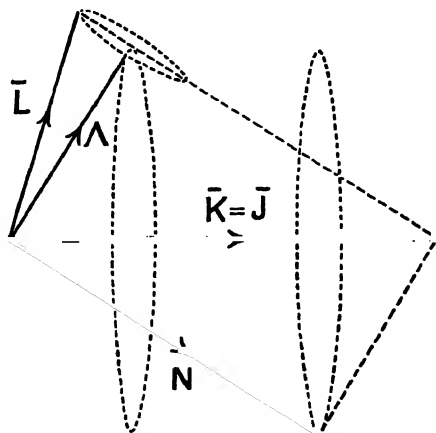


Fig. 46. Hund's Case (b) (all singlet states).

equation (23)). In $^1\Sigma$ states $\phi(K)$ of (72) vanishes. In $^1\Pi$ states it does not do so, but has a value $\delta J(J+1)$. Owing to Λ -type doubling (see Section (g)) δ is double-valued.

(d) STAGES INTERMEDIATE BETWEEN (a) AND (b)

We have just seen that Case (b') applies to all singlet states. We have also seen that Σ states are necessarily Case (b), while Π , Δ , Φ , states of higher multiplicity than singlet, may be Case (a) or Case (b), or in some stage intermediate between these two. If the coupling of S (the resultant spin) to Λ is strong, we approximate to Case (a). If it is not very strong, it is not uncommon to find an approximation to Case (a) for low values of J and a gradual transition to Case (b) at high values of J .

The form which the rotational function takes in such an intermediate stage has been studied by Hill and Van Vleck.* For the term $B_1 N^2$ they derive :

$$F(J) = B_1 \left[(J + \frac{1}{2})^2 - \Lambda^2 \pm \sqrt{(J + \frac{1}{2})^2 - \frac{\Lambda^2 A}{B_1} \left(1 - \frac{A}{4B_1}\right)} \right] + \phi(J) \quad (76)$$

in the case of doublet states (i.e. $S = \frac{1}{2}$). Neglecting Λ -type doubling, the two signs correspond to the two components of the electronic doublet. The smallest J -value $\Lambda - \frac{1}{2}$ is necessarily single. We see this either from (76) since it is obvious $F(J)$ cannot be negative, or by consideration of the limiting Cases (a) and (b). Thus in Case (a), since $J \geq \Omega$, $J = \frac{1}{2}$ occurs in the $^2\Pi_1$ series of rotational levels, but not in $^2\Pi_{1/2}$. Or in Case (b), since $J = K \pm \frac{1}{2}$ and $J \geq \Lambda = 1$, we

* *Phys. Rev.*, vol. 32, p. 250 (1928).

have as J -values $\frac{1}{2}$ and $1\frac{1}{2}$ for $K = 1$, $1\frac{1}{2}$, and $2\frac{1}{2}$ from $K = 2$, &c. Thus $J = \frac{1}{2}$ occurs only once.

The formula (76) does not include the energy corresponding to the small term γ in (74). The coefficient A is the same in both these formulae. It is the same A as was used in Chapter VI (c) to measure the separation of the component levels of the multiplet. If A is large we see from the derivation of the terms of (74) that this means a strong linkage of \bar{S} with \bar{L} , and thus approximates to Case (a). If A

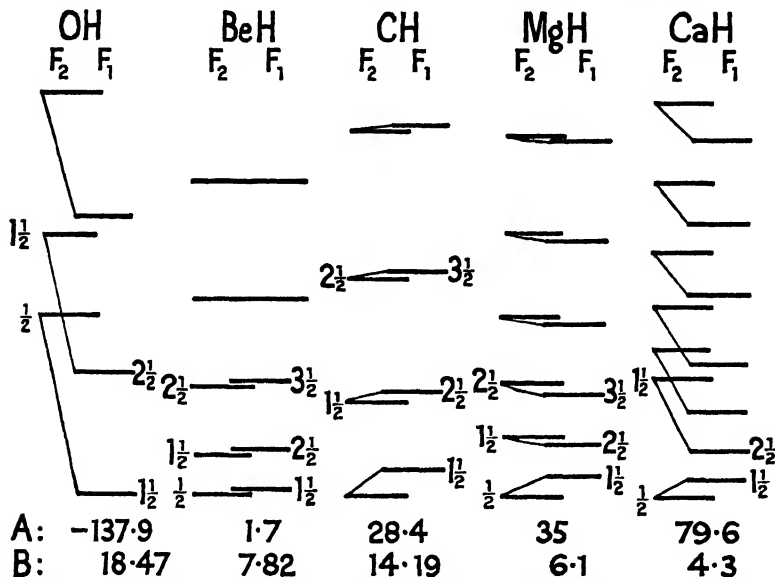


Fig. 47. Rotational energy levels for some typical $^2\Pi$ states, $v = 0$. (After Mulliken.)

is positive, the doublet is normal; if negative, it is inverted. If we expand (76) for large positive values of A/B_v we get:

$$F(J) = \pm \frac{A\Lambda}{2} + B_v \left\{ (J + \frac{1}{2})^2 - (\Lambda \pm \frac{1}{2})^2 \right\} \pm \frac{B_v^2}{A\Lambda} \{ (J + \frac{1}{2})^2 - \Lambda^2 \} + \phi_v(J) \quad (77)$$

which conforms with (71), Hund's Case (a), if B_v is replaced by the slightly modified value $B_v \left[1 \pm \frac{B_v}{A\Lambda} \right]$. At the other extreme we have A/B_v approximating to 0 or ± 4 . We then have

$$\begin{aligned} F(J) &= B_v [(J + \frac{1}{2})^2 - \Lambda^2 \pm (J + \frac{1}{2})] \\ &= B_v [K(K + 1) - \Lambda^2] \end{aligned}$$

if the $+\sqrt{}$ sign is associated with $J = K - \frac{1}{2}$ (the F_2 terms), and the $-\sqrt{}$ sign is associated with $J = K + \frac{1}{2}$ (the F_1 terms). We observe from (76) that if $A/B_v > 4$ or is negative, we shall have $F_1(K + \frac{1}{2}) < F_2(K - \frac{1}{2})$, while for values of $A/B_v > 0 < 4$, $F_1(K + \frac{1}{2}) > F_2(K - \frac{1}{2})$. This will be observed in Fig. 47.

In Fig. 47 we see (neglecting Λ -type doubling described in Section (g)) a set of rotational levels (for $v=0$) associated with each component of a ${}^2\Pi$ state. The series of molecules for which data are given range from CaH approximating to Case (a) normal, or OH Case (a) inverted, to BeH Case (b) and MgH ($A/B_v = 5.7$) which is also close to +4 of Case (b).

Midway between BeH and MgH is CH an almost exact example of $A/B_v = +2$. If this value is substituted in (76) the rotational term takes the special form

$$F(J) = B_v[\sqrt{J(J+1)} - \Lambda^2 \pm \tfrac{1}{2}]^2 \quad . \quad . \quad (78)$$

which chances to be a form suggested many years ago by Kramers and Pauli.

Several comments on Fig. 47 may be made here. Case (a) multiplicity is much larger than that of Case (b). (The Comet-Tail bands of Plate IV show an inverted Case (a) doubling. The minor doublet is due to Q heads.) Some of the J -values are appended in Fig. 47. Levels which in Case (b) would have the same K -value are linked by sloping lines. Mulliken describes the F_1 and F_2 sub-levels respectively as those belonging to $J = K + \tfrac{1}{2}$ and $J = K - \tfrac{1}{2}$, so that normal ${}^2\Pi_1$ and ${}^2\Pi_{11}$ would correspond to F_1 and F_2 (or inverted ${}^2\Pi_{11}$ and ${}^2\Pi_1$). Similarly for a triplet level, F_1, F_2, F_3 correspond to $J = K + 1, K, K - 1$, respectively, which in a normal ${}^3\Pi$ state are ${}^3\Pi_0, {}^3\Pi_1$ and ${}^3\Pi_2$, respectively.

(e) HUND'S CASE (c)

This is theoretically a possible type of coupling, but in practice will be rare. It may perhaps be found among the less stable states

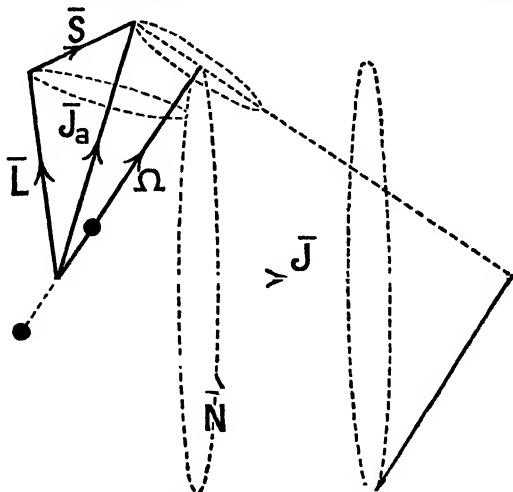


Fig. 48. Hund's Case (c).

of molecules with heavy atoms. In Case (c) the inter-nuclear electric field is not strong enough to break down the coupling of \vec{L} and \vec{S} ,

which therefore have a resultant $\bar{J}_a = \sqrt{J_a(J_a + 1)}$. (This particular notation recalls the analogy with the *atomic* coupling.) J_a will precess round the inter-nuclear axis at such angles as correspond to the quantum number Ω . This quantum number can take any of the values ranging from J_a to 0 (or $\frac{1}{2}$). It is then Ω and N which continue to give the resultant \bar{J} , and they will precess around the latter. It is clear that to describe electronic states as Σ , Π , or Δ has no significance now, since Λ does not exist. Ω , however, is a quantum number, and the numerical values of Ω —viz. 0, 1, 2, &c.—may be used to characterize such states. The rotational term in this case has the form :

$$F(J) = \frac{1}{2}A\{J_a(J_a + 1) - L(L + 1) - S(S + 1)\} \\ + F(\Omega) + B\{J(J + 1) - \Omega^2 + H^2\} + \phi(J) \quad . \quad . \quad (79)$$

Here H^2 stands for $L_{\text{perp}}^2 + S_{\text{perp}}^2$.

(f) HUND'S CASE (d)

This is one where \bar{L} is not coupled to the inter-nuclear axis to give a quantum number Λ , but to the angular momentum of the nuclei $\sqrt{N(N + 1)}$, which is now quantized, so that $N = 0, 1, 2, \dots$. These give a resultant $\bar{K} = \sqrt{K(K + 1)}$ about which they both pre-

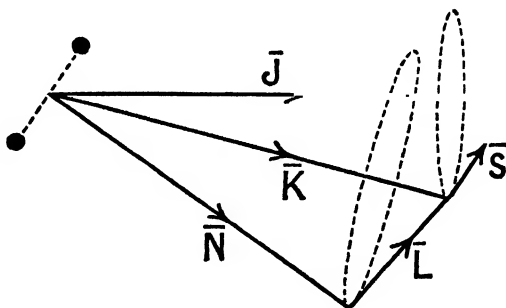


Fig. 49. Hund's Case (d).

cess. The quantum number K will have $2L + 1$ values ranging from $N + L$ to $N - L$. Finally \bar{S} combines with \bar{K} to give \bar{J} , where J takes $2S + 1$ values between $K + S$ and $K - S$. The special case in which $S = 0$ when $J = K$ is called by Mulliken Case (*d'*).

Case (*d*) may possibly occur in some high-energy states of H_2 and He_2 . It will occur when the \bar{L} is associated with an orbit, or orbits, very large compared with the distance between the nuclei. The only significant axis will in such a case be that of rotation of the whole system. We shall have

$$F(N) = B_i\{N(N + 1) + L_{\text{perp}}^2\} \quad . \quad . \quad . \quad (80)$$

(g) Λ -TYPE DOUBLING

The discussion of the formation of molecular multiplets (Chapter VI (c)) which was itself based on the behaviour of an atom in a strong electric field showed us that $F(\Lambda) = F(-\Lambda)$. Whether Λ was

parallel or antiparallel to the nuclear axis the energy value was the same. We there, however, neglected the effect of molecular rotation, which through its magnetic field causes a separation of these two energy values. In the rotating molecule each rotational level becomes a narrow doublet whose sub-levels we may distinguish arbitrarily by letters *c* and *d*: the doublet separation in general increases with *K* or *J*. There is necessarily no Λ-type doubling for Σ states (for which Λ = 0), while in Δ states it is too small to be observed, as a rule. We are therefore concerned in practice with Λ-type doubling only in Π states. The theory of the effect has been given by Van Vleck* and Kronig† and we shall here only summarize the results obtained.

Singlet States.

The energy separation of the two component levels is given by

$$\Delta W = \text{const } (J - \Lambda + 1)(J - \Lambda + 2) \dots (J + \Lambda) \quad (81)$$

which gives for ¹Π states Δ*W* = const *J*(*J* + 1). The constant is of the order $B_0 \left(\frac{B_0}{h\nu} \right)^{2\Lambda-1}$, where *B*₀ is the usual rotational band constant, so that *B*₀/*h* is of the order of a rotational frequency, while ν is of the order of an electronic frequency. Clearly the constant is vanishingly small for Δ states (Λ = 2). Moreover the doubling is pronounced only in ¹Π states of hydride molecules for which *B*₀ is comparatively large.

Referring back to equation (72) and to the subsequent remarks (see Section (c) also), we see that the effect of Λ-type doubling in ¹Π states is expressed by making δ double-valued, say either δ_{*a*} or δ_{*c*}.

Doublet States

Here the effect is different according as the conditions approximate to Case (a) or (b). If the latter, then since the spin is no longer coupled to the inter-nuclear axis, and the multiplet separation is small, the effect is similar to that above, where *K* replaces *J*, viz. Δ*W* = const *K*(*K* + 1). This simply means a double-valued ϕ(*K*) of the form δ_{*a*}*K*(*K* + 1) or δ_{*c*}*K*(*K* + 1) in equation (73). Owing to the loose coupling of the spin, the Λ-type doubling is the same in both sub-states *J* = *K* + *S* and *J* = *K* - *S*.

In Case (a), however, calculations show

$$\left. \begin{aligned} {}^2\Pi_1: \Delta W &= \text{const } (J + \tfrac{1}{2}) & \text{Constant of order } B_0 \frac{\Delta\nu}{\nu}, \\ {}^2\Pi_{11}: \Delta W &= \\ &\text{const } (J - \tfrac{1}{2})(J + \tfrac{1}{2})(J + \tfrac{3}{2}) & \text{Constant of order } B_0 \frac{B_0}{h\Delta\nu} \frac{B_0}{h\nu}, \end{aligned} \right\} \quad (82)$$

where Δν is the spin doublet separation of Section (b). The separation of the Λ-type components is thus much smaller in ²Π₁₁ than in ²Π₁ (cf. Fig. 50).

* *Phys. Rev.*, vol. 32, p. 250 (1928), also *Phys. Rev.*, vol. 33, p. 467 (1929).

† *Band Spectra and Molecular Structure*, p. 49 (C.U.P., 1930).

Triplet States

The result is the same as in doublet states where conditions approximate to Case (b). In Case (a) the splitting differs in the three sub-states. The energy difference of the two components is as follows :

$$\left. \begin{aligned} {}^3\Pi_0 : \Delta W &= \text{const} && \text{Constant of order } \frac{(\Delta\nu)^2}{\nu}, \\ {}^3\Pi_1 : \Delta W &= \text{constant } J(J+1) && \text{Constant of order } \frac{B_0^2}{h\nu}, \\ {}^3\Pi_2 : \Delta W &= \text{const } J^2(J+1)^2 && \text{Constant vanishingly small} \end{aligned} \right\} \quad (83)$$

If transition takes place from conditions of Case (a) to those of

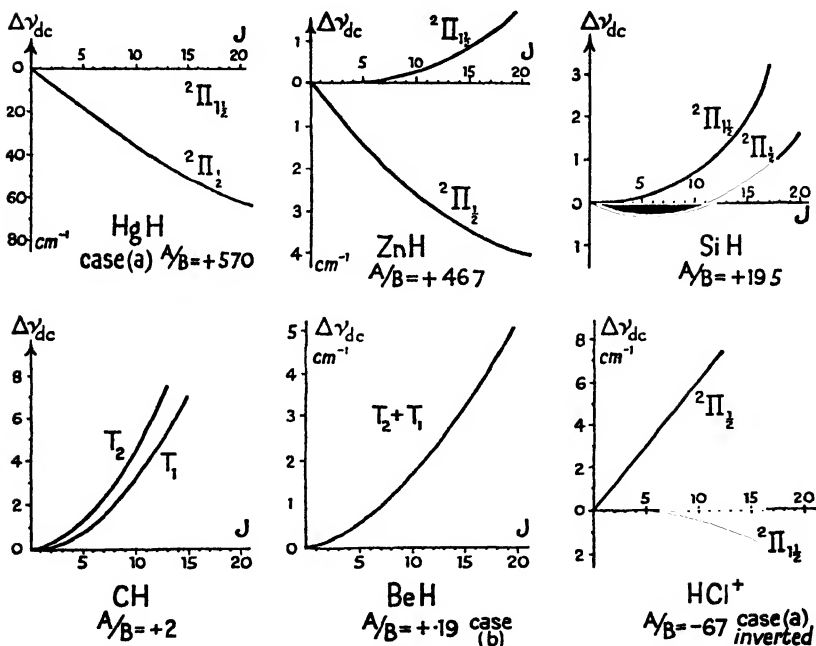


Fig. 50. Δ -type doubling in some ${}^3\Pi$ states of molecules ranging from Case (a) to Case (b) conditions. (Data from Mulliken and Christy, *Phys. Rev.*, vol. 38, p. 105 (1931).)

Case (b) with increasing J , then the Δ -type doubling may take a variety of intermediate forms, such as are illustrated in Fig. 50. As discussed in Section (d), the transition from Case (a) to (b) can be expressed as a function of A/B , which is large in Case (a), and either 0 (or +4) in Case (b). In Fig. 50 note the change from Case (a) to Case (b) conditions with increasing rotational speed, slowly in ZnH , but more rapidly in SiH . For fuller details the paper of Mulliken and Christy should be consulted.

CHAPTER VIII

FINE STRUCTURE: GENERAL CONSIDERATIONS

(a) TYPES OF BRANCHES

IN Chapter I (c) the fine structure of a simple type of band was described. In Plate II the Ångström CO band (${}^1\Sigma \rightarrow {}^1\Pi$) does not reveal the Λ -type doubling and illustrates the three simple branch-types P , Q , and R . In Plate III the Case (b) spin-doubling of the CN (${}^2\Sigma \rightarrow {}^2\Sigma$) band is not big enough to show, so that we have the appearance of the simple (${}^1\Sigma \rightarrow {}^1\Sigma$) type of band consisting only of a P and R branch. The Q branch, which theoretically can exist, is of zero intensity (Chapter X (b)).

The simple rotational quantum number gave rise to these three types of branch by changes of $+1$, 0 , and -1 . In Chapter VII we have seen that the rotational 'quantum number' N is in fact not a true quantum number at all (it is not subject to a selection principle), but it is, in general, a complex function of other more fundamental electronic and rotational quantum numbers. In equation (66) we recorded the selection principles which prescribe electronic transitions, and therefore define the possible band systems. We have now to consider the selection principle applicable to the rotational quantum number J (and also to the rotational quantum number K in Hund's Case (b)). These are :

$$\left. \begin{array}{l} \text{Change of } J = \pm 1 \text{ or } 0 \text{ (excluding } 0 \rightarrow 0), \\ \text{Change of } K = \pm 1 \text{ or } 0 \text{ (in Case (b) but not otherwise).} \end{array} \right\} \quad (84)$$

The changes of J give rise to P , Q , and R branches such as we have considered. The changes of K give rise to additional types of branches when we are dealing with electronic multiplet levels approximating to Case (b) coupling. The above restrictions on change of K are relaxed, so that changes of ± 2 or even ± 3 may occur, if the coupling is intermediate between Cases (a) and (b).

A branch corresponds not merely to a constant value of $J' - J''$ but to a constant value of $K' - K''$. Consistent with (84) nine types of branches will arise as shown in the following table. (${}^Q P$ is read Q -form P , &c.)

$K' - K'' :$		-2	-1	0	+1	+2
$J' - J'' \left\{ \begin{array}{l} -1 \\ 0 \\ +1 \end{array} \right.$	-1	${}^o P$	P	${}^Q P$	${}^s P$	${}^s P$
	0	${}^o Q$	${}^P Q$	Q	${}^s Q$	${}^s Q$
	+1	${}^o R$	${}^P R$	${}^Q R$	R	${}^s R$

The strongest branches are P , Q , and R , in which $K' - K''$ has the same change as $J' - J''$. Other branches of less strength are sometimes described as satellites. In Fig. 51 we have taken a single rotational level ($K = 2$) of one sub-level of a quintet

electronic state and drawn some of the rotational transitions which are possible.

(b) POSITIVE AND NEGATIVE ROTATIONAL LEVELS

We have already made reference (Chapter VI (d)) to the existence of 'positive' and 'negative' *electronic* states, a distinction based upon their wave-mechanical character. For similar reasons based on wave-mechanics, the *rotational* levels of all diatomic molecules are classed as positive (+) or negative (-). This involves still another selection principle governing rotational transitions which is

$$+ \rightleftharpoons - \text{ for rotational transitions } \dots (85)$$

(This rule is not, of course, to be confused with that of (67) for *electronic* transitions.) The selection rules (84) and (85) account for all

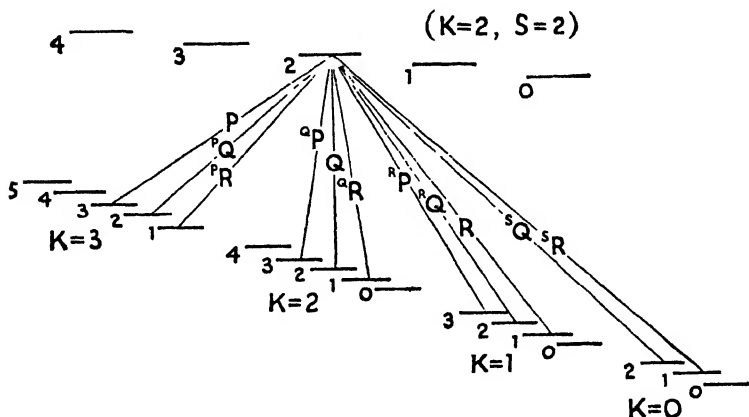


Fig. 51. Diagram to illustrate some of the great variety of branches which may arise. Transitions from a single rotational level of a quintet state to various rotational levels of a lower quintet state are drawn. The numbers attached to levels are J -values.

the great variety of band structures found in practice, provided the assignment of + and - characters to rotational levels is made in accordance with Fig. 52 or the table on p. 107. It will be observed that $^1\Sigma^+$ states have $J = 0$ and all even-numbered rotational levels positive, while $^1\Sigma^-$ states have $J = 0$ and all even-numbered levels negative. The Λ -type sub-levels of $^1\Pi$ and $^1\Delta$ states have opposite signs, being alternatively + and - (though unresolved in the latter). In multiplet electronic states we have a similar alternation with the provision that the 'corresponding' rotational levels of different components, viz. those for which J ranges from $K + S$ to $K - S$, all being derived from the same value of K , must be given the same sign (+ or -).

In the case of homonuclear molecules (C_2 , N_2 , &c.) the + and - levels have different statistical weights. In $^1\Sigma_g^+$ states (see (68) and text) the + levels, which are the even-numbered ones, are stronger than - levels. In $^1\Sigma_u^-$ the reverse is the case. In $^1\Sigma_g^-$ the + levels

are the stronger, and in $^1\Sigma_u^-$ the — levels are stronger. Similarly in $^1\Pi_g$ states + levels are the stronger, and in $^1\Pi_u$ states — levels are stronger, &c. These facts account for the alternating intensities characteristic of the band structure of elementary molecules of the type X_2 . Fuller consideration is given in Chapter X (f).

A system of notation used by Mulliken, which has proved convenient for describing rotational levels and types of transition, must now be recorded. It is an alternative system to the distribution of

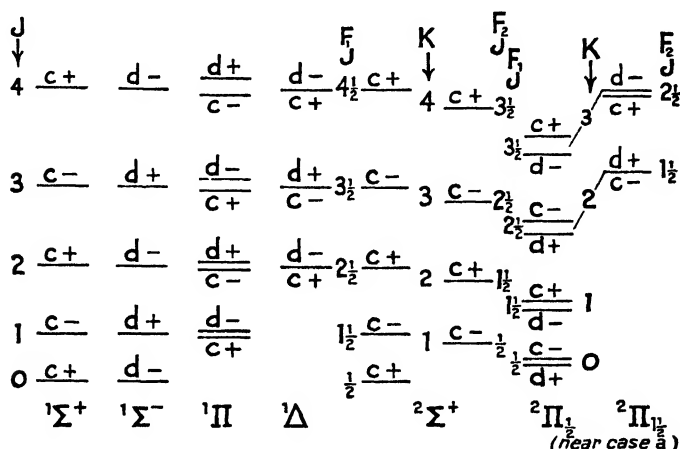


Fig. 52. Character (+ or -) of rotational levels of various electronic states. Mulliken's *cd* notation is also given.

+ and — characters of Fig. 52 and to the associated selection principle (85), but the one system can, of course, be completely correlated with the other. Mulliken describes all rotational levels by the letters *c* or *d*,

TABLE SHOWING ASSOCIATION OF *c* AND *d* (Λ-TYPE DOUBLING) WITH + AND - LEVELS

Nature of state	Sign of lowest rotational level	Mulliken's notation cord
Σ ⁺	+	<i>c</i>
Σ ⁻	-	<i>d</i>
Other singlet states and Case (b)	+ or -	<i>c</i> or <i>d</i>
Normal Case (a) doublets (e.g. $^2\Pi_1$)	- or +	<i>c</i> or <i>d</i>
Inverted Case (a) doublets	+ or -	<i>c</i> or <i>d</i>
Normal and Inverted Case (a) triplets	+ or -	<i>c</i> or <i>d</i>

The lowest rotational level in Case (b) is that group with lowest *K* and in Case (a) that with lowest *J*.

and he makes the assignment of *c* and *d* as shown in Fig. 52 and

summarized in the table. This accounts for band structures satisfactorily if the following rules apply :

$$\left. \begin{array}{l}
 \text{Transitions between electronic states having same} \\
 \Lambda \ (\Sigma \rightarrow \Sigma, \Pi \rightarrow \Pi, \text{ \&c.}) \\
 \text{Q-form branches (also O-form and S-form) : } c \rightleftharpoons d. \\
 \text{P-form and R-form branches : } c \rightarrow c \text{ and } d \rightarrow d. \\
 \text{Transitions between electronic states of different } \Lambda \ (\Sigma \rightleftharpoons \Pi, \text{ \&c.}) \\
 \text{Q-form branches (also O-form and S-form) : } c \rightarrow c \text{ and } d \rightarrow d. \\
 \text{P-form and R-form branches : } c \rightleftharpoons d.
 \end{array} \right\} (86)$$

We shall see the convenience of this system in describing band types and band lines in Chapter IX.

(c) THE COMBINATION PRINCIPLE

The fine structure of an ideally simple type of band has been given by (7) and (8) or more correctly by (23) and (24). The evaluation of the molecular constants $B' = h/8\pi^2 I'$ and $B'' = h/8\pi^2 I''$ could be determined by fitting the branch lines to quadratic formulae, but this method is not the most satisfactory. Without, however, assuming any particular form for the rotational energy function we have :

$$\begin{aligned}
 R(J) &= \nu_e + \nu_i + F'(v', J+1) - F''(v'', J), \\
 Q(J) &= \nu_e + \nu_n + F'(v', J) - F''(v'', J), \\
 P(J) &= \nu_e + \nu_i + F'(v', J-1) - F''(v'', J).
 \end{aligned}$$

From these we see

$$\left. \begin{aligned}
 R(J) - Q(J) &= Q(J+1) - P(J+1) \\
 &= F'(v', J+1) - F'(v', J) \\
 &= \Delta_1 F'(v', J), \text{ say.} \\
 R(J) - Q(J+1) &= Q(J) - P(J+1) \\
 &= F''(v'', J+1) - F''(v'', J) \\
 &= \Delta_1 F''(v'', J).
 \end{aligned} \right\} (87)$$

In the absence of a Q branch we still have the relations :

$$\left. \begin{aligned}
 R(J) - P(J) &= F'(v', J+1) \\
 &\quad - F'(v', J-1) = \Delta_2 F'(v', J), \text{ say.} \\
 R(J-1) - P(J+1) &= F''(v'', J+1) \\
 &\quad - F''(v'', J-1) = \Delta_2 F''(v'', J), \text{ say.}
 \end{aligned} \right\} (88)$$

Hence it is possible to find expressions for $F'(J)$ and $F''(J)$ by taking these differences and fitting them to a formula. Moreover, all the bands of a system can be utilized in obtaining the best values of these rotational functions. For example, bands (0,0) (0,1) (0,2) (0,3), &c., can all be used to derive $\Delta_1 F'(0, J)$ while bands (0,0) (1,0) (2,0) (3,0), &c., can all be used to derive $\Delta_1 F''(0, J)$.

Using the rotational function of (52) viz. $F(J) = BJ(J+1) + DJ^2(J+1)^2$ and dropping the vibrational quantum number we see from (88)

$$\left. \begin{aligned} R(J) - P(J) &= (4J + 2)[B' + 2D'(J^2 + J + 1)], \\ R(J - 1) - P(J + 1) &= (4J + 2)[B'' + 2D''(J^2 + J + 1)]. \end{aligned} \right\} (89)$$

Hence it is clear that these combination differences are to a close approximation a linear function of J and should vanish at $J = -\frac{1}{2}$. If this is not found in practice it indicates that an incorrect assignment of rotational quantum numbers has been made.

One method of determining B' and B'' is to plot the combination differences $R(J) - P(J)$ and $R(J - 1) - P(J + 1)$ as a function of J . All lines should intersect at $J = -\frac{1}{2}$, while the values of $2B'$ and $2B''$ are read off at $J = 0$.

The most accurate method of finding B' and B'' is illustrated in

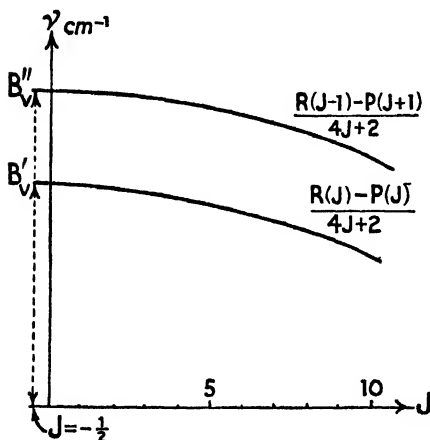


Fig. 53. Illustrates best method of evaluating B_v' and B_v'' .

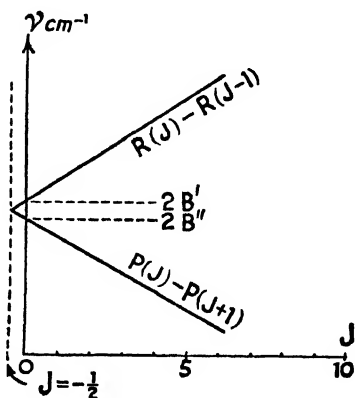


Fig. 54

Fig. 53. From (89) it is clear if we plot

$$\frac{R(J) - P(J)}{4J + 2} \quad \text{and} \quad \frac{R(J - 1) - P(J + 1)}{4J + 2}$$

as functions of J we shall obtain parabolae whose vertices are at the wave-numbers B_v' and B_v'' when $J = -\frac{1}{2}$.

Another method sometimes used to check as rapidly as possible the correct J -assignment to branch lines is to plot first differences of the lines as a function of J . Thus we shall have

$$\left. \begin{aligned} R(J) - R(J - 1) &= B' + B'' + C(2J + 1), \\ P(J) - P(J + 1) &= B' + B'' - C(2J + 1). \end{aligned} \right\} \quad \cdot \quad \cdot \quad (90)$$

It is clear that these functions intersect at $J = -\frac{1}{2}$ as shown in Fig. 54 and that the values they take at $J = 0$ are respectively $2B'$ and $2B''$.

We shall not discuss the combination principle further at this point. Its application to particular band types will be given in the next chapter.

CHAPTER IX

THE FINE STRUCTURE OF TYPICAL BANDS

(a) ${}^1\Sigma \rightarrow {}^1\Sigma$ BANDS

THESE bands alone conform to the ideally simple type already discussed. As mentioned in Chapter VII (c), here we have no resultant spin, therefore $S = 0$. In addition, $\Lambda = 0$ and the rotational term has the simple form BN^2 , where $N = \sqrt{J(J+1)}$. These bands have single P and R branches only, and Plate III gives a typical picture of

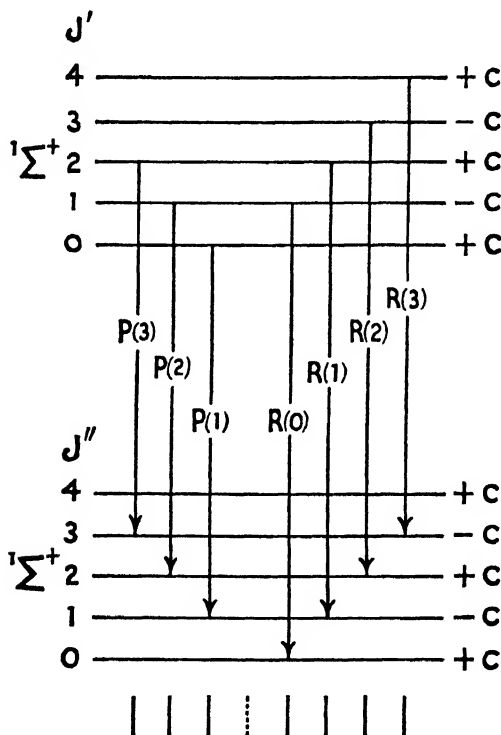


Fig. 55. Structure of ${}^1\Sigma^+ \rightarrow {}^1\Sigma^+$ band showing formation of P and R branches in conformity with the $+\rightleftharpoons -$ selection rule.

this type (since although it is actually ${}^2\Sigma \rightarrow {}^2\Sigma$, the Case (b) spin doubling is not perceptible).

As we saw in Chapter VIII (b), we distinguished two kinds of Σ states: Σ^+ and Σ^- , according to certain wave-mechanical properties. Fig. 55 shows that, in conformity with the $+\rightleftharpoons -$ selection rule for rotational levels, ${}^1\Sigma^+ \rightarrow {}^1\Sigma^+$ bands consist of P and R branches only.

Q branches are inadmissible. ${}^1\Sigma^- \rightarrow {}^1\Sigma^-$ bands are similar and Fig. 55 is applicable if all signs are changed and d is written for c .

Transitions between ${}^1\Sigma^+$ and ${}^1\Sigma^-$ states would in conformity with the $+\rightleftharpoons-$ rule yield only Q branches. It transpires, however, that such branches have zero intensity, so that no band system arises. We thus have the explanation of (67). Fig. 55 is applicable to the structure of vibration-rotation bands if the two sets of rotational levels are associated with two different vibrational levels of the same electronic state. (Σ^+ electronic states constitute the great majority of known Σ states. There is only one excited ${}^2\Sigma^-$ state of CH, a ${}^1\Sigma^-$ state of O_2 , and a few ${}^3\Sigma^-$ states associated with NH, PH, O_2 , S_2 , and SO known at present.)

(b) ${}^1\Pi \rightleftharpoons {}^1\Sigma$ BANDS

An example of a ${}^1\Sigma \rightarrow {}^1\Pi$ band is given in Plate III, which shows the (0,3) band of the Ångström CO system. The diagram of Fig. 56 shows that, consistent with the selection rules, we shall have a single P , Q , and R branch in each band. For the ${}^1\Sigma$ state $J_{\min} = \Lambda = 0$; for the ${}^1\Pi$ state $J_{\min} = \Lambda = 1$. Hence for a ${}^1\Pi \rightarrow {}^1\Sigma^+$ band, the first lines of each branch would be designated $P_d(2)$, $Q_c(1)$, $R_d(0)$. For ${}^1\Sigma^+ \rightarrow {}^1\Pi$ the first lines would be $P_d(1)$, $Q_c(1)$, and $R_d(1)$. In each type of band we should find two missing lines between the P and R branch-series. The use of c and d as suffixes has been explained in Chapter VIII (c). If we were dealing with a ${}^1\Sigma^-$ state the results are those given above, provided c and d are interchanged. The doublet character of the ${}^1\Pi$ levels is, of course, Λ -type in nature.

It now remains to consider the effect of this Λ -type doubling on the combination relations discussed in the preceding chapter. The equations (88) now become for a ${}^1\Sigma^+ \rightarrow {}^1\Pi$ band

$$\left. \begin{aligned} R(J) - P(J) &= F_c'(J+1) - F_c'(J-1) = \Delta_2 F_c'(J), \\ R(J-1) - P(J+1) &= F_d''(J+1) - F_d''(J-1) = \Delta_2 F_d''(J), \end{aligned} \right\} \quad (91)$$

while (87) gives place to :

$$\left. \begin{aligned} R(J) - Q(J) &= [F_c'(J+1) - F_c'(J)] - [F_d''(J) - F_c''(J)] \\ &= \Delta_1 F_c'(J + \tfrac{1}{2}) - z(J), \\ Q(J+1) - P(J+1) &= [F_c'(J+1) - F_c'(J)] + [F_d''(J+1) - F_c''(J+1)] \\ &= \Delta_1 F_c'(J + \tfrac{1}{2}) + z(J+1). \end{aligned} \right\} \quad (92)$$

$$\left. \begin{aligned} R(J) - Q(J+1) &= F_c''(J+1) - F_d''(J) \\ &= \Delta_1 F_c''(J + \tfrac{1}{2}) - z(J), \text{ or } \Delta_1 F_d''(J + \tfrac{1}{2}) - z(J+1), \\ Q(J) - P(J+1) &= F_d''(J+1) - F_c''(J) \\ &= \Delta_1 F_c''(J + \tfrac{1}{2}) + z(J+1), \text{ or } \Delta_1 F_d''(J + \tfrac{1}{2}) + z(J). \end{aligned} \right\} \quad (93)$$

It will be observed that from (91), $F_c'(J)$, we can find, as explained in Chapter VIII (c), B and D , the constants of the rotational function (see (89) of the ${}^1\Sigma^+$ state). Similarly from (91) we can derive from $F_d''(J)$ the constants $B + \delta_d$ and D for the ${}^1\Pi$ state. As mentioned

in Chapter VII (*g*), we do not find B , but $B + \delta$. From (93) we can subsequently determine $F_c''(J)$, since

$$F_c''(J+1) = F_d''(J) + R(J) - Q(J+1),$$

also

$$F_c''(J) = F_d''(J+1) - Q(J) + P(J+1).$$

This will give $B + \delta_c$. The value of B alone cannot be determined.

In the case of ${}^1\Pi \rightarrow {}^1\Sigma^+$ bands we have analogous to (91), (92), and (93)

$$\left. \begin{aligned} R(J) - P(J) &= \Delta_2 F_d'(J), \\ R(J-1) - P(J+1) &= \Delta_2 F_c''(J). \end{aligned} \right\} \quad \cdot \quad \cdot \quad \cdot \quad (94)$$

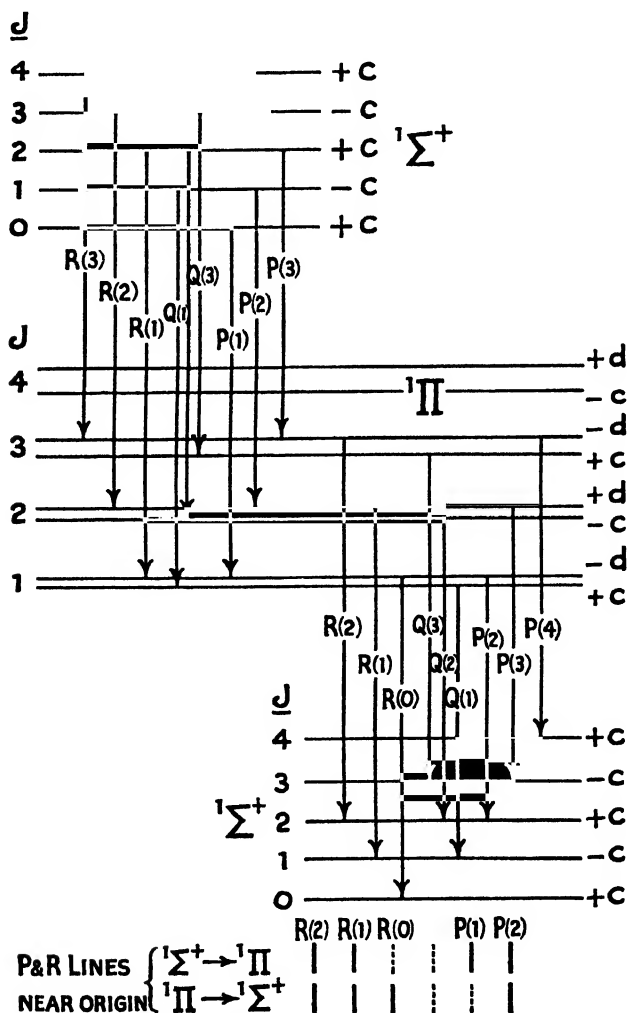


Fig. 56. Branches in ${}^1\Sigma^+ \leftrightarrow {}^1\Pi$ bands.

$$\left. \begin{aligned} R(J) - Q(J) &= \Delta_1 F_c'(J + \tfrac{1}{2}) + z(J + 1) \text{ or } \Delta_1 F_d'(J + \tfrac{1}{2}) + z(J), \\ Q(J + 1) - P(J + 1) &= \Delta_1 F_c'(J + \tfrac{1}{2}) - z(J) \text{ or } \Delta_1 F_d'(J + \tfrac{1}{2}) - z(J + 1), \end{aligned} \right\} \quad (95)$$

and

$$\left. \begin{aligned} R(J) - Q(J + 1) &= \Delta_1 F_c''(J + \tfrac{1}{2}) + z(J + 1), \\ Q(J) - P(J + 1) &= \Delta_1 F_c''(J + \tfrac{1}{2}) - z(J). \end{aligned} \right\} \quad (96)$$

In all these expressions $z(J)$ represents $F_d(J) - F_c(J)$, the width of

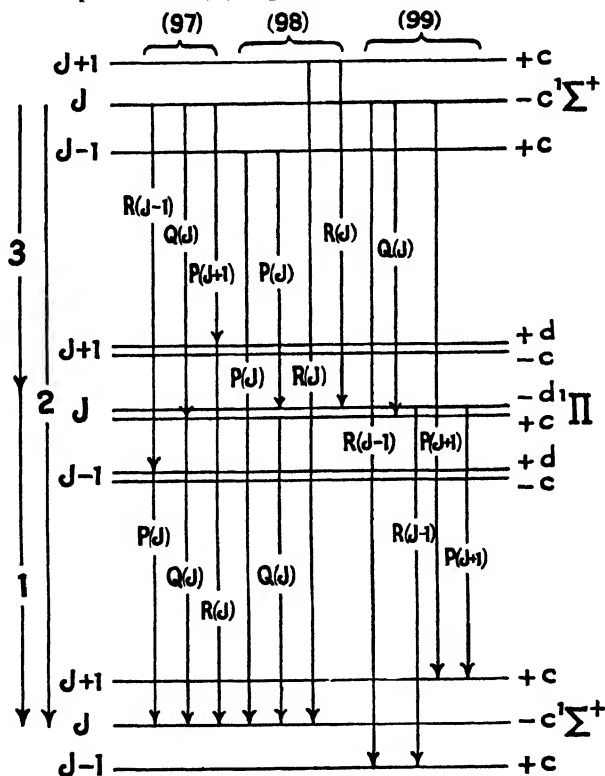


Fig. 57. Illustrates combination relations between three related systems; so that knowing two, the third could be calculated.

the Λ -type doubling of the J -rotational level of the ${}^1\Pi$ state. What used to be described as a 'combination defect' when the simple form of combination principle expressed in (87) was used, is clearly explained by (91)–(96). It may, of course, be the case that $z(J)$ is inappreciable, especially for low values of J , and this actually is the case for the Ångström bands (${}^1\Sigma^+ \rightarrow {}^1\Pi$), of which one (the 0,3 band) is shown in Plate II. Where all three band systems between three levels are known, as illustrated in Fig. 57, (1) ${}^1\Pi \rightarrow {}^1\Sigma^+$, (2) ${}^1\Sigma^+ \rightarrow {}^1\Sigma^+$, (3) ${}^1\Sigma^+ \rightarrow {}^1\Pi$ (or as in Fig. 40 for the doublet levels of the CO^+ molecule),

a number of useful relations exist between them. Indeed, from the data of two of the band systems it is clearly possible to calculate the third system. These relations are given in equations (97), (98), and (99) and are clearly deducible from Fig. 57. The prefix 1, 2, or 3 refers to the system :

$${}^1P(J) + {}^3R(J-1) = {}^1Q(J) + {}^3Q(J) = {}^1R(J) + {}^3P(J+1) \quad . \quad (97)$$

$${}^2P(J) - {}^3P(J) - {}^1Q(J) = {}^2R(J) - {}^3R(J) - {}^1Q(J) = z(J) \quad . \quad (98)$$

$$\begin{aligned} {}^3Q(J) + {}^1R(J-1) - {}^2R(J-1) \\ = {}^1P(J+1) + {}^3Q(J) - {}^2P(J+1) = z(J) \quad . \quad (99) \end{aligned}$$

(c) ${}^1\Pi \rightarrow {}^1\Pi$ BANDS

Here the selection rules (84) and (85) give rise to bands in the manner shown in Fig. 58. The Λ -type doubling and the absence of $J=0$ are obvious features. The first lines of the respective branches are therefore $P_c(2)$, $P_d(2)$, $Q_{cd}(1)$, $Q_{dc}(1)$, $R_c(1)$, $R_d(1)$. As shown in Fig. 59, there will be three missing doublets; one in each of the P and R branches and the null line. While a Q branch is theoretically possible, the intensity in it falls off so rapidly that the branch may not even be detected. The six branches found are obviously expressed by :

$$\left. \begin{aligned} R_d(J) &= \nu_0 + F_d'(J+1) - F_d''(J) \text{ and} \\ R_c(J) &= \nu_0 + F_c'(J+1) - F_c''(J), \\ Q_{cd}(J) &= \nu_0 + F_c'(J) - F_d''(J) \text{ and} \\ Q_{dc}(J) &= \nu_0 + F_d'(J) - F_c''(J), \\ P_d(J) &= \nu_0 + F_d'(J-1) - F_d''(J) \text{ and} \\ P_c(J) &= \nu_0 + F_c'(J-1) - F_c''(J), \end{aligned} \right\} \quad (100)$$

and the combination principle (88) clearly gives us

$$\left. \begin{aligned} R_d(J) - P_d(J) &= \Delta_2 F_d'(J) \text{ and} \\ R_c(J) - P_c(J) &= \Delta_2 F_c'(J), \\ R_d(J-1) - P_d(J+1) &= \Delta_2 F_d''(J) \text{ and} \\ R_c(J-1) - P_c(J+1) &= \Delta_2 F_c''(J). \end{aligned} \right\} \quad (101)$$

By the methods of Chapter VIII (c) we can thus find values of $B + \delta_c$ and $B + \delta_d$ (as mentioned on p. 109). As we shall subsequently consider in Chapter X (c), in the case of a homonuclear molecule (X_2) the statistical weights of the components of the Λ -doubling are unequal. In a particular electronic state all the $+$ levels or all the $-$ levels are stronger or weaker, as the case may be. This gives the alternating intensities of Fig. 58 (a). In the case of a homonuclear molecule without nuclear spin all the $+$ or all the $-$ levels are missing, giving the staggered effect of Fig. 58 (b). This feature is found in a ${}^1\Pi \rightarrow {}^1\Pi$ system of the C_2 molecule, and in the ${}^2\Pi \rightarrow {}^2\Pi$ system of the O_2^+ molecule.

(d) ${}^1\Pi \rightleftharpoons {}^1\Delta$ BANDS

These transitions are not common among band systems. We have, however, a ${}^1\Delta \rightarrow {}^1\Pi$ system of He_2 (0,0 band at λ 6110). There is a

${}^1\Pi \rightarrow {}^1\Delta(0,0)$ band of NH at λ 3240, and we shall use Dieke's observations * of this band to illustrate this section.

In conformity with Fig. 52 and the selection rules (85) and (86), we have constructed Fig. 59 to illustrate the formation of a ${}^1\Pi \rightarrow {}^1\Delta$

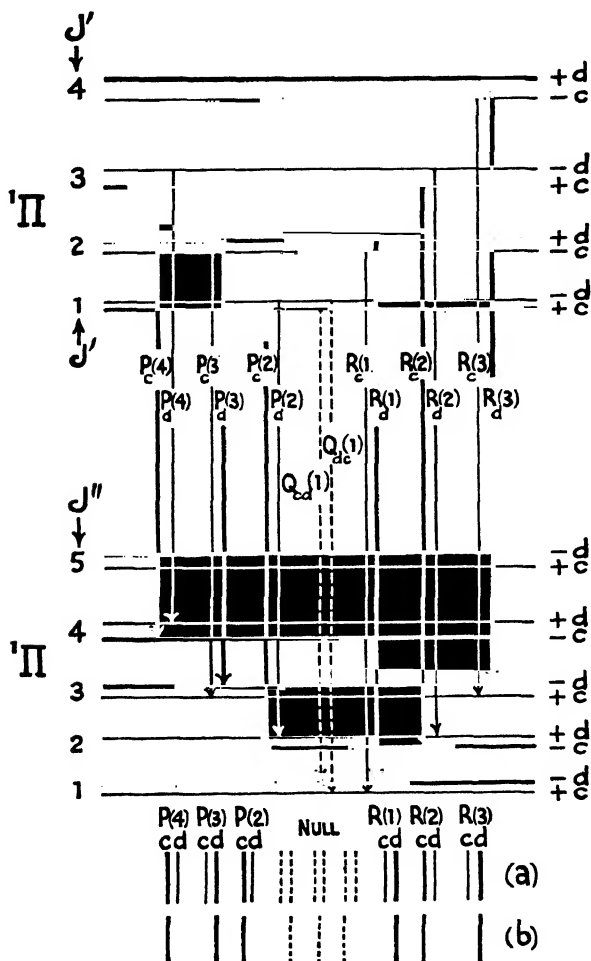


Fig. 58. ${}^1\Pi \rightarrow {}^1\Pi$ transitions. (a) Homonuclear molecule with nuclear spin. (b) Homonuclear molecule without nuclear spin.

band. The unequal intensities shown would, of course, occur only in a homonuclear molecule. Fig. 60 is constructed from experimental data of the NH band mentioned. There is, as we see from

* *Phys. Rev.*, vol. 45, p. 395 (1934). (Data for the isotopic ND band are also given, and a photograph of both is included.)

Fig. 59, a gap of four lines near the band origin : one in the P branch, the null line, and two in the R branch. (In a ${}^1\Delta \rightarrow {}^1\Pi$ band there would be two missing in the P branch and one from the R branch.) The general expressions for the six observed branches are :

$$\left. \begin{aligned} P_{dc}(J) &= \nu_0 + F_d'(J-1) - F_c''(J), \\ P_{cd}(J) &= \nu_0 + F_c'(J-1) - F_d''(J), \\ Q_{dc}(J) &= \nu_0 + F_d'(J) - F_c''(J), \\ Q_{cd}(J) &= \nu_0 + F_c'(J) - F_d''(J), \\ R_{dc}(J) &= \nu_0 + F_d'(J+1) - F_c''(J), \\ R_{cd}(J) &= \nu_0 + F_c'(J+1) - F_d''(J). \end{aligned} \right\} \quad (102)$$

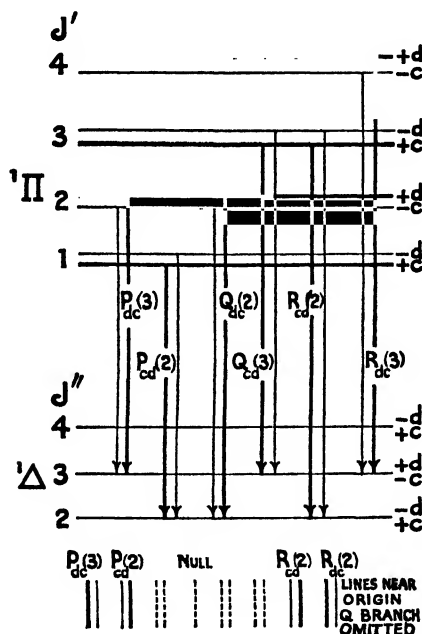


Fig. 59. ${}^1\Pi \rightarrow {}^1\Delta$ transitions (Δ -type doublets). Only the stronger component of each doublet labelled.

In contrast with the ${}^1\Pi \rightarrow {}^1\Pi$ band, the Q branches of ${}^1\Pi \rightleftharpoons {}^1\Delta$ bands are particularly strong.

(e) ${}^2\Sigma \rightarrow {}^2\Sigma$ BANDS

Many examples of this transition are known, and reference back to Plate VII may be made. This shows spectra of the ${}^2\Sigma \rightarrow {}^2\Sigma$ (violet) bands of CN. Since $\Lambda = 0$, the doubling is, of course, not Λ -type, but the Case (b) spin-type, which has been referred to in Chapter VII (c). Each doublet has a common K , and the two rotational components are given by $J = K \pm \frac{1}{2}$. They have a doublet separation which is proportional to $(K + \frac{1}{2})$. As Fig. 61 shows, we have theoretically six possible branches, consistent with the selection rules (84) and (85). Using the suffix 1 for the terms $J = K + \frac{1}{2}$

and suffix 2 for terms $J = K - \frac{1}{2}$, we may write these six branches as :

$$P_1(J), P_2(J), {}^PQ_{12}(J), {}^RQ_{21}(J), R_1(J), \text{ and } R_2(J).$$

The lowest level $K = 0$ is single, viz. $J = \frac{1}{2}$ only : this is clear from Fig. 61. Apart from this there is only the gap of the null line between the P and R branches.

A discussion of intensities (Chapter X (b)) shows that both Q branches are very weak (no trace is found in the CN bands). Further-

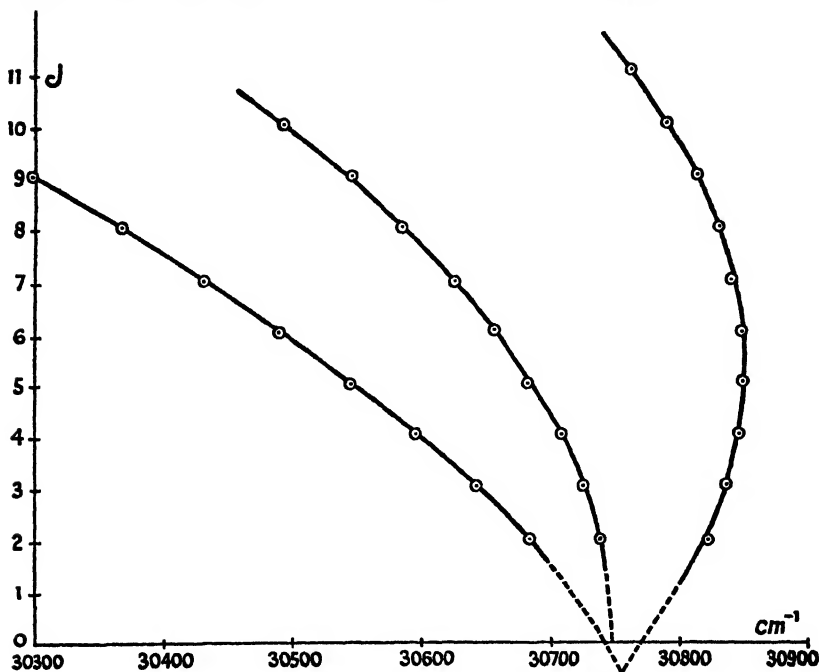


Fig. 60. Fortrat diagram of NH band at λ 3240 $^1\Pi \rightarrow ^1\Delta$ type. The doublet components which are only about 2 cm^{-1} apart at $J = 10$ do not show on the scale used.

more, for low rotational levels theory predicts that the components of the doublets will be quite unequal in intensity, P_1 and R_1 being stronger. Strip F of Plate VII shows this feature clearly in the region of the origin of the (10,10) band. For high rotational levels their intensities equalize (strip D of Plate VII). The correct assignment of subscripts 1 and 2 is not always easy, and this intensity criterion is then valuable.

The wave-numbers of the branches will be given by :

$$\left. \begin{aligned} P_1(J) &= F_1'(J-1) - F_1''(J), \text{ and} \\ R_1(J) &= F_1'(J+1) - F_1''(J), \\ P_2(J) &= F_2'(J-1) - F_2''(J), \text{ and} \\ R_2(J) &= F_2'(J+1) - F_2''(J), \\ {}^PQ_{12}(J) &= F_1'(J) - F_2''(J), \text{ and} \\ {}^RQ_{21}(J) &= F_2'(J) - F_1''(J), \end{aligned} \right\} \quad (103)$$

and the combination principle (88) gives at once $\Delta_2 F_1'(J)$, $\Delta_2 F_2'(J)$, $\Delta_2 F_1''(J)$, and $\Delta_2 F_2''(J)$. From (73) and (74) we have for a ${}^2\Sigma$ rotational term

$$\left. \begin{aligned} F_1(J) &= F_1(K + \tfrac{1}{2}) \\ &= \nu_0 + B_v K(K+1) + \tfrac{1}{2}\gamma K + D_v K^2(K+1)^2, \\ F_2(J) &= F_2(K - \tfrac{1}{2}) \\ &= \nu_0 + B_v K(K+1) - \tfrac{1}{2}\gamma(K+1) + D_v K^2(K+1)^2. \end{aligned} \right\} \quad (104)$$

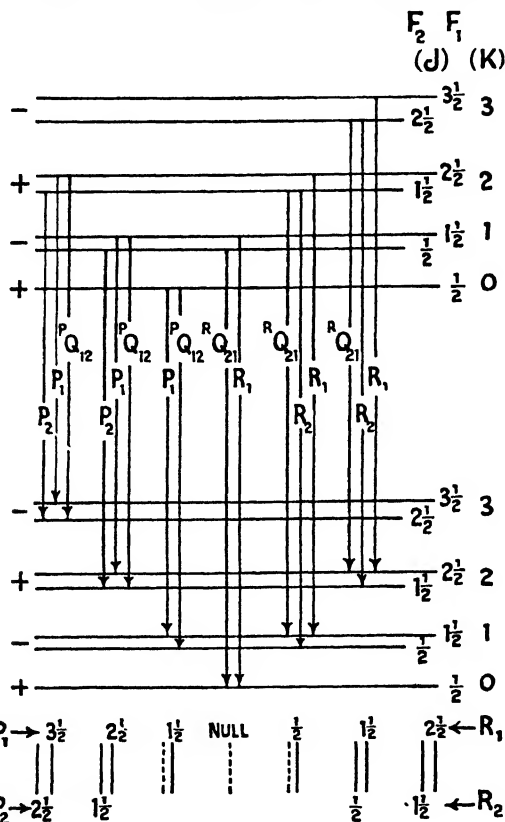


Fig. 61. Rotational transitions for ${}^2\Sigma^+ \rightarrow {}^2\Sigma^+$ bands. The two Q branches, while permissible, fade out rapidly in intensity and may be too weak to see.

From these we derive :

$$\left. \begin{aligned} \Delta_2 F_1(K + \tfrac{1}{2}) &= 4B_v(K + \tfrac{1}{2}) + \gamma + 8D_v(K + \tfrac{1}{2})(K^2 + K + 1), \\ \Delta_2 F_2(K - \tfrac{1}{2}) &= 4B_v(K + \tfrac{1}{2}) - \gamma + 8D_v(K + \tfrac{1}{2})(K^2 + K + 1), \end{aligned} \right\} \quad (105)$$

and from these γ can be derived

$$\gamma = \tfrac{1}{2}[\Delta_2 F_1(K + \tfrac{1}{2}) - \Delta_2 F_2(K - \tfrac{1}{2})] \quad . \quad . \quad (106)$$

and also B_v and D_v .

Sometimes the R_1 and R_2 heads (or the P_1 and P_2 heads, as the case may be) are well resolved, especially so when the heads are formed

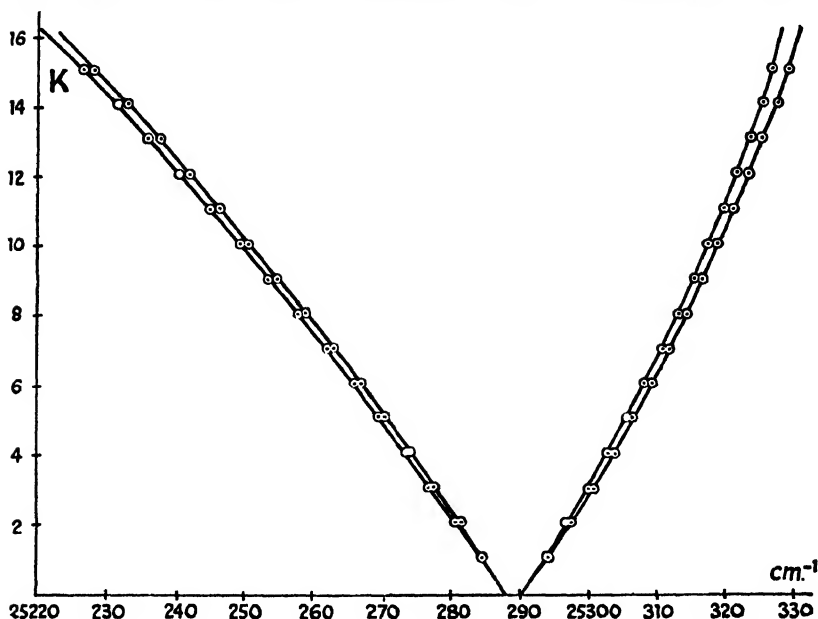


Fig. 62. Fortrat diagram of the (12,12) band at λ 3953, of the ${}^2\Sigma \rightarrow {}^2\Sigma$ violet CN system. (Data from Jenkins, *Phys. Rev.*, vol. 31, p. 543 (1928).)

at a substantial distance from the band origin. This is clearly illustrated in Spectrum 3 on Plate VI in the case of a ${}^2\Sigma \rightarrow {}^2\Sigma$ system of BaF. Molecules such as CaF, SrF, ScO, LaO, YO, all have similar spectra.

(f) ${}^2\Pi \rightleftharpoons {}^2\Sigma$ BANDS

The ${}^2\Sigma$ levels are always Case (b). We are faced, however, with the possibility that ${}^2\Pi$ states may be either Case (a) or Case (b) or intermediate between these extremes. Moreover, they will exhibit Λ -type doubling, and they may also be 'normal' or 'inverted'. The ${}^2\Sigma$ states will have spin doubling, which may or may not be appreciable. All these features make the study of ${}^2\Pi \rightleftharpoons {}^2\Sigma$ bands one of some complexity, and Chapter VII, Sections (a), (b), and (d), may be revised with advantage at this point.

Rotational Terms

We there saw that for an intermediate stage between Case (a) and Case (b) the rotational terms would be, according to Hill and Van Vleck, equation (76),

$$F(J) = B_v \left[\left(J + \frac{1}{2} \right)^2 - \Lambda^2 \pm \sqrt{\left(J + \frac{1}{2} \right)^2 - \frac{\Lambda^2 A}{B_v} \left(1 - \frac{A}{4B_v} \right)} \right] + \phi(J),$$

where for ${}^2\Pi$ states $\Lambda = 1$, $S = \frac{1}{2}$.

For A/B_r large, this gives the form of Case (a), where the + sign leads to ${}^2\Pi_{11}$ and the - sign to ${}^2\Pi_1$. The form of the terms would then reduce to

$${}^2\Pi_1 \left\{ \begin{aligned} F_{1c}(J) &= W + \frac{1}{2}a(J + \frac{1}{2}) + B_1J(J + 1), \\ F_{1a}(J) &= W - \frac{1}{2}a(J + \frac{1}{2}) + B_1J(J + 1), \end{aligned} \right\} \quad (107)$$

$${}^2\Pi_{11} : F_{2c}(J) = F_{2a}(J) = W + A + B_2J(J + 1).$$

In these

$$B_1 = B_r \left(1 - \frac{B_r}{A\Lambda} \right) + \delta_{c \text{ or } d},$$

and

$$B_2 = B_r \left(1 + \frac{B_r}{A\Lambda} \right) + \delta_{c \text{ or } d} \text{ (see equation (77))},$$

while the terms $\frac{1}{2}a(J + \frac{1}{2})$ represent $\phi(J)$ the Λ -type doubling (see equation (82)). Λ -type doubling, as we saw, was practically negligible for the ${}^2\Pi_{11}$ state.

At the other extreme we have seen that the rotational term (76) reduces for $A/B_r = 0$ or $+4$ to $F(J) = B_r[K(K + 1) - \Lambda^2]$ which is that of Hund's Case (b). To this we must add as per (74) the spin terms which correspond to $J = K + \frac{1}{2}$ and $J = K - \frac{1}{2}$. We see from Chapter VII (b) that the typical rotational terms of the ${}^2\Sigma$ state will therefore be

$$\left. \begin{aligned} {}^2\Sigma \quad J = K + \frac{1}{2} : \\ F_1(J) &= W + \frac{1}{2}\gamma K + BK(K + 1) + \dots \\ &= W + \frac{1}{2}\gamma(J - \frac{1}{2}) + B(J - \frac{1}{2})(J + \frac{1}{2}) + \dots, \\ {}^2\Sigma \quad J = K - \frac{1}{2} : \\ F_2(J) &= W - \frac{1}{2}\gamma(K + 1) + BK(K + 1) + \dots \\ &= W - \frac{1}{2}\gamma(J + \frac{3}{2}) + B(J + 1)(J + \frac{3}{2}) + \dots \end{aligned} \right\} \quad (108)$$

The ${}^2\Pi$ state, if it approximates to Hund's Case (b), will be represented by equations similar to (108) apart from Λ -type doubling. As mentioned in Chapter VII, (g) the Λ -type doubling is here represented by the replacement of B by $B + \delta_c$ and by $B + \delta_a$, giving $F_{1c}(J)$ and $F_{1a}(J)$. Λ -type doubling is now the same in both sub-states, so that we have also $F_{2c}(J)$ and $F_{2a}(J)$ similarly.

Correlation of Case (a) and (b)

We have already observed in Chapter VII (d) that the term of (76) reduces to the standard Case (b) type provided the

$$\begin{aligned} + \sqrt{} \text{ sign is associated with } J = K - \frac{1}{2} \text{ (} F_2 \text{ terms),} \\ - \sqrt{} \text{ sign is associated with } J = K + \frac{1}{2} \text{ (} F_1 \text{ terms).} \end{aligned}$$

We also saw in Chapter VII (d) that for A/B_r large and positive (76) became

$$F(J) = W \pm \frac{A\Lambda}{2} + B_1[J(J + 1) - (\Lambda \pm \frac{1}{2})^2] \dots + \phi(J),$$

while similarly for A/B_v large and negative it would give

$$F(J) = W \mp \frac{A\Lambda}{2} + B_1[J(J+1) - (\Lambda \mp \frac{1}{2})^2] \dots + \phi(J).$$

The conditions A/B_v large is Case (a) and $\Omega = \Lambda \pm \frac{1}{2}$.

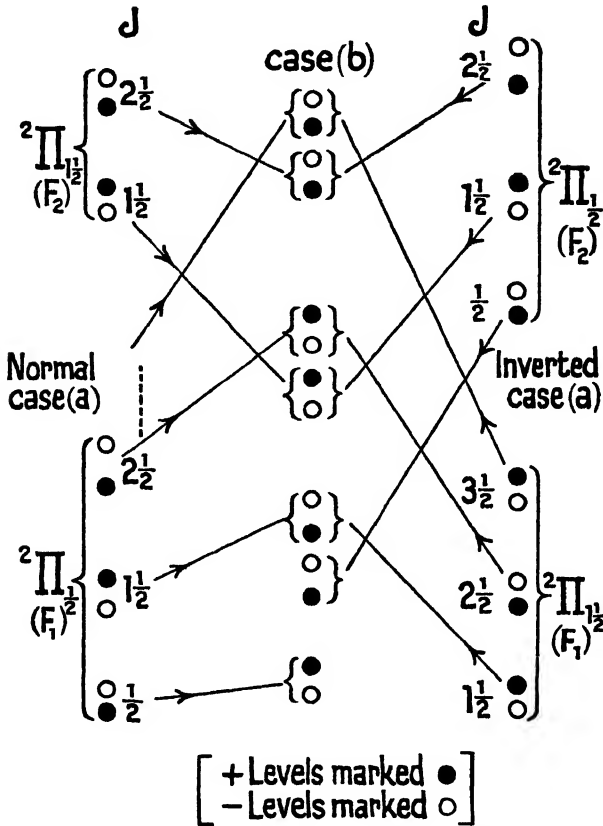


Fig. 63. Transition of ${}^2\Pi$ states from Case (a) to Case (b) conditions.

It is clear therefore that in the transition from Case (a) to Case (b) the correlation of terms is as follows :

$$\left. \begin{array}{l} A \text{ positive :} \\ \text{Normal } \left\{ \begin{array}{l} \Pi_{1,1} \Omega = 1\frac{1}{2} \text{ goes over to } F_2 \text{ terms } (J = K - \frac{1}{2}), \\ \Pi_{1,1} \Omega = \frac{1}{2} \text{ goes over to } F_1 \text{ terms } (J = K + \frac{1}{2}). \end{array} \right\} \\ A \text{ negative :} \\ \text{Inverted } \left\{ \begin{array}{l} \Pi_{1,1} \Omega = \frac{1}{2} \text{ goes over to } F_2 \text{ terms } (J = K - \frac{1}{2}), \\ \Pi_{1,1} \Omega = 1\frac{1}{2} \text{ goes over to } F_1 \text{ terms } (J = K + \frac{1}{2}). \end{array} \right\} \end{array} \right\} \quad (109)$$

These features have been shown diagrammatically in Fig. 63 where

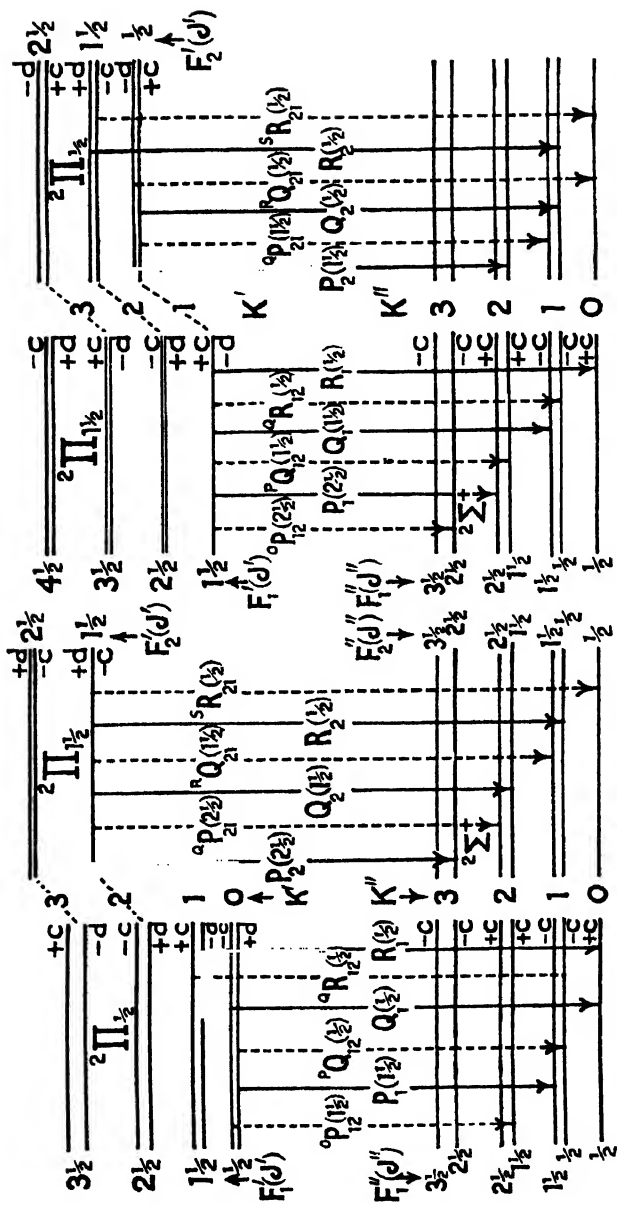


Fig. 64. Rotational transitions producing the first lines of each branch: (1) normal $2\Pi \rightarrow 2\Sigma^+$, (2) Inverted $2\Pi \rightarrow 2\Sigma^+$. (Broken lines indicate weak branches.)

corresponding labels have been attached. It will be noted for *normal* ${}^2\Pi$ states that the sub-state ${}^2\Pi_{11}$, where $J_{\min} = \Omega = 1\frac{1}{2}$, corresponds to $K = 2$, while the sub-state ${}^2\Pi_1$, where $J_{\min} = \Omega = \frac{1}{2}$, corresponds to $K = 0$. On the right of Fig. 63, where the ${}^2\Pi$ states are inverted, we have ${}^2\Pi_{11} : J_{\min} = 1\frac{1}{2}$ corresponding to $K = 1$, while ${}^2\Pi_1 : J_{\min} = \frac{1}{2}$ corresponds also to $K = 1$. These are, of course, deductions from (109). We have placed the $F_1(K + \frac{1}{2})$ above the corresponding $F_2(K - \frac{1}{2})$ levels in Case (b) conditions of Fig. 63. This was explained in Chapter VII (d).

Branches

In Fig. 64 are shown the transitions giving rise to the first lines of each branch for ${}^2\Pi \rightarrow {}^2\Sigma$ bands. The levels are labelled in accordance with Fig. 52 and the table in Chapter VIII (b). The transitions are in accordance with selection rules (84) and (85). The appearance of ${}^2\Pi \rightarrow {}^2\Sigma$ bands depends very much on the value of A/B_r for the ${}^2\Pi$ state. If it is large corresponding to Hund's Case (a), we shall tend to get two independent well-separated sub-bands, ${}^2\Pi_{11} \rightarrow {}^2\Sigma$ and ${}^2\Pi_1 \rightarrow {}^2\Sigma$, which will be generally similar in appearance. Each of these, as we see from Fig. 64, gives rise to six branches. Of the twelve branches, six are always strong, P_1 , Q_1 , R_1 , P_2 , Q_2 , and R_2 , whether conditions are Case (a) or Case (b). The other six branches are strong under Case (a) conditions, but weaker as Case (b) is approached. The two branches ${}^oP_{12}$ and ${}^sR_{21}$ are then completely extinguished because they would violate the selection rule for K (see (84)). The other four branches, ${}^qP_{21}$, ${}^rQ_{12}$, ${}^RQ_{21}$, and ${}^Q R_{12}$, are often termed satellite branches. It is clear from Fig. 64 that if the spin doubling in the ${}^2\Sigma$ state is small, then branch lines ${}^rQ_{12}$ will be close satellites of P_1 , and similarly ${}^Q R_{12}$ of Q_1 , ${}^qP_{21}$ of Q_2 , and ${}^RQ_{21}$ of R_2 . Indeed, these may not be resolved from each other. This would give each sub-band the appearance of four branches only, or three branches only if ${}^oP_{12}$ and ${}^sR_{21}$ are not present. Fig. 65 is the Fortrat diagram for a typical Case (a) state, ${}^2\Pi \rightarrow {}^2\Sigma$ showing the (0,0) band structure of BaH.* For this band $A = 462 \text{ cm.}^{-1}$, $B = 3.45 \text{ cm.}^{-1}$, and therefore $A/B = 133$. In Fig. 66 we have a Fortrat diagram for the (0,0) band of BeF † for which $A = 22.1 \text{ cm.}^{-1}$, $B = 1.41$, and $A/B = 15.67$. The spin doubling of ${}^2\Sigma$ is very small, and conditions are approaching those of Case (b). We have not constructed the counterpart of Fig. 64 for transitions. The student may do this as an exercise and verify that the first lines of the possible branches are

$$\begin{aligned} {}^2\Sigma \rightarrow {}^2\Pi_{11} \text{ (normal)} & \left\{ {}^oP_{12} (1\frac{1}{2}), P_2 (1\frac{1}{2}), {}^rQ_{12} (1\frac{1}{2}), Q_2 (1\frac{1}{2}), {}^Q R_{12} (1\frac{1}{2}), \right. \\ & \quad \left. {}^sR_{21} (1\frac{1}{2}), \right. \\ {}^2\Sigma \rightarrow {}^2\Pi_1 \text{ (normal)} & \left\{ P_1 (1\frac{1}{2}), {}^qP_{21} (1\frac{1}{2}), Q_1 (1\frac{1}{2}), {}^RQ_{21} (1\frac{1}{2}), R_1 (1\frac{1}{2}), {}^sR_{21} (1\frac{1}{2}), \right. \\ {}^2\Sigma \rightarrow {}^2\Pi_{11} \text{ (inverted)} & \left\{ P_1 (1\frac{1}{2}), {}^qP_{21} (1\frac{1}{2}), Q_1 (1\frac{1}{2}), {}^RQ_{21} (1\frac{1}{2}), R_1 (1\frac{1}{2}), \right. \\ & \quad \left. {}^sR_{21} (1\frac{1}{2}), \right. \\ {}^2\Sigma \rightarrow {}^2\Pi_1 \text{ (inverted)} & \left\{ {}^oP_{12} (1\frac{1}{2}), P_2 (1\frac{1}{2}), {}^rQ_{12} (1\frac{1}{2}), Q_2 (1\frac{1}{2}), {}^Q R_{12} (1\frac{1}{2}), R_2 (1\frac{1}{2}). \right. \end{aligned}$$

* Data from Fredrickson and Watson, *Phys. Rev.*, vol. 39, p. 753 (1932).

† Data from F. A. Jenkins, *Phys. Rev.*, vol. 35, p. 315 (1930).

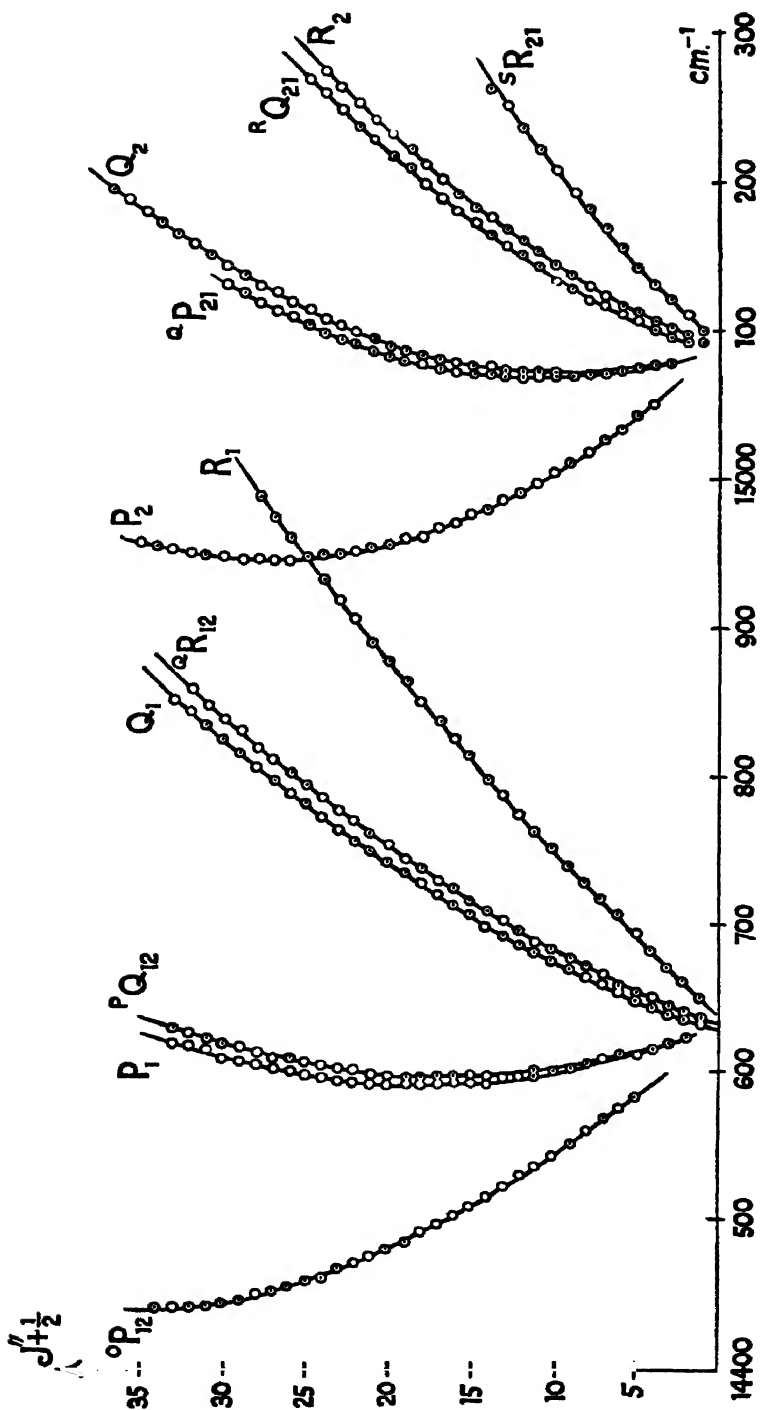


Fig. 65. Fortrat diagram for (0,0) band of BaH ($^2\Pi \rightarrow ^2\Sigma$) typical Case (a) conditions of the $^2\Pi$ state.

Combination Relations (${}^2\Pi \rightarrow {}^2\Sigma$)

As is evident by examination of Fig. 64, the typical lines of the twelve possible branches are given by :

$$\left. \begin{aligned} R_1(J) &= F_{1d}'(J+1) - F_{1c}''(J), \\ {}^sR_{21}(J) &= F_{2c}'(J+1) - F_{1c}''(J), \\ {}^qR_{12}(J) &= F_{1c}'(J+1) - F_{2c}''(J), \\ R_2(J) &= F_{2d}'(J+1) - F_{2c}''(J), \\ Q_1(J) &= F_{1c}'(J) - F_{1c}''(J), \\ {}^RQ_{21}(J) &= F_{2d}'(J) - F_{1c}''(J), \\ {}^PQ_{12}(J) &= F_{1d}'(J) - F_{2c}''(J), \\ Q_2(J) &= F_{2c}'(J) - F_{2c}''(J), \\ P_1(J) &= F_{1d}'(J-1) - F_{1c}''(J), \\ {}^qP_{21}(J) &= F_{2c}'(J-1) - F_{1c}''(J), \\ {}^oP_{12}(J) &= F_{1c}'(J-1) - F_{2c}''(J), \\ P_2(J) &= F_{2d}'(J-1) - F_{2c}''(J). \end{aligned} \right\} \quad (110)$$

From these we can at once write down certain line differences from which the rotational function can be evaluated or the values of $B' + \delta_d$,

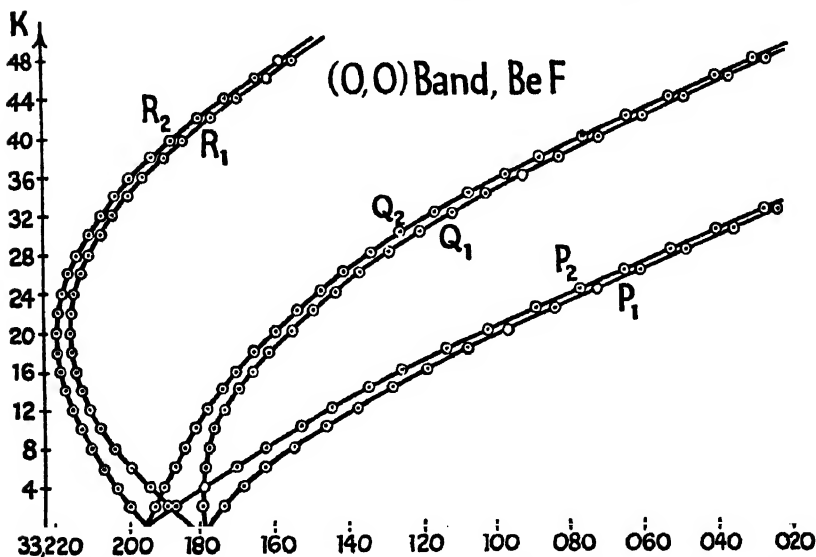


Fig. 66. Fortrat diagram for (0,0) band of BeF (${}^2\Pi \rightarrow {}^2\Sigma$), this is approaching Case (b) conditions of the ${}^2\Pi$ state. (After Jenkins.)

$B' + \delta_c$ (see Chapter VII (g)) for the ${}^2\Pi$ state, and B'' for the ${}^2\Sigma$ state can be found. Thus for the upper ${}^2\Pi$ state :

$$\left. \begin{aligned} R_1(J) - P_1(J) &= \Delta_2 F_{1d}'(J), \\ R_2(J) - P_2(J) &= \Delta_2 F_{2d}'(J), \\ {}^qR_{12}(J) - {}^oP_{12}(J) &= \Delta_2 F_{1c}'(J), \\ {}^sR_{21}(J) - {}^qP_{21}(J) &= \Delta_2 F_{2c}'(J), \end{aligned} \right\} \quad (111)$$

where $\Delta_2 F(J)$ stands for $F(J+1) - F(J-1)$ and $\Delta_1 F(J + \frac{1}{2})$ stands for $F(J+1) - F(J)$.

The spin separation $F_1'(K + \frac{1}{2}) - F_2'(K - \frac{1}{2})$, which, as we see from Fig. 63, is the same as $F_1'(J+1) - F_2'(J)$, is given directly by the following differences:

$$\left. \begin{aligned} R_1(J) - {}^R Q_{21}(J) &= {}^R Q_{12}(J+1) - P_2(J+1) \\ &= F_{1d}'(J+1) - F_{2d}'(J), \\ {}^Q R_{12}(J) - Q_2(J) &= Q_1(J+1) - {}^Q P_{21}(J+1) \\ &= F_{1c}'(J+1) + F_{2c}'(J). \end{aligned} \right\} \quad (112)$$

The Λ -type doublet interval

$$F_{1d}'(J) - F_{1c}'(J) = Z_1(J), \text{ say,}$$

and

$$F_{2d}'(J) - F_{2c}'(J) = Z_2(J), \text{ say,}$$

do not correspond to any particular wave-number difference.

But since $R_1(J) - Q_1(J) = \Delta_1 F_{1d}'(J + \frac{1}{2}) + Z_1(J)$,

and $Q_1(J+1) - P_1(J+1) = \Delta_1 F_{1d}'(J + \frac{1}{2}) - Z_1(J+1)$,

we have by subtraction the sum of the widths of adjacent Λ -doublets:

$$\begin{aligned} R_1(J) - Q_1(J) - Q_1(J+1) + P_1(J+1) \\ = Z_1(J) + Z_1(J+1) \quad . \quad . \quad (113) \end{aligned}$$

and to a close approximation this might be taken as $2Z_1(J + \frac{1}{2})$. An expression for $2Z_2(J + \frac{1}{2})$ is obtained by replacing 1 by 2 in (113). For the lower ${}^2\Sigma$ state the obvious relations are:

$$\left. \begin{aligned} R_1(J-1) - P_1(J+1) \\ = {}^S R_{21}(J-1) - {}^Q P_{21}(J+1) = \Delta_2 F_1''(J), \\ R_2(J-1) - P_2(J+1) \\ = {}^Q R_{12}(J-1) - {}^O P_{12}(J+1) = \Delta_2 F_2''(J). \end{aligned} \right\} \quad (114)$$

The spin doublet interval in this state $F_1''(K + \frac{1}{2}) - F_2''(K - \frac{1}{2})$, which is therefore $F_{1c}''(J+1) - F_{2c}''(J)$, can, as we see from (110), be derived from the four equal quantities

$$\begin{aligned} R_2(J) - {}^R Q_{21}(J+1) &= {}^Q R_{12}(J) - Q_1(J+1) \\ &= Q_2(J) - {}^Q P_{21}(J+1) = {}^R Q_{12}(J) - P_1(J+1) \quad . \quad . \quad (115) \end{aligned}$$

It should be a linearly increasing interval as per equation (108), viz. $\gamma(J-1)$.

(g) ${}^2\Pi \rightarrow {}^2\Pi$ BANDS

The structure of these bands depends to some extent on whether both ${}^2\Pi$ states are Case (a), both Case (b), or one Case (a) and the other Case (b). We shall deal with two of these possibilities, the first and the third, which are illustrated respectively by the β -bands of NO and the ultra-violet bands of O_2^+ (see Plate V).

We saw that in Case (a), where spin is coupled to the nuclear axis, its projection gives a quantum number Σ (see (66)), the restriction upon which results in two distinct sub-bands ${}^2\Pi_{11} \rightarrow {}^2\Pi_{11}$ and ${}^2\Pi_1 \rightarrow$

${}^2\Pi_1$. We have seen in (82) that the Λ -type doubling is negligibly small in Π_{11} states, hence we find three apparently single branches in the first of these, but six branches in the latter sub-band. Q branches are theoretically possible, but their intensities are low, so that not more than the first few lines are likely to be visible in practice. There will only be the usual null line missing between the P_1 and R_1 branches, since $\Omega' = \frac{1}{2}$, $\Omega'' = \frac{1}{2}$, and $J = \Omega + 1$, $\Omega + 2$, &c. But besides the null line the first doublet of each of the P_2 and R_2 branches will be missing in the $\Pi_{11} \rightarrow \Pi_{11}$ band, since $\Omega' = 1\frac{1}{2}$ and $\Omega'' = 1\frac{1}{2}$. The missing doublets will be $P_2(1\frac{1}{2})$ and $R_2(1\frac{1}{2})$.

The combination principle as described for ${}^1\Pi \rightarrow {}^1\Pi$ bands is applicable to ${}^2\Pi \rightarrow {}^2\Pi$ bands (see (100) and (101)). In the case of ${}^2\Pi_1 \rightarrow {}^2\Pi_1$ the letters c or d should have 1 before them; in the case of ${}^2\Pi_{11} \rightarrow {}^2\Pi_{11}$ they should have the prefix 2 before them.

Fig. 67 (2) represents transitions from a ${}^2\Pi$ state under Hund's Case (b) conditions to a ${}^2\Pi$ state under Case (a) conditions. Since in Case (b) the spin is not linked to the nuclear axis and there is no consequent quantum number Σ , there is no restriction $\Delta\Sigma = 0$ as per (66). We observe, as a consequence, that additional branches are possible. In Fig. 67 (2) the Q_2 and Q_1 branches which are theoretically possible have not been shown because of their very low intensity. For the same reason, ${}^nQ_{21}$ and ${}^nQ_{12}$, which are theoretically possible, are not shown. Each sub-band will thus appear to have four branches of close Λ -type doublets. The alternating strengths of the levels have been referred to at the end of Section (c). It is found in all homonuclear molecules. In the case of O_2^+ the weaker levels of Fig. 67 (ii) are entirely absent, so that one component of each Λ -type doublet is absent, and this gives a staggered effect of the branch lines.

In Fig. 68 is shown a Fortrat diagram* for the (0,8) band (see Plate V) of the O_2^+ ultra-violet system. In the case of this spectrum the Λ -type doubling was found to be negligible in the upper ${}^2\Pi$ state, but appreciable in the lower one. The use of the ${}^n P_{12}$, ${}^n R_{12}$, ${}^n P_{21}$, and ${}^n R_{21}$ branches in evaluating the rotational functions F' and F'' and the extent of the Λ -type doubling are illustrated in the original paper to which reference may be made.

(h) ${}^2\Delta \rightarrow {}^2\Pi$ BANDS

There are not many bands known corresponding to this type of transition. One of these due to a CH molecule with its head near λ 4315 is familiar to all spectroscopists and can easily be photographed from the blue cone of a bunsen flame or a carbon arc burning in hydrogen. It is the (0,0) band of the system, and apart from a faint (1,1) band the only representative of the electron transition

$$(1s\sigma)^2(2s\sigma)^2(2p\sigma)(2p\pi)^2 \rightarrow (1s\sigma)^2(2s\sigma)^2(2p\sigma)^2(2p\pi).$$

The ${}^2\Pi$ end-state is normal and near Case (b), since $(A/B) = 2.00$. In Fig. 69 we see the spin doubling and Λ -type doubling. The ${}^2\Delta$ -state also has spin doubling and Λ -type doubling, although the latter is too small to be resolved. Theoretically twenty branches are

* Data from D. S. Stevens, *Phys. Rev.*, vol. 38, p. 1292 (1931).

possible, but the eight shown with broken lines are much fainter than the other twelve, and are in fact of the 'satellite' type. (Intensities

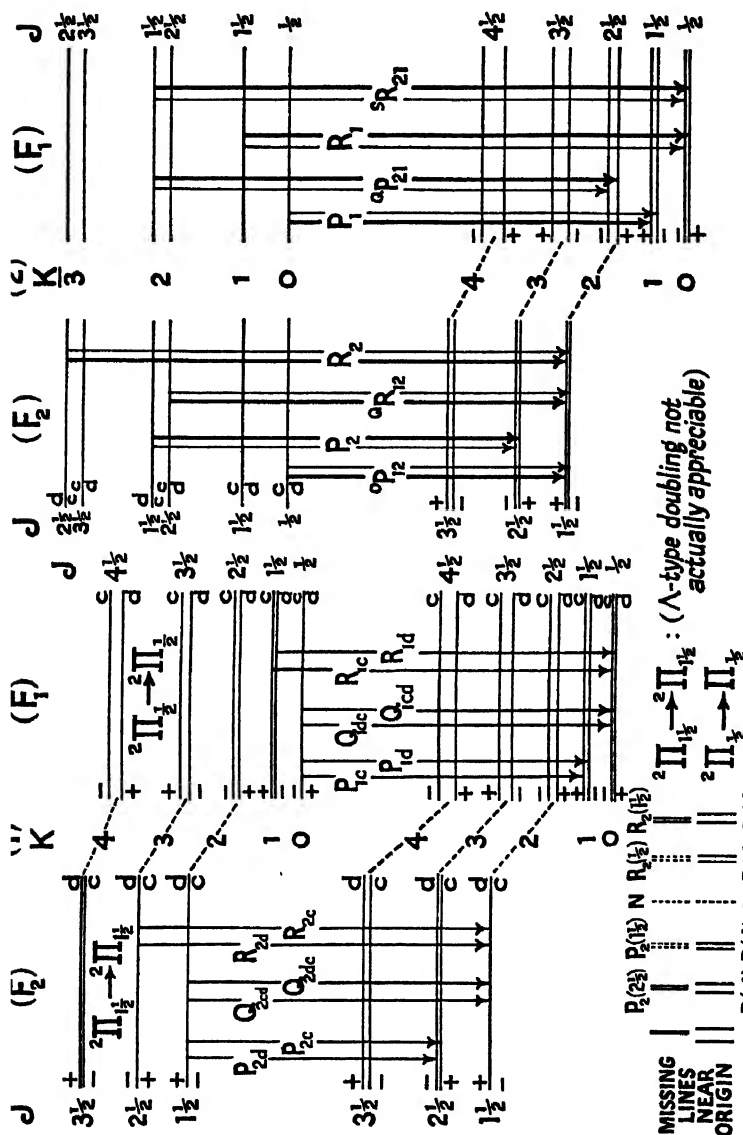


Fig. 67. Rotational transitions ($\Pi \rightarrow {}^2\Pi$).

(i) Case (a) \rightarrow Case (a), e.g. β -NO bands. (ii) Case (b) \rightarrow Case (a), e.g. O_2^+ bands in the ultra-violet.

on a relative scale are shown in brackets.) In accordance with the minimum values of J , viz. F_1' ($1\frac{1}{2}$), F_2' ($1\frac{1}{2}$), F_1'' ($1\frac{1}{2}$), and F_2'' ($\frac{1}{2}$) the first observed lines of the various branches will be P_1 ($3\frac{1}{2}$), Q_1 ($2\frac{1}{2}$), R_1 ($1\frac{1}{2}$), and P_2 ($2\frac{1}{2}$), Q_2 ($1\frac{1}{2}$), R_2 ($\frac{1}{2}$).

The student may easily write down for himself the combination relations which are useful, bearing in mind that the lines of the twelve main branches are :

$$\left. \begin{aligned} R_{1dc}(J) &= F_{1d}'(J+1) - F_{1c}''(J), \\ R_{1cd}(J) &= F_{1c}'(J+1) - F_{1d}''(J), \\ Q_{1c}(J) &= F_{1c}'(J) - F_{1c}''(J), \\ Q_{1d}(J) &= F_{1d}'(J) - F_{1d}''(J), \\ P_{1dc}(J) &= F_{1d}'(J-1) - F_{1c}''(J), \\ P_{1cd}(J) &= F_{1c}'(J-1) - F_{1d}''(J), \end{aligned} \right\} \quad . \quad (116)$$

with six similar expressions in which the suffix 2 replaces 1.

(i) ${}^3\Sigma \rightarrow {}^3\Sigma$ BANDS

Upon reference back to Chapter VII (b), it will be found that the rotational terms of a ${}^3\Sigma$ state should be represented by

$$F(K) = B_v K(K+1) + D_v K^2(K+1)^2 + f(K, J-K) \quad . \quad (117)$$

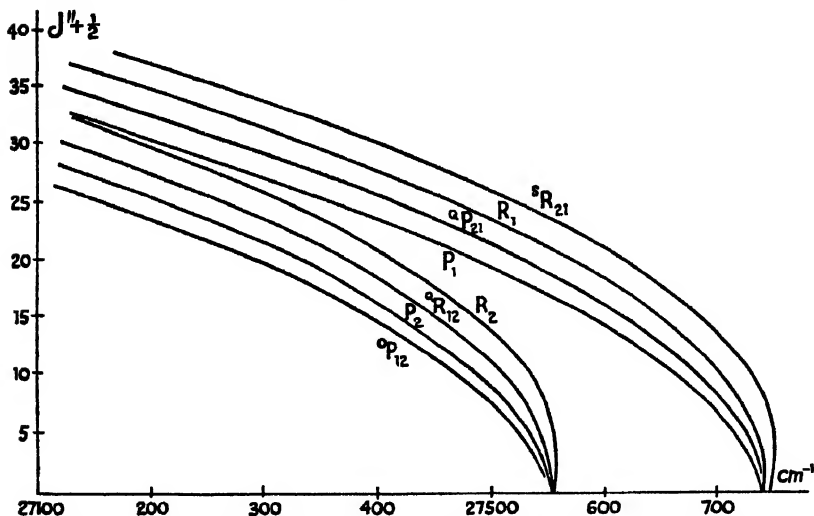


Fig. 68. Fortrat diagram of the (0,8) band of ${}^2\Pi_u \rightarrow {}^2\Pi_g$ system of O_2^+ .

The three components F_1 , F_2 , and F_3 correspond respectively to $J = K+1$, K , and $K-1$, the spin S being 1. The three values of $f(K, J-K)$ given in (75) may be repeated here for convenience :

$$f_1(K, +1) = K \left(\gamma - \frac{2\varepsilon}{2K+3} \right); \quad f_2(K, 0) = -\gamma + 2\varepsilon;$$

$$f_3(K, -1) = -(K+1) \left(\gamma + \frac{2\varepsilon}{2K-1} \right).$$

The structure of ${}^3\Sigma$ rotational levels is thus triple, and, as Fig. 71 indicates, we have, consistent with the selection rules (84) and (85) ten possible branches. (The first members $R(0)$ and $P(1)$ are, of

course, exceptional.) The two RQ and the two PQ branches* are faint except for low K values, hence the main structure consists of triplets. When we get a little way from the origin, the above-quoted expressions for $f(K, J - K)$ show that we shall have an approximately

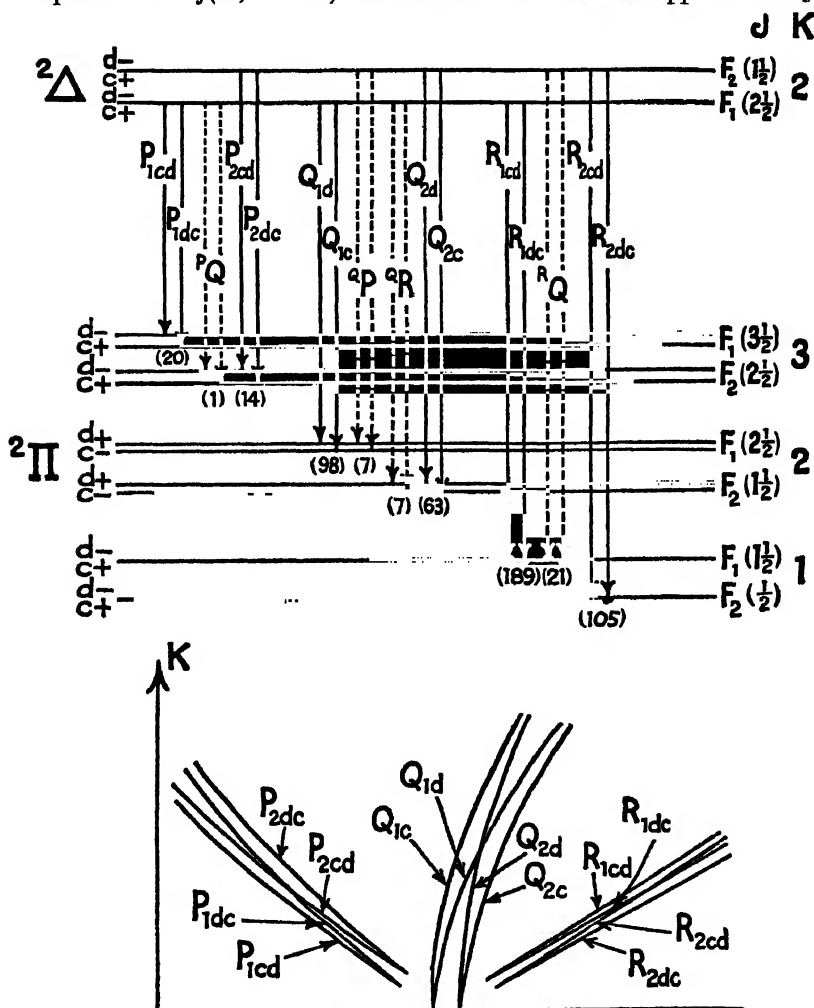


Fig. 69. Transitions giving rise to the CH λ 4315 band $2\Delta \rightarrow 2\Pi$ (Case (b)); also Fortrat diagram showing twelve observed branches (not drawn to scale). (After Jevons.)

linear divergence of $F_1(K)$ and $F_3(K)$ on opposite sides of $F_2(K)$, for when K becomes reasonably large the above expressions reduce to :

$$\begin{aligned} f_1(K, +1) &= K\gamma - \varepsilon; & f_2(K, 0) &= -\gamma + 2\varepsilon; \\ f_3(K, -1) &= -\varepsilon - \gamma(K+1) \end{aligned} \quad (118)$$

* When speaking we refer to these as 'R-form Q' and 'P-form Q'.

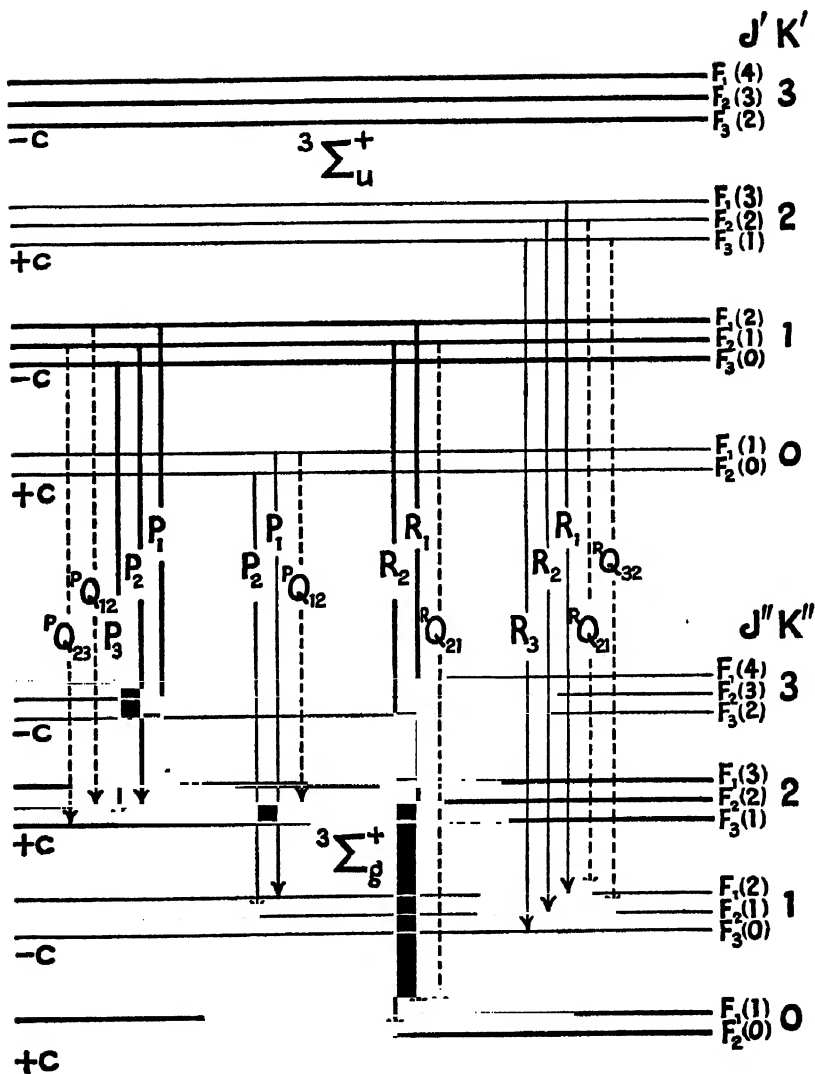


Fig. 70

Notes.

(1) Had we been dealing with a $3\Sigma^- \rightarrow 3\Sigma^-$ transition, the lowest rotational levels $K = 0$ would have been $-$, and the others alternating $+$ and $-$. Also all the levels would be d (see table in Chapter VIII (b)).

(2) In a $3\Sigma_g$ state the $+$ levels are statistically stronger and in a $3\Sigma_u$ state the $-$ levels are stronger. Above we have assumed $u \rightarrow g$. In a homonuclear molecule with zero spin (o.g. S_2) the weaker triplets are absent altogether.

(3) The satellite branches shown in broken lines are theoretically possible but are only of appreciable intensity for low values of K , where they are probably indistinguishable from the main branches.

Typical lines of the R and P branches are given by

$$\begin{aligned} R_i &= \nu_0 + F_i'(K+1) - F_i''(K), \\ P_i &= \nu_0 + F_i'(K-1) - F_i''(K), \end{aligned}$$

where $i = 1, 2$, or 3 .

Hence we have

$$R_i(K) - P_i(K) = F_i'(K+1) - F_i'(K-1) = \Delta_2 F_i'(K),$$

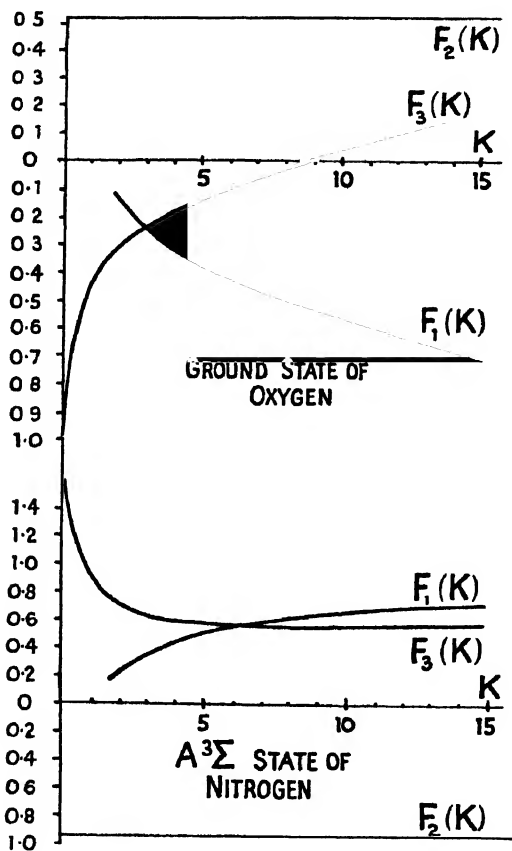


Fig. 71. Separation of components of the rotational spin components F_1, F_2, F_3 of $^3\Sigma$ states.

which from (117) and (118) gives

$$\begin{aligned} i=1 \quad \Delta_2 F_1'(K) &= 2(B_v' + 2D_v' + \gamma') + 4(B_v' + 3D_v')K + 8D_v'K^3, \\ i=2 \quad \Delta_2 F_2'(K) &= 2(B_v' + 2D_v') + 4(B_v' + 3D_v')K + 8D_v'K^3, \\ i=3 \quad \Delta_2 F_3'(K) &= 2(B_v' + 2D_v' - \gamma') + 4(B_v' + 3D_v')K + 8D_v'K^3. \end{aligned}$$

From these, values of B_v' , D_v' , and γ' can be found. Similarly we have $\Delta_2 F_i''(K) = R_i(K-1) - P_i(K+1)$, which gives three similar expressions to the above with $(')$ replacing $(')$.

The values of γ' and γ'' can easily be found otherwise, for it is easy to show

$$\left. \begin{aligned} 2\gamma' &= [R_1(K) - R_2(K)] - [P_1(K) - P_2(K)] \\ &= [R_2(K) - R_3(K)] - [P_2(K) - P_3(K)], \\ 2\gamma'' &= [R_1(K-1) - R_2(K-1)] - [P_1(K+1) - P_2(K+1)] \\ &= [R_2(K-1) - R_3(K-1)] - [P_2(K+1) - P_3(K+1)]. \end{aligned} \right\} \quad (119)$$

The values ϵ' and ϵ'' cannot be found separately from a ${}^2\Sigma \rightarrow {}^3\Sigma$ system, but the value of $(\epsilon' - \epsilon'')$ is determinable. It is easy to show

$$\left. \begin{aligned} 6(\epsilon' - \epsilon'') &= [R_2(K+1) - R_3(K+1)] - [R_1(K) - R_2(K)] \\ &= [P_2(K+1) - P_3(K+1)] - [P_1(K) - P_2(K)] \end{aligned} \right\} \quad (120)$$

For the smaller values of K these results do not hold precisely. In Fig. 70 we have arbitrarily drawn $F_1(K+1) > F_2(K) > F_3(K-1)$, but what will be the relative disposition of the three components for low values of K depends on the magnitude and sign of the constants γ and ϵ . To illustrate this in two typical cases we have in Fig. 71 plotted the values of $f_1(K, +1)$, $f_2(K, 0)$, and $f_3(K, -1)$ of (75) as a function of K for the ground state of O_2 ($\gamma = -0.025$, $\epsilon = +0.242$), and the $A({}^3\Sigma)$ state of N_2 for which $\gamma = -0.003$, $\epsilon = -0.433$. For low values of K it is clear that in the ${}^3\Sigma$ state of O_2 we have $F_2(K) > F_1(K+1) > F_3(K-1)$.

Well-known band systems of the ${}^3\Sigma_u^- \rightarrow {}^3\Sigma_g^-$ are the Schumann-Runge system of O_2 in the ultra-violet, and the strong band systems of S_2 , Se_2 , &c., also that of SO .

(j) ${}^3\Pi \rightleftharpoons {}^3\Sigma$ BANDS

The nature of ${}^3\Sigma$ states has been considered in the preceding section. The appearance of the bands and the number of branches possible will depend on whether the ${}^3\Pi$ state is Case (a) or Case (b), although often in practice we find an approximation to Case (a) for low values of J and a transition to Case (b) for increasing values of J , as the spin detaches itself from the inter-nuclear axis and associates with the rotation axis.

In Case (a) ${}^3\Pi$ falls into three well-separated sub-states ${}^3\Pi_2$, ${}^3\Pi_1$, and ${}^3\Pi_0$, corresponding to $\Omega = 2, 1$, and 0 . The minimum values of J in these three sub-states are there respectively $2, 1$, and 0 . Each level is, of course, subject to Λ -type doubling. For ${}^3\Pi_2$ levels (see Chapter VII (g)) it is very small, but increases in proportion to $J^2(J+1)^2$; for ${}^3\Pi_1$ it is not so small and increases with $J(J+1)$; for ${}^3\Pi_0$ it is the greatest, but should be approximately constant. This difference is a convenient criterion of whether a state is normal or inverted: if it is normal ${}^3\Pi_2$ is above ${}^3\Pi_1$, and ${}^3\Pi_1$ above ${}^3\Pi_0$, and vice versa. (The missing lines near the origin provide another criterion as to a state being normal or inverted.)

In Case (b), on the other hand, the quantum number Ω has no meaning and to a first approximation the rotational energy is $B_1[K(K+1) - \Lambda^2]$, but the spin $S = 1$ splits this up into a triplet term whose components F_1 , F_2 , and F_3 are characterized by $J = K + 1$, $J = K$, and $J = K - 1$. These three levels with a common K draw

closer together as K increases. In passing over from Case (a) to Case (b) we have the following association :

$$\left. \begin{array}{l} \text{Normal} \left\{ \begin{array}{l} {}^3\Pi_2 \rightarrow F'_3(J)_{J=\Lambda-1} \leftarrow {}^3\Pi_0 \\ {}^3\Pi_1 \rightarrow F'_2(J)_{J=K} \leftarrow {}^3\Pi_1 \\ {}^3\Pi_0 \rightarrow F'_1(J)_{J=K+1} \leftarrow {}^3\Pi_2 \end{array} \right\} \\ \text{Case (a)} \end{array} \right\} \text{Inverted Case (a)} \quad (121)$$

In Case (b) the Λ -type doubling is approximately the same in each of the three states F'_1 , F'_2 , and F'_3 , and is proportional to $J(J+1)$. In Fig. 72 is shown one line of each branch in a Case (a) ${}^3\Pi \rightarrow {}^3\Sigma$

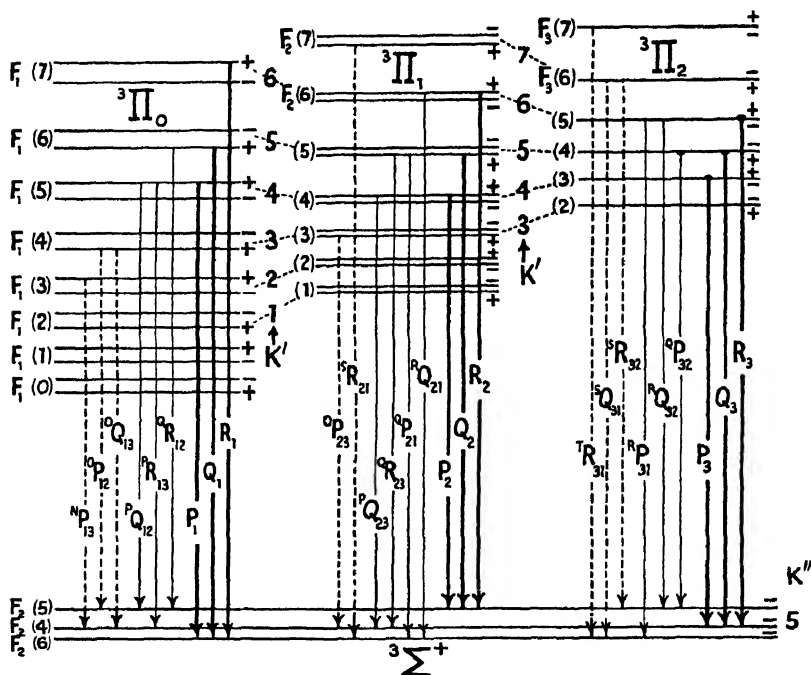


Fig. 72. ${}^3\Pi$ Case (a) \rightarrow ${}^3\Sigma$ transition.

transition. Each sub-band has nine branches, giving a total of twenty-seven branches, and it is interesting to observe that twenty-six branches were actually observed by Naudé* in his analysis of the (6,3) band λ 6623 of the First Positive system of N_2 , although the ${}^3\Pi$ state is an intermediate one between Cases (a) and (b).

Under Case (b) conditions eight of the branches (shown by dotted lines) will be impossible, because the selection principle for K then limits changes strictly to ± 1 , or 0. This leaves nineteen branches in Case (b), as in Fig. 74. Moreover, if it should happen that the spin-multiplicity in the ${}^3\Sigma$ state is negligible, then Case (a) bands will appear to have only fifteen resolved branches, and Case (b) bands only nine (the satellite branches disappearing). This was observed to be the case in the ${}^3\Sigma \rightarrow {}^3\Pi$ Third Positive system of CO analysed by

* Proc. Roy. Soc., A, vol. 136, p. 114 (1932).

Dieke and Mauchly.* The rotational terms for a triplet state are given by Hill and Van Vleck † in a form which is similar to that of (72) and reduces for large values of A/B (Case (a) conditions) to :

$$\left. \begin{aligned} \Omega = \begin{cases} 2 \\ 0 \end{cases} & F(J) = \pm A\Lambda - 2B_v \left(\frac{B_v}{A} \pm \Lambda \right) \\ & + B_v \left(1 \pm \frac{2B_v}{A} \right) [J(J+1) - \Lambda^2], \\ \Omega = 1 & F(J) = 2B_v \left(1 + \frac{2B_v}{A} \right) + B_v [J(J+1) - \Lambda^2]. \end{cases} \quad (122)$$

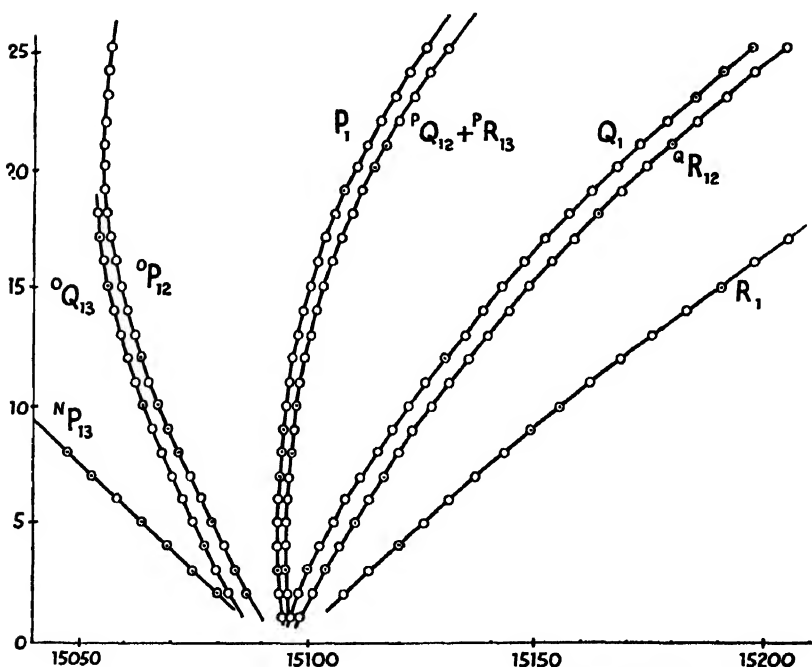


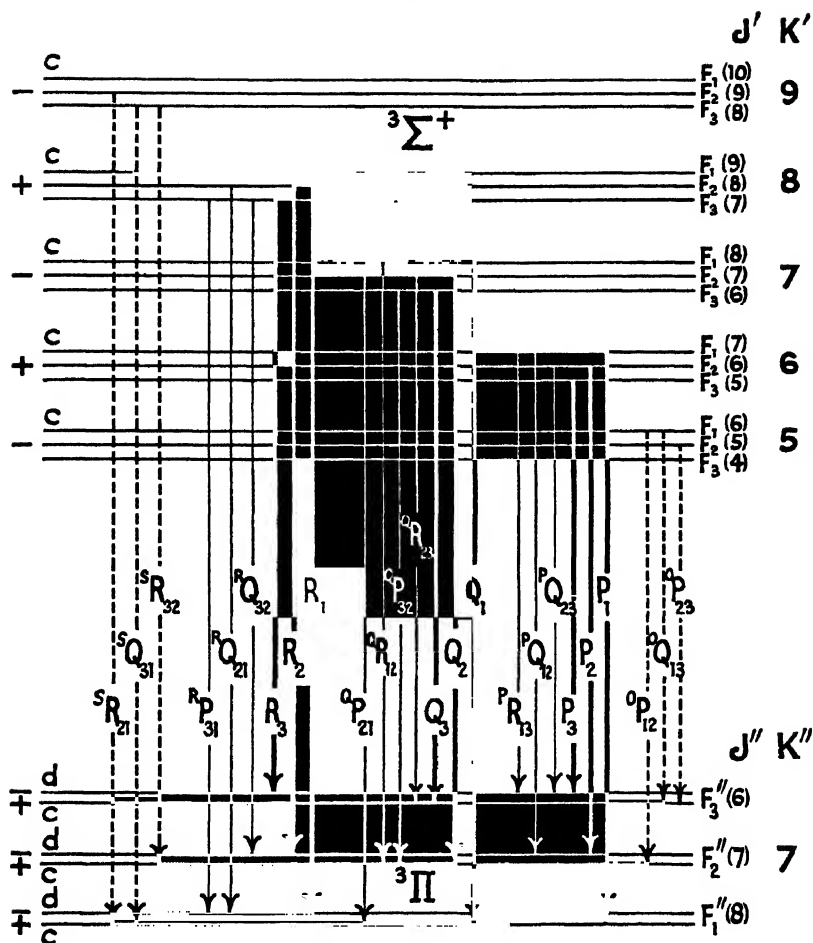
Fig. 73. Fortrat diagram showing nine branches of the ${}^3\Pi_0 \rightarrow {}^3\Sigma$ sub-band of (6,3) First Positive N_2 system.

These are slightly different from the formula (77) for doublet states. It will be observed that the separations of the upper and lower sub-states from the middle one are not quite the same, but of the order $A\Lambda$. Also it will be noted that the effective value of ' B_v ' becomes in the ${}^3\Pi_2$ and ${}^3\Pi_0$ sub-states $B_v \left(1 + \frac{2B_v}{A} \right)$ and $B_v \left(1 - \frac{2B_v}{A} \right)$, respectively. The double-valued term $\phi(J)$ which accounts for Λ -type doubling must be added to the expressions (122).

The rotational terms for a ${}^3\Pi$ state in Case (b), except for a constant

* *Phys. Rev.*, vol. 43, p. 12 (1932).

† *Phys. Rev.*, vol. 32, p. 250 (1928); vol. 33, p. 467 (1929).

Fig. 74. $^3\Sigma \rightarrow ^3\Pi$ Case (b) transition.

and the double-valued $\phi(K)$ which accounts for Λ -type doubling, are given by (117), where the values of $f(K, J - K)$ are

$$f_1 = \frac{A}{K+1} + K\left(\gamma - \frac{2\varepsilon}{2K+3}\right), \quad f_2 = -\frac{A}{K(K+1)} - \gamma + 2\varepsilon, \\ f_3 = -\frac{A}{K} - (K+1)\left[\gamma + \frac{2\varepsilon}{2K-1}\right] \quad . \quad . \quad (123)$$

For detail refer back to Chapter VII (b).

Details of the combination principle as applicable to these bands may be worked out by the student (see Naudé's paper).

(k) $^3\Pi \rightarrow ^3\Pi$ BANDS

The remarks in the preceding section about $^3\Pi$ states are applicable, of course, to these bands; moreover, the remarks applicable to

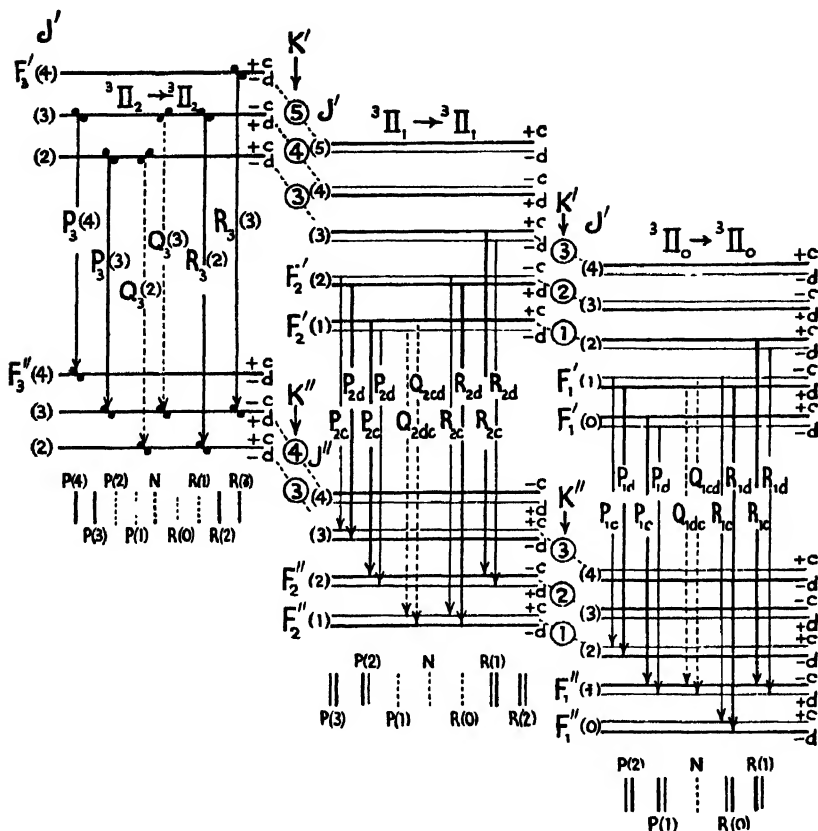


Fig. 75. $^3\Pi_v \rightarrow ^3\Pi_u$. Case (a) normal for both states.

Notes.

(1) The Λ -type doubling in both F'_2 and F'_1 sub-bands has been made far too large to make clear the effect. It is vanishingly small in F'_3 sub-band.

(2) In $^3\Pi_v$ states the + levels are statistically stronger. In $^3\Pi_u$ the - levels are stronger. This applies only to a homonuclear molecule.

$^3\Pi \rightarrow ^3\Pi$ transitions have a general bearing here also. It is possible to have transitions between two Case (a) states, in which case there will be three distinct sub-bands, as illustrated in Fig. 75. Each sub-band will have a strong P and a strong R branch with Λ -type doubling. The Q branches which are theoretically possible are very weak, and (see next chapter) are in $^3\Pi_2 \rightarrow ^3\Pi_2$, $^3\Pi_1 \rightarrow ^3\Pi_1$, and $^3\Pi_0 \rightarrow ^3\Pi_0$

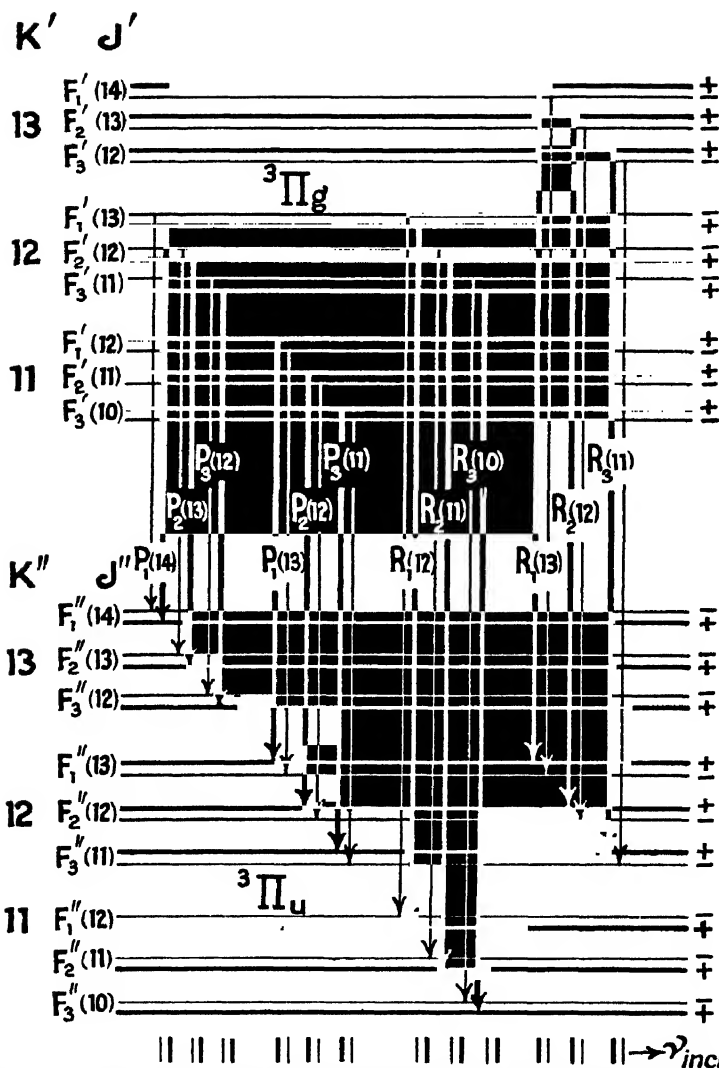


Fig. 76. ${}^3\Pi_g \rightarrow {}^3\Pi_u$. Both states Case (b) and *inverted* showing typical members of R and P branches.

Notes. The notes relevant to Fig. 75 apply here also. In addition :

(1) We have assumed that the spin separation is smaller in the upper than in the lower electronic state for the same value of K . Then (for inverted levels) as we pass outwards from the band origin the order of the triplet components is $R_1(K+1)$, $R_2(K)$, $R_3(K-1)$ and in the P branch $P_1(K-1)$, $P_2(K)$, $P_3(K+1)$. But for normal ${}^3\Pi$ states the order would have been reversed.

(2) We have also assumed in Fig. 75 that the Λ -type doubling was slightly smaller in the upper than the lower state.

(3) In a homonuclear molecule such as C_2 , with zero nuclear spin, the weaker components are absent altogether giving a 'staggering' effect in the branches. In a heteronuclear molecule the two component states have equal weight.

proportional to the values of Ω^2 , so that they are in the ratio 4 : 1 : 0 (absent in the last case). An example of such bands is the blue-green system of TiO, for which A/B is about 135 in the initial state and 132 in the final state. The 'high-pressure' C_2 system and the so-called 'triplet' system of CO, both shown under low dispersion on Plate IV, are probably of this type.

At the other extreme we may have both $^3\Pi$ states in Case (b), in which case the six branches will form triplets P_1, P_2, P_3 , and R_1, R_2, R_3 . The Swan system of C_2 seen under low dispersion in Plate I, is a close approximation to this. So also is the Second Positive N_2 system.* In both of these we have the common phenomenon of a transition from approximately Case (a) conditions at low J -values to Case (b) condi-

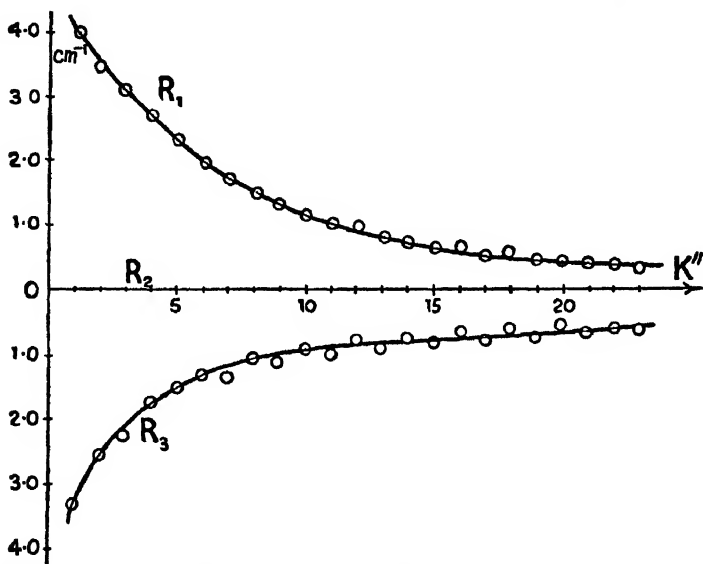


Fig. 77. Triplet separations in the R branch of the (0,0) band λ 5165 of the Swan system of C_2 .

tions at higher J -values. This is apparent from the contraction of the triplet intervals as J increases—a feature associated with the diminishing value of the term involving A in (123) above. Fig. 77 illustrates this feature in the R branch of the (0,0) band of the Swan system of C_2 . The Λ -type doubling might be expected to have shown itself, each branch splitting into components such as $R_{1c}, R_{1d}, R_{2c}, R_{2d}, R_{3c}, R_{3d}$. The C_2 molecule has, however, zero nuclear spin, so that the dotted components of Fig. 76 are absent. The triplets shown are alternately members of the c and d branches. Instead of joining alternate members in Fig. 77, which would reveal the Λ -type doubling, a smooth curve has been drawn through all the points, and there is therefore a slight 'staggering' perceptible with the points first on one side and then on the other of the curve drawn. In the

* For high dispersion photographs see *Phil. Trans.*, A, vol. 226, Plate 4 (1927).

preceding section we remarked that the Λ -type doubling was approximately the same in all three components for Case (b), but that for Case (a) conditions it was largest in the ${}^3\Pi_0$ sub-state, smaller in the ${}^3\Pi_1$ sub-state, and imperceptible in the ${}^3\Pi_2$ sub-state. Until the equality of Case (b) conditions is attained, it follows, therefore, from (121) that the staggering will be most marked in the earlier members of the R_3 branch, and imperceptible in earlier members of the R_1 branch (since the ${}^3\Pi$ states giving the Swan band system are inverted.)

It will be appreciated from Figs. 75 and 76 that the observed Λ -type doubling in branches may in general be either the difference or the sum of the Λ -type doubling in the rotational terms of the two ${}^3\Pi$ states. Which it is cannot be decided from the ${}^3\Pi \rightarrow {}^3\Pi$ system. If, however, another band system, such as ${}^3\Pi \rightleftharpoons {}^3\Sigma$ having its ${}^3\Pi$ state in common, is subject to analysis, the Λ -type doubling which is thus determined for this particular state may allow the question to be settled. Thus Naudé's analysis of the First Positive system ${}^3\Pi \rightarrow {}^3\Sigma$ of N_2 (see Fig. 73) showed the Λ -type doubling of the ${}^3\Pi$ state was larger than that observed in the Second Positive N_2 system which has its final ${}^3\Pi$ state in common. Hence it would appear that in the latter the 'difference' of the Λ -type doublings of the two ${}^3\Pi$ states is involved.

(l) MIXED TRANSITION ${}^3\Pi \rightarrow {}^1\Sigma$

A few band systems are known in which the resultant spin changes so that the initial and final electronic states have different multiplicity. There are, for example, the red atmospheric O_2 bands which can be photographed in absorption ${}^1\Sigma \leftarrow {}^3\Sigma$ and the Hopfield-Birge system of CO near $\lambda 1190$ ${}^3\Sigma \rightleftharpoons {}^1\Sigma$. We take here an example of an inter-system transition, the ${}^3\Pi \rightleftharpoons {}^1\Sigma$ system known as the Cameron system* of CO. The visible absorption bands of ICl and those in the near infra-red of IBr are attributed to the same transition. Fine-structure analysis of the Cameron system shows three fairly close sub-bands, each with three branches. The structure will be clear from a study of Fig. 78, and it is unnecessary to go into further detail.

(m) PERTURBATIONS

It is not uncommon to find that a certain band line or a small group of lines is displaced from the expected positions. Sometimes this is associated with an intensity reduction also, and sometimes with the appearance of additional lines, as though splitting had taken place. Such phenomena are described as perturbations, and their cause is now in a general sense understood. The perturbation is fundamentally one of the rotational energy levels, and thus if it is a level J' (associated with the initial electronic state) which is perturbed, the phenomenon will show itself in both branches by perturbation of $P(J' + 1)$ and $R(J' - 1)$, whereas if a rotational level J'' (associated with the final electronic state) is perturbed, it will reveal itself in $P(J'')$ and $R(J'')$.

* *Phys. Rev.*, vol. 52, p. 467 (1937).

Fig. 21 (e) and (f) provide a picture of how perturbations may arise as a type of resonance between the levels of two intersecting $U(r)$ curves. Such intersections as these cannot cause pre-dissociation, but it is probable that some mutual disturbance results. Thus if a band system arises by transitions $A \rightarrow X$ (where X is a lower electronic state) and another band system is possible such as $B \rightarrow X$ or $B \rightarrow Y$, then a 'leaking away' of the molecular emitters from the first to the second band system may take place. Hence some of the lines of the first system may be abnormally weakened. Moreover, the

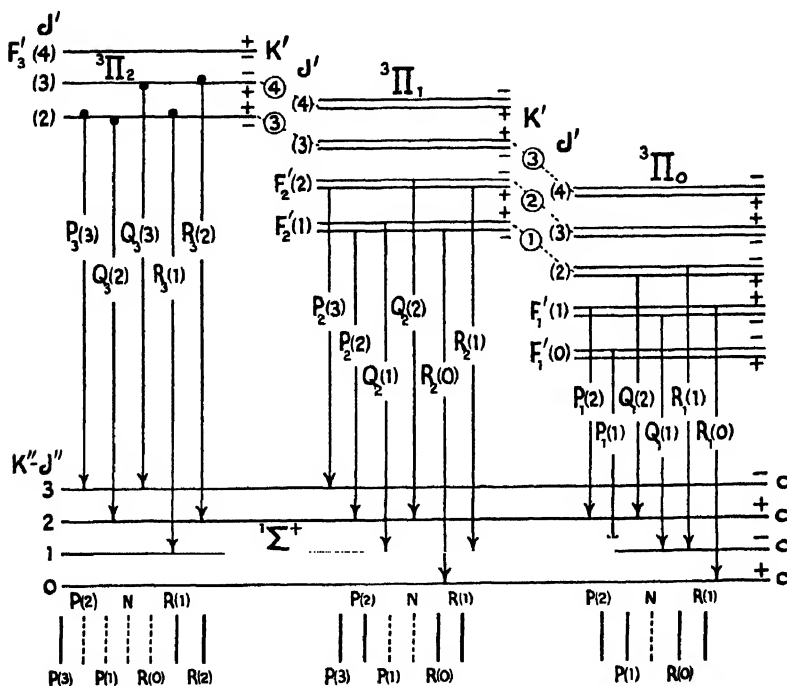


Fig. 78. Rotational transitions for $\text{Case (a)} \left\{ \begin{array}{l} \text{normal} \end{array} \right\} 3\Pi \rightarrow 1\Sigma$.

appearance of additional sporadic lines (the apparent 'splitting' referred to above) may be due to lines of the system $B \rightarrow X$ thus excited, even though the stronger part of this latter system may be located in another region of the spectrum.

It does not necessarily follow that all intersecting $U(r)$ states will be mutually perturbed. It appears that certain conditions must be satisfied, and these were stated by Kronig to be :

- (a) The states must have equal energy for the same total quantum number J (i.e. $\Delta J = 0$).
- (b) $\Delta \Lambda = \pm 1$ or 0, and $\Delta S = 0$.
- (c) Symmetry properties must be the same in both (both c , or both d).

(d) In the case of homonuclear molecules both states must be g , or both u .

(e) The inter-nuclear distances in the two states must not be too different.

These, except for (b), are in contrast with the normal conditions for radiative transitions (68) $u \rightleftharpoons g$, (84) $\Delta J = \pm 1$ or 0, and (86).

Dieke made an early study of these conditions in relation to the He_2^* band spectrum, and showed that the observed perturbations took place when these conditions were fulfilled. He later investigated

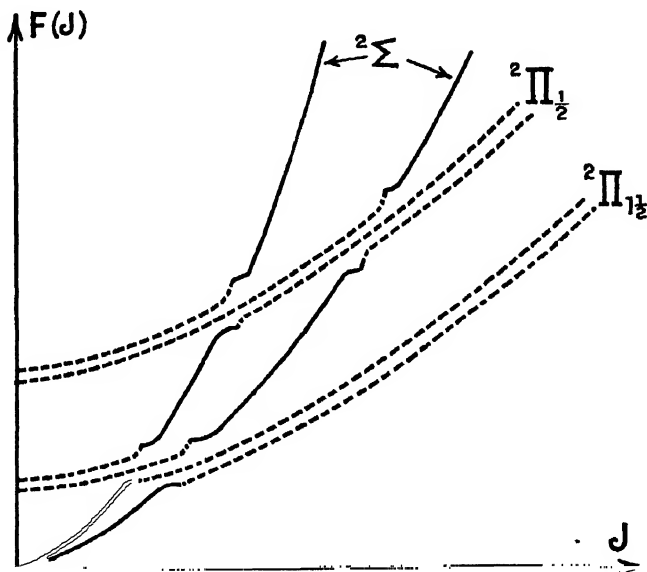


Fig. 79. Perturbation of Inverted ${}^2\Pi$ levels and ${}^2\Sigma$ levels. (The Λ -type doubling of the dotted lines is shown diagrammatically only. It is in practice very small for the ${}^2\Pi_{1/2}$ state.)

the H_2^+ spectrum from this point of view. Ittmann[†] extended Kronig's work and showed that the mutual perturbation of a ${}^2\Sigma$ and ${}^2\Pi_{\text{inv}}$ intersection would be as illustrated in Fig. 79. Passing from low to higher values of J , we observe that from the point of view of the ${}^2\Sigma$ rotational levels those prior to the perturbation are displaced to the low-frequency side, and those after the perturbation to the high-frequency side. The intersection of ${}^2\Pi_{\text{inv}}$ and ${}^2\Sigma$ levels giving rise to perturbation will be illustrated by the spectra of CN. It is well known that CN has two strong band systems, the violet bands ${}^2\Sigma \rightarrow {}^2\Sigma$ (see Plate VII) and the red bands ${}^2\Pi \rightarrow {}^2\Sigma$ (see Plate VIII). They have their final ${}^2\Sigma$ state, which is the ground state of the mole-

* *Phys. Rev.*, vol. 38, p. 646 (1931).

† *Ibid.*, vol. 48, p. 610 (1935); vol. 50, p. 797 (1936).

‡ *Z. Physik*, vol. 71, p. 616 (1931).

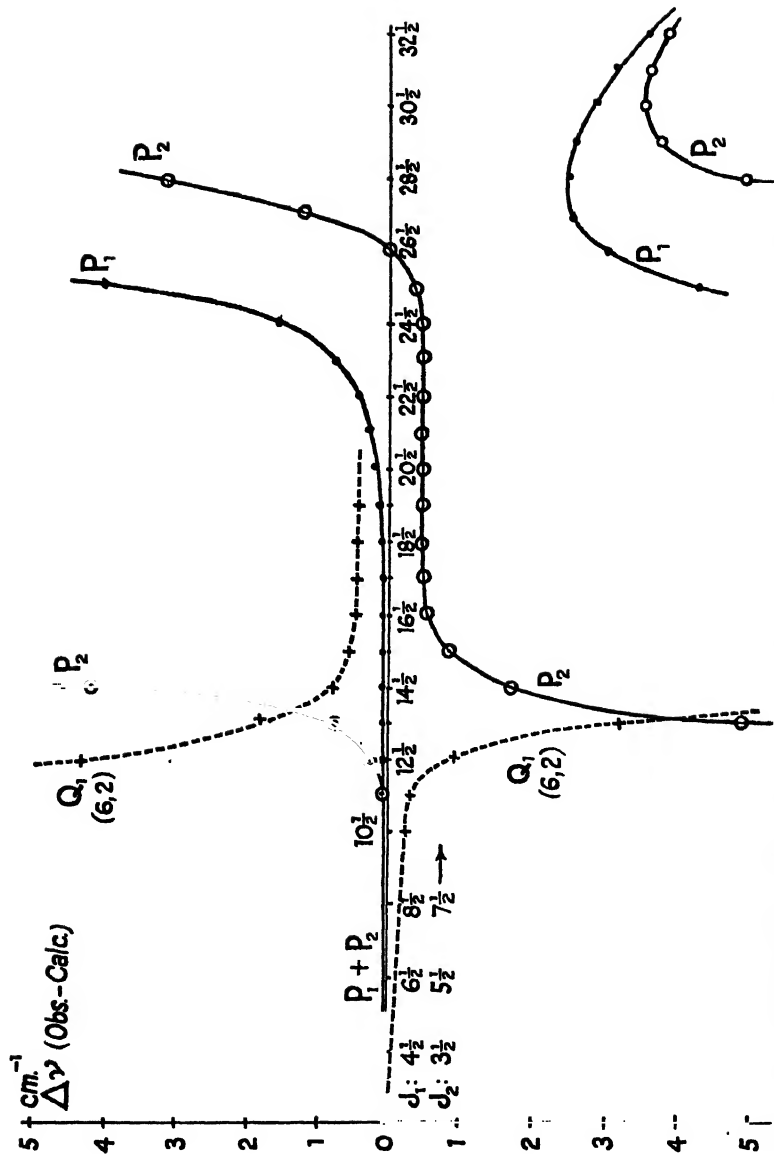


Fig. 80. Perturbations in CN bands. Full curve: (11,11) band $2\Sigma \rightarrow 2\Sigma$ violet CN. Broken curve: (6,2) band $2\Pi \rightarrow 2\Sigma$ red CN. (After Rosenthal and Jenkins.)

cule, in common. The perturbations of CN * were first studied by Rosenthal and Jenkins, and later more completely by Jenkins, Roots, and Mulliken. In Fig. 80 is a graph showing the lines of the P branch of the (11,11) band of ${}^2\Sigma \rightarrow {}^2\Sigma$. The perturbation occurs by reason of a near coincidence of certain rotational levels $J = 13\frac{1}{2}$, $25\frac{1}{2}$, and $27\frac{1}{2}$, of the level $v'' = 11$ of the lower (ground state) ${}^2\Sigma$ with the levels of ${}^2\Pi_{11}$ ($v' = 6$), $J = 13\frac{1}{2}$, and $25\frac{1}{2}$, and ${}^2\Pi_1$ ($v' = 6$), $J = 27\frac{1}{2}$. This has been demonstrated with considerable precision by Jenkins, Roots, and Mulliken, to whose paper reference may be made. In the same Fig. 80 is constructed the date of the Q_1 branch of the (6,2) red CN band to illustrate the reciprocal perturbation. The diagram was constructed by plotting the deviations of observed lines from their positions as calculated from a smooth function derived to fit the unperturbed lines of the branch. The displacement is reminiscent of the anomalous dispersion type of curve found in textbooks of optics.

Although perturbations in the P branch only of the (11,11) ${}^2\Sigma \rightarrow {}^2\Sigma$ band is shown in Fig. 80, the corresponding lines of the R branch (with the same J values) are likewise displaced. The positions can be located from a knowledge of the combination differences $\Delta_2 F'(J)$, viz. $R(J) = P(J) + \Delta_2 F'(J)$.

The question may be raised as to which branches of the (6,2) red CN band will be perturbed. In Fig. 80 we have only plotted deviations of the Q_1 branch. If reference is made to Fig. 64 (2), we see the various types of branch found in these bands. If the ${}^2\Pi$ levels there corresponded to $v = 6$, and the ground level ${}^2\Sigma$ to $v = 11$, then, as we have seen, it is a coincidence in the case of ${}^2\Pi_{11}$ and ${}^2\Sigma$ at $J = 13\frac{1}{2}$ and $25\frac{1}{2}$ which causes perturbations, and in the case of ${}^2\Pi_1$ and ${}^2\Sigma$ at $J = 27\frac{1}{2}$. But the symmetry conditions referred to (viz. c perturbed only by c) are satisfied only by the Q_1 and the ${}^oP_{12}$ and ${}^oR_{12}$ branches (and the last two are too faint to observe); also by the Q_2 and the ${}^sR_{21}$ and ${}^oP_{21}$ branches (and again the last two are too faint to observe).

The 'Negative Nitrogen' system ${}^2\Sigma_u^+ \rightarrow {}^2\Sigma_g^+$ of N_2^+ , which is the analogous spectrum to the violet CN system, has been studied by Childs,[†] and later by Parker.[‡] The bands from initial levels $v' = 0, 1, 3, 5, 8$, and 13 show perturbations, and a detailed study of the (0,0) band $\lambda 3914$ shows effects somewhat similar to those of Fig. 80. There is evidence that a number of vibration levels of an intersecting ${}^2\Pi_u$ state are involved.

Another example of perturbations studied in some detail by Rosenthal and Jenkins[§] and others is found in the Ångström system of CO (see Plates II and IV). This well-known system ${}^1\Sigma \rightarrow {}^1\Pi$ has some of the rotational levels associated with final vibrational states perturbed. This is probably by reason of intersection with levels of a ${}^3\Pi$ state which lies just below it, and is the initial state of Merton-Johnson triplet system (${}^3\Pi \rightarrow {}^3\Pi$) of Plate IV. The perturbations recorded in the Ångström bands are approximately at positions given

* *Proc. Nat. Acad. Sc.*, vol. 15, p. 381 (1929); *Phys. Rev.*, vol. 39, p. 16 (1932).

† *Proc. Roy. Soc., A*, vol. 137, p. 641 (1932).

‡ *Phys. Rev.*, vol. 44, p. 90 (1933); vol. 44, p. 914 (1933).

§ *Proc. Nat. Acad. Sc.*, vol. 15, p. 896 (1929).

PERTURBATIONS OF SOME LEVELS OF $^1\Pi$ STATE OF CO

v''	<i>P</i> and <i>R</i> branches	<i>Q</i> branch
0	$J = 9, 16, 27, > 30$	$J = 12, 29, > 35$
1	26, > 35	24, > 29
2	25, 33	29
3	31	28, 34

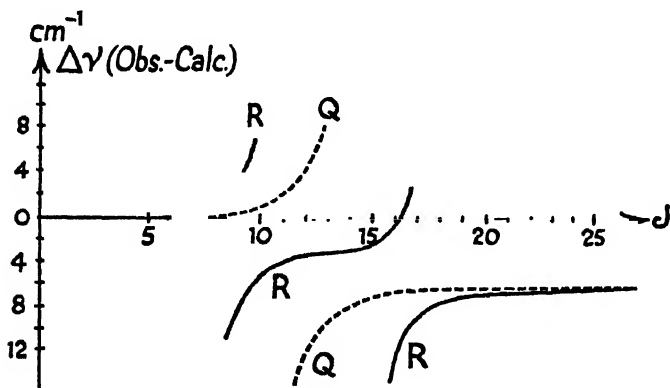


Fig. 81. *R*-branch data of an Angstrom band plotted to show deviations from the equation $R(J) = 22,175.3 + 4.194J + 0.3676J^2 - 0.000546J^3$.

below. The deviations of *R*-branch and *Q*-branch lines are shown in Fig. 81.

It may be remarked that here we have a violation of one of Kronig's theoretical conditions: that interacting states should be of the same multiplicity ($\Delta S = 0$). There appears to be no doubt, however, of the facts themselves.

Another feature to which attention is drawn is the 'permanent displacement of band lines subsequent to the perturbations, so that if, for example, the band head were formed subsequent to $J = 18$, it would appear to be displaced by about 6.5 cm^{-1} from its expected position. Such displacements are actually found in $v'' = 0$ and 1.

The fact that perturbation of the *Q* branch takes place for different values of J from that of the *P*: *R* branch perturbations is due to the necessity of satisfying Kronig's condition (c) on p. 141. As Fig. 56 shows, the lines of *P* and *R* branches in the $^1\Pi$ state terminate on *d*-levels, while the *Q*-branch lines terminate on *c* levels. These rotational levels of the intersecting $^3\Pi$ state which are

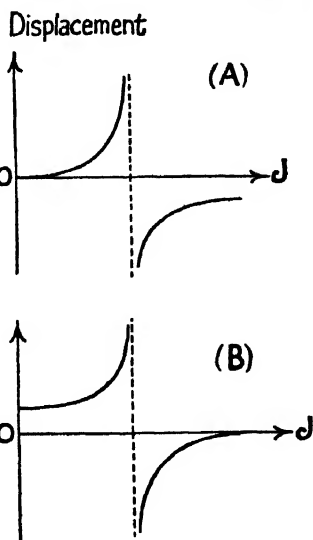


Fig. 82. Dieke's two classes of perturbation.

capable of perturbing *P* and *R*-branch lines at a certain *J*-value cannot, therefore, perturb the *Q*-branch lines at the same *J*-value.

In a theoretical paper Dieke * has grouped perturbations into two classes, *A* and *B*. Class *A* perturbations are due, according to Dieke, to the disturbing force caused by molecular rotation. There can be no displacement at the band origin $J = 0$, but there is a permanent residual displacement following a perturbation. This should obtain in band systems for which $\Lambda' = -\Lambda'' \pm 1$. Class *B* perturbations, which are possible for band systems where $\Lambda' = \Lambda''$, are not primarily rotational in origin, according to Dieke, and in these cases, while there is no residual displacement following a perturbation, there may be a 'vibrational displacement' of the band origin at $J = 0$.

* *Phys. Rev.*, vol. 47, p. 870 (1935).

INTENSITY DISTRIBUTION WITHIN BANDS

(a) GENERAL CONSIDERATIONS

THE appearance of a band will depend on two things : the disposition of the lines which constitute it, and the distribution of intensities among these lines. The first of these has been already considered (equation (24)), and we have seen how the relative values of B' and B'' , both their absolute magnitude and the difference $B' \sim B''$ between them, affects this appearance. Thus a small value of $B' \sim B''$ results in a large interval between band head and origin (Chapter II (b)). The distribution of intensities among the band lines will depend jointly on the population of molecules in the various initial rotational states, and on the probabilities of transition from the initial to the final states. If the initial energy distribution is assumed to be controlled by temperature (T) alone, the energy E in each state will be proportional to the Boltzmann factor $\exp(-E/kT)$, and we can write for the intensity of band lines

$$I = Ci \exp(-E/kT) \quad . \quad . \quad . \quad . \quad (124)$$

Here i is called the intensity factor, and is the product of the statistical weight $(2J+1)$ of the initial state and a fraction which represents the transition probability. (The statistical weight arises because each rotational state is capable of sub-division into $2J+1$ magnetic sub-states in the presence of a magnetic field.) The sum of the i -factors for those band lines which arise from the same initial rotational level J' is therefore $2J'+1$, and the sum of the i -factors for those band lines ending on the same final rotational level J'' is $2J''+1$. The i -factor is a function of J , the rotational quantum number, and the form of this function depends on the type of electronic transition ${}^2\Pi \rightarrow {}^2\Sigma$, ${}^1\Pi \rightarrow {}^1\Pi$, &c., and the type of branch involved. It does not depend at all on the conditions of excitation of the spectrum, on temperature, or on the nature of the molecule. It is considered in detail in the next section.

The total energy E in (124) is $E_e + E_v + E_r$. Since E_e and E_v are constant for a particular band, we may write E_r as the only variable, when considering the intensity within a band. Then (124) may be replaced by

$$I = Ci \exp\left(-\frac{E_r}{kT}\right) = Ci \exp\left(-\frac{hB'J'(J'+1)}{kT}\right) \div Ci \exp\left(-\frac{B'J'(J'+1)}{0.7T}\right) \quad . \quad (125)$$

The question, of course, arises as to how far the rotational energy distribution is governed by temperature. We should expect that just as gas molecules have a statistical distribution of linear velocities about a most probable value which is determined by the gas temperature, so there should be a statistical distribution of angular velocities

about a most probable value also determined by temperature. The characteristic maxima of intensity found at corresponding points in the branches of a band are evidence of this. In practice it is found, however, that the 'effective' temperature as determined from intensity measurements is not always the same as the gas temperature. So far as absorption spectra or thermally excited emission spectra are concerned, there is excellent agreement, but certain types of excitation of emission spectra give 'effective' temperatures (as deduced from the intensity of band lines) vastly higher than the gas temperature. This is discussed in Sections (d) and (e).

The factor C in (124) and (125) calls for comment. Theory shows that we must put (g being a constant)

$$\left. \begin{aligned} C &= g\nu^4 \text{ for emission band lines,} \\ C &= \left(\frac{g}{8\pi hc} \right) \nu \text{ for absorption band lines} \end{aligned} \right\} \quad \cdot \quad \cdot \quad (126)$$

Here ν is the frequency of the band line. Where a band does not extend over too wide a frequency range, C may be regarded as a constant. In comparing the intensities of different bands, or even sub-bands, this variation may, however, sometimes be appreciable. (The theory of intensities has been worked out with matrices. The factor ν^4 comes from the 'correspondence' with the classical theory of an oscillating doublet which radiates energy at a rate proportional to ν^4 . Again in absorption the energy of radiation absorbed per second by an oscillator is proportional to the magnitude of the incident quantum (ν).)*

If absorption band lines are involved, B'' of the lower state replaces B' in (125) and I is the absorption coefficient of the line which is α as defined by the equation $J = J_0 e^{-\alpha x}$, where J_0 is the incident and J the emergent light intensity after a path of length x is traversed. Strictly, α is the integral ($\int \alpha_\nu d\nu$) of the absorption coefficient taken through the absorption line, but if the line widths are constant the peak values will be relatively satisfactory measures of these. The experimentalist should, however, beware of many pitfalls.†

(b) INTENSITY FACTORS (i)

The intensity factors to which we have referred have been calculated for the many different types of transition giving rise to band lines. The various pairs of electronic states, the types of branch, and the types of coupling (whether Hund's Case (a) or (b) or intermediate between them) have been investigated by many investigators. In 1925 Kronig, Russell, Sommerfeld, and Hönsl solved some of the simplest cases by applying the so-called correspondence principle to a simple vector model of the molecule. The Case (a) type of vector coupling was studied by Hönsl and London‡ in 1925. The Case (b)

* See Ruark and Urey, *Atoms, Molecules, and Quanta*, p. 697 (McGraw Hill Book Co., 1930), or Kronig, *Band Spectra and Molecular Structure*, p. 70 (C.U.P., 1930).

† e.g. J. C. Slater, *Phys. Rev.*, vol. 25, p. 783 (1925).

‡ *Zeit. f. Phys.*, vol. 33, p. 803 (1925).

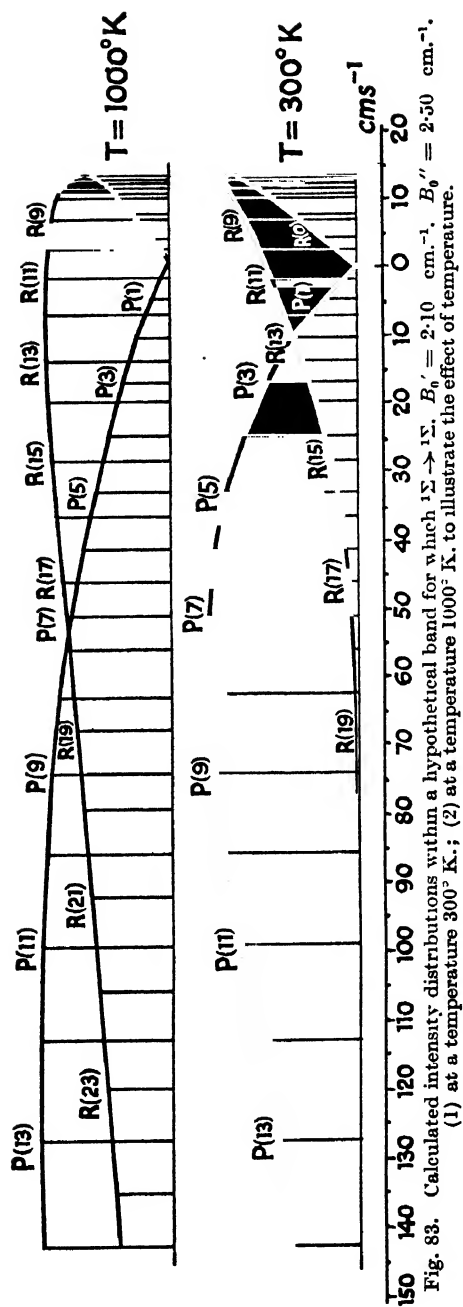


Fig. 83. Calculated intensity distributions within a hypothetical band for which $1\Sigma \rightarrow 1\Sigma$, $B' = 2.10 \text{ cm}^{-1}$, $B'' = 2.50 \text{ cm}^{-1}$. (1) at a temperature 1000°K ; (2) at a temperature 300°K ; to illustrate the effect of temperature.

type and intermediate types were studied by Mulliken,* Van Vleck,† and others, and the use of matrices and wave-mechanics largely confirms the results of the earlier method.‡ In this section we shall therefore record only these results and illustrate their application in particular cases.

TABLE 1
Intensity Factors for Two Singlet States

Branch	$\Sigma \rightarrow \Sigma,$ $\Pi \rightarrow \Pi,$ $\Delta \rightarrow \Delta$ ($\Omega \rightarrow \Omega$)	$\Pi \rightarrow \Sigma, \Delta \rightarrow \Pi$ ($\Omega \rightarrow \Omega - 1$)	$\Sigma \rightarrow \Pi, \Pi \rightarrow \Delta$ ($\Omega - 1 \rightarrow \Omega$)
$P(J)$	$\frac{J^2 - \Omega^2}{J}$	$\frac{(J - \Omega)(J - \Omega + 1)}{2J}$	$\frac{(J + \Omega)(J + \Omega - 1)}{2J}$
$Q(J)$	$\frac{(2J + 1)\Omega^2}{J(J + 1)}$	$\frac{(2J + 1)(J + \Omega)(J - \Omega + 1)}{2J(J + 1)}$	$\frac{(2J + 1)(J + \Omega)(J - \Omega + 1)}{2J(J + 1)}$
$R(J - 1)$	$\frac{J^2 - \Omega^2}{J}$	$\frac{(J + \Omega)(J + \Omega - 1)}{2J}$	$\frac{(J - \Omega)(J - \Omega + 1)}{2J}$

The above intensity factors apply also to pairs of Case (a) states having the same multiplicity, e.g. ${}^2\Pi \rightarrow {}^2\Pi$, ${}^3\Pi \rightarrow {}^3\Pi$, ${}^2\Delta \rightarrow {}^2\Pi$, &c. In practice, however, conditions seldom approximate closely to Case (a) in both states, and tend with increasing J towards Case (b). It may be verified that the sum of the intensity factors for $P(J)$, $Q(J)$, and $R(J)$ for any of the three columns is $2J + 1$, and likewise for $P(J + 1)$, $Q(J)$, and $R(J - 1)$, this being the statistical weight of the level J on which three transitions end, and on which three also begin.

The intensities of typical lines in a simple ${}^1\Sigma_0 \rightarrow {}^1\Sigma_0$ band would be

$$\left. \begin{aligned} P(J) : I_P &= C'J \exp(-B'J(J - 1)/kT), \\ R(J - 1) : I_R &= C'J \exp(-B'J(J + 1)/kT). \end{aligned} \right\} \quad (127)$$

The exponential factor for $P(J + 1)$ will be the same as for $R(J - 1)$, so that these pairs of lines (except for low J -values) will be approximately equal in intensity. We can express the same fact by saying that the P branch will be slightly stronger than the R branch when compared at corresponding branch lines.

In Fig. 84 are constructed the band structures of typical singlet transitions to illustrate the appearance of the intensity distribution. The lengths of the lines represent the intensity values, and are drawn to a relatively correct scale for each band (for particular values of B_0' , B_0'' , and temperature).

A few general remarks may be made from Table 1. We see that such a transition as ${}^1\Sigma_0 \rightarrow {}^1\Sigma_0$ will have no Q branch. Bands of the type ${}^1\Pi_1 \rightarrow {}^1\Pi_1$, or ${}^1\Delta_2 \rightarrow {}^1\Delta_2$, will have a Q branch of rapidly diminishing intensity, which will be appreciable only at low J -values. In transitions of the type ${}^1\Pi \rightleftharpoons {}^1\Sigma$ and ${}^1\Delta \rightleftharpoons {}^1\Pi$ the Q branch will be

* *Phys. Rev.*, vol. 30, p. 787 (1927).

† *Ibid.*, vol. 32, p. 270 (1928); vol. 33, p. 484 (1929).

‡ General reference may be made to Ruark and Urey's book, pp. 716 *et seq.*

In Table 2 are shown the intensity factors for transitions involving

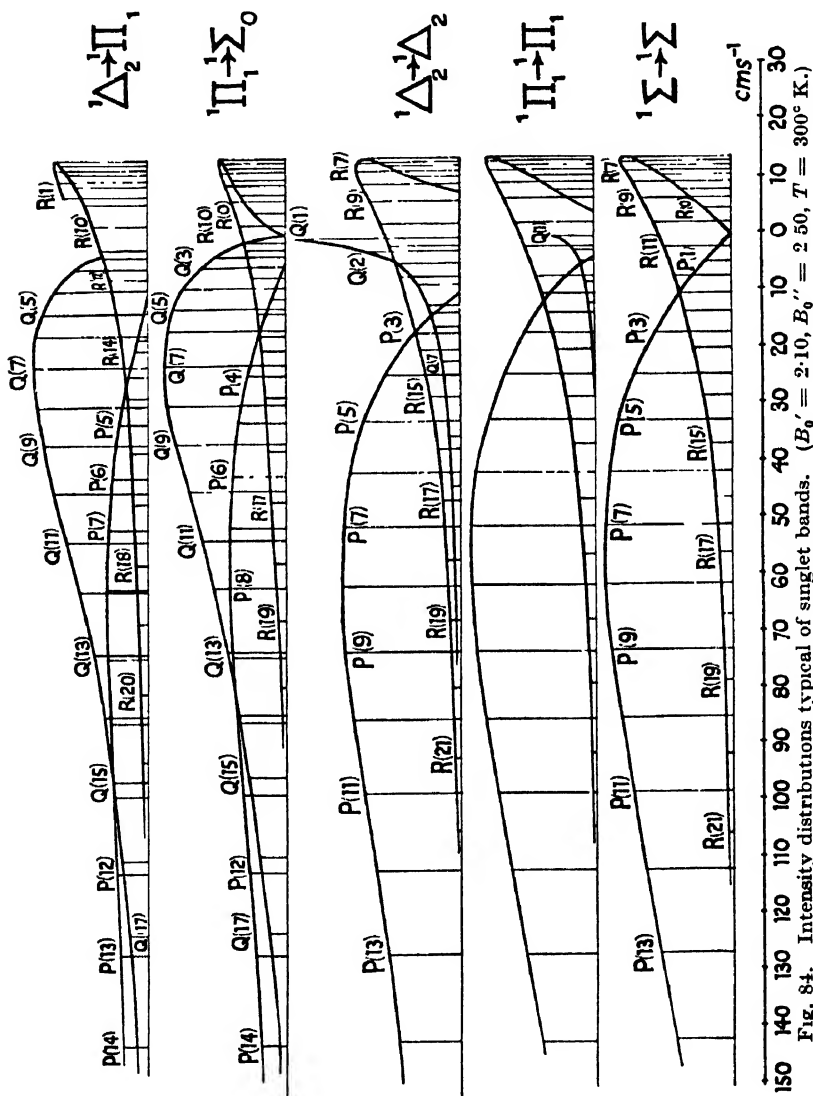


Fig. 84. Intensity distributions typical of singlet bands. ($B_0' = 2.10$, $B_0'' = 2.50$, $T = 300^\circ \text{K.}$)

two Case (b) states. Σ states are necessarily in this category. From the table it is clear that ${}^2\Sigma \rightarrow {}^2\Sigma$ and ${}^3\Sigma \rightarrow {}^3\Sigma$ bands have only six branches, and that the two satellite branches ${}^PQ_{12}$ and ${}^RQ_{21}$ fall off rapidly in intensity with J . Reference to Plate VII, showing the

TABLE 2
Intensity Factors (i). Doublet States, both Case (b)

	ΔJ	ΔK	Br	ΔJ	ΔK	Br	i
$\Lambda \rightarrow \Lambda$ -bands: ${}^2\Sigma \rightarrow {}^2\Sigma$, ${}^2\Pi \rightarrow {}^2\Pi$, ${}^2\Delta \rightarrow {}^2\Delta$.							
$J' = K'$ $J'' = K''$ $++ +$	$\left. \begin{matrix} J-1 \\ \rightarrow J \end{matrix} \right\}$	$K-1$ $\rightarrow K$	P_1	$\left. \begin{matrix} J+1 \\ \rightarrow J \end{matrix} \right\}$	$K+1$ $\rightarrow K$	R_1	$\frac{2(K+1)(K^2-\Lambda^2)}{K(2K+1)}$
$J' = K'$ $J'' = K''$ $-+ -$	$\left. \begin{matrix} J-1 \\ \rightarrow J \end{matrix} \right\}$	$K-1$ $\rightarrow K$	P_2	$\left. \begin{matrix} J+1 \\ \rightarrow J \end{matrix} \right\}$	$K+1$ $\rightarrow K$	R_2	$\frac{2(K-1)(K^2-\Lambda^2)}{K(2K-1)}$
$J' = K'$ $J'' = K''$ $++ -$	$\left. \begin{matrix} J \rightarrow J \end{matrix} \right\}$	$K-1$ $\rightarrow K$	${}^PQ_{12}$	$\left. \begin{matrix} J \rightarrow J \end{matrix} \right\}$	$K+1$ $\rightarrow K$	${}^2Q_{21}$	$\frac{2(K^2-\Lambda^2)}{K(4K^2-1)}$
$J' = K'$ $J'' = K''$ $-+ +$	$\left. \begin{matrix} J-1 \\ \rightarrow J \end{matrix} \right\}$	$K \rightarrow K$	${}^Q P_{21}$	$\left. \begin{matrix} J+1 \\ \rightarrow J \end{matrix} \right\}$	$K \rightarrow K$	${}^Q R_{12}$	$\frac{2\Lambda^2}{K(K+1)(2K+1)}$
$J' = K'$ $J'' = K''$ $++ +$	$\left. \begin{matrix} J \rightarrow J \end{matrix} \right\}$	$K \rightarrow K$	Q_1				$\frac{2(2K+3)\Lambda^2}{(K+1)(2K+1)}$
$J' = K'$ $J'' = K''$ $-+ -$	$\left. \begin{matrix} J \rightarrow J \end{matrix} \right\}$	$K \rightarrow K$	Q_2				$\frac{2(2K-1)\Lambda^2}{K(2K+1)}$

${}^2\Sigma \rightarrow {}^2\Sigma$ violet CN system, reveals that many of the bands appear to have only one P and one R branch, the three component branches being unresolved. In band types such as ${}^2\Pi \rightarrow {}^2\Pi$ (Chapter IX (g)) and ${}^3\Pi \rightarrow {}^3\Pi$ (Chapter IX (k)), it is clear from Table 2 that while Q branches are theoretically possible, they will die out rapidly in intensity. In band types such as ${}^2\Pi \rightleftharpoons {}^2\Sigma$, of the ten branches theoretically possible, the four satellite branches fall off rapidly in intensity with increasing rotational quantum number, but of these satellites the two Q -form branches are about twice as strong as PQ and RQ . The main Q branches are for high K -values about twice as strong as the P and R branches.

It is possible to construct another table dealing with transitions such as ${}^2\Pi \rightleftharpoons {}^2\Sigma$, where the ${}^2\Pi$ state is Case (a) coupling, but in practice such intensity factors are of little value. The nearest approach to Case (a) conditions known is that of HgH, in which (see Chapter VIII (f)) A/B (for which we shall in future use the parameter λ) is 560. Even in this case the observed intensity distribution is not that which theoretical Case (a) intensity factors will account for.

Hill and Van Vleck* in 1928 obtained formulæ for i involving the parameter λ for transitions between states, one or both of which were intermediate between Case (a) ($\lambda = \infty$) and Case (b) ($\lambda = 0$). These were reduced by Earls† to a comparatively simple form in the cases ${}^2\Pi \rightleftharpoons {}^2\Sigma$, and these are given in Table 3.

TABLE 3

${}^2\Pi \rightarrow {}^2\Sigma$		${}^2\Sigma \rightarrow {}^2\Pi$		Intensity factor i
P_2	${}^oP_{12}$	R_2	${}^sR_{21}$	$\frac{(2J+1)^2 + (2J+1)U(4J^2 + 4J + 1 - 2\lambda)}{32(J+1)}$
P_1	${}^oP_{21}$	R_1	${}^oR_{12}$	$\frac{(2J+1)^2 \mp (2J+1)U(4J^2 + 4J - 7 + 2\lambda)}{32(J+1)}$
Q_2	${}^PQ_{12}$	Q_2	${}^RQ_{21}$	$\frac{(2J+1)[(4J^2 + 4J - 1) \pm U(8J^3 + 12J^2 - 2J + 1 - 2\lambda)]}{32J(J+1)}$
Q_1	${}^RQ_{21}$	Q_1	${}^PQ_{12}$	$\frac{(2J+1)[(4J^2 + 4J - 1) \mp U(8J^3 + 12J^2 - 2J - 7 + 2\lambda)]}{32J(J+1)}$
R_2	${}^oR_{12}$	P_2	${}^oP_{21}$	$\frac{(2J+1)^2 + (2J+1)U(4J^2 + 4J - 7 + 2\lambda)}{32J}$
R_1	${}^sR_{21}$	P_1	${}^oP_{12}$	$\frac{(2J-1)^2 \mp (2J+1)U(4J^2 + 4J + 1 - 2\lambda)}{32J}$
				$U = [\lambda^2 - 4\lambda + (2J+1)^2]^{-\frac{1}{2}}$

In many bands as J increases we have a transition of the type of coupling of the ${}^2\Pi$ state from Case (a) or an intermediate condition, more towards Case (b). Table 3 is therefore of practical usefulness. The value of J given in the table is that in the ${}^2\Pi$ state: in other words, the intensity factors shown are for $P(J+1)$, $Q(J)$, and $R(J-1)$. These intensity factors are valid for both positive and negative values of λ (i.e. both normal and inverted doublets), for all

* *Phys. Rev.*, vol. 32, p. 250 (1928).

† *Ibid.*, vol. 48, p. 423 (1935).

values of $J > \frac{1}{2}$. For $J = \frac{1}{2}$ Earls gives the particular values shown (all other branch lines not referred to being zero). In Table 3 the positive sign is taken for U , while the + and - signs of the i -factor refer to the respective pairs of branches in the columns. Thus on

	$^3\Pi \rightarrow ^3\Sigma$	$^3\Sigma \rightarrow ^3\Pi$
$\lambda > 0$	$\begin{cases} {}^oP_{12} = P_1 = \frac{1}{2} \\ {}^oQ_{12} = Q_1 = \frac{1}{2} \end{cases}$	$\begin{cases} {}^sR_{21} = R_1 = \frac{1}{2} \\ {}^sQ_{21} = Q_1 = \frac{1}{2} \end{cases}$
$\lambda < 0$	$\begin{cases} P_2 = {}^oP_{21} = \frac{1}{2} \\ Q_2 = {}^oQ_{21} = \frac{1}{2} \end{cases}$	$\begin{cases} R_2 = {}^sR_{12} = \frac{1}{2} \\ Q_2 = {}^sQ_{12} = \frac{1}{2} \end{cases}$

the first row the + sign refers to P_2 (also to R_2); the - sign to ${}^oP_{12}$ (also to ${}^sR_{21}$). In the paper referred to, Earls has constructed several graphs of $i:J$ for a number of selected values of λ ranging between 0 and ∞ . Passing from Case (b), $\lambda = 0$, to Case (a), $\lambda = \infty$, these graphs show clearly the emergence of the two satellite branches oP and sR , which are forbidden in Case (b) (where $\Delta K = \pm 1$ or 0 strictly). They show clearly the rise of the other four satellite branches from weakness to a strength equal to the main branches (when $\lambda = \infty$).

The i -factors calculated from $\lambda = 560$ (HgH) have been found to agree well with the experimentally determined values.*

It has not been found possible to obtain general formulae for intensity factors of the type given in Table 2 to cover triplet transitions. The limiting types $^3\Pi$ Case (a) $\rightarrow ^3\Sigma$ and $^3\Pi$ Case (b) $\rightarrow ^3\Sigma$ have been evaluated. Nolan and Jenkins† investigated their applicability in the case of the $^3\Pi \rightarrow ^3\Sigma$ (0,0) band of PH at $\lambda 3400$. Plotting the experimentally determined i -factors as a function of J , they got reasonable agreement with the Case (b) values predicted above in all the main branches except for those values of $J = 5$. Pearse,‡ who first analysed this PH band, showed that its $^3\Pi$ state was inverted, and found ${}^3\Pi_0 - {}^3\Pi_1 = 121 \text{ cm.}^{-1}$, ${}^3\Pi_1 - {}^3\Pi_2 = 111 \text{ cm.}^{-1}$, also $B_0' = 7.85 \text{ cm.}^{-1}$, so that an intermediate type of coupling approximating to Case (b) is to be anticipated.

The intensity factors for certain 'mixed' transitions $^1\Sigma \rightleftharpoons ^3\Sigma$ and $^1\Sigma \rightleftharpoons ^3\Pi$ have been investigated by Schlapp,§ and reference may be made to his paper.

(c) TEMPERATURE DETERMINATIONS FROM BAND DATA

We shall defer until the next section a discussion of the results obtained for particular molecules, and the discrepancy which sometimes occurs between the true gas temperature and the temperature as found from the intensity distribution within bands. We concern ourselves here with three methods of analysing the intensity data to find this 'effective' temperature.

* Kapuscinski and Eymers, *Zeit. f. Phys.*, vol. 54, p. 206 (1929).

† Nolan and Jenkins, *Phys. Rev.*, vol. 50, p. 947 (1936).

‡ *Proc. Roy. Soc., A*, vol. 129, p. 328 (1930).

§ *Phys. Rev.*, vol. 39, p. 806 (1932).

(1) *Position of Maximum Intensity in the Branches*

By selecting the line of maximum intensity in a branch the effective temperature can be calculated as shown below. The value of J' corresponding to maximum intensity is given by applying $dI/dJ = 0$ to (125). This gives J'_{max} as the value of J' which satisfies the equation

$$\frac{di}{dJ} = i \frac{B'hc}{KT} (2J' + 1) \quad . \quad . \quad . \quad (128)$$

Thus for a simple band ${}^1\Sigma_0 \rightarrow {}^1\Sigma_0$, where $i_{P(J)} = J''$ and $i_{K(J)} = J'' + 1$, we have :

$$\left. \begin{aligned} P \text{ branch : } T &= \frac{B'hc}{K} J_m'' (2J_m'' - 1), \\ R \text{ branch : } T &= \frac{B'hc}{K} (J_m'' + 1)(2J_m'' + 3), \end{aligned} \right\} \quad . \quad . \quad (129)$$

where the constant $hc/K = 1.43$. This method is particularly simple in that the plate calibration (image density : light intensity) is not necessary. On the other hand, the intensity variation near the maximum is small, and an error of one unit in determining J_m will result in considerable error in determining T . For the Ångström bands ${}^1\Sigma \rightarrow {}^1\Pi$, for example, if $J_m = 9 \pm 1$ the corresponding temperatures are approximately $500 \pm 100^\circ$ abs.

(2) *The Line Intensity Graph Method*

We observe from (125) that if we plot $\log_e (I/i)$ against $B'J(J+1)$ we should have a straight line, always assuming that the rotational energy corresponds to a temperature-controlled type. The slope of this graph will then give $-\frac{1.43}{T}$, from which T is derived. This method was first used by Ornstein and Van Wijk.* It involves, of course, accurate measurement of line intensities upon the basis of plate calibration, and it is therefore not a rapid method.

A variant of it, which is more general, in that it can be applied to bands whose i -factors are not known, has been used by Nolan and Jenkins† and others. Making use of the sum-rule referred to in Section (a) we have

$$\sum_{J''} i = \text{const } (2J' + 1) \text{ and } \sum_{J'} i = \text{const } (2J'' + 1) \quad . \quad (130)$$

Hence from (125) we have by summing the intensities of all lines beginning on the same initial rotational level

$$\sum_{J''} I = C \exp \left(-\frac{E_r}{KT} \right) \sum_{J''} i = C(2J' + 1) \exp \left(-\frac{E_r}{KT} \right)$$

$$\text{and} \quad \log_e \left(\frac{\sum_{J''} I}{2J' + 1} \right) = -\frac{E_r}{KT} + \text{const.}$$

* *Zeit. f. Phys.*, vol. 49, p. 315 (1928).

† *Phys. Rev.*, vol. 50, p. 945 (1936).

Hence by plotting the logarithm on the left-hand side against $B'J'(J' + 1)$ we shall have a straight line, from the gradient of which,

$-\frac{1.43}{T}$, the temperature, may be found. An example of this method is

found in Nolan and Jenkins's paper on the PH band which was excited by a high-voltage discharge through hydrogen and phosphorus vapour. The three sub-bands ${}^3\Pi_{012} \rightarrow {}^3\Sigma$ yielded temperatures of 700° K., 694° K., and 689° K. A particularly interesting feature of this band was that upon replacing E_r by the total energy $E_r + hcA\Lambda\Sigma$ (in this case ${}^3\Pi_0 - {}^3\Pi_1 = 121$ cm. $^{-1}$ and ${}^3\Pi_1 - {}^3\Pi_2 = 111$ cm. $^{-1}$ ($\Lambda = 1$, $\Sigma = \pm 1$)) the three parallel graphs (131) coincided in one line, showing that the same temperature controlled both electronic and rotational energy. Expressed otherwise, we may say that after excitation there apparently takes place a redistribution of thermal energy in the PH molecule. This was not found to be the case for the HgH molecule, but in this case there is the gigantic spin-coupling energy ${}^2\Pi_{11} - {}^2\Pi_1 = 3683$ cm. $^{-1}$

(3) The Intensity Coincidence Method

If the intensities of the various branch lines as determined by experiment are plotted against wave-length or frequency, smooth-

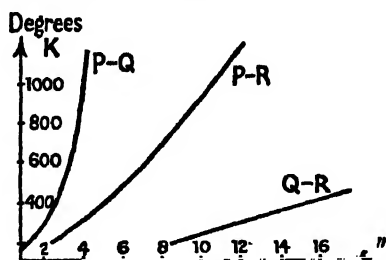


Fig. 85. Temperature correlation with the J'' -values at which the intensity envelopes intersect for the (0,3) Ångström band λ 5610 (after Knauss and McCay). Values of J'' (R) are plotted for the PR and QR intersections, and J'' (Q) for the PQ intersection.

flowing curves of the various branches will intersect at certain points (see Figs. 84 and 85). There will be three such points corresponding to the intersection of the PR, QR, and PQ envelopes. In practice all that it is necessary to do is to construct the smooth envelopes through the micro-photometered band and identify the pairs of J -values corresponding to each intersection. Thus in Fig. 84 we note (for $T = 300^\circ$ K.) that the intensities coincide at $P(2)$ and $R(12\frac{1}{2})$ for the ${}^1\Sigma \rightarrow {}^1\Sigma$ band. Such pairs of values satisfy the two conditions

$$\nu_P = \nu_R \text{ and } I_P = I_R. \quad (132)$$

If J_P and J_R are two values of J'' from the respective branches which satisfy these conditions, then

$$i_{J_P} \exp\left(-\frac{B'hc}{KT} J_P(J_P - 1)\right) = i_{J_R} \exp\left(-\frac{B'hc}{KT} (J_R + 1)(J_R + 2)\right),$$

$$\left. \begin{aligned} \text{and thence } T &= \frac{B'hc}{K} \left[\frac{J_P(J_P - 1) - (J_R + 1)(J_R + 2)}{\log_e (i_P/i_R)} \right], \\ \text{and similarly for the } PQ \text{ and } QR \text{ intersecting envelopes :} \\ T &= \frac{B'hc}{K} \left[\frac{J_P(J_P - 1) - J_Q(J_Q + 1)}{\log_e (i_P/i_Q)} \right], \\ T &= \frac{B'hc}{K} \left[\frac{J_Q(J_Q + 1) - (J_R + 1)(J_R + 2)}{\log_e (i_Q/i_R)} \right]. \end{aligned} \right\} \quad (133)$$

The pairs of values (J_P , J_R), &c., will not generally be integers, but the fractional value corresponding to the points of intersection must be used. Fig. 86 is adapted from a paper of Knauss and McCay,* by whom this method was developed. Its application to the Ångström bands of CO showed excellent agreement with other methods.

(d) FACTORS ON WHICH 'EFFECTIVE' TEMPERATURE DEPENDS

Many observers have used one or other of these methods to derive an 'effective' temperature. The important question to be considered is under what conditions this approximates to the true gas temperature. Arc 'temperatures' have been determined from the CN and AlO bands observed in the arc as 3900° C. and 4500° C. Birge obtained 4000° C. for the temperature of the solar reversing layer using the CN bands, and Richardson temperatures between 5000° C. and 5700° C. using the λ 5165 C_2 band. Wilson found a value of 5000° C. from the OH band obtained in absorption from an under-water spark. On the other hand, its emission in an oxy-hydrogen flame was found by one observer to give 3000° C. and in a copper arc to correspond to over 6000° C. The generation of spectra by means of active nitrogen has given temperatures ranging from 15° C. to 80° C. as determined from the bands of SiN and NO. When, and under what conditions, can these 'effective' temperatures be relied upon?

Oldenberg † has attempted to give a review of conditions in which abnormal rotation of molecules is to be expected. He has also suggested conditions under which true gas temperatures are likely. Most observers will agree with three of his conditions under which true temperatures are likely, viz.

- (1) in absorption spectra of unexcited molecules,
- (2) in emission spectra excited by heat, provided self-absorption by cooler surrounding layers does not vitiate the result,
- (3) in emission spectra in the presence of a large excess of rare gas (particularly helium) which permits molecules to come to thermal equilibrium during the life of the excited state.

Of course, these conditions cover only a fraction of those which occur in practice.

Knauss and McCay did some careful work using a high-frequency (electrodeless) discharge to excite a slow stream of pure CO at a pressure of about 0.09 mm. Hg. The tube was enclosed in an electric

* *Phys. Rev.*, vol. 52, p. 1147 (1937).

† *Ibid.*, vol. 46, p. 213 (1934).

furnace of which the temperature could be determined. With a furnace temperature of 353°K. , the average 'effective' temperature was determined as $438 \pm 42^{\circ}\text{K.}$; with the furnace at 383°K. the 'effective' temperature was $467 \pm 30^{\circ}\text{K.}$; with the furnace at 638°K. the 'effective' temperature was $630 \pm 24^{\circ}\text{K.}$ The apparent conclusion is that at the lower gas temperature the 'effective' temperature exceeded it by about 85°C. The two were coincident, however, at the higher gas temperature 638°K.

Along with this we may consider experiments of Duffendack, Revans, and Roy.* They examined the N_2^+ bands produced in a low-voltage arc between a tungsten filament and a nickel plate about 15 mm. distant. A current of 100 milliamp. was passed. A white-hot tungsten spiral filament was the source of electrons, and the temperature of the gas inside the helix was estimated to be about 2600°C. With a gas pressure of 2 mm. photographs taken of various parts of the discharge from the inside of the helix to what must have been a much cooler layer adjacent to the anode showed no variation from an 'effective' band temperature of 1425°K. Moreover, replacement of the tungsten filament by an oxide-coated one running at a dull red temperature certainly not above 1000°C. (the other conditions being the same) gave just the same effective temperature (1425°K.) from the band-line intensities. In such a low-voltage arc, where a dense stream of electrons was the exciting agent, it would appear that the gas temperature had no relevance. When, however, an electrodeless discharge excited the same bands, these gave an 'effective' temperature of 330°K. , while with a 60-cycle 14,000-volt transformer they gave an 'effective' temperature of about 430°K. Both of these values, it was thought, could not have been much above the true gas temperature.

Without attempting to picture the mechanism, or say why it should be, we must simply record that the impinging electronic impacts of the D.C. arc apparently result in some measure of transfer of electronic energy into rotational energy of the molecule. Further experiments showed that the arc voltage was able to influence the effective temperature to an appreciable extent, values of 25 volts, 100 volts, and 200 volts corresponding to temperatures of 855°K. , 1078°K. , and 1425°K. For the 100-volt arc it was calculated that 0.009 electron-volt only, if transformed into molecular rotational energy, would give rise to the observed effective temperature. These general results were supported by similar experiments on the negative oxygen bands (O_2^-) and the negative CO^+ bands.

The present writer † found effective temperatures as high as 7000°K. from the rotational energy distribution in the Swan bands of C_2 obtained by running an ordinary 200-volt D.C. carbon arc in low-pressure hydrogen, and no one would claim a temperature as high as this for the gases between the poles of a carbon arc. We mention but one other experiment. Duffendack and others observed that when a mixture of 10% N_2 and 90% helium was excited, whether in the low-voltage arc or otherwise, the effective temperature was probably but little above the true temperature. The excitation of N_2^+ bands

* *Phys. Rev.*, vol. 45, p. 807 (1934).

† *Phil. Trans.*, A, vol. 226, p. 184 (1927).

was presumably due to metastable helium atoms. The same result was obtained with a mixture of 10% N_2 and 90% CO when presumably impacts of the second kind of excited CO^+ ions (in the upper $^1\Sigma$ state having 19.8 volts energy) excited the N_2^+ bands (of which the initial state is 19.6 volts above the ground level of N_2).

What general conclusions may we draw from all these experiments? The type of excitation used is of primary importance. In the case of the low-voltage arc where an electron stream of high-current density is the exciting agent, it would seem that it is the mechanics of this interaction of electrons and molecules which *alone* controls the effective temperature. Otherwise it is impossible to explain Duffendack's experiments, and in particular to explain how the effective temperature of 1425° K. was *less* than the estimated gas temperature of 2600° C. inside the white-hot helical tungsten filament. In an A.C. transformer type of discharge with currents of a few milliamps we probably have an intermediate stage where the mechanics of electron impact gives an effect superposed on the gas-temperature distribution. With the 'field' type of excitation typical of the high-frequency electrodeless discharge (where the current density is zero), we appear to approximate closely to the gas temperature distribution.

There is, however, one consideration which is likely to modify the above conclusions, viz. there is likely to be a difference between experiments where the molecule to be excited is already formed (e.g. CO) and experiments where it has to be formed by a synthesis or a disintegration of another molecule (e.g. CN, OH, He_2 , and C_2). This is discussed in the next section.

Meanwhile, the influence of the presence of other gases on the effective temperature is one which merits further consideration. The present writer found that by excitation of the Swan system of C_2 in an A.C. transformer discharge through a tube with carbon electrodes containing a little hydrogen in a large excess (20–30 mm.) of argon, the effective temperature was about 700° K. This was in marked contrast with the effective temperature, already referred to, of the bands produced by a carbon arc in hydrogen.

The detailed investigations by Duffendack, Revans, and Roy of the low-voltage arc through mixtures of nitrogen and helium, and carbon monoxide and helium, showed conclusively that the presence of the foreign gas in increasing proportions lowered the effective temperature of the N_2^+ and CO^+ bands. In Fig. 86 is shown in the case of N_2^+ the extent of this effect. For a trace of nitrogen in a large excess of helium it is apparent that the effective temperature is but little, if any, above the gas temperature.

Oldenberg* has made the observation that the abnormal intensity distribution found in the OH band at λ 3064, when it is excited by a transformer discharge through water vapour, is transformed to a normal temperature distribution corresponding to 670° K. when the discharge takes place through a trace of water vapour in 20 mm. of helium. His view is that by arranging for numerous collisions of the abnormally excited molecule, during the lifetime of its excited state, with light atoms of helium, we enable it to part with its excess of

* *Phys. Rev.*, vol. 46, p. 212 (1934).

rotational kinetic energy. The rotation of OH would substantially be that of a light H atom round the more massive O atom, necessitating another light body if collision is to result in the transfer of

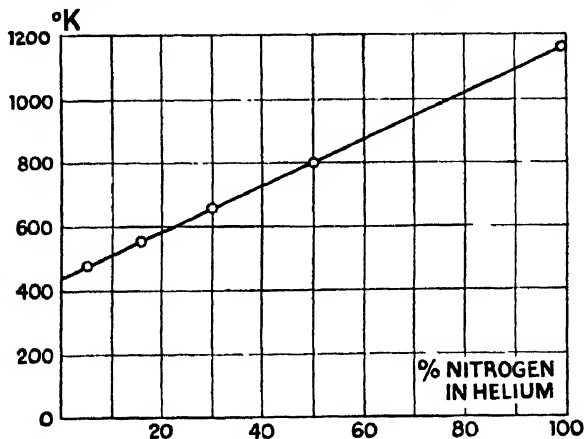


Fig. 86. Relation between 'effective' temperature determined from the N_2^+ bands, and the percentage of the mixture used. (Data from Duffendack, Revans, and Roy.)

kinetic energy. Argon atoms are likely to be quite effective in the same way in relation to C_2 molecules, since they are of comparable masses.

(e) ABNORMAL MOLECULAR ROTATION (OH AND HgH)

It was mentioned in the last section that where the emitting molecule has to be first produced by a synthesis or a disintegration, there is the possibility of abnormal molecular rotation occurring. Spurious 'effective' temperatures may arise, or we may find no energy distribution of the Boltzmann type at all.

Lochte-Holtgreven * photographed simultaneously the band spectra of C_2 and CH from the same light sources, viz. discharges through acetylene (C_2H_2), ethylene (C_2H_4), and methane (CH_4). The interesting result was obtained that the 'effective' temperatures deduced from the intensity distribution within the bands of C_2 and CH differed greatly. The discharge in ethylene gave for C_2 , 3800° K., and for CH, 1600° K. In acetylene they were respectively 4700° K., and 2000° K. The processes by which these two emitters were produced from the hydrocarbons used must be very different, and this is certainly reflected in the widely divergent rotational speeds of these molecular fragments. A systematic study of these 'effective' temperatures (both of the electronic and vibration-rotation band spectra) for the products of breakdown of various hydrocarbons should throw a good deal of light on the mechanism of disintegration.

Examination by van Wijk † of the spectra of N_2 and N_2^+ from the

* *Zeit. f. Phys.*, vol. 67, p. 590 (1931).

† *Ibid.*, vol. 59, p. 315 (1930).

same discharge showed that they had a common effective temperature. The process of ionization apparently leaves unaffected (in nitrogen) the rotational energy distribution.

Knauss and McKay, in their experiments already described with CO, found that the substitution of a substantial proportion of CO₂ at 383° K. gave an effective temperature in the Ångström CO bands that was indistinguishable from that of pure CO (viz. about 80–90° C. higher than the furnace temperature). In this case apparently the breakdown of CO₂ and excitation of CO resulted in a product which reached approximate thermal equilibrium prior to radiation.

The high effective temperature of the carbon arc in hydrogen as determined from the C₂ (Swan) bands is clearly to be regarded as much more closely related to the mechanism of production of the C₂ molecule (presumably from some hydrocarbon formed) than it is to the true gas temperature of the arc. Similar remarks would apply to the CN bands presumably formed by a breakdown of C₂N₂, to the fantastic 'temperature' of the OH absorption band derived from a spark under water, and to the 'temperature' of an electrically fused aluminium wire in H₂, as deduced from the AlH bands.

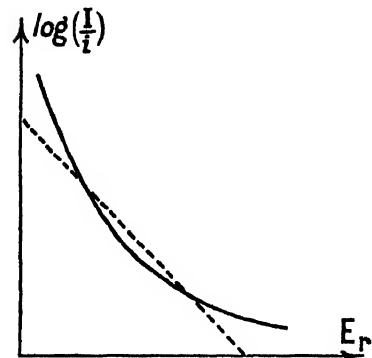


Fig. 87. Illustrates the type of departure from thermal equilibrium found in the OH band, λ 3064.

Special studies have been made of the OH band at λ 3064, and the HgH band at λ 4017 from the point of view of the abnormal rotation they exhibit. The OH band at λ 3064 is the (0,0) band of a $^3\Sigma \rightarrow ^2\Pi_{inv}$ system. The H₂O molecule has its O atom subtending an angle of 105° with the two H atoms, and when in an electric discharge it is dissociated into O and an excited OH

molecule it seems very probable that the latter will acquire rotational energy quite different from that characteristic of the gas temperature. The extent to which this will reveal itself depends on the ability of collisions to bring it down to the normal value within the lifetime of the excited state. Oldenberg showed that excess of helium was able to do this. E. R. Lyman* subsequently investigated normal transformer discharges and high-frequency electrodeless discharges through water vapour alone at various pressures, also at various pressures from 10⁻⁵ mm. to 7 mm. in the presence of 7 mm. of helium or argon. Plotting $\log(I/i)$ against $B'K'(K' + 1)$ in no case gave a straight line, showing that thermal equilibrium of the usual Boltzmann type was never established. Fig. 87 shows qualitatively the type of curve obtained. Among the very low levels there is an excess of energy, which, it is suggested, may be caused by temperature inhomogeneity in the discharge. The striking excess energy among the higher rotational states is presumably due to the mechanics of production of the OH molecule.

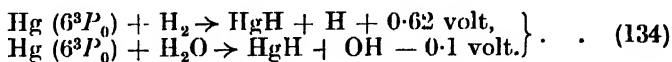
The HgH band at λ 4017 is (0,0) of $^2H_1 \rightarrow ^3\Sigma$. Its intensity dis-

* *Phys. Rev.*, vol. 53, p. 379 (1938).

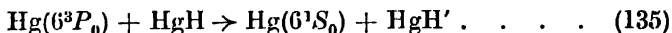
tribution has been studied by Rieke * and others, and the same type of departure from the normal has been found, viz. excess energy in the higher rotational quantum numbers over that corresponding to thermal equilibrium. It was first discovered in 1928 by Gaviola and Wood that the HgH bands could be produced by what is called 'sensitized fluorescence' by a discharge through a tube under the following conditions :

- (1) a little Hg vapour + a few thousandths mm. H_2 + a few mm. N_2 ;
- (2) a little Hg vapour + a few mm. H_2O vapour.

It is presumed that HgH molecules are produced in the respective cases thus :



The resulting HgH molecule is excited by metastable $Hg(6^3P_0)$ atoms thus :



and subsequently radiates the bands. Now experiment shows that whereas conditions (1) yield bands with highly abnormal rotation (and inasmuch as temperature has any meaning) in the region of $3000^\circ K.$, conditions (2) give an effective 'temperature' distribution in the region $300^\circ K.$ It was originally supposed that the energetics of the formation of HgH yielding an excess energy of 0.62 volt in the first case and a deficit of 0.1 volt in the second, accounted for this 'temperature' difference. But if the 0.62 volt energy does in fact produce excessive rotation, then since the concentration of $Hg(6^3P_0)$ atoms is only about 10^{-5} that of the N_2 molecules, it would involve the persistence of this abnormal rotation through thousands of collisions with these N_2 molecules before the excitation process (135) took place. This explanation is clearly improbable. It is more plausible that process (135) gives rise (on the basis of the Franck-Condon principle, see Chapter III (a)) to considerable vibrational energy. Now it is well known that in a collision between two particles, interchange of kinetic energy only takes place freely between particles of comparable mass. Where the particles differ widely, the lighter may change its direction but there is little energy interchange. For practical purposes the rotating HgH' molecule is a hydrogen atom rotating round a Hg nucleus. So light an atom will not part with much kinetic energy to a comparatively heavy N_2 molecule, but may be expected to do so to H_2O molecules with their light fast-moving H atoms. The collision of vibrating HgH' molecules with N_2 molecules, though not leading to loss of rotational energy, probably gives rise to transformation of some of its vibrational energy into rotational energy. Hence the marked differences in (1) and (2) are accounted for.

* *Jour. Chem. Phys.*, vol. 4, p. 513 (1936).

(f) ALTERNATING INTENSITIES OF BAND LINES

The experimental facts are simple. It has been observed that the fine structure of bands arising from *homonuclear* diatomic molecules exhibits the phenomenon of alternating intensity. Alternate lines are strong and weak. Thus in the case of the N_2^+ band shown in Fig. 88 the ratio of the intensity of one of the strong lines to the mean of the intensity of its neighbours on each side has been found to be exactly 2 : 1. Other homonuclear molecules have been found to present characteristic intensity ratios ranging between 1 (which means no perceptible fluctuation) and ∞ (which means that alternate band lines are missing altogether). The term homonuclear means, of course, identity of mass of the nuclei, and not merely that we are dealing with an elementary molecule. Thus the spectrum of

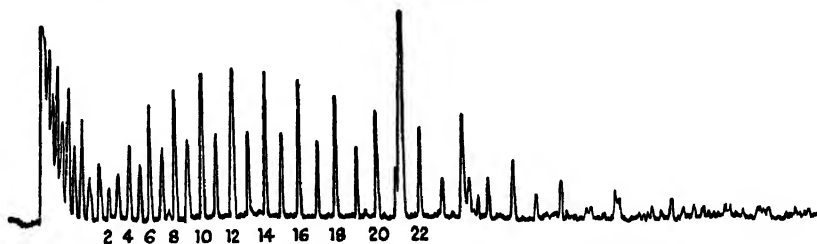


Fig. 88. Intensity distribution in the (0,0) band of $^2\Sigma \rightarrow ^2\Sigma$ system of N_2^+ at λ 3914 showing the alternating intensity ratio 2 : 1. (After Duffendack, Revans, and Roy.)

$Cl^{35}Cl^{37}$, $O^{16}O^{18}$, and Li^6Li^7 will not show alternating intensities, but $(Cl^{35})_2$, $(O^{16})_2$, and $(Li^7)_2$ will do so.

Empirically we can introduce a further principle of classification of rotational levels to account for the facts. First, let us recall the classifications of levels we have already had.

Electronic States (see Chapter VI (d)). (1) There is a special classification as + or -, which, however, need concern us only for Σ states, when it restricts transitions thus: $\Sigma^+ \rightarrow \Sigma^+$ or $\Sigma^- \rightarrow \Sigma^-$. (2) There is a special classification of the electronic states of all *elementary* molecules as *g* (even) or *u* (odd), and a restriction $g \rightleftharpoons u$.

Rotational States (see Chapter VIII (b)). (1) There is a classification of *all* levels as + or -, and a restriction $+\rightleftharpoons -$. To this we must now add another. (2) There is a special classification for *homonuclear* molecules as *s* or *a* (symmetrical or anti-symmetrical) with a further restriction $s \rightarrow s$ and $a \rightarrow a$.

What is significant for our purpose at present is that *s* levels and *a* levels are respectively strong and weak. Expressed more precisely, the statistical weight of any *s* level is greater than that of the mean of the two *a* levels on each side of it. Thus while the statistical weights of all rotational levels of a heteronuclear molecule are $2J + 1$, the statistical weights of the rotational levels of a homonuclear molecule are either $g_s(2J + 1)$ or $g_a(2J + 1)$, where $g_s > g_a$. In equation (125), and others derived from it, we should in this case replace the constant *c* by either g_s or g_a . When using a method such as that of

equation (131) to evaluate an effective temperature we should expect to obtain two parallel straight lines from the intensity data of the strong lines and the weak lines respectively. These two lines should be separated on the E_r -axis by the interval $\log_e (g_s/g_a)$. This was verified by Ornstein and Van Wijk * for N_2^+ , who obtained two parallel lines separated by $\log_e (2)$.

For the moment we offer no explanation, but record that the value of the alternating intensity ratio g_s/g_a is simply related to the angular momentum quantum number N of the atomic nucleus (of which two constitute the diatomic molecule). Thus

$$\frac{g_s}{g_a} = \frac{N+1}{N} \quad . \quad . \quad . \quad . \quad . \quad (136)$$

It is now well known that each atomic nucleus must have ascribed to it angular momentum $\sqrt{N(N+1)} \frac{h}{2\pi}$, to account for the facts of hyperfine structure in line spectra. (The above mechanical moment has a magnetic moment associated with it which perturbs the electronic motion.) It is known that for the proton $N = \frac{1}{2}$ and also that half-integral nuclear spins are always associated with odd atomic masses. It is believed that intra-nuclear electrons lose their spin when linked up with a proton to form a neutron, so that both protons and neutrons in atomic nuclei have a spin of $\frac{1}{2}$. It is possible that protons and neutrons may form closed shells, as far as possible, in a manner analogous to the disposition of electrons outside atomic nuclei, and that the unbalanced spins constitute N the resultant. In practice, values of N occur between 0 and $4\frac{1}{2}$. Thus we see from (136) that the intensity ratios to be expected are as in the table.

N	g_s/g_a	Examples (X_2)
0	∞	He ⁴ , C ¹² , O ¹⁶ , S ³² , Cu ⁴⁰
$\frac{1}{2}$	3/1	H ¹ , F ¹⁹ , P ³¹ , Tl ²⁰³ , Tl ²⁰⁵ , Pb ²⁰⁷
1	2/1	H ² , N ¹⁴
$1\frac{1}{2}$	5/3	Li ⁷ , Na ²³ , K ³⁹ , Cu ⁶³ , Cu ⁶⁵ , Br ^{79, 81}
2	3/2	
$2\frac{1}{2}$	7/5	Cl ³⁵ , Rb ⁸⁵ , Sb ¹²¹ , I ¹²⁷
3	4/3	
$3\frac{1}{2}$	9/7	Cs ¹³³ , La ¹³⁹ , Ta ¹⁸¹
4	5/4	

As already mentioned, in the case of $N = 0$ or $g_s/g_a = \infty$ we have alternate lines missing. Such is the case with He₂, C₂¹², O₂¹⁶, S₂³², and in general with all homonuclear molecules whose atomic masses are a multiple of four. Moreover, it is notable that the odd atomic masses correspond to half-integral values of N , and the even atomic masses to integral values of N .

It is at first sight not at all apparent how a property which is essentially intra-nuclear can affect the intensities of band lines which are a product of changes in the rotational speeds of the molecules as

* *Zeit. f. Phys.*, vol. 49, p. 315 (1928).

a whole. So long as we continue to seek an explanation in terms of the Old Quantum Theory and a precisely visualized model, it will remain difficult to perceive such a connexion.

Instead of this we must talk about Ψ , a wave-function for the molecule. To a first approximation it can be regarded as made up of three factors

$$\Psi = \psi_e \cdot \psi_r \cdot \psi_{nu}$$

so far as our study of an individual band is concerned. ψ_e is the electronic component for a 'frozen' molecule (non-vibrating). If we take the origin of x , y , and z axes at the mid-point of the inter-nuclear axis and regard ψ_e as a $f(x, y, z)$, it is regarded as an *even* electronic state and labelled g if $\psi_e = f(-x, -y, -z)$, i.e. if ψ_e remains unchanged in sign upon reflexion in the origin. It is called an *odd* electronic state and labelled u if $f(-x, -y, -z) = -\psi_e$, i.e. if reflexion changes the sign of ψ_e . Since ψ_e depends on the symmetry of the electric forces in the molecule, this classification as g and u is of significance in all elementary molecules such as $\text{O}^{16}\text{O}^{17}$ or $\text{O}^{16}\text{O}^{18}$, as well as in $(\text{O}^{16})_2$, &c. Mulliken* has pointed out that even in molecules like CN , which are nearly symmetrical, the $g \rightleftharpoons u$ rule, which is strict in elementary molecules, is reflected in the much greater strength of transitions of this type than of those corresponding to $g \rightarrow g$ or $u \rightarrow u$.

The factor ψ_r is the rotational wave-function and is classified as $+$ or $-$ for the same reasons of symmetry as ψ_e was classified as g or u respectively.

The factor ψ_{nu} is the wave-function appropriate to the system of two nuclear spins, and is classified as either s or a for precisely similar reasons. The symmetrical (*Sy*) or anti-symmetrical (*An*) character of the molecular wave-function Ψ is then determined by the combination of these qualities in its three components:

$$\left. \begin{aligned} (g)(+)(s) \text{ or } (u)(-)(s) \text{ or } (g)(-)(a) \text{ or } (u)(+)(a) &= Sy, \\ (g)(+)(a) \text{ or } (u)(-)(a) \text{ or } (g)(-)(s) \text{ or } (u)(+)(s) &= An. \end{aligned} \right\} \quad (137)$$

If the nuclei of a homonuclear molecule each have an *even* mass, then it is found that the complete wave-function must be *Sy*; if an *odd* mass, then the complete wave-function must be *An*. It is on the basis of this principle that $+$ and $-$ rotational levels are further labelled as s or a .

As regards the greater strength of s levels than a levels, Mulliken† has shown that just as electronic spins couple with each other and also orientate at various positions in an external magnetic field, so there are various magnetic couplings of the two N -vectors, and of these the s -forms outnumber the a -forms in the g_s/g_a ratios given in (136).

In the special case of $N = 0$ we can now see that alternate rotational levels will be missing altogether, for ψ_{nu} can only be of the s -form, since interchanging the two nuclei would clearly make no

* Mulliken, *Review of Modern Physics*, vol. 3, p. 140 (1931). I am greatly indebted to this article for the exposition here given.

† *Trans. Faraday Soc.*, vol. 25, p. 634 (1929).

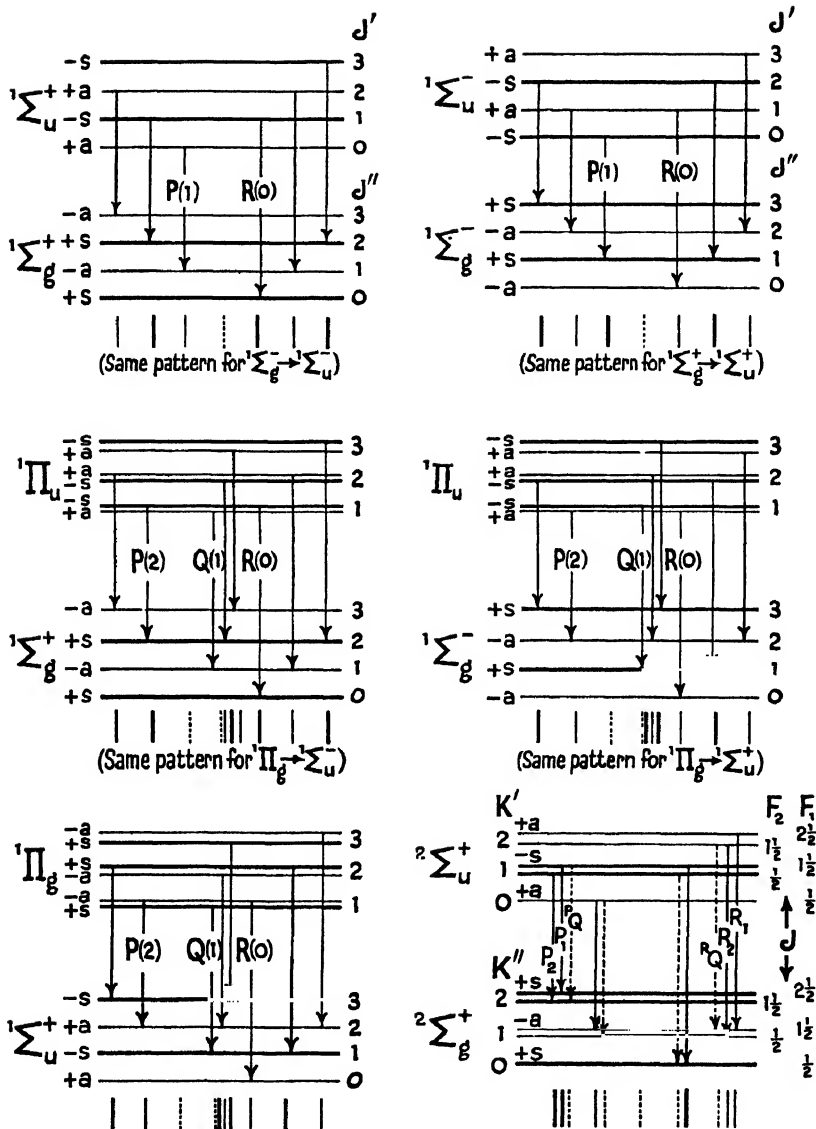


Fig. 89.—Simple types of band structure arising in homonuclear molecules.

difference. From (137) we then see that for atoms of even mass *g*-type electronic states can have only + rotational levels, and *u*-types electronic states only - rotational levels. For atoms of odd mass the converse is true.

In constructing rotational level diagrams to illustrate band structure for homonuclear molecules, as in Fig. 89, we must label our levels *s* and *a* as well as + and -, and see that the two restrictions $+\nleftrightarrow-$ and $s\rightarrow s$ or $a\rightarrow a$ are both satisfied. In Fig. 89 we have assumed the molecule has even nuclear masses, so that its resultant state must be *Sy*. The \pm designation accords with the principles of Chapter VIII (b), and the *s, a* designation can then be made in accordance with the first row of (137).

If we were dealing with a molecule whose resultant Υ was *An*, then *a* and *s* would be completely interchanged throughout Fig. 89, and of course the greater statistical weight goes with the *s*-level. The only multiplet transition shown is that of $^2\Sigma \rightarrow ^2\Sigma$, which corresponds to the case of the negative nitrogen bands of Fig. 88. The extension of the singlet diagrams of Fig. 89 to spin doubling and trebling is simply done, since the *s* and *a* assignments to the various *J* sub-levels derived from a particular *K* are all the same as that assigned to the corresponding *K* level in the singlet case. The $^RQ_{21}$ and $^RQ_{12}$ satellite branches are shown dotted because of their comparative weakness.

THE EFFECT OF ISOTOPY ON MOLECULAR SPECTRA

ISOTOPES of an element, as is well known, have the same nuclear charge, but differ in their nuclear masses. Thus H^1 has a nucleus of one proton, and H^2 a nucleus consisting of one proton and one neutron. Li^6 has a nucleus of three protons and three neutrons, while Li^7 has a nucleus containing three protons and 4 neutrons. Only those few physical properties of an element which involve the mass directly, such as the processes of diffusion evaporation or electrolysis, will permit of separation being made between the isotopes of an element. Nuclear mass enters into molecular spectra, however, in a very prominent

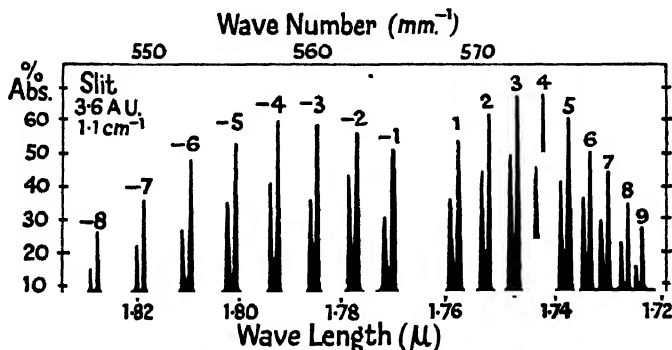


Fig. 90.—The (2,0) HCl absorption band showing the isotope effect due to HCl^{35} and HCl^{37} . (After Meyer and Levin.)

way. (1) The vibration frequency of isotopic molecules will be different. Thus for $B^{11}O$ we have $\omega_0'' = 1875 \text{ cm.}^{-1}$ and for $B^{10}O$ $\omega_0'' = 1927 \text{ cm.}^{-1}$. The restoring forces controlling vibration are the same, but the masses to be moved are different. (2) The fine structure of the bands of isotopic molecules will be relatively displaced, since the moments of inertia will differ. (3) The nuclear spins will differ. In atomic spectra this will result in different hyperfine structure patterns of the lines. In molecular spectra if X and X' are two isotopes it will show itself in different alternating intensity ratios in the molecular bands from X_2' , while XX' , being heteronuclear, will show no alternating intensities.

So long ago as 1919 Imes observed in the (2,0) vibration-rotation band of HCl at 1.76μ that the absorption lines were asymmetrical on the long wave-length side. This was interpreted later by Loomis and Kratzer as due to the presence of lines of HCl^{37} . Fig. 90 is a scale diagram based upon experimental work of Meyer and Levin * in which the isotopic band lines (about 4.5 cm.^{-1} apart) were completely resolved.

* *Phys. Rev.*, vol. 34, p. 44 (1929).

Imes's observation was historically the first observation of the different spectra of isotopic molecules, and is referred to more for the sake of its interest than its importance. The theoretical foundations of the isotope effect in band spectra were laid down by Mulliken* in a series of papers in 1925, and these were applied to the spectra of BO, CuI, and SiN. We proceed to outline the theory given by Mulliken.

(a) THE VIBRATIONAL EFFECT

From equation (2) we may regard the displacement between corresponding band lines of two isotopic molecules XY_1 and XY_2 (where Y_1 and Y_2 stand for the more abundant and less abundant isotopes of an element) as made up of three parts, electronic, vibrational, and rotational. Thus

$$v_2 - v_1 = (v_2^e - v_1^e) + (v_2^v - v_1^v) + (v_2^r - v_1^r) \quad (138)$$

The first of these will be considered in Section (c); the vibrational effect is our immediate interest. The vibrational function is

$$G(v) = \omega_e(v + \frac{1}{2}) - \omega_e x_e(v + \frac{1}{2})^2 + \omega_e y_e(v + \frac{1}{2})^3 \quad (139)$$

If reference is made to Chapter IV for the significance of the coefficients,† we find $\omega_e \propto \mu^{-1}$, $\omega_e x_e \propto \mu^{-1}$, and $\omega_e y_e \propto \mu^{-1}$, where μ (see (10)) is the reduced mass of the molecule. It will be convenient to let

$$\rho = \frac{\mu_2^{-1}}{\mu_1^{-1}} = \sqrt{\left(\frac{1}{M_2} + \frac{1}{M'}\right) / \left(\frac{1}{M_1} + \frac{1}{M'}\right)} \quad (140)$$

from which we have to a close approximation if $M_1 - M_2$ is small compared to each atom of the molecule,

$$\rho - 1 = \frac{M'(M_1 - M_2)}{2M_2(M_1 + M')} \quad (141)$$

The displacement of the vibrational energy levels of the two isotopic molecules may therefore be written :

$$G_2(v) - G_1(v) = (\rho - 1)\omega_e(v + \frac{1}{2}) - (\rho^2 - 1)\omega_e x_e(v + \frac{1}{2})^2 + \dots \quad (142)$$

The displacement of corresponding bands due to this effect is therefore

$$v_2^v - v_1^v = (\rho - 1)[\omega_e'(v' + \frac{1}{2}) - \omega_e''(v'' + \frac{1}{2})] - (\rho^2 - 1) \frac{[\omega_e'x'(v' + \frac{1}{2})^2 - \omega_e''x'(v'' + \frac{1}{2})^2]}{2} \quad (143)$$

To a close approximation we can put $\rho + 1 = 2$ in the coefficient of the second term which is small, and we have

$$v_2^v - v_1^v \doteq (\rho - 1)[\omega_e'(v' + \frac{1}{2}) - \omega_e''x'(v'' + \frac{1}{2})^2] \quad (144)$$

or approximately $v_2^v - v_1^v \doteq (\rho - 1)v_1^v$,

where v_1^v is the separation of the (v', v'') band of the more abundant isotope from the system origin. We see from (140) or (141) that the coefficient $\rho - 1$ is positive or negative according as the more abundant isotope has the greater mass or the smaller. It is clear, therefore, that the lighter isotope always presents a band pattern which is 'magnified'

* *Phys. Rev.*, vol. 25, p. 119 (1925); vol. 25, p. 259 (1925); vol. 26, p. 1 (1925); vol. 26, p. 319 (1925).

† For more precise expressions see Dieke, *Phys. Rev.*, vol. 47, p. 665 (1935).

compared to that of the heavier isotope: to be more precise, corresponding heads of the lighter molecule always fall farther away from the system origin. This is apparent in Fig. 91. The displacement of corresponding isotopic heads $\nu_2'' - \nu_1''$ will increase approximately linearly with distance from the system origin. A rapid and

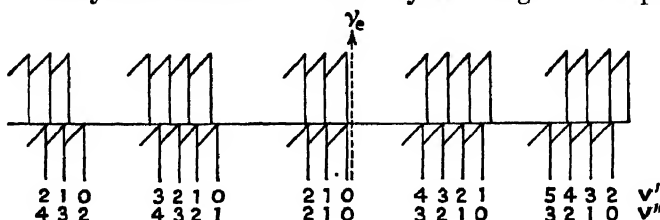


Fig. 91.—Illustrating vibrational isotopic displacements. The lighter molecule has been assumed the more abundant.

approximate determination of ρ from experimental data can be made from (144), since $\rho = \nu_2''/\nu_1''$, but a precise value should be obtained by expressing each isotopic system of band heads or origins by formulae of the usual type (21) and taking the ratio of the coefficients of $(\nu' + \frac{1}{2})$ and $(\nu'' + \frac{1}{2})$ for the two systems.

Examination of (141) shows upon what factors the magnitude of $(\rho - 1)$, and therefore the magnitude of the vibrational isotopic dis-

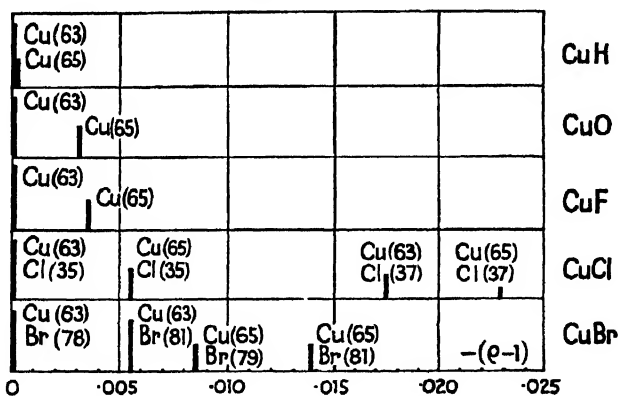


Fig. 92.—Calculated values of $\rho - 1$ for various molecules containing Cu. Relative abundance is proportional to the heights of the lines. (After Mulliken.)

placement, depends. It increases with M' , the non-isotopic component of the molecule, since the factor $\frac{M'}{M_1 + M'}$ is involved. This is seen in Fig. 92 comparing CuH, CuO, CuF, CuCl, and CuBr.

Again for a given isotopic mass difference, say $M_1 - M_2 = 2$, the value of $\rho - 1$ diminishes as the molecule gets heavier due to M_1 and M_2 increasing. Compare CuCl³⁵ and CuCl³⁷ with the pair CuBr⁷⁸ and CuBr⁸¹ in Fig. 92.

Where a long progression of bands shows a vibrational isotope effect it may exhibit at first sight rather unusual variations. Consider (143), where v'' has a fixed value and v' may take a long series of values—as in absorption, for example. We may write it

$$\nu_2^v - \nu_1^v = (\rho - 1)[\omega_e'(v' + \tfrac{1}{2}) - (\rho + 1)\omega_e'x_e'(v' + \tfrac{1}{2})^2] - A \quad (145)$$

where A depends on the particular value of v'' . It is clear that the isotopic separation, if followed to large values of v' , will rise to a maximum, fall to zero, and ultimately grow in the reverse direction. This will be clear from Fig. 93, embodying data on ICl bands of Curtis and Patkowski, and of Darbyshire.

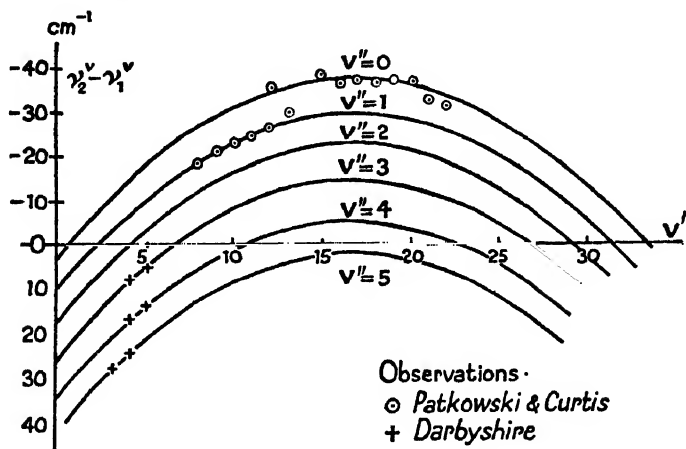


Fig. 93.— $(\nu_2^v - \nu_1^v)$ plotted against v' for several long progressions of ICl. (After Jevons, *Report*, p. 215.)

The vibrational isotope effect has proved to have a number of useful applications:

(1) *Making a correct assignment of (v', v'') values.* From (143) we observe that the separation of isotopic heads vanishes at the origin of the band system (see (16)). Note that it does not quite vanish at the (0,0) band, but at a close point obtained by extrapolating to $v' = -\frac{1}{2}$, $v'' = -\frac{1}{2}$. In sorting out complex overlapping band systems this knowledge may be helpful.

(2) *Distinguishing between alternative emitters.* Experimental evidence is not always available, and sometimes if available it is not conclusive as to the nature of the molecule emitting a spectrum. A classical example of this was the case of the BO bands. They are produced brilliantly when BCl_3 is admitted into 'active' nitrogen, although unobtainable by a discharge through the vapour of BCl_3 , and it was naturally assumed from their simple structure that a nitride of boron, BN, was the emitter. The calculated value of $\rho - 1$ from (141) is 0.0276 for BN and 0.0292 for BO, and the experimentally determined value was found to be 0.0291. Careful investigation showed that the presence of a trace of oxygen in the 'active' nitrogen

was essential to their production. As Mulliken has pointed out, the variation of ρ with M' (see 141) is so pronounced that it is possible almost by inspection to distinguish between such possible emitters as MH , MO , or M_2 .

(3) *Discovery of rare isotopes.* The mass spectrograph in the hands of Aston had at the time of this work of Mulliken already surveyed the majority of the elements. The study of band spectra has, however, proved confirmatory evidence; it has elucidated some doubtful cases, and it subsequently revealed the existence of rare isotopes present only in very small amounts. It is well known that 'positive rays' such as are used in the mass spectrograph commonly contain simple molecular ions. Thus Si^{28} is the main isotope of silicon, but $Si^{28}H$ would, if present, obscure an Si^{29} , and $Si^{28}H_2$ or $Si^{29}H$ would obscure an Si^{30} . The existence of Si^{30} was definitely established by Mulliken from an examination of the band spectrum of SiN obtained by admitting $SiCl_4$ vapour into active nitrogen. Band-heads of $Si^{29}N$ and $Si^{30}N$ were both found in the expected positions.

In the same way, $C^{12}H$ would obscure a C^{13} , $N^{14}H$ would obscure a N^{15} , and $O^{16}H$ and $O^{16}H_2$ would obscure O^{17} and O^{18} , which places a limitation on the usefulness of the mass spectrograph unless extreme precautions in the matter of purity are taken. The study of band spectra has revealed all these isotopes present in small quantities. Giauque and Johnston * found rotational band lines in the O_2 absorption bands in the positions to be expected for $O^{16}O^{18}$ and $O^{16}O^{17}$ molecules. Mecke and Childs give the relative abundance of these isotopes $O^{16} : O^{18} : O^{17}$ as 630 : 1 : 0.2. King and Birge † first identified a faint head at λ 4744.5 in the Swan (C_2) spectrum as the (1,0) band of an isotopic molecule $C^{12}C^{13}$. This band can be faintly seen on Plate I just outside the main (1,0) band λ 4737. The abundance ratio $C^{12} : C^{13}$ may be 100 : 1 or greater. So also Naudé ‡ from the γ -bands of NO ($^2\Sigma \rightarrow ^2\Pi$) found band-heads due to $N^{15}O^{16}$ in between heads due to $N^{14}O^{16}$ and $N^{14}O^{18}$, and a rough estimate of the abundance ratio $N^{14} : N^{15}$ was 350 : 1. No great weight should be attached, however, to the numerical values of these ratios, for widely different intensities are notoriously difficult to measure with precision, and moreover it would appear that under different experimental conditions the relative band line intensities of isotopic molecules sometimes differ.

(4) *Determination of atomic weights.* If the abundance ratios of the isotopes of an element are determined with care, whether from band-line intensities or mass-spectrograph data, then from the precise values of the atomic weights of the isotopes (which can be determined correct to 1 in 10,000 by the mass spectrograph), the ordinary atomic weight of the element can be calculated.

This gives a value probably as reliable as the best chemical determinations. It should be observed that while the *chemical* standard is taken as 16.0000 for ordinary oxygen (which is a mixture of three isotopes), the *physical* standard of the mass spectrograph takes 16.0000 for the main isotope of oxygen. On this latter standard the atomic

* *Jour. Amer. Chem. Soc.*, vol. 51, p. 1436 and p. 3528 (1929).

† *Phys. Rev.*, vol. 34, p. 376 (1929).

‡ *Ibid.*, vol. 36, p. 333 (1930).

weight as calculated from mass-spectrograph data must be multiplied by the factor $16/16.0044$ or 0.99973 to reduce them to the chemical scale. Taking the abundance ratio of $B^{11} : B^{10}$ as $4.00 : 1$, we thus calculate a chemical atomic weight 10.81 which agrees well with the present chemically determined value 10.82 .

Atomic weights of isotopes		Atomic weights of isotopes	
(Neutron)	(1.00897)	C	12.00428 13.00761
H	1.00815 2.01478	N	14.00750 15.00489
He	4.00395	O	16.00000 18.00369
Li	7.01822	F	19.00452
Be	9.01517		
B	10.01633 11.01295		

(See Bainbridge & Jordan : *Phys. Rev.*, 51 385 (1937))

The closeness of the atomic weights of isotopes to whole numbers (usually called the mass numbers) will be remarked. The small but definite departure from integral values led Aston * to define a 'packing fraction' as $(\text{Isotopic At. Wt.} - \text{Mass Number}) \times 10^4 / \text{Mass Number}$. This is for the most part a smooth curve when plotted against mass number, and is an indication of the stability of the various nuclei.

In the determination of the abundance ratios of isotopes from molecular spectra we have several complicating factors.† The intensities of bands are, as we know, dependent on the population of the initial state, and will therefore, assuming a temperature equilibrium, depend on the Boltzmann factor $\exp(-(E'' + E')/KT)$. The heavier isotope will have a lower vibration frequency, and therefore lower E'' , and hence will be favoured. In absorption the same is true, but since $\nu'' = 0$ probably, there is only the half-quantum of residual vibrational energy, and the difference in the Boltzmann factor for the two isotopes will be negligible. The term in E' will operate in the same sense to favour the heavier molecule, which has the larger moment of inertia and therefore a smaller B_v . In the special case of elementary molecules such as $Cl^{35}Cl^{35} : Cl^{35}Cl^{37} : Cl^{37}Cl^{37}$ it is to be observed that if the abundance ratio of $Cl^{35} : Cl^{37}$ is $n : 1$, the relative abundance of these molecules is as $n^2 : 2n : 1$.‡ The abundance of

* *Proc. Roy. Soc., A*, vol. 115, p. 487 (1927).

† See J. L. Dunham, *Phys. Rev.*, vol. 36, p. 1553 (1930).

‡ A simple proof : if x is a very large number of atoms of the first isotope, and y a large number of the second isotope ($x/y = n$ above), the number of ways we can select atoms two at a time both from the first group is $x(x-1)/2$, and both from the second group is $y(y-1)/2$. The number of ways we can select atoms two at a time, one from each group is xy . Since x and y are very large these numbers are approx. $x^2/2 : xy : y^2/2$ or as $n^2 : 2n : 1$.

the species $\text{Cl}^{35}\text{Cl}^{35} : \text{Cl}^{35}\text{Cl}^{37}$ is therefore as $n/2 : 1$. In determining this abundance ratio from an intensity ratio of corresponding band lines, the presence of alternating intensity in the first case will necessitate taking the sum of the intensities of an even number of lines in the first case and comparing it with the sum of the intensities of the corresponding lines in the second case.

(b) THE ROTATIONAL EFFECT

Reference to Chapter IV gives the expression for the energy of a rotating molecule, including a small term representing vibration-rotational interaction, as

$$\begin{aligned} F(J) &= B_v J(J+1) - D_v J^2(J+1)^2 \\ &= [B_v - \alpha(v + \frac{1}{2})]J(J+1) - D_v J^2(J+1)^2. \end{aligned} \quad (146)$$

We have no need to consider more complicated types of rotational

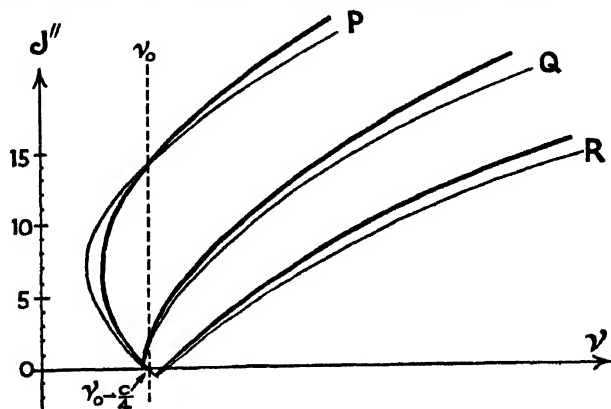


Fig. 94. Simple type of band to illustrate the rotational isotopic effect. The lighter isotope gives the band lines farther from the band origin.

term: it will suffice to consider this simple type. As before, we find B_v involves μ^{-1} , α involves μ^{-1} , and D involves μ^{-2} . The *rotational* displacement of corresponding band lines of the isotopic molecules is therefore:

$$\begin{aligned} \nu_2' - \nu_1' &= (\rho^2 - 1)[B_v' J'(J' + 1) - B_v'' J''(J'' + 1)] - (\rho^3 - 1) \\ &\quad [\alpha'(v' + \frac{1}{2})J'(J' + 1) - \alpha''(v'' + \frac{1}{2})J''(J'' + 1)] \\ &\quad - (\rho^4 - 1)[D_v' J'^2(J' + 1)^2 - D_v'' J''^2(J'' + 1)^2]. \end{aligned} \quad (147)$$

This can be simplified by approximation as in the case of (143) and (144). For most purposes we may write:

$$\nu_2' - \nu_1' = (\rho^2 - 1)\nu_1' \quad . \quad . \quad . \quad (148)$$

This gives rise to the rotational separation of isotopic band lines as illustrated in Fig. 94. The separation increases almost linearly with distance from the band origin, its value at the head of the band may be obtained by substituting for ν_1' from (26). It is necessary to

remind ourselves that the appearance of a duplicated pattern shown in Fig. 94 would not be seen unless according to (138) the vibrational and electronic effects were zero. Since ν_1' will be small compared to ν_1 , the vibrational displacement is much the more important.

(c) THE ELECTRONIC EFFECT

By an electronic effect we primarily mean the shift in the electronic frequency ν , i.e. of the origin of the band system, when one isotope is substituted for the other. The subdivision of the isotopic shift into three parts, as in (138), is a convenient fiction: in practice, terms occur which are due to the interaction of one type of motion with another. We shall consider electronic effects under four headings, of which the first is a purely electronic effect and the other three are of the 'interaction' type.

(1) Centre of mass effect

In the elementary Bohr theory of the hydrogen type of atom it is shown that the lines are given by $\nu = R\left(\frac{1}{n'^2} - \frac{1}{n^2}\right)$, where R is Rydberg's constant and stands for

$$R = \frac{2\pi^2\mu E^2 c^2}{ch^3} \quad . \quad . \quad . \quad . \quad . \quad . \quad (149)$$

Here E is the nuclear charge, e the electronic charge, and $\mu \left(= \frac{Mm}{M+m}\right)$ is called the 'reduced mass' of the electron. M is nuclear mass and m is the electronic mass, and the appearance of μ instead of m in (149) is due to the recognition that both nucleus and electron are moving round their common centre of mass. We should expect, therefore, slightly different values of the Rydberg constants for two isotopes, viz.

$$\frac{R_1}{R_2} = \frac{M_1(M_2 + m)}{M_2(M_1 + m)} \div 1 + \frac{m(M_1 - M_2)}{M_1 M_2} \quad . \quad . \quad (150)$$

This effect will only be appreciable for the very lightest atoms. The actual separation of corresponding lines of the isotopes will be

$$\nu_1' - \nu_2' = (R_1 - R_2) \left(\frac{1}{n'^2} - \frac{1}{n^2} \right) = \frac{m(M_1 - M_2)}{M_1 M_2} \nu_1' \quad . \quad (151)$$

It amounts to about 4.1 cm.^{-1} for $\text{H}\alpha$ and 22.2 cm.^{-1} for $\text{L}\alpha$, as calculated for the two isotopes of hydrogen of mass numbers 1 and 2. The effect will be much smaller in two-electron or three-electron atoms,* being of the order of 1 cm.^{-1} for lithium isotopes 6 and 7. While we may anticipate electronic displacements of this order in *molecular* spectra, for practical purposes only the lightest molecules, and in particular H_2 , HD, and D_2 ,† will show appreciable effects.

* *Phys. Rev.*, vol. 36, p. 694 (1930); vol. 38, p. 857 (1931).

† The hydrogen isotope of mass number 2 is called deuterium and the symbol D is used for it. The nucleus is called a deuteron (or deutron) analogous to the proton.

(2) *Nuclear reaction to precession of the electronic angular momentum round the inter-nuclear axis*

This effect, like the preceding one, is of importance only for the lightest molecules, and has been studied by Dieke * both theoretically and experimentally. He obtained an additional energy term by considering the interaction between the inter-nuclear axis and the precessing orbital momentum vector \bar{L} in a rotationless molecule, viz.

$$W/hc = [B_e - \alpha(v + \frac{1}{2})][L(L + 1) - \Lambda^2] . \quad (152)$$

From this we see that it is proportional to the square of the component of the orbital angular momentum perpendicular to the inter-nuclear axis. It is zero only for $S\Sigma$ levels for which $L = 0$, $\Lambda = 0$.

The first (constant) part of (152) will involve an electronic isotope shift. The displacements (in cm^{-1}) of the origins of two-band systems of hydrogen are given in the table (due to Dicke). Allowing for error

System	$\text{H}_2 - \text{HD}$		$\text{HD} - \text{D}^2$	
	Obs.	Calc.	Obs.	Calc.
$3p \ ^3\Pi \rightarrow 2s \ ^3\Sigma$. . .	5 01	7.55	4.94	7.61
$3p \ ^3\Sigma \rightarrow 2s \ ^3\Sigma$. . .	13 23	13.44	12.28	12.62

due to extrapolations, the agreement is reasonably good, and at least indicates that this interaction effect explains a large part of the electronic isotopic displacement.

The second part of (152) indicates that the vibrational frequency ω_e of the vibrational energy function should be replaced by $\omega_e - \alpha[L(L + 1) - \Lambda^2]$, and this will have a slight effect on the experimentally determined values of ρ to the extent of one part in a few thousand.

(3) *Nuclear reaction to precession of the spin momentum round the J-axis (spin multiplicity effect)*

During investigation of the (1,0) bands of OD and OH a substantial electronic shift (about 10 cm^{-1}) was recorded, and attributed to the effect of nuclear mass on the $K:S$ coupling of the $^2\Pi$ terms. The same effect, though smaller, was noted with B^{11}O and B^{10}O . Fig. 95 shows graphs of H. L. Johnston † in which the difference of the spin-doublet width of the $^2\Pi$ levels for the two isotopic molecules is portrayed. The circles represent experimental data: the full line is constructed from the theoretical relationship given in (153). Hill and Van Vleck showed that the doublet separation should be given by ‡

$$\begin{aligned} \Delta &= F_{2nd}''(K) - F_{1st}''(K) \\ &= B[4(K + \frac{1}{2})^2 + \lambda(\lambda - 4)\Lambda^2] - (2K + 1) \quad (153) \end{aligned}$$

where $\lambda = A/B$ (see p. 99).

This expression has been found to be only an indifferent repre-

* *Phys. Rev.*, vol. 47, p. 661 (1935).

† *Ibid.*, vol. 45, p. 79 (1934).

‡ See Dawson and Johnston, *Phys. Rev.*, vol. 43, p. 991 (1933).

presentation of the actual doublet width for large K values. The agreement shown in Fig. 95, where the difference in the isotopic Δ^S is plotted, is therefore as good as can be expected.

As another example of the isotopic effect on spin-doubling, this time in a $^2\Sigma$ state, we may take Watson's comparison of CaH and

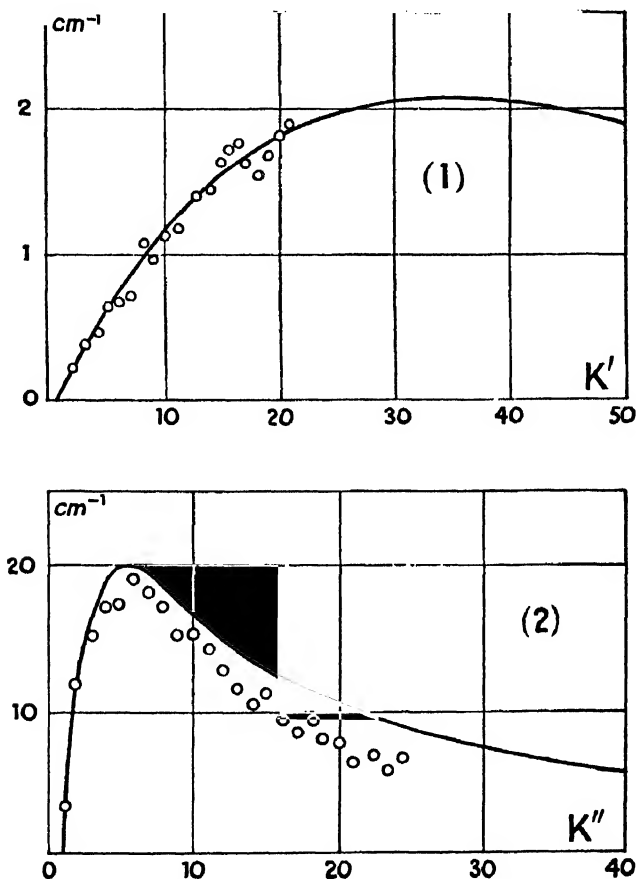


Fig. 95. Difference of the spin-doublet width Δ of the $^2\Pi$ components (1) $B^{11}O$ and $B^{10}O$, (2) DO and HO . The full line is the theoretical curve from the difference of the two values calculated by using (153). (After H. L. Johnston.)

CaD. According to theory the doublet separation should increase linearly: $\Delta v_{12}(K) = \gamma(K + \frac{1}{2})$. The linearity is very precise for CaD, the slope giving a value of $\gamma = -0.364$. In the case of CaH, due to perturbation, the slope changes from an initial value -0.945 to -0.543 . The ratio of the values of γ for CaD and CaH should theoretically be $\rho^2 (= 0.5127)$. This would require a value of γ for CaH of $-0.364/0.5127 (= -0.709)$.

(4) *A* Λ -type doubling effect

According to Van Vleck,* the Λ -type doublet separation should in Case (b) be $\delta_1 = \delta_2 = \frac{4B^2}{\nu} K(K+1)$, where 1 and 2 refer to the two $^2\Pi$ components and ν is the frequency ν^e of the electronic transition. For a Case (a) state $\delta_1 = a(J + \frac{1}{2})$ and $\delta_2 = 0$.

In the case of OH, Mulliken found the Λ -type doublet separation fitted empirically the formulæ $\delta_1 = 0.04(K + \frac{1}{2})^2$, $\delta_2 = 0.03(K - \frac{1}{2})^2$,

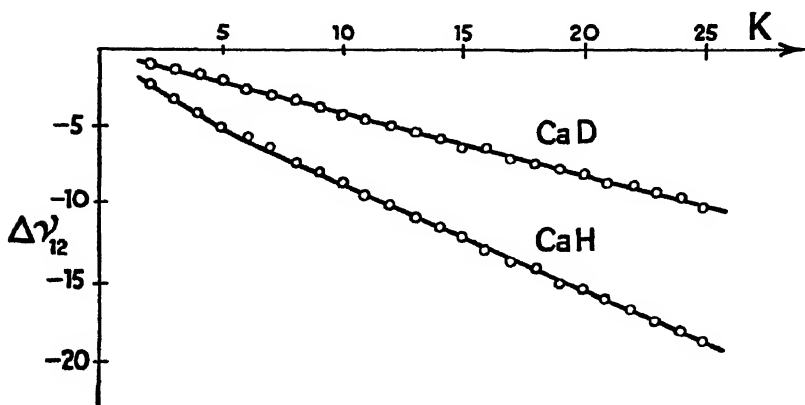


Fig. 96. Comparison of the spin-doubling in the upper $^2\Sigma$ state of the $B(^2\Sigma \rightarrow ^2\Sigma)$ band systems of CaH and CaD. (After W. W. Watson.)

which is in formal agreement with Van Vleck's Case (b) formula, although the constant differs from the predicted value $\frac{4B^2}{\nu}$ by a factor of about 10.

H. L. Johnston (*loc. cit.*) observed a very pronounced difference in the Λ -type doublet width for OH and OD. The experimental data based upon the (2,0), (1,0), and (0,0) bands for OH, and upon the (1,0) band for OD are shown in Fig. 97. According to Van Vleck, as we have seen, the factor controlling the doublet width involves B^2 . In Fig. 97 the best full line was constructed through the OH data. The broken line was then constructed by multiplying these ordinates by the factor p^4 ($= 0.284$), which is the ratio of the values of B^2 for OH and OD. The agreement is reasonably good. Similar results have been recorded for the Λ -doubling of the $^2\Pi$ state in the ($^2\Pi \rightarrow ^2\Sigma$) systems of BeH and BeD, and reference may be made with advantage to this work of Koontz.† The Λ -doubling of the $^1\Pi$ state of the ($^1\Pi \rightarrow ^1\Delta$) band of NH and ND also shows the same characteristic behaviour, and the paper of Dieke and Blue‡ may be referred to. An example of the Λ -doubling in a $^3\Pi$ state, viz. the $3p$ $^3\Pi$ level of H_2 , HD, and D_2 , is found in a paper by Dicke.§

* *Phys. Rev.*, vol. 33, p. 467 (1929).

† *Ibid.*, vol. 48, p. 711 (1935); see his Fig. 3.

‡ *Ibid.*, vol. 45, p. 400 (1934), see their Fig. 2.

§ *Ibid.*, vol. 48, p. 613 (1935).

(d) DEUTERIDE SPECTRA

Among the rare isotopes discovered in recent years * is that of hydrogen with mass number 2, commonly called deuterium. It occurs with an abundance ratio of about 1 : 5000 compared to H^1 . In no

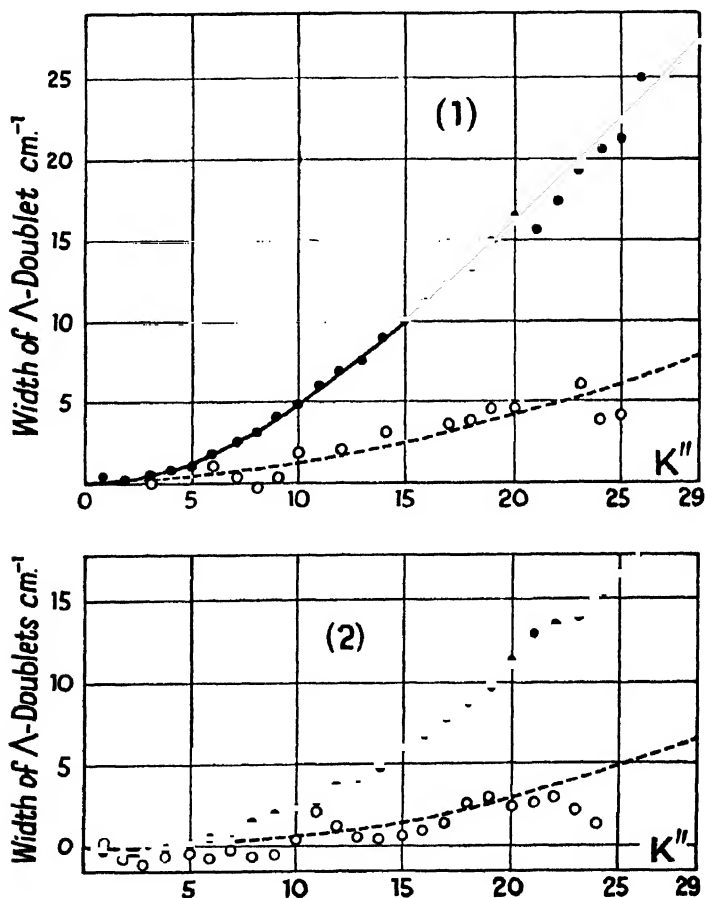


Fig. 97. Width of A-type doublets as a function of K'' . (1) $2\Pi_{1/2}$ state of OH and OD, (2) $2\Pi_1$ state of OH and OD. Experimental data on OH (full circle); on OD (open circle). The full line is drawn to fit the OH data. The dotted line through OD data is calculated as described in the text. (Both figs. after H. L. Johnston.)

case are isotopic effects in spectra likely to be so pronounced as those in which D is substituted for H in a molecule, one atom being replaced by an isotope of about twice its mass. The corresponding band systems of H_2 , HD, and D_2 have therefore been subject to close study

* Urey, Brickwedde, and Murphy, *Phys. Rev.*, vol. 39, p. 164 (1932).

by Dieke and others, for they provide the most favourable and searching tests of the theory of isotopic effects in band spectra.

The separation of gaseous isotopes has been effected by a number of ingenious methods. Some make use of repeated diffusion, based upon the rate of diffusion varying inversely as the square root of the molecular weight. Other methods make use of fractional evaporation and distillation since the rate of these processes follows a similar law. One of the most satisfactory methods has resulted in the concentration of 'heavy' water by the process of prolonged electrolysis. In electrolysis the light isotope is evolved preferentially, and by electrolysis of water down to about 10^{-5} of its original volume the concentration of D_2O rises to 99%. In the later stages of electrolysis the evolved gas is rich in deuterium: it is therefore burned and used for subsequent electrolysis. Heavy water has a density of 1.1079, a boiling point of $101.42^\circ C$. and freezing point of $3.82^\circ C$.

In the appended table is shown for six typical electronic states the variation of vibration frequency, of the rotational constant $B_e = \frac{h}{8\pi^2 \mu r_e^2}$, and of α , in the H_2 molecule and its isotopes. Data for the $2p\ ^1\Sigma$, $2s\ ^3\Sigma$, and $3p\ ^3\Pi$ states are of considerable precision, and it will be observed that the ratio of the ω_e -values is greater than ρ , and the ratio of the B_e -values greater than ρ^2 by a small but appreciable amount. The same feature will be noticed from the data of the second table, in which are collected some of the constants of hydride and deuteride spectra. An examination of the reasons for these small departures from the elementary theory would take us rather beyond the scope of this book. We shall therefore merely classify the causes and refer students to original papers:

(1) *Interaction of vibration and rotation*

Dunham, *Phys. Rev.*, vol. 41, p. 721 (1932).

Crawford and Jorgensen, *Phys. Rev.*, vol. 49, p. 745 (1936).

Dieke and Lewis, *Phys. Rev.*, vol. 52, p. 116 (1937).

(2) *Interaction of vibration and electronic motion*

Dieke (see Section (c) of this chapter).

Kronig, *Physica*, vol. 1, p. 617 (1934).

(3) *Interaction with other electronic states*

Van Vleck, *Jour. Chem. Phys.*, vol. 4, p. 327 (1936).

Mulliken and Christy, *Phys. Rev.*, vol. 38, p. 87 (1931).

Watson, *Phys. Rev.*, vol. 47, p. 30 (1935).

Note. The student who wishes to read additional papers illustrating isotopic effects in band spectra may consult the following:

Mulliken's papers on BO , CuI , and SiN (*loc. cit.*). Jenkins and McKellar on BO , *Phys. Rev.*, vol. 42, p. 464 (1932). Hardy and Sutherland on HCl , *Phys. Rev.*, vol. 41, p. 471 (1932). Brice on Silver Halides, *Phys. Rev.*, vol. 35, p. 960 (1930); vol. 38, p. 658 (1931). Brown on Br_2 , *Phys. Rev.*, vol. 38, p. 1179 (1931); vol. 39, p. 777 (1932). Watson on BeH , *Phys. Rev.*, vol. 37, p. 167 (1931).

TABLE OF VALUES OF ω_e (VIBRATION FREQUENCY), B_e THE ROTATIONAL CONSTANT, AND α GIVEN BY
 $B_e = B_e - \alpha(v + \frac{1}{2})$ FOR HYDROGEN : DEUTERIUM MOLECULES

	1. H_2	2. HD	3. D_2	2 : 1	3 : 1	3 : 2	ρ_{12}^n	ρ_{13}^n	ρ_{23}^n	n
$2p\ ^1\Sigma$	$\left\{ \begin{array}{l} \omega_e \\ B_e \\ \alpha \end{array} \right\}$ 1363.03 20.2485 1.227	$\left\{ \begin{array}{l} \omega_e \\ B_e \\ \alpha \end{array} \right\}$ 1180.77 15.1896 0.781	$\left\{ \begin{array}{l} \omega_e \\ B_e \\ \alpha \end{array} \right\}$ 965.25 10.1319 0.429	$\left\{ \begin{array}{l} \omega_e \\ B_e \\ \alpha \end{array} \right\}$ 0.86629 0.75016 0.6365	$\left\{ \begin{array}{l} \omega_e \\ B_e \\ \alpha \end{array} \right\}$ 0.70816 0.50038 0.3498	$\left\{ \begin{array}{l} \omega_e \\ B_e \\ \alpha \end{array} \right\}$ 0.81747 0.66703 0.5500	$\left\{ \begin{array}{l} \omega_e \\ B_e \\ \alpha \end{array} \right\}$ 0.86613 0.75019 0.6498	$\left\{ \begin{array}{l} \omega_e \\ B_e \\ \alpha \end{array} \right\}$ 0.70737 0.50038 0.3540	$\left\{ \begin{array}{l} \omega_e \\ B_e \\ \alpha \end{array} \right\}$ 0.81670 0.66700 0.5447	$\left\{ \begin{array}{l} \omega_e \\ B_e \\ \alpha \end{array} \right\}$ 1 2 3
$2s\ ^3\Sigma$	$\left\{ \begin{array}{l} \omega_e \\ B_e \\ \alpha \end{array} \right\}$ 2664.83 34.216 1.671	$\left\{ \begin{array}{l} \omega_e \\ B_e \\ \alpha \end{array} \right\}$ 2308.44 25.685 1.099	$\left\{ \begin{array}{l} \omega_e \\ B_e \\ \alpha \end{array} \right\}$ 1885.84 17.109 0.606	$\left\{ \begin{array}{l} \omega_e \\ B_e \\ \alpha \end{array} \right\}$ 0.86626 0.7507 0.658	$\left\{ \begin{array}{l} \omega_e \\ B_e \\ \alpha \end{array} \right\}$ 0.70768 0.5000 0.363	$\left\{ \begin{array}{l} \omega_e \\ B_e \\ \alpha \end{array} \right\}$ 0.81693 0.6661 0.551				
$2s\ ^1\Sigma$	$\left\{ \begin{array}{l} \omega_e \\ B_e \\ \alpha \end{array} \right\}$ 2588.9 32.679 —	$\left\{ \begin{array}{l} \omega_e \\ B_e \\ \alpha \end{array} \right\}$ 2204.4 24.568 —	$\left\{ \begin{array}{l} \omega_e \\ B_e \\ \alpha \end{array} \right\}$ 1784.5 16.373 —	$\left\{ \begin{array}{l} \omega_e \\ B_e \\ \alpha \end{array} \right\}$ 0.8514 0.7517 —	$\left\{ \begin{array}{l} \omega_e \\ B_e \\ \alpha \end{array} \right\}$ 0.6893 0.5010 —	$\left\{ \begin{array}{l} \omega_e \\ B_e \\ \alpha \end{array} \right\}$ 0.8095 0.6664 —				
$3p\ ^3\Sigma$	$\left\{ \begin{array}{l} \omega_e \\ B_e \\ \alpha \end{array} \right\}$ 2196.7 27.71 —	$\left\{ \begin{array}{l} \omega_e \\ B_e \\ \alpha \end{array} \right\}$ 1905.17 20.766 1.010	$\left\{ \begin{array}{l} \omega_e \\ B_e \\ \alpha \end{array} \right\}$ 1556.64 13.856 0.541	$\left\{ \begin{array}{l} \omega_e \\ B_e \\ \alpha \end{array} \right\}$ — — —	$\left\{ \begin{array}{l} \omega_e \\ B_e \\ \alpha \end{array} \right\}$ — — —	$\left\{ \begin{array}{l} \omega_e \\ B_e \\ \alpha \end{array} \right\}$ 0.81706 0.6672 0.534				
$3p\ ^3\Pi$	$\left\{ \begin{array}{l} \omega_e \\ B_e \\ \alpha \end{array} \right\}$ 2371.58 30.364 1.545	$\left\{ \begin{array}{l} \omega_e \\ B_e \\ \alpha \end{array} \right\}$ 2054.59 22.810 1.020	$\left\{ \begin{array}{l} \omega_e \\ B_e \\ \alpha \end{array} \right\}$ 1678.22 15.200 0.5520	$\left\{ \begin{array}{l} \omega_e \\ B_e \\ \alpha \end{array} \right\}$ 0.86634 0.7512 0.660	$\left\{ \begin{array}{l} \omega_e \\ B_e \\ \alpha \end{array} \right\}$ 0.70764 0.5006 0.357	$\left\{ \begin{array}{l} \omega_e \\ B_e \\ \alpha \end{array} \right\}$ 0.81682 0.6664 0.541				
$3d\ ^1\Pi$	$\left\{ \begin{array}{l} \omega_e \\ B_e \\ \alpha \end{array} \right\}$ 2265.22 29.790 1.515	$\left\{ \begin{array}{l} \omega_e \\ B_e \\ \alpha \end{array} \right\}$ 1962.14 22.36 1.21	$\left\{ \begin{array}{l} \omega_e \\ B_e \\ \alpha \end{array} \right\}$ 1600.14 14.739 0.526	$\left\{ \begin{array}{l} \omega_e \\ B_e \\ \alpha \end{array} \right\}$ 0.86621 0.7506 0.798	$\left\{ \begin{array}{l} \omega_e \\ B_e \\ \alpha \end{array} \right\}$ 0.70640 0.4948 0.347	$\left\{ \begin{array}{l} \omega_e \\ B_e \\ \alpha \end{array} \right\}$ 0.81551 0.6592 0.434				

Notes.

1. $3p\ ^3\Pi \rightarrow 2s\ ^3\Sigma$ is the so-called Fulcher system with $\nu^* = 16793.9$ (Dieke and Blue, *Phys. Rev.*, vol. 47, p. 261 (1935)).
 2. $2s\ ^1\Sigma \rightarrow 2p\ ^1\Sigma$ is in the near infra-red $\nu^* = 8375.6$ (Dieke, *Phys. Rev.*, vol. 50, p. 797 (1936)).
 3. $3p\ ^3\Sigma \rightarrow 2s\ ^3\Sigma$ is the near infra-red $\nu^* = 11839$ (Dieke, *Phys. Rev.*, vol. 48, p. 606 (1935)).
 4. $3d\ ^1\Pi \rightarrow 2p\ ^1\Sigma$ is in the visible region with $\nu^* = 21295.2$ (Dieke and Lewis, *Phys. Rev.*, vol. 52, p. 100 (1937)).
- B_e is a value of B_e to which several corrections have been applied (see Section (e)).

M	ω_e		Ratio MD/MH	B_e		Ratio MD/MH	Calculated	
	MH	MD		MH	MD		ρ	ρ^2
N 1Π	—	—	—	14.16 *	7.64	0.5388	0.73078	0.53404
1Σ	—	—	—	16.446	8.886	0.5372		
C $6_{\text{ground}} 2\Sigma'$	—	—	—	4.2776	2.196	0.5137		
	—	—	—	4.4918	2.2813	0.50788	0.71607	0.51276
Li $7_{\text{grd}} 1\Sigma'$	1405.65	1055.12	0.75062	7.5131	4.2338	0.56352		
	234.41	189.12	0.7812	2.8186	1.6080	0.5695	0.75049	0.56323
Ag $6_{\text{grd}} 1\Sigma'$	—	—	—	6.453	3.2595	0.50511	0.71061	0.50497
Be $6_{\text{grd}} 2\Sigma'$	2059.5	—	—	10.308	5.6807	0.55110		
Be $6_{\text{grd}} 1\Sigma'$	2220.0	1647.6	0.7420	10.813	5.9546	0.55073	0.7459	0.55062
Be $6_{\text{grd}} 1\Sigma'$	1476.1	1090.4	0.7430	7.2008	3.9712	0.55149		
Al $6_{\text{grd}} 1\Sigma'$	—	—	—	6.4040	3.3209	0.51443	—	0.51835
Cl $6_{\text{grd}} 1\Sigma'$	2989.2	2144.0	0.71724	10.5839	5.333	0.51855	0.71703	0.51414
Sr $6_{\text{grd}} 2\Sigma'$	—	—	—	3.8788	1.9427	0.50635	0.71136	0.50603
Sr $6_{\text{grd}} 1\Sigma'$	—	—	—	3.6751	1.8609	0.50085		
Cu $6_{\text{grd}} 1\Sigma'$	1939.9	1384.4	0.7135	7.935	4.0375	0.5085	0.7129	0.5082
	1699.9	1213.2	0.7129	6.878	3.5199	0.5116		
Cd $6_{\text{grd}} 1\Sigma'$	1775	1262.5	0.7113	6.070	3.075	0.5065	0.7105	0.5048
	1252	887.2	0.7086	4.851	2.451	0.5052		
Zn $6_{\text{grd}} 1\Sigma'$	1916	1364.8	0.7123	7.415	3.818	0.5155	0.7127	0.5079
	1365	974.4	0.7138	5.77	2.944	0.5098		
Na $6_{\text{grd}} 1\Sigma'$	—	—	0.72250	4.9012	2.5575	0.52181	0.72213	0.52147

N: Dicke and Blue, *Phys. Rev.*, vol. 45, p. 395 (1934).

Ca: Watson, *Phys. Rev.*, vol. 47, p. 27 (1935).

Li: Crawford and Jorgensen, *Phys. Rev.*, vol. 47, p. 358 (1935); vol. 49, p. 745 (1936).

Ag: Koontz, *Phys. Rev.*, vol. 48, p. 139 (1935).

Be: Koontz, *Phys. Rev.*, vol. 48, p. 707 (1935).

Cl: Hardy, Barker, and Dennison, *Phys. Rev.*, vol. 42, p. 279 (1932).

Sr: Watson, Fredrickson, and Hogan, *Phys. Rev.*, vol. 49, p. 150 (1936).

Cu: Jeppesen, *Phys. Rev.*, vol. 50, p. 445 (1936).

Cd: Zumstein, Gabel, and McKay, *Phys. Rev.*, vol. 51, p. 238 (1937).

Zn: Gabel and Zumstein, *Phys. Rev.*, vol. 52, p. 726 (1937).

Al: Holst and Huithen, *Nature*, vol. 133, pp. 496, 4796 (1934); *Zeit. f. Phys.*, vol. 90, p. 712 (1934).

Na: Olsson, *Nature*, vol. 134, p. 697 (1934); *Zett. f. Phys.*, vol. 93, p. 206 (1935).

* These values for nitrogen are all B_0 not B_e .

EFFECTS OF APPLIED MAGNETIC FIELDS

(a) WEAK FIELDS : THE ZEEMAN EFFECT

THE principle of the effect of a magnetic field is similar in the case of atoms * and molecules, although the effect itself is more complex in molecules than in atoms. In both cases the resultant magnetic moment is caused to precess like a spinning-top round the axis of the applied field. In an atom, provided the applied field is not strong enough to cause a breakdown of the coupling of \bar{L} and \bar{S} giving a resultant \bar{J} , this resultant magnetic moment in the direction of \bar{J} will precess round the field H at certain angles given by $\bar{J} \cos(\bar{J}H) = M$. Here M is called the magnetic quantum number, and takes $2J + 1$ (integral) values which lie between $+J$ and $-J$. There are thus $2J + 1$ orientations of the magnetic moment in the field, corresponding to different energies of precession, so that each non-field level now yields a symmetrical pattern of $2J + 1$ equi-spaced levels. Transitions between such sub-levels are governed by a selection principle controlling M , viz. $\Delta M = \pm 1$, or 0, and thus arises the Zeeman splitting of a spectral line. The states of polarization of the various component lines of the Zeeman pattern are summarized below.

	View parallel to H	View perpendicular to H
$\Delta M = \pm 1$. . .	Circular	Linear perpendicular to H
$\Delta M = 0$. . .	(Not visible)	Linear parallel to H

The energy of precession of a magnetic vector round a field H can be calculated simply by using Larmor's theorem, according to which the angular velocity Ω of the precession is given by

$$\Omega = H \frac{\text{Magnetic Moment}}{\text{Mechanical Moment}} \quad . \quad . \quad . \quad (154)$$

If the precessing entity is a simple electron orbit the above ratio is $\frac{e}{2mc}$. If it is a spinning electron, the ratio is $2\frac{e}{2mc}$. If it is a combination of a spin and an orbital motion, then the ratio is $g\left(\frac{e}{2mc}\right)$, where g , which is possibly fractional, is determined by the type of coupling between l and s , and is called the Landé g -factor. It can be calculated from

$$g = 1 + \frac{j(j+1) + s(s+1) - l(l+1)}{2j(j+1)} \quad . \quad . \quad (155)$$

In general therefore

$$\Omega = Hg\left(\frac{e}{2mc}\right) \quad . \quad . \quad . \quad . \quad (156)$$

* Reference may be made to *Atomic Spectra*, Chapter VI, for a brief account of this.

where $g = 1$ for an electronic orbit and 2 for a spinning electron. The energy of the precession will thus be given by

$$E^H = \frac{m}{2} [\dot{r}^2 + r^2 \dot{\theta}^2 + r^2 \sin^2 \theta (\dot{\phi} + \Omega)^2] - \frac{m}{2} [r^2 + r^2 \dot{\theta}^2 + r^2 \sin^2 \theta \dot{\phi}^2] \\ \doteq mr^2 \sin^2 \theta \dot{\phi} \Omega = p_\phi \Omega \quad . \quad . \quad . \quad (157)$$

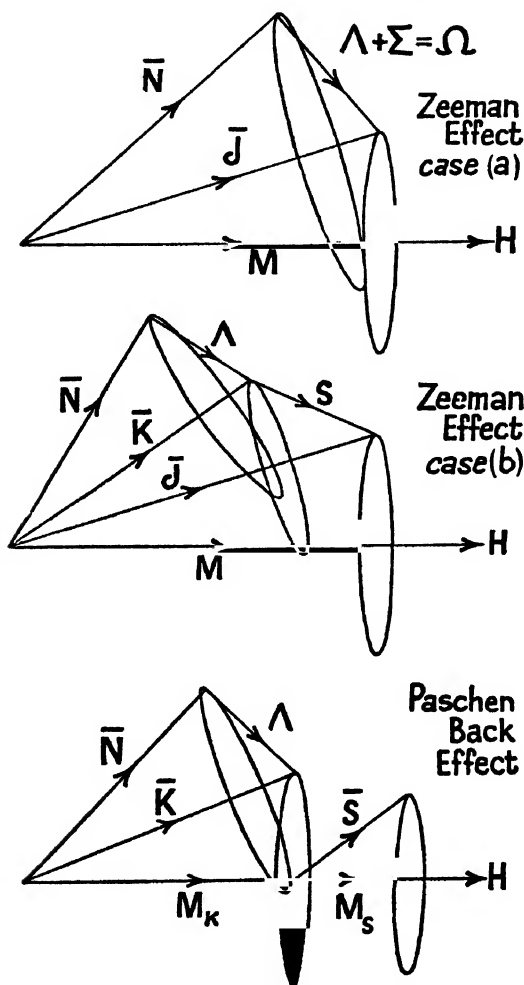


Fig. 98. Effects of applied magnetic field on molecular vectors.

Here p_ϕ is the component of the angular momentum of the vector along the axis of the field.

Alternatively, we may, by (154), write this

$$E^H = \mu_H H \quad . \quad . \quad . \quad . \quad (158)$$

where μ_* is the component of the resultant magnetic moment of the molecule along the axis of the field.

Let us apply these data to the molecular case. We recognize that the molecular magnetic moment will derive from electronic orbital motion, electronic spins, and nuclear rotation. The third of these will be much less important than the first two, and is for the present neglected (see Section (f)). The nature of the coupling (Hund's cases, see Chapter VII) will be important, and will, of course, determine the magnetic moment involved. In a molecule, owing to the rapid precession of the orbital vector L and the spin vector S , round the inter-nuclear axis, we are only concerned with Λ and Σ , their respective components along this axis. The components perpendicular to this axis vanish by averaging.

Case (a). Here the angular momentum associated with the inter-nuclear axis is $(\Lambda + 2\Sigma) \frac{h}{2\pi}$. (We have noted already that the spin precesses round any magnetic field, and therefore round the inter-nuclear axis with twice the precessional velocity of L .) The resultant magnetic moment is thus $(\Lambda + 2\Sigma) \frac{eh}{4\pi mc}$. The component along J is alone of importance because of the rapid precession round J . Then this component precesses round the external field. Hence by (158) we have

$$E^H = (\Lambda + 2\Sigma) \frac{eh}{4\pi mc} \cos(\Omega\bar{J}) \cos(\bar{J}H)H \quad . \quad (159)$$

where

$$\Omega = \bar{J} \cos(\Omega\bar{J}) \quad \text{and} \quad M = \bar{J} \cos(\bar{J}H).$$

Hence substituting

$$E^H = (\Lambda + 2\Sigma) \frac{eh}{4\pi mc} \frac{\Omega M}{J(J+1)} H.$$

Or we may write it

$$\Delta\nu = \frac{(\Omega + \Sigma)\Omega M}{J(J+1)} \delta \quad . \quad . \quad . \quad (160)$$

where $\delta = \frac{eH}{4\pi mc}$ is the Lorentz unit ($4.674 \times 10^5 H$ cm.⁻¹), and $\Delta\nu$ gives the separation of the component Zeeman levels from the undisplaced one.

From this result we may deduce several characteristic features of the Zeeman effect. (1) Those levels for which $\Omega = 0$, e.g. $3\Pi_0$, or for which $\Omega = -\Sigma$, e.g. $2\Pi_1$, are unsplit by the field. (2) Since M takes the series of $2J+1$ integral values lying between $\pm J$, the overall width of the Zeeman pattern of levels is $\pm \frac{(\Omega + \Sigma)\Omega\delta}{J+1}$, which diminishes with increasing J . We thus expect to find patterns of increasing numbers of components in a diminishing space as we pass outward from a band origin. Band lines near the origin are usually of low intensity. Hence the detail necessary to verify completely the Zeeman effect in bands requires enormous resolving power, and except near band origins all that is possible experimentally is to

verify overall widths and the intensity distributions through the broadened 'lines' (which we discuss later).

Case (b). As Fig. 98 reminds us, we here have the spin vector detached from the inter-nuclear axis and coupled with K which is the resultant of Λ and N . This coupling, as we know, is generally a loose one, as indicated by the smallness of the 'spin multiplicity' in most cases. It will therefore often happen that a Case (b) coupling to which a magnetic field is applied passes straight over to a Paschen-Back effect in which J , the resultant of K and S , is broken down, and the two latter rotate independently round H . Assuming this does not happen, we shall have a Zeeman effect. By (158) we can then write down for the magnetic energy of precession

$$E^H = [\Lambda \cos(\Lambda K) \cos(KJ) + 2\bar{S} \cos(SJ)] \frac{ehH}{4\pi mc} \cos(JH) \quad (161)$$

where

$$\begin{aligned} \cos(\Lambda K) &= \frac{\Lambda}{\sqrt{K(K+1)}}, \quad \cos(KJ) = \frac{J(J+1) + K(K+1) - S(S+1)}{2KJ}, \\ \cos(JH) &= \frac{M}{\sqrt{J(J+1)}}, \quad \cos(SJ) = \frac{J(J+1) - K(K+1) + S(S+1)}{2SJ}. \end{aligned}$$

Substituting

$$\begin{aligned} \Delta v &= \frac{E^H}{h} = \frac{M\delta}{J(J+1)} \left[\frac{\Lambda^2}{2K(K+1)} \{J(J+1) + K(K+1) - S(S+1)\} \right. \\ &\quad \left. + \{J(J+1) - K(K+1) + S(S+1)\} \right] \quad (162) \end{aligned}$$

This is a cumbersome expression of little practical value which reduces to

$$\Delta v = M\delta \left[\frac{\Lambda^2}{J(J+1)} + \frac{2}{J}(J-K) \right] \quad (163)$$

for large values J and K and by neglecting S . The overall width of the pattern of levels, putting $M = \pm J$ is $2\delta \left[\frac{\Lambda^2}{J+1} + 2(J-K) \right]$.

(b) STRONG FIELDS: THE PASCHEN-BACK EFFECT

Here, as indicated in Fig. 98, there is no coupling of K and S , and therefore no J or M . The vectors K and S precess round the applied field and give rise to two quantum numbers M_K and M_S , where M_K takes the $2K+1$ integral values between $\pm K$, and M_S the $2S+1$ values between $+S$ and $-S$. We have

$$\begin{aligned} \sqrt{K(K+1)} \cos(KH) &= M_K, \\ \sqrt{S(S+1)} \cos(SH) &= M_S, \end{aligned} \quad (164)$$

and the energy of precession about the magnetic field is

$$\begin{aligned} E^H &= [\Lambda \cos(\Lambda K) \cos(KH) + 2\bar{S} \cos(SH)] \frac{eh}{4\pi mc} H \\ &= \left[M_K \frac{\Lambda^2}{K(K+1)} + 2M_S \right] \delta \quad (165) \end{aligned}$$

The $2S + 1$ values of M_s correspond to the multiplicity of the term, and each of these sub-levels splits into $2K + 1$ components in the strong magnetic field. The range of the pattern is $\pm \left[\frac{\Lambda^2}{K+1} + 2S \right] \delta$.

It is when the strength of the field is such that the Zeeman components arising from adjacent multiplet levels become contiguous that asymmetry in the patterns develops, and conditions change over to the Paschen-Back effect. The end result for a very strong field is a grouping of the lines to form a 'normal' triplet. We have seen that in the presence of a field the spin vector desires to precess round it with twice the frequency of the orbital vector. A 'compromise' frequency is presumably attained, which with increase of field results in distortion of the molecule until finally independent precession takes place.

The earliest attempt to account for magnetic effects in molecular bands was made by Lenz in 1919. Kramers and Pauli in 1923 and Kemble about the same time considered a particular model. Hund in 1926 provided the theoretical views which, expressed in modern notation, have been given above.

(c) ZEEMAN EFFECT IN THE ÅNGSTRÖM CO BANDS (${}^1\Sigma \rightarrow {}^1\Pi$)

Experimental work on the effect of magnetic fields on band structure goes back many years. Dufour in 1906-9, Croze in 1914, Fortrat in 1913-15, Deslandres and others in 1913-14, to mention some of the early workers, made many careful observations; but in the absence of a guiding theory and a knowledge of what to look for, their data have little more than historical interest. The first experimental work specifically undertaken to test Hund's theoretical views was that of Kemble, Mulliken, and Crawford * on a well-known band system of CO, chosen because of its simple structure (${}^1\Sigma \rightarrow {}^1\Pi$) (see Plate II and Chapter IX (b)).

By equation (160) or (163), since $\Lambda = 0$ and the spin $S = 0$, we note that the upper electronic level will be unaffected by the field, and will contribute nothing to the Zeeman pattern of the band lines. For the lower state we have from (160), where $\Omega = 1$ and $\Sigma = 0$,

$$\Delta\nu = \frac{M''}{J''(J''+1)} \delta, \quad \text{where } J'' = 1, 2, 3, \text{ etc.} \quad (166)$$

From this we should expect the following simple line structures :

Lines	Zeeman components		Interval	Overall width
$R(1), Q(1), P(1)$	3	$M'' = \pm 1, 0$	$\delta/2$	δ
$R(2), Q(2), P(2)$	5	$M'' = \pm 2, \pm 1, 0$	$\delta/6$	$\frac{5}{3}\delta$
$R(3), Q(3), P(3)$	7	$M'' = \pm 3, \pm 2, \pm 1, 0$	$\delta/12$	$\frac{7}{3}\delta$
$R(4), Q(4), P(4)$	9	$M'' = \pm 4, \pm 3, \pm 2, \pm 1, 0$	$\delta/20$	$\frac{9}{5}\delta$

In Fig. 99 we indicate what the Zeeman patterns of a few of the early lines of each branch will be. The intensities were calculated from

* *Phys. Rev.*, vol. 30, p. 438 (1927), and vol. 33, p. 341 (1929).

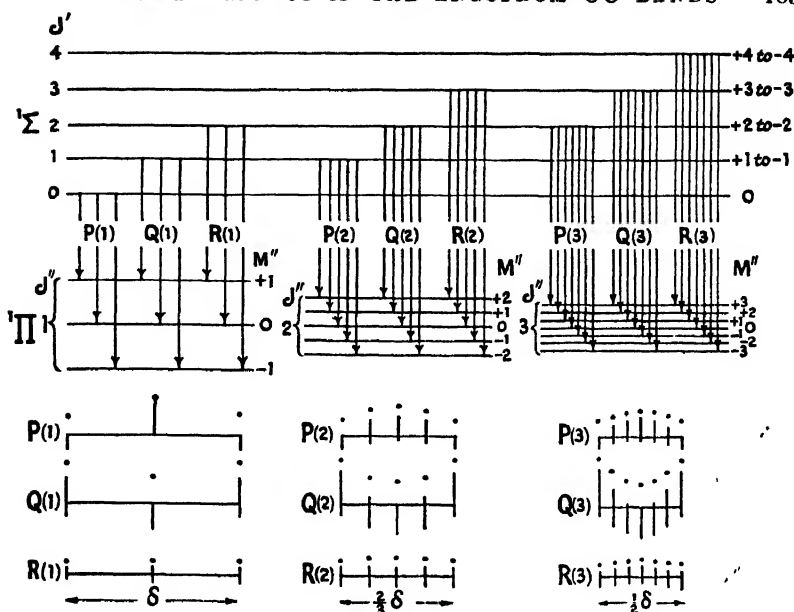


Fig. 99. Formation of Zeeman patterns of a few lines of $^1\Sigma \rightarrow ^1\Pi$ bands. The lengths of the lines represent total intensities. The parts of these lines above the horizontal base line are intensities of the components polarized parallel to the field ($\Delta M = 0$); the parts below the horizontal base line measure intensities of the components perpendicular to the field ($\Delta M = \pm 1$). The dots measure by their height above the base line the total intensities where these two polarized components are superposed.

formulae of Dennison,* which in the case of a $^1\Sigma \rightarrow ^1\Pi$ transition are :

$$\left. \begin{aligned}
 P \text{ branch : } I_0 &= \frac{3(J^2 - M^2)(J + 1)}{(2J - 1)(2J + 1)J}, \\
 I_{\pm 1} &= \frac{3(J \pm M)(J \pm M - 1)(J + 1)}{4J(2J - 1)(2J + 1)}, \\
 Q \text{ branch : } I_0 &= \frac{3M^2}{J(J + 1)}, \quad I_{\pm 1} = \frac{3(J \pm M)(J \pm M + 1)}{4J(J + 1)}, \\
 R \text{ branch : } I_0 &= \frac{3J[(J + 1)^2 - M^2]}{(J + 1)(2J + 1)(2J + 3)}, \\
 I_{\pm 1} &= \frac{3J(J \mp M + 1)(J \mp M + 2)}{4(J + 1)(2J + 1)(2J + 3)}.
 \end{aligned} \right\} \quad (167)$$

These formulae, as we see in Fig. 99, give patterns with a symmetrical intensity distribution, which, as we shall mention later, is not in accord with experimental data. What, then, are the experimental data?

In their later work Kemble, Mulliken, and Crawford used the arrangement pictured diagrammatically in Fig. 100. The important

* *Phys. Rev.*, vol. 28, p. 318 (1926).

part of the discharge was through a fine capillary tube of 0.3–0.5 mm. bore. Small cylinders of tube bored longitudinally with eight or ten half-millimetre holes and baked for five hours at 950° C. were used as traps to catch tungsten oxide vapours which otherwise diffused from the electrodes and rendered the capillary walls opaque. Fields up to 35,000 gauss were employed, the precise value being determined by the magnitude of Zeeman effect on some convenient atomic lines. For this purpose the zinc triplet (λ 4680, 4722, 4810) from a special arc, or the mercury lines λ 4047, 4358, 5461 from a special discharge tube were used. Most of the patterns corresponding to the first two lines of each branch of the strongest band at λ 5610 were resolved using Nicol prisms to separate the parallel and perpendicular polarization (the lines above and below the base lines in the lower part of Fig. 99). It is apparent that where the patterns are unresolved, as for the higher members of each branch, the *Q* lines (in parallel polarization)

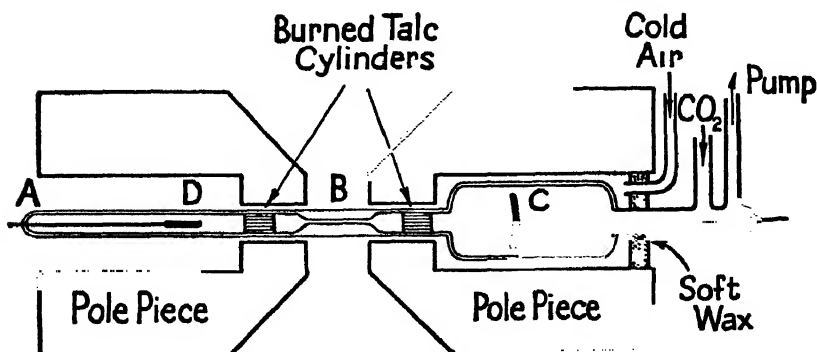


Fig. 100. Discharge tube arranged in a magnetic field to study the Angstrom CO bands. (Kemble, Mulliken, and Crawford.)

and the *P* lines (in perpendicular polarization) will tend to appear as doublets. This was found to be the case, and the overall width as determined from them was in good agreement with that anticipated theoretically from (166).

One of the most interesting features, unaccounted for by the simple theory which led to (167), was the asymmetrical intensity of these 'doublet' components. It was found that in the *Q* 'doublets' the low-frequency component was the stronger, in the *P* 'doublets' the high-frequency component was stronger. Kronig* investigated further the theoretical intensities of the components of a Zeeman band-line pattern, pointing out that the formulae of (167) were only valid in the limiting case of very weak fields ($H \rightarrow 0$). For appreciable fields Kronig showed that intensity perturbations would arise directly proportional to the field strength, and of such a nature that the decrease of intensity of a particular Zeeman component was associated with a corresponding increase of intensity of the symmetrically placed component in the other half of the pattern. The

* *Phys. Rev.*, vol. 31, p. 195 (1928).

expressions giving facts for the *relative* intensity changes of the components of the Zeeman pattern are rather cumbersome.

$$\left. \begin{aligned}
 P(J+1) & \left\{ \begin{array}{ll} M \rightarrow M \mp 1 & \epsilon = \mp k \frac{J \pm M}{(J \mp 1)^2}, \\ \text{(perp.)} & \\ M \rightarrow M & \epsilon = -k \frac{M}{(J \mp 1)^2}, \\ \text{(parallel)} & \end{array} \right. \\
 Q(J) & \left\{ \begin{array}{ll} M \rightarrow M \mp 1 & \epsilon = \mp k \left[\frac{(J^2 - 1)(J \pm M - 1)}{J^2(2J - 1)(2J + 1)} \right. \\ & \left. - \frac{J(J + 2)(J \mp M + 2)}{(J + 1)^2(2J + 1)(2J + 3)} \right] \\ M \rightarrow M & \epsilon = k \left[\frac{(J^2 - 1)(J^2 - M^2)}{J^2(2J - 1)(2J + 1)M} \right. \\ & \left. + \frac{J(J + 2)\{(J + 1)^2 - M^2\}}{(J + 1)^2(2J + 1)(2J + 3)M} \right], \end{array} \right. \\
 R(J-1) & \left\{ \begin{array}{ll} M \rightarrow M \mp 1 & \epsilon = \pm k \frac{J \mp M + 1}{J^2}, \\ M \rightarrow M & \epsilon = -k \frac{M}{J^2}, \end{array} \right.
 \end{aligned} \right\} \quad (168)$$

where k stands for $\frac{8\pi^2 I''}{h} \frac{eH}{4\pi m}$ and is of the order of the ratio of the precession frequency to the ordinary molecular rotation frequency $\left(\frac{eH}{4\pi mc} : \frac{Jh}{4\pi^2 Ic} \right)$.

These formulae account satisfactorily for the experimental data. Consider, for example, $Q(J)$, $M \rightarrow M$ in (180): ϵ is positive for positive values of M , and vice versa. Thus the positive values of M correspond in the pattern to stronger components than the negative values. As is clear from Fig. 99 or equations (160) or (163) positive values of M will correspond to the lower frequency components. Again, considering $P(J+1)$, $M \rightarrow M \mp 1$, we have ϵ negative for positive values of M and vice versa.

About the same time as this work on CO was done, Watson and Perkins * investigated a $^1\Sigma \rightarrow ^1\Sigma$ system of AgH, and found, as theory predicted, no Zeeman patterns even up to $H = 33,000$ gauss. The AlH band at ($^1\Pi \rightarrow ^1\Sigma$) behaved likewise as theory predicted.

(d) PERTURBED TERMS IN THE ÅNGSTRÖM CO BANDS

Perturbations in the band lines were discussed in Chapter IX (m) and mention was made in particular of violent perturbations in certain Ångström CO bands. The investigations of Rosenthal and Jenkins showed that these perturbations occurred in the lower ($^1\Pi$) state and they were able to assign correct rotational quantum numbers to the band lines (see Fig. 81) so as to secure smooth deviations from the expected positions, and to retain the correct $\Delta_2 F'(J)$ combination

* *Phys. Rev.*, vol. 30, p. 592 (1927).

differences. It was considered probable that the perturbing state was a $^3\Pi$ state lying close to the $^1\Pi$. As Fig. 81 shows, there are commonly two lines for each J -value near the centre of a perturbation. It was also found that the sum of the intensities of the two lines was about equal to that which an unperturbed line would have had, and that the greater a line's displacement the less its intensity. The appearance of two lines is explained by the interaction of the two-wave function corresponding to $^3\Pi$ and $^1\Pi$, so that transitions from $^1\Sigma$ to $^3\Pi$ may occur.

Crawford first noted the existence of large and irregular Zeeman effects on these perturbed lines. In 1932 Watson* made a detailed examination of these effects. He found a different type of Zeeman

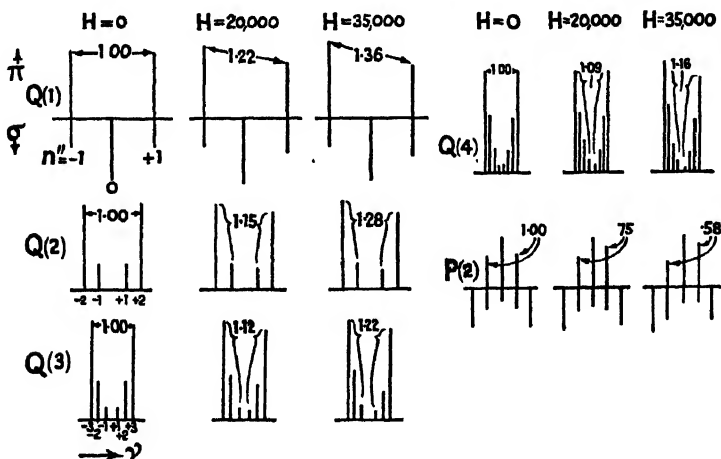


Fig. 101. Theoretical intensities of some Zeeman patterns of Ångström band lines according to Kronig's formulae. The parallel (polarized) components ($M \rightarrow M$) are drawn above the line and the perpendicular (polarized) components are shown below the line. The figures attached to the Q lines are the ratios of the sums of intensities of the low-frequency and the high-frequency components. (After F. H. Crawford.)

effect at each of the perturbations in the (0,0) band, and noticed that the most perturbed lines were magnetically the most sensitive. It was also observed that, in general, where the effect of the field was to produce a 'doublet' effect, these components were never symmetrically placed relative to the no-field position. Moreover, where in strong fields two separate blocks of radiation were produced, their intensities were never equal.

Let us consider specific perturbations. In the region about $Q(12)$ of the (0,0) band very little effect was produced by a field of $H = 10,000$ gauss. Stronger fields merely increased slightly the magnitude of the perturbation. On the other hand, P and R lines around $J = 16$ underwent a uniform symmetrical broadening with an overall width much greater than one would expect. Again, the $Q(30)$ pattern at high field strength was a narrow, sharp, but unsymmetrical doublet.

* *Phys. Rev.*, vol. 42, p. 509 (1932).

These different experimental features, as well as the multiple character of the perturbations, support the view that a state such as ${}^3\Pi$ with its components ${}^3\Pi_0$, ${}^3\Pi_1$, and ${}^3\Pi_2$ may be responsible. If, as seems likely, it is the ${}^3\Pi$ state which is the end state of 'third positive CO bands' (${}^3\Sigma \rightarrow {}^3\Pi$), we know that it has A of the order 50 to 60 cm^{-1} and is fairly near to Case (a) conditions. The Zeeman effect on these levels by (160) would be

$$\left. \begin{aligned} {}^3\Pi_0 \quad \Delta\nu &= -\frac{M}{J(J+1)} \delta, \\ {}^3\Pi_1 \quad \Delta\nu &= +\frac{M}{J(J+1)} \delta, \\ {}^3\Pi_2 \quad \Delta\nu &= +\frac{3M}{J(J+1)} \delta. \end{aligned} \right\} \dots \dots (169)$$

It is notable that the Zeeman splitting of ${}^3\Pi_1$ is the same as for a ${}^1\Pi$ state of the same J -value. For ${}^3\Pi_0$ the splitting is of the same magni-

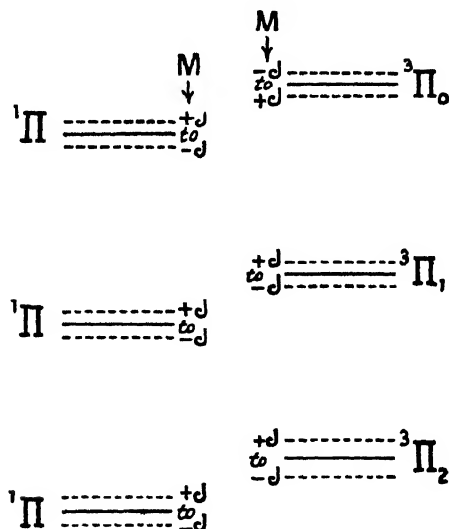


Fig. 102. Magnetic sub-levels associated with ${}^3\Pi_0$, ${}^3\Pi_1$, and ${}^3\Pi_2$ levels, which are supposed to be slightly above ${}^1\Pi$ levels. (After Watson.)

tude but the pattern is inverted; for ${}^3\Pi_2$ the pattern interval is three times as great as the others.

The conditions under which two levels may perturb each other were stated in Chapter IX (m). To these conditions we must now add another: the levels must have the same M -values.

Suppose we consider the case of a ${}^3\Pi_0$ level slightly above a ${}^1\Pi$ level of the same J -value, as in Fig. 102. The $2J+1$ magnetic sub-levels are not shown in the diagram, but only the two limiting sub-levels $M = +J$ and $M = -J$. Perturbation takes the form, as we saw, of an apparent mutual repulsion of levels. It therefore

follows that the close approach of $+M$ sub-levels of the two states will result in violent repulsion. The $-M$ sub-levels of the two states are moving farther from each other and will be mutually perturbed much less. The result is a tendency to inversion of the levels and spreading out of the pattern. In the case of ${}^1\Pi$ and ${}^3\Pi_1$, no effect of the magnetic field should appear unless ${}^3\Pi_1$ departs from Case (a) conditions (cf. $Q(12)$). In the case of ${}^1\Pi$ and ${}^3\Pi_2$ the $-M$ levels are forced closer together with increased perturbation, while the $+M$ levels separate from each other. Such is probably the case at $J = 16$ in the P and R branches. The $Q(30)$ pattern is possibly a ${}^1\Pi$, ${}^3\Pi_0$ interaction. Such are the general lines of explanation of these effects.

(c) ZEEMAN EFFECT IN DOUBLET BANDS (${}^2\Pi \rightleftharpoons {}^2\Sigma$)

According to equation (160) if we are dealing with a ${}^2\Pi$ state under Case (a) conditions, the two sub-levels ${}^2\Pi_1$ and ${}^2\Pi_{11}$ will behave very differently. For ${}^2\Pi_1$, since $\Omega = -\Sigma = -\frac{1}{2}$, we should expect no Zeeman splitting. For ${}^2\Pi_{11}$, where $\Sigma = +\frac{1}{2}$ and $\Omega = \Lambda + \Sigma = 1\frac{1}{2}$, we should have $\Delta\nu = \pm \frac{3M}{J(J+1)} \delta$, where $J = 1\frac{1}{2}, 2\frac{1}{2}, 3\frac{1}{2}$, etc.

Thus each rotational level of the ${}^2\Pi_{11}$ state splits in the Zeeman effect into $2J + 1$ components, the overall width of each pattern being $\frac{6\delta}{J+1}$. As Fig. 103 shows, the levels corresponding to $J' = 1\frac{1}{2}, 2\frac{1}{2}, 3\frac{1}{2}$, &c., have 4, 6, 8, components respectively.

In a ${}^2\Sigma$ state for which $\Lambda = 0$, and the spin $S = \frac{1}{2}$, the spin angular momentum is not linked with the inter-nuclear axis, but is very weakly coupled to the axis of rotation along which there will be a small magnetic field depending in value on K . The looseness of this coupling of the spin to the rotation axis is evident from the smallness of the 'spin-doubling' $F_1(K + \frac{1}{2}) - F_2(K - \frac{1}{2})$ which is $\gamma(K + \frac{1}{2})$ (see Chapter IX (e)). Any applied external magnetic field will therefore cause the spin $S = \frac{1}{2}$ to precess round it, giving the two values $M_s = +\frac{1}{2}$ and $M_s = -\frac{1}{2}$. This is, of course, a complete Paschen-Back effect: the only magnetic effect possible in a ${}^2\Sigma$ level till the magnetic field due to rotation becomes appreciable. By (165) the two components will be $\pm \delta$ from the no-field position. The slight magnetic field due to nuclear rotation is theoretically coupled still with S , and it is responsible for a slight broadening of the two components as K increases (see Fig. 103). Under extremely high resolving power presumably $2J + 1$ components would be observed.

It follows that the effect of a magnetic field on ${}^2\Sigma \rightarrow {}^2\Sigma$ bands will leave band lines apparently unchanged, since the selection rule $\Delta M_s = 0$ holds rigorously. If, however, one of the ${}^2\Sigma$ levels shows appreciable spin doubling there tends to be a separation giving a doublet appearance of this order of magnitude (see next section).

If the ${}^2\Pi$ state of a system (${}^2\Pi \rightleftharpoons {}^2\Sigma$) is Case (b), reference to (163) shows that for $J = K + \frac{1}{2}$, $\Delta\nu = M\delta \frac{J+2}{J(J+1)}$, and for $J = K - \frac{1}{2}$, $\Delta\nu = -\frac{M\delta}{J+1}$. Each of the spin doublet levels has $2J + 1$ Zeeman

components (except $K = 1, J = \frac{1}{2}$, which remains single). We observe also that the Zeeman pattern of the F_2 levels ($J = K - \frac{1}{2}$) is inverted (due to the minus sign). By substitution of the lower

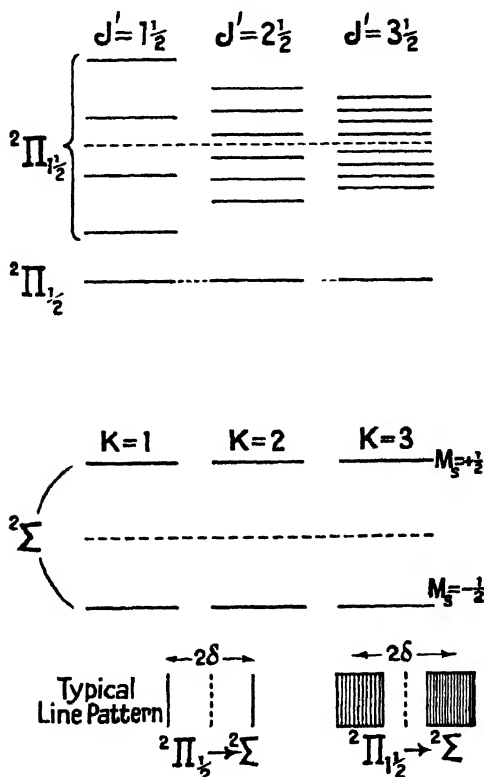


Fig. 103. The ${}^2\Pi$ state is assumed to be Case (a), and the Zeeman patterns are drawn to scale. The ${}^2\Sigma$ state is shown as giving the Paschen-Back doublet in an applied field. Arrows corresponding to transitions have not been shown, but a typical line pattern is constructed below.

values of K and J in (162) we obtained the overall widths given below :

$K \rightarrow$	1	2	3	4	... n
$J = K + \frac{1}{2}$	$\pm \frac{3\delta}{2}$	$\pm \frac{4\delta}{3}$	$\pm \frac{5\delta}{4}$	$\pm \frac{6\delta}{5}$	$\pm \frac{n+2}{n+1} \delta$
$J = K - \frac{1}{2}$	0	$\mp \frac{\delta}{2}$	$\mp \frac{2\delta}{3}$	$\mp \frac{3\delta}{4}$	$\mp \frac{n-1}{n} \delta$

and these are represented in Fig. 104.

The Paschen-Back effect on a ${}^2\Pi$ level is immediately clear from (165), where $\Lambda = 1$, and $S = \frac{1}{2}$. Two values of M_S occur, $+\frac{1}{2}$ and

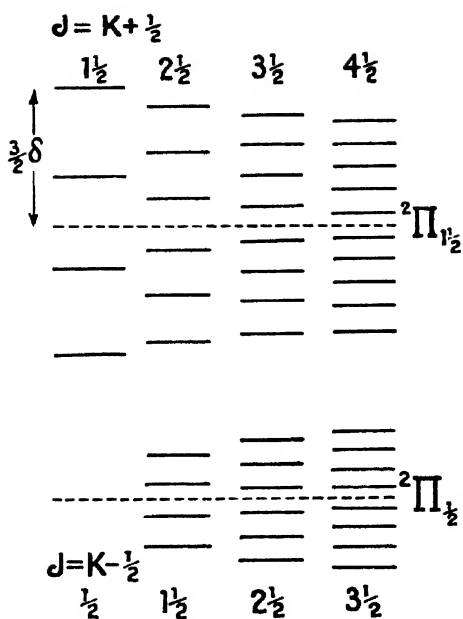


Fig. 104. Case (b) $^2\Pi$ levels in the Zeeman effect.

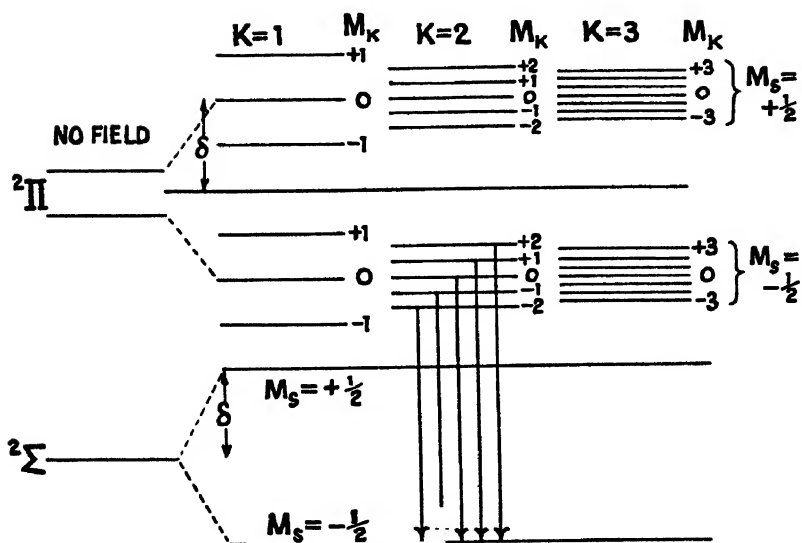


Fig. 105. Paschen-Back splitting of $^2\Pi \rightarrow ^2\Sigma$ band lines.

$-\frac{1}{2}$. These correspond to two levels $+\delta$ and $-\delta$ from the mid-position of the no-field doublet. Grouped round each of these are the $2K+1$ components corresponding to values of M_K between $+K$ and $-K$, as shown in Fig. 105. It will be clear that the two sets of

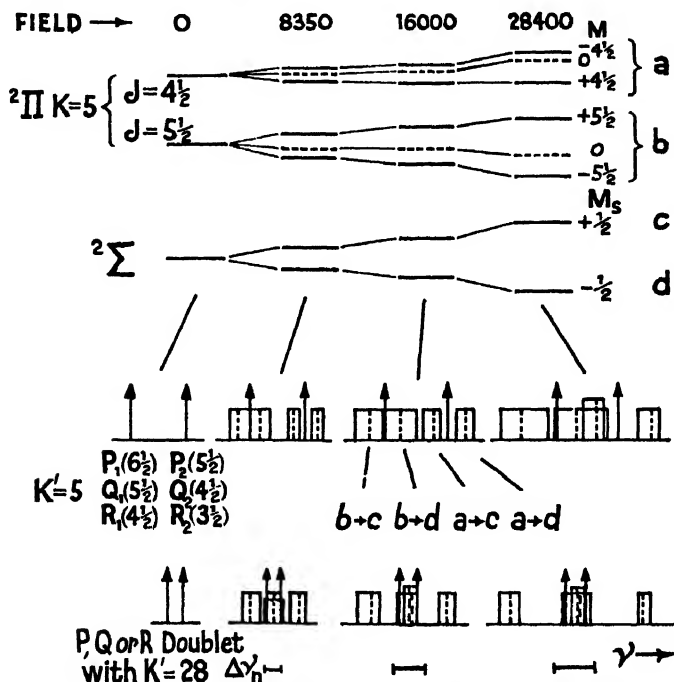


Fig. 106. Theoretical Zeeman splitting of the energy levels ${}^2\Pi$, ${}^2\Sigma$ in fields of different strength, also representative Zeeman patterns of the green MgH band at λ 5211. The number of Zeeman components in each ${}^2\Pi$ level is $2J+1$, but only the extreme components $M = \pm J$ have been constructed, while the no-field level is shown dotted. The resulting unresolved line patterns are shown as blocks. The position of the hypothetical transition from $M = 0$ to $M_s = \pm \frac{1}{2}$ is shown by a dotted line within the block. The long vertical lines show positions of the no-field spin doublets. For MgH $A/B = 5.7$ and while for low rotational states this may be regarded as a coupling intermediate between Cases (a) and (b), for high values of K it approximates closely to Case (b). At low K -values we thus observe that the low-frequency member of the doublet is a broad, nearly symmetrical block, while the high-frequency member is a doublet. At high K -values where the spin doubling becomes small as Case (b) conditions are approached, the intensity distribution in the block patterns varies markedly with strength of field. At $H = 8350$ gauss the two central overlapping blocks are faint, and the intensity is in the outer wings $\Delta M = \pm 1$. In strong fields the outer wings are very faint, and the central block is strong ($\Delta M_s = 0$), the Paschen-Back effect. (Adapted from Almy and Crawford's diagrams.)

transitions of $M_s(+\frac{1}{2} \rightarrow +\frac{1}{2})$ and $(-\frac{1}{2} \rightarrow -\frac{1}{2})$ will give patterns coincident in position, so that $K' = 1$ corresponds to one triplet, $K' = 2$ to one quintet, $K' = 3$ to one septet, &c., in the band lines arising from ${}^2\Pi \rightleftharpoons {}^2\Sigma$ under strong-field conditions.

If it is not a complete Paschen-Back effect, transitions in $M_s(-\frac{1}{2} \rightarrow \frac{1}{2})$ and $(\frac{1}{2} \rightarrow -\frac{1}{2})$ give rise to additional pattern blocks $\pm 2\delta$ from the mean position, but these diminish in intensity (finally vanishing) as the field is increased. With increase of molecular rotation, which not infrequently results in transition from Case (a) to Case (b) conditions, the same intensity reduction may be observed.

The pattern of splitting represented by equations (160), (162), and (165) deals strictly with limiting cases only. Hill* has provided a rather complex formula by which the patterns for states intermediate between Zeeman and Paschen-Back conditions may be predicted. A characteristic of this formula is the asymmetrical distribution of the magnetic sub-levels which is shown clearly in Fig. 106. The experimental work of Almy and Crawford† on MgH supports, and is interpreted satisfactorily by, Hill's theoretical predictions.

(f) SPIN DOUBLING AND Λ -TYPE DOUBLING

In the preceding section reference was made to the characteristic behaviour of $^2\Sigma$ levels in a magnetic field; breaking into two levels corresponding to $M_s = \pm \frac{1}{2}$, each $\pm \delta$ from the centre of the no-field level. In these circumstances, and because of the limitation $\Delta M_s = 0$ in the Paschen-Back effect, $^2\Sigma \rightarrow ^2\Sigma$ bands would be unaffected in structure by an applied magnetic field. Spin doubling in $^2\Sigma$ states due to the control of the spin vector by the magnetic field due to rotation, which is along K , will affect our conclusions. The spin doubling, as we know, is a linear function of K , viz. $v_{12} = \gamma(K + \frac{1}{2})$. A small value of γ in either level will result only in slight broadening of the $^2\Sigma \rightarrow ^2\Sigma$ band lines in presence of a field. Bearing in mind that the two spin components correspond to $J = K + \frac{1}{2}$ and $J = K - \frac{1}{2}$, each of these broadened components is really an unresolved complex of $2J + 1$ members in a field. If the constant γ is so large that $\gamma(K + \frac{1}{2})$ is of the order of δ due to the field, new considerations arise, and these Hill has investigated by quantum mechanics. The energy levels of a $^2\Sigma$ state in a field are given by Hill's expression

$$W = \pm \frac{1}{2} \left[v_{12}^2 + \frac{4Mv_{12}\delta}{K + \frac{1}{2}} + 4\delta^2 \right]^{\frac{1}{2}}. \quad (170)$$

where W is measured from the mid-point of the no-field levels. The positive sign applies to the $(K + \frac{1}{2})$ spin component, the negative sign to the $(K - \frac{1}{2})$ component. For the $J = K + \frac{1}{2}$ spin level, putting $M = \pm (K + \frac{1}{2})$ to get the two outermost magnetic components, we obtain from (170) $W = \frac{1}{2}v_{12} \pm \delta$. This is clearly a block of magnetic levels 2δ in extent. Fig. 107 shows an application of (170) which demonstrates in a specific case the modification of the simple Paschen-Back doublet (corresponding to $K = 1$) to produce two patterns each of width 2δ as the magnetic field due to rotation increases.

* *Phys. Rev.*, vol. 34, p. 1507 (1929).

† *Ibid.*, vol. 34, p. 1517 (1929).

Just as we have described a Paschen-Back effect as arising when the $\Lambda : S$ coupling is broken down by a strong field, or, to express it otherwise, when the Lorentz unit δ becomes of the order of A (the multiplet component interval), so we might visualize a new effect arising by the uncoupling of L from the inter-nuclear axis. This would mean that Λ would not continue to exist as a quantum number : there would be no significance in referring to Σ , Π , Δ states, but only of a complex of states derived from a particular value of L . Theoretically L could be uncoupled from the inter-nuclear axis by an applied magnetic field big enough to make δ of the order of the interval between corresponding Σ and Π levels. In practice this would not

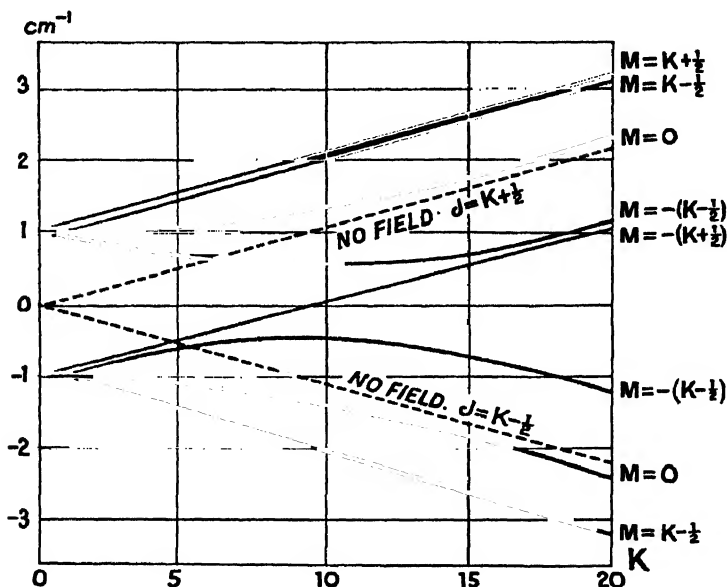


Fig. 107. Graph based on (170) showing the magnetic levels produced in the case of the $^2\Sigma$ state of OH for which $\gamma = 0.22$ and for a field of 20000 gauss. Only the outer components corresponding to $M = \pm J$ are shown. The broken lines are the no-field levels. (Adapted from Crawford.)

arise from this cause, but we do find occasionally due to nuclear rotation a so-called L -uncoupling, which may result in a change from Case (b) of Fig. 45 to Case (d) of Fig. 49. The L -uncoupling may be diagnosed by the degree of Λ -type doubling which it creates. As we saw in Chapter VII (g), the molecular field due to rotation is responsible for the slight difference in energy values of $F(\Lambda)$ and $F(-\Lambda)$ which we call Λ -type doubling. Uncoupling of L gives rise to an appreciable component L_{perp} along the rotation axis, increasing the magnetic field and therefore the Λ -type doubling.

The result of complete uncoupling in singlet states, as Fig. 49 shows ($S = 0$), would be a precession of N (now a quantum number) and L

round K . This would result in new energy levels in a magnetic field given according to Mills * by

$$W = M \frac{K(K+1) + L(L+1) - N(N+1)}{2K(K+1)} \delta,$$

and resulting in magnetic effects of a greater magnitude than are found normally.

The student desiring to study the subject matter of this chapter in more detail should consult the excellent account of F. H. Crawford, *Reviews of Modern Physics*, vol. 6, pp. 90-117 (1934)).

* *Phys. Rev.*, vol. 38, p. 1163 (1931).

THE SPECTRA OF POLYATOMIC MOLECULES

(a) INTRODUCTION

IN a general way we may say that the dozen years 1918-30 produced a systematic study of the spectra of diatomic molecules, and resulted in a reliable theory based upon accurate and ample experimental data. Every diatomic molecule has its peculiarities and features of interest, and many such molecules still await experimental investigation, but in broad outline such further study will be expected to illustrate the established theory.

In the same way we may regard the years 1930-40 as having laid the foundations of a theory of polyatomic molecular spectra; but here the vast number of molecular types is such that the possible experimental and theoretical work is almost unlimited. The fine structure of the heavier molecules will remain, however, quite outside the possibility of resolution, in the absence of much more powerful instruments than are at present available.

The problems associated with the *electronic* structure of molecules are very complex, and have been the subject of a long series of papers by Mulliken (1932-35) * and others. It appears that commonly the atomic nuclei retain their *K*-shells, and that the electronic structure external to these is best regarded as a large number of shells each containing two electrons only, and each having a distinctive ionization potential or term value. Brief reference will be made to electronic spectra and structures in a later section, but no detailed consideration will be presented because of the knowledge of Group Theory necessarily involved. A comprehensive review of this aspect has been made by Sponer and Teller.†

Vibration-rotation spectra and pure-rotation spectra occur respectively in the near and the far infra-red as in diatomic spectra. The vibrational and rotational energy of polyatomic molecules will be studied in subsequent sections of this chapter. If a molecule has n atoms and three degrees of freedom are ascribed to each atom, the total number for the whole system is $3n$. Of these, three are accounted for by the translational motion of the molecule as a whole, and three more are concerned with its free rotation (two only are involved in rotation if it is a linear molecule). The remaining $3n - 6$ degrees of freedom ($3n - 5$ for a linear molecule) must therefore represent modes of vibration of the system. Thus if ν_1 , ν_2 , and ν_3 were the frequencies of these normal modes in a typical triatomic molecule such as SO_2 , and if to a first approximation these vibrations were regarded as simple harmonic, we could write the vibrational energy of the molecule

$$E^v = h(\nu_1 + \frac{1}{2})\nu_1 + h(\nu_2 + \frac{1}{2})\nu_2 + h(\nu_3 + \frac{1}{2})\nu_3 \quad (171)$$

* *Phys. Rev.*, vol. 40, p. 55 (1932); vol. 41, p. 49 (1932); vol. 41, p. 751 (1932); vol. 43, p. 279 (1933); *Jour. Chem. Phys.*, vol. 1, p. 492 (1933); vol. 3, pp. 375, 506, 514, 517, 564, 573, 586, 635, 720 (1935).

† *Rev. Mod. Phys.*, vol. 13, p. 75 (1941).

In dealing with the modes of vibration of molecules there is a simplifying principle available, viz. that the nature of these fundamental vibrations can be deduced entirely from the geometry of the molecule. To predict their *absolute* values it would be necessary to know the potential function of the nuclei, and the correct values of the constants involved. For any simple molecular model which we like to formulate, it is possible, however, to infer the number of fundamental modes of vibration, to see how they arise, to predict for each of these the corresponding direction of oscillation of the electric moment of the molecule, and in general to decide which of the vibrations are likely to be stronger and which weaker. Theory indicates that only where there is an oscillation of the electric moment associated with the fundamental vibrations will these be 'active' in the infra-red, as absorption or emission bands. Likewise, pure-rotation bands in the far infra-red depend on the existence of a permanent electric moment in the molecule.

An interesting attempt was made in 1930 by Kettering, Shutts, and Andrews* to determine experimentally the modes of vibration of models of simple organic molecules. Steel balls of appropriate masses were used to represent the nuclei, and these were connected together with spiral springs, on the assumption that the important restoring forces lie along the chemical bonds, and that they would, for small oscillations, obey Hooke's Law. The model was excited by an eccentric drive attached to a variable speed motor, and viewed by a neon lamp flashing at a frequency 2% slower than the exciting one, which varied from 200 to 3500 cycles per minute. Thus a slow motion image of $1/50$ of the actual frequency enabled a close study of the characteristics of the motion of the model to be made. Tuning was found to be quite sharp as the exciting frequency of the motor was varied. A comparison of the frequencies found (multiplied by an appropriate factor) with those known from the infra-red and Raman spectra of such a molecule, showed an interesting correspondence in most cases, and confirmed theoretical suppositions as to how most of these vibrations occur. In 1934 Andrews and Murray improved the technique of this method by using photography of a bright spot on each 'atomic' nucleus which was illuminated more strongly at one extreme of its oscillatory path than at the other.

A considerable number of bands of the lighter polyatomic molecules have now been subjected to fine-structure analysis. Unlike the diatomic case, where only one moment of inertia is involved, we now have to deal with three moments of inertia, A , B , and C about the three principal axes of the molecule. If two of these are equal, we have a symmetrical top, and the rotation of such a top is comparatively simple from a mathematical standpoint. The rotational energy expression, as we shall see later, involves two rotational quantum numbers instead of only J , as in the diatomic case. If the two larger moments of inertia are equal we have the prolate type of molecule (spindle-shaped); if the two smaller moments of inertia are equal we have the oblate type of molecule (approximating to a plate or fly-wheel). The asymmetrical rotator, where the three moments of

* *Phys. Rev.*, vol. 36, p. 531 (1930); *Jour. Chem. Phys.*, vol. 2, p. 634 (1934); vol. 3, p. 175 (1935).

inertia are all unequal, has been successfully treated mathematically by a number of methods. Although the motion has three degrees of freedom, only two periodicities, and therefore only two rotational quantum numbers, are involved. The computations involved in determining the rotational levels of asymmetrical molecules are, however, of great complexity, and have not been attempted except in one or two simple cases (e.g. H_2O and D_2O).*

(b) THE VIBRATIONS OF MOLECULES

Triatomic Molecules (Triangular)

Following the line of Dennison's † work, we proceed to consider the three modes of vibration which are possible in a triatomic molecule.

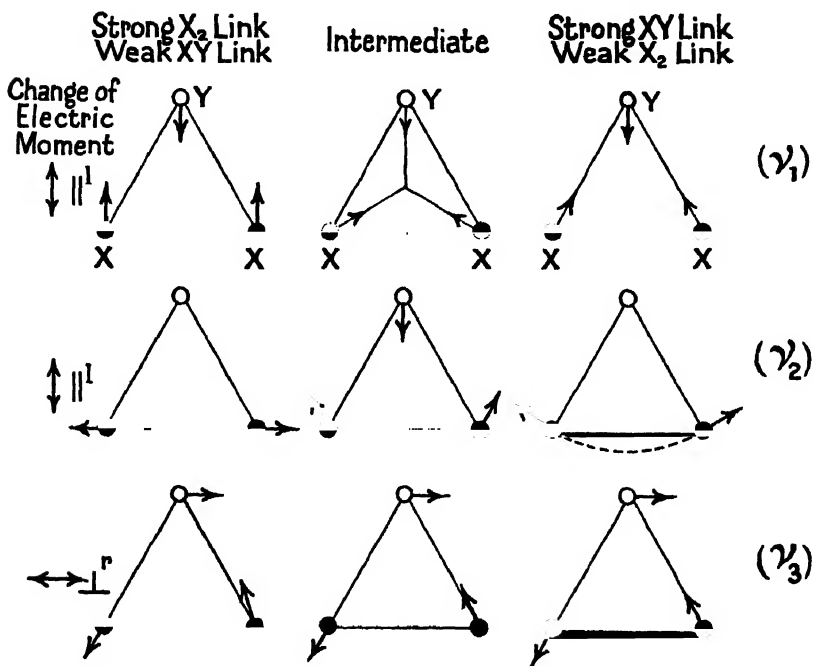


Fig. 108. The three normal modes of vibration of a triatomic molecule, such as YX_2 . (After Dennison.)

In the special case of a molecule such as X_3 with the atoms at the corners of an equilateral triangle, there would only be two modes (ν_2 and ν_3 of Fig. 108 would degenerate into one species); but no such molecule is known up to the present. In Fig. 108 we have considered a type of molecule which has an axis of symmetry bisecting the angle XYX . It is a type to which belong H_2O , H_2S , H_2Se , D_2O , D_2S ,

* Randall, Dennison, Ginsberg, and Weber, *Phys. Rev.*, vol. 52, p. 161 (1937); vol. 56, p. 982 (1939).

† *Rev. Mod. Phys.*, vol. 3, p. 289 (1931).

D_2Se , O_3 , NO_2 , SO_2 , Cl_2O , &c. The oscillations of the atomic nuclei must obviously be confined to the plane containing the three atoms, and Fig. 108 is designed to illustrate how they arise. Passing down the central column ('Intermediate'), the frequency ν_1 is often called the breathing frequency, which is a good description of the type of motion. The frequency ν_2 is one of which the main characteristic is an oscillation of the angle XYX about its mean value. The frequency ν_3 is a motion of one X atom nearer to Y and the other farther from Y , causing a movement of Y perpendicular to the axis of symmetry of the molecule.

The first column is an extreme case where the forces between the X_2 and XY pairs of atoms are very different and the X_2 band is much the stronger. In this case ν_1 is the comparatively low-frequency oscillation of Y perpendicular to a rigid rod. ν_3 is the comparatively low-frequency oscillation of Y created by a small rotational oscillation of the rod, and ν_2 is the high-frequency oscillation due to the bond X_2 , leaving Y unaffected.

The third column illustrates the other extreme, where the XY bonds are strong and the X_2 bond is weak. Here we can imagine the triatomic molecule as constructed from two XY molecules sharing the Y atom in common. Then ν_1 and ν_3 are two comparatively high frequencies, in which the two XY bonds oscillate, in one case in phase, and in the other out of phase by 180° . The lower frequency ν_2 due to the weaker X_2 bond can be pictured as a motion of two rigid rods YX due to oscillation of the angle XYX about its equilibrium value.

If the centre of the positive charge in a molecule does not coincide with the centre of negative charge, a permanent electric moment exists. The direction of oscillation of this moment is parallel to the axis of symmetry of the molecule for ν_1 and ν_2 , but perpendicular to it for ν_3 . Hence arise two different types of bands in molecular spectra. 'Parallel' bands have the familiar fine structure of P , Q , and R branches; 'perpendicular' bands have more complex fine structure consequent upon changes in the subsidiary rotation quantum number. This is discussed in Section (c).

The question now arises what frequencies may be expected to appear in infra-red spectra. One general principle has been already stated: that a change of electric moment must take place. It will therefore be apparent that if in Fig. 108 we were dealing with a completely symmetrical molecule X_3 , the breathing frequency ν_1 would not be found in the infra-red spectrum, since it is not associated with a change of electric moment. For the same reason, vibration bands of homonuclear diatomic molecules X_2 are not found in the infra-red. In the same way, the frequency ν_1 of CO_2 (see Fig. 110), and ν_1 , ν_2 , and ν_5 of C_2H_2 (see Fig. 113) do not appear in infra-red spectra.

If molecular vibrations were strictly simple harmonic, as imagined in (171), changes in the quantum numbers would be confined to $\Delta\nu_1 = 1$, $\Delta\nu_2 = 1$, $\Delta\nu_3 = 1$, and moreover they would occur independently, so that there would be no combination frequencies such as $\nu = \nu_1 + \nu_2 + \nu_3$. Since, however, the oscillations are not strictly harmonic, we may have changes of $\Delta\nu_1$, $\Delta\nu_2$, and $\Delta\nu_3$ which are small

integers. There may also be bands having combination frequencies approximately given by

$$v = \Delta v_1 v_1 + \Delta v_2 v_2 + \Delta v_3 v_3 \quad . \quad . \quad . \quad (172)$$

Such bands are of the 'perpendicular' type if Δv_3 is odd and of the 'parallel' type if Δv_3 is even. Bands of the type $v = \Delta v_1 v_1 + \Delta v_2 v_2$ are necessarily 'parallel'. The proof of these statements depends on a wave-mechanical treatment which will not be attempted here. The correct vibrational energy expression replacing (171) should take account of anharmonicity and interaction terms, and would have the form

$$E/hc = \sum_k \omega_k (v_k + \frac{1}{2}) + \sum_{k,l} X_{kl} (v_k + \frac{1}{2})(v_l + \frac{1}{2}) \quad . \quad (173)$$

If we write it in the convenient form

$$E/hc = x_0 + x_1 v_1 + x_2 v_2 + x_3 v_3 + x_{11} v_1^2 + x_{22} v_2^2 + x_{33} v_3^2 + x_{12} v_1 v_2 + x_{13} v_1 v_3 + x_{23} v_2 v_3 \quad . \quad (174)$$

the constants may be determined by using the data on nine band centres, and from these it is easy to calculate the fundamental modes of vibration :

$$\left. \begin{aligned} \omega_1 &= x_1 - x_{11} - \frac{1}{2}x_{12} - \frac{1}{2}x_{13}, \\ \omega_2 &= x_2 - x_{22} - \frac{1}{2}x_{12} - \frac{1}{2}x_{23}, \\ \omega_3 &= x_3 - x_{33} - \frac{1}{2}x_{13} - \frac{1}{2}x_{23}. \end{aligned} \right\} \quad . \quad . \quad (175)$$

We shall illustrate the theory outlined by reference to the H_2O molecule, which is one of the most investigated non-linear triatomic molecules. Its vibration-rotation bands are numerous, and found in the region 0.5μ – 8.5μ . The pure-rotation band structure ranges from 15μ to 500μ . Vibrational energy levels are given in the appended table, and vibration-rotation bands are found in absorption from the

VIBRATIONAL ENERGY LEVELS (H_2O)

Designation $v_1 \quad v_2 \quad v_3$	Position (cm^{-1})	Designation $v_1 \quad v_2 \quad v_3$	Position (cm^{-1})
0 1 0	1595.0	2 1 1	12151.2
0 2 0	3151.0	0 1 3	12565.0
1 0 0	3650.0	3 0 1	13830.9
0 0 1	3755.4	1 0 3	14318.8
0 1 1	5330.8	3 1 1	15347.9
1 0 1	7251.0	1 1 3	15832.4
1 1 1	8807.0	3 2 1	16821.6
2 0 1	10613.1	4 0 1	16899.0
0 0 3	11032.4	2 0 3	17495.5

ground state (0,0,0) to all of the levels tabulated. Fig. 109 sets out these vibrational levels in pictorial form, so as to illustrate the various combination bands arising in absorption. The figures 1, 2, and 3 represent the three fundamental frequencies ω_1 , ω_2 , and ω_3 . It may be remarked that neither $(2 + \frac{1}{2})\omega_3$ nor any other level with v_3 an even integer has been observed in combination with ω_1 and ω_2 . The reason for this is that levels corresponding to even values of v_3 have

a different symmetry character from those having odd values, and transitions can only occur between levels of the same symmetry character according to wave-mechanics.

The three fundamental vibrations are easily picked out of the spectrum: it is necessary to consider, however, which is which. In the infra-red ν 1595 and ν 3755 are very strong, but ν 3650, although present, is overlaid by strong absorption in its neighbourhood. The

Raman spectrum contains ν 3650 only. We have as guides in making a correct assignment the following criteria:

(1) ν_1 and ν_2 are 'parallel' bands with simple *P*, *Q*, and *R* branches; ν_3 is 'perpendicular' with more complex fine structure. It appears that ν 1595 is 'parallel' and ν 3755 is 'perpendicular', indicating that the latter is probably ν_3 .

(2) We expect ν_1 and ν_3 , being due to vibrations of the OH bond, to approximate more closely to each other than either does to ν_2 . This suggests that ν 3650 is probably ν_1 and ν 1595 is ν_2 . The OH bonds are therefore stronger than the HH interaction, and we should anticipate that the angle HOH might be obtuse.

(3) Some measure of guidance is provided by the order of the frequency associated with certain bonds. It is found, for example, that the OH bond is often associated with a frequency of about ν 3500. This frequency will, however, obviously be modified by the 'loading' of the molecule in which OH is a link, so that the criterion is not to be applied too rigorously.

(4) It has been mentioned previously that vibration relative to a

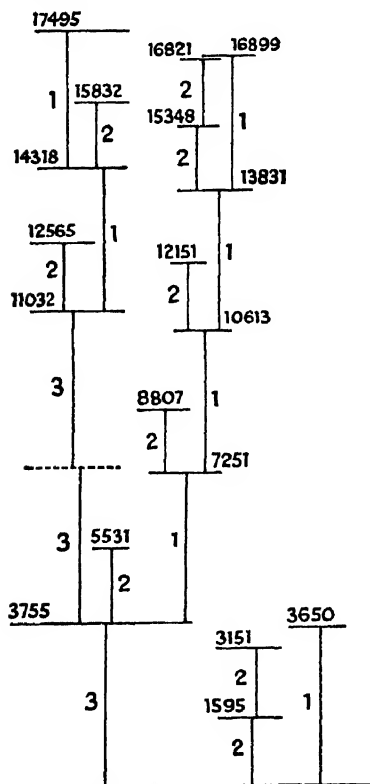


Fig. 109. Vibrational levels of H₂O.
(After E. F. Barkor.)

centre of symmetry results in no change of electric moment, and therefore in no infra-red bands. We shall see in the next chapter, however, that such frequencies are active in the Raman effect. The appearance of some fundamental frequencies in the infra-red and others exclusively in the Raman spectrum is therefore a criterion of such a point-centre of symmetry. For triatomic molecules of obtuse angle, approaching linearity (which possesses a point-centre of symmetry), we should expect to find the 'breathing' symmetrical type of vibration (e.g. ν_1) weakening in the infra-red and strengthening in the Raman spectrum as compared with the anti-symmetrical types of vibration (ν_2 and ν_3). It may be remarked that ν_1 appears strongly

in the infra-red spectrum of HDO, where the deuterium atom destroys any approach to a centre of symmetry.

These criteria are all consistent with the identification made in the table. Bonner * and subsequently Dennison † computed the constants of (173) from selected vibrational levels. Dennison's values were :

$$\begin{aligned}\omega_1 &= 3825.32, & X_{11} &= -43.89, & X_{12} &= -20.02, \\ \omega_2 &= 1653.91, & X_{22} &= -19.50, & X_{13} &= -155.06, & E_0/hc &= 4631.25. \\ \omega_3 &= 3935.59, & X_{33} &= -46.37, & X_{23} &= -19.81,\end{aligned}$$

E_0 is, of course, the zero-point energy corresponding to $v_1 = 0, v_2 = 0, v_3 = 0$. Dennison has shown how to calculate the constants of an appropriate potential function, but this will not be considered here.

We shall find later that from a knowledge of the moments of inertia

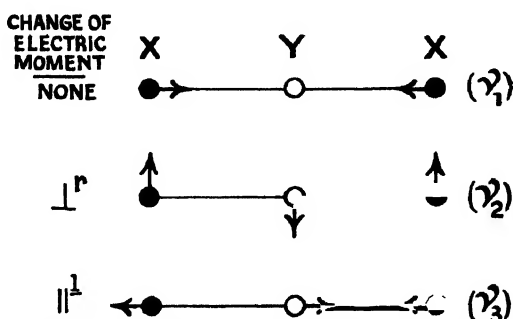


Fig. 110. Modes of vibration of linear triatomic molecule (e.g. CO_2).

of the H_2O molecule it is calculated in equilibrium to have an OH distance of 0.9580 A.U. and an angle HOH of $104^\circ 31'$.

Bailey and Cassie, ‡ assuming valence forces for a triangular molecule of the YX_2 type, have derived an expression involving the three fundamental frequencies $p_1 = 2\pi\nu_1, p_2 = 2\pi\nu_2, p_3 = 2\pi\nu_3$, the masses of the atoms and the semi-angle α ($-\frac{1}{2}\text{X Y X}$). The expression is

$$\frac{p_1^2 p_2^2}{p_3^2} \frac{x^3}{1 + \frac{2m}{M}} - (p_1^2 + p_2^2 + p_3^2)x + 2p_3^2 \left(1 + \frac{m}{M}\right) = 0.$$

This cubic equation may be solved for x , where x stands for $1 + \frac{2m}{M} \sin^2 \alpha$. Hence α may be calculated.

Triatomic Molecules (Linear)

We now turn to consider the vibration of triatomic molecules in which the atoms lie in a straight line. We can conveniently regard these in two groups: those with central symmetry, such as CO_2 and CS_2 , and those which are linear but without central symmetry, such as N_2O , COS , HCN , DCN , ClCN , BrCN , and ICN .

* *Phys. Rev.*, vol. 46, p. 462 (1934).

† *Rev. Mod. Phys.*, vol. 12, p. 188 (1940).

‡ *Proc. Roy. Soc., A*, vol. 137, p. 630 (1932).

We shall consider CO_2 as a type of the first group and use it as an illustration. Fig. 110 illustrates the three modes of vibration which are possible. For a *linear* triatomic molecule ($n = 3$) we should have expected $3n - 5$, i.e. four fundamental frequencies. The vibration ν_2 is really the degenerate representative of two equal frequencies. The atom Y is clearly free to vibrate in two dimensions in the plane perpendicular to the molecular axis, a motion which is necessarily isotropic.

In ν_1 the Y atom is stationary, and the electric moment is both zero and unchanging. No pure-rotation bands will therefore be found for CO_2 , and moreover the frequency ν_1 will not occur (except in combination) as a vibration-rotation band in the near infra-red, although it occurs strongly in the Raman spectrum.

There are found in the near infra-red spectrum of CO_2 two strong bands obviously corresponding to fundamentals: one is about 15μ (ν 667) and the other 4.7μ (ν 2349). The first of these is ν_2 and the second ν_3 , for we should expect the deformation type of oscillation perpendicular to the bonds to be substantially less than that along the bonds themselves. Moreover, ν 667 has a strong Q branch while ν 2349 has not, and these features are to be expected (see Section (c)) in bands whose changes of electric moment are respectively perpendicular to, and parallel to, the axis of symmetry (here the nuclear axis).

When we examine the Raman spectrum to find ν_1 we find not one, but *two* strong bands at ν 1285 and ν 1388. It will be observed that the mean of these, viz. ν 1337, is almost exactly $2\nu_2$. Fermi first explained this effect as a perturbation or 'resonance interaction' between two vibrational levels ν_1 and $2\nu_2$, both of which are thereby displaced from their normal positions. The same cause is responsible for the displacement of many combination bands from their normal positions. The whole effect is now accounted for by theory.

In addition to the two strong fundamental bands in the infra-red, many harmonics and combination bands are known. The appended table (after Dennison) gives a summary of the known vibrational

VIBRATIONAL LEVELS OF CO_2

ν_1	$\nu_2(0)$	ν_3	$(E - E_0)/hc$	ν_1	$\nu_2(0)$	ν_3	$(E - E_0)/hc$
0	1 ₁	0	667.3	{ 0	2 ₀	1	3609
{ 0	2 ₀	0	1285.5	{ 1	0 ₀	1	3716
{ 1	0 ₀	0	1388.4	{ 0	4 ₀	1	4859
0	2 ₂	0	1335.4	{ 1	2 ₀	1	4981
{ 0	3 ₁	0	1932.4	{ 2	0 ₀	1	5108
{ 1	1 ₁	0	2076.6	{ 0	6 ₀	1	6077
0	3 ₂	0	—	{ 1	4 ₀	1	6231
0	0 ₀	1	2349.4	{ 2	2 ₀	1	6351
{ 0	4 ₀	0	2553.6	{ 3	0 ₀	1	6510
{ 1	2 ₀	0	—	0	0 ₀	3	6976
{ 2	0 ₀	0	2804.4	0	0 ₀	5	11496
{ 0	4 ₂	0	—	{ 0	2 ₀	5	12672
{ 1	2 ₂	0	2761.3	{ 1	0 ₀	5	12774

levels: the bands bracketed together arise from resonance interaction between almost coincident levels as already explained. Fig. 111 (after

Barker) presents a picture of these levels. A part of the main diagram has been constructed on a larger scale to show detail of the transitions. (The description of a level by a symbol such as 2_1^3 means we are dealing with the third harmonic of ν_2 , i.e. $\nu_2 = 3$. The suffix 1 means $l = 1$. The nature of l , a subsidiary quantum number to ν_2 , will be explained immediately.)

We have mentioned that the frequency ν_2 is degenerate, because of the two-dimensional motion possible to the carbon atom. In the wave-mechanical treatment of the molecule this subsidiary quantum number labelled l arises. It measures in units of $h/2\pi$ the angular

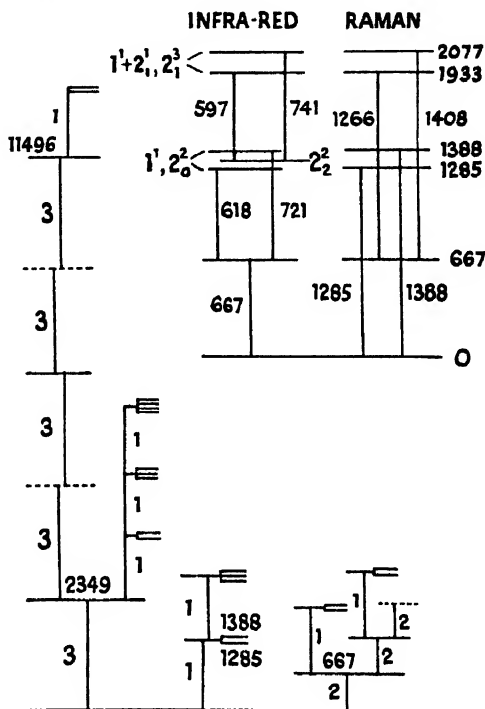


Fig. 111. Vibrational levels of CO₂. (After Barker.)

momentum which the carbon atom may have round the inter-nuclear axis. In the elementary wave-mechanical treatment of the CO₂ molecule, neglecting anharmonicity and mutual interaction of vibrations, the vibrational energy expression has the simple form (not involving l)

$$\frac{E}{hc} = (\nu_1 + \frac{1}{2})\omega_1 + (\nu_2 + 1)\omega_2 + (\nu_3 + \frac{1}{2})\omega_3 \quad (176)$$

A more accurate treatment of the non-rotating molecule by Adel and Dennison * gives the expression :

* *Rev. Mod. Phys.*, vol. 12, p. 185 (1940).

$$\begin{aligned} \frac{E}{hc} = & \omega_1(v_1 + \tfrac{1}{2}) + \omega_2(v_2 + 1) + \omega_3(v_3 + \tfrac{1}{2}) + X_{11}(v_1 + \tfrac{1}{2})^2 \\ & + X_{22}(v_2 + 1)^2 + X_{33}(v_3 + \tfrac{1}{2})^2 + X_u(l^2 - 1) \\ & + X_{12}(v_1 + \tfrac{1}{2})(v_2 + 1) + X_{13}(v_1 + \tfrac{1}{2})(v_3 + \tfrac{1}{2}) \\ & + X_{23}(v_2 + 1)(v_3 + \tfrac{1}{2}) \quad \dots \quad (177) \end{aligned}$$

There is here a small term involving l .

The ten constants of the above expression could not, however, be determined directly from the band data because of the perturbation of position introduced by resonance interaction of $(1,0,0)$ and $(0,2,0)$. Making an appropriate correction for this, the constants for CO_2 were found to be :

$$\begin{array}{lll} \omega_1 = 1351.2, & X_{11} = -0.3, & X_{12} = 5.7, \\ \omega_2 = 672.2, & X_{22} = -1.3, & X_{13} = -21.9, \\ \omega_3 = 2396.4, & X_{33} = -12.5, & X_{23} = -11.0, \\ & & X_u = 1.7. \end{array}$$

The wave-mechanical investigation shows that for each value of the quantum number v_2 , the quantum number l takes $(v_2 + 1)$ values, viz. $\pm v_2, \pm (v_2 - 2), \pm (v_2 - 4), \dots$. Thus we have

$$\begin{array}{cccccc} v_2: & 0 & 1 & 2 & 3 & 4 \\ l: & 0 & \pm 1 & \pm 2, 0 & \pm 3, \pm 1 & \pm 4, \pm 2, 0 \end{array}$$

Normally there is a complete coincidence of the two levels (+ and -) constituting each pair. Under the influence of rotation of the molecule by reason of the magnetic field created, the components may gradually separate, giving an l -type doubling. This is precisely analogous to the Λ -type doubling in diatomic molecules. In the one case we have vibrational angular momentum l about the inter-nuclear axis, and in the other case electronic angular momentum Λ about the axis. Herzberg * has discussed this effect in the case of the linear molecules C_2H_2 , HCN , and CO_2 . Because of the analogous part played by l in the vibrational states of *linear* polyatomic molecules to that played by Λ in the electronic states of diatomic molecules, Mulliken † proposed that such *vibrational* states should be described as Σ^+ , Σ^- , Π , Δ , &c., according to their value of l . If multiple perpendicular vibrations were excited in a molecule the resultant l would be derived from the individual values of l_i . Just as Λ -type doubling is appreciable in Π states only, so this is found to be the case for $l = 1$. Its magnitude is approximately given by $\Delta\nu = kJ(J + 1)$.

If the expression for a typical combination band is approximately $\nu = \Delta\nu_1\omega_1 + \Delta\nu_2\omega_2 + \Delta\nu_3\omega_3$, the following selection principles are found to govern the appearance of such bands in triatomic linear symmetrical molecules :

Always $\Delta v_2 + \Delta v_3$ must be an *odd* integer (Δv_1 is unrestricted).
 If Δv_2 is *odd* and $\Delta l = \pm 1$ we have a perpendicular band.
 If Δv_3 is *odd* and $\Delta l = 0$ we have a parallel band. } (178)

We may immediately deduce from this why it is that in such a molecule the sum of the frequencies of two observed bands is never

* *Rev. Mod. Phys.*, vol. 14, p. 219 (1942).

† *Jour. Phys. Chem.*, vol. 41, p. 159 (1937).

observed as another band. Suppose that another observed band is given by $\nu' = \Delta\nu_1'\omega_1 + \Delta\nu_2'\omega_2 + \Delta\nu_3'\omega_3$, then the sum of these would be $\nu + \nu' = (\Delta\nu_1 + \Delta\nu_1')\omega_1 + (\Delta\nu_2 + \Delta\nu_2')\omega_2 + (\Delta\nu_3 + \Delta\nu_3')\omega_3$. This cannot possibly satisfy the first condition of (178) that $\Delta\nu_2 + \Delta\nu_2' + \Delta\nu_3 + \Delta\nu_3'$ must be odd, for the sum of two odd integers ($\Delta\nu_2 + \Delta\nu_3$) and ($\Delta\nu_2' + \Delta\nu_3'$) is necessarily even. The absence of any band whose frequency is the sum of two others may be regarded as evidence that we are dealing with the spectrum of a linear molecule with a centre of symmetry. Reference to Fig. 111 shows strong harmonic bands associated with $\Delta\nu_3 = 1, 3$, and 5 , but not with $\Delta\nu_3 = 2$ or 4 in harmony with (178).

Let us consider now the features which will be characteristic of linear molecules, such as HCN or NNO, which have no centre of symmetry. All three fundamental frequencies will now be active in the infra-red, for clearly ν_1 will be associated with a changing electric moment. For HCN the calculations of Adel and Barker gave $\omega_1 = 2037$; $\omega_2 = 712.1$; $\omega_3 = 3364.2$. Fig. 112 shows the vibrational levels calculated for this molecule together with transitions observed. The restrictions of (178) do not apply. All combinations of $\Delta\nu_1$, $\Delta\nu_2$, and $\Delta\nu_3$ are now possible. If the change $\Delta\nu_2$ is odd (this is associated with $\Delta l = \pm 1$), we have perpendicular bands with Q branches. If, however, the change in $\Delta\nu_3$ is even (associated with $\Delta l = 0$), we have parallel bands with no Q branches.

The cyanogen halides were investigated by West and Farnworth,* who give for the fundamental vibration bands values in the table. It

	ν_1	ν_2	ν_3
ClCN . .	729	397	2201
BrCN . .	580	368	2187
ICN . .	470	321	2158

seems probable from a consideration of the magnitude of the bond vibrations that these molecules are of the nitrile structure $X-C\equiv N$ rather than the carbilamine structure $X-N\equiv C$.

The question may be raised: how do we know these molecules are linear rather than triangular? The primary evidence comes from a knowledge of the band fine structures. We shall see in Section (c) that the parallel bands of *linear* molecules have P and R branches only, while perpendicular bands have P , Q , and R branches. In triangular molecules, parallel bands have P , Q , and R branches, while perpendicular bands become very complex. The fine structure of the $14\ \mu$ band (ν_2) of HCN has been satisfactorily resolved and shows a simple P , Q , R structure such as we should expect from a perpendicular band if the molecule were linear.

Another simple criterion of linearity is available, however. It can be shown that for a stable linear arrangement of three masses m_1 , m_2 , and m_3

$$\frac{\nu_3}{\nu_1} + \frac{\nu_1}{\nu_3} > 2 \left(1 - \frac{\mu_{12}^2 \mu_{23}^2}{m_2^2} \right),$$

* *Jour. Chem. Phys.*, vol. 1, p. 402 (1933).

where

$$\mu_{12} = \frac{m_1 m_2}{m_1 + m_2} \quad \text{and} \quad \mu_{23} = \frac{m_2 m_3}{m_2 + m_3}.$$

For the cyanogen halides the left- and right-hand sides of the inequality

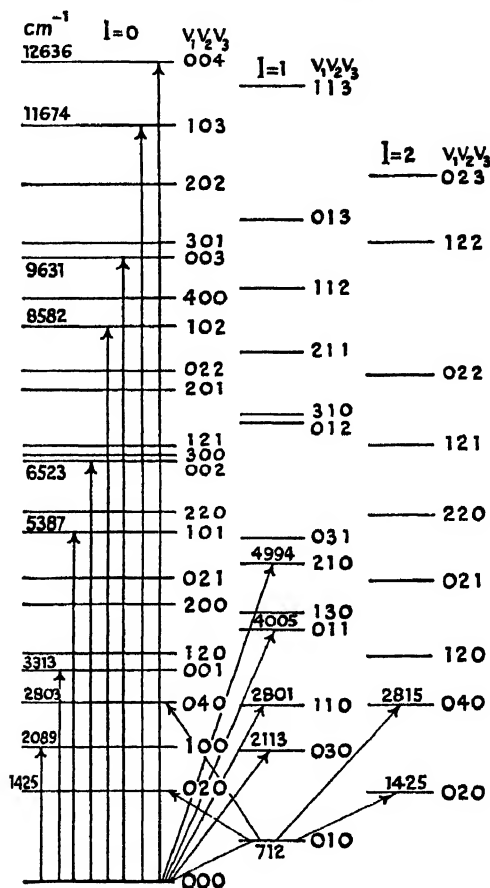


Fig. 112. Vibrational Energy Levels of HCN showing observed transitions. (After Adel and Barker, *Phys. Rev.*, vol. 45, p. 278 (1934).)

are: chloride, 3.36 and 2.60; bromide, 4.00 and 2.74; iodide, 4.84 and 2.80.

Four-Atom Linear Molecule (Y_2X_2)

A well-known example of this is acetylene HCCH , which is a special case of the linear type, in that it has a centre of symmetry. Having four atoms, it should possess seven internal modes of vibration. Of these only five are known, as illustrated in Fig. 113, but clearly ν_4

and ν_5 are degenerate, since they correspond to the possibility of two-dimensional vibration in a plane perpendicular to the axis. ν_1 is primarily the vibration of the C_2 bond in which the CH groups move as units. ν_2 and ν_3 are essentially CH bond vibrations in phase, and out of phase respectively. ν_4 and ν_5 are 'deformation' vibrations of the CH groups in pendulum-like fashion, respectively, in and out of phase.

There is clearly no change in electric moment arising from ν_1 , ν_2 , or ν_5 , since these are completely symmetrical modes with respect to the centre of the molecule. They will not be anticipated in the infrared, where, however, ν_3 and ν_4 should appear. In the low-frequency region ($< 3500 \text{ cm.}^{-1}$), where fundamentals are likely to occur, acetylene has three strong bands at 3288 cm.^{-1} , 1327 cm.^{-1} , and 729 cm.^{-1} . It is safe to identify $\nu 729$ with ν_4 , since deformation vibrations are

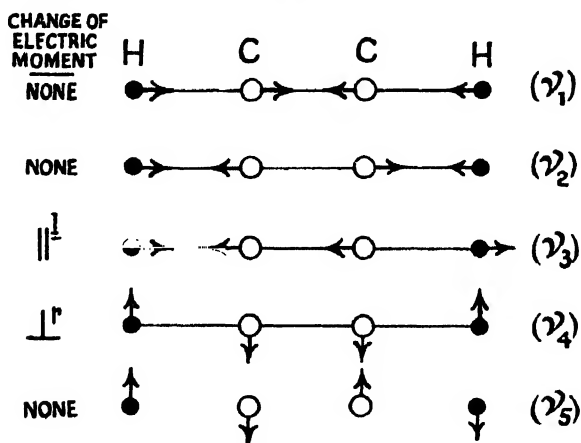


Fig. 113. Modes of vibration of the acetylene molecule, C_2H_2 .

likely to be much less than valence vibrations. The frequency 3288 is identified with ν_3 since the CH bond has a characteristic value in the region of 3000 cm.^{-1} . The Raman spectrum has two marked bands at 1975 cm.^{-1} and 3372 cm.^{-1} , of which the latter may be regarded as ν_2 (which is primarily a CH oscillation) and the former is therefore ν_1 . The unidentified frequency $\nu 1327$ must be regarded as a combination band $\nu_4 + \nu_5$ which would be reasonable, in that ν_5 (then 598 cm.^{-1}) would be expected to be of the same order as ν_4 being a deformation type of oscillation.

A large number of combination bands have been recorded in the absorption spectrum of acetylene. Data in the appended table are from Sutherland.* Fig. 114 shows pictorially the lower vibrational energy levels identified in C_2H_2 . The observed transitions (in absorption) are shown built upon the two active fundamentals ω_3 and ω_4 . The thickened arrows correspond to perpendicular bands: the thin arrows to parallel bands.

* *Phys. Rev.*, vol. 43, p. 885 (1933).

VIBRATION-ROTATION BANDS OF C_2H_2

$\nu_{cm^{-1}}$	Description	Band	$\nu_{cm^{-1}}$	Description	Band
730	ν_4	Perpendicular	6500	$\nu_2 + \nu_2$	Parallel
1326	$\nu_4 + \nu_5$	Parallel	8450	$\nu_1 + \nu_2 + \nu_3$	Parallel
2643	$\nu_2 - \nu_4$	Perpendicular	9641	$2\nu_2 + \nu_3$	Parallel
2670	—	Perpendicular	9835	$3\nu_1$	Parallel
2683	$\nu_4 - \nu_5$	Perpendicular	10400	$3\nu_4 + \nu_5$	Perpendicular
2702	$\nu_1 + \nu_4$	Perpendicular	11599	$\nu_1 + 2\nu_2 + \nu_3$	Parallel
3288	ν_3	Parallel	11783	$\nu_1 + 3\nu_3$	Parallel
3882	$\nu_3 + \nu_5$	Perpendicular	12676	—	Parallel
3910	$3\nu_4 + 3\nu_5$	Parallel	13033	$3\nu_2 + \nu_3$	Parallel
4092	$\nu_2 + \nu_4$	Perpendicular	15600	$4\nu_2 + \nu_3$	Parallel
4690	$\nu_2 + \nu_4 + \nu_5$	Parallel	18430	$5\nu_2 + \nu_3$	Parallel
5250	$\nu_1 + \nu_4$	Parallel			

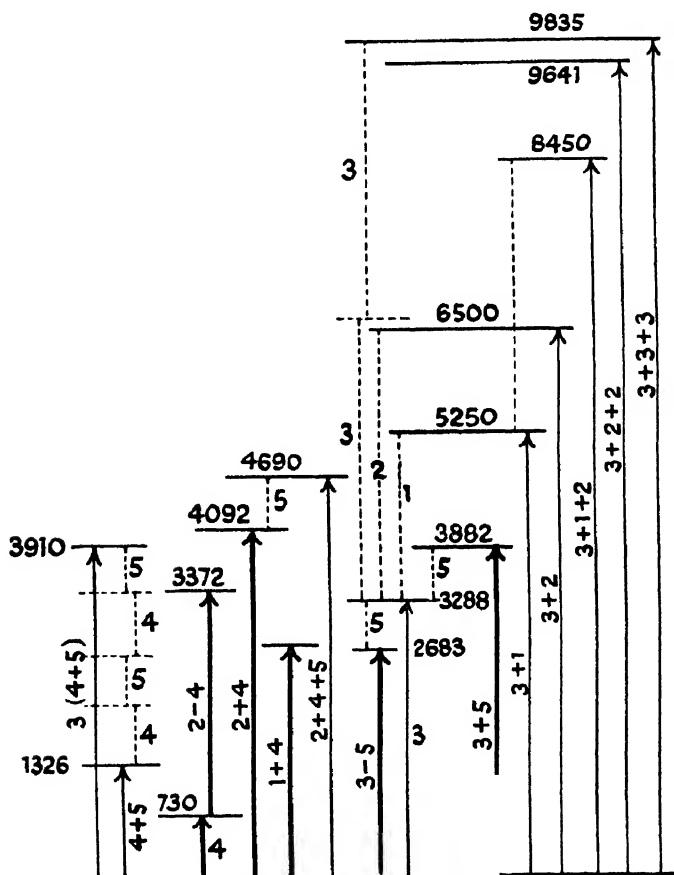


Fig. 114. Vibrational energy levels and absorption transitions observed in C_2H_2 (infra-red).

To a first approximation the vibrational energy expression for the molecule is shown by wave-mechanics to be :

$$\frac{E}{hc} = (v_1 + \frac{1}{2})\omega_1 + (v_2 + \frac{1}{2})\omega_2 + (v_3 + \frac{1}{2})\omega_3 \\ + (v_4 + 1)\omega_4 + (v_5 + 1)\omega_5 \quad \dots \quad (179)$$

If we make a closer approximation we should also have five additional terms of the type $x_{11}(v_1 + \frac{1}{2})^2 \dots x_{55}(v_5 + 1)^2$ and ten interaction terms such as $x_{12}(v_1 + \frac{1}{2})(v_2 + \frac{1}{2}) \dots x_{25}(v_2 + \frac{1}{2})(v_5 + 1)$, &c.

Sutherland gives the values of the fundamentals as :

$$\omega_1 = 1974, \omega_2 = 3372, \omega_3 = 3288, \omega_4 = 730, \omega_5 = 605 \text{ cm.}^{-1}$$

Strictly, there should also be two terms involving l_4 and l_5 as in (177). These two subsidiary quantum numbers bear the same relation to v_4 and v_5 that l did to v_2 in CO_2 . There are also certain selection principles restricting changes of the vibrational quantum numbers, somewhat as in (178) for CO_2 .

$\Delta v_3 + \Delta v_4$ must be odd (Δv_1 and Δv_2 are unrestricted).
 If $\Delta v_4 = \Delta v_5$ (or $\Delta l_4 = \Delta l_5$) we have parallel bands.
 If $\Delta v_4 = \Delta v_5 \pm 1$ (or $\Delta l_4 = \Delta l_5 \pm 1$) we have perpendicular bands. } (180)

The description of the bands in the table conforms to these rules. We shall see later (Section (c)) that parallel bands of linear molecules have no Q branches, while perpendicular bands have Q branches. These features are also found to be consistent with the above band descriptions.

Sutherland has drawn attention to the fact that large values of interaction constants in the vibrational energy expression, such as x_{22} and x_{23} , are probably to be associated with the strong series of overtone bands $v_3 + v_2$, $v_3 + 2v_2$, $v_3 + 3v_2$, $v_3 + 4v_2$, $v_3 + 5v_2$.

The Four-Atom Molecule (YX_3)

A type of this molecule is NH_3 , which is a pyramidal structure with the N atom at the apex and an equilateral triangle of H atoms as the base. There should be $3n - 6$ internal vibrations where $n = 4$, viz. six fundamental frequencies. Owing to the axial symmetry only four distinct frequencies occur, two of them (v_2 and v_4) being degenerate two-dimensional oscillations. In a substituted ammonia such as NH_2D the whole six would be expected to arise.

If the binding of Y was extremely weak v_1 would be a symmetrical breathing oscillation of the X atoms, remaining at the corners of an equilateral triangle in their own plane. With appreciable XY binding the Y atom will oscillate along the axis of symmetry of the molecule, and the X atoms will be also directed somewhat upwards. An oscillating electric moment will result.

In v_2 of Fig. 115 we have oscillatory movements of the three X atoms in their own plane which represent a degenerate blend of the v_2 and v_3 type of motion of Fig. 108. This is associated with an induced oscillation of Y in a plane parallel to the X_3 base. The motion of Y may perhaps be visualized as of a precessing ellipse in this plane.

The oscillation ν_3 of Fig. 115 may be visualized as an expansion and upward lift of the X_3 triangle as Y approaches it, and vice versa. It is virtually an oscillation of the apical angle of the pyramid about its mean value.

The oscillation ν_4 is associated with a movement of the Y atom in a plane parallel to the base (similar to that in ν_2). It is associated, however, with a 'tipping oscillation' of the X_3 plane in a manner somewhat similar to the 'tipping oscillation' of the X_2 rod in ν_3 of Fig. 108.

The bands arising from ν_1 and ν_3 of the YX_3 molecule will be of the parallel type, while ν_2 and ν_4 will be perpendicular. The axis of

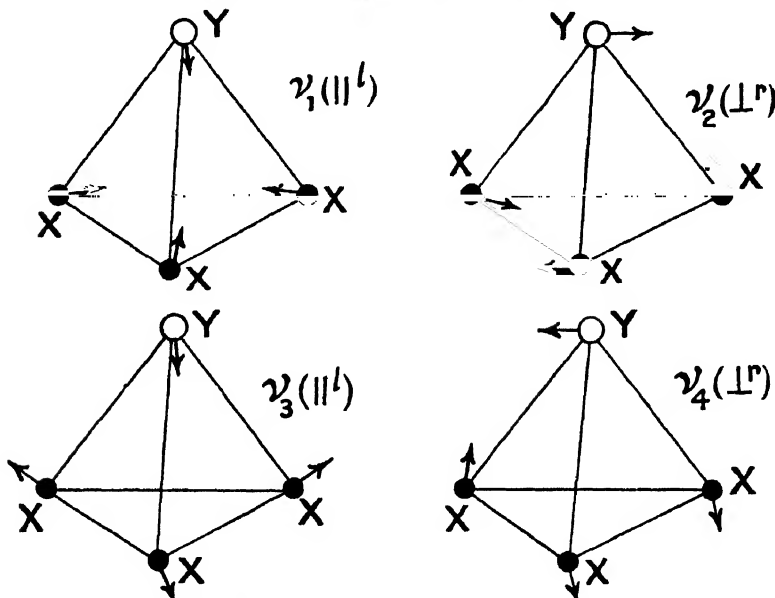


Fig. 115. Fundamental vibrations of YX_3 .

symmetry is, of course, a line through Y perpendicular to the X_3 plane.

A considerable amount of work has been done on the spectrum of NH_3 , which shows it to be a pyramidal molecule with the following dimensions: HH distance 1.631 A.U.; NH distance 1.014 A.U.; height of pyramid 0.377 A.U.; HNH angle $107^\circ 3'$. The centres of the two parallel bands are found to be at 3μ (ν_1 : 3336), and 10.5μ (ν_3 : 949.9). The centre of the weaker ν_2 band which is confused with ν_1 structure is at ν 3414, while ν_4 is an intense band at ν 1627.5.

The question as to what combination bands are permissible, i.e. of the selection principles governing changes of ν_1 , ν_2 , ν_3 , and ν_4 , and the nature (parallel or perpendicular) of the resulting bands, depends on the 'symmetry' properties of the states involved. These we shall not consider here.

There is a feature of the vibration of the NH_3 molecule which has

given rise to several investigations and is known as the 'tunnel' effect. There are obviously two equivalent equilibrium positions of the N nucleus, one on each side of the H_3 plane. It will be clear from Fig. 115 that it is a vibration of the ν_3 type which may make possible a passage of the N atom through the plane on to the other side. The potential function corresponding to this vibration is assumed to have two minima, as in Fig. 116.

In many molecules the energy necessary to surmount the barrier will be too great to permit the transition, but in NH_3 the barrier is

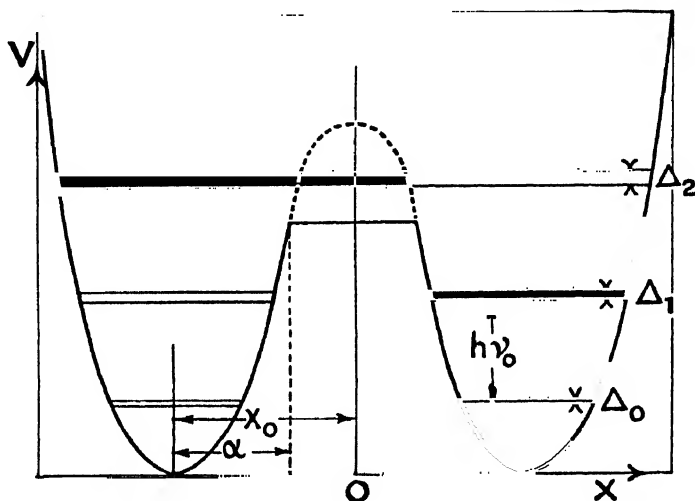


Fig. 116. Two-minima potential function applicable to the ν_3 vibration of NH_3 . (The diagram is not to scale, and the level doubling is greatly magnified)

probably about 2070 cm.^{-1} in height, and the transition is quite possible. Dennison and Uhlenbeck* treated this problem by the methods of wave-mechanics. From the spectroscopic point of view the most important consequence of a potential function of this type is that the vibrational levels are split into pairs (one component being 'symmetrical' and the other 'anti-symmetrical' in the vibrational wave-functions). If V is the potential and E the energy of a pair of levels which are separated by ν from the neighbouring vibrational pair, the separation Δ of the two components was found theoretically to be

$$\Delta_\nu = \frac{h\nu}{\pi A_\nu^2} \quad . \quad . \quad . \quad . \quad . \quad (181)$$

where

$$A_\nu = \exp \left[\frac{2\pi}{h} \int_0^{x_1} \sqrt{2m(V - E_\nu)} dx \right],$$

provided we are well below the barrier summit. The form of V as a function of x is, of course, unknown. With the known data

* *Phys. Rev.*, vol. 41, p. 313 (1932).

$\nu_3 = 950 \text{ cm.}^{-1}$, $\Delta_0 = 0.67 \text{ cm.}^{-1}$, and $\Delta_1 = 30.9 \text{ cm.}^{-1}$, Dennison and Uhlenbeck made the assumption that the curve for V might approximate to two parabolae joined by a flat barrier of length $2(x_0 - \alpha)$, as shown in Fig. 116. Approximate expressions for Δ_0 and Δ_1 were computed for this particular form of potential function

$$\Delta_0/h\nu = \left(\frac{2\alpha}{\pi^{\frac{1}{2}}}\right) \exp[-\alpha^2 - 2(x_0 - \alpha)(\alpha^2 - 1)^{\frac{1}{2}}],$$

$$\Delta_1/h\nu = \left(\frac{4\alpha^3 - 4\alpha}{\pi^{\frac{1}{2}}}\right) \exp[-\alpha^2 - 2(x_0 - \alpha)(\alpha^2 - 3)^{\frac{1}{2}}],$$

and from these the values of α and x_0 were found, viz. $\alpha = 1.930$, $x_0 = 3.182$. The height of the pyramid can be calculated from $\frac{x_0}{2\pi} \sqrt{\frac{h}{\mu\nu}}$ to be 0.38 A.U. It is clear from (181) that as E_v increases (that is, for higher overtones), A_v will diminish, and therefore Δ will increase rapidly. We also note from the above expressions for Δ_0 and Δ_1 that larger values of these quantities arise as x_0 diminishes, i.e. as the pyramid becomes flatter.

Manning* assumed another specific form for V , viz.

$$V = -A \operatorname{sech}^2\left(\frac{r}{2\rho}\right) + B \operatorname{sech}^4\left(\frac{r}{2\rho}\right)$$

where A , B , and ρ are arbitrary constants. This function has two symmetrical minima at $r = \pm r_0$, where $\operatorname{sech}^2\left(\frac{r_0}{2\rho}\right) = \frac{A}{2B}$. The height of the barrier at $r = 0$ is $(2B - A^2)/4B$. Manning evaluated A , B , and ρ and found a pyramidal height of 0.37 A.U. or 0.40 A.U., according as he substituted the reduced mass of the vibrating system as calculated at the end of the tunnel (equilibrium position), or in the centre of the tunnel (N passing through the H_3 plane).

A few remarks may be made about the special YX_3 molecule in which all the atoms are co-planar in the stable position. The CO_3 and NO_3 ions are such molecular groups. Here ν_1 will be a completely symmetrical breathing frequency in which the carbon or nitrogen atom does not move. No change of electric moment results, and therefore ν_1 is inactive in the infra-red.

Mode	CO_3'	NO_3'	Active in
ν_1 'breathing'	1088	1050	Raman
ν_2 trans-planar	880	830	Infra-red
ν_2 } degenerate	1438	1360	Raman and
ν_4 } in plane	714	720	infra-red

The infra-red absorption spectra of carbonate crystals, such as CaCO_3 , are characterized by three strong bands at about 7μ , 11.5μ , and 14μ . Moreover it is found that the absorption spectrum with light polarized parallel to the crystal axis contains 11.5μ only; polarized perpendicular to the axis it contains only 7μ and 14μ . The first is clearly ν_3 , and the latter are ν_2 and ν_4 .

* *Jour. Chem. Phys.*, vol. 3, p. 136 (1935).

The Five-Atom Molecule (ZYX₃)

The pyramidal model of Fig. 115 may be imagined as having a further atom *Z* beyond *Y* and on the axis of symmetry. This is represented in Fig. 117. Such molecules will have permanent electric moments and therefore pure-rotation spectra. The possible vibration modes are nine in number. Six of these (four active and two degenerate) associated with the *YX*₃ pyramid will remain substantially similar to those in Fig. 115. To these must be added ν_5 , a 'parallel' oscillation fundamentally of the *ZY* bond, i.e. of the *Z* atom relative to the *YX*₃ pyramid. In addition, we should have ν_6 , which will be a two-dimensional oscillation in a plane parallel to the base and therefore perpendicular in type. It may be visualized as due to a 'tipping' oscillation of the *YX*₃ pyramid, or of a pendulum-like motion of the bond *YZ* about the fixed point *Y*. The methyl halides are a type of this molecule which has been extensively studied. A summary has been made by Dennison* of the fundamental frequencies identified, and the table illustrates the progressive change as the atom *Z* is altered. In the region of ν_1 (about 2900 cm.⁻¹) there is found, instead of a single parallel band, a pair of comparable intensity, separated by about 100 cm.⁻¹. The effect is generally regarded as a resonance interaction between ν_1 and the parallel component of $2\nu_4$. The angle *ZYX* (Fig. 117) for all these halides is calculated to be about 107.5°, very little different from the value 109.5° for methane, CH₄. The *ZY* distance which in methane is 1.093 A.U. is calculated from the data on moments of inertia to have values shown in the table.

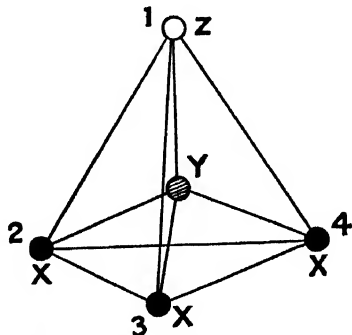


Fig. 117. Model of *ZYX*₃ molecule, e.g. methyl halides.

		CH ₃ F	CH ₃ Cl	CH ₃ Br	CH ₃ I
Parallel	ν_1	2862	2920	2930	2940
	ν_3	1460	1356	1305	1252
	ν_5	1048	732	610	532
Perpendicular	ν_2	2987	3045	3061	3074
	ν_4	1476	1460	1450	1445
	ν_6	1200	1020	957	885
<i>ZY</i> A.U.		1.40	1.71	1.90	2.2

From a knowledge of the bands observed in a molecular spectrum we always desire to get a more fundamental knowledge of the potential function of the molecule from which, of course, the possible modes can be derived. Rosenthal and Voge found that a twelve-constant

* *Rev. Mod. Phys.*, vol. 12, p. 188 (1940).

function was involved, but there are insufficient experimental data to make this usable. Dennison and others have therefore attempted to use plausible expressions for V , containing fewer constants to be determined. The principles governing the choice of expression by Slawsky and Dennison and by Linnett were as follows. Molecules with several H atoms attached to another atom, such as CH_4 , NH_3 , OH_2 , are commonly found to have the dominant forces along the valence bonds. The potential function, to a first approximation, in these cases includes squares of displacements along the bonds and squares of bond-angular displacements. For other heavy atom linkages a simple valence bond potential may, however, be insufficient. Thus the function used was

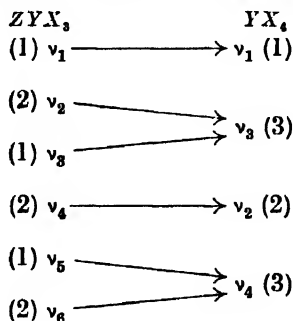
$$2V = k_1 \Sigma (\Delta r_i)^2 + k_2 R^2 \Sigma (\Delta \alpha_i)^2 + k_3 R^2 \Sigma (\Delta \beta_i)^2 + c (\Delta x_0)^2 + 2k_4 R (\Delta x_0) \Sigma (\Delta \beta_i),$$

where Δr_i ($i = 1, 2, 3$) is the change in CH bonds; $\Delta \alpha_i$ is the change in an HCH bond-angle; $\Delta \beta_i$ is the change in the ZCH bond-angle; Δx_0 is the change in the ZC bond distance.

One of the commonly occurring difficulties in evaluating molecular constants accurately is the insufficiency of data. The absence of overtone bands clearly makes it impossible to determine the anharmonic constants, X_{11} , X_{22} , &c., of (177). Any evaluation of constants of the molecule must therefore make use of the data ν_1 , ν_2 , ν_3 , &c., since the true frequencies ω_1 , ω_2 , ω_3 , &c., are unknown. If data of a convenient isotopic molecule are available, an approximate evaluation of the true frequencies can be made (see Section (e)).

Methane (CH_4)

A special case of ZYX_3 arises when Z is also an X atom. Such a case is methane, where the H atoms are at the corners of a tetrahedron and the C atom is at its centre. This high degree of 'spherical' symmetry in a molecule results in fewer distinct frequencies, and these are highly degenerate. As the Z atom approaches more to the likeness of an X atom a mathematical correlation of the possible frequencies of the two molecules can be made as shown :



It is not possible, however (excepting for ν_1), to form a clear physical picture of this transition to YX_4 . ν_1 is the completely symmetrical breathing frequency and is therefore inactive in the infra-red.

If in Fig. 117 we picture Z as an X atom and label the four atoms

1, 2, 3, and 4, they can be imagined as all undergoing elliptical types of motion on the surface of a sphere. The atom-pair 1 : 2 can be imagined mutually approaching at the same time as 3 : 4 is doing so, or, we might have taken the pairs 1 : 3 and 2 : 4, or 1 : 4 and 2 : 3. In ν_2 this surface type of oscillation takes place while leaving Y undisturbed, so that the frequency ν_2 is also inactive in the infra-red.

If, however, we imagine these pairs of moving particles out of phase, e.g. 1 : 2 approaching and 3 : 4 receding, &c., there result three-dimensional oscillations of both X and Y atoms. The atoms each oscillate, as it were, in a little spherical zone of their own. In some such manner the two active but triply-degenerate frequencies ν_3 and ν_4 are imagined to arise. In methane ν_3 lies in the region 3.3μ (origin at 3019 cm.^{-1}), ν_4 about 7.7μ (origin at 1306 cm.^{-1}). In the region 2.3μ are combination bands $\nu_1 + \nu_4$ and $\nu_3 + \nu_4$. All of these have been resolved into fine structure by A. H. Nielsen and H. H. Nielsen.* The frequency ν_1 occurs strongly in the Raman spectrum at 2914 cm.^{-1} ; the Raman band ν_2 has not apparently been recorded, but its overtone $2\nu_2$ occurs at 3071.5 cm.^{-1} .

It may be remarked that while CH_4 has four fundamentals, CDH_3 , as we should expect, has six,[†] and CD_2H_2 has all nine fundamental frequencies.

The vibrations of nickel carbonyl Ni(CO)_4 were studied by Duncan and Murray ‡ by means of the Raman spectrum, and also through using a mechanical model such as we have already referred to.§ As a nine-atom molecule there should be twenty-one internal vibration modes in all, and the remaining twelve are presumably associated with vibrations of the CO bonds, and their oscillation about the four nickel-carbon axes.

The Six-Atom Molecule : Ethylene (C_2H_4)

Ethylene is a plane six-atom molecule with twelve internal degrees of vibrational freedom. These modes are illustrated in Fig. 119. The table gives, in addition to the usual notation (given by Sutherland and Dennison),|| a notation devised by Teller and Topley.¶ They classify vibrations by a subscript which indicates with respect to what plane or planes the vibration is symmetrical. The plane α is perpendicular to the CC bond; the plane β contains the CC bond and is perpendicular to the paper; the plane γ is that of the paper. If a vibration is totally symmetrical with respect to all three planes, the subscript t is used. This does not uniquely classify the vibrations. A superscript is therefore also used which indicates the dominant feature of the vibrations. Thus, CH is used to indicate primarily a CH bond vibration; CC primarily a CC bond vibration; CH_2 primarily an oscillation of the bond angle HCH ; M a bending of the CH_2 group as a whole from the axis of the molecule.

* *Phys. Rev.*, vol. 48, p. 866 (1935).

† Ginsburg and Barker, *Jour. Chem. Phys.*, vol. 31, p. 668 (1935).

‡ *Jour. Chem. Phys.*, vol. 2, p. 636 (1934).

§ Kettering, Shuttles, and Andrews, *Phys. Rev.*, vol. 36, p. 531 (1930); also *Jour. Chem. Phys.*, vol. 2, p. 634 (1934); vol. 3, p. 175 (1935).

|| *Proc. Roy. Soc.*, vol. 148, p. 250 (1935).

¶ *Jour. Chem. Soc.*, July 1935, p. 885.

The actual assignment of frequencies in the third column is a little uncertain: values in parentheses are quite uncertain at present. Bands marked *R* should appear in the Raman spectrum: the vibration

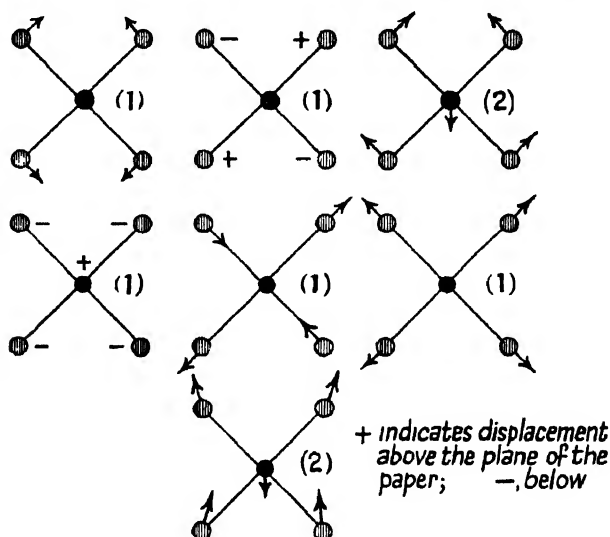


Fig. 118. Vibrations of four CO groups in $\text{Ni}(\text{CO})_4$ to illustrate a plane 'five'-atom type.

Description		ν_{cm}^{-1}	
Sutherland and Donnison	Teller and Topley		
ν_1	$\nu_{\text{CH}}^{\text{CH}}$	2088	Parallel
ν_2	$\nu_{\text{CH}}^{\text{CH}}$	3019	Parallel <i>R</i>
ν_3	$\nu_{\text{CH}}^{\text{CH}}$	1444	Parallel
ν_4	$\nu_{\text{CH}}^{\text{CH}}$	1343	Parallel <i>R</i>
ν_5	$\nu_{\text{CH}}^{\text{CH}}$	3110	Perpendicular
ν_6	$\nu_{\text{CH}}^{\text{CH}}$	3240	<i>R</i>
ν_7	$\nu_{\text{CH}}^{\text{CH}}$	(950)	<i>R</i>
ν_8	$\nu_{\text{CH}}^{\text{CH}}$	1623	Parallel <i>R</i>
ν_9	$\nu_{\text{CH}}^{\text{CH}}$	(1160)	Perpendicular
ν_{10}	$\nu_{\text{CH}}^{\text{CH}}$	(1097)	<i>R</i>
ν_{11}	$\nu_{\text{CH}}^{\text{CH}}$	(730)	Perpendicular
ν_{12}	$\nu_{\text{CH}}^{\text{CH}}$	(1110)	<i>R</i>

results in no change of electric moment, so that they will be inactive in the infra-red.

The notation of Teller and Topley permits us to group the vibration modes into a number of symmetry classes. Thus ν_1 , ν_3 , and ν_{12} are in one class, ν_2 , ν_4 , and ν_8 are in another, ν_5 and ν_9 in another, ν_6 and ν_{10} in

another, while ν_7 and ν_{11} are in separate classes. This grouping corresponds to the symmetry properties of the wave-functions—a knowledge of which is important in relation to such matters as selection principles, and the structure (parallel or perpendicular) of combination bands.

The treatment of ethylene as a dynamical system, so far as its vibrations parallel to the molecular axis are concerned, has been given by Sutherland and Dennison.* The co-ordinates used were x_0 , the relative displacement of C_1 and C_2 from equilibrium; x_1 , the relative displacement of C_1 from A the centre of gravity of H_1 and H_2 ;

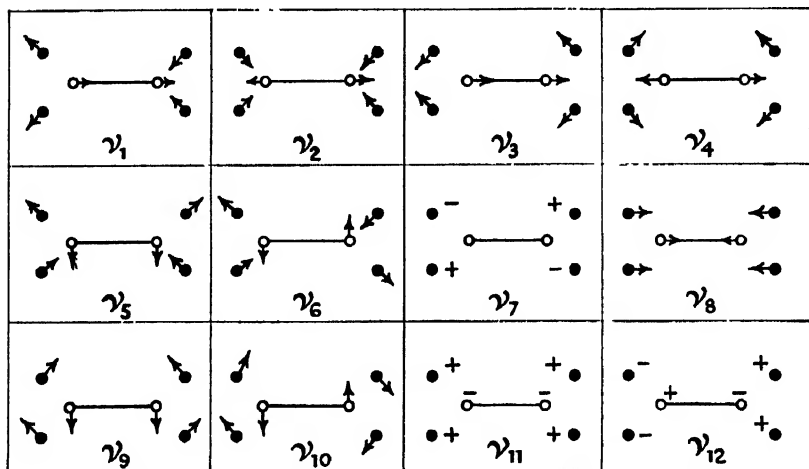


Fig. 119. Vibrational modes of ethylene, C_2H_4 .

x_2 applies similarly to the displacement of C_2 from B ; q_1 is the relative displacement of H_1 and H_2 from equilibrium; q_2 applies similarly to H_3 and H_4 . The expression for the potential energy of one of the CH_2 groups is in general

$$V = \frac{1}{2}(ax_1^2 + bq_1^2 + 2dx_1q_1).$$

The assumption is now made that the potential energy between the two CH_2 groups depends only on the distance between the two carbon nuclei. This gives a four-constant formula for the potential energy of the whole molecule

$$V = \frac{1}{2}\{a(x_1^2 + x_2^2) + b(q_1^2 + q_2^2) + cx_0^2 + 2d(x_1q_1 + x_2q_2)\},$$

and the values of a , b , c , and d were subsequently determined. A relation was found in the course of investigation between the five parallel frequencies :

$$\nu_1^2 + \nu_3^2 + \frac{M + 2m}{M} \frac{\nu_2^2 \nu_4^2 \nu_8^2}{\nu_1^2 \nu_3^2} = \nu_2^2 + \nu_4^2 + \nu_8^2. \quad (182)$$

* *Proc. Roy. Soc.*, vol. 148, p. 250 (1935).

where M and m are masses of the carbon and hydrogen atoms respectively. It is of interest to find that with the values of the table, the left-hand side is 13.73×10^6 and the right-hand side 13.55×10^6 , which indicates the accuracy of the assumption made.

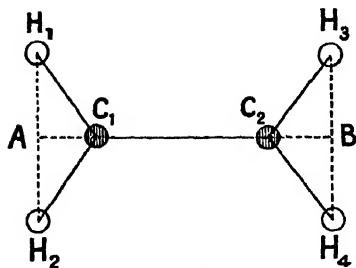


Fig. 120.

The importance of this type of investigation is to show that we can reduce the number of constants in a potential function to a small and determinable number, thus demonstrating that we can consider groups of atoms vibrating as larger units in complex molecules.

The chlorine derivatives of ethylene have been investigated by Ta-You Wu * and others. As anticipated, there is good evidence of the twelve fundamental frequencies. It is of interest to observe that the *cis*- and *trans*-forms of $C_2H_2Cl_2$, $\begin{matrix} Cl & & Cl \\ & \backslash & / \\ H & > C = C < \\ & / & \backslash \\ & H & & H \end{matrix}$ and $\begin{matrix} Cl & & H \\ & \backslash & / \\ H & > C = C < \\ & / & \backslash \\ & H & & Cl \end{matrix}$ have some of their fundamental frequencies modified as between one molecule and the other.

Ethane (C_2H_6)

As an eight-atom molecule it should have eighteen internal vibrations, but examination shows that only twelve would be expected as distinct, six being degenerate. The molecule may be regarded as two CH_3 groups linked together by a single C-C bond. Reference to Fig. 115 shows the four vibrations appropriate to each methyl group. The way that the two CH_3 pyramids are put together may be envisaged easily from Fig. 119 if we imagine a third H atom at each end of the ethylene molecule. The first eight modes of ethane are thus accounted for. ν_7 represents a free rotation of the pyramids about the molecular axis. ν_8 is a mutual oscillation of the two pyramids along the CC bond. ν_{11} and ν_{12} are two degenerate oscillations conical-wise round the molecular axis. No attempt has been made to assign experimental values of the frequencies to the particular modes tabulated. Sutherland and Dennison † treated the problem of ethane along similar lines to that of ethylene, using a four-constant potential energy formula satisfactorily.

It is along these lines that we may hope to gain information about very complex molecules. A group of atoms will have its own characteristic modes of vibration which are understood. A complex molecule may be regarded as a number of such groups coupled together. So far as the frequencies of these couplings are concerned, the group behaves as a unit. The internal vibrations of the group will be somewhat modified by its setting—but not fundamentally changed.

* *Phys. Rev.*, vol. 46, p. 465 (1934); *Jour. Chem. Phys.*, p. 392 (1937).

† *Proc. Roy. Soc.*, vol. 148, p. 250 (1935).

CH ₃ mode, <i>see</i> Fig. 119	Relative phase of the two CH ₃ groups	C ₂ H ₆ modes		
		Sutherland and Dennison	Teller and Topley	
ν_1	{ out of	ν_1	ν_1^{CH}	Parallel <i>R</i>
	{ in	ν_2	ν_1^{CH}	Parallel <i>R</i>
ν_2	{ out of	ν_3	$\nu_3^{\text{CH}_2}$	Parallel
	{ in	ν_4	$\nu_4^{\text{CH}_2}$	Parallel <i>R</i>
ν_3	{ in	(2) ν_5	ν_5^{CH}	Perpendicular
	{ out of	(2) ν_6	ν_6^{CH}	Perpendicular <i>R</i>
ν_4	{ in	(2) ν_9	$\nu_9^{\text{CH}_2}$	Perpendicular
	{ out of	(2) ν_{10}	$\nu_{10}^{\text{CH}_2}$	Perpendicular <i>R</i>
	free rotation	ν_7	ν_7^R	—
	in	ν_8	ν_8^{CO}	Parallel <i>R</i>
	in	(2) ν_{11}	ν_{11}^M	Perpendicular
	out of	(2) ν_{12}	ν_{12}^M	Perpendicular <i>R</i>

R — should appear in Raman spectrum.

Moreover, when an atom or a group of atoms in a molecule is replaced by a homologous series of atoms or groups of atoms, we commonly find that while new bands corresponding to the internal vibrations of the group are added, the basic absorption spectrum of the couplings shows gradual displacements of the chief bands.

With the recognition that the vibrations within a group do vary a few per cent., according to the nature of the molecule of which it forms a part, and also that the vibration of a coupling between two atoms or groups of atoms may be somewhat affected by other outside bonds, we do nevertheless find a remarkable constancy of frequency associated with certain couplings. This is of considerable assistance in assigning experimental frequency data to certain modes of vibration.

A collection of data is made in the table on p. 226. The force-constants have been taken from Sutherland and Dennison and also from Hibben.* Where the molecule is stated, by investigation of which *k* was found, it is given in the first column. The frequency of the corresponding bond oscillation for the *two* atoms given has been calculated from

$$c\nu = \frac{1}{2\pi} \sqrt{\frac{k}{\mu m_0}} \quad . \quad . \quad . \quad . \quad . \quad (183)$$

where $\mu = \frac{m_1 m_2}{m_1 + m_2}$ is the reduced mass of the pair of atoms whose atomic masses are m_1 and m_2 , and m_0 is the mass of an atom of unit atomic weight, viz. 1.649×10^{-24} gm.

The formula for ν in cm.^{-1} becomes

$$\nu = 4.125 \sqrt{\frac{k}{\mu}} \quad . \quad . \quad . \quad . \quad . \quad (184)$$

* *The Raman Effect and its Chemical Applications.*

FORCE-CONSTANTS AND VIBRATION FREQUENCIES OF SOME BONDS

Mole- cule	Bond	$k \times 10^{-5}$ dyne/cm. ⁻¹	$\nu_{\text{cm}^{-1}}$	Mole- cule	Bond	$k \times 10^{-5}$ dyne/cm. ⁻¹	$\nu_{\text{cm}^{-1}}$
C ₂ H ₂	C—H	5.88	3288	—	N—H	6.20	3370
CH ₄	C—H	5.04	3050	—	O—H	6.80	3650
CH ₃	C—H	4.67	2851	—	O=O	11.40	1556
C ₂ H ₆	C—C	4.96	1187	—	N=O	20.90	2224
C ₂ H ₄	C=C	9.79	1668	H ₂	H—H	5.63	4370
C ₂	C=C	9.52	1641	HCl	H—Cl	4.75	2880
C ₂ H ₂	C≡C	15.71	2113	HBr	H—Br	3.80	2558
CH ₃ OH	C—O	5.00	1030	—	H—S	3.78	2572
H ₂ CO	C=O	13.45	1829	—	C—S	2.14	650
CO ₂	C=O	15.4	1957	CH ₃ F	C—F	5.76	1048
CO	C≡O	19.0	2155	CH ₃ Cl	C—Cl	3.44	732
	C—N	4.85	1033	CH ₃ Br	C—Br	2.85	610
	C=N	10.40	1650	CH ₃ I	C—I	2.26	532
	C≡N	17.50	2150				

If attached to each atom of the bond is a group which moves with it, the greater load to be moved by the same restoring force will, of course, reduce the frequency, which may be calculated from (184).

It is interesting to observe that three such bonds as C—C, C=C, and C≡C have their force constants approximately in the ratio 1 : 2 : 3.

Examination of the same bond, such as C—H, in different molecules, makes it clear that there are differences in its strength. While in CH the bond is built from a (2s)²(2p)³ carbon atom and a (1s) hydrogen atom, in methane and acetylene it is probably built from a (2s)(2p)³ carbon atom and a (1s) hydrogen atom. Moreover, there is as between these two molecules a different degree of association of the two atoms. The same type of variation occurs for the C=O bond in different molecules, as the table shows.

The flexural force-constant concerned with angular deformations is certainly always much smaller than that concerned with vibrations along a bond. The constant 'b', which may be taken to give an approximate idea of the force separating the pairs of H atoms in ethylene, was found by Sutherland and Dennis to be 1×10^{-5} dyne/cm. —approximately one-fifth of the k value associated with extension of a bond.

(c) THE ROTATION OF MOLECULES

In the preceding section we have considered the vibrational energy of molecules, which roughly we may say corresponds to emission or absorption in the near infra-red up to 20μ (500 cm^{-1}). Simultaneous vibrational and rotational changes give rise to bands, and with adequate resolving power the fine structure of these can be revealed. If a molecule has a permanent electric moment, such as H₂O and NH₃ (but not CO₂), it will also have a pure-rotation band beyond 100μ (100 cm^{-1}). This region presents greater experimental difficulties, however.

In general the polyatomic molecule will have three principal moments

of inertia, which we will call A , B , and C , where $A < B < C$. If they are all unequal, we have the asymmetrical top. This rotator can be described as executing pure rotation about either the greatest or least axis of inertia while this axis makes a precession and a nutation (of commensurable period) round the axis of total angular momentum. It is a spinning top whose angle to the vertical is oscillating.

If two of the moments of inertia are equal, we have the symmetrical rotator. The motion of this can be represented as a pure rotation about either the greatest or least axis of inertia, with this axis making a precession round that of total angular momentum. If the two smaller moments of inertia are equal, i.e. $A = B$, we have an oblate type (a disk or plate in the extreme case); if the two larger are equal, i.e. $B = C$, we have a prolate type (spindle-shape).

Special cases arise when $A = B = C$, which may be described as a spherical molecule. We may take CH_4 as an example of this. If one of the moments of inertia is zero, and the other two are equal, we have the linear molecule. We shall consider these in the order of increasing complexity.

Linear Molecules

We have already discussed the vibrations of such molecules as CO_2 , HCN , C_2H_2 , &c. The fine structure arising from rotation of these molecules is similar in all essential respects to that of diatomic molecules. The selection principle which governs changes in J , the rotation quantum number, is different for parallel or perpendicular bands. These terms, it will be recalled, describe bands in which the electrical moment oscillates parallel or perpendicular to the axis of symmetry (here the molecular axis). Parallel bands have only P and R branches; perpendicular bands have P , Q , and R branches.

$$(\text{Linear Molecules}) \left\{ \begin{array}{ll} \Delta J = \pm 1 & (\text{parallel bands}), \\ \Delta J = \pm 1, 0 & (\text{perpendicular bands}). \end{array} \right\} \quad (185)$$

Fig. 121 (after Choi and Barker, *Phys. Rev.*, vol. 42, p. 779 (1932)) shows a typical vibration-rotation band of the perpendicular type with a strong Q branch extending beyond the limit of the figure. The rotational and vibrational energy may, if we neglect interaction terms, be simply added

$$E(v, J) = (v + \frac{1}{2})h\nu_0 + \frac{h^2}{8\pi^2 I} J(J+1) \quad (186)$$

Hence we have for typical branches arising in emission by a change in v ($1 \rightarrow 0$)

$$\left. \begin{array}{l} R \text{ branch} \\ J+1 \rightarrow J \quad \nu = \nu_0 + \frac{h}{4\pi^2 I} (J+1) \quad J = 0, 1, 2, \dots, \\ R \text{ branch} \\ J-1 \rightarrow J \quad \nu = \nu_0 - \frac{h}{4\pi^2 I} J \quad J = 1, 2, 3, \dots, \\ Q \text{ branch } J \rightarrow J \quad \nu = \nu_0. \end{array} \right\} \quad (187)$$

Q

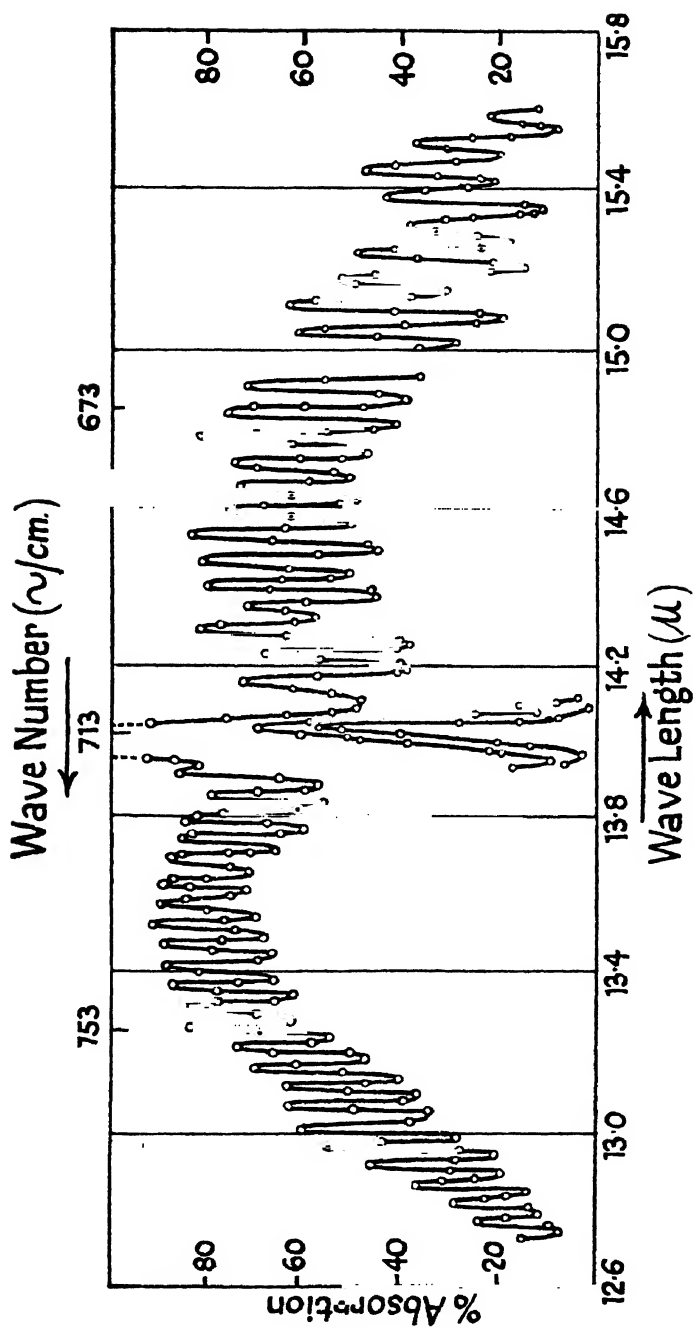


Fig. 121. Fine structure of the 14μ band of HCN (after Choi and Barker). It is associated with the fundamental ν_1 ($= 712\text{ cm}^{-1}$), and has a strong Q branch ($I = 18.32 \times 10^{-40}$).

The Q branch is in practice not one single line but usually a somewhat broad though unresolved peak due to interaction of vibration and rotation. Clearly if I for $v = 1$ is slightly greater than for $v = 0$ we should expect formulae like (24) with C negative; there would be a slight degradation to the low-frequency side. There would be a smaller term in J^2 in (187). All the well-resolved CO_2 bands have been reported as showing this effect.

It is clear that where a symmetrical linear molecule such as CO_2 has its moment of inertia determined, we can calculate the inter-atomic distances. Taking the best value for $h/4\pi^2 Ic$ as 0.785 we deduce $I = 71.30 \times 10^{-40}$ gm.-cm.² giving O-O as 2.317×10^{-8} cm. In the case of an unsymmetrical linear molecule such as HCN a knowledge of $I = 18.72 \times 10^{-40}$ gm.-cm.² is insufficient to determine the HC or CN distance. Similar information for the isotopic molecule DCN, viz. $I = 22.92 \times 10^{-40}$ gm.-cm.², allows this determination to be made: H-C = 1.06 Å., and C-N = 1.15 Å. The isotopic effect in bands is discussed more fully in Section (e).

If band structure is unresolved, an approximate estimate of I may be made by measuring $\Delta\nu$, the separation of the two maxima of the P and R envelopes. From (129) we have approximately $K T = 2hcBJ_m^2$. Since $2BJ_m = \frac{1}{2}\Delta\nu$, the separation of the line of maximum intensity from the origin, we have:

$$\Delta\nu_{\text{cm}^{-1}} = \frac{1}{\pi c} \sqrt{\frac{KT}{I}} \quad . \quad . \quad . \quad . \quad (188)$$

From this I may be found. K is Boltzmann's constant (1.37×10^{-16}).

Spherical Molecules

Methane CH_4 , silane SiH_4 , and germane GeH_4 are analogues and probably 'spherical' molecules having $A = B = C$. These molecules have all had the fine structure of leading vibration-rotation bands analysed by H. H. Nielson* and his collaborators. The four hydrogen atoms are presumably at the corners of a regular tetrahedron.

Fig. 122 shows one of these bands, viz. ν_3 at 4.7μ , for the molecule GeH_4 . The energy expression (186) applies to a first approximation to spherical molecules. The selection principle is $\Delta J = \pm 1$ or 0.

Symmetrical Rotators

These constitute a large and important group of molecules of which we may cite as examples NH_3 , methyl halides, ethane, and ethylene, and the Y-shaped molecule formaldehyde H_2CO . We shall derive an expression for the rotational energy of such a top—the disk or cylinder of Fig. 123. Let (x', y', z') be its own proper axes for rotations, about which the moments of inertia are respectively A , A , and C . If p , q ,

* CH_4 : *Phys. Rev.*, vol. 48, p. 864 (1935); SiH_4 : *Phys. Rev.*, vol. 47, p. 828 (1935); GeH_4 : *Phys. Rev.*, vol. 48, p. 861 (1935).

and r are the angular velocities about these axes we have for the kinetic energy τ

$$2\tau = Ap^2 + Aq^2 + Cr^2.$$

Let us change the co-ordinates to three angular ones (θ, ψ, ϕ) which

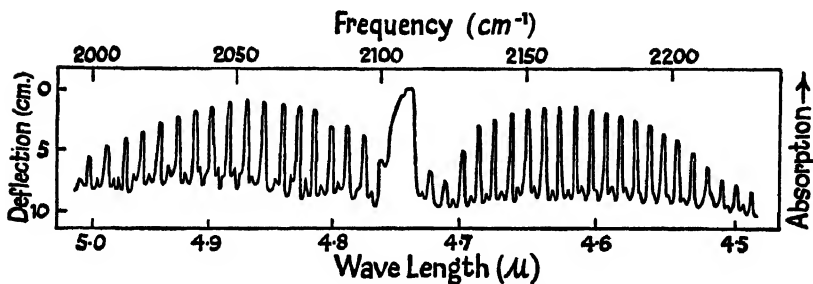


Fig. 122. 4.7μ band of GeH_4 , a 'spherical' molecule.

$$A = B = C = 7 \times 10^{-40} \text{ gm.-cm.}^2.$$

$$\text{GeH} = 1.37 \text{ A.U.}$$

$$\text{H-H} = 2.06 \text{ A.U.}$$

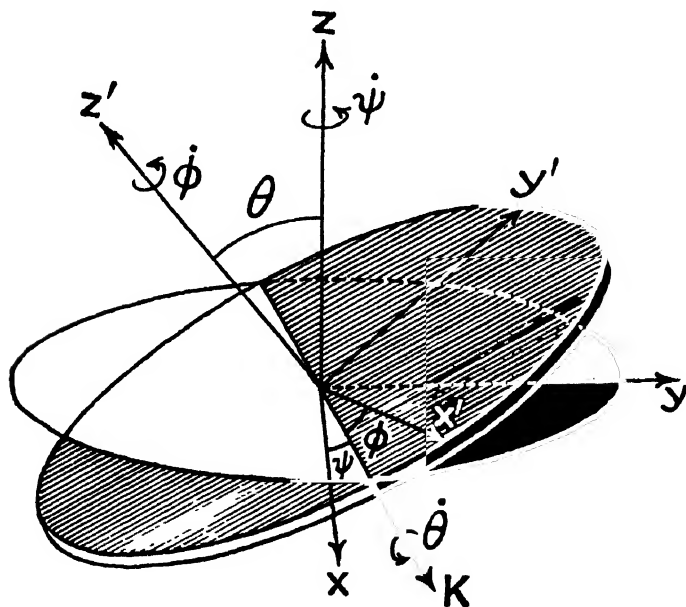


Fig. 123. Symmetrical top (a disk).

are known as Eulerian angles. If (x, y, z) are a set of fixed axes of reference, θ is the angle the top's axis z' makes with z . In pure precession it is a constant, as in a symmetrical rotator. In an asymmetrical body it might vary. The plane $x'y'$ of the top intersects the fixed plane xy in a line OK , and this line OK rotates in the xy -

plane with an angular velocity ψ , where ψ measures the angle $K'Ox$. ϕ measures the angle between Ox' and the moving line OK . We can express p , q , and r in terms of θ , ϕ , and ψ :

$$\begin{aligned} p &= \theta \cos \phi + \psi \sin \theta \sin \phi, \\ q &= -\theta \sin \phi + \psi \sin \theta \cos \phi, \\ r &= \phi + \psi \cos \theta. \end{aligned}$$

Hence $2\tau = A(\theta^2 + \psi^2 \sin^2 \theta) + C(\phi^2 + 2\phi\psi \cos \theta + \psi^2 \cos^2 \theta)$.

The angular momenta associated with θ , ϕ , and ψ can now be written down:

$$\begin{aligned} p_\theta &= \frac{\partial \tau}{\partial \dot{\theta}} = A\dot{\theta}, \\ p_\psi &= \frac{\partial \tau}{\partial \dot{\psi}} = C \cos \theta (\psi \cos \theta + \phi) + A\psi \sin^2 \theta, \\ p_\phi &= \frac{\partial \tau}{\partial \dot{\phi}} = C(\phi + \dot{\psi} \cos \theta). \end{aligned}$$

By substitution we can write for 2τ

$$\begin{aligned} 2\tau &= \frac{p_\theta^2}{A} + p_\psi \dot{\psi} + p_\phi \dot{\phi}, \\ &= \frac{p_\theta^2}{A} + p_\psi \dot{\psi} + p_\phi \left(\frac{p_\phi}{C} - \dot{\psi} \cos \theta \right) \text{ by eliminating } \dot{\phi}, \\ &= \frac{p_\theta^2}{A} + \frac{p_\phi^2}{C} + \frac{(p_\psi - p_\phi \cos \theta)^2}{A \sin^2 \theta} \text{ by eliminating } \dot{\psi}. \end{aligned}$$

Since ϕ and ψ do not occur in this, p_ψ and p_ϕ are constants. We are dealing with a uniform precession round the z -axis along which the resultant angular momentum vector R of the top is directed. p_ψ is obviously R , and $p_\phi = R \cos \theta$. Since there is no nutation $\theta = \text{constant}$, and $p_\theta = 0$.

The quantum conditions are

$$\int_0^{2\pi} p_\psi d\psi = \bar{J}h \text{ or } 2\pi p_\psi = \bar{J}h \quad (\bar{J} = \sqrt{J(J+1)}),$$

and

$$\int_0^{2\pi} p_\phi d\phi = kh \text{ or } 2\pi p_\phi = kh,$$

so that $\cos \theta = k/\bar{J}$.

Substituting in τ we have

$$\tau = \frac{h^2}{8\pi^2 A} J(J+1) + \frac{h^2}{8\pi^2} \left(\frac{1}{C} - \frac{1}{A} \right) k^2 \quad \dots \quad (189)$$

$$= \frac{h^2}{8\pi^2 A} [J(J+1) + \beta k^2] \quad \dots \quad (190)$$

where $\beta = \frac{A}{C} - 1$. We observe that two rotational quantum numbers are involved: J , which measures the total angular momentum, and k , which measures the top's angular momentum about its own axis of symmetry. The quantum number k may take a series of integral values up to J , i.e. $k \leq J$, but in practice it is usually confined to reasonably low values. The values taken by J will then be the series $k, k+1, k+2$, &c.

We may also note that where the top has the form of a disk $A = \frac{C}{2}$, so that $\beta = -\frac{1}{2}$, while for a very thin spindle or rod for which $C \rightarrow 0$ we have $\beta \rightarrow \infty$.

The selection rules which govern changes of the two quantum numbers are

$$(\text{Symmetrical Top}) \left\{ \begin{array}{l} \Delta J = \pm 1, 0 \text{ with } \Delta k = 0 \\ \hspace{10em} (\text{parallel band}), \\ \Delta J = \pm 1, 0 \text{ with } \Delta k = \pm 1 \\ \hspace{10em} (\text{perpendicular band}). \end{array} \right\} \quad (191)$$

It is obvious, therefore, that the parallel bands of these molecules have P , Q , and R branches precisely as indicated in (187). The perpendicular bands show, however, a much more complex structure which we now proceed to examine.

For every specific change in k such as $1 \rightarrow 0$, $2 \rightarrow 1$, $3 \rightarrow 2$, &c., we shall have a complete band with P , Q , and R branches. These may be called positive subsidiary bands, since they occur on the high-frequency side of ν_0 , the vibrational origin. Similarly each change in k such as $0 \rightarrow 1$, $1 \rightarrow 2$, &c., corresponds to a negative subsidiary band. Writing $B = h/8\pi^2 A$ we have

$$\left. \begin{array}{l} k+1 \rightarrow k \\ \text{(Positive subsidiary bands)} \\ J+1 \rightarrow J \quad \nu = \nu_0 + 2B[(J+1) + \beta(k + \frac{1}{2})] \quad R(J) \\ J \rightarrow J \quad \nu = \nu_0 + 2B[\beta(k + \frac{1}{2})] \quad Q(J) \\ J-1 \rightarrow J \quad \nu = \nu_0 + 2B[-J + \beta(k + \frac{1}{2})] \quad P(J) \\ \hline k-1 \rightarrow k \\ \text{(Negative subsidiary bands)} \\ J+1 \rightarrow J \quad \nu = \nu_0 + 2B[(J+1) - \beta(k - \frac{1}{2})] \quad R(J) \\ J \rightarrow J \quad \nu = \nu_0 + 2B[-\beta(k - \frac{1}{2})] \quad Q(J) \\ J-1 \rightarrow J \quad \nu = \nu_0 + 2B[-J - \beta(k - \frac{1}{2})] \quad P(J) \end{array} \right\} \quad (192)$$

The arrows are pointed as corresponding to *emission* of radiation: if reversed we have the changes in absorption bands.

Fig. 124 shows a diagram (after Dennison) to illustrate the structure of a typical perpendicular band. The missing lines to be expected in each subsidiary band are as follows:

First Positive $k' = 1, k'' = 0, \therefore J' \geq 1, J \geq 0$
Missing: $P(1)$

First Negative $k' = 0, k'' = 1, \therefore J' \geq 0, J'' \geq 1$
Missing: $R(0)$

Second Positive $k' = 2, k'' = 1, \therefore J' = 2, J'' = 1$
 Missing : $R(0), P(1), P(2)$

Second Negative $k' = 1, k'' = 2, \therefore J' = 1, J'' = 2$
 Missing : $R(0), R(1), P(1)$

and so on. The value of β used by Dennison in Fig. 124 is about 4. The figure would correspond to a temperature distribution appropriate

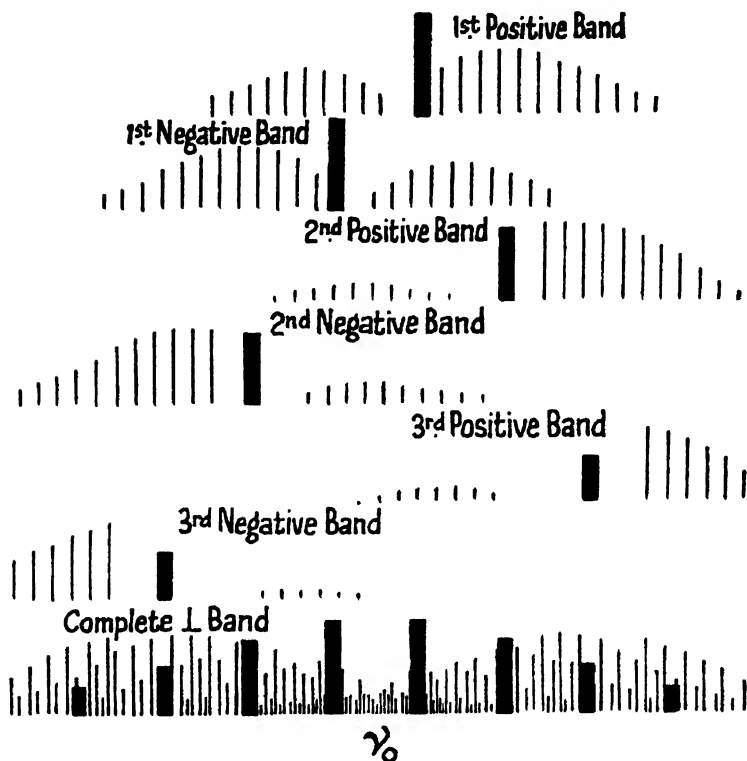


Fig. 124. Structure of a perpendicular band of a symmetrical rotator.
 (After Dennison.)

to $\tau = 790^\circ \text{ K.}$ for NH_3 (taking $A = 2.782 \times 10^{-40} \text{ gm.-cm.}^2$). Dennison* has given intensity factors for the various branches and subsidiary bands, but for these reference may be made to the original paper. The positive subsidiary bands, it will be noted, have stronger R branches, and the negative subsidiary bands have stronger P branches. The outstanding (unresolved) Q branches are a feature of the diagram. The intervals between these are $2B\beta$ or $\frac{h}{4\pi^2} \left(\frac{1}{C} - \frac{1}{A} \right)$, so that if A is known from the analysis of parallel bands C is calcul-

* *Rev. Mod. Phys.*, vol. 3, p. 289 (1931).

able. For reasons which we shall outline briefly difficulties, however, arise: the values of $\frac{h}{4\pi^2} \left(\frac{1}{C} - \frac{1}{A} \right)$ are found to differ in different perpendicular bands, because of the interaction of rotation and vibration.

It has been observed that where degenerate perpendicular vibrations take place, as e.g. ν_2 of Fig. 110 or ν_2 and ν_4 of Fig. 115, an internal angular momentum $\zeta h/2\pi$ may arise. The quantity ζ depends on the vibrational properties of the molecule only, i.e. masses, force-constants, &c. Forces of interaction are set up between this angular momentum of vibrational origin and the angular momentum due to molecular rotation, the net result of which is to replace the second term in (189) by $\frac{h}{8\pi^2} \left[\frac{1-\zeta}{C} - \frac{1}{A} \right] k^2$. The values of the intervals between the

Q branches should therefore be $\frac{h}{4\pi^2} \left[\frac{1-\zeta}{C} - \frac{1}{A} \right]$, and these will be different for each perpendicular band. Johnston and Dennison * have shown that $\Sigma \zeta = \frac{C}{2A} - 1$ for the molecules such as YX_3 , and $\Sigma \zeta = \frac{C}{2A}$ for molecules such as ZYX_3 , so that the sums of the Q -branch spacings in the several perpendicular bands of these molecules are quantities from which reliable values of C are determinable.

NH_3 has been cited as an example of a symmetrical rotator, and some of the data will be used to illustrate the principles of band structure already given. It is obvious that since there is no permanent electric moment associated with rotation about the axis of symmetry, the *pure-rotation* bands in the far infra-red will be due to rotation about an axis at right angles. So far as (189) is concerned, $\Delta k = 0$ and $\Delta J = +1$, so that the pure-rotation band will be a single positive branch $\nu = 2BJ$ for $J \rightarrow J-1$.

Wright and Randall † have investigated NH_3 and PH_3 in this region. Barnes ‡ has investigated NH_3 and ND_3 . In NH_3 the lines from $J = 3$ at 168.4μ to $J = 12$ at 42.47μ have been recorded and found to fit the formula $\nu = 19.880 J - 0.00176 J^3$. The small cubic term arises from the slight deformation of the molecule due to the centrifugal effects of rotation. As previously mentioned in connexion with NH_3 , the vibrational levels are all double, due to the special potential function involved (Fig. 116). In Fig. 125 are shown three consecutive rotational levels with possible transitions, all associated with $v = 0$. The states α have wave-functions of which the vibrational part is 'symmetrical' so far as an interchange of two H-nuclei is concerned; β states are 'anti-symmetrical' in this respect. For pure-rotation bands and for parallel vibration-rotation bands the selection principle is $\alpha \leftrightarrow \beta$. This means that in pure-rotation bands the doublet interval (associated with $v = 0$) will be $2\Delta_0$. In the vibration-rotation band lines of ν_3 the doublet-separation will be $\Delta_1 + \Delta_0$. Wright and Randall give $\Delta_0 = 0.67 \text{ cm.}^{-1}$ and $\Delta_1 = 30.9 \text{ cm.}^{-1}$.

* *Phys. Rev.*, vol. 48, p. 868 (1935).

† *Ibid.*, vol. 44, p. 391 (1933).

‡ *Ibid.*, vol. 47, p. 658 (1935).

The α and β states have different statistical weights according to the values of k and J . These are

α	β	Condition
0	$2(2J + 1)$	For $k = 0$ and J even
$2(2J + 1)$	0	For $k = 0$ and J odd
$2J + 1$	$2J + 1$	For $k \neq 0$ but not a multiple of 3
$2(2J + 1)$	$2(2J + 1)$	For $k \neq 0$ but a multiple of 3

For both the pure-rotation band and parallel type vibration-rotation bands $\Delta k = 0$, but the intensities of the branch lines will arise as a summation of all the intensities due to the values of k that can exist. As might be anticipated, therefore, from the above statistical weights, alternating intensities will arise in both the $\beta \rightarrow \alpha$ and the $\alpha \rightarrow \beta$ bands.

In Fig. 126 (after Dennison and Hardy) are shown the calculated intensities for the ν_1 fundamental at 3μ and the ν_3 fundamental at 10.5μ . The value of A may be found easily from these bands, but C , the moment of inertia about the symmetry axis, requires detailed structure of the perpendicular bands giving $\left(\frac{1}{C} - \frac{1}{A}\right)$. In practice it may be calculated from a knowledge of the corresponding ND_3 bands.

There is no theoretical reason against transitions between adjacent component levels α and β of each pair of Fig. 125. Such radiation would be of wave-number $\Delta_0 = 0.67 \text{ cm.}^{-1}$, or wave-length 1.5 cm. Cleeton and Williams * produced electromagnetic waves of this wave-length and demonstrated their strong absorption by NH_3 .

Asymmetrical Rotators

In this class will be the great majority of molecules for which $A \neq B \neq C$. Some simple triatomic molecules such as H_2O and SO_2 are asymmetric tops. These, being plane molecules, will be expected to have a relationship of the type $A + B = C$ between the three moments of inertia. There is no simple expression of the type (189) from which the rotational levels can be derived. The mathematical problem has, however, been solved by several investigators, and we follow here in outline the detailed account given by Dennison.† There

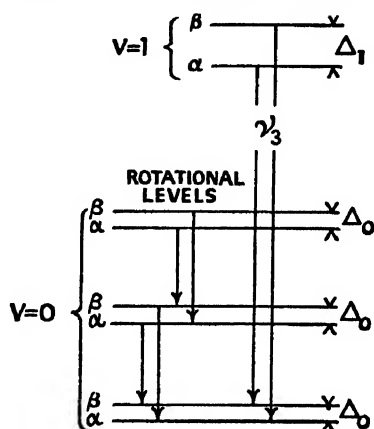


Fig. 125. Vibrational and rotational transitions typical of those in NH_3 . The doubling of vibrational levels is due to the 'tunnel' effect.

* *Phys. Rev.*, vol. 45, p. 234 (1933).

† *Rev. Mod. Phys.*, vol. 3, p. 289 (1931).

is a total quantum number J as before, but associated with each value of J there are $2J + 1$ sub-levels. Each of these is distinguished by an index number r ranging from $+J$ for that of highest energy to $-J$ for that of lowest energy. r is not a quantum number but merely a distinguishing index.

These $2J + 1$ levels associated with a particular value of J have their energy values W_r computed by calculation of the $2J + 1$ values of x_r . The energy levels are then given by

$$\frac{8\pi^2}{h^2} W_r = x_r + \frac{J(J+1)}{C} \quad . \quad . \quad . \quad (193)$$

or by a similar expression in which A or B may replace C , depending on which axis is that of molecular rotation. The values of x_r are

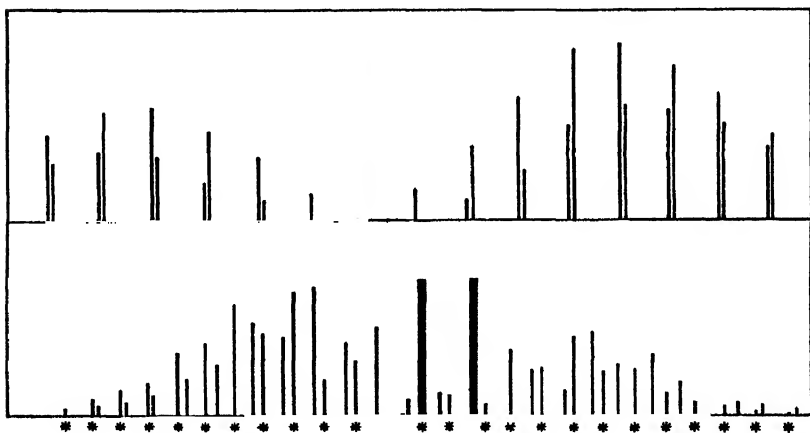


Fig. 126. (a) Structure of 3μ band. (b) Structure of 10.5μ band of NH_3 . (After Dennison and Hardy.)

found as solutions of certain equations and these equations have been tabulated up to $J = 8$ by Dennison.

To indicate the labour involved we reproduce the equations for $J = 5$

$$\left. \begin{aligned} x^3 - 35\alpha_1 x^2 + (259\alpha_1^2 + 528\beta_1)x - 225\alpha_1^3 - 4560\alpha_1\beta_1 &= 0, \\ x^2 - 20\alpha x + 64\alpha^2 + 108\beta &= 0. \end{aligned} \right\}$$

There are three values of α , and β , which are computed from the moments of inertia A , B , and C

$$\begin{aligned} \alpha_1 &= \frac{1}{A} + \frac{1}{B} - \frac{2}{C}, & \beta_1 &= \left(\frac{1}{A} - \frac{1}{C}\right)\left(\frac{1}{B} - \frac{1}{C}\right), \\ \alpha_2 &= \frac{1}{B} + \frac{1}{C} - \frac{2}{A}, & \beta_2 &= \left(\frac{1}{B} - \frac{1}{A}\right)\left(\frac{1}{C} - \frac{1}{A}\right), \\ \alpha_3 &= \frac{1}{C} + \frac{1}{A} - \frac{2}{B}, & \beta_3 &= \left(\frac{1}{C} - \frac{1}{B}\right)\left(\frac{1}{A} - \frac{1}{B}\right). \end{aligned}$$

Each of these three cubics has, of course, three solutions, and the quadratic has two more, thus giving the eleven values of x , required for $J = 5$. Consider now the complex of band lines arising from the J transition $5 \rightarrow 4$. The question now arises as to the selection principle governing transitions from the eleven initial sub-levels to the nine final sub-levels. Each sub-level has two 'symmetry' classifications assigned to it: these are labelled a and b in Fig. 127. We shall not consider their significance, but merely remark that the assignment is done as follows (where $+$ means 'even,' and $-$ means 'odd'). To assign a begin with $r = +J$ and label it $+$, then passing downwards label the next two $-$, the next two $+$, &c. To assign b begin with $r = -J$, which is labelled $+$, then, passing upward, label the next two $-$, the next two $+$, &c. The selection principle for J , as we expect, is $\Delta J = \pm 1, 0$. Apart from this the sub-level transitions permitted depend on the particular axis along which the electric moment or change of electric moment lies. Let us take $A < B < C$. If the change is along the axis about which the moment of inertia is least (viz. A), transitions can take place between levels having a different sign under a and the same sign under b concurrently.

τ	$J=5$	a	b
$+5$	_____	$+$	$-$
$+4$	_____	$-$	$-$
$+3$	_____	$-$	$+$
$+2$	_____	$+$	$+$
$+1$	_____	$+$	$-$
0	_____	$-$	$-$
-1	_____	$-$	$+$
-2	_____	$+$	$+$
-3	_____	$+$	$-$
-4	_____	$-$	$-$
-5	_____	$-$	$+$

Fig. 127. Sub-levels associated with $J = 5$ of an asymmetrical rotator (after Dennison).

	a	b	} . (194)	
<i>Electric moment (along)</i>	$A :$	Different		Same
	$B :$	Different		Different
	$C :$	Same		Different

The number of such transitions associated with a few lines of the R branch are: $R(0)$, 1; $R(1)$, 4; $R(2)$, 9; $R(3)$, 16; $R(4)$, 25, &c. Clearly for $R(J)$ the number of lines associated is $(J + 1)^2$.

Since the $(2J + 1)$ energy levels are not spaced at any regular or regularly varying intervals, there is no obvious order in the line complex. The bands of asymmetric rotators will thus be expected to consist of a very complicated and numerous assembly of lines, if they are resolved.

The pure-rotation spectra of H_2O and D_2O have been resolved and

studied in this detailed way.* Practically all observed lines (160 out of 173) were accounted for by going up to $J = 14$ in the case of H_2O , and by applying the selection principle of (194) appropriate to the molecule's structure in which, as we know, the permanent electric moment is along the middle axis B .

The method of identifying the lines was based upon Mecke's approximate determination of the moments of inertia from a study of the vibration-rotation bands of H_2O . These were then used to calculate the expected positions of pure rotation band lines. A knowledge also

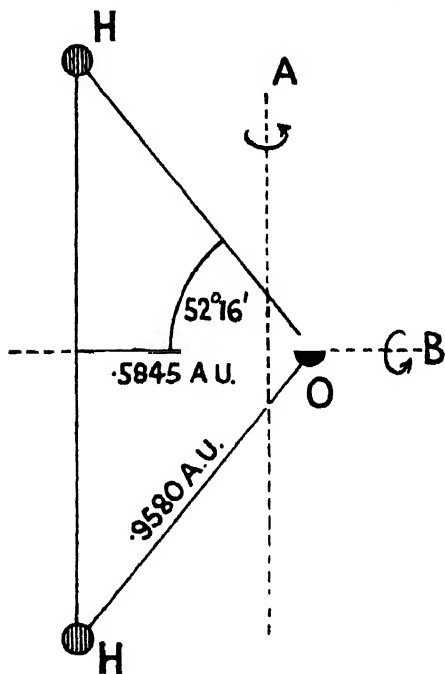


Fig 128.

of approximate intensity variations assisted in the identification of individual lines. The actual differences of observed position from those calculated were found to increase substantially with J , a result of the centrifugal distortion of the molecule. It was calculated that whereas in rotationless equilibrium the OH distance is 0.9558 A.U. and the bond-angle $104^\circ 36'$, for $J = 11$, the OH distance becomes 0.9640 A.U. and the angle $98^\circ 52'$.

It was also found that the highest r states of each J group correspond fairly well to simple spinning of the molecule about the axis of least moment of inertia A (see Fig. 128). For the lower r states of each J group the motion approximates more to a spin about the axis of greatest moment of inertia C .

A study of the moments of inertia based upon vibration-rotation band data showed a definite discrepancy in the expected equality $C = A + B$ which should hold for a plane molecule. The discrepancy was found to be a linear function of the vibrational quantum numbers :

$$C - (A + B) = [0.1644(v_2 + \frac{1}{2}) - 0.0122(v_3 + \frac{1}{2})]10^{-40} \text{ gm.-cm.}^2$$

with a negligible coefficient of $(v_1 + \frac{1}{2})$. The reason for this is the dependence of moment of inertia on vibration, so that actually

$$\left. \begin{aligned} A_v &= A_0[1 + \Sigma a_i(v_i + \frac{1}{2})], \\ B_v &= B_0[1 + \Sigma b_i(v_i + \frac{1}{2})], \\ C_v &= C_0[1 + \Sigma c_i(v_i + \frac{1}{2})], \end{aligned} \right\} \dots (195)$$

* Randall, Dennison, Ginsberg, and Weber, *Phys. Rev.*, vol. 52, p. 161 (1937); also *Phys. Rev.*, vol. 56, p. 982 (1939).

where i takes the values 1, 2, 3, corresponding to the three fundamental modes of vibration.

It is instructive to observe from Fig. 129 (after Dennison) the effect on the rotational energy levels of a change from a symmetrical oblate type of rotator through asymmetry to a symmetrical prolate type. The energy levels of a symmetrical rotator are by (201)

$$W = \frac{h^2}{8\pi^2 A} J(J+1) + \frac{h^2}{8\pi^2} \left(\frac{1}{C} - \frac{1}{A} \right) k^2,$$

where C is in this expression the moment of inertia about the axis of symmetry. Putting $C = 2$, $A = 1$, we have the levels $k = 0$ to 3 on the left-hand side of Fig. 129. For the levels on the right-hand

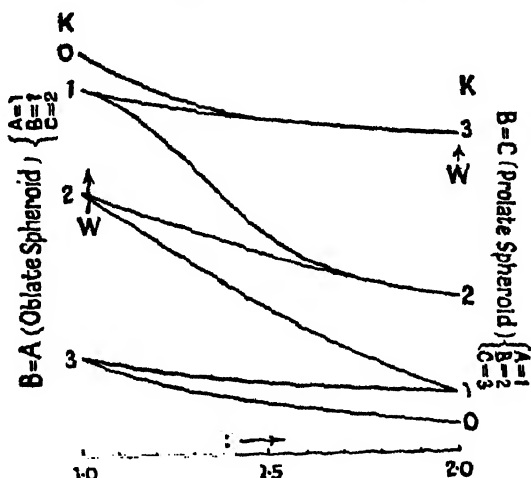


Fig. 129. Energy level diagram to show the effect of transition from an oblate to a prolate symmetrical rotator. (After Dennison.) $A = 1$, $C = 2$, and B changes from 1 to 2.

side, where $A = 1$, $B = 2$, $C = 1$, since the A -axis is now that of symmetry, the above energy expression becomes

$$W = \frac{h^2}{8\pi^2 C} J(J+1) + \frac{h^2}{8\pi^2} \left(\frac{1}{A} - \frac{1}{C} \right) k^2.$$

The levels in between have been evaluated by Dennison by the laborious calculation of x_i values (in 193). The association of the various energy levels in Fig. 129 by curves may be made on the assumption that they do not intersect.

In the parallel type vibration-rotation bands of H_2O the oscillating electric moment is along the B -axis; in the perpendicular type of band it will be along the A -axis (see Fig. 128). Different selection principles obtain in these two cases (see (194)). Dennison* has mapped the expected rotational structure of these two types of band for a given value of $C = A + B$, and for a series of values of the

* *Rev. Mod. Phys.*, vol. 3, p. 289 (1931).

ratio A/B . His diagrams show that where the oscillation of electric moment is along the least axis, the change from symmetry $A = B$ to increasing asymmetry $A = \frac{B}{10}$ results in increasing accumulation of band lines near the origin. In contrast, where oscillation of the electric moment is along the middle axis, increasing asymmetry results in a dispersal of lines away from the band origin.

(d) ENVELOPES OF INFRA-RED ABSORPTION BANDS

Unless far more powerful instruments than are at present available can be devised, the fine structure of the bands of heavy molecules will remain largely unresolved. Much information, however, is possible from the shape of the contours or envelopes of the bands of sym-

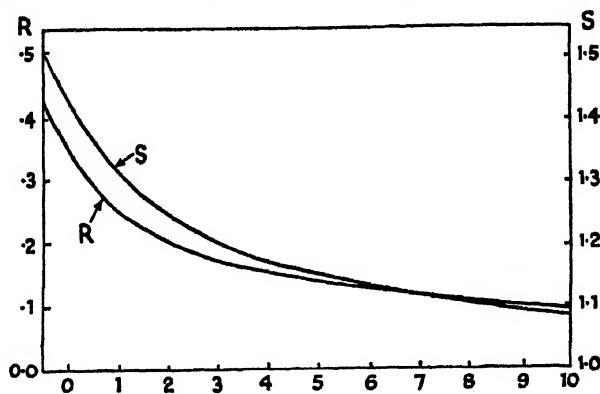


Fig. 130. Variation of R and of S with β . (After Gerhard and Dennison.)

metrical rotators, as Gerhard and Dennison * have shown. It is not possible to reproduce here the mathematics involved, but the results may be given.

In the case of parallel bands of symmetric rotators they obtained expressions for the ratio R of the intensity of the Q branch to that of the whole band. These ratios are :

$$\frac{\log [\beta^{\frac{1}{2}} + (1 + \beta)^{\frac{1}{2}}] - [\beta/1 + \beta]^{\frac{1}{2}}}{\beta[\beta/1 + \beta]^{\frac{1}{2}}} \quad \text{for } \beta > 0; \quad \frac{1}{2} \text{ for } \beta = 0;$$

and

$$\frac{[-\beta/1 + \beta]^{\frac{1}{2}} - \sin^{-1}(-\beta)^{\frac{1}{2}}}{-\beta[-\beta/1 + \beta]^{\frac{1}{2}}} \quad \text{for } \beta < 0;$$

where $\beta = \left(\frac{A}{C} - 1\right)$. It has a value $-\frac{1}{2}$ for a disk-shaped molecule, 0 for a spherical molecule, and $+\infty$ for a linear molecule.

The values of R as a function of β are shown in Fig. 130. For a parallel band, as we know, as $\beta \rightarrow +\infty$, $R \rightarrow 0$. We see, then, that if R is determinable from experiment, β can be determined from Fig. 130.

* *Phys. Rev.*, vol. 43, p. 197 (1932).

The interval $\Delta\nu$ between the maxima of the P and R branches of parallel bands was also found to be

$$\Delta\nu = \frac{S(\beta)}{\pi c} \sqrt{\frac{KT}{A}} \quad \dots \quad (196)$$

which may be compared with (188). Here $S(\beta)$ may be termed the separation function, and it has been shown as a function of β in Fig. 130. It varies from about 1.5 for $\beta = -\frac{1}{2}$ to $\sqrt{2}$ for $\beta = 0$, and approaches 1 for a linear molecule. Empirically Gerhard and Dennison find it can be approximately given from $\beta = -\frac{1}{2}$ to $+100$ by

$$\log_{10} S = \frac{0.721}{(\beta + 4)^{1.13}} \quad (197)$$

Hence, if β is already known, S can be found, and thus if $\Delta\nu$ is also determined by experiment, A may be calculated from (196).

If, on the other hand, A is known, $\Delta\nu$ allows S to be found, and hence β from (197), and thus C the other moment of inertia.

In the case of perpendicular-type bands a similar investigation gave the absorption coefficient through the band envelope. This is plotted

in Fig. 131 against $x = \frac{\nu}{\alpha} \sigma^{\frac{1}{2}}$, where

$$\alpha = \frac{h}{4\pi^2 A} \quad \text{and} \quad \sigma = \frac{h^2}{8\pi^2 A K T}$$

The dotted line gives the absorption due to the Q branches alone of all the various subsidiary bands. (These were represented in Fig. 124 as a group of black lines.) The total absorption due to the whole of the perpendicular band is represented by the full line of Fig. 131. The two vertical lines show the doublet separation of a parallel band with the same values of β . For $\beta = 0$, which means a 'spherical' molecule, the parallel and perpendicular band envelopes would be identical. Some conception of the order of β should therefore be possible by an inspection of a band contour. Unfortunately the reliability of inferences of this sort from perpendicular-band contours is vitiated by the effect of the

internal angular momentum $\frac{3h}{2\pi}$ mentioned previously.

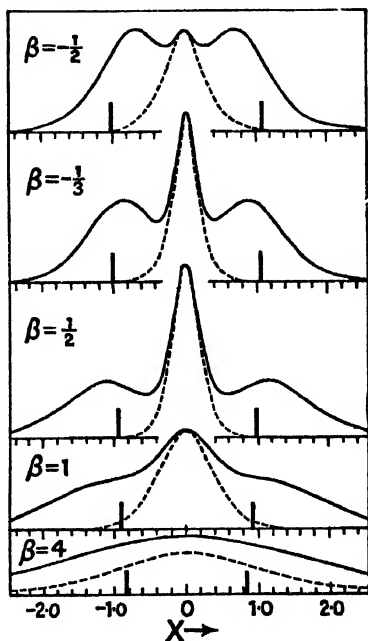


Fig. 131. Envelopes of perpendicular-type bands of a symmetric rotator, for various values of β . (After Gerhard and Dennison.)

(e) ISOTOPIC EFFECTS

In Chapter XI we have considered the effect of isotopy in detail in the case of diatomic molecules. The effect in polyatomic molecules has a variety of aspects, and these will be mentioned very briefly.

It is assumed that the forces between the atoms and the distances between them are unaffected when an atom is replaced by its isotope. The whole system of vibration-rotation bands will therefore occur in different positions. In addition to this, however, the introduction of a deuterium atom in place of a hydrogen atom will remove the degeneracy which arises in symmetrical molecules such as NH_3 and CH_4 . Thus in Fig. 115 the ν_2 and ν_4 vibrations should each be replaced by two vibrations in the molecules NDH_2 or NHD_2 . Similarly in methane, as we have pointed out, the four degenerate vibrations are replaced by six in CH_3D and CDH_3 (which are of the type of Fig. 117). In CH_2D_2 the complete number of nine fundamental frequencies probably occurs.

The most generally used application of this information from isotopic molecules is to calculate constants of the potential function of a

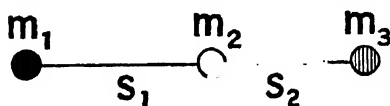


Fig. 132.

molecule. Consider a linear molecule as in Fig. 132. If q measures the relative displacement of the two outer atoms, z the axial displacement of the middle atom relative to the centre of gravity of the two outer atoms, and r the

displacement of the middle atom perpendicular to the axis, the simplest potential function, assuming simple harmonic vibrations, is

$$V = \frac{1}{2}[k_{11}q^2 + 2k_{13}qz + k_{33}z^2 + k_{22}r^2].$$

We know that such molecules as Fig. 132 depicts have three fundamental frequencies, and these data are therefore insufficient to determine the four constants.

Adel* has shown that for this molecule the following relationships hold:

$$\lambda_1 + \lambda_3 = \frac{k_{11}}{\mu_q} + \frac{k_{33}}{\mu_z}, \quad \lambda_1\lambda_3 = \frac{k_{11}k_{33}}{\mu_q\mu_z} - \frac{k_{13}}{\mu_q\mu_z}, \quad \lambda_2 = \frac{k_{22}}{\mu_r},$$

$$I_0 = m_1s_1^2 + m_3s_2^2 - \frac{m_1^2s_1^2 + m_3^2s_2^2 + 2m_1m_3s_1s_2}{m_1 + m_2 + m_3},$$

where $\lambda = 4\pi^2\omega^2$, ω_1 , ω_2 , and ω_3 being the fundamental vibration frequencies,

$$\mu_q = \frac{m_1m_3}{m_1 + m_3}, \quad \mu_z = \frac{m_2(m_1 + m_3)}{m_1 + m_2 + m_3},$$

$$\mu_r = \mu_z \left[\frac{1}{m_1} \left(\frac{s_2}{s_1 + s_2} \right)^2 + \frac{1}{m_3} \left(\frac{s_1}{s_1 + s_2} \right)^2 + \frac{1}{m_2} \right].$$

Suppose we had the values of I_0 for two isotopic molecules, we could find s_1 and s_2 . We can then calculate μ_r and then k_{22} . To calculate k_{11} , k_{13} , and k_{33} we now need ω_1 and ω_3 of one molecule and either ω_1 or ω_3 of its isotope.

Similarly if we consider a bent molecule subtending an angle α at m_3 , instead of being collinear, as in Fig. 132, we might use a potential function such as

$$V = \frac{1}{2}[K_1(\Delta s_1)^2 + K_2(\Delta s_2)^2 + k(s\Delta\alpha)^2],$$

* *Phys. Rev.*, vol. 46, p. 222 (1934).

where s is some length and α the apex angle. The relations which follow have been shown to hold :

$$\begin{aligned}\omega_1^2 + \omega_2^2 + \omega_3^2 &= \frac{K_1}{\mu_1} + \frac{K_2}{\mu_2} + \frac{k}{\mu_4}, \\ \omega_1^2 \omega_2^2 + \omega_2^2 \omega_3^2 + \omega_1^2 \omega_3^2 &= \frac{K_1 K_2}{\mu_1 \mu_2} \left(1 - \frac{\mu_1 \mu_2 \cos^2 \alpha}{m_2^2} \right) \\ &\quad + \frac{k}{\mu_4} \left(\frac{K_1}{\mu_1} + \frac{K_2}{\mu_2} \right) - \frac{k s^2 \sin^2 \alpha}{m_2^2} \left(\frac{K_1}{s_2^2} + \frac{K_2}{s_1^2} \right), \\ \omega_1^2 \omega_2^2 \omega_3^2 &= \frac{K_1 K_2 k}{\mu_1 \mu_2 \mu_4} \left(1 - \frac{\mu_1 \mu_2}{m_2^2} \right),\end{aligned}$$

where

$$\frac{1}{\mu_1} = \frac{1}{m_1} + \frac{1}{m_2}, \quad \frac{1}{\mu_2} = \frac{1}{m_2} + \frac{1}{m_3} \quad \text{and} \quad \frac{1}{\mu_4} = s^2 \left(\frac{1}{\mu_1 s_1^2} + \frac{1}{\mu_2 s_2^2} - \frac{2 \cos \alpha}{m_2 s_1 s_2} \right).$$

Thus if s_1 , s_2 , and α are known from fine structure data, there remain three constants, K_1 , K_2 , and ks^2 , to be found.

In the special case of a symmetrical molecule $K_1 = K_2$, $m_1 = m_3 = m$, say, $m_2 = M$ and $r_1 = r_2 = s$ these relationships are :

$$\begin{aligned}\omega_3^2 &= K_1 \left(\frac{1}{\mu} - \frac{\cos \alpha}{M} \right), \\ \omega_3^2 (M + 2m) K_a &= m^2 M \omega_1^2 \omega_2^2 \left(\frac{1}{\mu} - \frac{\cos \alpha}{M} \right), \\ \omega_1^2 + \omega_2^2 &= K_1 \left(\frac{1}{\mu} + \frac{\cos \alpha}{M} \right) + \frac{K_a}{s^2} \left(\frac{1}{\mu} - \frac{\cos \alpha}{M} \right),\end{aligned}$$

where $K_a = 2ks^2$ and $\frac{1}{\mu} = \frac{1}{M} + \frac{1}{m}$.

Salant and Rosenthal* have obtained some simple relationships in the case of YX_2 molecules. If the Y atom of mass M is replaced by $M + \Delta M$ they deduce

$$\left. \begin{aligned}\frac{\Delta \omega_1}{\omega_1} + \frac{\Delta \omega_3}{\omega_3} &= - \frac{m \Delta M}{(M + \Delta M)(2m + M)}, \\ \frac{\Delta \omega_2}{\omega_2} &= - \frac{m \Delta M}{M(M + \Delta M) \left(\frac{1}{\mu} + \cot^2 \alpha \right)},\end{aligned} \right\} \quad \dots \quad (198)$$

where in this case $\mu = \frac{M}{M + 2m}$ and 2α is the apex angle. These relationships (and the ones below) are, however, true only if ΔM is small compared to M , so that they would not apply to hydrogen : deuterium. The interesting feature of these expressions is their independence of the force constants of the molecule (which will be different in different electronic states). The sum of the effects $\frac{\Delta \omega_1}{\omega_1}$, and $\frac{\Delta \omega_3}{\omega_3}$

* *Phys. Rev.*, vol. 42, p. 812 (1932).

or the two parallel bands is seen to be a constant. The effect $\Delta\omega_2/\omega_2$ could be used to evaluate the molecular angle α . For a collinear molecule the relations (198) become, since $\alpha = 180^\circ$,

$$\left. \begin{aligned} \Delta\omega_1 &= 0, \\ \frac{\Delta\omega_2}{\omega_2} &= \frac{\Delta\omega_3}{\omega_3} = - \frac{m\Delta M}{(M + \Delta M)(2m + M)} \end{aligned} \right\} . \quad (199)$$

which would provide a test of the linearity of a molecule. In band spectra involving electronic transitions the angle α may change. It is therefore of some interest to observe what the effect of change of angle will be on the isotope effect. For a collinear molecule, the inactive frequency shows no isotope effect, while the two active frequencies show, for ΔM positive, equal displacements to the low-frequency side. From (198) we observe that as α diminishes, the effect $\frac{\Delta\omega_2}{\omega_2}$ in the perpendicular bands diminishes, approaching zero as

the two X atoms get close together. The value of $\frac{\Delta\omega_1}{\omega_1}$ increases, and in the opposite sense to $\frac{\Delta\omega_3}{\omega_3}$, but which increases and which decreases cannot be predicted without information about the force constants of the molecule.

The variation of $\frac{\Delta\omega_2}{\omega_2}$ with angle has been calculated from (198) for a few molecules.

	m	M	ΔM	$2\alpha = 180^\circ$	150°	120°	90°	60°
ClO_2	16	35	2	-0.01293	-0.01245	-0.0101	-0.00849	-0.00502
MgI_2	127	24	1	-0.0182	-0.0181	-0.0177	-0.0168	-0.0143
H_2S	1	32	1	-0.00089	-0.00089	-0.00083	-0.00068	-0.00023

A heavy end-atom such as iodine results in a much smaller degree of angular change.

If one of the X atoms of mass m is replaced by $m + \Delta m$ this is called by Salant and Rosenthal an 'end' isotope effect, as distinct from the previous 'central' one. In this case they obtain

$$\left. \begin{aligned} \frac{\Delta\omega_1}{\omega_1} + \frac{\Delta\omega_3}{\omega_3} &= - \frac{(\mu + 1)\Delta m}{2(2m + \Delta m)}, \\ \frac{\Delta\omega_2}{\omega_2} &= - \frac{(1 + \cot^2 \alpha)\Delta m}{2\left(\frac{1}{\mu} + \cot^2 \alpha\right)(2m + \Delta m)}, \end{aligned} \right\} . \quad (200)$$

or for a collinear molecule ($\alpha = 90^\circ$)

$$\mu \frac{\Delta\omega_1}{\omega_1} = \frac{\Delta\omega_2}{\omega_2} = \frac{\Delta\omega_3}{\omega_3} = - \frac{\mu\Delta m}{2(2m + \Delta m)} \quad . \quad (201)$$

The calculation values for a few molecules of $\Delta\omega_2/\omega_2$ are given :

	M	m	Δm	$2\alpha = 180^\circ$	120°	90°	60°	0°
CS_2	12	32	1	-0.00121	-0.00154	-0.00210	-0.00340	-0.00769
MgCl_2	24	35	2	-0.00354	-0.00436	-0.00565	-0.00802	-0.0140
HgCl_2	200	35	2	-0.0101	-0.0108	-0.0117	-0.0127	-0.0140

showing that, in contrast with the central isotope effect, the end isotope effect increases as angle diminishes. The effects where *both* X atoms are replaced by their isotopes would be approximately twice the effects where one only is replaced.

Salant and Rosenthal have investigated similarly the YX_3 type, of which we may take Cl^{35}O_3 and Cl^{37}O_3 or B^{10}I_3 and B^{11}I_3 as examples of the central isotope effect, or PCl_3^{35} and PCl_3^{37} as an example of the end effect. References should be made to their paper for these data.

(f) ELECTRONIC BANDS OF TRIATOMIC MOLECULES

Let us consider a bent triatomic molecule of the type YX_3 shown in Fig. 133, where $I_a < I_b < I_c$. Such a molecule will necessarily be an asymmetrical rotator with three unequal moments of inertia :

$$I_a = \frac{2Mm}{M+2m} r^2 \cos^2 \alpha; \quad I_b = 2mr^2 \sin^2 \alpha; \quad I_c = I_a + I_b. \quad (202)$$

There is, however, a particular angle for which $I_a = I_b = \frac{1}{2}I_c$, viz. α_0 , where

$$\tan \alpha_0 = \sqrt{\frac{M}{M+2m}} \quad \dots \quad (203)$$

If this relation is satisfied we clearly have an oblate symmetrical top. For angles close to this value we may expect to find band structure closely related to that of the symmetrical top. (For SO_2 we may calculate $2\alpha_0 = 70^\circ 32'$; for H_2O , $2\alpha_0 = 86^\circ 37'$.) On the other hand, for angles far removed from this angle we should have what may be described as a near-prolate type of symmetrical top. In Fig. 133 if α was quite acute, I_b would be small, and hence $I_a \approx I_c$: this would be a near-prolate symmetrical top with the I_b -axis as that of symmetry. On the other hand, if α became much larger than the critical value α_0 , I_a would be small, and this axis would be that of near-symmetry of the prolate top, while $I_b \approx I_c$. This latter case $\alpha \gg \alpha_0$, which may be described as the obtuse near-prolate case, is probably much commoner than the acute near-prolate case. As an example of the former, take SO_2 with $2\alpha = 120^\circ$, $I_a = 13.9$, $I_b = 83.2$, $I_c = 97.1$, all in $\text{gm.-cm.}^2 \times 10^{40}$.

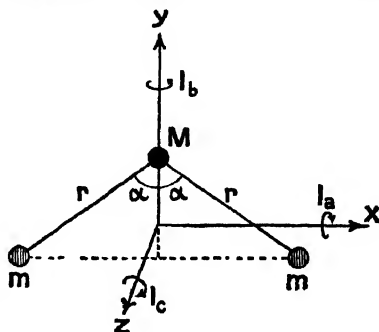


Fig. 133.

The possibility of carrying out fine-structure analysis of many asymmetrical top molecules, as reasonably close approximations to oblate or prolate symmetrical tops, is a great simplification of procedure. In the oblate top the symmetry axis of the molecule will be that of greatest moment of inertia, in the prolate top it will be that of least moment of inertia. In the acute near-prolate molecule parallel bands will therefore have the electric moment oscillating along the I_b -axis, in the obtuse near-prolate case along the I_a -axis, and in the near-oblate case along the I_c -axis.

The main question for us to consider is that of the characteristics of band structure where an electronic change has taken place. Let us write the expression for the rotational energy of a symmetrical top (189) as

$$F = BJ(J + 1) + Hk^2 \quad . \quad . \quad . \quad (204)$$

The characteristic of electronic change is that the moments of inertia will be appreciably different in the initial and final states. Thus we shall have values B' and H' in the initial state and B'' and H'' in the final state. The parallel bands corresponding to $\Delta k = 0$ will no longer have the simple form of (187), and the perpendicular bands given by $\Delta k = \pm 1$ will no longer have the form of (192).

Parallel bands would be given by

$$\nu = \nu_0 + \left\{ (B' + B'')m + (B' - B'')m^2 \text{ (R and P),} \right. \\ \left. + (H' - H'')k^2 + \left\{ (B' - B'')J + (B' - B'')J^2 \text{ (Q),} \right\} \right\} \quad (205)$$

where we put $m = J + 1$ for the R branch and $m = -J$ for the P branch. $R(J)$ means a transition $J + 1 \rightarrow J$ and $P(J)$ means $J - 1 \rightarrow J$, as usual.

The perpendicular bands would be given by

$$\nu = \nu_0 + H' \pm 2H'k + \left\{ (B' + B'')m + (B' - B'')m^2, \right\} \\ + (H' - H'')k^2 + \left\{ (B' - B'')J + (B' - B'')J^2, \right\} \quad (206)$$

where the above remarks also apply.

An electronic parallel band will therefore appear to consist of a number of sub-bands whose origins, corresponding to $k = 0, 1, 2, 3$, &c., are disposed in the manner of Q -branch lines. Each of these has ordinary P , Q , and R branches.

An electronic perpendicular band will consist of sub-bands disposed about the origin in the manner of P - and R -branch structure, while each sub-band has P , Q , and R branches. The sub-bands may be appropriately labelled $q(0)$, $q(1)$, $q(2)$, &c., in the parallel type or $r(0)$, $r(1)$, $p(1)$, $p(2)$, &c., in the perpendicular case, as in Fig. 134. The λ 2491 band of NO_2 and the λ 3879 band of SO_2 are cited by Mulliken* as typical examples of these types, and photographs are reproduced in the paper mentioned. N. Metropolis† has also plotted carefully diagrams of band structures corresponding to (205) and (206) in the near-prolate case. It should be remarked that sub-bands will in general have a considerable number of missing lines near their origins. Thus, since $J \geq k$, in an $r(6)$ sub-band for which $k' = 7$

* *Rev. Mod. Phys.*, vol. 14, p. 204 (1942).

† *Phys. Rev.*, vol. 60, p. 283 (1941).

and $k'' = 6$ the first branch lines would be $R(6)$, $Q(7)$, and $P(8)$. In a $p(6)$ sub-band for which $k' = 5$ and $k'' = 6$ the first lines would be $R(6)$, $Q(6)$, and $P(6)$. In a $q(6)$ sub-band for which $k' = 6$, $k'' = 6$, the first lines would be $R(6)$, $Q(6)$, $P(7)$.

In electronic bands it is also apparent that the J -structure and the

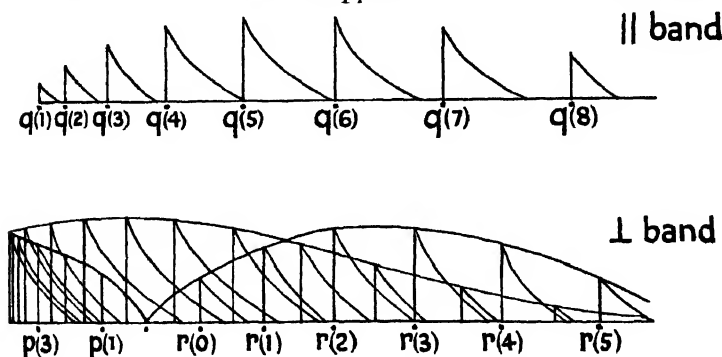


Fig. 134. Structure of electronic bands

k -structure may both degrade the same way or in opposite senses, giving four possible cases. The significance of these features must now be considered. Just as the direction of degradation of bands of diatomic molecules informed us of the relative sizes of r_e' and r_e'' , we should be able to correlate the degradation of J - and k -structures with the relative changes in r and α which may occur in the electronic transition.

Near-Prolate Type of Molecule

In the obtuse near-prolate type the constants B and H of (204) will be

$$B = \frac{h}{8\pi^2} \frac{1}{2} \left[\frac{1}{I_b} + \frac{1}{I_c} \right], \quad H = \frac{h}{8\pi^2} \left[\frac{1}{I_a} - \frac{1}{2} \left(\frac{1}{I_b} + \frac{1}{I_c} \right) \right] \quad (207)$$

For the rarer acute-angled near-prolate case I_a and I_b would be interchanged. From (202) we know the values of B and H as functions of r and α . In Fig. 135 we follow Metropolis in showing B and H as functions of α . The full lines show these functions for a definite bond-distance $r_2 = 1.43$ A.U. which is appropriate to the normal state of the SO_2 molecule, and the broken lines are for a smaller bond-distance 0.85×1.43 A.U.

Fig. 135 will repay close study. It is easy to deduce from it that the following changes in α and r affect the band structure as indicated.

Change in α and r	B	H	J -structure degrades to	k -structure degrades to
$\alpha' > \alpha''$ $r' = r''$	$B' < B''$	$H' > H''$	Red	Violet
$\alpha' < \alpha''$ $r' = r''$	$B' > B''$	$H' < H''$	Violet	Red
$\alpha' = \alpha''$ $r' > r''$	$B' < B''$	$H' < H''$	Red	Red
$\alpha' = \alpha''$ $r' < r''$	$B' > B''$	$H' > H''$	Violet	Violet

As is customary, we keep the single accent for the higher and the double accent for the lower electronic state. Metropolis points out that the acute-angled near-prolate case would give curves which are deducible from Fig. 135 by reflexion in the line $\alpha = 45^\circ$, so that the above predictions would only need to be modified in this case by reversing the inequality signs between α' and α'' on the first two lines of the table.

It would, of course, be a special case in which *only* the angle or

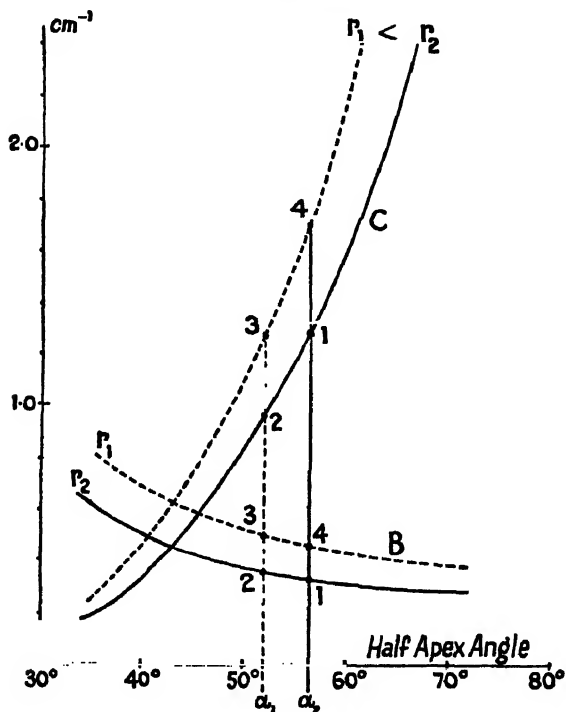


Fig. 135. Graphs showing B and H of (207) as functions of α , the semi-angle at the apex. The full line is for $r_2 = 1.43$ A.U. The dotted line is for $r_1 = 0.85 r_2$. The data are for SO_2 . (After Metropolis.)

only the bond-distance changed in an electronic transition. We must therefore deduce from Fig. 135 what is likely to happen when both of these change. We obviously have four possible combinations to consider. Writing $\Delta\alpha = \alpha' - \alpha''$ and $\Delta r = r' - r''$, these are $\Delta\alpha (+)$, $\Delta r (-)$; $\Delta\alpha (-)$, $\Delta r (-)$; $\Delta\alpha (+)$, $\Delta r (-)$; $\Delta\alpha (-)$, $\Delta r (+)$. Let us take one of these by way of example—say, $\Delta\alpha (-)$, $\Delta r (-)$. Let $\alpha'' = \alpha_2$, corresponding to the point 1 in Fig. 135. In passing to the point 2, $\alpha' = \alpha_1$, clearly $B' > B''$ and $H' < H''$. If now we move from point 2 to point 3 corresponding to $r' < r''$, it is clear that B' is still $> B''$, but whether H' will then be greater or less than H'' will depend on the magnitudes of the two changes in r and α and the slopes of the curves. Similarly we see that there are, for each of

the four pairs $\Delta\alpha$, Δr , two possible alternatives which are set out in the table. We have used the sign (+) to indicate degradation to the

DIRECTIONS OF SHADING OF *k*- AND *J*-STRUCTURES CORRESPONDING TO VARIOUS CHANGES IN $\Delta\alpha$, Δr

$\Delta\alpha = r' - r''$	$\Delta r = r' - r''$	<i>k</i> -structure	<i>J</i> -structure
+	+	{ + —	— —
—	—	{ + —	+ +
+	—	{ + +	— +
—	+	{ — —	+ —

high-frequency side ($B' > B''$) or ($H' > H''$) and the sign (—) to indicate the reverse.

In the table which follows the data are rearranged to show that for each of the four possible combinations of band-shading there are two alternatives as regards $\Delta\alpha$ and Δr .

	Shading		Molecular changes	
	<i>k</i>	<i>J</i>	$\Delta\alpha$	Δr
I	+	—	{ + +	+ —
II	—	+	{ — —	— +
III	—	—	{ + —	+ +
IV	+	+	{ — +	— —

Are there any criteria for distinguishing between the two alternatives in each case? Thus, for example, in Case I, if *k*-structure shades away to the high-frequency side and the *J*-structure to the low-frequency side, it is clear that $\alpha' > \alpha''$, but it is not clear whether $r' > r''$ or $r' < r''$. Let us look at this particular case in the light of Fig. 135. Start at point 3 corresponding to $\alpha' = \alpha_1$, and move to point 4 corresponding to $\alpha' = \alpha_2$. This increase in α alone (i.e. $\Delta\alpha$ (+)) means that $B' < B''$, and therefore *J*-structure, degrades (—), while $H' > H''$, and therefore *k*-structure, degrades (+). If from point 4 we move towards point 1, corresponding to Δr (+), this will reduce the quantity $H' - H''$ and increase the quantity $B'' - B'$, which is probably not going to be of significance as a criterion. If, however, from point 4 we move away from point 1, i.e. Δr (—), this will increase the quantity $H' - H''$ and probably reduce $B'' - B'$ to a very small quantity. As we recall by reference to Chapter II, equations (25) and (26), a very small value of $B' - B''$ would imply a very slow

convergence of J -structure to form a head, indeed, the possibility of headless bands.

In Case I we may therefore regard a very slow convergence of the J -structure with well-marked convergence of the k -structure as favouring Δr (-). Similarly in Case II very slow convergence of the J -structure would favour Δr (+).

In Cases III and IV there are precise criteria for picking the correct alternative. The doubt exists as to whether $\Delta\alpha$ is positive or negative. It can be easily shown that if the J -structure converges more rapidly to a head than the k -structure, then $\alpha' > \alpha''$, and vice versa. This may be determinable by inspection or, alternatively, it may be inferred if the numerical value of $\frac{B'}{B''} = \frac{B''}{B''}$ is less than that of $\frac{H' + H''}{H' - H''}$. In this case $\frac{H' + B'}{B'} > \frac{H'' + B''}{B''}$.

From (207) we have $\frac{1}{I_a'} / \left(\frac{1}{I_b'} + \frac{1}{I_c'} \right) > \frac{1}{I_a''} / \left(\frac{1}{I_b''} + \frac{1}{I_c''} \right)$.

Approximately since $I_c \approx I_b$, $\left(\frac{I_b}{I_a} \right)' > \left(\frac{I_b}{I_a} \right)''$,

which gives by (202) $\tan^2 \alpha' > \tan^2 \alpha''$, or $\alpha' > \alpha''$.

We see, then, from the above table that while changes in both α and r will in general occur, the principal change is likely to be one of angle if the k - and J -structure shade in opposite senses, while the change is likely to be chiefly in r if the structures shade in the same sense.

Since v_1 and v_3 of Fig. 108 are chiefly involved in changes of r , and v_2 in changes of α , we should expect to find that in absorption from the ground state we had strong v_1' - and v_3' -progressions in the first case, and v_2' -progressions in the second case. The general principles of the Franck-Condon theory (Chapter III, Section (a)) are presumably applicable to triatomic molecules. Very little change in r would be expected to yield only a strong (0,0) band of the ($v_1' \leftarrow v_1''$) and ($v_3' \leftarrow v_3''$) transitions; very little change in α would give only the (0,0) band of ($v_2' \leftarrow v_2''$). Big changes would favour long progressions, also possibly molecular dissociation.

Reference may be made by way of illustration to the paper by Metropolis * dealing with one of the absorption systems of SO_2 in the ultra-violet. The bands are fitted to a formula

$$\nu = 29622 + 770v_1' + 320v_2' + 813v_3' - 6v_1'^2 - 2.5v_2'^2 - 20v_1'v_2' - 25v_2'v_3' - 15v_1'v_3',$$

where v_1' , v_2' , and v_3' are the symmetrical, the deformation, and the anti-symmetrical vibration quantum numbers of the excited state. The bands were found to fit into a series of progressions from the ground level (0,0,0) to (0, v_2' ,0), (1, v_2' ,0), (2, v_2' ,0), (3, v_2' ,0), (4, v_2' ,0), and (5, v_2' ,0), where v_2' ranged from 0 to 8, together with a few v_2' -progressions to (0, v_2' ,1), (0, v_2' ,2), (1, v_2' ,2), and (0, v_2' ,4). The three fundamental frequencies determined from Raman and infra-red data for the ground electronic state are $\nu_1'' = 1152 \text{ cm.}^{-1}$, $\nu_2'' = 525 \text{ cm.}^{-1}$, and $\nu_3'' = 1361 \text{ cm.}^{-1}$.

* *Phys. Rev.*, vol. 60, p. 295 (1941).

Near-Oblate Type of Molecule

In the near-oblate type of molecule where $I_a \approx I_b = \frac{1}{2}I_c$, the constants B and H of (204) will be given by

$$B = \frac{h}{8\pi^2} \frac{1}{2} \left[\frac{1}{I_a} + \frac{1}{I_b} \right], \quad H = \frac{h}{8\pi^2} \left[\frac{1}{I_c} - \frac{1}{2} \left(\frac{1}{I_a} + \frac{1}{I_b} \right) \right] \quad (208)$$

where H will now be a negative quantity.

From (202) we know I_a , I_b , and I_c as functions of α . In Fig. 136 we have constructed B and $-H$ as functions of α . Analogous to Fig. 135 we have used also $r_2 = 1.43$ A.U. for the full curves and $r_1 = 0.85 r_2$ for the broken lines. The specific values are of no importance: we are concerned merely to understand the general characteristics associated with change in r and α . We observe that B has a characteristic minimum and H (since it is negative) a maximum at about 40° . The angle at which this occurs is easily demonstrated as given by $\tan \alpha = \left(\frac{M}{M + 2m} \right)^{\frac{1}{2}}$. It is not the angle α_0 of (203), which is about $35^\circ 16'$ and is marked in Fig. 136 as the line of the strictly symmetrical top. The angle corresponding to B_{\min} is necessarily greater than α_0 .

It is perhaps desirable to point out that the *strictly* oblate symmetrical top in the case of a *triatomic* molecule would have neither pure-rotation bands nor vibration-rotation bands, since no electric moment or oscillation thereof can take place along the I_c -axis (see Fig. 133). In the case of more complex molecules for which vibrations may take place perpendicular to the xy -plane, the general analysis is valid. Consider, for example, the CO_3' ion or NO_3' ion or a shallow pyramidal YX_3 molecule. In this particular case we have $\alpha_0 = 30^\circ$, since $M = m$, and we may consider vibrations of this type of molecule as practical examples of the conclusions given below.

For near-oblate molecules we may deduce the following effects on band structure of changes in α and r .

Change in α and r	B	H	J -structure degrades to	k -structure degrades to
$\alpha' > \alpha''$ $r' = r''$	$B' < B''$	$H' > H''$	—	+
$\alpha' < \alpha''$ $r' = r''$	$B' > B''$	$H' < H''$	+	—
$\alpha' = \alpha''$ $r' > r''$	$B' < B''$	$H' > H''$	—	+
$\alpha' = \alpha''$ $r' < r''$	$B' > B''$	$H' < H''$	+	—

(+ means high frequency and — means low frequency.)

Because of the proximity of the minimum of B (and maximum of H) a few degrees above α_0 there is obviously the possibility of a substantial change in α reversing the effects in the above table, or producing non-converging structure. We will assume, however, that the effects are appropriate to a region around or near to the angle of the true oblate top.

It will be observed that as a consequence of the similarity of the B and $-H$ curves in Fig. 136 we expect no cases where the k -structure and J -structure degrade in the same direction. For each of the two

SHADING OF J - AND k -STRUCTURE FOR VARIOUS CHANGES IN $\Delta\alpha$ AND Δr

$\Delta\alpha = \alpha' - \alpha''$	$\Delta r = r' - r''$	k -structure	J -structure
+	+	+	-
-	-	-	+
+	-	{	{
-	+	{	{

cases ($k+$, $J-$) and ($k-$, $J+$) there are three possible combinations of ($\Delta\alpha$, Δr). If the J structure converges more rapidly than the k -structure it can be shown that $\alpha' < \alpha''$ or $\Delta\alpha$ must be negative. A unique determination on this basis is clearly not always possible.

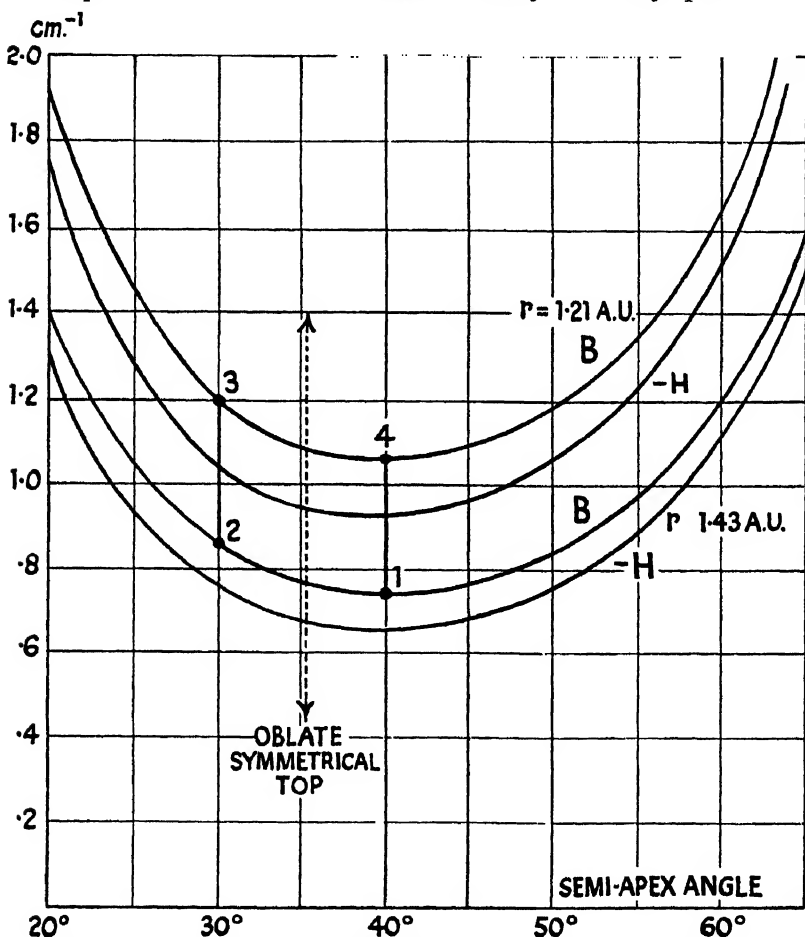


Fig. 136. R and $-H$ of (208) as functions of α , the semi-apex angle.

(g) ELECTRONIC STRUCTURES OF MOLECULES

A discussion of this is beyond the scope of the present book. Just as in Chapter VI we outlined the principles of orbital classification for diatomic molecules, we are faced with the vastly more complex task of classification in polyatomic molecules. The electronic structure of such molecules has to be expressed by a very large number of shells, each containing only two electrons. A simple account of these shells for typical triatomic molecules has been given by Mulliken.* The rotation-vibration levels of triatomic molecules are considered in detail in two other papers by Mulliken.† A proper understanding of electronic structures of molecules requires a knowledge of Group Theory,‡ for it is in these terms that classification of molecules has been made. When this is mastered, a paper by Sponer and Teller§ provides an excellent review of the whole subject. The historical development of Mulliken's ideas prior to this may be read in a series of papers || he wrote between 1932 and 1935. The most comprehensive account of the subject matter of this chapter is probably in *Infra-Red and Raman Spectra* by Herzberg (D. van Nostrand Co., N.Y., 1945).

* *Rev. Mod. Phys.*, vol. 14, p. 204 (1942).

† *Phys. Rev.*, vol. 51, p. 873 (1941); vol. 60, p. 506 (1941).

‡ Rosenthal and Murphy, *Rev. Mod. Phys.*, vol. 8, p. 317 (1936).

§ *Rev. Mod. Phys.*, vol. 13, p. 75 (1941).

|| *Phys. Rev.*, vol. 40, p. 55 (1932); vol. 41, p. 49 (1932); vol. 41, p. 751 (1932); vol. 43, p. 279 (1933). *Jour. Chem. Phys.*, vol. 1, p. 492 (1933); vol. 3, pp. 375, 506, 514, 517, 564, 573, 586, 635, 720 (1935).

THE RAMAN EFFECT

IN 1923 it had been predicted by Smekal that when light of any frequency ν was scattered by matter, the scattered light should include radiations such as $\nu \pm \nu_0$, where $h\nu_0$ represented an amount of energy emitted or absorbed by the molecules of the scattering substance. In 1928 Raman announced the discovery of this effect experimentally, and since that time there has been an enormous output of experimental work dealing with thousands of chemical compounds in various physical states—solid, liquid, and gaseous. The lines on the low-frequency side, such as $\nu - \nu_0$, may be called 'Stokes' lines, and those on the high-frequency side, such as $\nu + \nu_0$, 'anti-Stokes' lines. Raman initially looked upon the effect as an optical analogue of the Compton effect, in which a quantum of X-radiation is scattered by an electron to become a quantum of lower frequency, endowing the electron with the balance of energy.

The Raman effect should be distinguished from fluorescence. Fluorescence is preceded by light absorption of a quantum $h\nu$, and as the excited electron of the atom or molecule falls back to the normal, which it may do in various ways, there is re-radiation of the energy as a fluorescent spectrum. The lines of this spectrum must naturally be of lower frequency than the exciting radiation. The amount of light emitted in this way is of the same order as that which is incident upon the substance. Moreover, the fluorescent spectrum can only be excited by a specific frequency which is capable of being absorbed by the atom or molecule. The Raman spectrum, in contrast with this, is extremely weak, but may be excited by light of any frequency.

The scattering of light by matter is really of two kinds, ordinary Rayleigh scattering, and Raman scattering. It arises provided the particles involved are small compared to the impinging wave-lengths, and we have for both these types the familiar variation of the intensity of the scattered light with the inverse fourth power of the wave-length. Rayleigh scattering involves no change in wave-length of the scattered light: Raman scattering does. Both effects arise from the polarization of the atoms or molecules by the incident light. Because they are polarizable at all, we have the former effect, and because this polarizability varies with motions within the molecule, we have the latter effect.

Consider the ideally simple case of a spherical molecule or atom subject to an electric field E . It becomes an electric doublet, or, as we say, it is 'polarized' by reason of a relative displacement of the centre of gravity of the positive and negative charge. The electric moment M is given by

$$M = \alpha E \quad . \quad . \quad . \quad . \quad . \quad . \quad (209)$$

where α is called the polarizability. Under the influence of the

light-wave for which $E = E_0 \cos 2\pi\nu t$ there would therefore result a variable electric moment, and this on the classical view would radiate the scattered light of the Rayleigh effect. Because, however, of molecular changes (rotation, vibration, &c.) the polarizability is itself variable, and may be written, let us suppose, as $\alpha = \alpha_0 + \alpha_1 \cos 2\pi\nu_0 t$. Substituting in (209) we have

$$M = E_0(\alpha_0 + \alpha_1 \cos 2\pi\nu_0 t) \cos 2\pi\nu t \\ = E_0\alpha_0 \cos 2\pi\nu t + \frac{1}{2}E_0\alpha_1 [\cos 2\pi(\nu + \nu_0)t + \cos 2\pi(\nu - \nu_0)t] \quad (210)$$

showing both the Rayleigh and the Raman scattering. We would reiterate that the induced polarizability under the light wave gives the Rayleigh scattering, while the variations of this polarizability give the Raman effect.

The intensity of the Rayleigh line is proportional to α_0^2 , and the intensity of the Raman lines is proportional to $\frac{\alpha_1^2}{4}$. The latter is generally only a few thousandths of the value of the former in gases, although in liquids it may rise to a few hundredths of its value.

If a molecule is of the simple type we have pictured, viz. with an equal facility for polarization in all directions, equation (209) applies. We might write down $M_x = \alpha E_x$, $M_y = \alpha E_y$, $M_z = \alpha E_z$: in other words, the moment of the induced doublet is along the axis of the applied field. In general, because of the unequal polarizability along different axes of the molecule, these simple relations must be replaced by

$$\left. \begin{aligned} M_x &= \alpha_{xx}E_x + \alpha_{xy}E_y + \alpha_{xz}E_z, \\ M_y &= \alpha_{yx}E_x + \alpha_{yy}E_y + \alpha_{yz}E_z, \\ M_z &= \alpha_{zx}E_x + \alpha_{zy}E_y + \alpha_{zz}E_z, \end{aligned} \right\} \quad . \quad . \quad (211)$$

where there are six coefficients of polarizability, since $\alpha_{xy} = \alpha_{yx}$, &c. A coefficient such as α_{xy} means the moment induced in the x -direction by unit field (E_y) polarized along the y -axis. The physical picture is that the induced dipole moment makes an angle with the electric vector E . (The vector E is usually taken to define the 'polarization' of the incident light wave.) We can, however, find three axes in the molecule along which the directions of M and E will coincide, and taking these as axes we have $M_\xi = \alpha_\xi E_\xi$, $M_\eta = \alpha_\eta E_\eta$, $M_\zeta = \alpha_\zeta E_\zeta$. It is helpful to visualize fixed to a molecule an 'ellipsoid of polarizability', whose semi-axes are $(\alpha_\xi, \alpha_\eta, \alpha_\zeta)$, viz. the moments induced by unit electric force in these directions. The Raman effect arises due to the rotation of this ellipsoid as the molecule rotates, and due to the change of shape of this ellipsoid because of vibrations within the molecule.

If a molecule could be fixed in a known position relative to the incident light (which is possible in the case of crystals only), we could determine the six coefficients of (211) or α_ξ , α_η , and α_ζ . In general, the molecular orientation is a random one, and appropriate allowance for this must be made.

In the ideally simple case first considered, where the ellipsoid of polarizability becomes a sphere, the scattered radiation is wholly polarized in the same direction as the incident radiation. Thus suppose the incident light is incident along the z -axis and plane

polarized along the x -axis, the light scattered, whether along the y - or z -axes, will still be polarized along the x -axis. If, however, we have to deal with an ellipsoid of polarizability, this is not the case, and a 'de-polarization factor' is defined which is measured by the ratio of intensity of the scattered light polarized perpendicular to x , to the intensity of the scattered light polarized parallel to x . We may say that the depolarization factor is zero for the simple case of a 'sphere' of polarizability, while it will rise to $6/7$ for unpolarized scattered light. The experimental determination of the depolarization factor is of assistance in assigning Raman frequencies to the particular mode of vibration to which they belong. Theory indicates that the depolarization factor will rise to $6/7$ for unsymmetrical fundamentals; for symmetrical vibrations it is between 0 and $6/7$; while for the highly symmetrical 'breathing' vibrations it is zero or very small.

RAMAN DATA ON CHCl_3 (CHLOROFORM)

ν cm. ⁻¹	Mode	$\frac{I_{\text{Raman}}}{I_{\text{Rayleigh}}} \times 10^3$ (after Rao)	Depolarisation Factor ρ
667	ν_1 sym.	2.10	0.06
366	ν_3 anti-sym.	1.90	0.18
3020	ν_5 CH valency	0.67	0.25
759	ν_2 degenerate	0.49	0.86
261	ν_4 degenerate	2.50	0.86
1213	ν_6 CH (deform.)	0.31	0.86

We may take by way of illustration the depolarization data for CHCl_3 . The probable assignment of the modes of vibration to the observed frequencies is given in the table. Reference may be made to the previous chapter describing such modes for a molecule of the type ZYX_3 . We shall find that ν_1 , ν_3 , and ν_5 all apply to the parallel type of band, i.e. a change of electric moment parallel to the axis of symmetry. The most symmetrical mode, the quasi-breathing frequency, where the CH group approaches the three chlorine atoms, corresponds to the highly polarized band $\rho = 0.06$.

Structurally similar molecules, e.g. others of the type ZYX_3 , are found to have their corresponding lines depolarized to the same degree. Depolarization is a function, largely, if not entirely, of the mode of vibration. Observations made on the depolarization of the vibrational lines of diatomic or linear molecules in the gaseous state according to Bhagavantam gives values of ρ in the region 0.2 to 0.3. Thus

	H_2	D_2	N_2	O_2	CO_2	C_2H_2	CO	NO
ν	4156	2993	2331	1557	1389	1974	2143	1876
ρ	0.13	0.18	0.19	0.26	<0.20	0.2	0.29	0.31

Rotational Raman lines always have a depolarization of 0.86.

It should be borne in mind that it is the *changes* in the coefficients of (109) and (111) which are responsible for the Raman frequencies. Hence in 'spherical' molecules there will be no pure-rotational Raman effect, though there may be vibration-rotation effects. Where there is, however, an ellipsoid of polarizability, pure-rotation Raman bands

are possible the line structure of which is given by $\nu \pm \nu_r$. Here ν is the exciting frequency and ν_r corresponds to the rotation quanta which the molecule may possess. In the case of linear molecules the polarizability ellipsoid is one of symmetry round the figure axis. Since these molecules execute pure rotation round an axis perpendicular to this, the ellipsoid returns to its original position each half-revolution of the molecule. In other words, the polarizability goes through a cycle of twice the rotation frequency: ν_r -intervals in the Raman band therefore correspond approximately to alternate lines of a far infra-red rotation band. The two branches of the Raman rotation band might be interpreted as due to a selection principle for the rotational quantum number of ± 2 . In the case of the symmetrical top molecule, the molecule does not reproduce its position by rotation through 180° . Here both the precession frequency and the octave occur, corresponding to selection principles ± 1 , ± 2 .

The effect of vibration will usually be to cause a periodic change of shape of the ellipsoid of polarizability, and vibrational frequencies ν_v will be found associated with ν (the incident frequency), giving $\nu \pm \nu_v$. These will, in general, become the origins of Raman bands such as we have discussed. We may summarize the effects thus:

(1) A spherical molecule which remains completely symmetrical under the influence of vibration, e.g. the 'breathing' frequency of methane, would be represented in the Raman spectrum by strong lines at $\nu \pm \nu_1$, without any band structure.

(2) A spherical molecule whose symmetry is changed by vibration will give rise to Raman bands at $\nu \pm \nu_2$, where ν_2 is approximately the vibration frequency involved: these will have the fine structure appropriate to a spherical top molecule. We have examples of this in the non-symmetrical frequencies of methane.

(3) If the polarizability is not spherical, but remains unaffected by vibration, we should have the rotational Raman structure surrounding the exciting line. If, as is common, we have an ellipsoid of polarizability affected by vibration, we shall have vibration-rotation Raman bands. A more detailed statement than this of the criteria that modes of vibration (including overtones and combination tones) should be active or inactive in the Raman effect depends on the terminology of Group Theory, and is therefore not included here.

(b) THE STRUCTURE OF RAMAN BANDS

The picture of a quantum of molecular energy added on to, or subtracted from, that of the exciting radiation proves to be too simple. It does not account for the fact that some strong Raman bands have no counterpart in absorption spectra, and vice versa. Nor does it account for the intensities with which the Raman radiations occur. The Raman effect is now recognized to involve a third level C other than the initial level A and the final level B of the molecule. We must visualize the process as a molecular absorption of energy $A \rightarrow C$, followed by an emission $C \rightarrow B$. The difference of the energy levels A and B gives the Raman shift. If B is above A the corresponding Raman line is on the low-frequency side of the exciting line, and vice versa. This picture of the process shows that

the intensity of the Raman line depends on the product of the transition probabilities ($A \rightarrow C$) and ($C \rightarrow B$), and not on that of ($A \rightarrow B$).

Fig. 137 shows in detail how a typical rotation-vibration band may be excited in the Raman effect, viz. the ($1 \leftarrow 0$) band, which will appear on the low-frequency side of the exciting line. We have shown the cases where two higher electronic states $y^1\Sigma^+$ or $^1\Pi$ might act as the 'intermediate' level (called C above). Consistent with the selection rules $\Delta J = \pm 1, 0$ and $+\nleftrightarrow -$, we see that this vibration rotation band will consist of three branches, a Q branch ($\Delta J = 0$), an S branch ($J + 2 \rightarrow J$), and an O branch ($J - 2 \rightarrow J$). These are so named by an extension of the R, Q, P notation for branches. The particular lines shown in Fig. 137 are $S(3)$, $Q(3)$, and $O(3)$. In the lower part of Fig. 137 is shown the assembly of band lines of the ($1 \leftarrow 0$) Raman band. The first lines of each band are as shown: $S(0)$, $Q(0)$, and $O(2)$, and they should be expressed by

$$\left. \begin{aligned} S(J) &= \nu - [\nu^{(1,0)} + F''(J+2) - F''(J)], \\ Q(J) &= \nu - [\nu^{(1,0)} + F''(J) - F''(J)], \\ O(J) &= \nu - [\nu^{(1,0)} + F''(J-2) - F''(J)], \end{aligned} \right\} \quad (212)$$

where F'' and F''' represent the rotational energy functions for $v = 1$ and $v = 0$. If the vibrational energy function of the ground state is $E/hc = \omega_e(v + \frac{1}{2}) - \omega_e x_e(v + \frac{1}{2})^2$, then $\nu^{(1,0)}$ is clearly $\omega_e - 2\omega_e x_e$. Furthermore, if $F(J) = BJ(J+1)$, the spacing of the lines around the origin of the band ($\nu - \nu^{(1,0)}$) may be set out as below, neglecting the differences between B_0 and B_1 and a term in higher powers of J . The positions of R - and P -branch lines are given for purposes of comparison.

$J \rightarrow$	0	1	2	3	4	5
$S(J)$	$6B$	$10B$	$14B$	$18B$	$22B$	$26B$
$R(J)$	$2B$	$4B$	$6B$	$8B$	$10B$	$12B$
$-P(J)$	—	$2B$	$4B$	$6B$	$8B$	$10B$
$-O(J)$	—	—	$6B$	$10B$	$14B$	$18B$

If in Fig. 137 the Raman spectrum had involved, instead of the molecular vibrational change ($1 \leftarrow 0$), the change ($1 \rightarrow 0$), the disposition of the branches can be envisaged by reflecting the band portrayed in the thick line, labelled 'exciting line'.

If the Q branch is unresolved, and the S and O branches are faint, we may have the appearance of a strong dark Raman 'line' coincident in position with what would be the null line or gap in the corresponding infra-red vibration-rotation band.

If the molecular end-state is the same vibrational level as the initial state we shall have a pure-rotation Raman band centred round the exciting line. The intermediate energy level involved need not imply an *electronic* change: a transition from $v = 0$ to $v = 1$ and then back to $v = 0$ is possible.

In the case of homonuclear molecules, which necessarily have no permanent electric moment, no infra-red bands exist. There are, however, Raman bands due to the oscillating electric moment induced

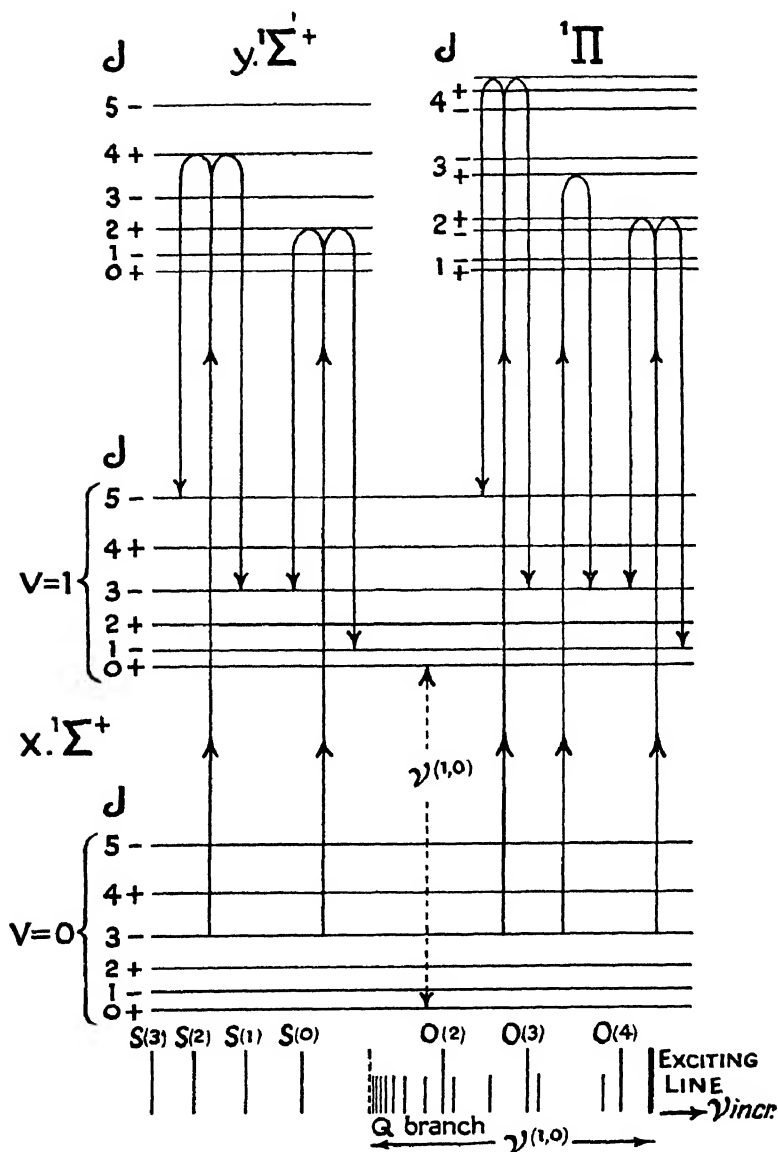


Fig. 137. The formation of typical lines of a Raman vibration-rotation band, also (below), the fine structure of a typical $(1 \leftarrow 0)$ band of a 1Σ state.

by the light wave. These will have alternating intensities in the band lines, appropriate to the nuclear spin.

The necessity of a permanent electric moment to make possible a pure-rotation absorption band is not difficult to account for. In the

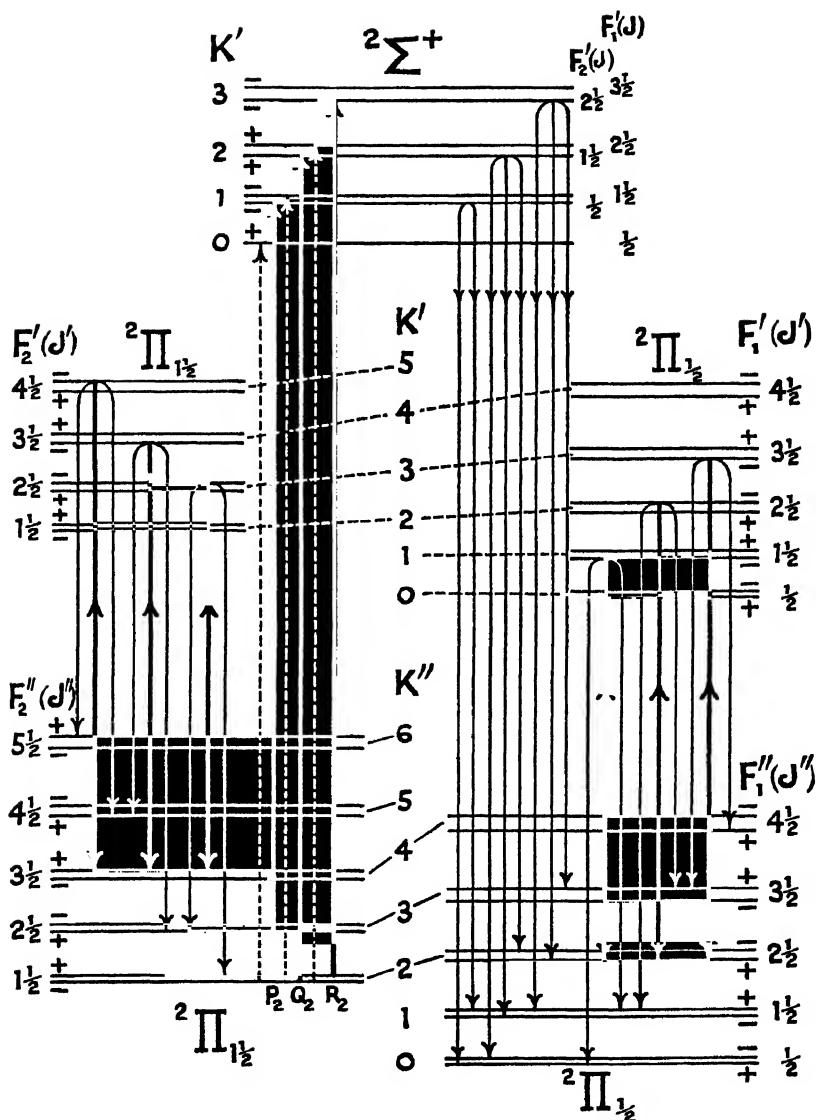


Fig. 138. Illustrating the formation of Raman pure-rotation bands in the case of NO. The upper 2Π level provides the intermediate level on the right and left of the diagram. The central part makes an upper 2Σ level the intermediate one and illustrates the formation of an electronic Raman band by a transition from $2\Pi_{1/2} \rightarrow 2\Pi_{1/2} = 124 \text{ cm}^{-1}$, which would appear on the high-frequency side of the exciting line.

absence of such a moment the alternating electric force in the light wave cannot produce a couple so as to rotate the molecule. Likewise a vibrating electric moment of the same periodicity as the electric vector of the light wave would appear a prerequisite of the absorption of vibrational energy.

It has been mentioned that the precessing symmetrical top molecule gives rise to *S*, *R*, *Q*, *P*, and *O* branches in Raman bands. Such are also found in the case of the diatomic molecule NO, which is in a ${}^2\Pi$ state normally. Fig. 138 shows how this may arise. On the right- and the left-hand sides of the diagram are shown the formation of pure-rotation Raman bands associated with the two electronic levels ${}^2\Pi_{11}$ and ${}^2\Pi_1$. For the sake of clearness only one of the components of the Λ -type doublet is drawn. The Raman lines represented on the left-hand side are *O*($5\frac{1}{2}$), *P*($4\frac{1}{2}$), *Q*($3\frac{1}{2}$), *R*($2\frac{1}{2}$), and *S*($1\frac{1}{2}$), all arising from the initial rotational level $J = 3\frac{1}{2}$. The Raman lines represented on the right-hand side of Fig. 138 are *S*($\frac{1}{2}$), *R*($1\frac{1}{2}$), *Q*($2\frac{1}{2}$), *P*($3\frac{1}{2}$), and *O*($4\frac{1}{2}$), all arising from the rotational level $J = 2\frac{1}{2}$. The typical band structure will be a strong *Q* branch with origin at $\nu \pm \nu_v$ (where ν is the exciting line and ν_v the vibrational contribution, if any). The four branches corresponding to $\Delta J = \pm 2, \pm 1$ will be disposed round the origin as follows (taking the rotational function $F(J) = B[J(J+1) - \Omega^2]$):

$J \rightarrow$	$\frac{1}{2}$	$1\frac{1}{2}$	$2\frac{1}{2}$	$3\frac{1}{2}$	$4\frac{1}{2}$	$5\frac{1}{2}$	$6\frac{1}{2}$
<i>S</i> (<i>J</i>) and $-O$ (<i>J</i>)	8 <i>B</i>	12 <i>B</i>	16 <i>B</i>	20 <i>B</i>	24 <i>B</i>	28 <i>B</i>	32 <i>B</i>
<i>R</i> (<i>J</i>) and $-P$ (<i>J</i>)	3 <i>B</i>	5 <i>B</i>	7 <i>B</i>	9 <i>B</i>	11 <i>B</i>	13 <i>B</i>	15 <i>B</i>

The lines corresponding to $J = \frac{1}{2}$ will not be present in ${}^2\Pi_{11}$.

The central part of Fig. 138 illustrates the possibility of a Raman band arising from a transition ${}^2\Pi_{11} \rightarrow {}^2\Pi_1$ or ${}^2\Pi_1 \rightarrow {}^2\Pi_{11}$ via the higher ${}^2\Sigma$ level. The first of these will be on the high-frequency side and the second on the low-frequency side of the exciting line. The broken lines ascending are satellite branches which are not taken into account on the descending side. The Raman lines shown in the figure are

$(K' = 2, J' = 1\frac{1}{2}) \rightarrow (K'' = 3, J'' = 3\frac{1}{2})$: <i>P</i> <i>O</i>	one line.
$(K' = 2, J' = 1\frac{1}{2}) \rightarrow (K'' = 2, J'' = 2\frac{1}{2})$: <i>Q</i> <i>P</i>	two lines.
$(K' = 2, J' = 1\frac{1}{2}) \rightarrow (K'' = 1, J'' = 1\frac{1}{2})$: <i>R</i> <i>Q</i>	three lines.
$(K' = 2, J' = 1\frac{1}{2}) \rightarrow (K'' = 0, J'' = \frac{1}{2})$: <i>S</i> <i>R</i>	two lines.

(c) RAMAN SPECTRA OF CO₂, OCS, NH₃, H₂O, &c.

The study of Raman spectra as mentioned at the beginning of this chapter has covered a vast range of chemical substances, and several books have classified the data and given bibliographies.* All that will be attempted in this chapter is therefore the presentation of a few examples to illustrate the theory or indicate the kind of information the Raman effect can provide. We shall only expect to find

* *E.g.*, Hibben, *The Raman Effect and its Chemical Applications* (Reinhold Pub. Corp., N.Y., 1939).

rotational Raman structure in the case of the lighter gases: bands have in fact been observed in H_2 , D_2 , O_2 , N_2 , NO , NH_3 , &c. If the structure is unresolved, it will give rise to the appearance of a broad or diffuse line. Unresolved 'wings' are found to exhibit considerable variations in intensity as between one substance and another. As anticipated from what we said earlier, in spherically symmetrical molecules the 'wings' are negligible; in anisotropic molecules they may be extensive. It should be added, however, that the 'wings' often found in the liquid state are far more extensive than can be accounted for on any rotational basis. Raman spectra recorded thus correspond very largely to *vibrational* molecular changes.

Carbon Dioxide (CO_2)

As mentioned in the previous chapter, this linear symmetrical molecule has two fundamental infra-red bands: the band ν_2 (667 cm.^{-1}), and the band ν_3 (2349 cm.^{-1}). The completely symmetrical vibration ν_1 does not appear in the infra-red spectrum. On the other hand, while ν_2 and ν_3 are not found in the Raman spectrum either alone or in combination, ν_1 does occur there. Owing to Fermi resonance of $2\nu_2$ with ν_1 , the latter is found to be represented by two frequencies ν 1285 and ν 1384, which are approximately 50 cm.^{-1} on each side of what would probably have been the position of ν_1 in the absence of resonance. These frequencies have been observed in both liquid and solid CO_2 . Rotational Raman lines have also been observed in the gas.

Carbonyl Sulphide (OCS)

This may be taken as a type of the linear but unsymmetrical molecule. The frequencies observed in the Raman spectrum, with their identification, are as follows: ν_2 (524), ν_1 (859), $2\nu_2$ (1041), $\nu_1 + \nu_2$ (1383), ν_3 (2055), $2\nu_1 + \nu_2$ (2233). Of these 859 cm.^{-1} is much stronger than any others. From X-ray measurements it has been inferred that the inter-atomic separations are: $O-C$ (1.10 A.U.) and $C-S$ (1.96 A.U.). Observers of the infra-red* have reported these bands also, with the exception of 2233 and 1383. The following additional bands are reported in the infra-red: $\nu_2 + \nu_3$ (2575), $\nu_1 + \nu_3$ (2919), $2\nu_2 + \nu_3$ (3096), $2\nu_1 + \nu_3$ (3739), $2\nu_3$ (4101) cm.^{-1} . The single $C-S$ bond probably has a frequency of about 650 cm.^{-1} . It would seem probable that in the OCS molecule both the OC and CS bonds are doublet ones.

Ammonia (NH_3)

This molecule to which Fig. 115 is applicable had, in the infra-red, strong absorption bands ν_1 (3336), ν_3 (950), and ν_4 (1627). The ν_2 perpendicular band, if present, is weaker, and being probably in the region 3414 cm.^{-1} , would be confused with the ν_1 structure. The ν_1 band is dominant in the Raman spectrum of NH_3 in both gaseous, liquid, and solid states, and the structure of the branches $\Delta J = 0$, ± 1 , ± 2 has been recorded. The ν_3 band is of medium strength in the gaseous state, but does not appear to have been recorded in the liquid or solid state: ν_2 and ν_4 are possibly present but are weak.

* Bartunck and Barker, *Phys. Rev.*, vol. 48, p. 516 (1935).

Water (H₂O)

The infra-red spectrum of water vapour contains ν_1 (3650) rather weak or overlaid with other structure, and strong bands ν_2 (1595) and ν_3 (3755). The Raman spectrum of the liquid has three peaks at or about 3190, 3440, and 3650 cm.⁻¹. Various observers differ as to their precise location, but they are obviously associated with ν_1 , the symmetrical OH vibrations. The effect of raising the water temperature

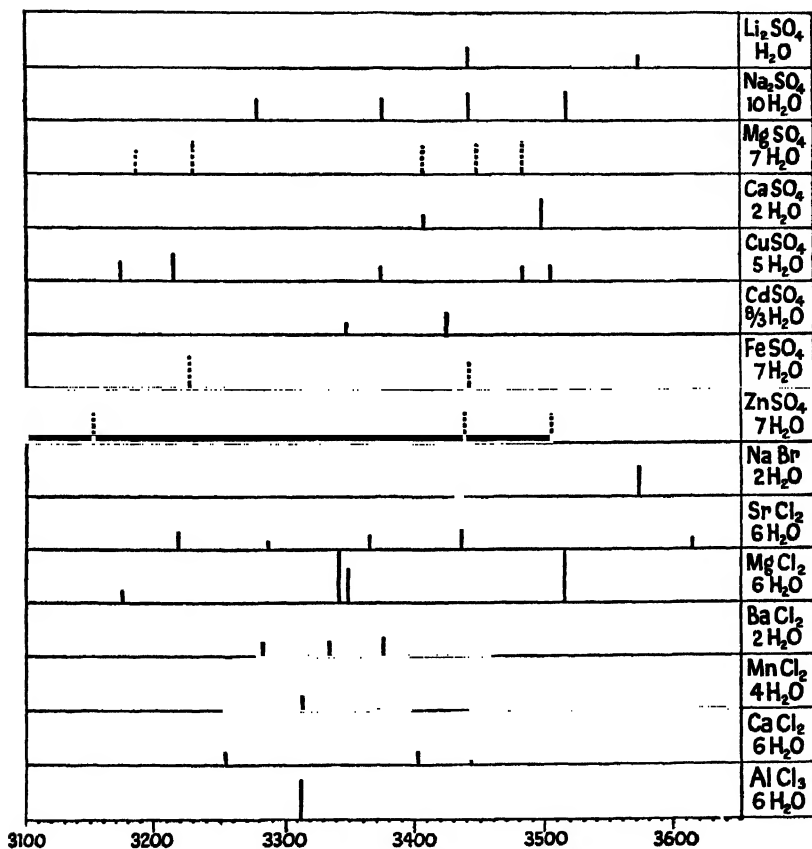


Fig. 139. Raman bands arising from the water of crystallization in various salts.

from 0° to 100° C. is to displace the energy from the lowest of these towards the highest (3650 cm.⁻¹). Though by no means as strong as ν_1 , the frequency ν_2 has been definitely recorded in the Raman spectra.

In addition to these, a number of low-frequency bands have been found: ν 170 and 500 are found in both water and ice, and they have been shown to occur in infra-red absorption also. The first of these remains unaffected in heavy water, and is presumably due to some inter-molecular effect; the second at 500 cm.⁻¹ has been ascribed

to hindered rotation of the hydrogen atoms. There can be little doubt that the polymers such as $(\text{H}_2\text{O})_2$ and $(\text{H}_2\text{O})_3$ are present in water. It is indeed possible that these polymers are respectively responsible for the bands at 3440 and 3190 to which reference has been made. The temperature effect would be consistent with this view. Modification of these bands induced by dissolved substances are of interest. Thus, for example, the presence of hydroxyl ion produced by adding a little caustic soda reduces the intensity of the low-frequency bands, and presumably therefore favours de-polymerization. Crystalline sodium hydroxide has been found to give a sharp band at 3630 cm.^{-1} , which is virtually that of the OH oscillation in H_2O .

These characteristic water bands have been subject to much study in so far as they are modified in crystalline hydrates. The water of crystallization in most salts gives rise to a group of much sharper maxima in the region $3050\text{--}3650\text{ cm.}^{-1}$ than occur otherwise. These bands are shown in Fig. 139 for a series of chlorides. The frequency near 3380 cm.^{-1} does not occur in pure water. An understanding of the various forms of association of the H_2O molecules in the crystal will probably in due course lead to a satisfactory account of these spectra. The displacement in various crystals of what is obviously the same band must also be related in some way not yet understood to the ionic forces or radii of the specific molecule.

(d) RAMAN SPECTRA OF SOME ACIDS

The study of Raman spectra provides an additional method by which the phenomenon of ionization in solution may be studied. If the time of photographic exposure is increased in the same ratio as the dilution, we should anticipate no change in intensity provided the scattering particles do not change. A departure from constancy would, however, indicate a change in dissociation, and the extent of this could be calculated.

One of the features of the Raman spectra, which we have already observed, is the appreciable displacement of the Raman bands of a substance under varying physical conditions. This may be illustrated by the cases of HCl and HBr as solid, liquid, and gas, and dissolved in various solvents :

	Gas	Liquid	Solid	In CHCl_3	In $\text{C}_6\text{H}_6\text{Br}$
HCl .	2880	2778	2760	2826	2797
HBr .	2558	2487	2465	2500	2471

There is evidence which suggests that the large wave-number displacement in various solvents is closely connected with high dielectric constant of these liquids. As there is no evidence of polymerization of HCl , the variability of the vibration frequency must presumably correspond to some measure of polarization of the neighbouring solvent molecules by the dipole. As might be anticipated from the high degree of ionization of HCl in aqueous solution, the above characteristic HCl Raman band is not observed.

Sulphuric acid has been the subject of numerous investigations, and

exhibits many features of interest. Fig. 140 based upon the work of Woodward and Horner * shows that certain Raman bands disappear, and other new ones appear, as we pass from pure acid to dilute aqueous solution. Apart from this there is also a displacement of some of those bands which persist through a substantial range of concentrations. Thus the band which is at about 1030 cm^{-1} in 90% acid is at about 1050 cm^{-1} in 10% solution. The band at 982 cm^{-1} remains constant in position. According to observations of Bell and Jeppeson † the bands

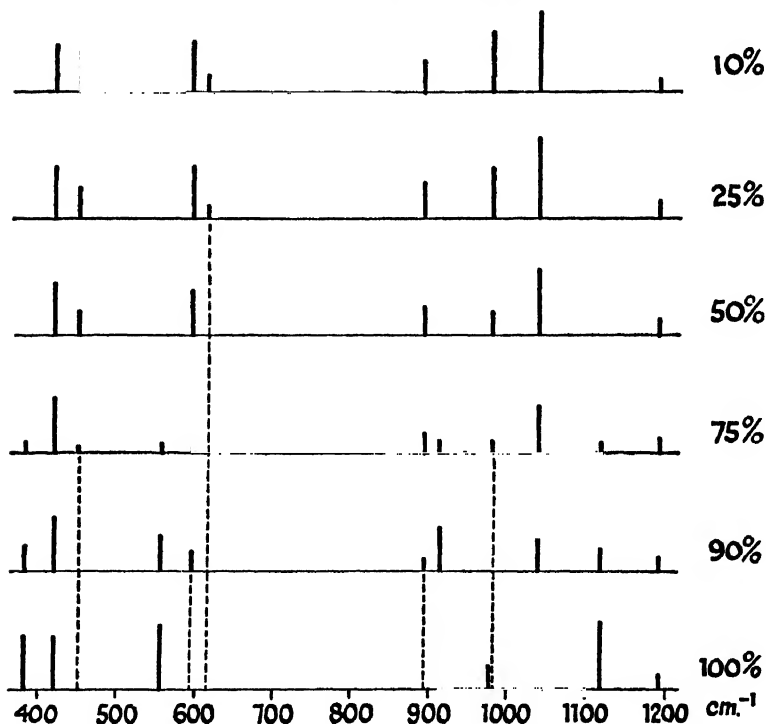


Fig. 140. Raman spectra of sulphuric acid in solutions of varying concentration. (After Woodward and Horner.)

which are at 417 cm^{-1} and 575 cm^{-1} in high concentrations are displaced $15\text{--}20\text{ cm}^{-1}$ to the high-frequency side in dilute solution, but these may be only apparent displacements accounted for by the changes of intensity of components of unresolved bands, as we see from Fig. 140.

The origins of the various lines is a matter of considerable interest. The frequencies at 381 , 555 , 910 , 978 , 1121 , and 1360 cm^{-1} , which are attributed to the molecule H_2SO_4 , decrease rapidly in intensity with dilution. The frequencies at 595 , 895 , and 1036 cm^{-1} attributed to the HSO_4^- ion begin with slight dilution and increase substantially in strength. The frequencies at 452 , 617 , and 982 cm^{-1} are attributed

* *Proc. Roy. Soc., A*, vol. 44, p. 129 (1934).

† *Jour. Chem. Phys.*, vol. 3, p. 245 (1935).

to the SO_4^{--} ion. These begin at greater dilution and then increase in strength with dilution.

The small depolarization factor for the strong line 910 cm^{-1} ($\rho = 0.16$) has led to the suggestion that this vibration probably corresponds to the quasi-symmetrical 'breathing' frequency of the tetrahedron $(\text{HO})_2\text{SO}_2$. The absence of any SH frequency which would be about 2600 cm^{-1} is consistent with the tetrahedral structure in which the H atoms occur in hydroxyl groups. A Raman vibration reported at about 3000 cm^{-1} would be due to the OH vibration.

Fuming sulphuric acid, which contains SO_3 , has been studied by means of the Raman effect. As the concentration of SO_3 increases, the bands characteristic of H_2SO_4 diminish in intensity, fading out at about 36% additional SO_3 . Meanwhile new bands attributable to $\text{H}_2\text{S}_2\text{O}_7$ have made their appearance at 300, 327, 480, 735, 970, and 1250 cm^{-1} . As the concentration of SO_3 is further increased, additional bands appear due to the vibrations of the SO_3 molecule, and at higher concentrations, of S_2O_6 .

The Raman spectrum of anhydrous HNO_3 is shown in Fig. 141,

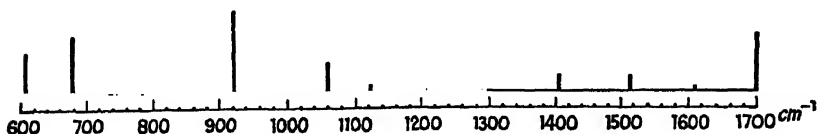


Fig. 141. Raman spectrum of anhydrous HNO_3 .

using the data of Angus and Leckie.* It has been observed that some of the bands show marked displacement with dilution of the acid. Thus 608 cm^{-1} in concentrated HNO_3 is displaced to 657 cm^{-1} in 52% acid, while 674 cm^{-1} is displaced to 726 cm^{-1} in 17.6% acid. Other bands vary much less than these. It is, of course, possible that, as in sulphuric acid, the intensity variations of unresolved components may be responsible for the apparent displacements. A frequency in the region $3300\text{--}3400\text{ cm}^{-1}$ (not shown in Fig. 141) is almost certainly an OH vibration.

There is a very great increase in intensity of the band about 1050 cm^{-1} upon dilution of the acid. In addition, the band 674 cm^{-1} (displaced to 726 cm^{-1}) strengthens with dilution. As the most characteristic frequencies of the NO_3^- ion, as inferred from a study of the metallic nitrates, are in the region 729(2), 1050(10), and 1360(2), the interpretation of the two bands mentioned is not in doubt. There are, however, several indications that the structure of nitric acid differs in important respects from that of organic nitrates. Thus, alkyl nitrates are found to have strong bands at 1290(10) and 1644(5), but the characteristic frequency at 1050 is not present. The structure of nitric acid may be $\text{HO}-\text{N}^+\begin{smallmatrix} \text{O} \\ \diagup \\ \text{O} \end{smallmatrix}-$. The small depolarization factors of 920 cm^{-1} , and 1297 cm^{-1} , suggest that they are symmetrical vibrations, but which particular vibrations of the molecule they correspond to is as yet uncertain.

* *Proc. Roy. Soc., A*, vol. 149, p. 327 (1935).

(e) SOME ORGANIC COMPOUNDS

Paraffins

The simplest of organic compounds are the paraffins in which the normal quadrivalence of carbon is satisfied. It is therefore desirable to consider the series of molecules which are expressed by C_nH_{2n+2} , so that we find the effect of increasing molecular complexity by easy stages. We saw in the last chapter that CH_4 (methane), by reason of its spherical symmetry, would only be expected to have four fundamental modes of vibration: ν_1 (2914 cm^{-1}) the symmetrical 'breathing' frequency, ν_2 (about 1536 cm^{-1}) a doubly degenerate

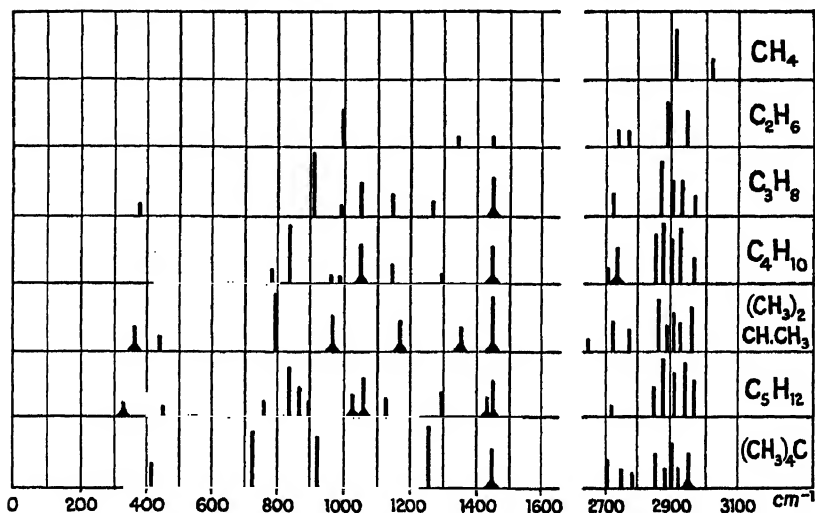


Fig. 142. Raman spectra of some straight chain paraffins. Length of line represents intensity. A broad base indicates diffuseness.

vibration which, like ν_1 , is inactive in the infra-red, ν_3 (3019 cm^{-1}) and ν_4 (1306 cm^{-1}), both triply degenerate but active vibrations.

When the spherical symmetry is lost by substitution, as in CH_3D and CHD_3 , six of the vibrations occur; in CH_2D_2 the full theoretical nine arise. The higher the degree of symmetry in a vibration the more complete the polarization of the line. In CH_4 , ν_1 has therefore a very small depolarization factor, ν_2 is intermediate, while for ν_3 and ν_4 the factor is large ($6/7$). As we should expect, ν_1 appears strongly in the Raman spectrum, while ν_3 and $2\nu_2$ are present but weak. Examination of Fig. 142 shows at once the increasing complexity of the Raman spectrum with molecular building. The spectra may for convenience be regarded as falling into four parts: the CH valence vibrations in the region ($2700\text{--}3000\text{ cm}^{-1}$); the CH deformation vibrations in the region ($1100\text{--}1600\text{ cm}^{-1}$); the CC valence vibrations in the region ($700\text{--}1100\text{ cm}^{-1}$); the CC deformation vibrations in the region ($200\text{--}700\text{ cm}^{-1}$). Consider the CH valence vibrations (as collected by Hibben) in the following table.

CH VALENCE VIBRATIONS

CH ₄ . . .	—	—	—	—
C ₂ H ₆ . . .	—	—	—	—
C ₃ H ₈ . . .	—	2728(3)	2767(1)	2874(10)
C ₄ H ₁₀ . . .	2665(1)	2706(1)	2736(2)	2864(4)
CH ₄ . . .	—	2918(10)	—	—
C ₂ H ₆ . . .	—	2913(9)	2943(10)	—
C ₃ H ₈ . . .	2903(3)	2920(3)	2948(3)	2968(3)
C ₄ H ₁₀ . . .	2879(8)	2910(3)	2938(6)	2964(3)

The various CH pairs in the molecules no longer have exactly the same vibration frequency, so that the single characteristic frequency of methane is replaced by a complex of lines. Although attempts have been made to assign these to specific CH pairs, there is no general agreement on this. A precisely similar complexity is introduced if the CC oscillation is studied in molecules of increasing length (data after Hibben). Again there is no certainty about the assignment of these vibrations.

CC VIBRATIONS

C ₂ H ₆ . . .	—	—	—	—	—
C ₃ H ₈ . . .	—	377(2)	—	867(10)	—
C ₄ H ₁₀ . . .	320(0)	430(6)	793(4)	834(10)	960(3)
C ₂ H ₆ . . .	993(5)	—	—	—	—
C ₃ H ₈ . . .	—	1055(2)	—	1155(2)	—
C ₄ H ₁₀ . . .	983(3)	1060(6)	1067(0)	1146(4)	1303(3)

A Series of Octanols

These are aliphatic alcohols containing eight carbon atoms, and having the resultant formula C₈H₁₇OH. There are many octanols corresponding to (1) the position of the OH group along the carbon chain, and (2) isomeric forms in which one (or more) CH₃ groups projects laterally from various positions of the chain. G. Collins * investigated a series of nineteen octanols, with results shown in Fig. 143. The interest of this type of investigation is in the information it provides of the effect on vibration of slight changes of molecular form.

The CH valence vibrations in the region 2900 cm.⁻¹ are presumably present, but not shown in Fig. 143. One of the difficulties of satisfactory interpretation is that the force-constants of the C—C and the C—OH vibrations are not very different. A few general conclusions may be drawn. The low-frequency vibrations in the region 200–500 cm.⁻¹ are undoubtedly C—C deformation vibrations in which we can picture the side-chains anchoring the molecule, as at a node, and the two lengths of the molecule on each side of this point oscillating like flexible rods. The two vibrations about 1300 cm.⁻¹ and 1450 cm.⁻¹ are very probably transverse or deformation vibrations of the CH bond. They are almost the same as the vibrations in Fig. 142 corre-

* *Phys. Rev.*, vol. 40, p. 829 (1932).

sponding to this. This figure also shows that the CC valence vibrations may be expected in the region 800–1100 cm^{-1} . There is a strong frequency at 1030 cm^{-1} in CH_3OH , obviously characteristic of the C—OH vibration, and it is possible that the vibration of Fig. 143 about this position is due to this bond.

It may be remarked that as the side-chains move towards the

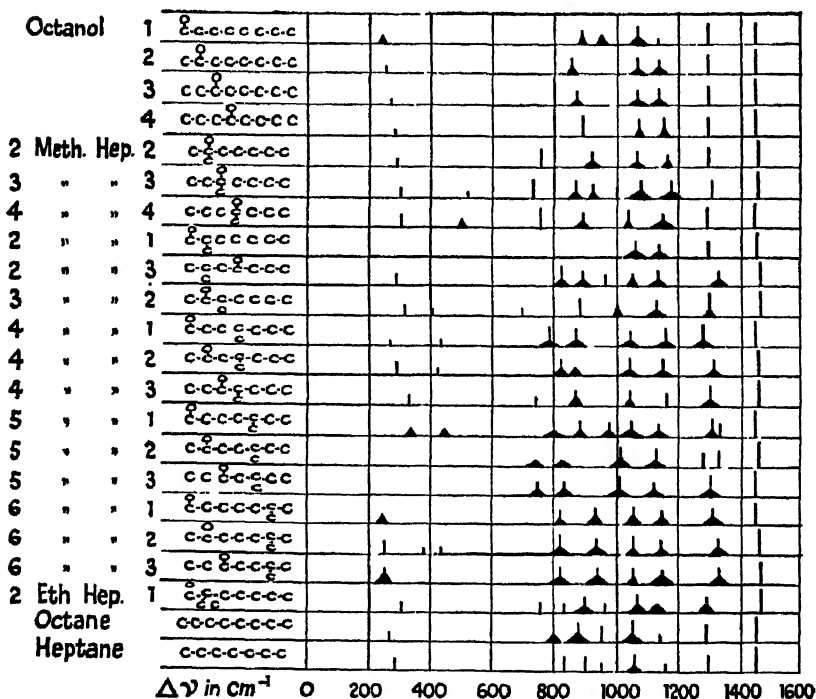


Fig. 143. Raman spectra of a series of octanols. (After G. Collins.)

centre the CC deformation frequency increases, which is intelligible on the picture formulated, if we regard the observed frequency as produced by the longer portion of the chain. It will be observed that the attachment of OH and CH_3 groups on opposite sides of the same carbon atom gives rise to a new frequency about 750 cm^{-1} , probably due to the vibration $\text{HO}\rightarrow\text{C}\leftarrow\text{CH}_3$.

Compounds of Ethylene

If reference is made to Fig. 119 and the table descriptive of the modes of vibration of the molecule, it is obvious that while the theoretical modes of vibration are clear, the precise identification of some of the observed frequencies with these modes is as yet uncertain. In Fig. 144 are shown the Raman frequencies arising from ethylene $\text{H}_2\text{C}=\text{CH}_2$ and three pentenes. The increasing complexity of the Raman spectra is obvious. It seems clear that the group

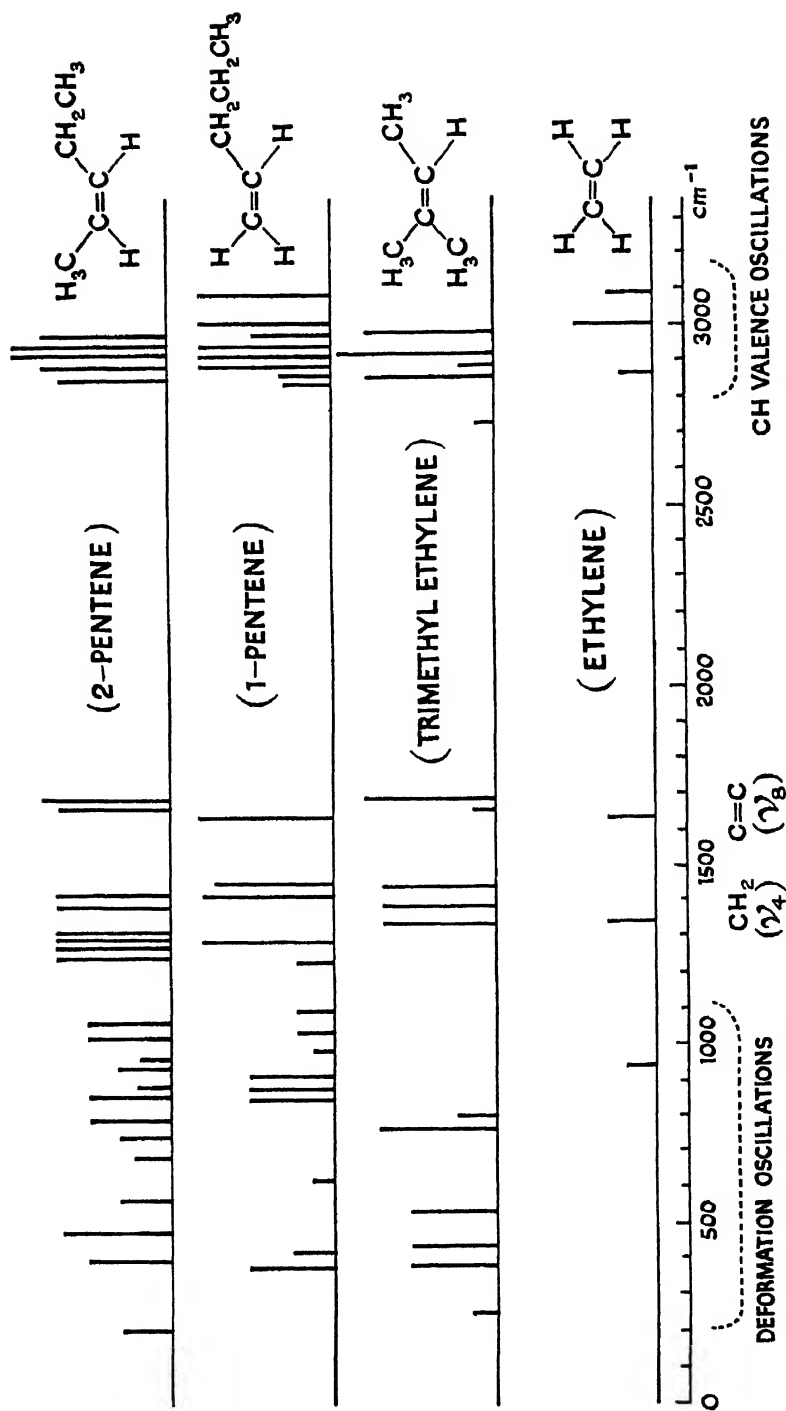


Fig. 144. Raman spectra of ethylene and three pentenes (C_5H_{10}).

around 3000 cm^{-1} is due to the various CH valence vibrations, and those about 1620 cm^{-1} are due to the C=C double bond (ν_8 of Fig. 119). It seems probable that those near 1340 cm^{-1} are due to the anti-symmetrical oscillation (ν_4 of Fig. 119), and the two lower frequency groups are deformation vibrations relative to the double-bond axis. One group may be in the plane of the paper, the ν_{10} type, and the other group perpendicular to the plane of the paper, the type ν_{12} .

The applications of the Raman effect are very numerous: to such problems as the identification of substances in a mixture, the structure of organic molecules, the nature of crystals, the nature of the liquid state, &c. A comprehensive summary and a bibliography of over 500 papers are given by Glockler in *Reviews of Modern Physics*, vol. 15, pp. 111-173 (1943). An excellent and simpler account will also be found in the book of Bhagavantam, *Scattering of Light and the Raman Effect* (Andhra Univ., Waltair, India).

VARIOUS APPLICATIONS OF MOLECULAR SPECTROSCOPY

THE interpretation of molecular spectra presented in preceding chapters will have shown the reader how much may be inferred about the structure of a molecule from analysis of the light which it will absorb or emit under certain conditions. In the present chapter it is proposed to give a survey of the wider applications of this knowledge of molecular spectra. The data given are not to be regarded as complete or detailed, but as illustrative.

(a) ASTROPHYSICS

(1) *The Night Sky and Aurorae*

Many investigations have been made of the light of the night sky. Because of its faintness, the most powerful light-gathering spectrographs are necessary. Thus in the paper of Elvey, Swings, and Linke on the spectrum of the night sky * the arrangement used consisted of a narrow mirror reflecting the sky, and this itself acted as the slit of the spectrograph. The light from it was reflected in a mirror 75 ft. distant, and then passed into an objective prism camera consisting of two quartz prisms mounted in front of an $f/1$ Schmidt camera. The slit being virtually 150 ft. away, no collimating lens was necessary.

The 'normal' light of the night sky is sometimes called the permanent aurora, or non-polar aurora, since its strongest feature is the well-known green line λ 5577.35 due to oxygen. The next strongest feature is another oxygen line which has as its initial state the final state of the green line. This 'red' line is a triplet, but only two of the components λ 6300, 6364 are observed. The green line $^1S_0 \rightarrow ^1D_2$ and the red line $^1D_2 \rightarrow ^3P_{2,1,0}$, which takes the oxygen atom down to its normal or ground state, are, it will be observed, both forbidden transitions. In addition to these, the yellow sodium lines $\lambda\lambda$ 5890, 5896 appear in the twilight when sunlight is illuminating a layer of the atmosphere about 60–80 km. above the earth. Observations made cover the spectral range 3000–8600 A.U., but apart from the above-mentioned lines the spectrum is wholly molecular, and largely due to the N_2 molecule (see Fig. 22).

The Vegard-Kaplan ($A^3\Sigma \rightarrow X^1\Sigma$) system of N_2 with an electronic excitation potential of 6.2 volts is a transition from a metastable state down to the ground state. The observed bands which occur in the near ultra-violet and extend to the blue consist chiefly of a few bands of the sequences $v'' - v' = 10, 11$, and 12.

Babcock observed eleven bands which are attributed to the First Positive band system of N_2 ($B^3\Pi \rightarrow A^3\Sigma$). Their vibrational quantum numbers are (11,5) + (10,4), (16,11), (14,9), (12,7), (13,9), (8,4), (4,0), (11,8), (9,6), (8,5), and (7,4) (see Fig. 23). The highest excitation

* *Astrophys. Jour.*, vol. 93, p. 337 (1941).

potential involved in this is about 10 volts. There is also a possibility of four or five bands (0,19) to (0,23) of the Lyman-Birge-Hopfield system occurring, but this identification is uncertain. The excitation potential of these would be only about 8.5 volts.

There is some evidence of CH. The Q -branch lines of ($A^2\Delta \rightarrow X^2\Pi$) may account in part for a band near λ 4316. In addition, the system ($C^2\Sigma \rightarrow X^2\Pi$) is probably represented by the (0,0) band at λ 3143 and (1,1) band at λ 3157, but there is no evidence of the $B^2\Sigma \rightarrow X^2\Pi$ system near λ 3900. These CH bands (if such is their origin) appear of constant intensity from zenith to horizon, unlike the Vegard-Kaplan bands, and an interplanetary origin has therefore been suggested for them.

There is no evidence of OH_2 bands in the night sky, but it is possible that the so-called 'C' band (1,3,1) \rightarrow (0,0,0) may account in part for the broad line at λ 6560. Swings* has made a number of tentative identifications of the Herzberg bands of O_2 (the forbidden transition $^3\Sigma_u^+ \rightarrow ^3\Sigma_g^-$) between λ 3110 and λ 4174 with bands of the night sky.

The polar aurora, like the non-polar aurora, has the two oxygen lines as a prominent component. The dominant bands in a polar aurora are those of the ionized N_2^+ molecule ($^2\Sigma \rightarrow ^2\Sigma$). The Vegard-Kaplan bands are unimportant; a few of the First Positive bands are present, and some of the Second Positive bands ($C^3\Pi \rightarrow B^3\Pi$) are also quite strong. The order of excitation of the negative nitrogen bands of N_2^- is 19 volts. Slipher made the discovery that for a limited period, before dawn and after sunset, the polar aurora appears with some strength superposed on the normal spectrum of the night sky. While the excitation of the polar aurora is probably through charged particles from the sun entering the upper atmosphere, the energy of excitation of the non-polar aurora is, according to Chapman's theory,† derived from the energy of recombination of oxygen atoms. His views are briefly as follows. The main constituents of the upper atmosphere are thought to be N_2 molecules and O atoms, the latter having been produced by sunlight and possessing an energy of recombination of 5.1 volts. Their recombination requires, however, the participation of a third particle so that conservation of energy and momentum may be secured. If the third particle is a N_2 molecule it will not be excited, since about 6.2 volts is necessary, but if the third particle is an oxygen atom the latter may be raised to the 1S state (4.2 volts), and the balance of energy becomes kinetic energy or energy of excitation of the O_2 molecule formed. The 1S oxygen atoms which emit the green line descend to the metastable 1D state (1.96 volts above the normal). Should these 1D atoms recombine with normal 3P oxygen atoms, the total energy available, viz. $5.1 + 1.96$ volts, will, if the third particle is now a N_2 molecule, be able to excite the latter. In this way the main features of the non-polar aurora may be accounted for. The detailed application of this theory has been given in a review by Elvey.‡

* *Astrophys. Jour.*, vol. 97, p. 72 (1943).

† *Phil. Mag.*, vol. 23, p. 657 (1937).

‡ *Rev. Mod. Phys.*, vol. 14, p. 140 (1942).

(2) *Cometary Spectra*

Although the spectra of comets have been studied extensively in recent years there still remain problems associated with the structure and behaviour of these bodies. The nucleus of a comet is assumed to be an aggregation of meteorites. At a great distance from the Sun there is little or no perceptible luminosity. Under the increasing influence of solar radiation occluded gases are set free. Some of these molecules are polyatomic, containing chiefly the elements carbon, hydrogen, oxygen, and nitrogen. Photo-dissociation and excitation of such molecules take place under the action of sunlight. With the approach of the comet to the Sun it develops around its nucleus a luminous atmosphere which is called the head or coma. The brightness of this increases (in an absolute manner) with diminishing solar distance. The tails of the comets appear usually at something under 2 astronomical units,* and it is calculated that under radiation pressure

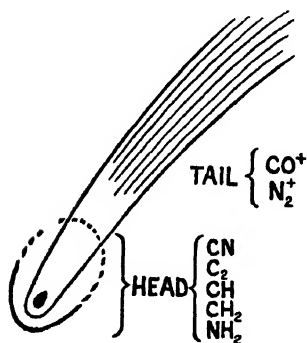


Fig. 145.

from the Sun the molecules constituting the tail may be driven away by a force several thousand times as large as the gravitational attraction, corresponding to velocities of several km./sec.

Many of the properties of comets, their activity in producing gaseous fans and jets, their shape, their luminosity, and their spectra, depend on the heliocentric distance, but it is not safe to make generalizations. It is clear that comets differ greatly in their ability to generate gases out of their nuclei, that the constituents may differ in their proportions in different comets, and in the same comet at successive appearances.

The spectra of comets have been observed between λ 3000 and λ 6600, but inevitably not under high dispersion. The molecules whose spectra have been established are: OH, CN, C₂, NH, NH₂, CH, CH₂, CH⁺, CO⁺, and N₂⁺, and these are distributed in various parts of the cometary structure (see Fig. 145). Most of the molecules are confined to the head, but CO⁺ and N₂⁺ are exclusive to the tail; the bands of CO⁺ (² $\Pi \rightarrow$ ² Σ) known as the Comet-Tail bands are shown in Plate IV. In addition to molecular spectra, continua are found both in the head and tail. The obvious explanation is in terms of fine dust particles reflecting sunlight, but the progressive shift in the maximum of intensity from the violet to λ 4700 in passing from the nucleus down the tail, recorded by some observers, suggests that the continuous spectrum may not be exclusively of the origin mentioned.

The dominant band systems of the heads of comets are the Swan system of the C₂ molecule (³ $\Pi \rightarrow$ ³ Π) (see Plate I) and the violet CN system (² $\Sigma \rightarrow$ ² Σ) (see Plate VII). The violet CH band at λ 4315 (² $\Delta \rightarrow$ ² Π) is usually strong. A well-known strong group of bands about λ 4050 for long puzzled spectroscopists, but has recently been

* 1 astronomical unit = distance of Earth from Sun.

assigned by Herzberg to a CH_2 molecule. Recent detailed investigation of the yellow-red region of cometary spectra, and comparison with the spectrum of the oxy-ammonia flame, leaves little doubt of the existence of NH_2 and NH molecules in the former. These are presumably formed by photochemical decomposition of NH_3 .

In addition to the continuous spectrum and molecular bands, the yellow sodium lines occasionally appear in emission. This is generally in the case of comets which make a comparatively close approach to the Sun, and occurs over this part of the path.

One of the significant things about all the molecular spectra appearing is that they represent electronic transitions to the ground state. This is consistent with the generally held view that the excitation of these band systems is by the absorption of the corresponding frequencies from the solar spectrum and their re-emission, a resonance-fluorescence mechanism. Calculations based on this assumption of the luminosity of comets give the estimated partial pressure of C_2 molecules as 10^{-10} mm. in the cometary nucleus. In the rest of the head and in the tail the pressures must be much less than this. It is at any rate clear that the mean free paths of the molecules will be so great that collisions will be a rarity. From this it follows that the distribution of energy among the rotational states of molecules will not necessarily be related to temperature in the usual way.

Intensity measurements on CN and CH bands in comets have recently been made by McKellar and others, with a view to elucidating some of these problems. It has been known since 1908 that the intensity distribution in the $\lambda 3883$ (0,0) CN band of most comets was peculiar, suggesting a duplicity of structure or an over-population of a group of rotational states. It was thought that the phenomenon might be similar to one found in the spectrum of CN, excited in active nitrogen, and attributed to intersection of a $^2\Pi$ state with the upper $^2\Sigma$ state. But the transfer of molecules from a $^2\Pi$ to $^2\Sigma$ state involves collisions, and the low cometary density precludes this. Another theory supposed that the production of CN by photo-dissociation of a parent molecule C_2N_2 might lead to the over-population of certain rotational states of CN. What now appears to be the true explanation was suggested by Swings,* and based upon the resonance-fluorescence mechanism of excitation. It is simply that we should anticipate that the number of CN molecules raised to an upper level will depend on the intensity of sunlight of that frequency. In other words, allowing for the radial velocity of the comet relative to the Sun, the cometary emission bands should reflect the contour of solar emission in that region. Intensity measurements have given strong support to the correctness of this view.†

Careful examination of the intensity maximum of the $\lambda 3883$ CN band also revealed that the maximum was displaced towards higher rotational quantum numbers as heliocentric distance decreased, corresponding to an increase of 'effective' rotational temperature. In the case of Comet 1940 (c) the curve of intensity distribution for $r = 0.92$ Ast. U. corresponded to a rotational temperature of 300°K. , for $r = 0.54$ Ast. U. the temperature was 435°K.

* *Luck Obs. Bull.*, vol. 19, p. 131 (1941).

† See *Rev. Mod. Phys.*, vol. 14, p. 179 (1942).

An abnormal intensity feature found in the CN bands of several comets is the unusual strength of $P(3)$ and $R(1)$, i.e. of $K' = 2$. This level appears to contain two or three times the normal number of molecules. It should be remembered, however, that in computing the anticipated intensity distribution, a Boltzmann distribution of rotational energies in the lower state is assumed, and this may not be the case under cometary conditions.

The rotational temperature deduced from the $\lambda 4315$ CH band was about 200°K. , considerably less than that inferred from CN. Two suggestions made by Wurm may possibly explain the lower value. The first suggestion is that because of its greater asymmetry CH has a larger dipole moment than CN, hence the mean lifetime of CH on its various rotational levels may be expected to be shorter, and hence pure-rotation transitions in the far infra-red should be more frequent, and hence the lower rotational levels would become more populated. The second suggestion made is that the strong Q branches of CH ($\Delta K = 0$) would reduce by their presence the tendency of molecules by absorption and emission of solar radiation to reach larger values of K' .

The mechanism of ionization of CO and N_2 to give the dominant band spectra of comet tails is mysterious. For CO the ionization energy is 14.1 volts (corresponding to $\lambda 880$); for N_2 the ionization energy is 15.5 volts (corresponding to $\lambda 800$). Photo-ionization by solar radiation is improbable, because if the Sun radiates as a black body at 6000°C its continuum will be weak in this region, and will be further reduced by the continuous absorption beyond the Lyman series limit at $\lambda 912$. Ionization of CO and N_2 may possibly be by solar electrons, or it may be achieved in several stages.

Some interesting papers on cometary spectra are mentioned below.*

(3) Planetary Spectra

It is well known that the Earth's atmosphere is opaque to radiations of shorter wave-length than $\lambda 2900$. The absorption below $\lambda 2400$ is due to a forbidden $\Sigma^+ \leftarrow \Sigma^-$ transition of the O_2 molecule and the continuum associated with this system. The oxygen atoms formed by this are responsible for the production of O_3 (ozone) molecules, and these have a strong absorption in the region $\lambda 3000\text{--}2400$. In the infra-red beyond 13μ the absorption of H_2O and CO_2 in the Earth's atmosphere cuts off most radiation from outside. Between these limits, various absorption bands, collectively called the telluric bands, have been carefully measured, and are due to the following molecules in the Earth's atmosphere: O_2 , CO_2 , H_2O , O_3 , N_2O , N_2O_5 , and HDO . The existence of the three last-named has been demonstrated by Adel by a detailed analysis of the solar spectrum in the infra-red.

A precise knowledge of the absorption of the Earth's atmosphere is clearly of great importance before proper interpretation of any

* Several aspects in: *Rev. Mod. Phys.*, vol. 14, p. 172 (1942). CH_2 : Herzberg, *Astrophys. Jour.*, vol. 96, p. 314 (1942). CH: McKellar, *Astrophys. Jour.*, vol. 98, p. 1 (1943). NH_3 : Swings, McKellar, and Minkowski, *Astrophys. Jour.*, vol. 98, p. 142 (1943). CN: McKellar, *Astrophys. Jour.*, vol. 100, p. 69 (1944). Comet 1942 (c): McKellar, *Astrophys. Jour.*, vol. 99, p. 162 (1944). Comet 1940 (c): Bobrovnikoff, *Astrophys. Jour.*, vol. 99, p. 173 (1944).

celestial spectra is possible. It would seem that absorption bands due to certain molecules in the Earth's atmosphere would make impossible the detection of these same absorption bands in planetary spectra. Fortunately, however, the Doppler effect will give rise to a lack of precise coincidence of the bands from these two sources. Of course gases not present in the Earth's atmosphere, such as methane (found on Jupiter, Saturn, Uranus, and Neptune), are easily detected.

	Radius	Mass	Density	g	v	Atmosphere
Moon .	0.273	0.01226	3.33	0.1645	0.212	None
Mercury	0.403	0.034	2.86	0.2093	0.290	None
Venus .	0.989	0.820	4.86	0.8383	0.910	O ₂ and H ₂ O doubtful; CO ₂ abundant.
Earth .	1.000	1.000	5.52	1.0000	1.000	N ₂ , O ₂ , CO ₂ , H ₂ O, rare gases
Mars .	0.538	0.081	3.84	0.3717	0.447	O ₂ and H ₂ O, traces CO ₂ ?
Jupiter	11.26	317.1	1.30	2.501	5.32	NH ₃ , CH ₄ , H ₂
Saturn.	9.45	95.02	0.69	1.064	3.17	NH ₃ , CH ₄ , H ₂
Uranus	4.19	14.74	1.10	0.840	1.88	NH ₃ (trace); CH ₄ abundant, H ₂
Neptune	3.89	17.27	1.62	1.111	2.12	NH ₃ (trace); CH ₄ abundant, H ₂
Pluto .	—	1.0 ± 0.1	—	—	—	Probably none

Data for the Earth: radius, 6378.39 km.; mass, 5.966×10^{27} gm.; $g = 980.6$ gm. sec.⁻²; $v = 11.188$ km./sec.

The spectra of the Moon and Mercury are the same as that of the illuminating sunlight, and are almost certainly devoid of atmosphere, for the following reasons:

(1) They do not have a sufficient gravitational attraction to retain one. We can calculate, for example, that if a body were thrown off the surface of the Earth with a velocity of less than 5 miles/sec. it would return; if its velocity were between 5 miles/sec. and 7 miles/sec. it would move round the Earth in an orbit; if its velocity were greater than 7 miles/sec. it would escape from the Earth's gravitational field. The velocities of escape from the various planets are given in column 6 of the table.* The mean velocities of various molecules can easily be

calculated by kinetic theory from $v = 0.158 \sqrt{\frac{T}{M}}$ km./sec., where T is the absolute temperature and M the molecular weight. The Earth should therefore only lose very slowly even so light a gas as H₂, for its mean velocity at 273° K. is but 1.85 km./sec. Jeans has given an approximate formula for the rate of escape of a gas: but a phenomenon such as possible high temperatures in the F layer of the stratosphere may invalidate its results. It is possible, therefore, to calculate whether a given gas will be lost from any planetary atmosphere, provided that an approximate value of the temperature is known. The bright side of the Moon is about hot enough to boil water; the bright side of Mercury is possibly 350° C., although the dark side (it is not rotating) is probably extremely low.

* Data from Wildt, *Rev. Mod. Phys.*, vol. 14, p. 152 (1942).

(2) The albedo (which is the per cent. reflexion of the total light falling on it) is too low to suggest an atmosphere. In the case of both the Moon and Mercury the albedo is only 7%. Even a clear atmosphere would give a higher albedo than this. Venus, in contrast, which is covered with dense cloud entirely obscuring the surface, has an albedo of 59%. From the intensity of Earthshine reflected from the dark part of the Moon, it is calculated that the Earth's albedo is at least six times that of the Moon.

(3) The suddenness of the occultation of a star by the Moon's disk, revealing the apparent absence of refraction and dimming also suggests that there is no atmosphere on the Moon.

The planet Venus has been studied intensively by the spectrograph. The brilliant and dense cloud stratum covering the planet limits this study to the atmosphere above the cloud layer. The atmosphere of Venus has been shown by Adams and Dunham to contain abundance of CO_2 . Estimates made suggest several hundred metre-atmospheres, at least a few hundred times the abundance in the Earth's atmosphere. On the other hand, tests for O_2 and H_2O reveal that these must be scarce, if not absent. Upper limits to the amount of oxygen are 1 metre-atmosphere, and as regards H_2O , the equivalent of 1 mm. of precipitable water. If the cloud stratum of Venus is composed of water vapour, the failure to detect H_2O in the atmosphere above it is remarkable, since it is calculated that the huge mass of CO_2 would produce a 'greenhouse' effect, and raise the temperature beneath it probably close to the boiling point of water. It has been suggested that in the absence of a protective screen of O_2 and O_3 , CO_2 and H_2O might interact under the influence of the Sun's ultra-violet radiation to produce formaldehyde $\text{H}\cdot\text{CHO}$, and that the cloud stratum on Venus might consist of this substance. No trace, however, of the formaldehyde bands $\lambda\lambda$ 3500–3000 has been found, and this hypothesis now seems improbable.* Possibly all the H_2O which might otherwise have existed in a free state on Venus is bound in hydrated minerals.

Some of the most interesting work on the atmosphere of Venus has been done by Adel† through his study of the CO_2 bands. The infra-red emission of CO_2 must play an important role in the radiation of Venus. The active fundamentals ν_2 ($14\cdot97\ \mu$) and ν_3 ($4\cdot27\ \mu$) are completely absorbed by the 3 metre-atmospheres of terrestrial CO_2 . There are, however, other emission bands of CO_2 which do not occur in a region of strong terrestrial absorption, viz. $\nu_3 \rightarrow (\nu_1, 2\nu_2)$ which centre round $10\cdot41\ \mu$ and $9\cdot40\ \mu$ and have *P* and *R* branches; also $(\nu_1, 2\nu_2) \rightarrow \nu_2$ near $12\ \mu$, and $(\nu_1 + \nu_2, 3\nu_2) \rightarrow (\nu_1, 2\nu_2)$ near $13\ \mu$. These have been located as emission bands from Venus.

The planet Mars exhibits much surface detail, and the variable character of its appearance suggests a changeable atmosphere. The white strip on the east side of the planet, seen just after sunrise, may be a morning frost, which means, of course, precipitation from an atmosphere. A twilight zone effect due to refraction of the Sun's rays on to the planet after sunset also supports the existence of an atmosphere. Photographs of the planet taken through violet and

* Wildt, *Astrophys. Jour.*, vol. 96, p. 312 (1942).

† Adel, *ibid.*, vol. 93, p. 397 (1941).

infra-red screens, corresponding to wave-lengths of very different penetrating power in the atmosphere, led W. H. Wright to calculate an atmospheric depth of about 60 miles. The polar caps are believed to be frozen water, while the reddish colour of much of the surface suggests an abundance of oxides of iron, in which form much of the oxygen formerly free in the atmosphere may now be combined. Adams and Dunham* have calculated that the free oxygen-abundance on Mars cannot be more than 1% of that found in the Earth's atmosphere. The strengthening of the terrestrial water-vapour bands in the spectrum of Mars is at most 5%. The scarcity of oxygen and the considerably lower temperatures of the planet would make it unfavourable for animal life of the kind we know.

Jupiter, with a diameter eleven times that of the Earth, exceeds both in mass and volume the totality of the other planets. It is characterized by a number of dark belts of cloud crossing the planet and lying parallel to the equator. The spectrum of the planet shows evidence of NH_3 (λ 6400) and also of CH_4 ($\lambda\lambda$ 7260, 6190). Calculations of the surface temperature based on the amount of heat it will receive from the Sun, and also observations made with the radiometer, suggest about -120°C . to -140°C . At such temperatures all water vapour would be precipitated as ice. Possibly the cloud belts are of condensed NH_3 and hydrocarbons.

The surface temperature of Saturn is probably about -150°C . Methane predominates in the spectrum: the NH_3 bands are weaker, possibly due to the precipitation of NH_3 at this low temperature. The very low density of the planet suggests that it has a denser core surrounded by a cloudy atmosphere of very great extent. For Jupiter and Saturn it has been calculated that the methane content may correspond to 0.5 mile-atmosphere. Uranus and Neptune also show the methane bands markedly.

Kuiper† has recently published spectrograms of the major planets and some of their satellites, and has shown that Titan the largest satellite of Saturn, has an atmosphere with appreciable CH_4 content.

It is quite possible that large quantities of molecular H_2 and N_2 may exist in some planetary atmospheres, but being homonuclear their dipole moment is zero, and they have therefore no vibration-rotation bands. Herzberg‡ has recently considered the possibility of detecting these gases either by the faint quadrupole radiation they should emit, or by the expected radiation of the isotopic molecules HD and $\text{N}^{14}\text{N}^{15}$.

(4) Stellar Spectra

The Harvard classification of stars according to their spectra is given in outline. Each class has many subdivisions, and the information supplied under the heading 'Spectral character' gives no more than a general picture of the whole class. As would be anticipated, molecular bands are not found until the temperature falls below a certain level which is possibly about 6000°C . The detection of one

* *Astrophys. Jour.*, vol. 79, p. 308 (1935).

† Kuiper, *ibid.*, vol. 100, p. 378 (1944).

‡ Herzberg, *ibid.*, vol. 87, p. 428 (1938).

Classification	Approx. temp. °C.	Spectral character
<i>P</i>	—	Nebulae. Continuum and bright lines of H, He ⁺
<i>O</i>	To 50000	Bluish-white stars. Bright lines H, He ⁺ and multiply ionized C, N, and O
<i>B</i>	20000	Bluish-white stars. Dark lines of H, He, ionized O, N, Si, etc.
<i>A</i>	10000	White. Hydrogen dominant. Ionized metallic lines
<i>F</i>	7000	Yellowish-white. Metallic lines stronger. Ca ⁺ stronger than H
<i>G</i>	6000	Yellow, e.g. Sun. Neutral metals stronger than ionized. Molecules begin
<i>K</i>	4000	Orange. Lines of Ca ⁺ (H and K) reach maximum. TiO and other molecules
<i>M</i>	3000	TiO bands strong and low temperature lines of metals
<i>S</i>	3000	Similar to <i>M</i> stars but ZrO takes place of TiO. Both may appear
<i>R</i>	< 3000	Very red. Carbon bands C ₂ , CN, NH and continuum. Metallic lines
<i>N</i>	< 3000	Very red. Stronger C ₂ and CN bands, some metallic lines

or two isolated and perhaps faint bands depends very much, however, on the dispersion which can be employed. Thus we are aware of many molecules in the Sun such as MgH, CaH, CH, OH, &c., because of the powerful grating photographs which the intensity of the sunlight has made it possible to obtain. The brightest stars have also been studied under reasonably good dispersion, say 4 or 5 A.U./mm., but in the fainter stars the failure to distinguish bands of some molecules is probably due to inadequate dispersion.

Up to the present no bands of polyatomic molecules have been identified in stellar spectra. Moreover, the observed band spectra of diatomic molecules are practically all resonance spectra, i.e. they represent absorption from the ground state, and not from excited molecular states. The resonance system of H₂ involves a transition of some 11–12 volts which would correspond to a system at about λ 1000, so that no evidence of this molecule can be obtained in stellar spectra, although it may in fact be present. Similarly O₂, CO, and N₂, which may all be present in stellar atmospheres, are unlikely to appear spectroscopically, since their resonance system is below λ 3000.

The *M*-type stars are very remarkable in having their spectra dominated by strong absorption bands of TiO. The ground state is $^3\Pi \leftarrow ^3\Pi$, $^3\Sigma \leftarrow ^3\Pi$, and $^1\Pi \leftarrow ^1\Sigma$. If the last is in fact present it is exceptional as being a system from an excited $^1\Sigma$ level.

The *S*-type stars appear to be a side-branch of the main sequence, lying between *K2* and *M5*, and very similar to the *M* stars, except that ZrO replaces TiO. Sometimes, however, both oxides occur in these stars.

The *R* and *N* classes appear as another side-branch of the main sequence, and are often described as carbon stars. In *R*-type stars the CN bands increase in strength from *R0* to *R5* in which they obtain

their maximum, while the C_2 (Swan) bands increase in intensity from $R0$ to $R8$. In N -type stars the CN bands are very weak, or absent, while the C_2 bands progressively increase.

The molecules so far identified in stellar spectra are :

Hydrides : OH, NH, MgH, AlH, CH, NaH, SiH, CaH, CuH, PH.

Oxides : MgO, AlO, TiO, ScO, YO, VO, SrO, ZrO, MnO, CrO, BO, CaO.

Others : CN, C_2 , CP, SiN, SiF.

The problem of explaining why some molecular spectra are strong, some weak, and others absent, in terms of temperature and relative abundance of the elements, is very complex. Russell made an attempt to explain stellar spectra on the basis of the same relative abundance of the elements as occurs in the Sun, and which was adjudged from the intensities of atomic lines in the solar spectrum. Many other factors may be involved, such as the stratification of some molecules and their opacity to radiations emitted beneath them. It has been suggested that an unusual intensity decrement down the Balmer series found in Me variable stars may be due to a superposed TiO layer above the hydrogen. Recent reviews of molecules appearing in stellar spectra have been made by Bobrovnikoff * and by Howell.†

(b) CHEMISTRY

The study of the spectra of complex molecules is inevitably one of *absorption* spectra. The number of molecules that can be studied in the vapour state is limited, and the spectra of complex polyatomic molecules are difficult to interpret. The moment of inertia may be so large that fine structure even in the vapour state is unresolvable, and the variety of vibrations and their mutual interactions make their identification with particular bands difficult. The examination of solutions has the disadvantages that the close molecular packing results in the broadening of all the bands, so that often little more than a synthesis of band contours is recorded. Also the absorption of the solvent itself may limit investigation considerably. Substances which are water-soluble but not fat-soluble cannot, for example, be investigated in the infra-red. Here, however, Raman spectra provide a line of investigation, since the monochromatic radiation used can be in the visible or ultra-violet, in which region the absorption of water is very small.

Absorption spectra in the visible and ultra-violet are subject to the limitation already mentioned, that free rotation is eliminated and vibration is substantially modified by the molecules of the solvent medium, so that we have to deal usually with an absorption contour with a few possibly ill-defined maxima and minima. An absorption curve such as that shown in Fig. 146 may be regarded as typical, and Brode's analysis into component vibrational bands is given also. It is probable that in this particular case we have the formation of $CoCl_4^{--}$ ions. The vibrations of this type of structure have already been

* *Astrophys. Jour.*, vol. 89, p. 301 (1939).

† *Proc. of Seventh Summer Conference on Spectroscopy at Massachusetts Inst. of Technology*, p. 128 (John Wiley and Son, 1939).

considered, where the metallic atom is probably at the centre of a tetrahedron of halogen atoms. The component frequencies are presumably among those described on p. 219 (Fig. 117), possibly comprising overtones and combinations of them. The associated electronic absorption which brings these bands into the visible region is possibly due to an electron transition from the $4s$ orbit to the incomplete $3d$ shell of the metal.

A few generalizations as to the correlation of chemical structure

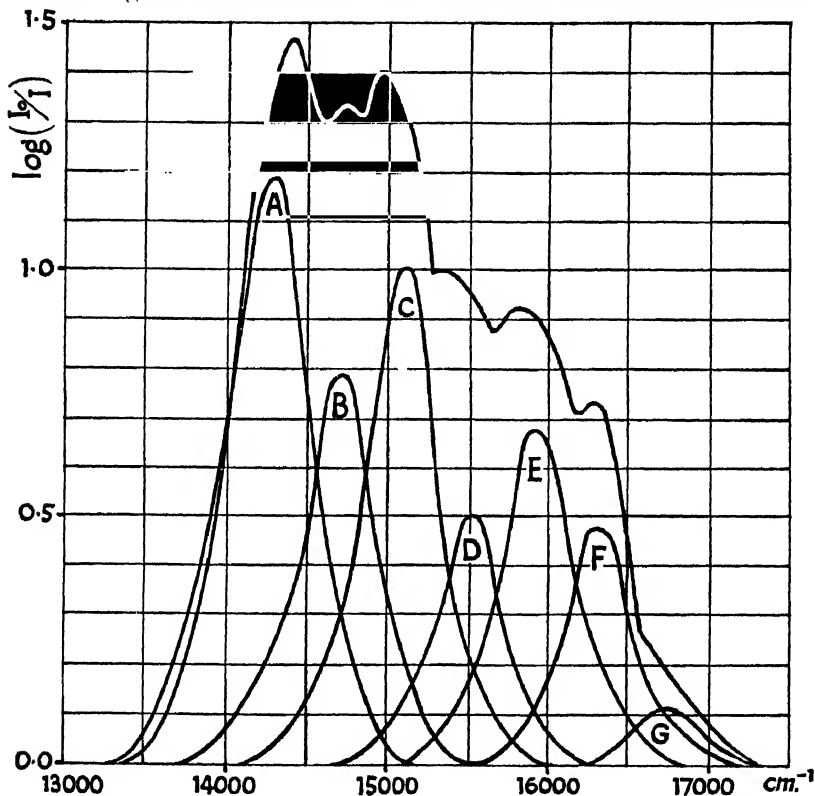


Fig. 146. Absorption of CoCl_2 in conc. HCl , and its analysis into component vibrational bands. (After Brode, *Proc. Roy. Soc.*, vol. 118, p. 286 (1928).

and spectra have been made. The following are taken from a review by Loofbrouw * of *Borderland Problems in Biology and Physics* :

(1) Absorption spectra associated with an electronic transition and the vibration of unsaturated bonds are generally in the region $\lambda\lambda$ 8000–2000, while those of saturated bonds are in the far ultra-violet.

(2) As we should anticipate, the attachment of a heavier atom or group to a bond results in a diminution of the associated vibration frequency.

* *Rev. Mod. Phys.*, vol. 12, p. 317 (1940).

(3) The effect of single, i.e. saturated, linkages in a chain, tends to isolate vibrating groups from each other, with the result that the total absorption tends to become the sum of the unmodified individual absorption bands.

(4) In contrast with this, double bonds, unsaturated linkages, transmit vibration along a chain to a considerable extent, and this 'loading' effect, as expected, results in a displacement towards lower frequencies.

(5) The loading of a vibration, whether as described in (2) or (4) above, results, in general, in increased absorption.

(6) Other factors are also responsible for changes in absorption spectra, such as salt formation due to change in pH , 'association' effects, and molecular re-arrangements (tautomerism). An example of the first of these factors is given by Callow,* who showed that oestrone showed an increase in the absorption peak intensity, and a shift from λ 2800 in acid solution to λ 2950 in alkaline solution. Fig. 147 is taken from a paper of E. F. Holiday,† and shows the variation of extinction coefficient with pH of the solution. There is a large class of substances used as indicators in which change in pH results rather in a change in the intensity of an absorption band than a displacement. Commonly, the absorption in one part of the visible spectrum will increase, and in another part of the visible it will simultaneously decrease, resulting in a colour change.‡

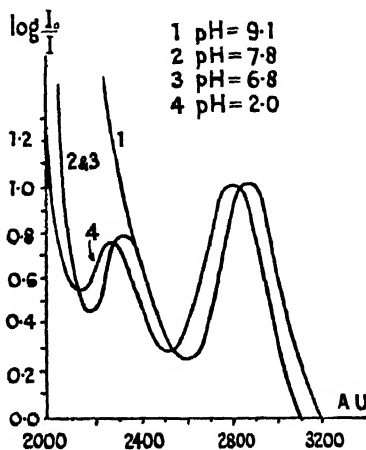


Fig. 147. Uric acid absorption showing the effect of hydrogen-ion concentration. (After Holiday.)

The phenomenon of 'association', more especially associated with the hydrogen bond, as in CH , OH , or NH , is as follows. The H atom may come into close association with another atom or group X (perhaps on another part of the same molecule or possibly on a different molecule), and a loose bond with it may thus be created such as $OH-X$. The result of this will be, in general, a modification both in position and in intensity of the normal OH vibration. The CH vibration is about 3000 cm^{-1} , the OH and NH vibrations are about $3400\text{--}3500\text{ cm}^{-1}$. They or their overtones in the region 7000 cm^{-1} may be examined in the near infra-red if the parent substance is dissolved in CCl_4 as solvent. Pauling§ has listed scores of substances in this way, and it is found that where conditions favourable to a strong H -association bond are present, the expected absorption peaks are weak and diffuse. If such an association-bond is not possible

* *Biochem. Jour.*, vol. 30, p. 906 (1936).

† *Ibid.*, *Jour.*, vol. 24, p. 621 (1930).

‡ Stenstrom and Reinhard, *Jour. Phys. Chem.*, vol. 29, p. 1477 (1925).

§ *Nature of the Chemical Bond*, p. 318 (Cornell Univ. Press, 1939).

the OH or NH vibration is strong and sharp. The OH group in phenol, for example, has a strong peak about 7050 cm^{-1} , but in ortho-nitrophenol the formation of an association bond, as in Fig. 148 (b), results in its virtual disappearance. On the other hand, substitution of the nitro-group in the meta- or para-positions leaves the absorption peak unaffected. In the case of another class of molecules, such as ortho-chlorophenol, there is no strong association bond formed between the H and Cl atoms, but because of the slightly ionic character of the C—Cl and OH bonds giving Cl a negative character and H a positive one, there is an appreciable interaction which displaces the absorption peak of OH to 6890 cm^{-1} . As indicated in Fig. 148 (c) and (d), since two forms of the molecule are possible, we should expect two absorption peaks, one displaced as mentioned above, and the other undis-

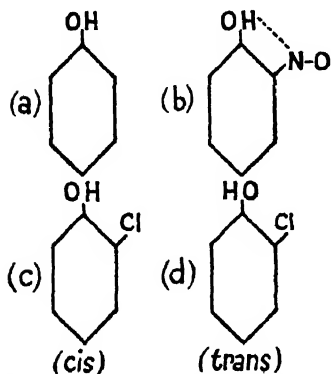


Fig. 148. (a) Phenol, (b) *o*-Nitrophenol, (c) *o*-Chlorophenol (*cis*), (d) *o*-Chlorophenol (*trans*) to illustrate 'association' effects.

placed at about 7050 cm^{-1} , and this is in fact observed. The *cis*-form is the more favoured one, the 6890 peak having an area about ten times that of 7050 . Still another absorption band at 6620 cm^{-1} observed in the liquid *o*-chlorophenol has been attributed to further modification of the OH frequency through an association bond formed between pairs of molecules. The O atom of the *cis*-form forms this bond with the H atom of the hydroxyl group of the *trans*-form. For fuller details of H association bonds Pauling's book should be consulted.

The influence of molecular rearrangement on absorption bands is, of course, a fundamental subject. Upon an understanding of this depends the possibility of using absorption spectra

to help in unravelling chemical constitution. The demonstration that synthetic substances are identical with natural products depends also on this. The mass of data accumulated for a great variety of substances is enormous. The student will find a brief résumé with many references to original papers in Loofbourrow's review (*loc. cit.*), or may study the principal features in Brode's book.* Brode published a series of papers on the relation between absorption spectra and chemical constitution of certain azo-dyes, and we use below by way of illustration some of the data and results of the first of these papers.† In Fig. 149 is shown the absorption of benzene azophenol in a 3% aqueous solution of NaOH. Close examination shows that the main absorption band at about $23,300\text{ cm}^{-1}$ is a synthesis of two close components of which the low-frequency one may be called *A*, and the high-frequency one *B*.

The absorption spectra of the mono-methyl substitution derivatives and of di-methyl substitution derivatives were determined so that the effect of 'position isomerism' could be known.

In the table on p. 235 the second column describes the position

* *Chemical Spectroscopy* (John Wiley and Son, N.Y., 1939).

† *J.A.C.S.*, vol. 51, p. 1204 (1929).

of the substituted methyl group or groups. A and B are the intensities of the two components of the peak at $23,300\text{ cm}^{-1}$. The sum $A + B$ measures the total band intensity, and the last column but one gives the ratio $A/(A + B)$. Brode drew the following conclusions for this particular dye: (a) The ratio of the intensities of the two components depended on the nature of the solvent and on the position of the substituted group. An *o*-substitution favours A at the expense of B ; an *m'*- or *o'*-substitution does the reverse, while *m'* and *p'* practically

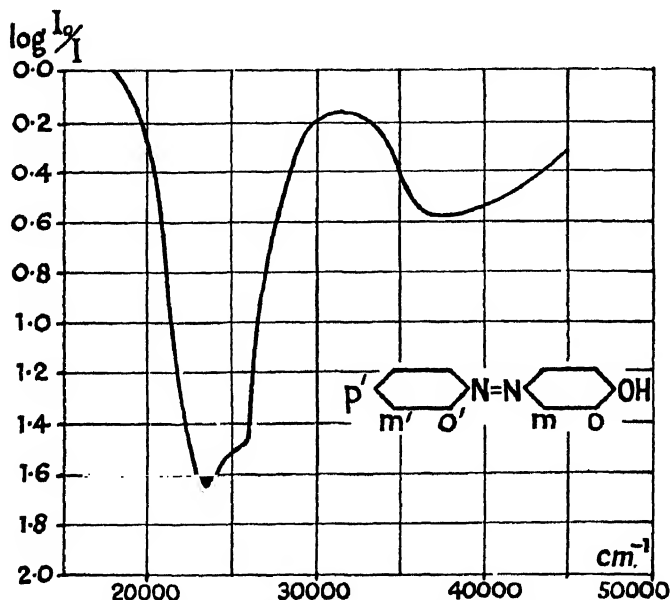


Fig. 149. Absorption spectrum of benzene azophenol. (After Brode.)

give no change. (b) Substitution in the p' -position causes an increase in the total intensity $A + B$ whatever the solvent. (c) Substitution in the o' -position, in contrast, causes a fall in total intensity. (d) The

Compound	Position of CH_3	A	B	$A + B$	$\frac{A}{A + B}$	Group
Benzene azophenol .	—	1.53	1.29	2.82	0.543	(4)
Benzene azo- <i>o</i> -cresol .	<i>o</i>	1.82	0.85	2.67	0.682	(5)
Benzene azo- <i>m</i> -cresol .	<i>m</i>	1.38	1.29	2.67	0.518	(3)
<i>o</i> -Toluene azophenol .	<i>o'</i>	1.18	1.40	2.58	0.457	(2)
<i>m'</i> -Toluene azophenol .	<i>m'</i>	1.50	1.26	2.76	0.543	(4)
<i>p</i> -Toluene azophenol .	<i>p'</i>	1.57	1.32	2.89	0.542	(4)
<i>o</i> -Toluene azo- <i>o</i> -cresol .	<i>o'o</i>	1.47	1.06	2.53	0.581	(5)
<i>o</i> -Toluene azo- <i>m</i> -cresol .	<i>o'm</i>	1.06	1.34	2.40	0.442	(1)
<i>m</i> -Toluene azo- <i>o</i> -cresol .	<i>m'o</i>	1.92	0.90	2.82	0.680	(5)
<i>m</i> -Toluene azo- <i>m</i> -cresol .	<i>m'm</i>	1.40	1.31	2.71	0.517	(3)
<i>p</i> -Toluene azo- <i>o</i> -cresol .	<i>p'o</i>	2.05	1.02	3.07	0.668	(5)
<i>p</i> -Toluene azo- <i>m</i> -cresol .	<i>p'm</i>	1.52	1.42	2.94	0.517	(3)

effect of the di-substituted derivatives is to some extent what may be expected as the resultant of the two mono-methyl substitution effects.

The same general characteristics are found (see Fig. 150) for other substituted groups.

The ratios of $\frac{A}{(A+B)}$ appear to fall into about five groups, which

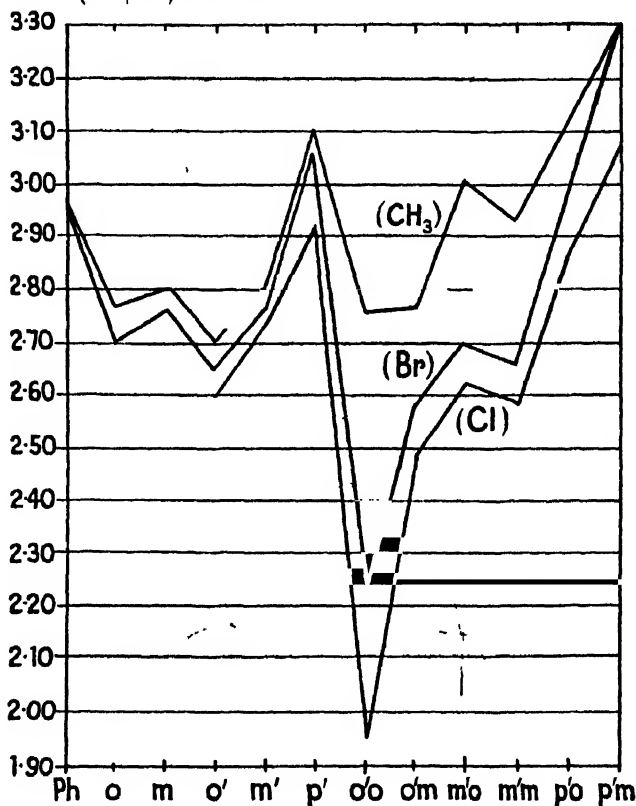


Fig. 150. Extinction values for the substitution of CH_3 , Cl , and Br respectively in benzene azophenol. (After Brode, *Proc. of Sixth Summer Conference on Spectroscopy at Massachusetts Inst. of Technology*, p. 130 (John Wiley and Son, 1939).)

are labelled in the last column of the above table. The determination of $\frac{A}{A+B}$ for an unknown methyl substitution product of benzene azophenol should therefore be of value in determining its structure.

Although the precise feature of the molecule's structure responsible for these two close absorption peaks is not clear, the empirical knowledge outlined may be of practical use. Much of the correlation of absorption spectra and chemical structure is at present of this empirical kind.

(c) BIOCHEMISTRY

The field of application of absorption spectrophotometry to substances of biochemical interest such as carbohydrates, fatty acids, amino acids, proteins, purines, and pyrimidines, and polycyclic hydrocarbons is enormous. Loofbourow's review * of this may be consulted for numerous references to original papers.

(1) *Proteins*

In the case of proteins their absorption is accounted for by the sum of the amino-acid absorptions, which means in practice those of tyrosine, tryptophane, and phenylalanine, since the others have only general absorption rising slowly from λ 2500 towards shorter wavelengths. In the nucleo-proteins the nucleic acid contributes materially to the spectrum, and the absorption of the latter is largely due to the contained purines and pyrimidines. One of the most promising applications of absorption spectrophotometry is to the detection of small amounts of such substances in biological fluids. The possibility of greater success in this field appears to depend, in part, upon the preliminary separation of various fractions by physical or chemical means, in order that the superposition of absorption curves does not obscure the maxima and minima looked for. Such a procedure is described in a paper of Lavin † due to Dobriner, and applied to urine and blood. The ether-soluble compounds were treated with sodium carbonate and then with sodium hydroxide, so as to separate the acid and phenolic compounds. The neutral substances are retained by the ether. The phenolic substances were subdivided by steam distillation into volatile and non-volatile compounds.

In the case of the amino acids, tyrosin, tryptophane, and phenylalanine, a certain amount of detailed structure ‡ (presumably vibrational in origin) facilitates the identification of these substances in the absorption spectra of proteins. The wave-lengths of these bands are :

VIBRATIONAL BANDS OF AMINO ACIDS

Tyrosin . . .	—	—	—	—	—	—	—
Tryptophane . .	—	—	—	—	—	—	—
Phenylalanine . .	2366	2418	2466	2517	2574	2606	2635
Tyrosin . . .	2672	—	—	2747	—	2816	—
Tryptophane . .	—	2694	—	—	2794	—	2888
Phenylalanine . .	2671	—	2714	—	—	—	—

The absorption of blood serum is very substantially due to the contained tyrosin and tryptophane. The quantitative determination of these two acids by means of absorption spectrophotometry has been

* *Rev. Mod. Phys.*, vol. 12, p. 318 (1940).

† *Proc. of Seventh Summer Conference on Spectroscopy at Massachusetts Inst. of Technology*, p. 107 (John Wiley and Son, 1939).

‡ Coulter, Stono, and Kabot, *J. Gen. Physiol.*, vol. 19, p. 739 (1936).

worked out by Holiday.* A summary of this is given by R. A. Morton † in his book.

(2) *Hormones*

Where, as in the case of pituitary hormones, there is no specific absorption by which they can, in general, be differentiated from one another, but only the typical absorption of animal protein, special methods of estimation have been devised. The hormonal extracts as such may be unsuitable for testing, since the absorption they give may be quite obscured by that of inactive proteins. In the case of the androgens (male hormone-producing substances), the method used was to add a reagent with which the androgens would interact to form substances having strong absorption in a part of the spectrum where the absorption of the inactive substances was not strong. Zimmerman ‡ first showed that on treatment with *m*-dinitrobenzene in the presence of an alkali strongly coloured compounds were formed. Androsterone gives quite a different absorption from testosterone. Langstroth § has shown how spectrophotometry may then be used to determine the amounts of these two hormones present in a mixture.

(3) *Enzymes*

Enzymes are catalysts produced by living cells to facilitate some essential process, thus enabling it to proceed at an adequate speed under the comparatively low temperature conditions of living tissue. Enzymes are found to consist of two essential parts. One part is called the co-enzyme, which is a substance of relatively low molecular weight. This contains the 'prosthetic group', which is the site of the interaction between the enzyme as a whole and the 'substrate' or substance undergoing the change. The co-enzyme may be detached chemically from the enzyme as a whole and studied separately. The second part of the enzyme is a large protein molecule to which the co-enzyme is attached, and which in turn attaches it to the substrate. The particular protein carrier controls the specificity of the enzyme action: thus the same co-enzyme attached to different protein carriers produces specific and quite different functioning enzymes. R. A. Morton in Chapter X of his book (*loc. cit.*) has given a brief review of respiratory enzyme mechanisms. Hogness ¶ has also reviewed the data and the possibilities of spectroscopic study of respiratory enzyme action. It is familiar knowledge that sugar or some other substrate disappears when oxygen is used up, while CO₂ and H₂O appear, in the respiratory processes of cells. The steps by which this happens have been clarified by the use of absorption spectrophotometry. Oxidation commonly takes place in stages, which alternately consist

* *Biochem. Jour.*, vol. 24, p. 619 (1930); vol. 30, p. 1795 (1936); vol. 32, p. 1166 (1938).

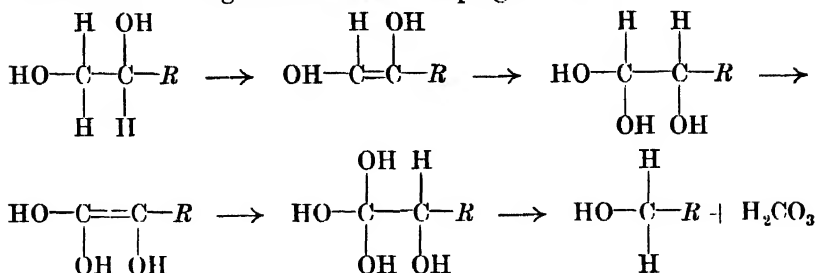
† *The Application of Absorption Spectra to the Study of Vitamins*, Chapter IX (Hilger, 2nd ed., 1942).

‡ *Zeit. physiol. Chem.*, 233, 257 (1935).

§ *Proc. of Seventh Summer Conference on Spectroscopy at Massachusetts Inst. of Technology*, p. 111 (John Wiley and Son, 1939).

¶ *Proc. of Sixth Summer Conference on Spectroscopy at Massachusetts Inst. of Technology* (John Wiley and Son, 1938).

in the removal of two H atoms followed by the addition of H_2O to the molecule. Hogness illustrates the progress thus :



The removal of two H atoms produces a double bond : the addition of H_2O in these circumstances restores the single carbon bond. The

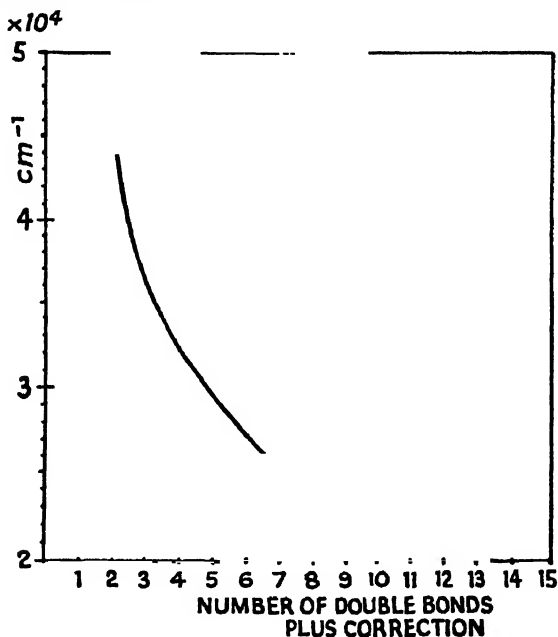


Fig. 151. Relation between position of absorption maximum of sixty-five related substances, and the number of conjugated double bonds. (After T. R. Hogness.)

number of conjugated double bonds in a long chain as we have seen (p. 283) affects both the position and intensity of the characteristic absorption peaks. Consider a series of compounds such as

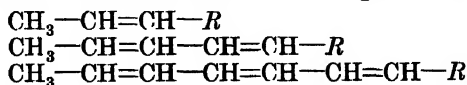


Fig. 151 shows the displacement of the main absorption peak towards long wave-lengths as the number of conjugate double bonds increases.

A correction was made for the nature of the end-group *R*. Thus if *R* was carboxyl (COOH) it was found to be the equivalent of one double bond; if a benzene ring, it was found equivalent to one and a half double bonds

In addition to the variation of *position* of the absorption peak just mentioned, the intensity of the peak was observed to vary linearly with the number of double bonds. Both these features therefore permit the process of oxidation of such compounds in tissues to be followed spectroscopically. The function of some of the respiratory enzymes is to accept the two H atoms from the substrate, and pass them on to other molecules involved in the chain of processes. Such respiratory enzymes frequently show a specific variation in their reduced form (with the two H atoms), as compared with the oxidized (normal) form, so far as the absorption spectrum is concerned. This spectroscopic feature also may be used to study the progress of a reaction.

Hogness and others * have also applied spectrophotometry to the study of chemical equilibria, and free energy changes. Thus, for example, by allowing an enzyme (such as cytochrome C) to come to an oxidation-reduction equilibrium with a coloured dyestuff of known potential, it is possible to calculate the hitherto unknown potential of the enzyme after spectrophotometric estimation of the concentrations of the different substances present. From a knowledge of the potential of the enzyme it is then possible to predict which substances it can react with and at what velocity.

Hogness makes the interesting suggestion that in view of the intimate relationship of cell growth and respiration, abnormal cell growth, as in cancer, will in all probability be associated with some abnormality of cell respiration, and that the spectrograph should be a powerful aid in our final understanding of this disease. With this suggestion the present writer finds himself in cordial agreement.

(4) *Vitamins*

The vast amount of research done on vitamins in recent years may be judged from the reviews of it in several books.† We shall not attempt to do more here than indicate briefly how spectrophotometry has been of assistance in this field. The uses have been chiefly these :

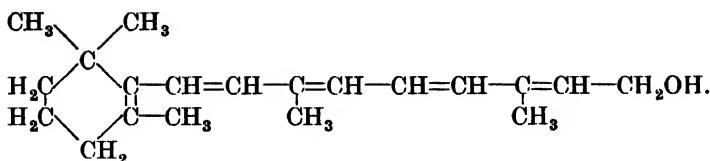
(1) In helping to establish the chemical structure of vitamins. This is a useful technique in the identification of the chemical nature of decomposition products, and also in checking up the identity of the synthetic vitamin and the natural product.

(2) In the work of assaying, or quantitative estimation of the concentration of the vitamin present.

Vitamin A is a fat-soluble alcohol whose formula is $C_{20}H_{20}OH$. Its detailed structure is now known and it can be synthesized :

* *Jour. Phys. Chem.*, vol. 41, p. 379 (1937), and *Jour. Biol. Chem.*, vol. 124, p. 11 (1938).

† Morton, *The Application of Absorption Spectra to the Study of Vitamins* (Hilger, 2nd ed., 1942); *The Nicholas Vitamins Manual* (Nicholas Pty, Ltd., Melbourne, 1943).



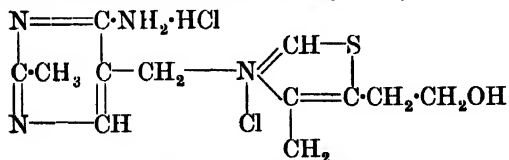
It is described as being 'growth-promoting, anti-xerophthalmic, and anti-infective'. It is produced in the animal body from carotenoids which are vegetable pigments having the formula $C_{40}H_{56}$. The vitamin-A molecule shown above results from the breaking of these carotenes into two and the introduction of H_2O into the gap. The carotenes and closely related pigments occur widespread in nature, in chestnuts, carrots, mountain-ash berries, green leaves and grass, yellow maize, egg-yolks, butter, &c. One of the earliest symptoms of vitamin-A deficiency is partial night blindness; the visual purple on which the functioning of the retinal rods depends is believed to be a conjugated protein with a carotenoid prosthetic group. In distinguishing between the various isomeric carotenes and related pigments the positions of absorption peaks, the general absorption contours, and the actual value of the extinction coefficient $E_{1\%}^{1\text{cm}}$ ($= \log_{10} \frac{I_0}{I}$)

are of great value. The optical rotation is of assistance also in some cases.

Vitamin A has a marked absorption peak at λ 3250, which probably accounts for its photochemical decomposition in the presence of ultra-violet light of this order. The extinction coefficient corresponding to this peak, and also the depth of the blue colour produced by an interaction of vitamin A with SbCl_5 , have been used in assay work. One of the richest sources of this vitamin is that of fish-oils, particularly those derived from the intestinal mucosa of halibut, herring, cod, sturgeon, and trout.

The blue vitamin $A + SbCl_3$ compound has a weak absorption peak at λ 6200, but it was also observed to have a peak of *variable* intensity at λ 6930. This led ultimately to the recognition of a closely related compound labelled vitamin A_2 , possibly $C_{22}H_{31}OH$, with one more double bond than A_1 . Its principal absorption peak in alcoholic solution is at λ 3450 compared with λ 3250 of vitamin A. Vitamin A_2 occurs naturally only in fish, though mammals can apparently store and use it. It only predominates over A_1 in the fresh-water fish.

Vitamin B is water soluble, and is now recognized as a complex of many substances with different physiological functions. Vitamin B₁ or aneurin is anti-beriberi in man. It was obtained pure and crystalline, after much chemical work, from extracts of yeast. The analysis of the vitamin C₁₂H₁₆ON₄S(2HCl), the determination of its structure by R. R. Williams and others, and finally its synthesis, is the record



(Vitamin B₁ hydrochloride)

of brilliant chemical work in which spectrophotometry was constantly used to identify the character of the decomposition products. The technique and the various steps have been described by R. A. Morton and are also reviewed by Ruehle.* We shall therefore not repeat it

here. Ruehle points out in his review that another kind of service was also rendered by absorption technique. The pyrimidine structure is frequently synthesized by coupling together at two places two chain compounds. If conditions are too mild it is possible for coupling to take place at only one point, leaving the ring unclosed. In this case the marked absorption peak found in the region λ 2600 in most pyrimidine compounds is absent. Without making quantitative determinations the organic chemist can thus determine whether he is forming the pyrimidine structure or not. The identity of the natural and synthetic vitamin B₁ was finally checked by an interesting technique. By means of spectrophotometry the absorption curves were compared over a substantial wave-length range of three saturated alcoholic solutions: of the synthetic product, the natural product, and of an equal mixture of the two. It was assumed that if the first two were not identical, then the absorption of the third solution would be approximately twice that of either the first or the second, and would certainly not match with either of them. In fact an excellent match of all three was obtained by experiment for all wave-lengths.

These examples of vitamin investigation will suffice to illustrate the usefulness of spectroscopic technique in this field.

It is not, I think, unreasonable to predict that one of the important applications of absorption spectrophotometry will, at some future date, be in the field of diagnostic medicine. Disorders of metabolism, and the toxins of disease, should reveal themselves to the spectrograph. It may also be shown that in the fields of therapeutic medicine and preventive medicine the irradiation of a patient with light of specific wave-lengths for specific reasons may be of recognized value.

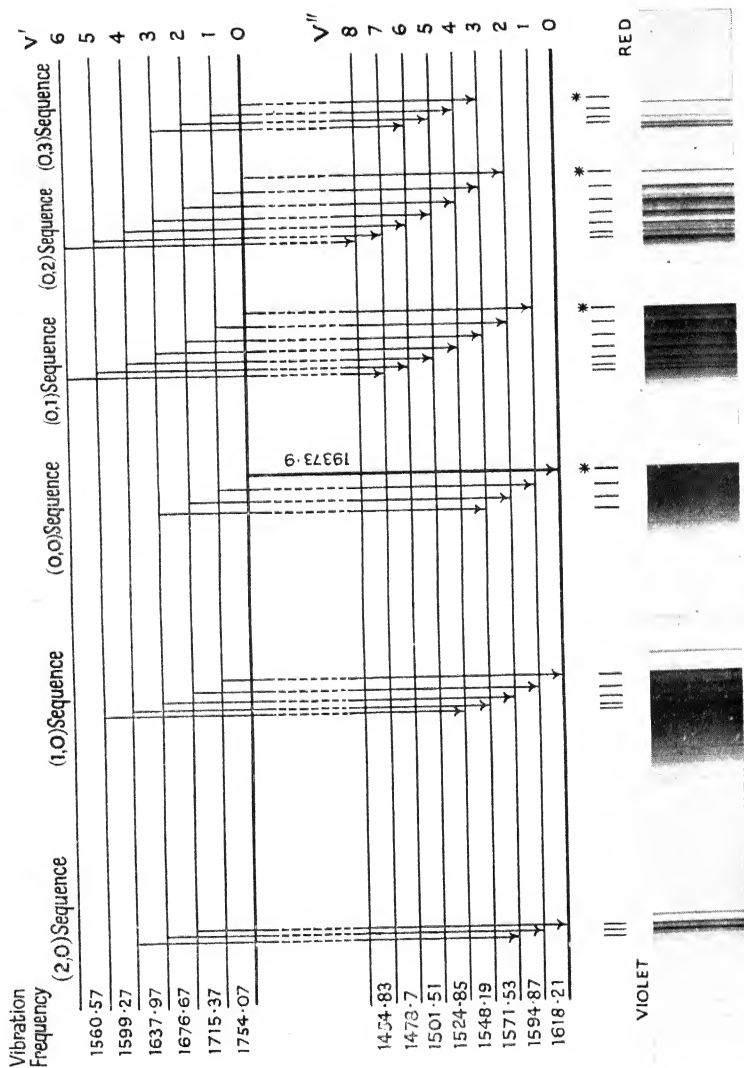
* *Proc. of Sixth Summer Conference on Spectroscopy at Massachusetts Inst. of Technology*, p. 27 (John Wiley and Son, 1938).

INDEX

- ABEGG**, 60
Adams and Dunham, 278, 279
Adel, 209, 211, 278
 and Longair, 55
Andrews, 202
Ångström system, 7, 9, 25, 188 ff.,
 Plate II
Angus and Leckie, 266
Astrophysics, 272
Atom, electronic states of, Ch. VI (b),
 80 ff.
Atomic type of binding, 67
 vectors, precession in a field, 82
Auroræ, 272
Babcock, 272
Badger, 57
Bailey and Cassin, 207
Bands, branches, 7, 9, 12, 105, 108, 110,
 112, Fig. 56
 degradation of, 9, 21
 fine structure of, Ch. I (c), Ch. IX
 heads, 10, 13, 17, 19, 64
 infra-red, 10
 lines and half-width, 78
 multiplicity in, 23
 origins, 10
 progressions, 5
 rotation, 14
 sequences, 5
 system-origins, 15
 ' tails ' in sequences, 27
 vibration-rotation, 11, 12, 60
Barker, 211
Barnes, 234
Bell and Jeppeson, 265
Bengtsson and Rydberg, 78
Bhagavantam, 256, 271
Binding, atomic type (homopolar), 60,
 63, 66, 67
 ionic type (heteropolar), 60, 62, 63,
 66, 67
 of molecules, 91
 Van der Waals, 70
Birge, 54, 55, 62, 73, 158, 173
Bobrovnikoff, 281
Boltzmann, 147, 162, 174, 229
Bonds and vibration frequency, 226
 association effects, 283 ff.
 effect on spectra, 282, 289
Bonner, 207
Brode, 281, 284, 285
Broglie, de, 46
Brown and Gibson, 43
Callow, 283
Childs, 173
Choi and Barker, 227
Clark, 54, 55
Cleeton and Williams, 235
Combination principle, Ch. VIII (c)
Condon, 49. *See* Franck-Condon
Cram, S. W., 72
Crawford, F. H., 181, 188, 189, 200
Crozo, 188
Curtis, 172
Darbyshire, 172
Debye, 43
Dennison, 189, 203, 207, 209, 217, 220,
 223, 225, 232, 234, 235, 236, 238,
 240, 241
Depolarization factors, 256
Deslandres, 188
Deuterium, 176
 deuteride spectra, 180 ff.
Dieke, 142, 146, 177, 179, 181
 and Mauchly, 135
Dissociation, molecular, Ch. V, 93
 through rotation, Ch. V (f)
Doppler, 65, 277
Doubling, Λ -type, 25, Ch. VII (f),
 102 ff., 107, 111, 113
Duffendack, 45, 159, 160
Dufour, 188
Duncan and Murray, 221
Electric fields, effect on atom, 83
 moment, 11, 202, 204, 237
**Electronic configurations and molec-
 ular states**, 86
 states. *See* Molecules
Elliott, 76
Elvey, Swings, and Linke, 272
Energy of Atoms and Molecules, 1
 electronic, 2
 rotational, 2, 13, 59, 95
 vibrational, 2, 13, 59, 95
 of dissociation, 60, 65, 67, 68, 72, 75,
 77
 of vibrating-rotating molecule, 50,
 Ch. IV (e)
Farnworth, 211
Fermi, 262
Fine structure of bands, Ch. IX, 110
Force, Law of. *See* Law
**Force-constants and vibration fre-
 quency**, 226
Fortrat Diagram, 9, 12, 117, 119, 124,
 125, 129, 135
Franck, 60
Franck-Condon theory, Ch. III (a), 35,
 38, 40, 46, 47, 59, 71, 250
Frank and Hognoss, 65
Frederick and Watson, 123
Gamow, 78

- Gaussian error curve, 48
 Gaviolo and Wood, 163
 Gerhard, 240, 241
 Giaque and Johnson, 173
 Ginsberg, 238
 Glockler, 73, 271
- Hardy, 235
 Harvey, 30
 Heitler and London, 40, 49, 62, 70;
 Method, Ch. VI (e), 88 ff.
 Henri, 41
 and Harris, 43
 Herzberg, 30, 43, 89, 93, 210, 273, 275
 Hibben, 225, 268
 Hill, 99, 119, 135, 150, 177
 Hogness, 289, 290
 Holiday, E. F., 283
 Honl, 148
 Hopfield and Birge, 140
 Howell, 281
 Hund, 86, 188, Case (a) Ch. VII, 95
 (b) Ch. VII, 97
 (b) Ch. VII, 98
 (c) Ch. VII, 101 ff.
 (d) Ch. VII, 102 ff.
 Herzberg and Mulliken, Method of,
 89 ff., Ch. VI (f)
- Intensity, alternating, 164 ff.
 factors, 148 ff.
 in a band, Ch. X
 in a system, Ch. III
 variability, 43, 44
 wave-mechanics treatment, 46
- Interval, between band head and
 origins, 19, 21
- Isotopes, effect on polyatomic molecules,
 241 ff.
 effect on spin-doubling, 178
 effect on A-type doubling, 179
 electronic effect, 176
 rare, 173
 rotational effect, 175
 vibrational effect, 170 ff.
- Isotopic multiplicity, 26, 55, Ch. XI
 boron-oxide, 169
 copper halides, 171
 hydrogen chloride, 169
 iodine chloride (ICl), 172
- Ittman, 142
- Jenkins, Dr. F. A., 3, 29, 30, 123, 191
 Jevons, W., Preface
 Johnson, 45
 Johnston, H. L., 177, 179, 234
- Kaplan, 41
 Kapuscinski and Eymers, 155
 Kemble, 188
 Kettering, 202
 King, 173
 Knauss and McCay, 158, 162
 Kondratjew, 65
- Koontz, 179
 Kramers, 101, 188
 Kratzer, 50, 55, 57, 58, 75, 169
 Kronig, 86, 103, 141, 142, 148, 181, 190
 Kuiper, 279
- Landé, 9, 18
 factor, 184
 interval rule, 84
 Langstroth, 288
 Lavin, 287
 Law of Force, internuclear, Ch. V
 Lenz, 188
 Linnett, 220
 Lochte-Holtgreven, 161
 London, 148
 Loofbourow, 282, 284, 287
 Loomis, 169
 Lyman, E. R., 162
- McKellar, 275
 Magnetic fields, Ch. XII
 Paschen-Back Effect, 187
 Zeeman Effect, 184 ff.
- Manning, 218
 Martin, 43, 78
 Mecke, 54, 55, 173, 238
 Metropolis, 248 ff.
 Mills, 199
 Molecular constants, empirical relation
 between, 54
- Molecule, abnormal rotation, 161
 anharmonic-rotating, 47
 dissociation of, Ch. V
 general principles, Ch. V (a)
 electrical moment of, 59, 60
 electronic states of, 54, Ch. VI
 homonuclear molecules, 106, 115,
 Fig. 58, 164 ff.
 internuclear distance, 10
 life period, 41
 metastable, 145
 moment of inertia, 10, 13
 valence bonds in, 93
- Morse, 51, 52, 54, 55, 57
 Morton, R. A., 288, 290, 292
 Mrozowski, 71, 72
 Mulliken, 76, 78, 89, 93, 107, 150, 166,
 170, 179, 181, 188, 201, 210, 246,
 253
- Naudé, 134, 136, 173
 Night sky, 272
 Nolan and Jenkins, 155, 156, 157
 Nuclear potential energy functions, 32
- Okubo and Hamada, 45
 Oldenberg, 54, 73, 78, 158, 162
 Ornstein, 156, 165
- Paschen-Back Effect. *See* Magnetic
 fields
 Patkowski, 172
 Pauli principle, 76, 82, 85, 91, 101, 188

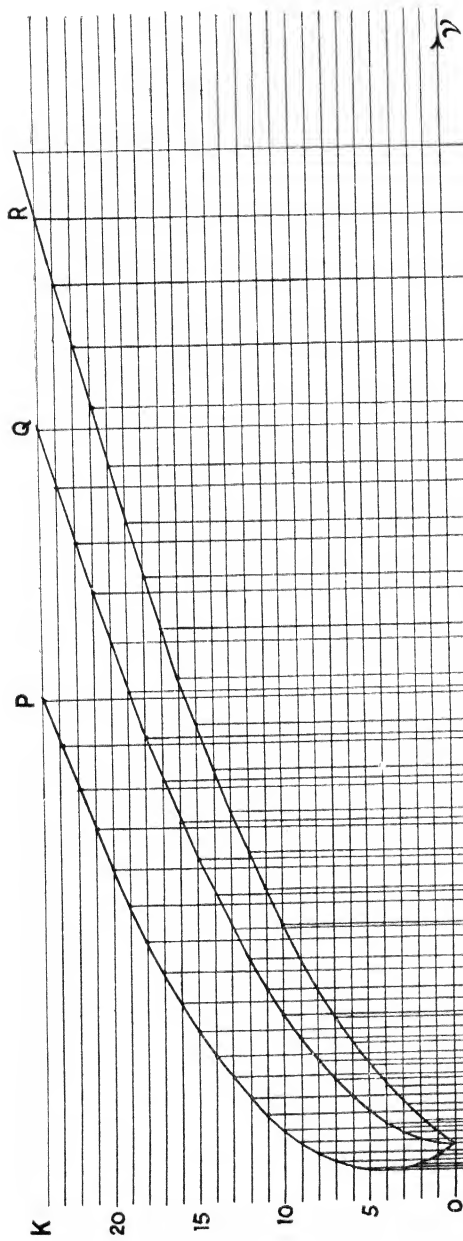
- Pekeris, 58
 Perturbations, 140 ff
 Polarizability, 255. *See also* Raman Effect
 Polyatomic molecules, Ch. XIII
 electronic structure of, 253
 isotopic effects, 241
 rotational spectra, 226 ff.
 asymmetrical molecules, 235 ff.
 electronic bands, 245 ff.
 envelopes of infra-red bands, 240
 linear molecules, 227
 spherical molecules, 229
 symmetrical molecules, 229 ff.
 vibrational spectra, 203 ff.
 ethane, 224
 four-atom molecules, 212 ff.
 five-atom molecules, 219 ff.
 six-atom molecules, 221 ff.
 triatomic molecules, 203 ff.
 Popov, 66
 Pro-dissociation, Ch. III (c), 40, 42, 62
 modification of, 43
 Q branches, 9, 11, 19, 24
 Quantum numbers, half-integral, 15
 Theory, New, 15, 47, 49, 58
 Old, 46, 47
 Raman Effect, Ch. XIV
 Spectra, Acids, 264 ff.
 CHCl_3 , 256
 CO_2 , 262
 NH_3 , 262
 OCS , 262
 organic compounds, 267 ff.
 water of crystallization, 263
 vibration-rotation bands, 257 ff.
 Randall, 238
 Rayleigh, 254
 Richardson, 158
 Rieke, 163
 Rotational levels, positive and negative, 106
 Ruark and Urey, 46, 48
 Ruehle, 292
 Russell, 148, 281
 Rydberg, 56, 176
 Salant and Rosenthal, 244
 Schumann, Schumann-Runge, 70
 Selection rules, Ch. VI (c), 81, 87
 Shutts, 202
 Slawsky, 220
 Smekal, 254
 Sommerfeld, 148
 Sommermeyer, 64
 Spectra, absorption, 281 ff.
 continuous, 14, 38, 40, 47, 49
 absorption spectra, 48, 66
 emission spectra, 48, 66
 hormones and enzymes, 288
 Molecular
 Angstrom, CO, 111, 113, 145
 Spectra,
 Molecular
 BaH system, 123, 124
 barium fluoride, 25, Plate VI, 26, 36
 beryllium fluoride, 25, 125
 beryllium oxide, 16
 BO system, 43
 cadmium, 71, 72
 CH Band, 127, 130, 273, 274
 CO^+ systems, 79
 comet-tail system, 23, Plate IV, 101, 274
 comets, 274
 cyanogen, 28, 116, 119, 274
 deuterides, 180
 Fourth positive system CO, 68
 high-pressure carbon, 23, 139
 night sky and aurorae, 272
 nitrogen, 1st positive, 23, 43, 44, 54, 134, 135, 272
 nitrogen, 2nd positive, 23, 41, 139, 273
 nitrogen, 4th positive, 41
 NO β system, 34, 38, 43, 47, 68, 126
 NO γ system, 43
 nitrogen afterglow, 43, 44
 oxygen systems, 69
 O_2^+ ultra-violet, 22, Plate V, 126, 129
 planets, 276 ff.
 sodium iodide, 64
 stars, 279 ff.
 Swan system, 1, Plate 1, 4, 5, 6, 15, 24, 33, 36, 139, 274
 Third positive CO, 134
 triplet system of CO, 24, Plate IV
 proteins, 287
 Raman. *See* Raman Effect
 recombination, 39
 vitamins, 290
 Spectrographs, vacuum, 70
 Spectroscopy
 applications of, Ch. XV
 infra-red, 11, 13
 in medicine, 292
 Sponer, 62, 67, 201
 Sutherland, 213, 215, 223, 225
 Teller and Topley, 221, 222
 Temperature, of comets, 275
 determinations, 155 ff.
 'effective,' 158 ff.
 Terenin, 64, 65, 66
 Terms, rotational, Ch. VII, Ch. IX
 Transitions, electronic, 8
 rotational, 8, 9
 vibrational, 5
 Uhlenbeck, 217, 218
 United atom, 84, 85, 91
 Units, 4



Gross structure of 'Swan bands' of C_2 molecule.

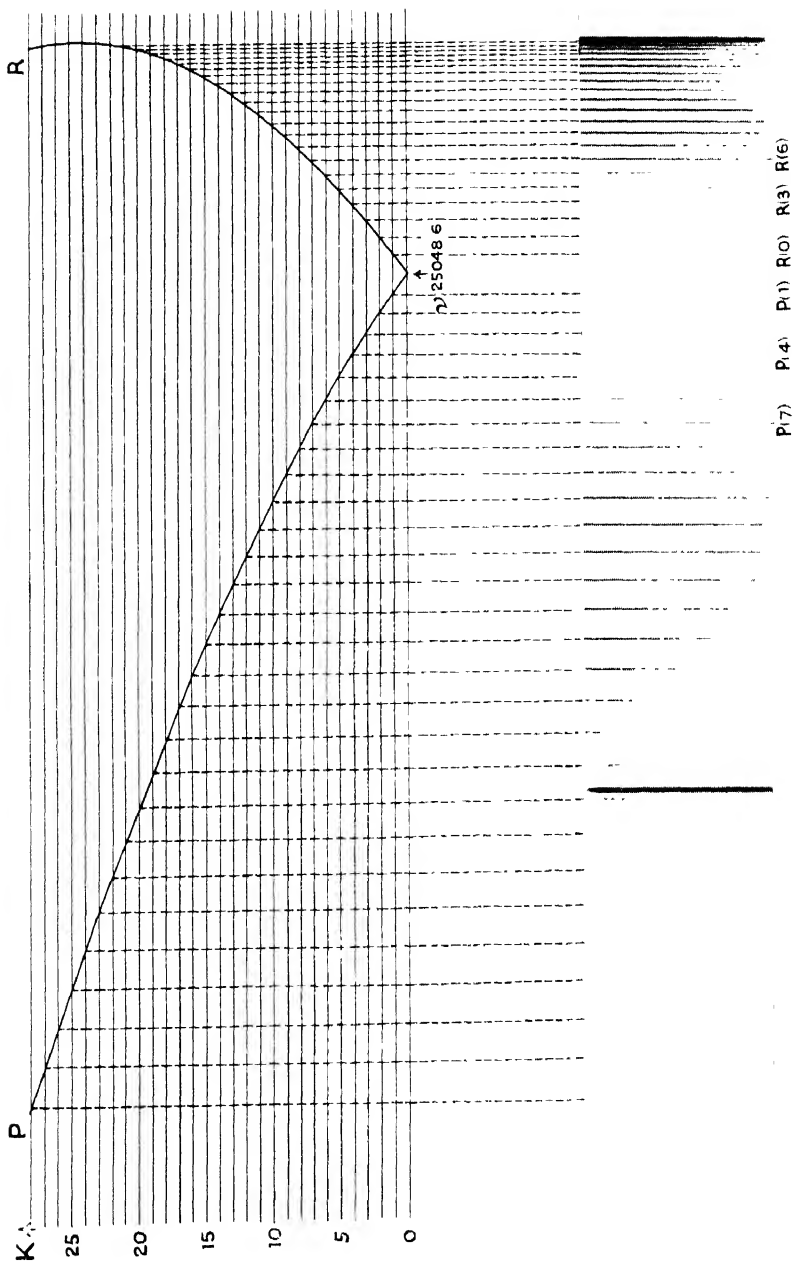
Ångstrom band (0,3) at λ 5610, showing fine structure analysis.

[Photograph by Kemble, Mulliken, and Crawford]



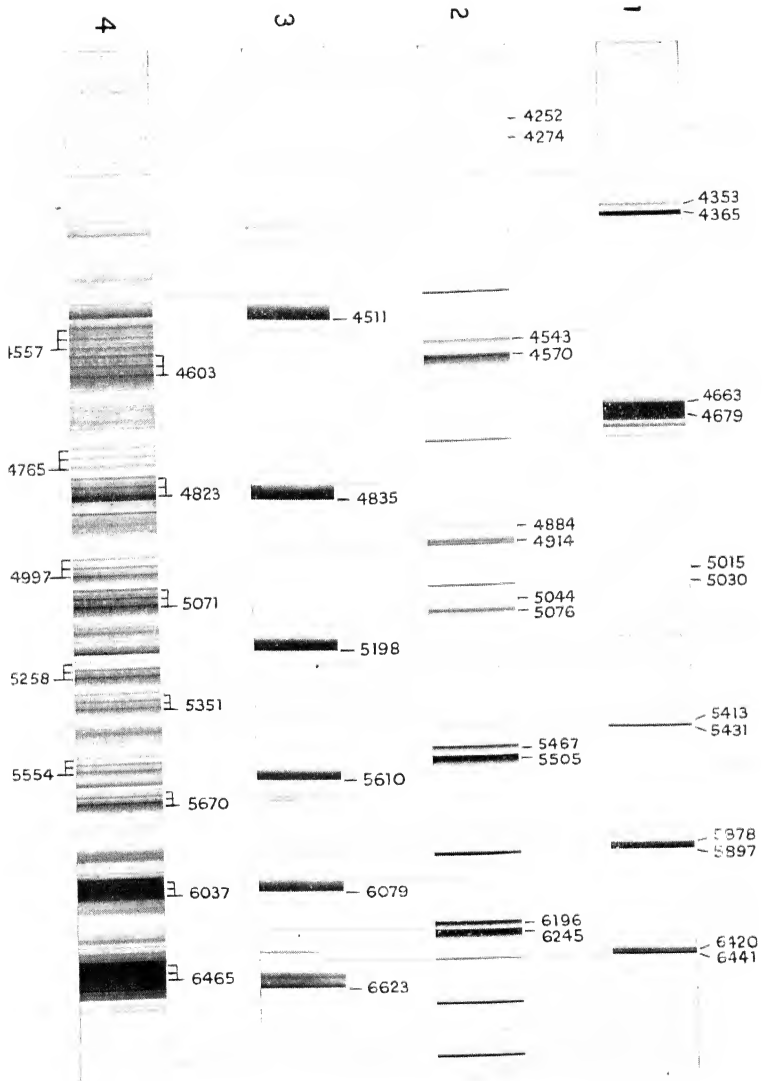
Fortrat diagram for the (13,13) band at λ 3991.11 of the CN
band system $^2\Sigma \longrightarrow ^2\Sigma$
The higher members of the R branch after the head formation are
too faint to be observed

[Photograph by P. A. Jenkins]

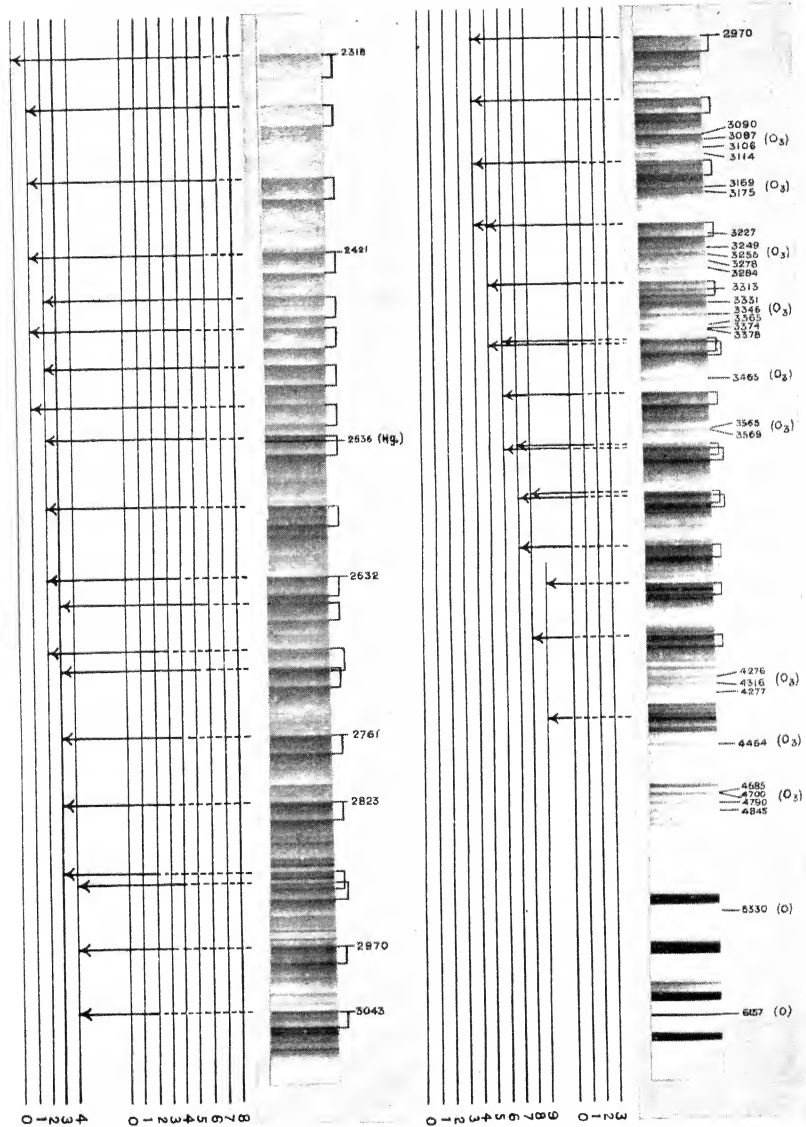


- (1) High-pressure C_2 bands, being a $^3\Pi \longrightarrow ^3\Pi$ system. This system is composed of a single v'' progression, and the bands seen are, from the left, (0,4), (0,5), (0,7), (0,8), (0,9), vide P.R.S. 124, 668 (1929).
- (2) Comet-tail bands, being a $^2\Pi \longrightarrow ^2\Sigma$ system of CO^+ . The bands seen are, from left to right, (2,0), (1,0), (0,0), (1,1), (0,1), and (0,2).
- (3) The Angstrom system of CO, $^1\Sigma \longrightarrow ^1\Pi$. The main heads shown are the (0,0), (0,1), (0,2), &c, reading from left to right.
- (4) The 'Triplet' system of CO $^3\Pi \longrightarrow ^3\Pi$. We have here two main progressions (0,0), (1,0), (2,0), &c., the first member of which is the strong band at λ 6465, and another progression (0,1), (1,1), (2,1), (3,1), (4,1), &c. The non-appearance of higher values of v'' than 0 and 1 is presumably due to the phenomenon discussed in Chapter IIIc.

PLATE IV



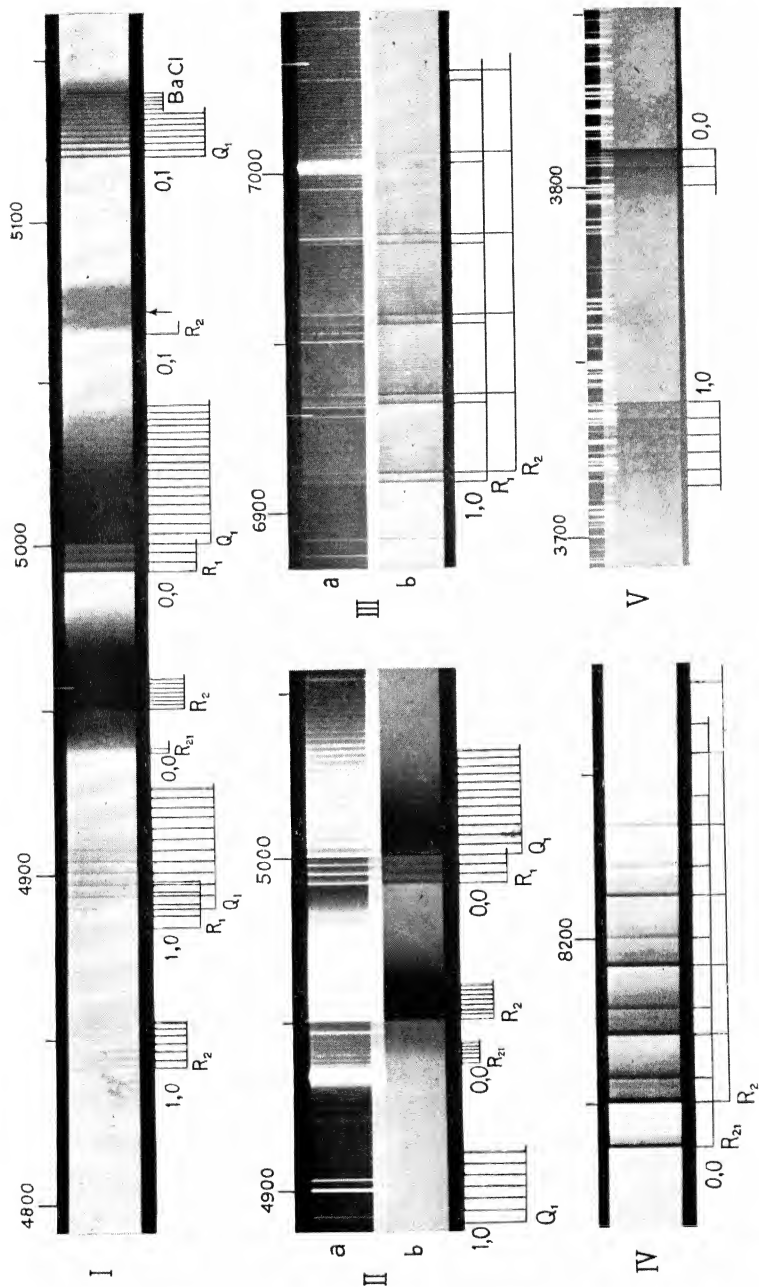
Ultra-violet system of O_2^+ (${}^2\Pi \longrightarrow {}^2\Pi$), photographed on a medium quartz spectrograph, and showing the vibrational analysis. The 'first negative' O_2^+ bands are strongly present in the visible region.



Band systems in emission and absorption of BaF (first order of 21-ft. concave grating).

- I. The entire green system ${}^2\Pi \longrightarrow {}^2\Sigma$ in absorption. The temperature of the absorption tube was about 1200° C.
- II. Central part of the green system (*a*) in emission, (*b*) in absorption.
- III. The +1 sequence of the extreme red system ${}^2\Sigma \longrightarrow {}^2\Sigma$ (*a*) in emission, (*b*) in absorption. The designation of the heads as R_1 and R_2 is arbitrary.
- IV. (0,0) sequence in absorption of the infra-red system ${}^2\Pi \longrightarrow {}^2\Sigma$ High-frequency component only.
- V. Part of high-frequency component of an ultra-violet system ($? \longrightarrow {}^2\Sigma$) in absorption

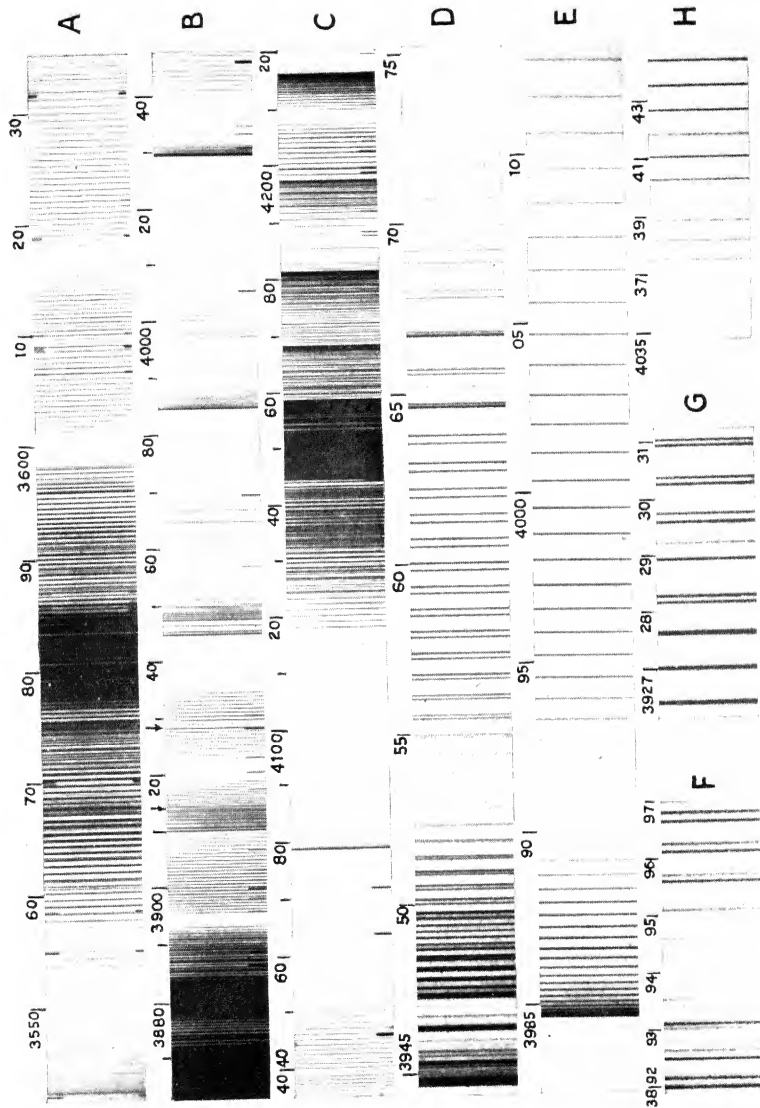
[Photograph by F. A. Jenkins and A. Harvey (Phys. Rev., 39, p. 922, 1932)]



CN 'Tail' bands in the second order of a 21-ft. concave grating produced by the interaction of active nitrogen with acetylene.

- (A) More intense portion of the sequence $v'' - v' = -1$. The head at $\lambda 3542.27$ is that of the A4 band, (14,12), of the next sequence to the violet. The intensity minimum at the null-line of the B1 band, (9,8), shows plainly at $\lambda 3617$. A few doublets of the *R* branch of the B2 band, (10,9), which does not form a head, are visible at the extreme right. Second order; iron arc comparison spectrum.
- (B) and (C) Tail bands C1 to C6, showing also the 4216 sequence of ordinary CN bands and the beginning of the 3883 sequence. First order, iron arc comparison spectrum. Cuts (D) to (H) are details from this set of tail bands with greater enlargement.
- (D) C3 band, (12,12), showing doubling and perturbations. Second order.
- (E) C4 band, (13,13). Second order.
- (F) Region of the null-line of the C1 band, (10,10). Note the unequal intensities of the doublet components. The long-wave component of *R*(1), at $\lambda 3893.1$, is strengthened by coincidence with a line of the (9,9) band. Second order.
- (G) Beginning of the perturbation in the *P* branch of C2 (11,11). Second order.
- (H) First few lines of the *P* branch of C5, (14,14). The perturbations of *P*(8), $\lambda 4039.6$, and *P*(11), $\lambda 4041.8$, are evident. First order.

[Photograph by F. A. Jenkins (Phys. Rev., 31, p. 546, 1928) and his descriptive notes above.]



Two bands of the red CN system'(${}^2\Pi \longrightarrow {}^2\Sigma$).

- (A) is the (8,3) band and shows the four heads marked, with the numeration of the Q_2 lines also.
- (B) shows the (6,2) band with a perturbation in the Q_1 branch marked below.
- (C) is a microphotometric curve of the region of the origin of the (8,3) band. P_2 are marked long and Q_2 are marked short.
- (D) is a microphotometric curve of the perturbed region in the (6,1) band corresponding to that in (B) above

(Photographs are by Jenkins, Roofs, and Mulliken (Phys. Rev., 39, p. 25, 1932) and were taken in the first order of a 21-ft grating.)

